The geometry of some tridimensional families of planar quadratic differential systems

Alex Carlucci Rezende

The geometry of some tridimensional families of planar quadratic differential systems

Alex Carlucci Rezende

Advisor: **Profa. Dra. Regilene Delazari dos Santos Oliveira**

Co-advisor: **Prof. Dr. Joan Carles Artés Ferragud**

Doctoral dissertation submitted to the *Instituto de Ciências Matemáticas e de Computação* - ICMC-USP, in partial fulfillment of the requirements for the degree of the Doctorate Program in Mathematics. *FINAL VERSION*.

USP – São Carlos
October 2014

Ficha catalográfica elaborada pela Biblioteca Prof. Achille Bassi
e Seção Técnica de Informática, ICMC/USP,
com os dados fornecidos pelo(a) autor(a)

R467t

Rezende, Alex Carlucci
The geometry of some tridimensional families of planar quadratic differential systems / Alex Carlucci Rezende; orientadora Regilene Delazari dos Santos Oliveira; co-orientador Joan Carles Artés Ferragud. -- São Carlos, 2014.
342 p.

Tese (Doutorado - Programa de Pós-Graduação em Matemática) -- Instituto de Ciências Matemáticas e de Computação, Universidade de São Paulo, 2014.

1. quadratic differential systems. 2. topological classification. 3. affine invariant polynomials. 4. global phase portrait. I. Oliveira, Regilene Delazari dos Santos, orient. II. Artés Ferragud, Joan Carles, co-orient. III. Título.

A geometria de algumas famílias tridimensionais de sistemas diferenciais quadráticos no plano

Alex Carlucci Rezende

Orientadora: **Profa. Dra. Regilene Delazari dos Santos Oliveira**

Co-orientador: **Prof. Dr. Joan Carles Artés Ferragud**

Tese apresentada ao Instituto de Ciências Matemáticas e de Computação - ICMC-USP, como parte dos requisitos para obtenção do título de Doutor em Ciências - Matemática. *VERSÃO REVISADA.*

USP – São Carlos
Outubro 2014

Ficha catalográfica elaborada pela Biblioteca Prof. Achille Bassi
e Seção Técnica de Informática, ICMC/USP,
com os dados fornecidos pelo(a) autor(a)

R467g

Rezende, Alex Carlucci
A geometria de algumas famílias tridimensionais de sistemas diferenciais quadráticos no plano / Alex Carlucci Rezende; orientadora Regilene Delazari dos Santos Oliveira; co-orientador Joan Carles Artés Ferragud. -- São Carlos, 2014.
342 p.

Tese (Doutorado - Programa de Pós-Graduação em Matemática) -- Instituto de Ciências Matemáticas e de Computação, Universidade de São Paulo, 2014.

1. sistemas diferenciais quadráticos. 2. classificação topológica. 3. polinômios invariantes afins. 4. retrato de fase global. I. Oliveira, Regilene Delazari dos Santos, orient. II. Artés Ferragud, Joan Carles, co-orient. III. Título.

It's not time to make a change
Just relax, take it easy
You're still young, that's your fault
There's so much you have to know
Find a girl, settle down
If you want, you can marry
Look at me, I am old
But I'm happy

I was once like you are now
And I know that it's not easy
To be calm when you've found
Something going on
But take your time, think a lot
I think of everything you've got
For you will still be here tomorrow
But your dreams may not

CAT STEVENS, *Father and Son*

Agradecimentos

Chega um momento em que o trabalho se torna a tarefa mais importante de nossas vidas e acabamos esquecendo que as pessoas que nos cercam são aquelas que fazem tudo valer a pena. Com tanta correria no dia a dia, ficamos acomodados e esquecemo-nos de agradecer por tudo que acontece conosco: a ajuda recebida, a graça alcançada. Neste momento, paro por um instante e tento agradecer aquele sorriso, aquele puxão de orelha, aquelas palavras de conforto e também de repreensão, aquele carinho, aquela tristeza e aquela alegria. Certamente, tudo isso me faz querer ser uma pessoa melhor a cada dia.

Em primeiro lugar, quero agradecer a Deus por minha vida, minha família, minha noiva, meus amigos, meus sentidos, minha sabedoria e pela dose diária de vontade e ânimo.

Agradeço e dedico este trabalho a minha mãe, Lucimary, a quem eu devo toda minha essência como pessoa e cidadão. Te amo incondicionalmente, mãe!

Agradeço também ao meu pai, Wagner, que pôde proporcionar-me a oportunidade de ter uma boa formação escolar básica; além de ensinar-me como (não) agir em determinadas situações.

Agradeço a Natália, meu amor, minha vida, meu tudo! Minha companheira dos momentos felizes e tristes, com quem eu quero dividir toda minha vida. Você faz parte desse trabalho tanto quanto eu, pois foi contigo que dividi o que me aconteceu de bom e de ruim em relação ao doutorado. E, se hoje estou com a tese pronta, é porque você compreendeu que às vezes minha atenção deve ser integral ao meu trabalho, além de aprender a suportar e administrar a distância que nos separa. Obrigado por tudo, meu amor! Te amo para sempre!

Aos meus irmãos, sobrinhos, padrasto, cunhada, avó, tios, primos e sogros, agradeço pelos momentos felizes em família, pois, toda vez que estive em sua presença, era motivo de festa e alegria.

Agradeço a todos os professores e funcionários do ICMC/USP, em especial a minha orientadora

Regilene Oliveira. Sem sua ajuda, Regilene, tenho certeza que não conseguiríamos chegar ao final deste trabalho. Obrigado pela atenção e disposição em ajudar, ensinar e aprender. Certamente foi um período de grande aprendizado e fortalecimento de laços para nós dois e espero que essa parceria perdure por muitos anos.

Agradezco también a los profesores y empleados del Departamento de Matemáticas de la UAB que me recibieron de brazos abiertos cuando llegué a Barcelona. Gràcies pel suport! Agradezco especialmente a Joan Carles que ha tenido mucha paciencia para enseñarme y hacerme un conocedor de la técnica empleada en este trabajo. Sin duda ya es más que un colaborador, es un gran amigo.

I would like to thank Nicolae and Dana for the opportunity of meeting you and working with you. I am pleased to know that, besides great professors, both of you are good friends that I will take for the rest of my life. Thank you for everything you could help me in these last years and I wish we could work together for many years more.

Aos amigos, irmãos que a vida me dá, muito obrigado pelo apoio, pelas conversas nas horas certas e pelas risadas e conversas jogadas fora. Não há vida nem construção e conquistas sem amigos do lado.

Agradeço à Coordenação de Aperfeiçoamento de Pessoal de Nível Superior (CAPES) pela bolsa de Doutorado no país e no exterior.

E por fim, fazendo minhas as palavras de Arthur Schopenhauer: *"a tarefa não é tanto ver aquilo que ninguém viu, mas pensar o que ninguém ainda pensou sobre aquilo que todo mundo vê"*!

Abstract

Planar quadratic differential systems occur in many areas of applied mathematics. Although more than one thousand papers have been written on these systems, a complete understanding of this family is still missing. Classical problems, and in particular Hilbert's 16th problem, are still open for this family. One of the goals of recent researchers is the topological classification of quadratic systems. As this attempt is not possible in the whole class due to the large number of parameters (twelve, but, after affine transformations and time rescaling, we arrive at families with five parameters, which is still a large number), many subclasses are considered and studied. Specific characteristics are taken into account and this implies a decrease in the number of parameters, which makes possible the study. In this thesis we mainly study two subfamilies of quadratic systems: the first one possessing a finite semi–elemental triple node and the second one possessing a finite semi–elemental saddle–node and an infinite semi–elemental saddle–node formed by the collision of an infinite saddle with an infinite node. The bifurcation diagram for both families are tridimensional. The family having the triple node yields 28 topologically distinct phase portraits, whereas the closure of the family having the saddle–nodes within the bifurcation space of its normal form yields 417. Invariant polynomials are used to construct the bifurcation sets and the phase portraits are represented on the Poincaré disk. The bifurcation sets are the union of algebraic surfaces and surfaces whose presence was detected numerically. Moreover, we also present the analysis of a differential system known as SIS model (this kind of systems are easily found in applied mathematics) and the complete classification of quadratic systems possessing invariant hyperbolas.

Key words: quadratic differential systems; topological classification; affine invariant polynomials; semi–elemental triple node; semi–elemental saddle–node; global phase portrait; SIS model; invariant hyperbola

Resumo

Sistemas diferenciais quadráticos planares estão presentes em muitas áreas da matemática aplicada. Embora mais de mil artigos tenham sido publicados sobre os sistemas quadráticos ainda resta muito a se conhecer sobre esses sistemas. Problemas clássicos, e em particular o XVI problema de Hilbert, estão ainda em aberto para essa família. Um dos objetivos dos pesquisadores contemporâneos é obter a classificação topológica completa dos sistemas quadráticos. Devido ao grande número de parâmetros (essa família possui doze parâmetros e, aplicando transformações afins e re–escala do tempo, reduzimos esse número a cinco, sendo ainda um número grande para se trabalhar) usualmente subclasses são consideradas nas investigações realizadas. Quando características específicas são levadas em consideração, o número de parâmetros é reduzido e o estudo se torna possível. Nesta tese estudamos principalmente duas subfamílias de sistemas quadráticos: a primeira possuindo um nó triplo semi–elemental e a segunda possuindo uma sela–nó semi–elemental finita e uma sela–nó semi–elemental infinita formada pela colisão de uma sela infinita com um nó infinito. Os diagramas de bifurcação para ambas as famílias são tridimensionais. A família tendo um nó triplo gera 28 retratos de fase topologicamente distintos, enquanto o fecho da família tendo as selas–nós dentro do espaço de bifurcação de sua forma normal gera 417. Polinômios invariantes são usados para construir os conjuntos de bifurcação e os retratos de fase topologicamente distintos são representados no disco de Poincaré. Os conjuntos de bifurcação são a união de superfícies algébricas e superfícies cuja presença foi detectada numericamente. Ainda nesta tese, apresentamos todos os retratos de fase de um sistema diferencial conhecido como modelo do tipo SIS (sistema suscetível–infectado–suscetível, muito comum na matemática aplicada) e a classificação dos sistemas quadráticos possuindo hipérboles invariantes. Ambos sistemas foram investigados usando de polinômios invariantes afins.

Palavras-chave: sistemas diferenciais quadráticos; classificação topológica; polinômios invari-

antes afins; nó triplo semi–elemental; sela–nó semi–elemental; retrato de fase global; modelo do tipo SIS; hipérbole invariante

List of abbreviations

We set here all of the abbreviations used in this thesis with their respective meaning.

QS: quadratic differential systems

QS$_f$ quadratic differential systems possessing a finite number of singularities (finite and infinite)

QsnSN: quadratic differential systems with a finite semi–elemental saddle–node and an infinite saddle–node of type $\overline{\binom{0}{2}}SN$

QT$\overline{\mathbf{N}}$: quadratic differential systems with a semi–elemental triple node

QVF: quadratic vector field

SIS: susceptible–infected–susceptible

Contents

List of Figures

List of Tables

Introduction

Closing problems is definitely the great pleasure of us mathematicians. We are also delighted when we have a long–time–ago theme concluded, when we write down the most famous quote *"quod erat demonstrandum"* in the end of the proof of a question formulated in the past. And this pleasure seems to be directly proportional to the time elapsed between the formulation of the question and the moment the answer is given.

With the advent of differential calculus, it became easy the possibility of solving many questions asked by ancient mathematicians, but at the same time some other questions were formulated any further. The searching for primitives for functions that could not be expressed algebraically or with a finite number of analytic terms has greatly complicated the future research and new areas of mathematics have even being created to answer these questions. And, besides the problem of searching for a primitive for a differential equation in one dimension we add more dimension, the problem became more complex.

As discussed above, the theory of ordinary differential equations became one of the basic tools of pure and applied mathematics. For instance, this theory makes it possible to study the population growth of species or the movement of a pendulum. If the derivation variable (well–known as the *time*) just plays an implicit role, the differential equation is said to be autonomous and, in this case, the systems can be considered as dynamical systems. The designation *time* for the derivation variable probably came from the evolution in time of a particle in space and is used in this sense since then. In addition, differential equations such as those used to solve real–life problems may not necessarily be directly solvable, i.e. their solutions do not have an explicit expression. Instead, solutions can be approximated using numerical methods.

Due to the complexity of solving generic differential systems and estimating their solutions, some strategies have been taken and developed in the attempt of "minimizing the problem".

Firstly, the birth of the qualitative theory of the differential equations introduced by Poincaré [47] was a great breakthrough in the study of differential systems and, secondly, the restriction in the analysis of families of differential systems with specific properties.

We recall, for example, the Hilbert's 16th problem [33, 34]. It is the most investigated mathematical problem in the qualitative theory of dynamical systems in the plane. In short, this problem discusses on the number of limit cycles in polynomial systems in the plane. Although the proposed family (the polynomial case) is already a subfamily of the set of all differential equations, this problem is still difficult to solve. In view of this difficulty, many researchers have been improving and giving new statements to the problem.

We dare say that the complete study of the huge family of generic differential systems is impossible and, hence, researchers have been studying only particular classes of such family.

In this thesis we restrict ourselves to the study and the topological classification of planar quadratic differential systems. By quadratic we mean that the functions which define the systems are polynomials of degree two. However, this subfamily is also generic and we have some reasons to restrict more this class of differential systems.

The first reason is that each particular subclass provide interesting results. For example, Artés, Llibre and Schlomiuk [6] have classified topologically the quadratic systems possessing a weak focus of second order. This class is interesting itself because all phase portraits with limit cycles in it can be produced by perturbations of symmetric (reversible) quadratic systems with a center.

Another reason is the existence of algebraic tools to deal with the problem of classifying topologically quadratic systems with peculiarities. Concerning this issue, in 1966, Coppel [22] believed that the classification of the quadratic systems could be completed purely algebraically, i.e. by means of algebraic equalities and inequalities, it would be possible to find the phase portrait of a quadratic system. At that time, his thoughts were not easy to be refuted. It is known that the finite singular points of a quadratic system can be found as the zeroes of a resultant of degree four, and its solutions can be calculated algebraically, as well as the infinite singular points. Additionally, limit cycles could be generated by Hopf bifurcation whose conditions were also determined algebraically.

However, as it is so often in mathematics that everything which is not perfectly proved may be completely false, Dumortier and Fiddelaers [26] proved in 1991 that starting with the quadratic systems (and following all subsequent systems) there exist geometric and topological phenom-

ena in their phase portrait whose determination cannot be fixed by means of algebraic relations. Specifically, most of the connections between separatrices and occurrence of double or semi–stable limit cycles is not determinable algebraically. This shows us that it is at least interesting and challenging the study of quadratic systems and the attempt to classify topologically all their phase portraits.

And the last reason (but not the less important nor, in fact, the last one) is the desire to classify all the codimension–one unstable quadratic systems. We explain a little more about it. Artés, Kooij and Llibre [4] have studied the structurally stable quadratic systems, modulo limit cycles. In their book, they proposed the determination of how many and which phase portraits a quadratic system can have after its coefficients suffer small perturbations. To obtain a structurally stable system modulo limit cycle we need few conditions. Simply, the existence of multiple singular points and separatrices connections are not allowed. Centers, weak foci, semi–stable limit cycles and all other unstable elements are "eliminated" by the quotient *modulo limit cycles*. The main result in the book [4] is that there exist exactly 44 topologically distinct phase portrait in the family of the structurally stable quadratic systems, modulo limit cycles.

As the main goal is the complete classification of the family of quadratic systems, and having classified topologically all the structurally stable quadratic systems, the natural continuation is to study the quadratic systems with a degree of degeneracy one higher, i.e. the codimension–one unstable quadratic systems, modulo limit cycles. We now allow the existence of multiple singular points and separatrices connections. Following a methodical and systematic study like the one conducted in [4], we can generate a family of topologically possible cases for this codimension. Moreover, we have the advantage that not all the topologically possible phase portraits can be realizable (fact that was learnt by constructing the 44 topological classes of structurally stable quadratic systems).

Following this methodology and other similar ones already applied in [4], we hope it will be possible to point out the candidates which are non–realizable and, using the extensive bibliography, it may be possible to find many of those realizable ones, either because they have previously appeared, or by some perturbation of them.

The state of the research is well advanced, remaining a few cases that refuse to find their example (or to prove their impossibility) and providing nearly 200 phase portraits to the collection of the 44. Again this is a very topological process with traces of qualitative theory.

Once we have completed the classification of the unstable quadratic systems of codimension

one, it would be the turn of the codimension–two systems. Although the entire process can be exhaustive, it can be subdivided into sections, and we also have the advantage that the higher degeneration the system possesses, the greater the existing bibliography is. Furthermore, the degree of codimension to further study is limited and, therefore, realizable.

Even if there exists a large literature from which we can take new examples of phase portraits still unknown, new families of quadratic systems must be studied in order to contribute to this systematic process.

The mainly used technique has been to produce a normal form for such family which fixes the position of two finite singular points, allowing the identification of the two other finite singular points (real or complex) by means of a quadratic equation. The study of singular points at infinity, even involving the study of a simple cubic, has become easier when assuming a single variable.

Sometimes, instead, this technique has forced a normal form which has behaved in a more complicated way in determining the bifurcation curves or surfaces, or simply which could have not be extended continuously to the boundaries of the parameter space. The alternative of fixing only one finite singular point is even more impracticable as it requires the use of a cubic to determine the other three finite singular points.

However, there comes to us in recent time great advances in the theory of invariants, mainly from the Sibirsky's school [57] in Moldova by the hand of one of his main students, N. Vulpe. The idea of the invariants is very simple and we will explain it with an example. We suppose that a quadratic system has generically four singular points (real or complex), but in some hypersurface of the parameter space a finite singular point goes to infinity and in another hypersurface another singular point also goes to infinity. The way to calculate them is to obtain the resultant of degree four in one of the variables. We denote by $\mu_0 x^4 + \mu_1 x^3 + \mu_2 x^2 + \mu_3 x + \mu_4$ such resultant. Therefore, in the union of the hypersurfaces in where a finite point has gone to infinity we must have $\mu_0 = 0$, so that the resultant gives exactly three (real or complex) solutions to the problem. And likewise, if two finite singular points have gone to infinity, then $\mu_0 = \mu_1 = 0$. Furthermore, the fact that a finite point collides with a point at infinity is an invariant under any affine transformation. We can modify the normal form as we desire, and the fact that $\mu_0 = 0$ will be maintained. In fact, we would have to be able (and we are) to obtain such expression not in terms of a certain normal form, but in terms of the general quadratic system with twelve coefficients. And so, having obtained these expressions, we can address classifications in wider parameter spaces since the position of the singular points has no longer any influence in calculating the bifurcations.

The great result of Sibirsky's school has been obtaining the "bricks" of these invariants, the tools to manipulate them, and obtaining a basis of elements which make up the ideal of invariant polynomials up to degree twelve. By now, these basic elements have proven to be sufficient to set all that can be determined algebraically in a quadratic system. Not only if a point goes to infinity or not, but also if two (or more) points collide, if a system has a certain degenerate singular point or not, if there exist invariant lines, if there exist centers and which global portrait they have, if there exist certain types of first integrals, if there exist weak points (foci or saddles) which are important to determine the possibility of creation of limit cycles. In short, everything that has been studied in some particular normal form can now be viewed in terms of invariants and we can obtain its bifurcations independently of the choice of the normal form.

From the papers of Artés, Llibre, Schlomiuk and Vulpe we obtain the classification of all possible combinations of finite singular points [8], of infinite singular points [53], systems with 6, 5 or 4 invariant straight lines, systems with weak focus or weak saddle, systems with polynomial first integral, systems with rational first integral of second or third order, and it is in progress the refinements of these works in terms of the tangential equivalence of singular points, i.e. in sense of distinguishing a generic node with two directions from non–generic nodes with one or infinite directions, or distinguishing the qualitative way a degenerate singular point is located at infinity. Likewise, it is also under construction a comprehensive classification of all quadratic systems in terms of their singular points. This still would not be the complete classification of phase portraits, but we would get very close to its completeness, besides being an essential step to achieve this.

Using these algebraic tools, together with numerical tools to determine the nonalgebraic bifurcations, in the recent years researchers have managed to classify families of quadratic systems that depend on four parameters. Turning to the projective space $\mathbb{RP}^3$ and by foliating it, it is possible to complete in a reasonable time studies which involve partitions of the parameter space of about 400 parts, which include about 125 different phase portraits. Many of these portraits provide new examples, which will be included in the great encyclopedia of the quadratic systems and are the first found representatives of a certain structurally stable configuration with a concrete number of limit cycles. Among these studies, we include the classification of quadratic systems possessing a focus of second order [6].

Recalling the last reason discussed above for restricting the family of quadratic systems to subfamilies with some specific characteristic, our purpose is to contribute to the classification of

the structurally unstable quadratic systems of codimension one. One way to obtain codimension–one phase portraits is considering a perturbation of known phase portraits of quadratic systems of higher codimension. This perturbation would decrease the codimension of the system and we may find a representative for a topological equivalence class in the family of the codimension–one systems and add it to the existing classification.

With this intention, we propose the study of two classes of quadratic systems. The first one possessing a finite semi–elemental triple node, and the other possessing a finite semi–elemental saddle–node and an infinite semi–elemental saddle–node formed by the collision of an infinite saddle with an infinite node. It is worth mentioning that this last class was divided into three subclasses according to the position of the infinite saddle–node.

Systems possessing a finite triple node depend on 3 parameters (and, then, their bifurcation space has dimension three — it is $\mathbb{R}^3$) and yields a partition in the parameter space of 63 parts, generating 28 topologically distinct phase portraits. The results on this family are contained in:

J. C. ARTÉS, A. C. REZENDE, R. D. S. OLIVEIRA, *Global phase portraits of quadratic polynomial differential systems with a semi–elemental triple node*, Internat. J. Bifur. Chaos Appl. Sci. Engrg. **23** (2013), 21pp.

Systems possessing the saddle–nodes as described above are divided into three subclasses according to the position of the infinite saddle–node, namely: (A) with the infinite saddle–node in the horizontal axis, (B) with the infinite saddle–node in the vertical axis and (C) with the infinite saddle–node in the bisector of the first and third quadrants. These systems are $4-$parametric, but, after affine transformations and time rescaling, one of these parameters can be fixed as 1 and, hence, their bifurcation spaces have dimension three — they are $\mathbb{RP}^3$). Doing this, we are able to provide the classification of the closure of each one of these families within the set of their representatives in the parameter space of the adopted normal forms for each family.

The parameter space of the closure of family (A) is partitioned in 85 parts, yielding 38 topologically distinct phase portraits; the parameter space of the closure of family (B) is partitioned in 43 parts, yielding 25 topologically distinct phase portraits; and the parameter space of the closure of family (C) is partitioned in 1034 parts, yielding 371 topologically distinct phase portraits. The results on this families are contained in:

J. C. ARTÉS, A. C. REZENDE, R. D. S. OLIVEIRA, *The geometry of quadratic polynomial differential systems with a finite and an infinite saddle–node* (A,B), Internat. J. Bifur. Chaos Appl.

Sci. Engrg. **24** (2014), 30pp.

and

J. C. ARTÉS, A. C. REZENDE, R. D. S. OLIVEIRA, *The geometry of quadratic polynomial differential systems with a finite and an infinite saddle–node* (*C*), Preprint, 2014.

For the analysis of the systems described above we have used the theory of invariant polynomials proposed by Sibirsky and his pupils. In addition to this algebraic tool, we have used the softwares *Mathematica*, *P4* and also an implementation in *Fortran*.

Besides these three works, we dare to go a little beyond. While we were studying the preliminaries for this thesis, we faced the problem of classifying topologically a quadratic system of type *SIS model*. Until that time, we had not had contact with the theory developed by the Sibirsky's school, so we had to use the classical results on qualitative theory of differential equations. It is a 4−parametric family which yields 3 topologically distinct phase portraits. The results on this family are contained in:

R. D. S. OLIVEIRA, A. C. REZENDE, *Global phase portraits of a SIS model*. Appl. Math. Comput. **219** (2013), 4924–4930.

Finally, but not less important, we also present in this thesis a joint work with Vulpe, which was done during the Brazilian summer of 2014 at ICMC–USP. In this work, we use the invariant polynomials to classify all the quadratic systems possessing a nondegenerate hyperbola given necessary and sufficient conditions by means of the invariant polynomials for these systems to possess at least one invariant hyperbola. Moreover, we provide their number and their multiplicity. The results on these family are contained in:

R. D. S. OLIVEIRA, A. C. REZENDE, N. VULPE, *Family of quadratic differential systems with invariant hyperbolas: a complete classification in the space* $\mathbb{R}^{12}$. Cadernos de Matemática. **15** (2014), 19–75.

This thesis is divided as follows. In Chapter 1 we provide basic concepts on the qualitative theory of differential equations and we also give an emphasis for the quadratic systems; the reader which is familiar to these concepts can skip this chapter. In Chapter 2 we present all the nomenclature concerning the singular points; they refer to "new" definitions more deeply related to the geometry of the singular points, their multiplicity and, especially, their Jacobian matrices.

Chapter 3 presents the notions of blow–up and Poincaré's compactification; in this chapter we discuss the results of the SIS model.

In Chapter 4 we describe the theory of invariant polynomials stated by Sibirsky and his pupils. This is the most important tool used in this thesis.

The results of the systems possessing a triple node are demonstrated in Chapter 5, while Chapters 6 and 7 discuss the systems having the two saddle–nodes, one finite and the other infinite.

In Chapter 8 we classify all the quadratic systems possessing an invariant nondegenerate hyperbola and, finally, in Chapter 9 we describe the further works to be done and ideas for the future.

I take this opportunity to thank the committee members Jaume Llibre, Dana Schlomiuk and Nicolae Vulpe for being present on the day of the defense (either in person or by videoconference) and also for the valuable comments and corrections which have enriched this thesis further. Moreover, I thank the advisors Joan Carles Artés and Regilene Oliveira for all patience and willingness to teach.

Have a good reading!

Chapter

1

Basic concepts on qualitative theory of ordinary differential equations

In this chapter we present some of the basic results on the qualitative theory of ordinary differential equations. Moreover, we define the class of differential systems we are going to study and present some peculiarities and related theories which will provide the basic tools in their analysis.

It is worth mentioning that the following theory is stated for differential equations in the plane $\mathbb{R}^2$. However, it is extendable for any euclidian space $\mathbb{R}^n$ (or even for Banach spaces) and it can be easily found in any book of classical ordinary differential equations (e.g. see [58] and [1]).

We also provide some definitions which will be very useful in the development of the applications we purpose to investigate. If not mentioned, all the results stated below as well as their proves can be found in [27].

1.1 Vector fields and flows in $\mathbb{R}^2$

We consider $U \subset \mathbb{R}^2$ an open subset of the plane $\mathbb{R}^2$. We define a **vector field of class** C^r on U as a C^r map

$$X : U \mapsto \mathbb{R}^2$$

where $X(x)$ represents a vector attached at the point $x \in U$. The r in C^r denotes a positive integer, $+\infty$ or ω, where C^ω stands for the set of analytic functions.

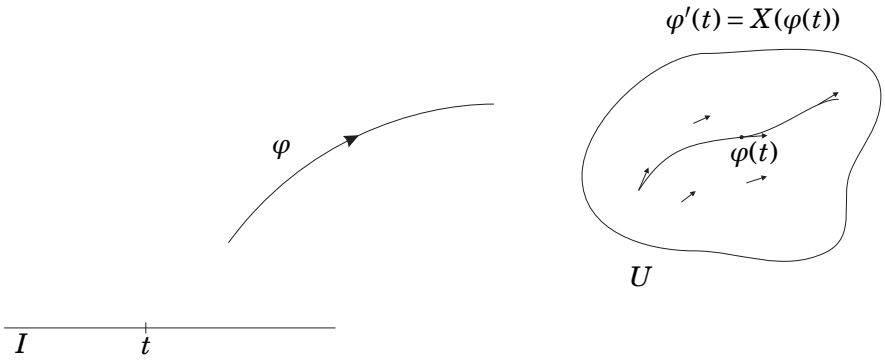

Figure 1.1: An integral curve

Figure 1.1 shows the graphical representation of a vector field on the plane which consists of a number of well chosen vectors $(x, X(x))$. Moreover, the notion of integrability of a vector field is based on the idea of looking for curves $x(t)$, with t belonging to some interval in $\mathbb{R}$, which are solutions of the *differential equation*

$$\dot{x} = X(x), \tag{1.1.1}$$

where $x \in U$, and $\dot{x}$ denotes dx/dt (i.e. the derivative of x with respect to t). In this sense, the variables x and t are called the *dependent variable* and the *independent variable* of the differential equation, respectively. The variable t is usually called the *time*.

If $X = X(x)$ does not depend on t, we say that the differential equation (1.1.1) is *autonomous*.

Solutions of this differential equation are differentiable maps $\varphi : I \mapsto U$ where I is an interval of $\mathbb{R}$ where the solution is defined, such that

$$\frac{d\varphi}{dt}(t) = X(\varphi(t)),$$

for every $t \in I$.

We can also represent the vector field by the differential operator

$$X = X_1 \frac{\partial}{\partial x_1} + X_2 \frac{\partial}{\partial x_2},$$

which operates on functions that are at least C^1. For such a function f, the image

$$Xf(x_1, x_2) = X_1 \frac{\partial f(x_1, x_2)}{\partial x_1} + X_2 \frac{\partial f(x_1, x_2)}{\partial x_2}$$

represents the derivative of $f \circ \varphi$ at $x = (x_1, x_2)$, for any solution φ at t with $\varphi(t) = x$.

Moreover, we associate to the vector field $X = (X_1, X_2)$ (or to the differential equation (1.1.1)) the 1−form

$$\omega = X_1(x_1, x_2)dx_2 - X_2(x_1, x_2)dx_1.$$

In this thesis, the notation of a vector field may also appear as a differential equation or an 1−form, but they will refer to the same object (according to the correspondences made above).

Definition 1.1.1. *A point $x \in U$ such that $X(x) = 0$ (respectively, $X(x) \neq 0$) is called a* ***singular point*** *(respectively,* ***regular point****) of X.*

Remark 1.1.2. *A singular point can also be called either a* singularity*, or a* critical point*, or an* equilibrium point*. In this thesis we use all these denominations indistinctly.*

Let $x \in U$ be a singular point of X. Then, $\varphi(t) = x$, with $-\infty < t < \infty$, is a solution of (1.1.1), i.e.

$$0 = \varphi'(t) = X(\varphi(t)) = X(x).$$

Definition 1.1.3. *Let $x_0 \in U$ and $\varphi : I \to U$ be a solution of* (1.1.1) *such that $\varphi(0) = x_0$. The solution $\varphi : I \to U$ is called* ***maximal*** *if, for every solution $\psi : J \to U$ such that $0 \in I \subset J$ and $\varphi = \psi\big|_I$, then $I = J$ and, consequently, $\varphi = \psi$.*

In the case of Definition 1.1.3, we denote $I = I_{x_0}$ and call it the *maximal interval*.

Definition 1.1.4. *Let $\varphi : I_{x_0} \to U$ be a maximal solution (either regular or constant). Its image $\gamma_\varphi = \{\varphi(t);\ t \in I_{x_0}\} \subset U$ endowed with the orientation induced by φ, in case φ is regular, is called* ***orbit****,* ***trajectory*** *or* ***(maximal) integral curve*** *associated to the maximal solution φ.*

We recall that for a solution defining an integral curve, the tangent vector $\varphi'(t)$ at $\varphi(t)$ coincides with the value of the vector field X at the point $\varphi(t)$ (see Figure 1.1).

Remark 1.1.5. *Let X be a vector field of class C^r, with $1 \leq r \leq \infty$ or $r = \omega$. We consider the set $\Omega = \{(t,x);\ x \in U,\ t \in I_x\}$. It is well-known that Ω is an open set in $\mathbb{R}^3$ and $\varphi : \Omega \to \mathbb{R}^2$ given by $\varphi(t,x) = \varphi_x(t)$ is a map of class C^r. (The proof of this fact can be found in [58].)*

We denote by $\varphi : \Omega \to \mathbb{R}^2$ the *flow generated by the vector field X*. We note that, if $I_x = \mathbb{R}$ for every x, the flow generated by X is defined on $\Omega = \mathbb{R} \times U$. But many times we have $I_x \neq \mathbb{R}$. For this reason, the flow generated by X is often called the *local flow generated by X*.

Definition 1.1.6. *Let $\varphi_x(t)$ be an integral curve of X. We say that it is **periodic** if there exists a real number $T > 0$ such that $\varphi_x(t+T) = \varphi_x(t)$, for every $t \in \mathbb{R}$.*

Having stated some definitions, geometrical elements and properties of differential equations, we need to discuss about the phase portrait of a planar differential system. The classification we want to do is based on the topological classification of all phase portraits of some families.

1.2 Phase portrait of a differential system

As discussed in Section 1.1, the orbit γ_p of a vector field $X : U \to \mathbb{R}^2$ through the point p is the image of the maximal solution $\varphi_p : I_p \to U$ endowed with an orientation, if the solution is regular.

Remark 1.2.1. *We note that the orbit passing through any point $q \in \gamma_p$ coincides with γ_p, i.e., if $q \in \gamma_p$, then $\gamma_q = \gamma_p$.*

By Remark 1.2.1, it follows that, if $q \in \gamma_p$, then there exists $t_1 \in I_p$ such that

$$q = \varphi(t_1, p), \quad \varphi(t, q) = \varphi(t + t_1, p) \quad \text{and} \quad I_p - t_1 = I_q.$$

In other words, given two orbits of X either they coincide or they are disjoint.

Roughly speaking, the next well-known result states that, given a solution φ of a vector field X, it is either a point, or a line, or a periodic orbit.

Proposition 1.2.2. *[27] If φ is a maximal solution of a C^r differential system* (1.1.1)*, then one of the following statements holds.*

(i) *φ is a bijection onto its image;*

(ii) *$I = \mathbb{R}$, φ is a constant function and γ_φ is a point;*

(iii) *$I = \mathbb{R}$ and φ is a periodic function of minimal period T (i.e. there exists a value $T > 0$ such that $\varphi(t+T) = \varphi(t)$, for every $t \in \mathbb{R}$, and $\varphi(t_1) = \varphi(t_2)$, if $|t_1 - t_2| < T$).*

Remark 1.2.3. *In statements (i) and (iii) of Proposition 1.2.2 we could add that γ_φ is C^r- diffeomorphic to $\mathbb{R}$ and that γ_φ is C^r- diffeomorphic to $\mathbb{S}^1$, respectively.*

An important object we are interested in this thesis is the global phase portrait of a differential system. All the classification we are going to present here are based on the topological classification of the global phase portraits of families of polynomial systems.

By a *phase portrait* of the vector field $X : U \to \mathbb{R}^2$ we mean the set of oriented orbits of X. It consists of singularities and regular orbits, oriented according to the maximal solutions describing them (and, consequently, in the sense of increasing t). In general, the phase portrait is represented by drawing a number of significants orbits, representing the orientation by arrows (in case of regular orbits). The notion of *global* phase portraits will be discussed later.

1.3 Topological equivalence and conjugacy

In this section we briefly present the notions of topological equivalence and conjugacy between two vector fields which allow the comparison of their phase portraits.

Let X_1 and X_2 be two vector fields defined on open subsets U_1 and U_2 of $\mathbb{R}^2$, respectively.

Definition 1.3.1. *The vector field X_1 is **topologically equivalent** (respectively, C^r- **equivalent**) **to** X_2 when there exists a homeomorphism (respectively, a C^r- diffeomorphism) $h : U_1 \to U_2$ which sends orbits of X_1 to orbits of X_2 preserving orientation.*

Definition 1.3.1 can be understood as follows. Let $p \in U_1$ and γ_p^1 be the oriented orbit of X_1 passing through p. Then, $h(\gamma_p^1)$ is an oriented orbit of X_2 passing through $h(p)$. Such a homeomorphism h is called *topological equivalence* (respectively, C^r- *equivalence*) between X_1 and X_2.

Now, let $\varphi_1 : \Omega_1 \to \mathbb{R}^2$ and $\varphi_2 : \Omega_2 \to \mathbb{R}^2$ be the flows generated by the vector fields $X_1 : U_1 \to \mathbb{R}^2$ and $X_2 : U_2 \to \mathbb{R}^2$, respectively.

Definition 1.3.2. *The vector field X_1 is **topologically conjugate** (respectively, C^r- **conjugate**) **to** X_2 when there exists a homeomorphism (respectively, a C^r- diffeomorphism) $h : U_1 \to U_2$ such that $h(\varphi_1(t,x)) = \varphi_2(t,h(x))$, for every $(t,x) \in \Omega_1$. In this case, it is necessary that the maximal intervals I_x for φ_1 and $I_{h(x)}$ for φ_2 be equal.*

The homeomorphism (respectively, diffeomorphism) h of Definition 1.3.2 is called a *topological conjugacy* (respectively, C^r- *conjugacy*) between X_1 and X_2. We note that any conjugacy is also an equivalence.

Remark 1.3.3. *A topological equivalence h defines an equivalence relation between vector fields defined on open sets U_1 and $U_2 = h(U_1)$ of $\mathbb{R}^2$. A topological equivalence h between X_1 and X_2 maps singular points to singular points and periodic orbits to periodic orbits. If h is a conjugacy, then the period of the periodic orbits is also preserved.*

1.4 Polynomial differential systems

We now consider P and Q two complex polynomials in the variables x and y of degrees m and n, respectively, and suppose that the two algebraic curves $P(x,y)=0$ and $Q(x,y)=0$ intersect in a finite number of points, i.e. that the polynomials P and Q have no common factor in the ring of complex polynomials. By Bézout's Theorem (see [32], page 47), the two algebraic curves $P(x,y)=0$ and $Q(x,y)=0$ intersect in at most mn points of the complex plane $\mathbb{C}^2$, and exactly in mn points of the complex projective plane $\mathbb{CP}^2$, if we take into account the multiplicity of the intersection points.

A differential system of the form

$$\begin{aligned} \dot{x} &= P(x,y), \\ \dot{y} &= Q(x,y), \end{aligned} \tag{1.4.1}$$

where P and Q are polynomials in the real variables x and y is called a *polynomial differential system* of degree m, if m is the maximum degree of the polynomials P and Q.

From Bézout's Theorem we conclude that a system (1.4.1) of degree m has either infinitely many singular points or at most m^2 singular points in $\mathbb{R}^2$.

Two important elements of a polynomial differential system are invariant algebraic curves and first integrals. They play an important role in the geometry of the system in the sense that they allow to draw its phase portrait.

Definition 1.4.1. *Let $f \in \mathbb{C}[x,y]$. We say that the algebraic curve $f(x,y)=0$ is an **invariant algebraic curve** of systems* (1.4.1)*, if there exists $K \in \mathbb{C}[x,y]$ such that*

$$P\frac{\partial f}{\partial x} + Q\frac{\partial f}{\partial y} = Kf. \tag{1.4.2}$$

*The polynomial K is called the **cofactor** of the invariant algebraic curve $f=0$.*

Definition 1.4.2. *Let V be an open and dense subset of $\mathbb{R}^2$. We say that a nonconstant function $H: V \to \mathbb{R}$ is a **first integral** of a system* (1.4.1) *on V, if $H(x(t),y(t))$ is constant for all of the values of t for which $(x(t),y(t))$ is a solution of this system contained in V.*

Clearly, H is a first integral of systems (1.4.1) if, and only if,

$$X(H) = P\frac{\partial H}{\partial x} + Q\frac{\partial H}{\partial y} = 0, \tag{1.4.3}$$

for all $(x,y) \in V$. When a system (1.4.1) has a first integral we say that this system is integrable. We note that, if in Definition 1.4.1 we have $K = 0$, then f is a polynomial first integral of system (1.4.1).

We now give the notion of *graphics*, which play an important role in obtaining limit cycles when they are due to connection of separatrices, for example.

Definition 1.4.3. *A **(nondegenerate) graphic** as defined in [28] is formed by a finite sequence of singular points $r_1,\ldots,r_n$ (with possible repetitions) and non–trivial connecting orbits γ_i for $i = 1,\ldots,n$ such that γ_i has r_i as α–limit set and r_{i+1} as ω–limit set for $i < n$ and γ_n has r_n as α–limit set and r_1 as ω–limit set. Also normal orientations n_j of the non–trivial orbits must be coherent in the sense that if γ_{j-1} has left–hand orientation then so does γ_j. A **polycycle** is a graphic which has a Poincaré return map.*

Definition 1.4.4. *A **degenerate graphic** is formed by a finite sequence of singular points $r_1,\ldots,r_n$ (with possible repetitions) and non–trivial connecting orbits and/or segments of curves of singular points γ_i for $i = 1,\ldots,n$ such that γ_i has r_i as α–limit set and r_{i+1} as ω–limit set for $i < n$ and γ_n has r_n as α–limit set and r_1 as ω–limit set. Also normal orientations n_j of the non–trivial orbits must be coherent in the sense that if γ_{j-1} has left–hand orientation then so does γ_j. For more details, see [28].*

1.5 A few basic properties of quadratic systems relevant for this study

Setting $m = 2$, we rewrite system (1.4.1) in the following generic form:

$$\begin{aligned} \dot{x} &= a + cx + dy + gx^2 + 2hxy + ky^2, \\ \dot{y} &= b + ex + fy + \ell x^2 + 2mxy + ny^2. \end{aligned} \tag{1.5.1}$$

Remark 1.5.1. *In systems* (1.5.1)*, we consider the coefficient of the terms xy in both equations multiplied by 2 in order to make easier the calculations of the algebraic invariants we shall compute later.*

We list below some results which play a role in the study of the global phase portraits of the real planar quadratic systems (1.5.1).

(i) A straight line either has at most two (finite) contact points with a quadratic system (which include the singular points), or it is formed by trajectories of the system; see Lemma 11.1 of [62]. We recall that by definition a *contact point* of a straight line L is a point of L where the vector field has the same direction as L, or it is zero;

(ii) If a straight line passing through two real finite[1] singular points r_1 and r_2 of a quadratic system is not formed by trajectories, then it is divided by these two singular points in three segments $\overline{\infty r_1}$, $\overline{r_1 r_2}$ and $\overline{r_2 \infty}$ such that the trajectories cross $\overline{\infty r_1}$ and $\overline{r_2 \infty}$ in one direction, and they cross $\overline{r_1 r_2}$ in the opposite direction; see Lemma 11.4 of [62];

(iii) If a quadratic system has a limit cycle, then it surrounds a unique singular point, and this point is a focus; see [22].

(iv) A quadratic system with an invariant straight line has at most one limit cycle; see [21].

(v) A quadratic system with more than one invariant straight line has no limit cycle; see [12].

Proposition 1.5.2. *A graphic must either*

(i) surround a singular point of index greater than or equal to +1, or

(ii) contain a singular point having an elliptic sector situated in the region delimited by the border, or

(iii) contain or surround an infinite number of singular points.

Proof. Let S be a simply connected closed bidimensional set which is invariant under the flow of a vector field. In [4] the *index of* ∂S is given by: $\sum_{i=1}^{n}(E_i - H_i + 2)/2$, where E_i (respectively, H_i) is the number of elliptic (respectively, hyperbolic) sectors which are inside the region delimited by S of the singular points forming the border. Also the *index of* S is given by the index of ∂S plus the sum of the indices of the singular points in the interior of S.

From the same paper, Proposition 4.8 claims that given a vector field X or $p(X)$ (the compactified vector field[2]) and S an invariant region topologically equivalent to $\mathbb{D}^2$ (the closed disk) containing a finite number of singular points (both in ∂S or its interior), then the index of S is always +1.

Now, assume that we have a graphic of a polynomial system. If it contains an infinite number of singular points (either finite or infinite) we are done. Otherwise, such a graphic together with

[1] See Chapter 3 for the definition of finite and infinite singular points

[2] See Chapter 3 for the definition of compactified vector field

its interior is an invariant region as defined in [4] and must have index +1. Since the index is positive, we must have some element, either in the interior or on the border which makes the index positive, and this implies the existence of either a point of index greater than or equal to +1 in its interior or at least one elliptic sector coming from a singular point on the border and situated in the region delimited by the graphic. ■

1.6 Intersection numbers for curves

According to [6], in this section we summarize the notion of intersection number of two algebraic curves at a point (see [30] for a complete explanation). This notion will be very useful in the definition of multiple singular point given in Chapter 2 and also in the description of the bifurcation surfaces (in Chapters 5, 6 and 7) combined with the notion of divisor and zero–cycles given in the end of Chapter 4.

Definition 1.6.1. *Let $C : f(x,y) = 0$ and $C' : g(x,y) = 0$ be two affine algebraic curves over $\mathbb{C}$. The **intersection number of** C **and** C' **over** $\mathbb{C}$ **at a point** $a \in \mathbb{C}^2$ is the number:*

$$I_a(f,g) = \dim_{\mathbb{C}} \frac{\mathbf{O}_a}{(f,g)},$$

where $\mathbf{O}_a$ is the local ring of the affine complex plane $\mathbf{A}^2(\mathbb{C}) = \mathbb{C}^2$ at a, i.e. $\mathbf{O}_a$ is the ring of rational functions $r(x,y)/s(x,y)$ which are defined at a (i.e. $s(a) \neq 0$), and (f,g) is the ideal generated by the functions f and g.

In the case that the polynomial differential systems are quadratic, the intersection numbers $I_a(P,Q)$ for P and Q as in (1.5.1), at the singular points a in $\mathbb{C}^2$ can be computed easily by using axioms in [30].

We can also define the intersection number for projective curves. See Section 3.3 (page 35) for the definition.

From now on, we assume that the reader knows most of the basic definitions and results on qualitative theory of differential systems on the plane $\mathbb{R}^2$ (see Chapter 1 of [27] for further reference). However, in Chapter 3 we shall discuss more emphatically the ideas of *blow–up* and *Poincaré's compactification* which play an important role in the application presented there.

Chapter

2

New nomenclature for singular points

2.1 New notation and representation for singular points

In this section we present new notation and designation for singular points which make part of a set of new definition more deeply related to the geometry of the singular points, their multiplicity and, especially, their Jacobian matrices.

We summarize here the definitions we shall use in this thesis. The entire new designation can be found in [7]. The purpose of these new nomenclature lays on the idea of introducing the *geometric equivalence relation* for singularities, finite or infinite, of planar quadratic vector fields. This equivalence relation is finer than the *qualitative equivalence relation* introduced by Jiang and Llibre in [35] since the first one distinguishes among the foci of different orders and among the various types of nodes. This equivalence relation also induces a finer distinction among the more complicated degenerate singularities.

Definition 2.1.1. *[7] Concerning the degeneracy of a singular point r of a quadratic vector field X, it can be called:*

(i) ***elemental****, if both eigenvalues of* $\mathrm{D}X(r)$ *are nonzero;*

(ii) ***semi–elemental****, if* $\mathrm{D}X(r)$ *has exactly one of its eigenvalues equal to zero;*

(iii) ***nilpotent****, if both of the eigenvalues of* $\mathrm{D}X(r)$ *are zero, but the matrix of* $\mathrm{D}X(r)$ *is not identically zero;*

(iv) ***intricate****, if the matrix of* $\mathrm{D}X(r)$ *is identically zero.*

Remark 2.1.2. *The equivalent names in the literature for the singular points given in Definition 2.1.1 are, respectively,* hyperbolic *(or* elementary*),* semi–hyperbolic *(or* semi–elementary*),* nilpotent *and* linearly zero*.*

Definition 2.1.3. *We say an elemental singular point is an* ***antisaddle****, if its index is* $+1$*, and it is a* ***saddle****, if its index is* -1*.*

Notation 2.1.4. *For the elemental singular points, we use the letters 's' and 'S' for saddles; 'n' and 'N' for nodes; 'f' for foci and 'c' for centers. The lower–case letters are for finite singularities and the capital letters are for the infinite ones.*

Being more specific, we distinguish the finite nodes as follows:

(i) 'n' for a node with two distinct eigenvalues (generic node);

(ii) $'n^d'$ *for a node with two identical eigenvalues whose Jacobian matrix cannot be diagonal (one–direction node);*

(iii) $'n^*'$ *for a node with two identical eigenvalues whose Jacobian matrix is diagonal (star node).*

Moreover, in the case of an elemental infinite generic node, we want to distinguish whether the eigenvalue associated to the eigenvector directed towards the affine plane is, in absolute value, greater or lower than the eigenvalue associated to the eigenvector tangent to the line at infinity. This difference is relevant to determine if all the orbits except one on the Poincaré disk arrive at infinity tangentially to the line at infinity or transversally to this line. We shall denote them by $'N^\infty'$ *and* $'N^f'$*, respectively.*

To distinguish among the foci (or saddles) of different orders we use the algebraic concept of Poincaré–Lyapunov constants.

Definition 2.1.5. *We call* ***strong focus*** *(or* ***strong saddle****) a focus (or a saddle) with nonzero trace of the linearization matrix at this point. Such a focus (or saddle) will be defined to have the order zero. A focus (or saddle) with trace zero is called a* ***weak focus*** *(or* ***weak saddle****).*

Notation 2.1.6. *According to Definition 2.1.5, finite elemental foci and saddles are classified as strong or weak. When the trace of the Jacobian matrix evaluated at those singular points is not zero, we call them strong saddles and strong foci and we maintain the standard notations 's' and 'f'. But when the trace is zero, except for centers and saddles of infinite order (i.e. saddles with*

all their Poincaré–Lyapounov constants equal to zero), it is known that the foci and saddles, in the quadratic case, may have up to 3 orders. We denote them by 's$^{(i)}$' and 'f$^{(i)}$', where $i = 1,2,3$ is the order. In addition, we have the centers which we denote by 'c' and saddles of infinite order (integrable saddles) which we denote by '$'.

For details on Poincaré–Lyapunov constants and weak foci we refer to [39].

The next definition sets the concept of multiplicity of singular points using the notion of intersection numbers for curves stated in Definition 1.6.1.

Definition 2.1.7. *[49] We say that a singular point r of system* (1.4.1) *has* ***multiplicity*** *k, if the intersection number of the curves $P = 0$ and $Q = 0$ at r is k, i.e. if $I_r(P,Q) = k$.*

Equivalently and roughly speaking, a singular point r of a polynomial differential system X is a *multiple singularity of multiplicity k*, if r produces k singularities, as close to r as we desire, in polynomial perturbations X_ε of this system and k is the maximal such number. In polynomial differential systems of fixed degree n we have several possibilities for obtaining multiple singularities:

(i) a finite singular point splits into several finite singularities in $n-$degree polynomial perturbations;

(ii) an infinite singular point splits into some finite and some infinite singularities in $n-$degree polynomial perturbations;

(iii) an infinite singularity splits only in infinite singular points of the systems in $n-$degree perturbations.

Another way to describe a singularity of multiplicity k is calling it a *collision of k singularities* in which we can add as information the type of the singularities that can be obtained after perturbations.

To all the previous cases it is possible to give a precise mathematical meaning using the notion of multiple intersection at a point r of two algebraic curves, in the sense of Definition 2.1.7.

The next definition standardizes the notation of certain singular points which will be the object of study in the next chapters.

Definition 2.1.8. *(i) A finite singular point is a* ***finite saddle–node****, if its neighborhood is formed by the union of two hyperbolic sectors and one parabolic sector;*

(ii) An infinite singular point is an ***infinite saddle–node****, if either:*

(ii.1) it is the collision of an infinite saddle with an infinite node;

(ii.2) it is the collision of a finite saddle (respectively, finite node) with an infinite node (respectively, infinite saddle).

Notation 2.1.9. *All nonelemental singular points are multiple points. For finite singular points we denote their multiplicity with a subindex as in '$\overline{s}_{(5)}$' or in '$\widehat{es}_{(3)}$' (the notation '$\overline{\ }$' indicates that the point is semi–elemental and '$\widehat{\ }$' indicates that the singular point is nilpotent). In order to describe the various kinds of multiplicity for infinite singular points we use the concepts and notations introduced in [53]. Thus we denote by '$\binom{a}{b}$...' the maximum number a (respectively, b) of finite (respectively, infinite) singularities which can be obtained by perturbation of the multiple point. For example, '$\overline{\binom{1}{1}}SN$' means a saddle–node at infinity produced by the collision of one finite singularity with an infinite one; '$\overline{\binom{0}{3}}S$' means a saddle produced by the collision of 3 infinite singularities.*

The semi–elemental points can either be nodes, saddles or saddle–nodes, finite or infinite. We will denote the semi–elemental ones always with an overline, for example '$\overline{sn}$', '$\overline{s}$' and '$\overline{n}$' with the corresponding multiplicity. In the case of infinite points we will put '$\overline{\ }$' on the top of the parenthesis with multiplicities. Semi–elemental nodes could never be 'n^d' or 'n^*' since their eigenvalues are always different. In case of an infinite semi–elemental node, the type of collision determines whether the point is denoted by 'N^f' or by 'N^∞', where '$\overline{\binom{2}{1}}N$' is an 'N^f' and '$\overline{\binom{0}{3}}N$' is an 'N^∞'.

The nilpotent points can either be saddles, or nodes, or saddle–nodes, or elliptic–saddles, or cusps, or foci, or centers. The first four of these could be at infinity. We denote the nilpotent singular points with a hat '$\widehat{\ }$' as in '$\widehat{es}_{(3)}$' for a finite nilpotent elliptic–saddle of multiplicity 3 and '$\widehat{cp}_{(2)}$' for a finite nilpotent cusp point of multiplicity 2. In the case of nilpotent infinite points, we will put the '$\widehat{\ }$' on top of the parenthesis with multiplicity, for example $\widehat{\binom{1}{2}}PEP-H$. The relative position of the sectors of an infinite nilpotent point, with respect to the line at infinity, can produce topologically different phase portraits. This forces us to use a notation for these points similar to the notation which we will use for the intricate points.

We recall that the neighborhood of any singular point of a polynomial vector field (except for foci and centers) is formed by a finite number of sectors which could only be of three types: parabolic, hyperbolic and elliptic (see [27]). Then, a reasonable way to describe intricate and nilpotent points at infinity is to use a sequence formed by the types of their sectors. The description we give is the one which appears in the clock–wise direction (starting anywhere) once the blow–down of the desingularization is done. Thus, in nondegenerate quadratic systems, we have just seven possibilities for finite intricate singular points of multiplicity four (see [8]) which are the following ones: $phpphp_{(4)}$, $phph_{(4)}$, $hh_{(4)}$, $hhhhhh_{(4)}$, $peppep_{(4)}$, $pepe_{(4)}$ *and* $ee_{(4)}$.

We use lower–case letters because they refer to finite singularities and add the subindex (4) *since they are all of multiplicity* 4.

For infinite intricate and nilpotent singular points, we insert a hyphen between the sectors to split those which appear on one side or the other of the equator of the sphere. In this way, we will distinguish between '$\binom{2}{2}PHP-PHP$*' and '*$\binom{2}{2}PPH-PPH$*'. Whenever we have an infinite nilpotent or intricate singular point, we will always start with a sector bordering the infinity in order to avoid using two dashes.*

It is worth mentioning that the finer distinctions of singularities can be obtained algebraically. The bifurcation diagram of the global configurations of finite and infinite singularities in quadratic vector fields can be obtained by using only algebraic means, for instance, the algebraic tool of invariant polynomials. In some purposes, algebraic information may not be significant for the local phase portrait around a singularity. For example, topologically there exists no distinction between a focus and a node or between a weak and a strong focus. However, algebraic information plays a fundamental role in the study of perturbations of systems possessing such singularities.

2.2 The normal form for semi–elemental singular points

In this section we present a well–known result which provides the normal form for a quadratic system to posses either a semi–elemental saddle–node, or a semi–elemental triple node, or a semi–elemental triple saddle at the origin. This normal form will be very useful in the next applications.

Proposition 2.2.1. *[2, 27] Let* $r=(0,0)$ *be an isolated singular point of the vector field* X *given by*

$$\begin{aligned} \dot{x} &= A(x,y), \\ \dot{y} &= y + B(x,y), \end{aligned} \tag{2.2.1}$$

where A *and* B *are analytic in a neighborhood of the origin starting with a degree at least 2 in the variables* x *and* y*. Let* $y=f(x)$ *be the solution of the equation* $y+B(x,y)=0$ *in a neighborhood of the point* $r=(0,0)$*, and suppose that the function* $g(x)=A(x,f(x))$ *has the expression* $g(x)=ax^{\alpha}+o(x^{\alpha})$*, where* $\alpha\geq 2$ *and* $a\neq 0$*. So, when* α *is odd, then* $r=(0,0)$ *is either an unstable multiple node, or a multiple saddle, depending if* $a>0$*, or* $a<0$*, respectively. In the case of the multiple saddle, the separatrices are tangent to the* x*–axis. If* α *is even, the* $r=(0,0)$ *is a multiple saddle–node, i.e. the singular point is formed by the union of two hyperbolic sectors with one parabolic sector. The stable*

separatrix is tangent to the positive (respectively, negative) x–axis at $r = (0,0)$ *according to* $a < 0$ *(respectively,* $a > 0$*). The two unstable separatrices are tangent to the y–axis at* $r = (0,0)$.

In the particular case where A and B from system (2.2.1) are real quadratic polynomials in the variables x and y, a quadratic system with a semi–elemental singular point at the origin can always be written into the form

$$\begin{aligned} \dot{x} &= gx^2 + 2hxy + ky^2, \\ \dot{y} &= y + \ell x^2 + 2mxy + ny^2. \end{aligned} \tag{2.2.2}$$

By Proposition 2.2.1, if $g \neq 0$, then we have a semi–elemental saddle–node $\overline{sn}_{(2)}$. If $g = 0$ and $h\ell \neq 0$, then, if $\ell < 0$, we have a triple node $\overline{n}_{(3)}$ and, if $\ell > 0$, we have a triple saddle $\overline{s}_{(3)}$.

The study of the case $g = 0$ and $\ell < 0$ is presented in Chapter 5 and the case $g \neq 0$ is discussed in Chapters 6 and 7. The remaining case $g = 0$ and $\ell > 0$ will be considered in near future (see Chapter 9).

Chapter

3

Blow–up, Poincaré's compactification and application

In this chapter we give some notions of *blow–up* and *Poincaré compactification*. They are the basic steps we need to learn concerning the qualitative theory of polynomial quadratic systems.

The blow–up is a tool used for studying the local behavior at nilpotent or intricate singularities by means of blowing up each such a singularity to a line or a circle (as many times as necessary), obtaining only elemental or semi–elemental singularities on this line (or circle); then we know their local sectors and separatrices and apply the inverse process (called blow–down), describing the local behavior of the given singular point. The blow–up is necessary if we want to construct the phase portrait of a vector field having nilpotent and intricate singularities.

In turn, Poincaré compactification is crucial if we want to draw the global phase portrait of a vector field on the plane. We shall be able to compactify the whole plane $\mathbb{R}^2$ and identify it to the unit disk $\mathbb{D}^2$, with the infinity of $\mathbb{R}^2$ being the circle $\partial\mathbb{D}^2 = \mathbb{S}^1$.

We also provide the notions of complex foliation with singularities on $\mathbb{CP}^2$ and of intersection number for complex curves.

Finally, we present an application using the tools presented until this chapter, including it. The reader who is familiarized with these concepts could skip Sections 3.1, 3.2, 3.3 and 3.4 and go directly to Section 3.5.

3.1 Blow–up: desingularization of nonelemental singularities

We now present the basic tool for studying nonelemental singularities of a differential system in the plane. This tool consists in applying changes in the variables called *blow–ups* and it is used for classifying nilpotent and intricate singularities. Another approach of blow–up is to show that, at isolated singularities, an analytic system has a finite sectorial decomposition.

The most–applied types of blow–up are the homogeneous one and the quasihomogeneous one. In this thesis we briefly introduce only the first type, and the second can be found in [27].

In spite of the fact that blow–up techniques are supposed to be known by the ones interested in studying quadratic differential systems, the aim of discussing them here is to reinforce the idea that, even if the singularity is nonelemental (as the nilpotent singular point), there exist techniques which help us to detect the behavior at the point.

It is worth mentioning that the homogeneous blow–up is a particular case of the quasihomogeneous blow–up, if we consider the weights $(1,1)$. In this sense, although we present only the notions on homogenous blow–up, the algorithm used in program P4 (Planar Polynomial Phase Portraits, see Chapter 10 of [27]; and also [3]) is based on the use of quasihomogeneous blow–up. For further information on these two types of blow–up, see [27].

We consider a vector field X on $\mathbb{R}^2$ of class C^∞ and let $p \in \mathbb{R}^2$ be a singularity of X. Via a translation (if necessary), we may assume p is the origin of $\mathbb{R}^2$. We consider the map

$$\begin{aligned} \phi : \mathbb{S}^1 \times \mathbb{R} &\to \mathbb{R}^2 \\ (\theta, r) &\mapsto (r\cos\theta, r\sin\theta). \end{aligned}$$

Thus, we can define a new vector field $\widehat{X}$ of class C^∞ on the cylinder $\mathbb{S}^1 \times \mathbb{R}$ such that $\phi_*(\widehat{X}) = X$, in the sense that

$$\mathrm{D}\phi_v(\widehat{X}(v)) = X(\phi(v)). \tag{3.1.1}$$

This property is called the *pull–back of X by ϕ* and it is nothing else but X written in polar coordinates.

Remark 3.1.1. *The map ϕ is a C^∞ diffeomorphism. Then, it is an authentic C^∞ coordinate change on $\mathbb{S}^1 \times (0,\infty)$, but not on $\{r = 0\}$. This map ϕ is called the* polar blow–up.

Indeed, it is easy to observe that ϕ maps the set $\{r = 0\}$ to the point $(0,0)$, but the inverse mapping ϕ^{-1} blows up the origin to a circle.

In order to study the phase portrait of X in a neighborhood V of the origin, it is sufficient to study the phase portrait of $\widehat{X}$ on the neighborhood $\phi^{-1}(V)$ of the circle $\mathbb{S}^1 \times \{0\}$ (we can even restrict to $\{r \geq 0\}$).

A priori analyzing $\widehat{X}$ seems to be a more difficult task than examining the vector field X itself, but its construction is very helpful. We note that, if the k–jet $j_k(X)(0)$ is zero, then $j_k(\widehat{X})(u) = 0$, for all $u \in \mathbb{S}^1 \times \{0\}$.

The cylinder is a good surface for having a global view of $\widehat{X}$ and its phase portrait. However, it is generally less suitable for making calculations, since we regularly have to deal with trigonometric expressions. In this sense, we always choose to perform the computations in different charts.

On the parts of the cylinder given, respectively, by $\theta \in (-\pi/2, \pi/2)$ and $\theta \in (\pi/2, 3\pi/2)$ we use a chart given by

$$K^x : (\theta, r) \mapsto (r\cos\theta, \tan\theta) = (\overline{x}, \overline{y}).$$

In this chart, the expression of the blow–up map ϕ is given by

$$\phi^x : (\overline{x}, \overline{y}) \mapsto (\overline{x}, \overline{xy}). \tag{3.1.2}$$

Indeed, we observe that

$$\begin{aligned} \phi = \phi^x \circ K^x : (\theta, r) &\overset{K^x}{\mapsto} (r\cos\theta, \tan\theta) \\ &\overset{\phi^x}{\mapsto} (r\cos\theta, r\cos\theta\tan\theta) = (r\cos\theta, r\sin\theta). \end{aligned} \tag{3.1.3}$$

The map ϕ^x defined in (3.1.2) is called *blow–up in the x–direction* and the pull–back of X by means of ϕ^x is denoted by $\widehat{X}^x$, i.e. $(\phi^x)_*(\widehat{X}^x) = X$.

Analogously, on the parts of the cylinder given, respectively, by $\theta \in (0, \pi)$ and $\theta \in (\pi, 2\pi)$ we use a chart given by

$$K^y : (\theta, r) \mapsto (\cot\theta, r\sin\theta) = (\overline{x}, \overline{y}).$$

So, this leads to the following expression of the blow–up map ϕ:

$$\phi^y : (\overline{x}, \overline{y}) \mapsto (\overline{xy}, \overline{y}), \tag{3.1.4}$$

which is such that $\phi = \phi^y \circ K^y$. The map ϕ^y defined in (3.1.4) is called *blow–up in the y–direction* and the pull–back of X by means of ϕ^y is denoted by $\widehat{X}^y$, i.e. $(\phi^y)_*(\widehat{X}^y) = X$.

Both ϕ^x and ϕ^y are called *directional blow–ups*.

If $j_k(X)(0) = 0$ and $j_{k+1}(X)(0) \neq 0$, then $j_k(\widehat{X}^x)(z) = 0$ and $j_k(\widehat{X}^y)(z) = 0$, for $z \in \{\overline{x} = 0\}$ and $z \in \{\overline{y} = 0\}$, respectively. In this case, the pull–back $\widehat{X}$ and likewise $\widehat{X}^x$ and $\widehat{X}^y$ are quite degenerate, and to make the situation less degenerate, we consider $\overline{X}$ defined as

$$\overline{X} = \frac{1}{r^k}\widehat{X}.$$

It is clear that $\overline{X}$ is also a C^∞ vector field on $\mathbb{S}^1 \times \mathbb{R}$. On $\{r > 0\}$ this division does not change the orbits of $\widehat{X}$ or their sense of direction, but only the parametrization by t. From the formulas above, we conclude that singularities of $\overline{X}\big|_{\{r=0\}}$ comes in pairs of opposite points.

For the directional blow–ups we use $(1/\overline{x}^k)\widehat{X}^x$ in case (3.1.2) and $(1/\overline{y}^k)\widehat{X}^y$ in case (3.1.4).

Remark 3.1.2. *We note that, on $\{\overline{x} \neq 0\}$ (respectively, $\{\overline{y} \neq 0\}$), the vector fields $(1/r^k)\widehat{X}$ and $(1/\overline{x}^k)\widehat{X}^x$ (respectively, $(1/\overline{y}^k)\widehat{X}^y$) are no longer equal up to analytic coordinate change, as were $\widehat{X}$ and $\widehat{X}^x$ (respectively, $\widehat{X}^y$), but they are the same up to analytic coordinate change and multiplication by a nonzero analytic function.*

Concerning the blow–up in the $x-$direction, since $\phi = \phi^x \circ K^x$, we conclude that $(K^x)_*(\widehat{X}) = \widehat{X}^x$. Hence,

$$(K^x)_*(\overline{X}) = (K^x)_*(\widehat{X}/r^k) = \frac{1}{r^k}(K^x)_*(\widehat{X}) = \frac{1}{r^k}\widehat{X}^x = \overline{X}^x\left(\frac{\overline{x}}{r}\right)^k.$$

Seen in $(\theta, r)-$coordinates, we have $\overline{x}/r = \cos\theta$, which is strictly positive on the part of the cylinder given by $\theta \in (-\pi/2, \pi/2)$.

Analogously, in the $y-$direction, we have $(K^y)_*(\widehat{X}) = \widehat{X}^y$ and $(K^y)_*(\overline{X}) = \overline{X}^y(\sin\theta)^k$, with $\sin\theta > 0$ on the part of the cylinder given by $\theta \in (0, \pi)$.

The directional blow–up ϕ^x (respectively, ϕ^y) can also be used for making a study on $\{(\theta, r);\ \theta \in (\pi/2, 3\pi/2),\ r \geq 0\}$ (respectively, $\{(\theta, r);\ \theta \in (\pi, 2\pi),\ r > 0\}$), but in the case we have $\cos\theta < 0$ (respectively, $\sin\theta < 0$).

If k is odd, this implies that in the phase portraits that we find for $\overline{X}^x\big|_{\{\overline{x}\leq 0\}}$ (respectively, $\overline{X}^y\big|_{\{\overline{y}\leq 0\}}$) we have to reverse the time. Such a time reversal could be avoided by using ϕ^x (respectively, ϕ^y) only for $\overline{x} \geq 0$ (respectively, $\overline{y} \geq 0$); adding two extra directional blow–ups

$$\phi^{-x}:(\overline{x}, \overline{y}) \mapsto (-\overline{x}, -\overline{xy}), \quad \phi^{-y}:(\overline{x}, \overline{y}) \mapsto (-\overline{xy}, -\overline{y}),$$

makes us limit to, respectively, $\overline{x} \geq 0$ and $\overline{y} \geq 0$.

Remark 3.1.3. *There exist some cases for which applying the blow–up only once is not sufficient to desingularize the singularity, i.e. there remains nonelemental singularities of* $\overline{X}\big|_{\{r=0\}}$ *at which we need to repeat the blow–up construction, leading to successive blow–up (see Example 3.2 of [27], page 95, for an illustration of this fact).*

Remark 3.1.4. *After a sequence of n blow–ups, we find some* C^∞ *vector field* $\overline{X}^n$ *defined on a domain* $U_n \subset \mathbb{R}^2$. *The vector field* $\overline{X}^n$ *remains analytic if we consider an analytic vector field* X. *We denote by* $\Gamma_n = (\phi_1 \circ \cdots \circ \phi_n)^{-1}(0) \subset U_n$. *Only one of the connected components of* $\mathbb{R}^2 \setminus \Gamma_n$, *call it* A_n, *has a noncompact closure. Furthermore, the border* $\partial A_n \subset \Gamma_n$ *is homeomorphic to* $\mathbb{S}^1$ *and consists of a finite number of analytic regular closed arcs meeting transversally. The map* $(\phi_1 \circ \cdots \circ \phi_n)\big|_{A_n}$ *is an analytic regular diffeomorphism which maps* A_n *onto* $\mathbb{R}^2 \setminus \{0\}$. *There exists a strictly positive function* F_n *on* A_n *such that* $\widehat{X}^n = F_n \overline{X}^n$ *and* $\widehat{X}^n\big|_{A_n}$ *is analytically diffeomorphic to* $X\big|_{\mathbb{R}^2\setminus\{0\}}$ *by means of the diffeomorphism* $(\phi_1 \circ \cdots \circ \phi_n)\big|_{A_n}$. *The function* F_n *extends in a* C^ω *way to* ∂A_n *where in general it is* 0.

By Remark 3.1.3, there appears some questions regarding successive blow–ups.

(a) How many times could we apply the blow–up to a vector field?

(b) Could this sequence of blow–ups be controlled in the sense that it leads to a desingularization?

(c) Is there any sufficient condition for applying successive blow–ups and obtain a desingularized vector field?

The answer to all these questions is *yes*!

In order to control a sequence of blow–ups and to guarantee it leads to a desingularization, we need the notion of a *Łojasiewicz inequality*.

Definition 3.1.5. *We say a vector field* X *on* $\mathbb{R}^2$ *satisfies a* ***Łojasiewicz inequality*** *at* 0 *if there exist* $k \in \mathbb{N}$, *with* $k \geq 1$, *and* $c > 0$ *such that* $\|X(x)\| \geq c\|x\|^k$ *on some neighborhood of* 0.

Remark 3.1.6. *We observe that for analytic vector fields at isolated singularities, a Łojasiewicz inequality always holds (see [14] for further information).*

The next theorem answers our questions. It provides a sufficient condition to obtain a desingularized vector field and it also states the type of the obtained singularities. We shall not give a proof for this theorem, but it can be found in [25].

Theorem 3.1.7. *[25] If a vector field* X *satisfies a Łojasiewicz inequality at* 0, *then there exists a finite sequence of blow–ups* $\phi_1 \circ \cdots \circ \phi_n$ *leading to a vector field* $\overline{X}^n$ *defined in the neighborhood*

of ∂A_n of which the singularities on ∂A_n are elemental. These elemental singularities can be as follows:

(i) isolated singularities p which are elemental or semi–elemental with flat behavior on the center manifold;

(ii) regular analytic closed curves (or possibly the whole ∂A_n when $n = 1$) along which $\overline{X}^n$ is normally elemental.

We treat the blow–up only as a technique to desingularize singularities. The method comes to be successful, at least if we apply it to a singularity of Łojasiewicz type, such as an isolated singularity of an analytic system. The reader may find more information on this technique as well as more examples in [27].

Having discussed a little about the (polar and directional) homogeneous blow–ups and their successive application, we find that they are sufficient for studying isolated singularities of an analytic vector field. Even though, there exist a more effective type of blow–up called the *quasi-homogeneous blow–up*. As said earlier, this approach of blow–up is the one used in the program P4 [3] due to the effectiveness of the desingularization compared to the homogeneous one. We refer to [27] for further information on this topic.

3.2 Poincaré compactification

The main goal of this section is to present a technique which enables us to join all the local behavior at each finite singular point with the behavior at infinite of a quadratic differential system by compactifying the whole plane $\mathbb{R}^2$ (in a "special" way), leading us to its global behavior (or global phase portrait).

The first approach we think when talking about compactifying the plane $\mathbb{R}^2$ is using the stereographic projection of the sphere onto the plane, in which case a single "point at infinity" is adjoined to the plane (see [13]). However, Poincaré [46] introduced a better technique for studying the behavior of trajectories near infinity by using the so called Poincaré sphere. Its advantage is that the singular points at infinity are displayed along the equator of the sphere and they are of a simpler nature than the singular points of the Bendixson sphere, but some of them being still very complicated. Nevertheless, for our purpose, the Poincaré compactification will be very useful.

In order to draw the phase portrait of a vector field, we were supposed to work over the complete plane $\mathbb{R}^2$, which is not very practical. As our approach in this thesis is to study only polyno-

mial vector fields, we can apply Poincaré compactification, which provides us a way to draw the phase portrait in a finite region.

In this sense, in order to reduce the study to a finite region of the plane, we have to introduce some notations.

In this section we shall use the coordinates (x_1, x_2) instead of (x, y). Let $X = P\,\partial/\partial x_1 + Q\,\partial/\partial x_2$ be a polynomial vector field (in the sense of Section 1.4), or, equivalently, the system

$$\begin{aligned} \dot{x}_1 &= P(x_1, x_2), \\ \dot{x}_2 &= Q(x_1, x_2). \end{aligned} \tag{3.2.1}$$

We recall that the degree of X is $d = \max\{\deg(P), \deg(G)\}$.

We consider $\mathbb{R}^2$ as the plane $(y_1, y_2, y_3) = (x_1, x_2, 1)$ in $\mathbb{R}^3$. Let $\mathbb{S}^2 = \{y \in \mathbb{R}^3;\ y_1^2 + y_2^2 + y_3^2 = 1\}$ be the sphere in $\mathbb{R}^3$, which we shall call it as *Poincaré sphere* and which is tangent to $\mathbb{R}^2$ at the point $(0, 0, 1)$.

We divide this sphere into three parts: $H_+ = \{y \in \mathbb{R}^3;\ y_3 > 0\}$, the northern hemisphere, $H_- = \{y \in \mathbb{R}^3;\ y_3 < 0\}$, the southern hemisphere, and $\mathbb{S}^1 = \{y \in \mathbb{R}^3;\ y_3 = 0\}$, the equator.

We consider the projection of the vector field X from $\mathbb{R}^2$ to $\mathbb{S}^2$ given by the central projections

$$f^+ : \mathbb{R}^2 \to \mathbb{S}^2 \text{ and } f^- : \mathbb{R}^2 \to \mathbb{S}^2,$$

where $f^+(x)$ (respectively, $f^-(x)$) is the intersection of the straight line passing through the point y and the origin with the northern (respectively, southern) hemisphere of $\mathbb{S}^2$, i.e.

$$f^+(x) = \left(\frac{x_1}{\Delta(x)}, \frac{x_2}{\Delta(x)}, \frac{1}{\Delta(x)}\right), \quad f^-(x) = \left(-\frac{x_1}{\Delta(x)}, -\frac{x_2}{\Delta(x)}, -\frac{1}{\Delta(x)}\right),$$

where $\Delta(x) = \sqrt{x_1^2 + x_2^2 + 1}$.

We observe that we obtain induced vector fields in each hemisphere which are analytically conjugate to X. The induced vector field on H_+ is $\overline{X}(y) = \mathrm{D}f^+(x)X(x)$, where $y = f^+(x)$, and, analogously, the one induced on H_- is $\overline{X}(y) = \mathrm{D}f^-(x)X(x)$, where $y = f^-(x)$. We note that $\overline{X}$ is a vector field on $\mathbb{S}^2 \setminus \mathbb{S}^1$ which is tangent to $\mathbb{S}^2$.

Remark 3.2.1. *The points at infinity of $\mathbb{R}^2$ (two for each direction) are in bijective correspondence to the points of the equator of $\mathbb{S}^2$.*

The natural procedure now is to try to extend the induced vector field $\overline{X}$ from $\mathbb{S}^2 \setminus \mathbb{S}^1$ to $\mathbb{S}^2$.

Unfortunately, in general it does not stay bounded as we get close to $\mathbb{S}^1$, obstructing the extension. However, by multiplying the vector field by the factor $\rho(x) = y_3^{d-1}$, the extension becomes possible.

Then, the extended vector field on $\mathbb{S}^2$ is called *Poincaré compactification* of the vector field X on $\mathbb{R}^2$ and it is denoted by $p(X)$. We notice that, on each hemisphere H_+ and H_-, the vector field $p(X)$ is no longer C^ω–conjugate to X, but it remains C^ω–equivalent.

3.2.1 Local charts on the sphere $\mathbb{S}^2$

Considering $\mathbb{S}^2$ as a smooth manifold, it provides us six local charts given by

$$U_k = \{y \in \mathbb{S}^2;\ y_k > 0\} \text{ and } V_k = \{y \in \mathbb{S}^2;\ y_k < 0\},$$

for $k = 1,2,3$. The corresponding local maps $\phi_k : U_k \to \mathbb{R}^2$ and $\psi_k : V_k \to \mathbb{R}^2$ are defined as

$$\phi_k(y) = -\psi_k(y) = \left(\frac{y_m}{y_k}, \frac{y_n}{y_k}\right),$$

for $m < n$ and $m, n \neq k$. We denote by $z = (u,v)$ the value of $\phi_k(y)$ or $\psi_k(y)$, for any k, such that (u,v) will play different roles depending on the local chart we are considering (but their meaning will be clear). Geometrically, the coordinates (u,v) can be expressed as in Figure 3.1. The points of $\mathbb{S}^1$ in any chart have $v = 0$.

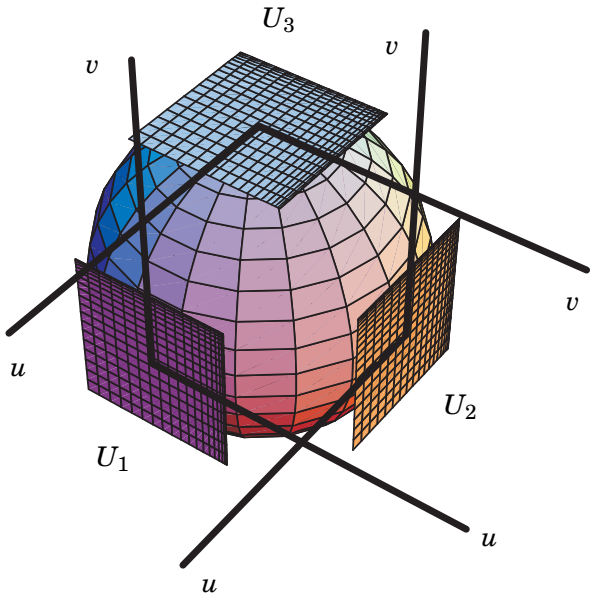

Figure 3.1: The local charts (U_k, ϕ_k) for $k = 1,2,3$ of the Poincaré sphere

3.2.2 The expression of the compactified vector field $p(X)$

We make here the calculations for the expression of $p(X)$ on the local chart U_1; for the other charts, the construction is analogous.

As we have $X(x) = (P(x_1,x_2), Q(x_1,x_2))$, then $\overline{X}(y) = \mathrm{D}f^+(x)X(x)$ with $y = f^+(x)$ and

$$\mathrm{D}\phi_1(y)\overline{X}(y) = \mathrm{D}\phi_1(y) \circ \mathrm{D}f^+(x)X(x) = \mathrm{D}(\phi_1 \circ f^+)(x)X(x).$$

Let $\overline{X}|_{U_1}$ denote the system defined as $\mathrm{D}\phi_1(y)\overline{X}(y)$. Then, since

$$(\phi_1 \circ f^+)(x) = \left(\frac{x_2}{x_1}, \frac{1}{x_1}\right) = (u,v),$$

we have

$$\begin{aligned}
\overline{X}|_{U_1} &= \begin{pmatrix} -\frac{x_2}{x_1^2} & \frac{1}{x_1} \\ -\frac{1}{x_1^2} & 0 \end{pmatrix} \begin{pmatrix} P(x_1,x_2) \\ Q(x_1,x_2) \end{pmatrix} = \\
&= \frac{1}{x_1^2}\left(-x_2P(x_1,x_2) + Q(x_1,x_2), -P(x_1,x_2)\right) = \\
&= v^2\left(-\frac{u}{v}\,P\left(\frac{1}{v},\frac{u}{v}\right) + \frac{1}{v}\,Q\left(\frac{1}{v},\frac{u}{v}\right), -P\left(\frac{1}{v},\frac{u}{v}\right)\right),
\end{aligned}$$

and

$$\rho(y) = y_3^{d-1} = \frac{1}{\Delta(x)^{d-1}} = \frac{v^{d-1}}{\Delta(z)^{d-1}} = v^{d-1}m(z),$$

where $m(z) = (1+u^2+v^2)^{(1-d)/2}$. Hence, it follows that

$$\rho(\overline{X}|_{U_1})(z) = v^{d+1}m(z)\left(-\frac{u}{v}\,P\left(\frac{1}{v},\frac{u}{v}\right) + \frac{1}{v}\,Q\left(\frac{1}{v},\frac{u}{v}\right), -P\left(\frac{1}{v},\frac{u}{v}\right)\right).$$

With the purpose to prove that the extension of $\rho\overline{X}$ to $p(X)$ is defined on the whole $\mathbb{S}^2$, we note that, while $\overline{X}|_{U_1}$ is not well defined when $v = 0$, the vector field $p(X)|_{U_1} = \rho\overline{X}|_{U_1}$ is well defined along $v = 0$, since the multiplying factor v^{d+1} cancels any factor of v which could appear in the denominator.

In order to simplify the extended vector field, we also make a change in the time variable and remove the factor $m(z)$ and we still obtain a vector field on $\mathbb{S}^2$ which is C^ω–equivalent to X on any of the hemispheres H_+ and H_-.

Thus, the expression for $p(X)$ in the local chart (U_1,ϕ_1) is given by

$$\dot{u} = v^d\left[-uP\left(\frac{1}{v},\frac{u}{v}\right)+Q\left(\frac{1}{v},\frac{u}{v}\right)\right], \quad \dot{v} = -v^{d+1}P\left(\frac{1}{v},\frac{u}{v}\right), \tag{3.2.2}$$

for (U_2,ϕ_2) is

$$\dot{u} = v^d\left[P\left(\frac{u}{v},\frac{1}{v}\right)-uQ\left(\frac{u}{v},\frac{1}{v}\right)\right], \quad \dot{v} = -v^{d+1}Q\left(\frac{u}{v},\frac{1}{v}\right), \tag{3.2.3}$$

and for (U_3,ϕ_3) is

$$\dot{u} = P(u,v), \quad \dot{v} = Q(u,v). \tag{3.2.4}$$

The expression for $p(X)$ in the charts (V_k,ψ_k) is the same as for (U_k,ϕ_k) multiplied by $(-1)^{d-1}$, for $k = 1,2,3$.

We remark that it is sufficient to work on $H_+\cup\mathbb{S}^1$ to study X in the complete plane $\mathbb{R}^2$. The set $H_+\cup\mathbb{S}^1$ is called the *Poincaré disk*. Computations can be done only in the three charts (U_1,ϕ_1), (U_2,ϕ_2) and (U_3,ϕ_3) using the expressions given by systems (3.2.2), (3.2.3) and (3.2.4), respectively.

Definition 3.2.2. *A **finite** (respectively, **infinite**) **singular point of** X **or** $p(X)$ is the singular point of $p(X)$ which lies in $\mathbb{S}^2\setminus\mathbb{S}^1$ (respectively, $\mathbb{S}^1$).*

Remark 3.2.3. *If $y\in\mathbb{S}^1$ is an infinite singular point, then $-y$ is also a singular point. Since the local behavior near $-y$ is the local behavior near y multiplied by $(-1)^{d-1}$, it follows that the orientation of the orbits changes when the degree is even.*

Due to the fact that infinite singular points appear in pairs of diametrally opposite points, it is enough to study half of them, and using the degree of the vector field, we can determine the other half (and this explains why it suffices to study only the local charts (U_k,ϕ_k), $k = 1,2,3$, previously mentioned).

Finally, we observe that the integral curves of $\mathbb{S}^2$ are symmetric with respect to the origin. In this sense, it is sufficient to represent the flow of $p(X)$ only in the closed northern hemisphere (the so called Poincaré disk). For practical purposes, in order to draw this as a disk in the plane, we can project the points of the closed northern hemisphere onto the disk $\{(y_1,y_2,y_3)\in\mathbb{R}^3 : y_1^2+y_2^2\le 1,\ y_3 = 0\}$. This could be done by projecting each point of the sphere onto the disk using a straight line parallel to the y_3-axis; however, we can project using a family of straight lines passing through a point $(0,0,y_3)$ with $y_3 < 0$. If y_3 is a value close to $-\infty$, we shall get the same result, but if y_3

is close to zero, then we might get a better representation of what is happening near infinity. In doing this we lose resolution in the regions close to the origin in the $(x_1, x_2)-$plane.

3.3 Complex (real) foliation with singularities on $\mathbb{CP}^2$ ($\mathbb{RP}^2$)

In this section we follow the ideas of Darboux's work [23]. Recalling the notation stated in Chapter 1, given $p(x,y)$ and $q(x,y)$ polynomials with real coefficients, we associate to the vector field $p\,\partial/\partial x + q\,\partial/\partial y$ the differential 1−form $\omega_1 = q(x,y)dx - p(x,y)dy$, and the differential equation

$$\omega_1 = 0. \tag{3.3.1}$$

Clearly, equation (3.3.1) defines a foliation with singularities on $\mathbb{C}^2$. The affine plane $\mathbb{C}^2$ is compactified on the complex projective space $\mathbb{CP}^2 = (\mathbb{C}^3 \setminus \{0\})/\sim$, where $(X,Y,Z) \sim (X',Y',Z')$ if, and only if, $(X,Y,Z) = \lambda(X',Y',Z')$, for some complex $\lambda \neq 0$. The equivalence class of (X,Y,Z) will be denoted by $[X:Y:Z]$.

The foliation with singularities defined by equation (3.3.1) on $\mathbb{C}^2$ can be extended to a foliation with singularities on $\mathbb{CP}^2$ and the 1−form ω_1 can be extended to a meromorphic 1−form ω on $\mathbb{CP}^2$ which yields an equation $\omega = 0$, i.e.

$$A(X,Y,Z)dX + B(X,Y,Z)dY + C(X,Y,Z)dZ = 0, \tag{3.3.2}$$

whose coefficients A, B, C are homogeneous polynomials of the same degree and satisfy the relation:

$$A(X,Y,Z)X + B(X,Y,Z)Y + C(X,Y,Z)Z = 0, \tag{3.3.3}$$

Indeed, consider the map $i : \mathbb{C}^3 \setminus \{Z=0\} \to \mathbb{C}^2$, given by $i(X,Y,Z) = (X/Z, Y/Z) = (x,y)$, and suppose that $\max\{\deg(p), \deg(q)\} = m > 0$. Since $x = X/Z$ and $y = Y/Z$ we have:

$$dx = \frac{ZdX - XdZ}{Z^2}, \quad dy = \frac{ZdY - YdZ}{Z^2},$$

the pull–back form $i^*(\omega_1)$ has poles at $Z = 0$ and yields the equation

$$i^*(\omega_1) = \frac{q(X/Z,Y/Z)(ZdX - XdZ)}{Z^2} - \frac{p(X/Z,Y/Z)(ZdY - YdZ)}{Z^2} = 0.$$

Then, the 1−form $\omega = Z^{m+2} i^*(\omega_1)$ in $\mathbb{C}^3 \setminus \{Z \neq 0\}$ has homogeneous polynomial coefficients of

degree $m+1$ and, for $Z=0$, the equations $\omega=0$ and $i^*(\omega_1)=0$ have the same solutions. Therefore, the differential equation $\omega=0$ can be written as (3.3.2), where

$$\begin{aligned} A(X,Y,Z) &= ZQ(X,Y,Z) = Z^{m+1}q(X/Z,Y/Z),\\ B(X,Y,Z) &= -ZP(X,Y,Z) = -Z^{m+1}p(X/Z,Y/Z),\\ C(X,Y,Z) &= YP(X,Y,Z) - XQ(X,Y,Z). \end{aligned} \tag{3.3.4}$$

We note that A, B and C are homogeneous polynomials of degree $m+1$ satisfying (3.3.3). Moreover, the straight line $Z=0$ is always an algebraic invariant curve of this foliation and its singular points are the solutions of the system: $A(X,Y,Z)=B(X,Y,Z)=C(X,Y,Z)=0$.

In order to study the foliation with singularities defined by the differential equation (3.3.2) subject to (3.3.3) with A, B, C satisfying the above conditions in the neighborhood of the line $Z=0$, we consider the two charts of $\mathbb{CP}^2$:

$$\begin{aligned} (u,z) &= (Y/X, Z/X), X\neq 0,\\ (v,w) &= (X/Y, Z/Y), Y\neq 0, \end{aligned}$$

covering this line. We note that in the intersection of the charts $(x,y)=(X/Z,Y/Z)$ and (u,z) (respectively, (v,w)) we have the change of coordinates $x=1/z$, $y=u/z$ (respectively, $x=v/w$, $y=1/w$). Except for the point $[0:1:0]$ or the point $[1:0:0]$, the foliation defined by equations (3.3.2) and (3.3.3) with A, B, C as in (3.3.4) yields in the neighborhood of the line $Z=0$ the foliations associated with the systems

$$\begin{aligned} \dot{u} &= uP(1,u,z) - Q(1,u,z) = C(1,u,z),\\ \dot{z} &= zP(1,u,z), \end{aligned} \tag{3.3.5}$$

or

$$\begin{aligned} \dot{v} &= vQ(v,1,w) - P(v,1,w) = -C(v,1,w),\\ \dot{w} &= wP(v,1,w). \end{aligned} \tag{3.3.6}$$

In a similar way we can associate a real foliation with singularities on $\mathbb{RP}^2$ to a real planar polynomial vector field.

3.4 Intersection number for complex curves

For two projective curves in $\mathbb{CP}^2$, $F(X,Y,Z)=0$ and $G(X,Y,Z)=0$, where F and G are homogeneous polynomials in the variables X, Y and Z which are relatively prime over $\mathbb{C}$, we can define

$I_W(F,G)$ regarding Definition 1.6.1.

Suppose, for example, that $W=[a:b:c]$, where $c\neq 0$. Hence, $W=[a/c:b/c:1]$. Let $f(x,y)=F(x,y,1)$ and $g(x,y)=G(x,y,1)$. Then, $I_W(F,G)=I_w(f,g)$, where $w=(a/c,b/c)$ (see Definition 1.6.1, page 17). It is known that $I_W(F,G)$ is independent of the choice of a local chart and of a projective change of variables (see again [30]).

Clearly, the above concept of intersection multiplicity extends to that of intersection multiplicity of several curves at a point of the projective plane. In particular, we will be interested in the way the projective curves $A=0$, $B=0$ and $C=0$ intersect and hence in the values of

$$I_a(A,B,C)=\dim_{\mathbb{C}}\frac{\mathbf{O}_a}{(A,B,C)}.$$

Here, $\mathbf{O}_a$ is the local ring at a of the complex projective plane (for more information see [30]) and (A,B,C) is the homogeneous ideal generated by these three polynomials.

If a is a finite or an infinite singular point of system (1.5.1) and A, B and C are defined as in (3.3.4), then we have that $I_a(P,Q)$, $I_a(C,Z)$ and $I_a(A,B,C)$ are invariant with respect to affine transformations of (x,y) ([51]) and

$$I_a(A,B,C)=\begin{cases} I_a(P,Q)=I_a(p,q), \text{ if } a \text{ is finite,}\\ I_a(P,Q)+I_a(C,Z), \text{ if } a=\infty. \end{cases} \tag{3.4.1}$$

3.5 Application: global phase portraits of a SIS model

The results presented in this section are based on the paper of Oliveira and Rezende [43].

Herein we analyze a quadratic system and provide its topological classification given all the possible distinct phase portraits it has. We can find many papers with this aim. Most of the studies rely on systems with real parameters and the study consists of outlining their phase portraits by finding out some conditions on the parameters.

We present the study of a susceptible–infected–susceptible (SIS) model described by the equations

$$\begin{aligned} \dot{x}&=-bxy-mx+cy+mk,\\ \dot{y}&=bxy-(m+c)y, \end{aligned} \tag{3.5.1}$$

where x and y represent, respectively, the portion of the population that has been susceptible to the infection and those who have already been infected. Such system describes an infectious

disease from which infected people recover with immunity against reinfection.

System (3.5.1) is a particular case of the class of classical systems known as SIS models, introduced by Kermack and McKendrick [37] and studied by Brauer [15], who has assumed that recovery from the nonfatal infective disease does not yield immunity. In system (3.5.1), k is the population size (susceptible people plus infected ones), mk is the constant number of births, m is the proportional death rate, b is the infectivity coefficient of the typical Lotka–Volterra interaction term and c is the recovery coefficient. As system (3.5.1) is assumed to be nonfatal, the standard term removing dead infected people $-ay$ in [15] is omitted. As usual in the literature, all the critical points of system (3.5.1) will henceforth be called (endemic) steady states (e.g. see [59]). In this section we shall study the phase portraits of the differential system (3.5.1) with $bm \neq 0$.

Remark 3.5.1. *If $b = 0$, then system* (3.5.1) *becomes linear, and if $m = 0$, then system* (3.5.1) *satisfies $\dot{x} + \dot{y} = 0$. These two cases are trivial and they are not interesting from a biological point of view.*

The integrability of system (3.5.1) has also been studied. For example, Nucci and Leach [42] have demonstrated that (3.5.1) is integrable using the Painlevé test. Later, Llibre and Valls [40] have proved that system (3.5.1) is Darboux integrable, and they have shown the explicit expression of its first integral and all its invariant algebraic curves.

Alternatively, the attempt of outlining the global phase portraits of differential systems is a possible way to determine their global behavior.

We propose to classify all the topological classes of the global phase portraits of system (3.5.1) using some information in [40]. The next theorem states the result obtained after the analysis of such a system.

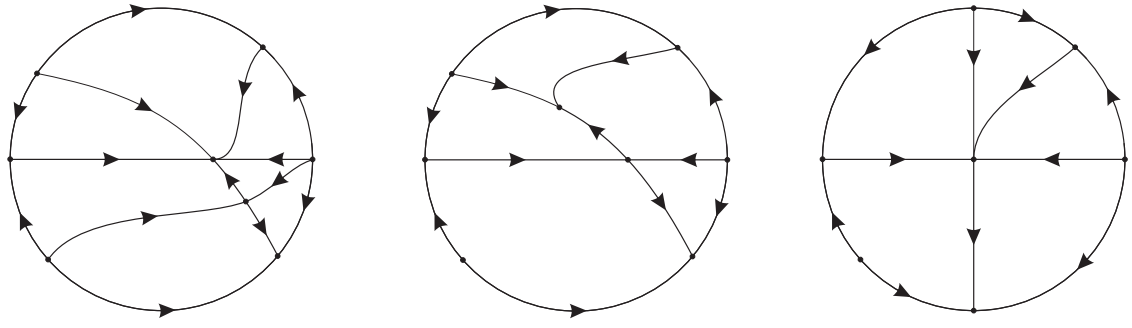

$(SIS)_1$ $(SIS)_2$ $(SIS)_3$

Figure 3.2: Global phase portraits of system (3.5.1) in the Poincaré disk

Theorem 3.5.2. *There exist three topological distinct phase portraits of system* (3.5.1) *and they are shown in Figure 3.2.*

Remark 3.5.3. *In Figure 3.2, we have plotted with wide curves the separatrices and we have added some orbits drawn on the picture with thinner lines to avoid confusion in some required cases (to show the invariant straight line).*

3.5.1 Analysis of the system (3.5.1)

Provided that $b \neq 0$, system (3.5.1) has only two finite singular points

$$p = \left(\frac{c+m}{b}, \frac{-c+bk-m}{b} \right) \quad \text{and} \quad q = (k, 0),$$

which are usually known, respectively, as endemic steady state and disease–free steady state. We note that both finite singular points p and q coincide if $bk - m = c$.

The names given above to each steady states are not an accident. In q, the number of susceptible individuals is equal to the population size k, whereas the number of infected people is null. On the other hand, the number of susceptible people in p is the recovery coefficient plus the death rate divided by the infection coefficient, while the infected ones are the rest of the population, which leads to the presence of infected people, since $bm \neq 0$. Finally, note that only non–negative values of x and y are interesting here, because they represent the number of individuals, even if we present the phase portraits in the whole Poincaré disk.

First, we start with the analysis of the endemic steady state p. Translating the singular point p to the origin in system (3.5.1), we obtain

$$\begin{aligned} \dot{x} &= -bkx + cx - my - bxy, \\ \dot{y} &= (-c + bk - m)x + bxy, \end{aligned} \tag{3.5.2}$$

which is equivalent to (3.5.1). The Jacobian matrix of (3.5.2) is given by

$$\mathrm{J}(x,y) = \begin{pmatrix} c - bk - by & -m - bx \\ -c + bk - m + by & bx \end{pmatrix},$$

which implies

$$\delta = (bk - c - m)m \quad \text{and} \quad \tau = -bk + c,$$

where δ and τ denote, respectively, the determinant and the trace of the matrix $J(0,0)$.

If $(bk-c-m)m<0$, then p is a saddle point. On the other hand, if $(bk-c-m)m>0$, then p is a node point, because $\tau^2-4\delta=(c-bk+2m)^2\geq 0$.

In the case that $(bk-c-m)m=0$, or equivalently, $m=bk-c$, then p is semi–elemental. Indeed, it is the case that both finite singular points are the same, i.e. $p=q=(k,0)$. Here, system (3.5.2) becomes

$$\begin{aligned}\dot{x}&=-mx-my-bxy,\\ \dot{y}&=bxy,\end{aligned}\tag{3.5.3}$$

whose Jacobian matrix at $(0,0)$ is

$$J(0,0)=\begin{pmatrix}-m & -m\\ 0 & 0\end{pmatrix},$$

so p is a semi–elemental point. By a linear change of coordinates, system (3.5.3) can be put on the form of system (2.2.1) and, applying Proposition 2.2.1, we conclude that p is a saddle–node.

From the biological point of view, when the death rate m is equal to the portion of the population which becomes infected (bk) minus the recovery coefficient, the dynamics around the steady states p and q changes and they become only one point which attracts (the node part) and repels (the saddle part) the orbits in its neighborhood.

Now, we analyze the disease–free steady state q. Translating the singular point q to the origin in system (3.5.1), we obtain

$$\begin{aligned}\dot{x}&=-mx+cy-bky-bxy,\\ \dot{y}&=(-c+bk-m)y+bxy,\end{aligned}\tag{3.5.4}$$

which is equivalent to (3.5.1). The Jacobian matrix of (3.5.4) is given by

$$J(x,y)=\begin{pmatrix}-m-by & c-b(k+x)\\ by & -c-m+b(k+x)\end{pmatrix}$$

which implies

$$\delta=-(bk-c-m)m \text{ and } \tau=bk-c-2m.$$

If $-(bk-c-m)m<0$, then q is a saddle point. In contrast, if $-(bk-c-m)m>0$, then q is a node point, because $\tau^2-4\delta=(c-bk)^2\geq 0$.

The case $(bk-c-m)m=0$, or equivalently $m=bk-c$, has already been studied, and $p=q$ is a semi–elemental saddle–node.

Finally, we have proved the following:

Proposition 3.5.4. *Consider system* (3.5.1) *with* $bm \neq 0$ *and its two finite steady states* p *and* q. *Then:*

1. *If either* $m > 0$ *and* $m > bk - c$, *or* $m < 0$ *and* $m < bk - c$, *then* p *is a saddle and* q *is a node;*
2. *If either* $m > 0$ *and* $m < bk - c$, *or* $m < 0$ *and* $m > bk - c$, *then* p *is a node and* q *is a saddle;*
3. *If* $m = bk - c$, *then* $p = q$ *is a semi–elemental saddle–node.*

Having classified all the finite singular points, we apply the Poincaré compactification to study the infinite singularities.

In the local chart U_1, where $x = 1/v$ and $y = u/v$, we have:

$$\begin{aligned} \dot{u} &= u(b + bu - cv - cuv - kmv^2), \\ \dot{v} &= v(bu + mv - cuv - kmv^2), \end{aligned} \tag{3.5.5}$$

whose infinite singular points are $(0,0)$ and $(-1,0)$, which are a saddle–node of type $\overline{\binom{1}{1}}SN$ (by Proposition 2.2.1) and a node, respectively.

In the local chart U_2, where $x = u/v$ and $y = 1/v$, the system

$$\begin{aligned} \dot{u} &= -bu - bu^2 + cv + cuv + kmv^2, \\ \dot{v} &= v(-bu + cv + mv) \end{aligned} \tag{3.5.6}$$

has two infinite singular points $(0,0)$ and $(-1,0)$. The latter one is a node and is the same as $(-1,0) \in U_1$, while the former one is a saddle–node of type $\overline{\binom{1}{1}}SN$.

We have just proved the following:

Proposition 3.5.5. *The infinite singular points of system* (3.5.1) *are the origin of charts* U_1, V_1, U_2 *and* V_2, *which are saddle–nodes of type* $\overline{\binom{1}{1}}SN$, *and* $(-1,0)$, *belonging to each of the charts* U_1 *and* U_2, *which is a node.*

Knowing the local behavior around finite and infinite singular points, another useful tool to describe the phase portraits of differential systems is the existence of invariant curves. The next result shows that system (3.5.1) has invariant straight lines.

Proposition 3.5.6. *Let* $bm \neq 0$. *System* (3.5.1) *always has two invariant straight lines given by* $f_1(x,y) \equiv y = 0$ *and* $f_2(x,y) \equiv k - x - y = 0$. *Additionally, if* $c = bk$, *then* $f_3(x,y) \equiv k - x = 0$ *is also an invariant straight line.*

Proof. By Definition 1.4.1, we can find $K_1(x,y) = bx - m - c$, $K_2(x,y) = -m$ and $K_3(x,y) = -m - by$ as the cofactors of $f_1(x,y)$, $f_2(x,y)$ and $f_3(x,y)$ (if $c = bk$), respectively. ∎

3.5.2 Proof of Theorem 3.5.2

From Propositions 3.5.4 and 3.5.5 we get all the information about the local behavior of finite and infinite singular points, respectively. Using the continuity of solutions and primary definitions and results of ordinary differential equations (e.g. ω-limit sets, existence and uniqueness of solutions, the Flow Box Theorem etc. [27]) and the existence of invariant straight lines of system (3.5.1) stated by Proposition 3.5.6, the global phase portraits can be easily drawn.

We have to analyze the three cases stated in Proposition 3.5.4.

The finite steady state q is the intersection of the invariant curves $f_1(x,y) = f_2(x,y) = 0$, and the other finite steady state p lies on the curve $f_2(x,y) = 0$.

According to items (1) and (2) of Proposition 3.5.4, p (respectively, q) is a saddle (respectively, a node) the one way and the other a node (respectively, a saddle).

In the case of item (1), a pair of opposite separatrices of the saddle p lies on the curve $f_2(x,y) = 0$ while the other pair must end (or start) in parabolic sectors. In this sense, each one of the separatrices of this second pair goes towards the nodal parts of different infinite saddle–nodes, as shown in the portrait $(SIS)_1$ in Figure 3.2.

Now, in the case of item (2), the singular point q is a saddle, which means that the four of its separatrices lie on the two invariant straight lines $f_1(x,y) = f_2(x,y) = 0$. However, the node p lies on the straight line $f_2(x,y) = 0$, which implies that p is a limit set of one of the separatrices of q and the other three separatrices end (or start) in three different infinite points, including a pair of infinite saddle–nodes, which produces a connection of separatrices, as seen in the portrait $(SIS)_2$ in Figure 3.2.

Another difference between the first two phase portraits in Figure 3.2 is that the corresponding singular points at infinity receives/sends a different number of separatrices from/to the finite singularities. Writing this characteristic in a sequence of digits, where each digit means the number of such separatrices, we can associate to the portraits $(SIS)_1$ and $(SIS)_2$ the sequences 211101 and 111010, respectively, which are clearly distinct.

Item (3) assures the existence of only one finite singular point, a saddle–node. Clearly, the corresponding phase portrait $(SIS)_3$ is different from the previous two portraits due to the presence of only one finite singular point.

Finally, Theorem 3.5.2 has been proved.

In this section we have proved the existence of only three classes of global phase portraits of the quadratic system (3.5.1). In general, in the qualitative theory of ordinary differential systems it is quite important to know the global behavior of solutions of systems and this sometimes is not an easy task. The most frequently used tools for this propose are the study of local behavior along with the (local and global) stability, integrability, and also the global phase portrait, which was employed in the present study.

From the biological point of view, in the case represented in phase portraits $(SIS)_1$ and $(SIS)_2$ in Figure 3.2, it is clear that while the steady state q characterizes the presence of only susceptible individuals, p indicates the mutual presence of susceptible and infected people. Besides, as q is an asymptotically stable node in $(SIS)_1$, the disease seems to be controlled and the whole population tends to be healthy but susceptible to be infected again. As p is an unstable saddle steady state, it suggests that there is no harmony between the number of susceptible people and infected ones, although some of the solutions tend to q, indicating the control of the disease. The same arguments are valid for $(SIS)_2$, but now considering p as the node and q as the saddle meaning that the infected population tends to increase as all solutions in a neighborhood of p tend to it.

In portrait $(SIS)_3$ in Figure 3.2, all the solutions tend to q (regarding that $x, y > 0$), i.e. if $m = bk - c$, the disease is supposed to be controlled and the whole population is inclined to be healthy but susceptible to the reinfection.

3.5.3 Equivalence between this SIS model and previous–studied normal form

After having stated and proved Theorem 3.5.2, we verified that, via an affine change in the variables and in the time, we can simplify system (3.5.1) in two normal forms which have already been classified by Schlomiuk and Vulpe in [54, 55].

These normal forms are given precisely by

$$\dot{u} = g + u, \quad \dot{v} = v(v - u), \tag{3.5.7}$$

where $g \in \mathbb{R}$ and $g(g-1) \neq 0$, and

$$\dot{u} = u, \quad \dot{v} = v(v - u). \tag{3.5.8}$$

The normal forms (3.5.7) and (3.5.8) are, respectively, the normal forms $(IV.16)$ and $(IV.17)$

from [54, Table 2, page 29] and [55, Table 2, page 17]. We note that system (3.5.8) is the particular case of system (3.5.7) when $g = 0$.

Lemma 3.5.7. *System* (3.5.1) *is equivalent to system* (3.5.7) *via an affine transformation in the variables and a homothety in the time.*

Proof. We need to construct the affine change in the variables and the homothety in the time which transforms system (3.5.1) into system (3.5.7). We consider these transformations having the forms:

$$\begin{pmatrix} u \\ v \end{pmatrix} = \begin{pmatrix} \alpha & \beta \\ \gamma & \delta \end{pmatrix} \begin{pmatrix} x \\ y \end{pmatrix} + \begin{pmatrix} \phi \\ \psi \end{pmatrix}, \quad \tau = \omega t. \tag{3.5.9}$$

Then, after applying these mappings to system (3.5.1), we obtain the system

$$\begin{aligned} \dot{u} &= a_{00} + a_{10}u + a_{01}v + a_{20}u^2 + 2a_{11}uv + a_{02}v^2, \\ \dot{v} &= b_{00} + b_{10}u + b_{01}v + b_{20}u^2 + 2b_{11}uv + b_{02}v^2, \end{aligned} \tag{3.5.10}$$

where

$$\begin{aligned}
a_{00} &= \left[km(\alpha\beta\gamma - \alpha\delta)^2 + \phi(m(\beta\gamma\alpha\delta)^2 + b(\alpha-\beta)\gamma\delta\phi) + b(-\alpha+\beta)(\beta\gamma+\alpha\delta)\phi\psi\right. \\
&\quad \left. + b\alpha(\alpha-\beta)\beta\psi^2 - c(\alpha-\beta)(-\beta\gamma+\alpha\delta)(-\gamma\phi+\alpha\psi)\right] / \left[(\beta\gamma-\alpha\delta)^2\omega\right], \\
a_{10} &= \left[-m(\beta\gamma-\alpha\delta)^2 - c(\alpha-\beta)\gamma(-\beta\gamma+\alpha\ \delta) + b(\alpha-\beta)(-2\gamma\delta\phi+\beta\ \gamma\psi+\alpha\delta\psi)\right] / \left[(\beta\gamma-\alpha\delta)^2\omega\right], \\
a_{01} &= \left[(\alpha-\beta)(c\alpha(-\beta\gamma+\alpha\ \delta) + b(\beta\gamma\phi+\alpha\delta\phi-2\alpha\beta\psi))\right] / \left[(\beta\gamma-\alpha\delta)^2\omega\right], \\
a_{20} &= \left[b(\alpha-\beta)\gamma\delta\right] / \left[(\beta\gamma-\alpha\delta)^2\omega\right], \\
a_{11} &= -\left[(b(\alpha-\beta)(\beta\gamma+\alpha\delta)\right] / \left[(\beta\gamma-\alpha\delta)^2\omega\right], \\
a_{02} &= \left[b\alpha(\alpha-\beta)\beta\right] / \left[(\beta\gamma-\alpha\delta)^2\omega\right], \\
b_{00} &= \left[\gamma(km\ (\beta\gamma-\alpha\delta)^2 + (\gamma-\delta)\ \phi(-c\beta\gamma+c\alpha\delta+b\delta\phi)) + ((\beta\gamma-\alpha\delta)\ ((c\alpha+m\beta)\gamma\right. \\
&\quad \left. -(c+m)\alpha\delta) - b(\gamma-\delta)(\beta\gamma+\alpha\delta)\ \phi)\psi + b\alpha\beta(\gamma-\delta)\psi^2\right] / \left[(\beta\gamma-\alpha\delta)^2\omega\right], \\
b_{10} &= \left[(\gamma-\delta)(c\gamma(\beta\gamma-\alpha\ \delta) + b(-2\gamma\delta\phi+\beta\gamma\psi+\ \alpha\delta\psi))\right] / \left[(\beta\gamma-\alpha\delta)^2\omega\right], \\
b_{01} &= \left[(-m(\beta\gamma-\alpha\delta)^2 + c\alpha(\gamma-\delta)(-\beta\gamma+\alpha\ \delta) + b(\gamma-\delta)(\beta\gamma\phi+\alpha\delta\ \phi-2\alpha\beta\psi)\right] / \left[(\beta\gamma-\alpha\delta)^2\omega\right], \\
b_{20} &= \left[b\gamma(\gamma-\delta)\delta\right] / \left[(\beta\gamma-\alpha\delta)^2\omega\right], \\
b_{11} &= -\left[(b(\gamma-\delta)(\beta\gamma+\alpha\delta)\right] / \left[(\beta\gamma-\alpha\delta)^2\omega\right], \\
b_{02} &= \left[b\alpha\beta(\gamma-\delta)\right] / \left[(\beta\gamma-\alpha\delta)^2\omega\right].
\end{aligned} \tag{3.5.11}$$

As we want to preserve the invariant straight line $\{y = 0\}$, we set $\gamma = \psi = 0$, then the expressions in (3.5.11) become

$$\begin{aligned}
&a_{00} = (m(k\alpha+\phi))/\omega, \qquad a_{10} = -m/\omega, \qquad a_{01} = ((\alpha-\beta)(c\alpha+b\phi))/(\alpha\delta\omega),\\
&a_{20} = 0, \qquad a_{11} = -((b(\alpha-\beta))/(2\alpha\delta\omega)), \qquad a_{02} = (b(\alpha-\beta)\beta)/(\alpha\delta^2\omega),\\
&b_{00} = 0, \qquad b_{10} = 0, \qquad b_{01} = -((c\alpha+m\alpha+b\phi)/(\alpha\omega)),\\
&b_{20} = 0, \qquad b_{11} = b/(2\alpha\omega), \qquad b_{02} = -((b\beta)/(\alpha\delta\omega)).
\end{aligned} \tag{3.5.12}$$

As $a_{10} = 1$ in system (3.5.7), then we set $\omega = -m$ and we compute:

$$\begin{aligned}
&a_{00} = -k\alpha-\phi, \qquad a_{10} = 1, \qquad a_{01} = -(((\alpha-\beta)(c\alpha+b\phi))/(m\alpha\delta)),\\
&a_{20} = 0, \qquad a_{11} = (b(\alpha-\beta))/(2m\alpha\delta), \qquad a_{02} = -((b(\alpha-\beta)\beta)/(m\alpha\delta^2)),\\
&b_{00} = 0, \qquad b_{10} = 0, \qquad b_{01} = (c\alpha+m\alpha+b\phi)/(m\alpha),\\
&b_{20} = 0, \qquad b_{11} = -(b/(2m\alpha)), \qquad b_{02} = -(b\beta)/(m\alpha\delta).
\end{aligned} \tag{3.5.13}$$

Now, in order to have $b_{11} = -1/2$, we set $\alpha = b/m$ and obtain:

$$\begin{aligned}
&a_{00} = -((bk+m\phi)/m), \qquad a_{10} = 1, \qquad a_{01} = ((-b+m\beta)(c+m\phi))/(m^2\delta),\\
&a_{20} = 0, \qquad a_{11} = -((-b+m\beta)/(2m\delta)), \qquad a_{02} = (\beta(-b+m\beta))/(m\delta^2),\\
&b_{00} = 0, \qquad b_{10} = 0, \qquad b_{01} = (c+m+m\phi)/m,\\
&b_{20} = 0, \qquad b_{11} = -1/2, \qquad b_{02} = \beta/\delta.
\end{aligned} \tag{3.5.14}$$

By solving the equation $a_{11} = 0$, we obtain $\beta = b/m$ and, then, we set $\delta = b/m$ in order to have $b_{02} = 1$. Finally, in order to have $b_{01} = 0$, we set $\phi = -(c+m)/m$ and we obtain the system:

$$\dot{u} = \frac{c-bk+m}{m} + u, \quad \dot{v} = v^2 - uv, \tag{3.5.15}$$

and the transformations (3.5.9) become:

$$\begin{pmatrix} u \\ v \end{pmatrix} = \begin{pmatrix} \frac{b}{m} & \frac{b}{m} \\ 0 & \frac{b}{m} \end{pmatrix} \begin{pmatrix} x \\ y \end{pmatrix} + \begin{pmatrix} \frac{-c-m}{m} \\ 0 \end{pmatrix}, \quad \tau = -mt. \tag{3.5.16}$$

Denoting $g := (c-bk+m)/m$ and verifying that

$$g(g-1) = \frac{(c-bk)(c-bk+m)}{m^2} \neq 0,$$

we arrive at system (3.5.8), proving the lemma. ■

From Lemma 3.5.7, studying system (3.5.1) is the same as studying system (3.5.8). And we refer to the reader the configurations Config. 4.16 and Config. 4.17 from [55, Diagram 1, page 13] which are the configurations of systems (3.5.7) and (3.5.8), respectively, concerning the position of the singular points and the invariant straight lines. Moreover, the reader could see the phase portraits in Figure 3.2 in their classification in [55, Table 3(a), Pictures 4.16(a), 4.16(b) and 4.17, page 31].

Chapter

4

Invariant polynomials: comitants and invariants

In this chapter we provide all the algebraic tools we shall use in future applications.

According to Olver [45] and Eves [29], the *classical invariant theory* has its origin in the investigations done by Lagrange, Gauss and, in particular, Boole [16].

This subject was intensely approached by Cayley and Sylvester, who made remarkable progress in this topic and in many different other areas of Mathematics, and followed by many other mathematicians from different parts of the world, as Hermite, Aronhold, Clebsch, Gordan and Hilbert. Researchers from many countries (and each one in his time) united their efforts in the common purpose to create and develop the classical invariant theory.

We consider the polynomial

$$p(x) = (x-3)^4\,(x+2)\,(x^2+1)^2 \in \mathbb{C}[x],$$

which is factorized and has four roots: $x_1 = 3$, $x_2 = -2$ and $x_{3,4} = \pm i$. Applying the affine transformation $\overline{x} = \alpha x + \beta$, $\alpha \neq 0$, $\alpha, \beta \in \mathbb{C}$, to the polynomial p, we obtain

$$\overline{p}(\overline{x}) = \frac{1}{\alpha^9}(\overline{x} - 3\alpha + \alpha\beta)^4\,(\overline{x} + 2\alpha + \alpha\beta)\,(\overline{x}^2 + \alpha^2 + 2\alpha\beta\overline{x} + \alpha^2\beta^2)^2.$$

After the transformation, the polynomial remains factorable and the multiplicity of the roots is unchanged, whereas the explicit value of the roots and the coefficients change. These properties

are called *intrinsic* and *non–intrinsic*, respectively.

The central problem in classical invariant theory is to find functions of the coefficients of a given polynomial which, after subjecting the variables of this polynomial to a general linear transformation, remain unchanged up to a factor involving only the coefficients of the transformation.

In this sense, there appears two problems regarding this intrinsic property. The first one is the problem of equivalence which discusses about conditions to transform a polynomial into another polynomial by a suitable change of coordinates which preserves the intrinsic properties equivalent. And the last one is the existence of an associated canonical form, i.e. the attempt to find out a system of coordinates in which the polynomial is transformed into a particular simple form. Remarkably, these two problems lead to the first goal of classical invariant theory: to determine the fundamental invariants.

We consider an example. Let

$$f(x,y) = ax^2 + 2bxy + cy^2 \in \mathbb{R}[x,y]$$

be a real quadratic form. If we consider the change

$$\overline{x} = \alpha x + \beta y, \quad \overline{y} = \gamma x + \delta y, \quad \alpha,\beta,\gamma,\delta \in \mathbb{R}, \tag{4.0.1}$$

where

$$A := \begin{pmatrix} \alpha & \beta \\ \gamma & \delta \end{pmatrix} \text{ is such that } \det A = \alpha\delta - \beta\gamma \neq 0,$$

then the polynomial $f(x,y)$ is transformed into the polynomial $\overline{f}(\overline{x},\overline{y})$ by the change (4.0.1), respecting the relation:

$$\overline{f}(\overline{x},\overline{y}) = \overline{f}(\alpha x + \beta y, \gamma x + \delta y) = f(x,y).$$

and we observe that the coefficients a, b and c of $f(x,y)$ relate to the coefficients $\overline{a}$, $\overline{b}$ and $\overline{c}$ of $\overline{f}(\overline{x},\overline{y})$ according to the identities:

$$a = \alpha^2\overline{a} + 2\alpha\gamma\overline{b} + \gamma^2\overline{c}, \quad b = \alpha\beta\overline{a} + (\alpha\delta - \beta\gamma)\overline{b} + \gamma\delta\overline{c}, \quad c = \beta^2\overline{a} + 2\beta\delta\overline{b} + \delta^2\overline{c}. \tag{4.0.2}$$

Using the identities in (4.0.2), we prove that there exists a relation between the discriminant

$\overline{\Delta}$ of $\overline{f}(\overline{x},\overline{y})$ and the discriminant Δ of $f(x,y)$. In fact, direct calculation leads to:

$$\Delta = b^2 - ac = (\alpha\delta - \beta\gamma)^2\,(\overline{b}^2 + \overline{a}\,\overline{c}) = (\alpha\delta - \beta\gamma)^2\,\overline{\Delta}. \tag{4.0.3}$$

Due to identity (4.0.3) we conclude that the types of the linear factors (which is the geometrical meaning of the discriminant for the quadratic form) of the polynomial $f(x,y)$ are preserved in the polynomial $\overline{f}(\overline{x},\overline{y})$ via the change (4.0.1). In Table 4.0.1 we present the classification of the family of quadratic forms.

Table 4.0.1: Classification of the family of quadratic forms

Sign of the discriminant	**Number of roots**	**Canonical form**
$\Delta > 0$	2 real (distinct)	xy
$\Delta < 0$	2 complex	$k(x^2+y^2)$, $k \in \{-1,1\}$
$\Delta = 0$, $f \not\equiv 0$	2 double (real)	kx^2, $k \in \{-1,1\}$
$\Delta = 0$, $f \equiv 0$	—	0

As we can see, the discriminant Δ is an invariant for the quadratic form $f(x,y)$, and it is one of the simplest example of an invariant in the classical invariant theory.

However, we are not interested here in the classical algebraic invariant theory. Our approach in this thesis is the study and application of the *algebraic invariants of differential systems*.

In effect, since 1963 in the city of Kishinev (Moldova), Sibirsky and his pupils have been working on the attempt of joining the concepts of invariant polynomials of autonomous differential equations with the action of groups of linear transformations of the phase space.

And this is the approach we use in our results in this thesis. We apply Sibirsky and his pupils' research and results in order to classify topologically planar differential systems in the space of parameters (see next chapters).

With the purpose of using this technique, we need to fix some notation and concepts in order to make the study clearer. The results of the next sections can be found in the book of Sibirsky [57].

4.1 Tensor notation of differential systems

We consider system (1.5.1) written in the form:

$$\begin{aligned}
\frac{dx^1}{dt} &= a_1^1 x^1 + a_2^1 x^2 + a_{11}^1 (x^1)^2 + a_{12}^1 x^1 x^2 + a_{21}^1 x^2 x^1 + a_{22}^1 (x^2)^2,\\
\frac{dx^2}{dt} &= a_1^2 x^1 + a_2^2 x^2 + a_{11}^2 (x^1)^2 + a_{12}^2 x^1 x^2 + a_{21}^2 x^2 x^1 + a_{22}^2 (x^2)^2,
\end{aligned} \tag{4.1.1}$$

where x^1 and x^2 are the dependent variable and t is the independent one. System (4.1.1) has degree 2 and the polynomials in the right–hand side have fixed coefficients in x^1 and x^2. They have no free terms and similar terms appear in the extent that $x^1x^2 = x^2x^1$. Moreover, it is always possible to consider $a^1_{12} = a^1_{21}$ and $a^2_{12} = a^2_{21}$. Clearly, any system of the form

$$\begin{aligned} \dot{x} &= ax + by + cx^2 + dxy + ey^2, \\ \dot{y} &= Ax + By + Cx^2 + Dxy + Ey^2, \end{aligned} \tag{4.1.2}$$

can be written in the form (4.1.1) via the identification:

$$x^1 = x,\ x^2 = y,\ a^1_{12} = a^1_{21} = \frac{d}{2},\ a^2_{12} = a^2_{21} = \frac{D}{2},\ \frac{dx^1}{dt} = \dot{x},\ \frac{dx^2}{dt} = \dot{y}.$$

Even though the form in (4.1.2) is more presentable, the form in (4.1.1) is more convenient, since it is possible to give it in the condensed form

$$\frac{dx^j}{dt} = \sum_{\alpha=1}^{2} a^j_\alpha x^\alpha + \sum_{\alpha,\beta=1}^{2} a^j_{\alpha\beta} x^\alpha y^\beta,\ (j = 1,2)$$

or, discarding the summation sign, in the form

$$\frac{dx^j}{dt} = a^j_\alpha x^\alpha + a^j_{\alpha\beta} x^\alpha y^\beta,\ (j,\alpha,\beta = 1,2). \tag{4.1.3}$$

Another way to display equation (4.1.3) is in the form

$$\frac{dx^j}{dt} = a^j_{j_1 j_2 \cdots j_\omega} x^{j_1} x^{j_2} \cdots x^{j_\omega},\ (j, j_1, j_2, \ldots, j_\omega = 1,2),$$

which is easily extended to multivariate systems with arbitrary polynomials or series on the right–hand sides:

$$\frac{dx^j}{dt} = \sum_{\omega\in\Omega} a^j_{j_1 j_2 \cdots j_\omega} x^{j_1} x^{j_2} \cdots x^{j_\omega},\ (j, j_1, j_2, \ldots, j_\omega = 1,2,\ldots,n), \tag{4.1.4}$$

where Ω is some set of positive integers distinct among themselves, while the coefficients $a^j_{j_1 j_2 \cdots j_\omega}$ are symmetrical with respect to the lower indices, i.e. their values are not dependent on the order of succession of these indices. We observe that, if the set Ω is infinite, then the right–hand sides are formal series.

4.2 The invariant polynomial

Let $x = (x^1, \dots, x^n)$ be the vector of the dependent variables of systems (4.1.4), a be the union of all the coefficients of systems (4.1.4), A be the space of the coefficients of systems (4.1.4) and $G = \{g\}$ be the group of linear transformations g of the $n-$dimensional space X of vectors x. We denote the linear transformation g in the form

$$y = gx, \tag{4.2.1}$$

where $y = (y^1, \dots, y^n)$ is the vector of the new dependent variables, while g is an $n \times n$ matrix.

Applying the transformation (4.2.1) to systems (4.1.4), we arrive at the systems

$$\frac{dy^r}{dt} = \sum_{\omega \in \Omega} b^r_{r_1 r_2 \cdots r_\omega} y^{r_1} y^{r_2} \cdots y^{r_\omega}, \ (r, r_1, r_2, \dots, r_\omega = 1, 2, \dots, n). \tag{4.2.2}$$

We analogously denote by b the union of all the coefficients of systems (4.2.2). It is clear that $b = b(a, g)$ and, consequently, we shall write $b = a(g)$.

Definition 4.2.1. *A **polynomial of an infinite set of variables** is a polynomial of any finite subset of these variables.*

Definition 4.2.2. *A polynomial $I(a)$ of coefficients from system* (4.1.4) *is called an **invariant polynomial** of those systems in the group G, if there exists a function $\lambda(g)$, depending only on elements of the group, for which this identity holds:*

$$I(b) = \lambda(g) I(a), \tag{4.2.3}$$

*for all $g \in G$ and any $a \in A$. The function $\lambda(g)$ is called a **multiplicator**. If $\lambda(g) \equiv 1$, then the invariant polynomial $I(a)$ is called **absolute**, otherwise it is **relative**.*

4.3 Invariant polynomials under linear transformations: a minimal basis

In this section we attain to the simple case $T = \{1\}$, $\Omega = \{1\}$, $n = 2$, $G = \mathrm{GL}(2, \mathbb{R})$. This conditions lead to the linear system $\dot{x} = ax$, where

$$a = \begin{pmatrix} a_1^1 & a_2^1 \\ a_1^2 & a_2^2 \end{pmatrix}.$$

We consider

$$g = \begin{pmatrix} \alpha & \beta \\ \gamma & \delta \end{pmatrix},$$

with $\Delta = \det g$. Then, from (4.2.1), we have $x = g^{-1}y$ and $\dot{y} = by$, where $b = gag^{-1}$, which is equivalent to $bg = ga$, i.e.

$$\begin{aligned} b_1^1\alpha + b_2^1\gamma &= a_1^1\alpha + a_1^2\beta, \qquad & b_1^1\beta + b_2^1\delta &= a_2^1\alpha + a_2^2\beta, \\ b_1^2\alpha + b_2^2\gamma &= a_1^1\gamma + a_1^2\delta, \qquad & b_1^2\beta + b_2^2\delta &= a_2^1\gamma + a_2^2\delta. \end{aligned} \tag{4.3.1}$$

Consequently, we find

$$\begin{aligned} \Delta\, b_1^1 &= \alpha\delta a_1^1 - \alpha\gamma a_2^1 + \beta\delta a_1^2 - \beta\gamma a_2^2, \qquad & \Delta\, b_2^1 &= -\alpha\beta a_1^1 + \alpha^2 a_2^1 - \beta^2 a_1^2 + \alpha\beta a_2^2, \\ \Delta\, b_1^2 &= \gamma\delta a_1^1 - \gamma^2 a_2^1 + \delta^2 a_1^2 - \gamma\delta a_2^2, \qquad & \Delta\, b_2^2 &= -\beta\gamma a_1^1 + \alpha\gamma a_2^1 - \beta\delta a_1^2 + \alpha\delta a_2^2. \end{aligned} \tag{4.3.2}$$

After a set of computations, we find that the homogeneous invariant polynomials of first degree have the form

$$I_1(a) = a_1^1 + a_2^2 = \mathrm{tr}(a),$$

while the homogeneous invariant polynomials of second degree are of the form

$$I_2(a) = a_1^1 a_2^2 - a_2^1 a_1^2 = \det(a),$$

(see Sibirsky [57] for details of the calculations).

For the third–degree invariant polynomials it is possible to show that they have the form

$$I_3(a) = k_1\,(\mathrm{tr}(a))^3 + k_2\ \mathrm{tr}(a)\ \det(a) = k_1\,(I_1(a))^3 + k_2\ I_1(a)\ I_2(a),$$

i.e. they are polynomially expressed by the previous obtained invariant polynomials of lesser degrees $I_1(a)$ and $I_2(a)$.

Definition 4.3.1. *An invariant polynomial $I(a)$ is called **reducible**, if it is polynomially expressed by invariant polynomials of lesser degrees.*

We note that the invariant polynomial $I_3(a)$ above is reducible. We denote $I(a) \equiv 0$ and say that $I(a)$ is congruent with zero. The notation $I(a) \equiv J(a)$ means that $I(a) - J(a) \equiv 0$.

We are likely to show that any invariant polynomial of the system (4.1.4) is polynomially ex-

pressed by means of $I_1(a)$ and $I_2(a)$. In this case, we say that $I_1(a)$ and $I_2(a)$ produce a polynomial basis of (affine) invariants.

Definition 4.3.2. *The set of all invariant polynomials* $\{I_\theta(a),\ \theta \in \Theta\}$ *of systems* (4.1.4) *under the group* G *is called a* ***polynomial basis of invariant polynomials*** *of those systems under the group* G*, if any invariant polynomial* $I(a)$ *of systems* (4.1.4) *under the group* G *can be expressed in the form of a polynomial of invariants* $I_\theta(a)$*. Here,* Θ *is some set of finite or transfinite integers.*

Definition 4.3.3. *A polynomial basis of invariants of systems* (4.1.4) *under the group* G *is called* ***minimal****, if after the removing of any invariant polynomial out of the set, it will cease to be a polynomial basis.*

Remark 4.3.4. *The minimality of a polynomial basis, consisting of the invariants* $\mathrm{tr}(a)$ *and* $\det(a)$*, follows from the fact that it is impossible to express* $\det(a)$ *by means of the square of* $\mathrm{tr}(a)$*.*

Sibirsky [57] provides more concepts concerning the tensor notation, for instance the operations on tensors: multiplication, (total) contraction, extended (total) contraction, (extended) alternation. By using these operations on tensors of systems (4.1.4), the obtained expressions will form a polynomial basis of affine (orthogonal) invariant polynomials of systems (4.1.4) (see [57], Theorem 6.1, page 12).

4.4 Comitants of systems of differential equations

Definition 4.4.1. *A polynomial* $U(a,x)$ *of coefficients of systems* (4.1.4) *and the dependent variable* $x = (x^1, x^2, \ldots, x^n)$ *is called a* ***comitant*** *of systems* (4.1.4) *under the group* G*, if there exists a function* $\lambda(g)$ *such that*

$$U(b,y) = \lambda(g)U(a,x), \tag{4.4.1}$$

for all $g \in G$*,* $a \in A$ *and* $x \in X$*. If* $\lambda(g) \equiv 1$*, then the comitant* $U(a,x)$ *is called* ***absolute****, otherwise it is* ***relative****.*

We observe that the invariants for systems (4.1.4) under the group G defined in Definition 4.2.2 are a particular case of comitants when they do not explicitly depend on the the variable x. Moreover, the theorem of a polynomial basis of comitants is easily extended from the theorem of a polynomial basis of invariants.

Let $U(a,x)$ be a comitant of systems (4.1.4). Applying the transformation (4.2.1) to systems (4.1.4), we obtain systems (4.2.2) with the comitant $U(b,y)$. Doing the same transformation within

the comitant $U(a,x)$ (as a polynomial), we obtain the polynomial $U(a,g^{-1}y)$, which we call the *transformed comitant*. In this sense,

$$U(b,y) = \lambda(g)U(a,x) = \lambda(g)U(a,g^{-1}y).$$

Then, we have the following result.

Proposition 4.4.2. *[57] The coefficients of a comitant of transformed systems are proportional to the coefficients of the transformed comitant.*

In continuation, Sibirsky [57] constructs some bases of invariant polynomials. For example, he shows that the polynomial basis of GL−invariants of systems (4.1.3) consists of 16 elements (from I_1 to I_{16}). Furthermore, if we add 20 more comitants (from K_1 to K_{20}) to those 16 invariants, we obtain a polynomial basis of GL−comitants of systems (4.1.3). We shall denote this basis of 36 GL−comitants by $\mathscr{K}$.

An important concept in this line is the definition of *syzygies*.

Definition 4.4.3. *Assume $\mathscr{K}$ is the basis of* GL*−comitants of systems* (4.1.3)*. A* ***syzygy*** *among comitants of systems* (4.1.3) *is any relation of the form $S(\mathscr{K}) = 0$, where $S(\mathscr{K})$ is a polynomial of comitants from $\mathscr{K}$, which is an identity with respect to the variables a and x, i.e. with respect to the coefficients and the dependent variable of such systems, and is not an identity with respect to comitants from $\mathscr{K}$.*

We consider a finite set of syzygies among comitants from $\mathscr{K}$ given by:

$$S_i(\mathscr{K}) = 0,\ (i = 1,2,\ldots,\kappa). \tag{4.4.2}$$

We shall say that the syzygy $S(\mathscr{K}) = 0$ is a *consequence* of syzygies (4.4.2), if it is possible to select polynomials $P_i(\mathscr{K})$ $(i = 0,1,\ldots,\kappa)$ of comitants from $\mathscr{K}$ with $P_0 \not\equiv 0$ relative to a and x, such that the equation

$$P_0 S = \sum_{i=1}^{\kappa} P_i S_i \tag{4.4.3}$$

appeared as identity with respect to the comitants which it contains. We shall call the system of syzygies (4.4.2) *independent*, if none of them is a consequence of the others and we shall say that a system of syzygies (4.4.2) is a *basis*, if every syzygy among the comitants from $\mathscr{K}$ is a consequence of syzygies (4.4.2).

The condition of independence is equivalent to the condition that for every set of polynomials $P_i(\mathscr{K})$ $(i = 1,2,\ldots,\kappa)$ from which at least one is not identical to zero with respect to a and x, the inequality

$$\sum_{i=1}^{\kappa} P_i S_i \not\equiv 0 \tag{4.4.4}$$

is fulfilled with respect to invariant polynomials.

We can prove that, among the invariant polynomials I_1 to I_{16} and K_1 to K_{20}, there exist 27 independent syzygies and every other syzygy among this set of invariant polynomials is a consequence of these 27 ones (see [57], Theorem 17.1, page 44).

The usage of invariants and comitants have been extensively applied in quadratic differential systems, as we can see in [41, 8, 6]. In the next section, we shall provide the main comitants used in the previous studies.

4.5 $T-$comitants governing the geometry of the singularities

Considering quadratic systems, we write system (1.5.1) in the form

$$\begin{aligned} \dot{x} &= p_0 + p_1(x,y) + p_2(x,y), \\ \dot{y} &= q_0 + q_1(x,y) + q_2(x,y), \end{aligned} \tag{4.5.1}$$

where p_i and q_i are homogenous polynomials in x and y of degree i with real coefficients, some of which may be zero. We denote the set of such systems by **QS**.

In accordance to Schlomiuk and Vulpe [53], the group $\mathrm{Aff}(2,\mathbb{R})$ of affine transformations on the plane acts on the set **QS** in the following way. Given $g \in \mathrm{Aff}(2,\mathbb{R})$, $g : \mathbb{R}^2 \to \mathbb{R}^2$, we have

$$g : \begin{pmatrix} \overline{x} \\ \overline{y} \end{pmatrix} = M \begin{pmatrix} x \\ y \end{pmatrix} + B \quad \text{and} \quad g^{-1} : \begin{pmatrix} x \\ y \end{pmatrix} = M^{-1} \begin{pmatrix} \overline{x} \\ \overline{y} \end{pmatrix} - M^{-1}B,$$

where $M = (M_{ij})$ is a 2×2 nonsingular matrix and B is a 2×1 matrix over $\mathbb{R}$. For every $S \in$ **QS**, we can form its transformed system $\tilde{S} = gS$:

$$\begin{aligned} \dot{\tilde{x}} &= \tilde{p}(\tilde{x},\tilde{y}), \\ \dot{\tilde{y}} &= \tilde{q}(\tilde{x},\tilde{y}), \end{aligned} \tag{4.5.2}$$

where

$$\begin{pmatrix} \tilde{p}(\tilde{x},\tilde{y}) \\ \tilde{q}(\tilde{x},\tilde{y}) \end{pmatrix} = M \begin{pmatrix} (p \circ g^{-1})(\tilde{x},\tilde{y}) \\ (q \circ g^{-1})(\tilde{x},\tilde{y}) \end{pmatrix}.$$

The map

$$\begin{array}{ccc} \mathrm{Aff}(2,\mathbb{R}) \times \mathbf{QS} & \to & \mathbf{QS} \\ (g,S) & \mapsto & \tilde{S} = gS \end{array}$$

verifies the axioms for a left group action. For every subgroup $G \subseteq \mathrm{Aff}(2,\mathbb{R})$, we obtain an induced action of G on **QS**.

We can identify the set **QS** of systems (4.5.1) with a subset of $\mathbb{R}^{12}$ via the embedding $\mathbf{QS} \hookrightarrow \mathbb{R}^{12}$ which associates to each system (4.5.1) the 12−tuple $a = (a_1, \ldots, a_{12})$ of its coefficients. For every group action $g \in \mathrm{Aff}(2,\mathbb{R})$, we consider the map $r_g : \mathbb{R}^{12} \to \mathbb{R}^{12}$ which corresponds to g via this action. It is known (see, for instance, Sibirsky [57]) that the map r_g is linear and the map $r : \mathrm{Aff}(2,\mathbb{R}) \to \mathrm{GL}(12,\mathbb{R})$ thus obtained is a group homomorphism. For every subgroup G of $\mathrm{Aff}(2,\mathbb{R})$, r induces a representation of G onto a subgroup $\mathscr{G}$ of $\mathrm{GL}(12,\mathbb{R})$.

We consider the polynomial ring $\mathbb{R}[a_1, \ldots, a_{12}, x, y]$ and denote it by $\mathbb{R}[a, x, y]$.

Rewriting Definition 4.4.1 in the previous notation, we say that a polynomial $U(a,x,y) \in \mathbb{R}[a,x,y]$ is a *comitant*, if there exists $\chi \in \mathbb{Z}$ such that

$$U(r_g(a), g(x,y)) = (\det(g))^{-\chi} U(a,x,y),$$

for every $(g,a) \in G \times \mathbb{R}^{12}$ and $(x,y) \in \mathbb{R}^2$. We note that, if $G = \mathrm{GL}(2,\mathbb{R})$ (respectively, $G = \mathrm{Aff}(2,\mathbb{R})$), then the comitant $U(a,x,y)$ of systems (4.5.1) is called GL−*comitant* (respectively, *affine comitant*).

Definition 4.5.1. *A subset $X \subset \mathbb{R}^{12}$ will be called G−**invariant** if, for every $g \in G$, we have $r_g(X) \subseteq X$.*

Let $T(2,\mathbb{R})$ be the subgroup of $\mathrm{Aff}(2,\mathbb{R})$ formed by translations. We consider the linear representation of $T(2,\mathbb{R})$ into its corresponding subgroup $\mathscr{T} \subset \mathrm{GL}(12,\mathbb{R})$, i.e. for every $\tau \in T(2,\mathbb{R})$, $\tau :\ x = \tilde{x} + \alpha,\ y = \tilde{y} + \beta$, we consider as above $r_\tau : \mathbb{R}^{12} \to \mathbb{R}^{12}$.

Definition 4.5.2. *A* GL−*comitant $U(a,x,y)$ of systems* (4.5.1) *is a T−**comitant**, if, for every $(\tau, a) \in T(2,\mathbb{R}) \times \mathbb{R}^{12}$, the relation $U(r_\tau(a),\ \tilde{x}, \tilde{y}) = U(a, \tilde{x}, \tilde{y})$ holds in $\mathbb{R}[\tilde{x},\ \tilde{y}]$.*

We now consider s polynomials $U_i(a,x,y) \in \mathbb{R}[a,x,y]$, $i = 1, \ldots, s$:

$$U_i(a,x,y) = \sum_{j=0}^{d_i} U_{ij}(a) x^{d_i - j} y^j, \quad i = 1, \ldots, s,$$

and assume that the polynomials U_i are GL$-$comitants of a system (4.5.1), where d_i denotes the degree of the binary form $U_i(a,x,y)$ in x and y with coefficients in $\mathbb{R}[a]$.

We denote by

$$\mathscr{U} = \left\{U_{ij}(a) \in \mathbb{R}[a];\ i = 1,\ldots,s,\ j = 0,1,\ldots,d_i\right\},$$

the set of the coefficients in $\mathbb{R}[a]$ of the GL$-$comitants $U_i(a,x,y)$, $i = 1,\ldots,s$, and by $V(\mathscr{U})$ its zero set, i.e.

$$V(\mathscr{U}) = \left\{a \in \mathbb{R}^{12};\ U_{ij}(a) = 0,\ \forall\ U_{ij}(a) \in \mathscr{U}\right\}.$$

Definition 4.5.3. *Let $U_1,U_2,\ldots,U_s$ be* GL$-$*invariant polynomials of a system* (4.5.1)*. A* GL$-$*comitant $U(a,x,y)$ of such a system is called a* ***conditional*** $T-$***comitant*** *(or $CT-$**comitant**), modulo the ideal generated by $U_{ij}(a)$ $(i = 1,\ldots,s;\ j = 0,1,\ldots,d_i)$ in the ring $\mathbb{R}[a]$, if the following two conditions are satisfied:*

(i) the algebraic subset $V(\mathscr{U}) \subset \mathbb{R}^{12}$ is affinely invariant (see Definition 4.5.1);

(ii) for every $(\tau,a) \in T(2,\mathbb{R}) \times V(\mathscr{U})$, we have $U(r_\tau(a),\tilde{x},\tilde{y}) = U(a,\tilde{x},\tilde{y})$ in $\mathbb{R}[\tilde{x},\tilde{y}]$.

In other words, a $CT-$comitant $U(a,x,y)$ is a $T-$comitant on the algebraic subset $V(\mathscr{U}) \subset \mathbb{R}^{12}$.

Definition 4.5.4. *A polynomial $U(a,x,y) \in \mathbb{R}[a,x,y]$, homogeneous of even degree in x and y, has* ***well–determined sign*** *on $V \subset \mathbb{R}^{12}$ with respect to x and y, if, for every $a \in V$, the binary form $u(x,y) = U(a,x,y)$ yields a function of constant sign on $\mathbb{R}^2$, except on a set of zero measure where it vanishes.*

Remark 4.5.5. *We draw the attention to the fact that, if a $CT-$comitant $U(a,x,y)$ of even weight is a binary form of even degree in x and y, of even degree in a and has well–determined sign on some affine invariant algebraic subset V, then its sign is conserved after an affine transformation and time rescaling.*

We consider the polynomials

$$P = p_0 + p_1 + p_2 \quad \text{and} \quad Q = q_0 + q_1 + q_2 \quad \text{in} \quad \mathbb{R}[a,x,y], \tag{4.5.3}$$

where

$$\begin{aligned} p_0 &= a_{00}, \quad p_1 = a_{10}x + a_{01}y, \\ p_2 &= a_{20}x^2 + 2a_{11}xy + a_{02}y^2, \\ q_0 &= b_{00}, \quad q_1 = b_{10}x + b_{01}y, \\ q_2 &= b_{20}x^2 + 2b_{11}xy + b_{02}y^2, \end{aligned} \tag{4.5.4}$$

and

$$\begin{aligned} C_i(a,x,y) &= y\,p_i(a,x,y) - x\,q_i(a,x,y) \in \mathbb{R}[a,x,y],\ i=0,1,2,\\ D_i(a,x,y) &= \frac{\partial}{\partial x}p_i(a,x,y) + \frac{\partial}{\partial y}q_i(a,x,y) \in \mathbb{R}[a,x,y],\ i=1,2. \end{aligned} \tag{4.5.5}$$

According to Sibirsky [57], the polynomials of degree one with respect to the coefficients of the initial systems, namely

$$\{C_0(a,x,y), C_1(a,x,y), C_2(a,x,y), D_1(a), D_2(a,x,y)\}, \tag{4.5.6}$$

are $GL-$comitants with respect to the coefficients of systems (4.5.1).

The next definition presents a differential operator which plays an important role in the next result.

Definition 4.5.6. *Let $f,g \in \mathbb{R}[a,x,y]$. The differential operator $(f,g)^{(k)} \in \mathbb{R}[a,x,y]$, given by*

$$(f,g)^{(k)} = \sum_{h=0}^{k} (-1)^h \binom{k}{h} \frac{\partial^k f}{\partial x^{k-h}\partial y^h}\ \frac{\partial^k g}{\partial x^h \partial y^{k-h}} \tag{4.5.7}$$

*is called **transvectant of index** k **of** f **and** g (see [31, 45] for further reference).*

The next result by Vulpe [60] states that we can obtain any GL$-$comitant by applying basic operations and the transvectant.

Proposition 4.5.7. *[60] Any* GL$-$*comitant can be constructed from the elements of the set* (4.5.5) *by using the operations: addition, subtraction, multiplication and the transvectant.*

We construct the following GL$-$comitants of second degree with respect to the coefficients of initial system:

$$\begin{array}{lll} T_1(a,x,y) = (C_0,C_1)^{(1)}, & T_4(a) = (C_1,C_1)^{(2)}, & T_7(a,x,y) = (C_1,D_2)^{(1)},\\ T_2(a,x,y) = (C_0,C_2)^{(1)}, & T_5(a,x,y) = (C_1,C_2)^{(1)}, & T_8(a,x,y) = (C_2,C_2)^{(2)},\\ T_3(a) = (C_0,D_2)^{(1)}, & T_6(a,x,y) = (C_1,C_2)^{(2)}, & T_9(a,x,y) = (C_2,D_2)^{(1)}. \end{array} \tag{4.5.8}$$

In order to be able to calculate the values of the needed invariant polynomials directly for every canonical system we shall express here a family of $T-$comitants expressed by means of C_i

($i=0,1,2$) and D_j ($j=1,2$):

$$
\begin{aligned}
\tilde{A} =& \left(C_1, T_8 - 2T_9 + D_2^2\right)^{(2)}/144,\\
\widetilde{B} =& \Big\{16D_1(D_2,T_8)^{(1)}(3C_1D_1 - 2C_0D_2 + 4T_2) + 32C_0(D_2,T_9)^{(1)}(3D_1D_2 - 5T_6 + 9T_7)\\
&+ 2(D_2,T_9)^{(1)}\left(27C_1T_4 - 18C_1D_1^2 - 32D_1T_2 + 32(C_0,T_5)^{(1)}\right)\\
&+ 6(D_2,T_7)^{(1)}[8C_0(T_8 - 12T_9) - 12C_1(D_1D_2 + T_7) + D_1(26C_2D_1 + 32T_5)\\
&+ C_2(9T_4 + 96T_3)] + 6(D_2,T_6)^{(1)}\left[32C_0T_9 - C_1(12T_7 + 52D_1D_2) - 32C_2D_1^2\right]\\
&+ 48D_2(D_2,T_1)^{(1)}\left(2D_2^2 - T_8\right) - 32D_1T_8(D_2,T_2)^{(1)} + 9D_2^2T_4(T_6 - 2T_7)\\
&+ 12D_1(C_1,T_8)^{(2)}(C_1D_2 - 2C_2D_1) + 6D_1D_2T_4\left(T_8 - 7D_2^2 - 42T_9\right)\\
&- 16D_1(C_2,T_8)^{(1)}\left(D_1^2 + 4T_3\right) + 12D_1(C_1,T_8)^{(1)}(T_7 + 2D_1D_2)\\
&+ 96D_2^2\left[D_1(C_1,T_6)^{(1)} + D_2(C_0,T_6)^{(1)}\right] - 16D_1D_2T_3\left(2D_2^2 + 3T_8\right)\\
&- 4D_1^3D_2\left(D_2^2 + 3T_8 + 6T_9\right) + 6D_1^2D_2^2(7T_6 + 2T_7) - 252D_1D_2T_4T_9\Big\}/(2^8 3^3),\\
\widetilde{D} =& \left[2C_0(T_8 - 8T_9 - 2D_2^2) + C_1(6T_7 - T_6) - (C_1,T_5)^{(1)} + 6D_1(C_1D_2 - T_5) - 9D_1^2C_2\right]/36,\\
\widetilde{E} =& \left[D_1(2T_9 - T_8) - 3(C_1,T_9)^{(1)} - D_2(3T_7 + D_1D_2)\right]/72,\\
\widetilde{F} =& \Big[6D_1^2(D_2^2 - 4T_9) + 4D_1D_2(T_6 + 6T_7) + 48C_0(D_2,T_9)^{(1)} - 9D_2^2T_4 + 288D_1\widetilde{E}\\
&- 24\left(C_2,\widetilde{D}\right)^{(2)} + 120\left(D_2,\widetilde{D}\right)^{(1)} - 36C_1(D_2,T_7)^{(1)} + 8D_1(D_2,T_5)^{(1)}\Big]/144,\\
\widetilde{K} =& (T_8 + 4T_9 + 4D_2^2)/72 \equiv \left(p_2(x,y), q_2(x,y)\right)^{(1)}/4,\\
\widetilde{H} =& (-T_8 + 8T_9 + 2D_2^2)/72.
\end{aligned}
\tag{4.5.9}
$$

The polynomials defined above in addition to (4.5.5) and (4.5.8) will serve as "bricks" in constructing affine invariant polynomials for systems (4.5.1).

In this sense, Boularas *et al.* [17] constructed a minimal polynomial basis of affine invariant polynomials of systems (4.5.1) of degrees up to 12 (as polynomials in the coefficients of the systems and the dependent variable) by using the affine invariant polynomials in (4.5.9). For this thesis, we need only the basis of affine invariant polynomials of 42 elements which are in the Table 4.5.1.

In the list of Table 4.5.1, the bracket "[" is used in order to avoid placing the otherwise necessary up to five parenthesis "(".

Using the basic elements (4.5.9) as well as the affine invariant polynomials A_i ($i=1,\ldots,42$) from Table 4.5.1, we can construct the invariant polynomials we are going to use in the next chapters.

Table 4.5.1: Minimal basis of affine invariant polynomials

$$
\begin{aligned}
A_1 &= \tilde{A},\\
A_2 &= (C_2,D)^{(3)}/12,\\
A_3 &= \left[C_2,D_2)^{(1)},D_2\right)^{(1)},D_2\right)^{(1)}/48,\\
A_4 &= (\widetilde{H},\widetilde{H})^{(2)},\\
A_5 &= (\widetilde{H},\widetilde{K})^{(2)}/2,\\
A_6 &= (\widetilde{E},\widetilde{H})^{(2)}/2,\\
A_7 &= \left[C_2,\widetilde{E})^{(2)},D_2\right)^{(1)}/8,\\
A_8 &= \left[\widetilde{D},\widetilde{H})^{(2)},D_2\right)^{(1)}/8,\\
A_9 &= \left[\widetilde{D},D_2)^{(1)},D_2\right)^{(1)},D_2\right)^{(1)}/48,\\
A_{10} &= \left[\widetilde{D},\widetilde{K})^{(2)},D_2\right)^{(1)}/8,\\
A_{11} &= (\widetilde{F},\widetilde{K})^{(2)}/4,\\
A_{12} &= (\widetilde{F},\widetilde{H})^{(2)}/4,\\
A_{13} &= \left[C_2,\widetilde{H})^{(1)},\widetilde{H}\right)^{(2)},D_2\right)^{(1)}/24,\\
A_{14} &= (\widetilde{B},C_2)^{(3)}/36,\\
A_{15} &= (\widetilde{E},\widetilde{F})^{(2)}/4,\\
A_{16} &= \left[\widetilde{E},D_2)^{(1)},C_2\right)^{(1)},\widetilde{K}\right)^{(2)}/16,\\
A_{17} &= \left[\widetilde{D},\widetilde{D})^{(2)},D_2\right)^{(1)},D_2\right)^{(1)}/64,\\
A_{18} &= \left[\widetilde{D},\widetilde{F})^{(2)},D_2\right)^{(1)}/16,\\
A_{19} &= \left[\widetilde{D},\widetilde{D})^{(2)},\widetilde{H}\right)^{(2)}/16,\\
A_{20} &= \left[C_2,\widetilde{D})^{(2)},\widetilde{F}\right)^{(2)}/16,\\
A_{21} &= \left[\widetilde{D},\widetilde{D})^{(2)},\widetilde{K}\right)^{(2)}/16,\\
A_{22} &= \left[C_2,\widetilde{D})^{(1)},D_2\right)^{(1)},D_2\right)^{(1)},D_2\right)^{(1)}D_2\right)^{(1)}/1152,\\
A_{23} &= \left[\widetilde{F},\widetilde{H})^{(1)},\widetilde{K}\right)^{(2)}/8,\\
A_{24} &= \left[C_2,\widetilde{D})^{(2)},\widetilde{K}\right)^{(1)},\widetilde{H}\right)^{(2)}/32,\\
A_{25} &= \left[\widetilde{D},\widetilde{D})^{(2)},\widetilde{E}\right)^{(2)}/16,\\
A_{26} &= (\widetilde{B},\widetilde{D})^{(3)}/36,\\
A_{27} &= \left[\widetilde{B},D_2)^{(1)},\widetilde{H}\right)^{(2)}/24,\\
A_{28} &= \left[C_2,\widetilde{K})^{(2)},\widetilde{D}\right)^{(1)},\widetilde{E}\right)^{(2)}/16,\\
A_{29} &= \left[\widetilde{D},\widetilde{F})^{(1)},\widetilde{D}\right)^{(3)}/96,\\
A_{30} &= \left[C_2,\widetilde{D})^{(2)},\widetilde{D}\right)^{(1)},\widetilde{D}\right)^{(3)}/288,\\
A_{31} &= \left[\widetilde{D},\widetilde{D})^{(2)},\widetilde{K}\right)^{(1)},\widetilde{H}\right)^{(2)}/64,\\
A_{32} &= \left[\widetilde{D},\widetilde{D})^{(2)},D_2\right)^{(1)},\widetilde{H}\right)^{(1)},D_2\right)^{(1)}/64,\\
A_{33} &= \left[\widetilde{D},D_2)^{(1)},\widetilde{F}\right)^{(1)},D_2\right)^{(1)},D_2\right)^{(1)}/128,\\
A_{34} &= \left[\widetilde{D},\widetilde{D})^{(2)},D_2\right)^{(1)},\widetilde{K}\right)^{(1)},D_2\right)^{(1)}/64,\\
A_{35} &= \left[\widetilde{D},\widetilde{D})^{(2)},\widetilde{E}\right)^{(1)},D_2\right)^{(1)},D_2\right)^{(1)}/128,\\
A_{36} &= \left[\widetilde{D},\widetilde{E})^{(2)},\widetilde{D}\right)^{(1)},\widetilde{H}\right)^{(2)}/16,\\
A_{37} &= \left[\widetilde{D},\widetilde{D})^{(2)},\widetilde{D}\right)^{(1)},\widetilde{D}\right)^{(3)}/576,\\
A_{38} &= \left[C_2,\widetilde{D})^{(2)},\widetilde{D}\right)^{(2)},\widetilde{D}\right)^{(1)},\widetilde{H}\right)^{(2)}/64,\\
A_{39} &= \left[\widetilde{D},\widetilde{D})^{(2)},\widetilde{F}\right)^{(1)},\widetilde{H}\right)^{(2)}/64,\\
A_{40} &= \left[\widetilde{D},\widetilde{D})^{(2)},\widetilde{F}\right)^{(1)},\widetilde{K}\right)^{(2)}/64,\\
A_{41} &= \left[C_2,\widetilde{D})^{(2)},\widetilde{D}\right)^{(2)},\widetilde{F}\right)^{(1)},D_2\right)^{(1)}/64,\\
A_{42} &= \left[\widetilde{D},\widetilde{F})^{(2)},\widetilde{F}\right)^{(1)},D_2\right)^{(1)}/16.
\end{aligned}
$$

The most significant elements for the finite singularities are $\mu_0(a)$ and $\mathbf{D}(a)$, which are given by

$$\mu_0(a) = \frac{\mathrm{Res}_x(p_2,q_2)}{y^4} \quad \text{and} \quad \mathbf{D}(a) = -\left(\left((\widetilde{D},\widetilde{D})^{(2)},\widetilde{D}\right)^{(1)},\widetilde{D}\right)^{(3)},$$

and they respectively determine when at least one finite singular point collides with an infinite one and when at least two finite singular points collide (see [8] for more details). It is to say that this two invariant polynomials (together with other ones) are responsible for the number and multiplicity of finite singular points.

There also exist the invariants which govern the types of the singular points. For instance, W_4 helps us to decide if an antisaddle is a node or a focus and it is given by

$$
\begin{aligned}
W_4(a) =& 1512A_1^2(A_{30}-2A_{29}) - 648A_{15}A_{26} + 72A_1A_2(49A_{25}+39A_{26})\\
&+ 6A_2^2(23A_{21}-1093A_{19}) - 87A_2^4 + 4A_2^2(61A_{17}+52A_{18}+11A_{20})\\
&- 36A_8(396A_{29}+265A_{30}) + 72A_{29}(17A_{12}-38A_9-109A_{11})
\end{aligned}
$$

$$+12A_{30}(76A_9-189A_{10}-273A_{11}-651A_{12})-648A_{14}(23A_{25}+5A_{26})$$
$$-24A_{18}(3A_{20}+31A_{17})+36A_{19}(63A_{20}+478A_{21})+18A_{21}(2A_{20}+137A_{21})$$
$$-4A_{17}(158A_{17}+30A_{20}+87A_{21})-18A_{19}(238A_{17}+669A_{19}).$$

And the most significant invariant polynomials which govern the number and multiplicity of infinite singular points of systems (4.5.1) are μ_0 and

$$\eta(a)=\frac{(\widetilde{M},\widetilde{M})^{(2)}}{384}=\text{Discrim}(C_2),$$

where $\widetilde{M}(a,x,y)=(C_2,C_2)^{(2)}$.

We can observe that, besides the fact that all these polynomials are invariant in the sense of Definition 4.2.2, they also carry geometrical properties of systems (4.5.1) as commented above. Suggestively, we can rewrite some of them in the forms below and understand their geometrical meaning:

$$C_2(a,x,y)=y\,p_2(x,y)-x\,q_2(x,y),$$
$$\widetilde{M}(a,x,y)=2\,\text{Hess}(C_2(a,x,y)),$$
$$\eta(a)=\text{Discrim}(C_2(a,x,y)),$$
$$\widehat{K}(a,x,y)=\text{Jacob}(p_2(x,y),q_2(x,y))=4\widetilde{K},$$
$$\mu_0(a)=\text{Res}_x(p_2,q_2)/y^4=\text{Discrim}(\widehat{K}(a,x,y))/16.$$

In what follows we present the expressions of invariants and comitants in terms of the basic ones presented above which we shall use in the classification problems we propose in the next chapters:

$$\widehat{H}(a,x,y)=-\text{Discrim}\left(\alpha p_2(x,y)+\beta q_2(x,y)\right)\big|_{\{\alpha=y,\beta=-x\}}=-4\widetilde{H},$$
$$\widetilde{N}(a,x,y)=\widehat{K}(a,x,y)+\widehat{H}(a,x,y),$$
$$\theta(a)=\text{Discrim}(\widetilde{N}(a,x,y)),$$
$$\mathscr{T}_4(a)=\mu_0\rho_1\rho_2\rho_3\rho_4,\quad \mathscr{T}_3(a)=\mu_0(\rho_1\rho_2\rho_3+\rho_1\rho_2\rho_4+\rho_1\rho_3\rho_4+\rho_2\rho_3\rho_4),$$
$$\mathscr{T}_2(a)=\mu_0(\rho_1\rho_2+\rho_1\rho_3+\rho_1\rho_4+\rho_2\rho_3+\rho_2\rho_4+\rho_3\rho_4),\quad \mathscr{T}_1(a)=\mu_0(\rho_1+\rho_2+\rho_3+\rho_4),$$

where ρ_i in $\mathscr{T}_i$ $(i=1,2,3,4)$, in generic case, is the trace of the Jacobian matrix at each singular point. The invariant polynomials $\mathscr{T}_4$ and $\mathscr{T}_i$ $(i=1,2,3)$ are defined in [61] and they are responsible for the weak singular points; see [61, Main Theorem] for further information.

We now consider the differential operator $\mathscr{L} = x\cdot\mathbf{L}_2 - y\cdot\mathbf{L}_1$ (see [11]) acting on $\mathbb{R}[a,x,y]$, where

$$\begin{aligned}\mathbf{L}_1 =& 2a_{00}\frac{\partial}{\partial a_{10}} + a_{10}\frac{\partial}{\partial a_{20}} + \frac{1}{2}a_{01}\frac{\partial}{\partial a_{11}} + 2b_{00}\frac{\partial}{\partial b_{10}} + b_{10}\frac{\partial}{\partial b_{20}} + \frac{1}{2}b_{01}\frac{\partial}{\partial b_{11}},\\ \mathbf{L}_2 =& 2a_{00}\frac{\partial}{\partial a_{01}} + a_{01}\frac{\partial}{\partial a_{02}} + \frac{1}{2}a_{10}\frac{\partial}{\partial a_{11}} + 2b_{00}\frac{\partial}{\partial b_{01}} + b_{01}\frac{\partial}{\partial b_{02}} + \frac{1}{2}b_{10}\frac{\partial}{\partial b_{11}}.\end{aligned}$$

Using this operator, we construct the following important set of invariant polynomials:

$$\mu_i(a,x,y) = \frac{1}{i!}\mathscr{L}^{(i)}(\mu_0),\ i = 1,\ldots,4, \tag{4.5.10}$$

where $\mathscr{L}^{(i)}(\mu_0) = \mathscr{L}(\mathscr{L}^{(i-1)}(\mu_0))$. These polynomials are in fact invariant polynomials of systems (4.5.1) with respect to the group $\mathrm{GL}(2,\mathbb{R})$ (see [11]).

Using the invariant polynomials μ_i $(i = 0,1,\ldots,4)$, we can construct the invariant polynomials **D**, **P**, **R**, **S**, **T**, **U** and **V**, which are responsible for the number and multiplicities of finite singularities of a nondegenerate quadratic system. They are expressed as follows:

$$\begin{aligned}\mathbf{D}(a) &= -(((\widetilde{D},\widetilde{D})^{(2)},\widetilde{D})^{(1)},\widetilde{D})^{(3)}/576,\\ \mathbf{P}(a,x,y) &= 12\mu_0\mu_4 - 3\mu_1\mu_3 + \mu_2^2,\\ \mathbf{R}(a,x,y) &= \mu_1^2 - 8\mu_0\mu_2,\\ \mathbf{S}(a,x,y) &= \mathbf{R}^2 - 16\mu_0^2\mathbf{P},\\ \mathbf{T}(a,x,y) &= 18\mu_0^2(3\mu_3^2 - \mu_2\mu_4) + 2\mu_0(2\mu_2^3 - 9\mu_1\mu_2\mu_3 + 27\mu_1^2\mu_4) - \mathbf{PR},\\ \mathbf{U}(a,x,y) &= \mu_3^2 - 4\mu_2\mu_4,\\ \mathbf{V}(a,x,y) &= \mu_4.\end{aligned}$$

We discuss now an application of the invariant polynomials from the former list. For this, we need the notion of a zero–cycle of the projective plane in order to describe the number and multiplicity of singular points of a quadratic system. This notion and the notion of the divisor of a line were used for purposes of classification of planar quadratic differential systems by Pal and Schlomiuk [51], Llibre and Schlomiuk [39], Schlomiuk and Vulpe [53, 54] and Artés, Llibre and Schlomiuk [6].

Definition 4.5.8. *We consider formal expressions $\mathscr{D} = \sum n(w)w$, where $n(w)$ is an integer and only a finite number of $n(w)$ are nonzero. Such an expression is called a* ***zero–cycle*** *of $\mathbb{CP}_2$, if all w appearing in $\mathscr{D}$ are points of $\mathbb{CP}_2$. We call* ***degree of the zero–cycle*** *$\mathscr{D}$ the integer* $\deg(\mathscr{D}) = \sum n(w)$. *We call* ***support of*** *$\mathscr{D}$ the set* $\mathrm{Supp}(\mathscr{D})$ *of w's appearing in $\mathscr{D}$ such that $n(w) \neq 0$.*

We recall that $\mathbb{CP}_2$ denotes the complex projective space of dimension 2. For a system S belonging to the family (4.5.1) we denote $\nu(P,Q) = \{w \in \mathbb{C}_2;\ P(w) = Q(w) = 0\}$ and we define the following zero–cycle $\mathscr{D}_S(P,Q) = \sum_{w\in\nu(P,Q)} I_w(P,Q)w$, where $I_w(P,Q)$ is the intersection number or multiplicity of intersection at w of the projective completions of the curves $P = 0$ and $Q = 0$ (see Section 3.4). It is clear that, for a nondegenerate quadratic system, $\deg(\mathscr{D}_S) \le 4$ and the number of points in $\mathrm{Supp}(\mathscr{D}_S)$ is lesser of equal to 4. The zero–cycle $\mathscr{D}_S(P,Q)$ is undefined for a degenerate system.

Having constructed the invariant polynomials $\mathbf{D}$, $\mathbf{P}$, $\mathbf{R}$, $\mathbf{S}$, $\mathbf{T}$, $\mathbf{U}$ and $\mathbf{V}$, their geometrical meaning is revealed in the next proposition.

Proposition 4.5.9. *[11, 61] The form of the divisor $\mathscr{D}_S(P,Q)$ for nondegenerate quadratic systems* (4.5.3) *is determined by the corresponding conditions indicated in Table 4.5.2, where we write $p+q+r^c+s^c$ if two of the finite points, i.e. r^c, s^c, are complex but not real.*

Table 4.5.2: Necessary and sufficient conditions: the number and multiplicity of the finite singular points of nondegenerate quadratic systems

No.	Zero–cycle $\mathscr{D}_S(P,Q)$	Invariant criteria	No.	Zero–cycle $\mathscr{D}_S(P,Q)$	Invariant criteria
1	$p+q+r+s$	$\mu_0 \neq 0, \mathbf{D} < 0, \mathbf{R} > 0, \mathbf{S} > 0$	10	$p+q+r$	$\mu_0 = 0, \mathbf{D} < 0, \mathbf{R} \neq 0$
2	$p+q+r^c+s^c$	$\mu_0 \neq 0, \mathbf{D} > 0$	11	$p+q^c+r^c$	$\mu_0 = 0, \mathbf{D} > 0, \mathbf{R} \neq 0$
3	$p^c+q^c+r^c+s^c$	$\mu_0 \neq 0, \mathbf{D} < 0, \mathbf{R} \le 0$ $\mu_0 \neq 0, \mathbf{D} < 0, \mathbf{S} \le 0$	12	$2p+q$	$\mu_0 = \mathbf{D} = 0, \mathbf{PR} \neq 0$
4	$2p+q+r$	$\mu_0 \neq 0, \mathbf{D} = 0, \mathbf{T} < 0$	13	$3p$	$\mu_0 = \mathbf{D} = \mathbf{P} = 0, \mathbf{R} \neq 0$
5	$2p+q^c+r^c$	$\mu_0 \neq 0, \mathbf{D} = 0, \mathbf{T} > 0$	14	$p+q$	$\mu_0 = \mathbf{R} = 0, \mathbf{P} \neq 0, \mathbf{U} > 0$
6	$2p+2q$	$\mu_0 \neq 0, \mathbf{D} = \mathbf{T} = 0, \mathbf{PR} > 0$	15	p^c+q^c	$\mu_0 = \mathbf{R} = 0, \mathbf{P} \neq 0, \mathbf{U} < 0$
7	$2p^c+2q^c$	$\mu_0 \neq 0, \mathbf{D} = \mathbf{T} = 0, \mathbf{PR} < 0$	16	$2p$	$\mu_0 = \mathbf{R} = 0, \mathbf{P} \neq 0, \mathbf{U} = 0$
8	$3p+q$	$\mu_0 \neq 0, \mathbf{D} = \mathbf{T} = 0, \mathbf{P} = 0, \mathbf{R} \neq 0$	17	p	$\mu_0 = \mathbf{R} = 0, \mathbf{P} = 0, \mathbf{U} \neq 0$
9	$4p$	$\mu_0 \neq 0, \mathbf{D} = \mathbf{T} = 0, \mathbf{P} = \mathbf{R} = 0$	18	0	$\mu_0 = \mathbf{R} = \mathbf{R} = 0, \mathbf{U} = 0, \mathbf{V} \neq 0$

Chapter

5

The topological classification of quadratic differential systems with a semi–elemental triple node

5.1 Motivation for the study

Artés, Kooij and Llibre [4] classified all the structurally stable quadratic planar systems modulo limit cycles, also known as the codimension–zero quadratic systems. Roughly speaking, those systems are characterized by having the properties: all singularities, finite and infinite, are simple, with no separatrix connection, and where any nest of limit cycles is considered as a single point with the stability of the outer limit cycle. The authors proved the existence of 44 topologically different phase portraits for such systems.

The natural continuation of this idea is the classification of the structurally unstable quadratic systems of codimension–one, modulo limit cycles. The next definition characterizes systems of codimension one.

Definition 5.1.1. *A differential system is said to be a* ***system of the first degree of structural instability*** *(or a* ***system of codimension one****) if, and only if, the following conditions are satisfied:*

(i) *A vector field, in the region of its definition, has one, and only one, simplest structurally unstable object, that is to say one of the following types:*

(i.1) *a multiple focus of multiplicity one;*

(i.2) *a limit cycle of multiplicity two;*

(i.3) *a saddle–node of multiplicity two (with divergence nonzero);*

(i.4) *a separatrix from one saddle point to another;*

(i.5) *a separatrix forming a loop for a saddle point (with divergence nonzero).*

(ii) *A vector field, in the region of its definition, has no structurally unstable limit cycles, saddle–point separatrices forming a loop, or equilibrium states other than those listed in* (i).

(iii) *If the vector field has a saddle–node, none of its separatrices may go to a saddle point and no two separatrices of the saddle–node are continuation one of the other.*

(iv) *The separatrix of a saddle point of the vector field in its region of definition may not go to a separatrix forming a loop as* $t \to -\infty$ *or as* $t \to \infty$. *The region of definition cannot contain two saddle point separatrices going to the same limit cycle of multiplicity two, one as* $t \to -\infty$ *and the other as* $t \to \infty$.

The above conditions, which are general for any class of vector fields, are easily reduced for the case of polynomial vector fields, and even more for quadratic vector fields, as for example condition (iv) which implies the existence of a saddle point inside the regions limited by a loop separatrix or a limit cycle, which cannot happen in quadratic vector fields, according to item (iii) of Section 1.5, on page 15.

Furthermore, these conditions are even simpler for the study done modulo limit cycles since we do not need to deal with multiple focus or limit cycles. So, the conditions will be reduced to:

(i) A vector field, in the region of its definition, has one, and only one, simplest structurally unstable object, that is to say one of the following types:

(i.1) a saddle–node of multiplicity two (with divergence nonzero);

(i.2) a separatrix from one saddle point to another;

(i.3) a separatrix forming a loop for a saddle point (with divergence nonzero).

(ii) A vector field, in the region of its definition, has no structurally unstable limit cycles, saddle–point separatrices forming a loop, or equilibrium states other than those listed in (i).

(iii) If the vector field has a saddle–node, none of its separatrices may go to a saddle point and no two separatrices of the saddle–node are continuation one of the other.

Even more, condition (i.3) of having a separatrix forming a loop for a saddle point with divergence nonzero can be considered without the requirement on the divergence as this means that

the loop is such that a limit cycle cannot bifurcate from it (compared with the fact that a limit cycle can bifurcate from a multiple focus). When considering specific examples, we will simply take care of this condition holding, but it is not needed when studying the topological possible phase portraits.

In short, a polynomial vector field is structurally unstable of codimension one modulo limit cycles if, and only if, they have one and only one of the following simplest structurally unstable objects: a saddle–node of multiplicity two (finite or infinite), a separatrix from one saddle point to another, and a separatrix forming a loop for a saddle point with its divergence nonzero. This study is already in progress [5], all topological possibilities have already been found, some of them have already been proved impossible and many representatives have been located, but still remain some cases without candidate.

It is worth mentioning that all the phase portraits of codimension one are split into four groups according to the possession of a structurally unstable element: (A) possessing a finite semi–elemental saddle–node, (B) possessing an infinite semi–elemental saddle–node $\overline{\binom{0}{2}}SN$, (C) possessing an infinite semi–elemental saddle–node $\overline{\binom{1}{1}}SN$, and (D) possessing saddle connection.

One way to obtain codimension–one phase portraits is considering a perturbation of known phase portraits of quadratic systems of codimension greater than one. This perturbation would decrease the codimension of the system and we may find a representative for a topological equivalence class in the family of the codimension–one systems and add it to the existing classification. In order to contribute to this classification, some families of quadratic systems of higher codimension are studied, e.g. systems with a weak focus of second order, see [6].

Besides, the complete characterization of the phase portraits for real planar quadratic vector fields is not known and attempting to classify topologically these systems, which occur rather often in applications, is quite a complex task. As mentioned before (see Section 4.5), this family of systems depends on twelve parameters, but due to the action of the group G of real affine transformations and time homotheties, the class ultimately depends on five parameters, but this is still a large number. So, we draw our attention to some subfamilies of quadratic systems possessing three and four parameters.

In this chapter our goal is to classify topologically all quadratic systems possessing a semi–elemental triple node as a finite singularity. This study is part of this attempt of classifying all the codimension–one quadratic systems.

We know that one phase portrait here will bifurcate to one of the codimension–one systems

still missing.

The results provided in this chapter can be also found in the paper of Artés, Rezende and Oliveira [9].

5.2 Statement of the results

The goal of this chapter is to study the class $\mathbf{QT\overline{N}}$ of all quadratic systems possessing a semi–elemental triple node. If we have a finite triple point, the possibility of having another finite singular point is present. Indeed, in case the remaining singularity did not go to infinity, then there is another singularity in the finite plane. In this study we follow the pattern set out in [6].

The class $\mathbf{QT\overline{N}}$ is partitioned into 63 parts: 17 three–dimensional ones, 29 two–dimensional ones, 15 one–dimensional ones and 2 points. This partition is obtained by considering all the bifurcation surfaces of singularities and one related to connections of separatrices, modulo "islands" (see Section 5.4.3).

Theorem 5.2.1. *There exist* 28 *distinct phase portraits for the quadratic vector fields having a semi–elemental triple node and given by the normal form* (5.3.1) *(class* $\mathbf{QT\overline{N}}$*). The bifurcation diagram for this class is the affine tridimensional space* $\mathbb{R}^3$*. All these phase portraits are shown in Figure 5.1. Moreover, the following statements hold:*

(a) There exist three phase portraits with limit cycles, and they are in the parts V_6*,* V_{15} *and* $5S_5$*;*

(b) There exist three phase portraits possessing a single graphic with two singular points both infinite which surrounds a focus. They are in the parts $5S_4$*,* $7S_1$ *and* $5.7L_1$*;*

(c) There exists exactly one phase portrait possessing a graphic with two singular points both infinite which surrounds an infinite number of graphics being all loops. It is in part $1.3L_2$*;*

(d) There exist 19 *phase portraits with two finite singular points and* 9 *with only one finite singular point.*

From the 28 topologically distinct phase portraits stated in Theorem 5.2.1, 9 occur in three–dimensional parts, 13 in two–dimensional parts, 5 in one–dimensional parts and 1 occurs in a single zero–dimensional part.

In Figure 5.1 we have denoted with a little disk the elemental singular points and with a little triangle the semi–elemental triple node. We have plotted with wide curves the separatrices and we have added some thinner orbits to avoid confusion in some required cases.

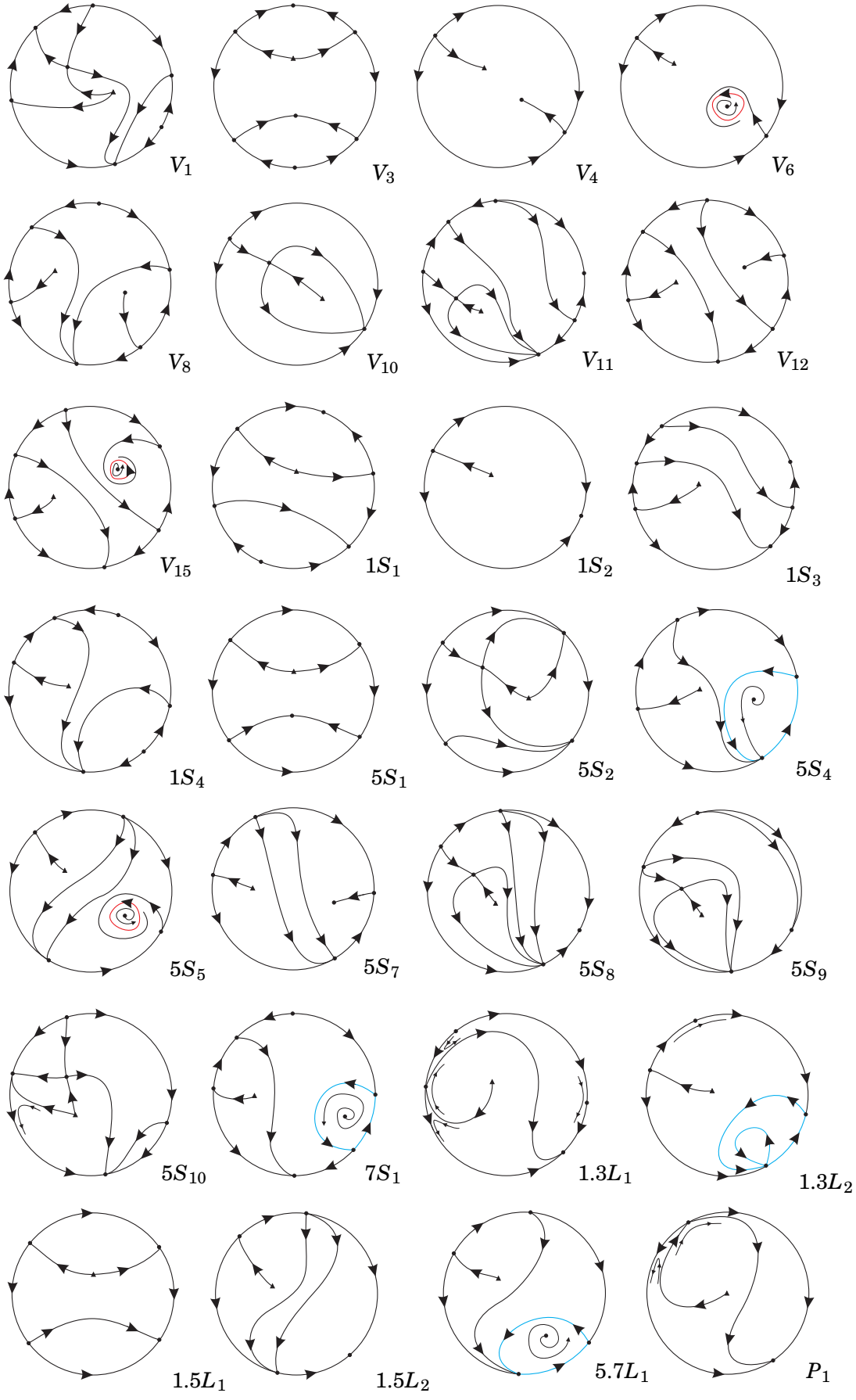

Figure 5.1: Phase portraits for quadratic vector fields with a semi–elemental triple node

Remark 5.2.2. *The phase portraits are labeled according to the parts of the bifurcation diagram where they occur. These labels could be different for two topologically equivalent phase portraits occurring in distinct parts. Some of the phase portraits in three–dimensional parts also occur in some two–dimensional parts bordering these three–dimensional parts. An example occurs when a node turns into a focus. An analogous situation happens for phase portraits in two–dimensional (respectively, one–dimensional) parts, coinciding with a phase portrait on one–dimensional (respectively, zero–dimensional) part situated on the border of it.*

Corollary 5.2.3. *After applying a perturbation, the phase portrait V_{11} in Figure 5.1 yields a new topologically possible phase portrait of codimension–one expected to exist.*

5.3 Quadratic vector fields with a semi–elemental triple node

According to Definition 2.1.1, a singular point r of a planar vector field X in $\mathbb{R}^2$ is semi–elemental, if the determinant of its Jacobian matrix, $DX(r)$, is zero, but its trace is different from zero.

We recall that in Proposition 2.2.1 (page 23) the normal form of a system possessing a semi–elemental singular point is presented. However, we want this semi–elemental singular point to be a triple node. The following result states the normal form for systems in $\mathbf{QT\overline{N}}$.

Proposition 5.3.1. *Every system with a finite semi–elemental triple node $\overline{n}_{(3)}$ can be brought via affine transformations and time rescaling to the following normal form:*

$$\begin{aligned} \dot{x} &= 2xy + ky^2, \\ \dot{y} &= y - x^2 + 2mxy + ny^2, \end{aligned} \tag{5.3.1}$$

where m, n and k are real parameters.

Proof. We start with system (2.2.2). By Proposition 2.2.1, we set $g = 0$ and $h\ell \neq 0$ in order to have a semi–elemental triple point at the origin. As the function $g(x) = -2h\ell x^3 + o(x^4)$ starts with odd degree, it implies that the triple point is either a node or a saddle. If $h\ell < 0$, we shall have a triple node. So, after applying the affine change $(x, y) \mapsto (\sqrt{-h\ell}x, hy)$, we obtain $h = 1$, $\ell = -1$ and, by renaming the other coefficients, we complete the proof. ∎

In view that the normal form (5.3.1) involves the coefficients m, n and k, which are real, the parameter space is $\mathbb{R}^3$ with coordinates (m, n, k).

Remark 5.3.2. *Instead of the normal form* (5.3.1) *we could have constructed another one in which case we would have considered the closure of the family* $\mathbf{QT\overline{N}}$. *According to the normal form* (2.2.2) *for semi–elemental singularities, for the existence of a triple singular point we must have* $h\ell < 0$ *(i.e.* $h\ell \neq 0$*). So, the closure would correspond to the cases:* (i) $h = 0$ *and* $\ell \neq 0$, (ii) $h \neq 0$ *and* $\ell = 0$, *and* (iii) $h = \ell = 0$, *which are related to either the presence of semi–elemental saddle–nodes of multiplicity* 4 *or higher degeneracy, e.g. the presence of lines of singularities. This means that the dimension of the bifurcation diagram would be greater than three. As our contact with the technique was recent, we avoided using a normal form depending on more parameters than* (5.3.1)*, so that the analysis would be less complicated than the one described in [6].*

Remark 5.3.3. *After applying the change* $(x, y, t) \mapsto (-x, y, t)$*, we note that system* (5.3.1) *is symmetric in relation to the real parameters* k *and* m *(the usual reflection in the axes* k *and* m*). So, we will only consider* $k \geq 0$ *and* $m \geq 0$.

We note that in this study we use the concept of intersection number for curves described in Section 1.6.

5.4 The bifurcation diagram of systems with a semi–elemental triple node

We recall that, in view that the normal form (5.3.1) involves the coefficients m, n and k, which are real, the parameter space here is $\mathbb{R}^3$ with coordinates (m, n, k).

5.4.1 Bifurcation surfaces due to the changes in the nature of singularities

For systems (5.3.1) we will always have $(0, 0)$ as a finite singular point, a semi–elemental triple node.

From Section 4.5 we get the formulas which give the bifurcation surfaces of singularities in $\mathbb{R}^{12}$, produced by changes that may occur in the local nature of finite and infinite singularities. These bifurcation surfaces are all algebraic and they are the following:

Bifurcation surfaces in $\mathbb{R}^3$ due to multiplicities of singularities

($\mathscr{S}_1$) This is the bifurcation surface due to multiplicity of infinite singularities as detected by the coefficients of the divisor $\mathscr{D}_{\mathbb{R}}(P, Q; Z) = \sum_{W \in \{Z=0\} \cap \mathbb{CP}^2} I_W(P, Q) W$, (here $I_W(P, Q)$ denotes the intersection multiplicity of $P = 0$ with $Q = 0$ at the point W situated on the line at infinity, i.e.

$Z = 0$) whenever $\deg(\mathscr{D}_{\mathbb{R}}(P,Q;Z)) > 0$. This occurs when at least one finite singular point collides with at least one infinite singular point. More precisely, this happens whenever the homogenous polynomials of degree two, p_2 and q_2 in p and q, have a common root. The equation of this surface is

$$\mu = k^2 + 4km - 4n = 0.$$

($\mathscr{S}_5$)[1] This is the bifurcation surface due to multiplicity of infinite singularities as detected by the coefficients of $\mathscr{D}_{\mathbb{C}}(C,Z) = \sum_{W\in\{Z=0\}\cap\mathbb{CP}^2} I_W(C,Z)W$, i.e. this bifurcation occurs whenever at a point W of intersection of $C = 0$ with $Z = 0$ we have $I_W(C,Z) \geq 2$, i.e. when at least two infinite singular points collide at W. This occurs whenever the discriminant of $C_2 = C(X,Y,0) = Yp_2(X,Y) - Xq_2(X,Y)$ is zero. We denote by η this discriminant. The equation of this surface is

$$\eta = -32 - 27k^2 - 72km + 16m^2 + 32km^3 + 48n + 36kmn - 16m^2n - 24n^2 + 4m^2n^2 + 4n^3 = 0.$$

The surface of C^∞ bifurcation due to a strong saddle or a strong focus changing the sign of their traces (weak saddle or weak focus)

($\mathscr{S}_3$) This is the bifurcation surface due to finite weak singularities, which occurs when the trace of a finite singular point is zero. The equation of this surface is given by

$$\mathscr{T}_4 = 8 + k^2 + 4n = 0,$$

where the invariant $\mathscr{T}_4$ is defined in Section 4.5. We note that this bifurcation surface can either produce a topological change, if the weak point is a focus, or just a C^∞ change, if it is a saddle, except when this bifurcation coincides with a loop bifurcation associated with the same saddle, in which case, the change may also be topological (for an example of this case we refer to Chapter 7).

The surface of C^∞ bifurcation due to a node becoming a focus

($\mathscr{S}_6$) This surface will contain the points of the parameter space where a finite node of the system turns into a focus (and conversely). This surface is a C^∞ but not a topological bifurcation surface. In fact, when we only cross the surface ($\mathscr{S}_6$) in the bifurcation diagram, the topological phase portraits do not change. However, this surface is relevant for isolating the parts where a limit cycle

[1] The numbers attached to these bifurcations surfaces do not appear here in increasing order. We just kept the same enumeration used in [6] to maintain coherence even though some of the numbers in that enumeration do not occur here.

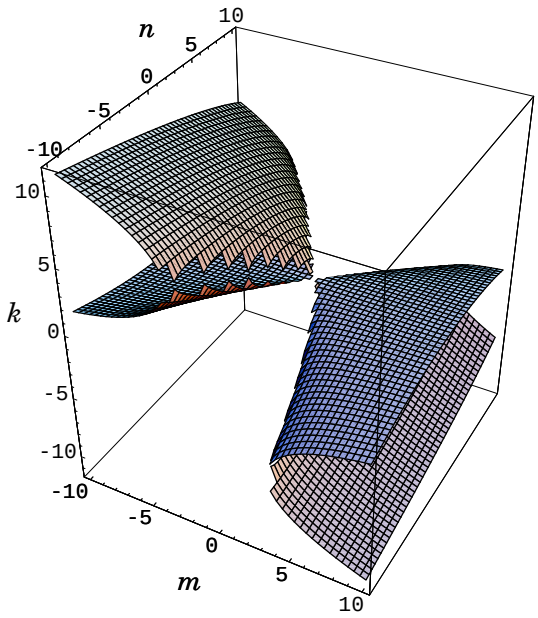

Figure 5.2: The 3−dimensional picture of the surface ($\mathscr{S}_6$) (when a finite node becomes a focus)

surrounding an antisaddle (different from the triple node) cannot exist. Using the expressions in Section 4.5, the equation of this surface is given by $W_4 = 0$, where

$$W_4 = 64 + 48k^2 + k^4 + 128km - 64n + 8k^2n + 16n^2.$$

Remark 5.4.1. *Even though we can draw a* 3*−dimensional picture of the algebraic bifurcation surfaces of singularities in* $\mathbb{R}^3$ *(see Figure 5.2, for an example), it is pointless to try to see a single* 3*−dimensional image of all these four bifurcation surfaces together in the space* $\mathbb{R}^3$*. As we shall see later, the full partition of the parameter space obtained from all these bifurcation surfaces has 63 parts.*

Due to Remark 5.4.1 we shall foliate the 3−dimensional bifurcation diagram in $\mathbb{R}^3$ by planes $k = k_0$, k_0 constant. We shall give pictures of the resulting bifurcation diagram on these planar sections on an affine chart on $\mathbb{R}^2$. In order to detect the key values for this foliation, we must find the values of parameters where the surfaces intersect each other. As we mentioned before, we will be only interested in non–negative values of k to construct the bifurcation diagram.

As the final bifurcation diagram is quite complex, it is useful to introduce colors which will be used to talk about the bifurcation points:

(a) the curve obtained from the surface ($\mathscr{S}_1$) is drawn in blue (a finite singular point collides with an infinite one);

(b) the curve obtained from the surface $(\mathscr{S}_3)$ is drawn in green (when the trace of a singular point becomes zero);

(c) the curve obtained from the surface $(\mathscr{S}_5)$ is drawn in red (two infinite singular points collide);

(d) the curve obtained from the surface $(\mathscr{S}_6)$ is drawn in black (an antisaddle different from the triple node is on the verge of turning from a node into a focus or vice versa); and

(e) the curve obtained from the surface $(\mathscr{S}_7)$ is drawn in purple (the connection of separatrices).

The following set of eight results study the singularities of each surface and the simultaneous intersection points of the bifurcation surfaces, or the points or curves where two bifurcation surfaces are tangent.

Lemma 5.4.2. *Concerning the singularities of the surfaces, it follows that:*

(i) $(\mathscr{S}_1)$ *and* $(\mathscr{S}_3)$ *have no singularities;*

(ii) $(\mathscr{S}_5)$ *has a curve of singularities given by* $4m^2+3n-6=0$*;*

(iii) $(\mathscr{S}_6)$ *has a singularity on the straight line* $(m,2,0)$ *on slice* $k=0$*. Besides, this surface restricted to* $k=0$ *is part of the surface* $(\mathscr{S}_5)$*.*

Proof. It is easy to see that the gradient of $(\mathscr{S}_1)$ and $(\mathscr{S}_3)$ is never null for all $(m,n,k)\in\mathbb{R}^3$; so *(i)* is proved. In order to prove *(ii)* we compute the gradient of η and we verify that it is null whenever $m=-3\sqrt[3]{k}/2$ and $n=2-3\sqrt[3]{k^2}$, for all $k\geq 0$. It is easy to see that these values of m and n for all $k\geq 0$ lie on the curve $4m^2+3n-6=0$. Finally, considering the gradient of the surface $(\mathscr{S}_6)$, it is identically zero at the point $(0,2,0)$ which lies on the straight line $(m,2,0)$ whenever $k=0$. Moreover, if $k=0$, we see that the equation of $(\mathscr{S}_6)$ is $(-2+n)^2$, which is part of $(\mathscr{S}_5)$, proving *(iii)*. ■

Lemma 5.4.3. *Surfaces* $(\mathscr{S}_1)$ *and* $(\mathscr{S}_3)$ *do not intersect on* $k=0$*. For all* $k\neq 0$*, they intersect in the point* $(-(4+k^2)/2k,-2-k^2/4,k)$*.*

Proof. By solving simultaneously both equations of the surfaces $(\mathscr{S}_1)$ and $(\mathscr{S}_3)$ for all $k\neq 0$, we obtain the point $(-(4+k^2)/2k,-2-k^2/4,k)$. We also note that, if $k=0$, there is no intersection point. ■

Lemma 5.4.4. *Surfaces* $(\mathscr{S}_1)$ *and* $(\mathscr{S}_5)$ *intersect at the points* $(-\sqrt{2},0,0)$ *and* $(\sqrt{2},0,0)$ *on* $k=0$*, and, for all* $k\neq 0$*, they intersect along the surface* $\gamma_1(m,n)=-64+32m^2+16n-n^2=0$ *and they have a* 2*–order contact along the surface* $\gamma_2(m,n)=1+2m^2+2n+m^2n+n^2=0$*.*

Proof. By solving simultaneously both equations of the surfaces $(\mathscr{S}_1)$ and $(\mathscr{S}_5)$ for $k = 0$, we obtain the two solutions $m_1 = -\sqrt{2},\ n_1 = 0$ and $m_2 = \sqrt{2},\ n_2 = 0$, proving the first part of the lemma. For all $k \neq 0$, the simultaneous solutions of the equations are the three points: $r_1 = (-\sqrt{2}-k/4, -\sqrt{2}k, k)$, $r_2 = (\sqrt{2}-k/4, \sqrt{2}k, k)$ and $r_3 = (-(4+k^2)/2k, -2-k^2/4, k)$. By computing the resultant with respect to k of $(\mathscr{S}_1)$ and $(\mathscr{S}_5)$, we see that $\mathrm{Res}_k[(\mathscr{S}_1),(\mathscr{S}_5)] = -16\,\gamma_1(m,n)\,(\gamma_2(m,n))^2$, where $\gamma_1(m,n)$ and $\gamma_2(m,n)$ are as stated in the statement of the lemma. It is easy to see that $\gamma_1(m,n)$ has two simple roots which are r_1 and r_2, and r_3 is a double root of $(\gamma_2(m,n))^2$. Then, the surfaces intersect transversally along the curve $\gamma_1(m,n)$ and they have a $2-$order contact along the curve $\gamma_2(m,n)$. ∎

Lemma 5.4.5. *Surfaces $(\mathscr{S}_1)$ and $(\mathscr{S}_6)$ do not intersect on $k = 0$. For all $k \neq 0$, they have a $2-$order contact along the surface $1 + 2m^2 + 2n + m^2n + n^2 = 0$.*

Proof. By solving the system formed by the equations of the surfaces $(\mathscr{S}_1)$ and $(\mathscr{S}_6)$, we find the point $r = (-(4+k^2)/2k, -2-k^2/4, k)$, for all $k \neq 0$, which lies on the curve $1+2m^2+2n+m^2n+n^2 = 0$. We claim that the surfaces $(\mathscr{S}_1)$ and $(\mathscr{S}_6)$ have a $2-$order contact point at r. Indeed, we have just shown that the point r is a common point of both surfaces. Applying the change of coordinates given by $n = (v + km + k^2)/4$, $v \in \mathbb{R}$, we see that the gradient vector of $(\mathscr{S}_1)$ is $\nabla\mu(r) = (0,0,0)$ while the gradient vector of $(\mathscr{S}_6)$ is $\nabla W_4(r) = (0,0,8(-4 + 16/k^2 + 5k^2))$, whose last coordinate is always positive for all $k \neq 0$. As it does not change its sign, the vector $\nabla W_4(r)$ will always point upwards in relation to $(\mathscr{S}_1)$ restricted to the previous change of coordinates. Then, the surface $(\mathscr{S}_6)$ remains only on one of the two topological subspaces delimited by the surface $(\mathscr{S}_1)$, proving our claim. ∎

Lemma 5.4.6. *If $k = 0$, the surfaces $(\mathscr{S}_3)$ and $(\mathscr{S}_5)$ intersect at the points $(-2,-2,0)$ and $(2,-2,0)$. For all $k \neq 0$, they intersect at the points $r_1 = ((32k - k^3 - \sqrt{(64-k^2)^3})/256, -2-k^2/4, k)$, $r_2 = (-(4+k^2)/2k, -2-k^2/4, k)$ and $r_3 = ((32k - k^3 + \sqrt{(64-k^2)^3})/256, -2-k^2/4, k)$.*

Proof. The result follows easily by solving the system formed by the equations of the surfaces. ∎

Corollary 5.4.7. *If $k = 2\sqrt{2}$, the points r_1 and r_2 of Lemma 5.4.6 are equal and they correspond to the singularity of the surface $(\mathscr{S}_5)$.*

Proof. Replacing $k = 2\sqrt{2}$ at the expressions of the points r_1, r_2 and r_3 described in Lemma 5.4.6, we see that $r_1 = r_2$ and they are equal to the singularity $(-3\sqrt{2}/2, -4, 2\sqrt{2})$ of the surface $(\mathscr{S}_5)$. ∎

Remark 5.4.8. *We observe that the values $k = 0$ and $k = 2\sqrt{2}$ will be very important to describe the bifurcation diagram due to the "rich" change on the behavior of the curves on specific surfaces as we change the slices.*

Lemma 5.4.9. *If $k = 0$, the surfaces $(\mathscr{S}_5)$ and $(\mathscr{S}_6)$ intersect along the straight line $(m, 2, 0)$, for all $m \in \mathbb{R}$. For all $k \neq 0$, they have a 2–order contact point at $(-(4+k^2)/2k, -2-k^2/4, k)$.*

Proof. Replacing $k = 0$ in the equations of the surfaces and solving them in the variables m and n, we find that $m \in \mathbb{R}$ and $n = 2$, implying the existence of intersection along the straight line $(m, 2, 0)$, $m \in \mathbb{R}$. For all $k \neq 0$, the solution of the equations of the surfaces is the point $r = (-(4+k^2)/2k, -2-k^2/4, k)$. We claim that the surfaces $(\mathscr{S}_5)$ and $(\mathscr{S}_6)$ have a 2–order contact point at r. We shall prove this claim by showing that each one of the surfaces $(\mathscr{S}_5)$ and $(\mathscr{S}_6)$ remains on only one of the half–spaces delimited by the plane $(\mathscr{S}_1)$ and their unique common point is r. Indeed, it is easy to see that the point r is a common point of the three surfaces. By applying the change of coordinates given by $n = (v + km + k^2)/4$, $v \in \mathbb{R}$, as in the proof of Lemma 5.4.5, we see that the surface $(\mathscr{S}_6)$ remains on only one of the two topological subspaces delimited by the plane $(\mathscr{S}_1)$. On the other hand, numerical calculations show us that the surface $(\mathscr{S}_5)$ is zero valued around the point r and it assumes negative values otherwise, showing that $(\mathscr{S}_5)$ remains on the other half–space delimited by the plane $(\mathscr{S}_1)$. ∎

Lemma 5.4.10. *The curve $r(k) = (-3\sqrt[3]{k}/2, 2 - 3\sqrt[3]{k^2}, k)$ of $(\mathscr{S}_5)$ (i.e. its set of singularities) cannot belong to the part where $W_4 > 0$ and $\mu < 0$.*

Proof. We consider the real continuous function $g = (\mu W_4)\big|_{r(k)} = \left(\sqrt[3]{k^2} - 2\right)^6 \left(\sqrt[3]{k^2} + 6\right) \sqrt[3]{k^4}$, whose zeroes are 0 and $2\sqrt{2}$. It is easy to see that g is always positive in $(0, 2\sqrt{2}) \cup (2\sqrt{2}, \infty)$, implying that the functions μ and W_4 calculated at $r(k)$ cannot have different signs, proving the lemma. ∎

Now we shall study the bifurcation diagram having as reference the values of k where significant phenomena occur in the behavior of the bifurcation surfaces.

According to Remark 5.4.8, these values are $k = 0$ and $k = 2\sqrt{2}$. So, we only need to add two more slices with some intermediate values.

We take, then, the values:

$$\begin{aligned} k_0 &= 0, & k_1 &= 1, \\ k_2 &= 2\sqrt{2}, & k_3 &= 3. \end{aligned} \tag{5.4.1}$$

The values indexed by positive even indices correspond to explicit values of k for which there is a bifurcation in the behavior of the systems on the slices. Those indexed by odd ones are just intermediate points (see Figures 5.3 to 5.6).

Notation 5.4.11. *We now describe the labels used for each part of the bifurcation space. The subsets of dimensions 3, 2, 1 and 0, of the partition of the parameter space will be denoted respectively*

by V, S, L and P for Volume, Surface, Line and Point, respectively. The surfaces are named using a number which corresponds to each bifurcation surface which is placed on the left side of the letter S. To describe the portion of the surface we place an index. The curves that are intersection of surfaces are named by using their corresponding numbers on the left side of the letter L, separated by a point. To describe the segment of the curve we place an index. Volumes and Points are simply indexed (since three or more surfaces may be involved in such an intersection).

We consider an example: the surface ($\mathscr{S}_1$) *splits into 5 different two–dimensional parts labeled from* $1S_1$ *to* $1S_5$*, plus some one–dimensional arcs labeled as* $1.iL_j$ *(where* i *denotes the other surface intersected by* ($\mathscr{S}_1$) *and* j *is a number), and some zero–dimensional parts. In order to simplify the labels in Figures 5.10 to 5.13 we see* ***V1*** *which stands for the TEX notation* V_1*. Analogously,* ***1S1*** *(respectively,* ***1.2L1****) stands for* $1S_1$ *(respectively,* $1.2L_1$*). And the same happens with many other pictures.*

Some bifurcation surfaces intersect on $k = 0$ or have singularities there. The restrictions of the surfaces on $k = 0$ are: the surface ($\mathscr{S}_5$) has a singularity at the point $(0,2,0)$ and it is the union of a parabola and a straight line of multiplicity two, which in turn coincides with the bifurcation surface ($\mathscr{S}_6$); the surface ($\mathscr{S}_1$) coincides with the horizontal axis and the bifurcation surface ($\mathscr{S}_3$) becomes a straight line parallel to the horizontal line having intersection points only with the surface ($\mathscr{S}_5$).

As an exact drawing of the curves produced by intersecting the surfaces with slices gives us very small parts which are difficult to distinguish, and points of tangency are almost impossible to recognize, we have produced topologically equivalent figures where parts are enlarged and tangencies are easy to observe. The reader may find the exact pictures in the web page http://mat.uab.es/~artes/articles/qvftn/qvftn.html.

As we increase the value of k, other changes in the bifurcation diagram happen. When $k = 1$, the surface ($\mathscr{S}_5$) has two connected components and a cusp point as a singularity which remains on the left side of the surface ($\mathscr{S}_6$) until $k = 2\sqrt{2}$ (see Figure 5.4). At this value, the cusp point is the point of contact among all the surfaces, as we can see in Figure 5.5, and when $k = 3$, the cusp point of ($\mathscr{S}_5$) lies on the right side of surfaces ($\mathscr{S}_6$) and ($\mathscr{S}_1$) (see Figure 5.6 and Lemma 5.4.10). In order to comprehend that the "movement" of the cusp point of the surface ($\mathscr{S}_5$) implies changes that occur in the bifurcation diagram, we see that when $k = 1$ we have a "curved triangular" part formed by the surfaces ($\mathscr{S}_3$) and ($\mathscr{S}_5$), the cusp point of ($\mathscr{S}_5$) and the points of intersection between both surfaces. The "triangle" bounded by these elements yields 15 subsets: three 3−dimensional

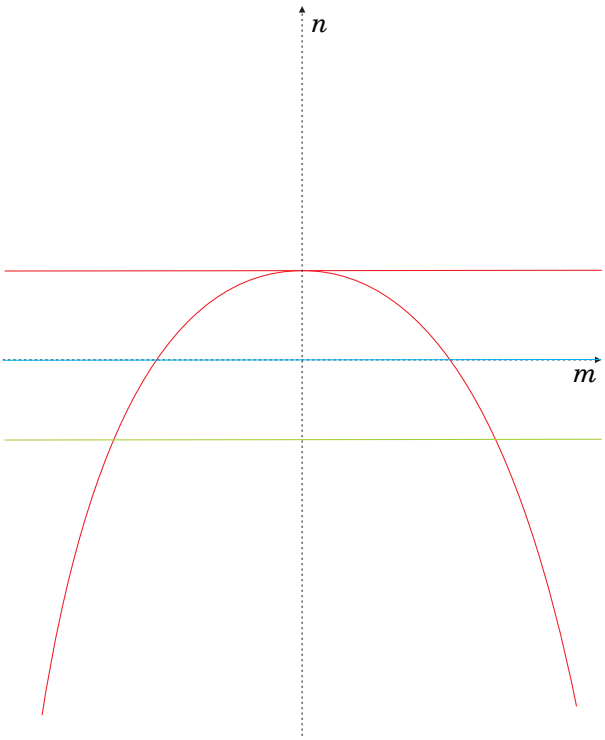

Figure 5.3: Slice of the parameter space when $k = 0$

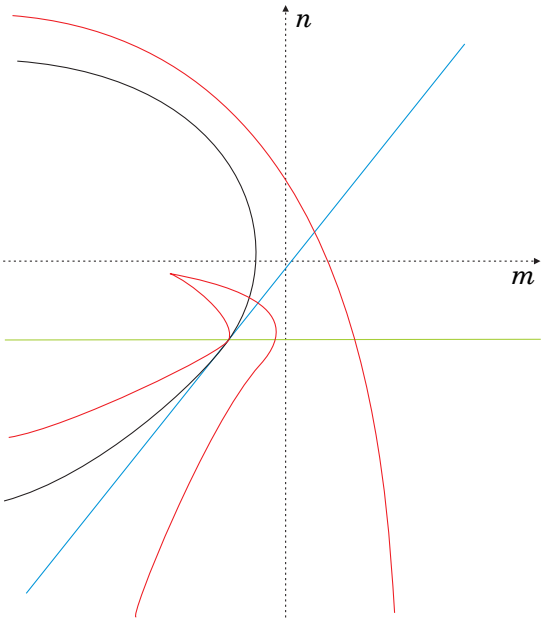

Figure 5.4: Slice of the parameter space when $k = 1$

subsets, seven 2−dimensional ones and five 1−dimensional ones. In Figure 5.5 we see that the "triangle" has disappeared and it has become a unique point which corresponds to the point of contact of all the surfaces and the cusp point of surface $(\mathscr{S}_5)$. Finally, when $k = 3$, the "triangle" reappears and yields also 15 subsets of same dimensions, but different from the previous ones.

All other parts of the parameter space related to singular points remain topologically the same with respect to the algebraic bifurcations of singularities when moving from Figures 5.4 to 5.6.

We recall that the black curve $(\mathscr{S}_6)$ (or W_4) means the turning of a finite antisaddle different from the triple node from a node into a focus. Then, according to general results about quadratic systems in Section 1.5, we could have limit cycles around such focus for any set of parameters having $W_4 < 0$.

Remark 5.4.12. *Wherever two parts of equal dimension d are separated only by a part of dimension $d-1$ of the black bifurcation surface $(\mathscr{S}_6)$, their respective phase portraits are topologically equivalent since the only difference between them is that a finite antisaddle has turned into a focus without change of stability and without appearance of limit cycles. We denote such parts with different labels, but we do not give specific phase portraits in pictures attached to Theorem 5.2.1*

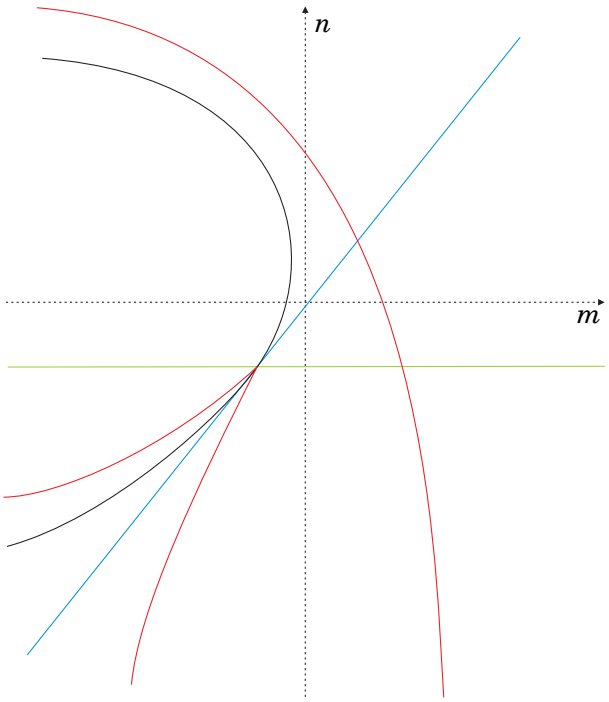

Figure 5.5: Slice of the parameter space when $k = 2\sqrt{2}$

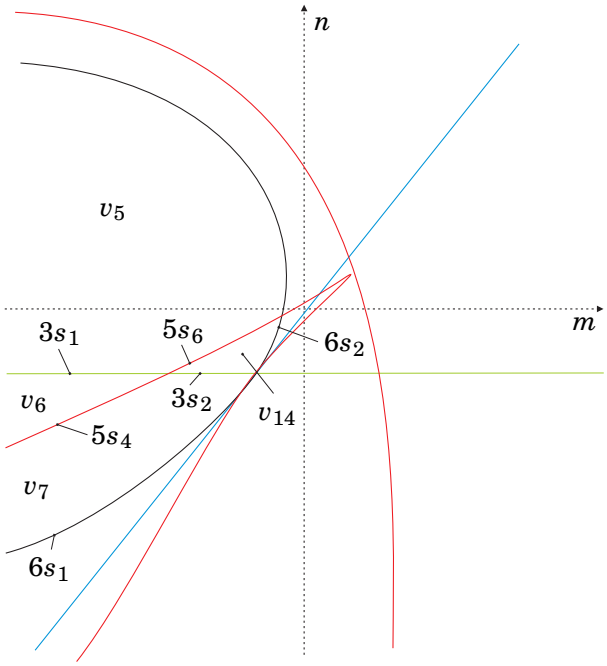

Figure 5.6: Slice of the parameter space when $k = 3$

for the parts with the focus. We only give portraits for the parts with nodes, except in the case of existence of a limit cycle or a graphic where the singular point inside them is portrayed as a focus. Neither do we give specific invariant description in Section 5.5 distinguishing between these nodes and foci.

5.4.2 Bifurcation surfaces due to connections

We now place for each set of the partition on $k = 3$ the local behavior of the flow around all the singular points. For a specific value of parameters of each one of the sets in this partition we compute the global phase portrait with the numerical program P4 [3, 27]. In fact, many (but not all) of the phase portraits in this work can be obtained not only numerically but also by means of perturbations of the systems of codimension one.

In this slice we have a partition in 2−dimensional parts bordered by curved polygons, some of them bounded, others bordered by infinity. From now on, we use lower–case letters provisionally to describe the sets found algebraically so not to interfere with the final partition described with capital letters.

For each 2−dimensional part we obtain a phase portrait which is coherent with those of all

their borders. Except one part. Consider the segment $3s_1$ in Figure 5.6. On it we have a weak focus and a Hopf bifurcation. This means that either in v_5 or v_6 we must have a limit cycle. In fact it is in v_6. The same happens in $3s_2$, so a limit cycle must exist either in v_{14} or v_7. However, when approaching $6s_1$ or $6s_2$, this limit cycle must have disappeared. So, either v_7 or v_{14} must be split in two parts separated by a new surface ($\mathscr{S}_7$) having at least one element $7S_1$ such that one part has limit cycle and the other does not, and the border $7S_1$ must correspond to a connection between separatrices. Numerically it can be checked that it is the part v_7 the one which splits in V_7 without limit cycles and V_{15} with one limit cycle. It can also be analytically proved (see Proposition 5.4.13) that the segment $5s_4$ must be split in two segments $5S_4$ and $5S_5$ by the 1–dimensional subset $5.7L_1$. The other border of $7S_1$ must be $1.3L_1$ for coherence. We plot the complete bifurcation diagram in Figure 5.13. We also show the sequence of phase portraits along these subsets in Figure 5.7.

Notice that the limit cycle which is "born" by Hopf on $3S_1$ either "dies" on $5S_4$ or "survives" when crossing $\eta = 0$, if we do it through $5S_5$, and then it "dies" either on $7S_1$ or again by Hopf in $3S_2$.

Surface ($\mathscr{S}_7$), for a concrete $k > 2\sqrt{2}$, is a curve which starts on $1.3L_1$ and may either cut $5s_4$, or not. We are going to prove that, at least for a concrete k_0, ($\mathscr{S}_7$) must cut it, and consequently it must do the same for an open interval around k_0, thus proving the existence of subsets $5S_4$, $5S_5$ and $5.7L_1$ which have different phase portraits.

Proposition 5.4.13. *The following statements hold:*

(i) System (5.3.1) *with* $(m,n,k) = (-29/2, -105/4, 7)$ *has an even number of limit cycles (counting their multiplicities), and possibly this number is zero;*

(ii) System (5.3.1) *with* $(m,n,k) = (-49/2, -185/4, 12)$ *has an odd number of limit cycles (counting their multiplicities), and possibly this number is one;*

Proof. *(i)* We see that the system with rational coefficients

$$\dot{x} = 2xy + 7y^2, \quad \dot{y} = y - x^2 - 29xy - \frac{105}{4}y^2 \tag{5.4.2}$$

is a representative of the red surface ($\mathscr{S}_5$) which belongs to the subset $5s_4$.

We have to show that there exists a hyperbola

$$\mathscr{H} \equiv ax^2 + bxy + y^2 + dx + ey + f = 0$$

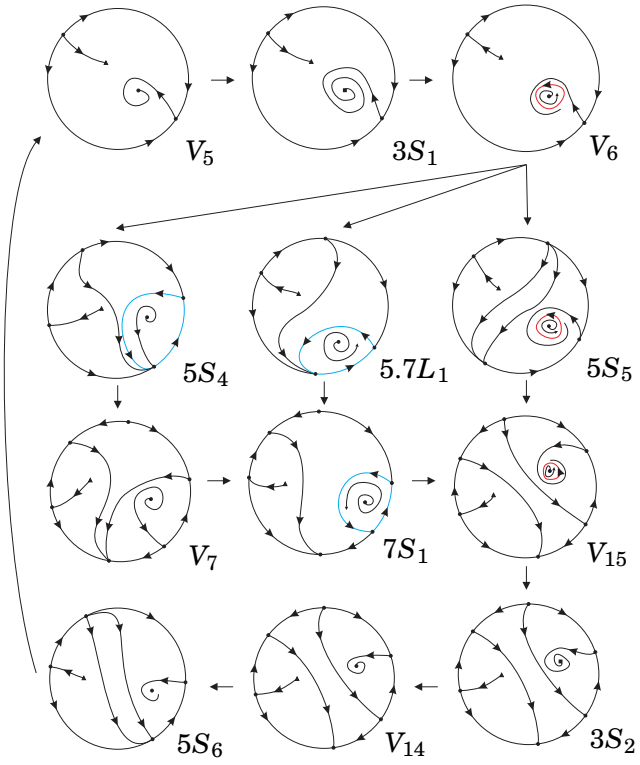

Figure 5.7: Sequence of phase portraits in slice $k = 3$. We start from v_5. We recall that the phase portrait $3S_1$ is equivalent to the phase portrait V_5 up to a weak focus (represented by a little black square) in place of the focus. When crossing $3s_1$, we shall obtain the phase portrait V_6 in subset v_6. From this point we may choose three different ways to reach the subset v_7 by crossing $5s_4$: (1) from the phase portrait $5S_4$ to the V_7; (2) from the phase portrait $5.7L_1$ to the $7S_1$; and (3) from the phase portrait $5S_5$ to the V_{15}, from where we can move to V_{14}. Finally, from V_{14} we can pass through $5S_6$ and reach V_5

which isolates the focus of (5.4.2) on the region where $\mathscr{H} < 0$ and $x > 0$, and with the property that at each of its points the flow crosses the hyperbola in only one direction, as we can see in Figure 5.8. By proving the existence of this hyperbola, we shall prove that (5.4.2) has an even number of limit cycles.

For convenience and making easier the calculations, we impose that the hyperbola passes through two infinite singular points of (5.4.2) with the same tangencies of the affine separatrices. With all these features we have just one free parameter which is used to force the hyperbola to pass through a concrete finite point. In resume, we take $a = 1/14$, $b = 57/28$,

$$d = \frac{1}{392}\left(\sqrt{148225e^2+1}+399e-1\right), \quad f = \frac{e^2-28de+e\sqrt{(28d-e)^2}}{1516\sqrt{(28d-e)^2}-110}$$

and $e = -324/10000$.

This hyperbola has a component fully included in the fourth quadrant and it is easy to check

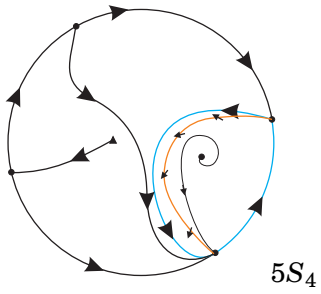

Figure 5.8: The hyperbola in the phase portrait of $5S_4$

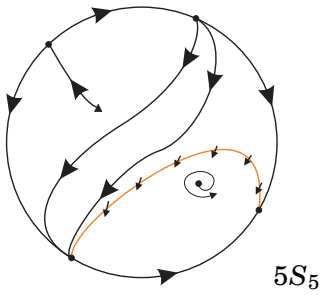

Figure 5.9: The hyperbola in the phase portrait of $5S_5$

that the scalar product of its tangent vector with the flow of the vector field does not change its sign and the flow moves outwards the region $\mathscr{H} < 0$. Since the focus is repellor, this is consistent with the absence of limit cycles (or with an even number of them, counting their multiplicities).

(ii) We see that the system with rational coefficients

$$\dot{x} = 2xy + 12y^2, \quad \dot{y} = y - x^2 - 49xy - \frac{185}{4}y^2 \tag{5.4.3}$$

is a representative of the red surface ($\mathscr{S}_5$) which belongs to the subset $5s_4$.

Analogously, we have to show that there exists a hyperbola $\mathscr{H} \equiv ax^2 + bxy + y^2 + dx + ey + f = 0$ which isolates the focus of (5.4.3) on the region where $\mathscr{H} < 0$ and $x > 0$, and with the property that at each of its points the flow crosses the hyperbola in only one direction, as we can see in Figure 5.9. By proving the existence of this hyperbola, we shall prove that (5.4.3) has an odd number of limit cycles.

By using the same technique as before, we take $a = 1/24$, $b = 97/48$,

$$d = \frac{1}{1152}\left(\sqrt{1299600e^2 + 1} + 1164e - 1\right), \quad f = \frac{e^2 - 48de + e\sqrt{(48d - e)^2}}{4516\sqrt{(48d - e)^2} - 190}$$

and $e = -18663/100000$.

This hyperbola has a component fully included in the fourth quadrant and it is easy to check that the scalar product of its tangent vector with the flow of the vector field does not change its sign and the flow moves inwards the region $\mathscr{H} < 0$. Since the focus is repellor, this is consistent with the presence of one limit cycle (or with an odd number of them, counting their multiplicities). ∎

Remark 5.4.14. *We cannot be sure that this is all the additional bifurcation curves in this slice. There could exist others which are closed curves which are small enough to escape our numerical research. For all other two–dimensional parts of the partition of this slice whenever we join two points which are close to two different borders of the part, the two phase portraits are topologically equivalent. So we do not encounter more situations than the one mentioned above.*

As we vary k in $(2\sqrt{2},\infty)$, the numerical research shows us the existence of the phenomenon just described, but for the values of k in $[0,2\sqrt{2})$, we have not found the same behavior.

In Figures 5.10 to 5.13 we show the complete bifurcation diagrams. In these figures, we have colored in light yellow the parts with one limit cycle. In Section 5.5 the reader can look for the topological equivalences among the phase portraits appearing in the various parts and the selected notation for their representatives in Figure 5.1.

5.4.3 Other relevant facts about the bifurcation diagram

The bifurcation diagram we have obtained for $\mathbf{QT\overline{N}}$ is completely coherent. By this, we mean that if we take any two points in the parameter space and join them by a continuous curve, along this curve the changes in phase portraits that occur when crossing the different bifurcation surfaces we mention can be completely explained.

However, we cannot be sure that this bifurcation diagram is the complete bifurcation diagram for $\mathbf{QT\overline{N}}$ due to the possibility of "*islands*" inside the parts bordered by unmentioned bifurcation surfaces. In case they exist, these "islands" would not mean any modification of the nature of the singular points. So, on the border of these "islands" we could only have bifurcations due to saddle connections or multiple limit cycles.

In case there were more bifurcation surfaces, we should still be able to join two representatives of any two parts of the 63 parts found until now with a continuous curve either without crossing such bifurcation surface or, in case the curve crosses it, it must do it an even number of times

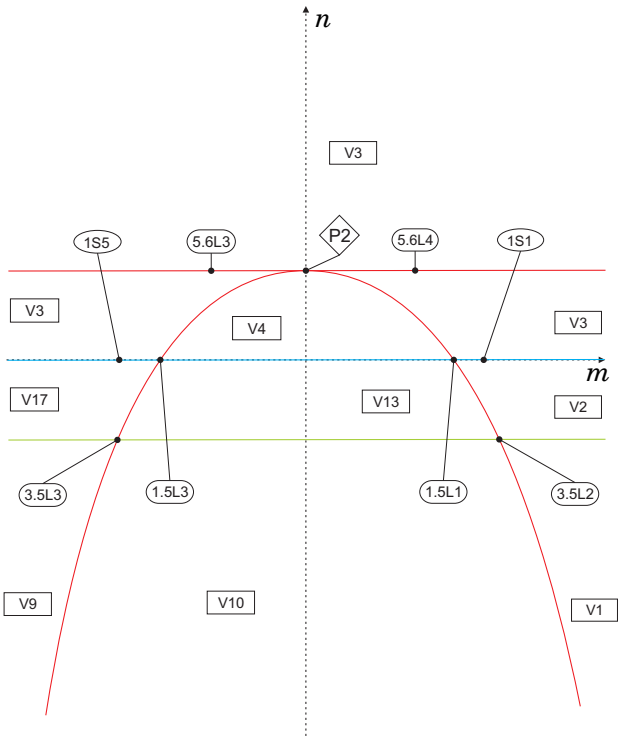

Figure 5.10: Complete bifurcation diagram for slice $k = 0$

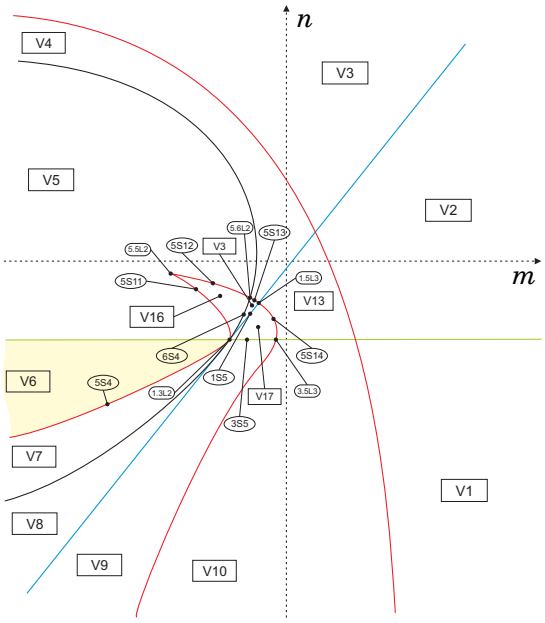

Figure 5.11: Complete bifurcation diagram for slice $k = 1$

without tangencies, otherwise one must take into account the multiplicity of the tangency, so the total number must be even. This is why we call these potential bifurcation surfaces "islands".

To give an example of such a potential "island", we consider part V_1 where we have a phase portrait having a finite antisaddle, a saddle and two pairs of infinite antisaddles and one pair of infinite saddles. This phase portrait is topologically equivalent (modulo limit cycles and associating to the triple node a simple antisaddle) with the phase portrait 9.1 from [4] where all structurally stable quadratic vector fields were studied, (see the first phase portrait of Figure 5.14).

We note that in [4] it is proved that structurally stable (modulo limit cycles) quadratic vector fields can have exactly 44 different phase portraits. In the case of system (5.3.1), we have a semi–elemental triple node which topologically behaves like an elemental node, and the phase portraits in generic parts on the bifurcation diagram will look like structurally stable ones. From those 44, two have no singular points, one has no finite antisaddles and 33 have four finite singular points, so obviously they cannot appear in $\mathbf{QT\overline{N}}$. From the remaining 8, only 7 appear in our description of $\mathbf{QT\overline{N}}$. There are two potential reasons for the absence of the remaining case: (1) it cannot be realized within $\mathbf{QT\overline{N}}$, or (2) it may live in such "islands" where the conditions for the singular

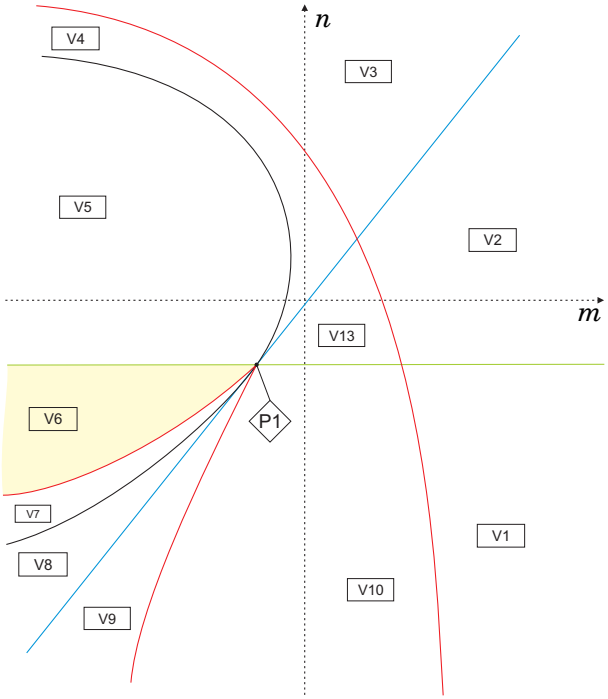

Figure 5.12: Complete bifurcation diagram for slice $k = 2\sqrt{2}$

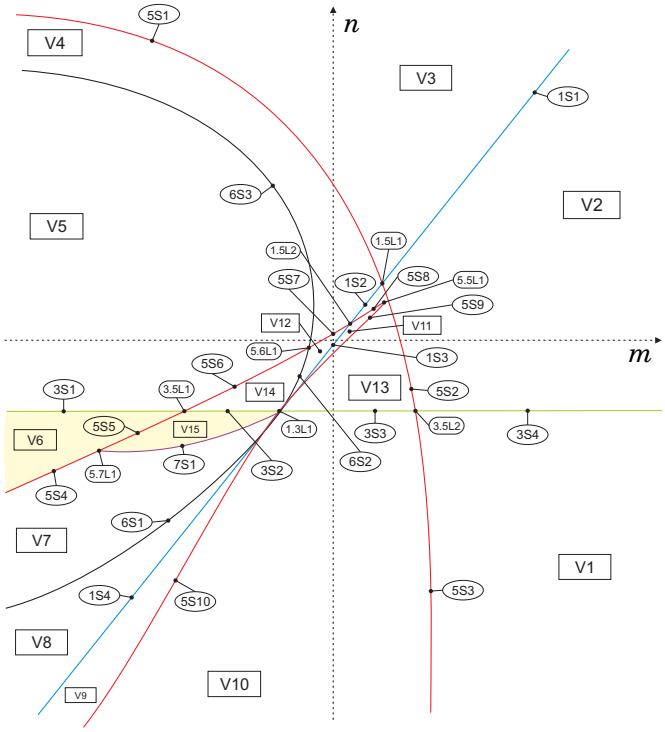

Figure 5.13: Complete bifurcation diagram for slice $k = 3$

points are met, but the separatrix configuration is not the one that we have detected as needed for the coherence.

For example, the structurally stable phase portrait 9.2 has so far not appeared anywhere, but it could perfectly lie inside an "island" of V_1 (or V_{11}) where we have phase portrait 9.1. The transition from 9.1 to 9.2 consists in the existence of a heteroclinic connection between the finite saddle and one of the infinite saddles as it can be seen in Figure 5.14. We also show (in the middle of this figure) the unstable phase portrait from which could bifurcate and also has the potential to be on the bifurcation surface delimiting the "island".

5.5 Completion of the proof of the main theorem

In the bifurcation diagram we may have topologically equivalent phase portraits belonging to distinct parts of the parameter space. As here we have 63 distinct parts of the parameter space, to help us identify or to distinguish phase portraits, we need to introduce some invariants and we actually choose integer–valued invariants. All of them were already used in [39, 6]. These integer–valued invariants yield a classification which is easier to grasp.

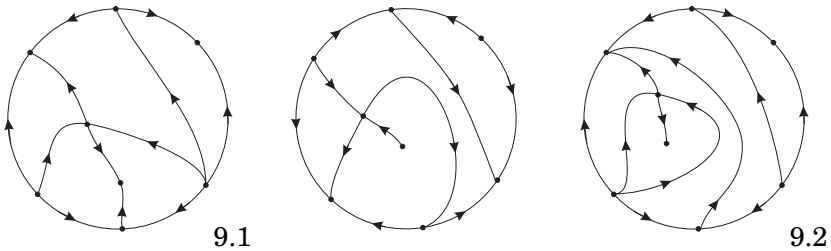

Figure 5.14: Example of a potential "island" in the bifurcation diagram of family $\mathbf{QT\overline{N}}$

Definition 5.5.1. *[6] We denote by $I_1(S)$ the number of the real finite singular points.*

Definition 5.5.2. *[6] We denote by $I_2(S)$ the sum of the indices of the real finite singular points.*

Definition 5.5.3. *[6] We denote by $I_3(S)$ the number of the real infinite singular points.*

Definition 5.5.4. *For a given infinite singularity s of a system S, let ℓ_s be the number of global or local separatrices beginning or ending at s and which do not lie on the line at infinity. We have $0 \leq \ell_s \leq 4$. We denote by $I_4(S)$ the sequence of all such ℓ_s when s moves in the set of infinite singular points of the system S.*

In our case we have used the clockwise sense beginning from the top–most infinite singular point in the pictures shown in Figure 5.1.

Definition 5.5.5. *We denote by $I_5(S)$ a digit which gives the number of limit cycles.*

As we have noted previously in Remark 5.4.12, we do not distinguish between phase portraits whose only difference is that in one we have a finite node and in the other a focus. Both phase portraits are topologically equivalent and they can only be distinguished within the C^1 class. In case we may want to distinguish between them, a new invariant may easily be introduced.

Theorem 5.5.6. *Consider the family $\mathbf{QT\overline{N}}$ of all quadratic systems with a semi–elemental triple node. Consider now all the phase portraits that we have obtained for this family. The values of the affine invariant $\mathcal{I} = (I_1, I_2, I_3, I_4, I_5)$ given in the following diagram yield a partition of these phase portraits of the family $\mathbf{QT\overline{N}}$.*

Furthermore, for each value of $\mathcal{I}$ in this diagram there corresponds a single phase portrait; i.e. S and S' are such that $I(S) = I(S')$, if and only if S and S' are topologically equivalent.

The bifurcation diagram for $\mathbf{QT\overline{N}}$ has 63 parts which produces 28 topologically different phase portraits as described in Table 5.5.1. The remaining 35 parts do not produce any new phase

portrait which was not included in the 28 previous. The difference is basically the presence of a strong focus instead of a node and vice versa.

The phase portraits having neither limit cycle nor graphic have been denoted surrounded by parenthesis, for example (V_1); the phase portraits having one limit cycle have been denoted surrounded by brackets, for example $[V_6]$; the phase portraits having one graphic have been denoted surrounded by {}, for example $\{5S_4\}$.

Proof of Theorem 5.5.6. The above result follows from the results in the previous sections and a careful analysis of the bifurcation diagrams given in Section 5.4, in Figures 5.10 to 5.13, the definition of the invariants I_j and their explicit values for the corresponding phase portraits. ■

We first make some observations regarding the equivalence relations used in this study: the affine and time rescaling, C^1 and topological equivalences.

The coarsest one among these three is the topological equivalence and the finest is the affine equivalence. We can have two systems which are topologically equivalent but not C^1-equivalent. For example, we could have a system with a finite antisaddle which is a structurally stable node and in another system with a focus, the two systems being topologically equivalent but belonging to distinct C^1-equivalence classes, separated by a surface ($\mathscr{S}_6$ in this case) on which the node turns into a focus.

In Table 5.5.2 we listed in the first column 28 parts with all the distinct phase portraits of Figure 5.1. Corresponding to each part listed in column 1 we have in its horizontal block, all parts whose phase portraits are topologically equivalent to the phase portrait appearing in column 1 of the same horizontal block.

In the second column we have put all the parts whose systems yield topologically equivalent phase portraits to those in the first column but which may have some algebro–geometric features related to the position of the orbits.

In the third (respectively, fourth, and fifth) column we list all parts whose phase portraits have another antisaddle which is a focus (respectively, a node which is at a bifurcation point producing foci close to the node in perturbations, a node–focus to shorten, and a finite weak singular point).

Whenever phase portraits appear on a horizontal block in a specific column, the listing is done according to the decreasing dimension of the parts where they appear, always placing the lower dimensions on lower lines.

Table 5.5.1: Geometric classification for the family $\mathbf{QT\overline{N}}$

$$
I_1 = \left\{
\begin{array}{l}
2 \;\&\; I_2 = \left\{
\begin{array}{l}
2 \;\&\; I_3 = \left\{
\begin{array}{l}
3 \;\&\; I_4 = \left\{
\begin{array}{l}
110110\,(V_3),\\
112110\,(V_7),\\
111111 \;\&\; I_5 = \left\{ \begin{array}{l} 1\,[V_{15}],\\ 0\,(V_{12}), \end{array} \right.\\
110111\,\{7S_1\},
\end{array} \right.\\
2 \;\&\; I_4 = \left\{
\begin{array}{l}
1212 \;\&\; I_5 = \left\{ \begin{array}{l} 1\,[5S_5],\\ 0\,(5S_6), \end{array} \right.\\
1111\,(5S_1),\\
1131\,\{5S_4\},\\
1122\,(5S_{10}),\\
1121\,\{5.7L_1\},
\end{array} \right.\\
1 \;\&\; I_4 = \left\{ 11 \;\&\; I_5 = \left\{ \begin{array}{l} 1\,[V_6],\\ 0\,(V_4), \end{array} \right. \right.
\end{array} \right.\\
0 \;\&\; I_3 = \left\{
\begin{array}{l}
3 \;\&\; I_4 = \left\{ \begin{array}{l} 111201\,(V_1),\\ 101311\,(V_{11}), \end{array} \right.\\
2 \;\&\; I_4 = \left\{ \begin{array}{l} 1122\,(5S_2),\\ 2041\,(5S_8),\\ 1132\,(5S_9), \end{array} \right.\\
1\,(V_{10}),
\end{array} \right.
\end{array} \right.\\
1 \;\&\; I_2 = \left\{
\begin{array}{l}
1 \;\&\; I_3 = \left\{
\begin{array}{l}
3 \;\&\; I_4 = \left\{ \begin{array}{l} 110110\,(1S_1),\\ 102110\,(1S_4),\\ 101111\,(1S_3), \end{array} \right.\\
2 \;\&\; I_4 = \left\{ \begin{array}{l} 1200\,(1.3L_1),\\ 1011\,\{1.3L_2\},\\ 1111\,(1.5L_1),\\ 1202\,(1.5L_2), \end{array} \right.\\
1 \;\&\; I_4 = \left\{ \begin{array}{l} 10\,(1S_2),\\ 21\,(P_1). \end{array} \right.
\end{array} \right.
\end{array} \right.
\end{array} \right.
$$

Table 5.5.2: Topological equivalences for the family $\mathbf{QT\overline{N}}$

Presented phase portrait	Identical under perturbations	Finite antisaddle focus	Finite antisaddle node–focus	Finite weak point
V_1	V_2, V_9, V_{17}			$3S_4$, $3S_5$
V_3		V_{16}	$6S_4$	
V_4	P_2	V_5, $5.5L_2$	$6S_3$	$3S_1$
V_6				
V_8		V_7	$6S_1$	
V_{10}	V_{13}, $5.5L_1$			$3S_3$
V_{11}				
V_{12}		V_{14}	$6S_2$	$3S_2$
V_{15}				
$1S_1$	$1S_5$			
$1S_2$				
$1S_3$				
$1S_4$				
$5S_1$	$5S_{13}$	$5S_{11}$, $5S_{12}$	$5.6L_2$, $5.6L_3$, $5.6L_4$	
$5S_2$	$5S_3$, $5S_{14}$			$3.5L_2$, $3.5L_3$
$5S_4$				
$5S_5$				
$5S_7$		$5S_6$	$5.6L_1$	$3.5L_1$
$5S_8$				
$5S_9$				
$5S_{10}$				
$7S_1$				
$1.3L_1$				
$1.3L_2$				
$1.5L_1$	$1.5L_3$			
$1.5L_2$				
$5.7L_1$				
P_1				

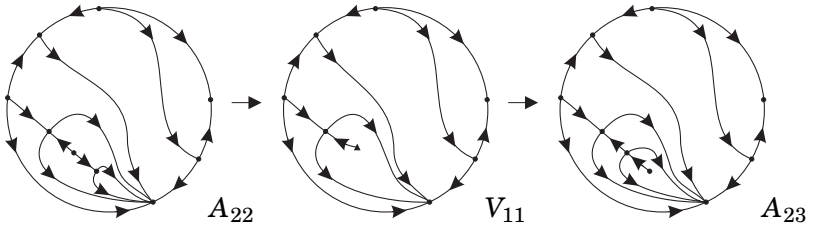

Figure 5.15: The perturbations of phase portrait V_{11} yielding the structurally unstable phase portraits A_{22} and A_{23}

5.5.1 Proof of the main theorem

The bifurcation diagram described in Section 5.4, plus Table 5.5.1 of the geometrical invariants distinguishing the 28 phase portraits, plus Table 5.5.2 giving the equivalences with the remaining phase portraits lead to the proof of the main statement of Theorem 5.2.1.

In [5] the authors are studying all phase portraits of quadratic systems having exactly one saddle–node or one connection of separatrices. By using a similar technique as the one used in [4] for the structurally stable ones, they have produced a complete list of topologically possible structurally unstable systems of codimension one (modulo limit cycles), they have erased many of them proving their impossibility and they have proved the existence of many others (180 just before this work is published), and it remains 24 which escape up to now both the proof of their impossibility and finding an example.

In the family $\mathbf{QT\overline{N}}$, system V_{11} yields an example of their "wanted" case A_{23}. Indeed, by adding a small perturbation of the form εx^2 in a representative of the part V_{11} we obtain the following system:

$$\begin{aligned} \dot{x} &= 2xy + 10y^2 + \varepsilon x^2, \\ \dot{y} &= y - x^2 - 2(3.7)xy - 14y^2, \end{aligned} \tag{5.5.1}$$

whose finite singularities are a saddle–node, a node and a saddle, and infinite singularities are a node, a saddle and a saddle–node $\overline{\binom{1}{1}}SN$. Depending on how we "split" the triple node of V_{11}, we may obtain two structurally unstable phase portraits, namely $\mathbb{U}^1_{A,22}$ and $\mathbb{U}^1_{A,23}$ as it may be seen in Figure 5.15. Then, Corollary 5.2.3 is proved.

Chapter

6

The topological classification of quadratic differential systems with a finite and an infinite semi–elemental saddle–nodes (A,B)

6.1 Motivation for the study

Recalling what was discussed in Section 5.1, we continue with the attempt of constructing families of quadratic differential systems with codimension greater than one in order to obtain by perturbations all the phase portraits containing elements of codimension one (see Section 5.1 to recall this background). Moreover, we continue classifying the quadratic systems possessing semi–elemental singularities, as discussed in the end of Section 2.2.

Only one phase portrait of quadratic vector fields possessing a semi–elemental triple node can yield a new codimension–one phase portrait after a small perturbation, according to Corollary 5.2.3. See Chapter 5 for details.

However, this single case is not enough to cover all the missing proofs, so that we need to advance and construct new families which could yield more codimension–one phase portraits.

With the intention to demonstrate that we may obtain all these missing phase portraits by perturbation, we propose the study of a whole family of quadratic systems having a finite semi–

elemental saddle–node and an infinite semi–elemental saddle–node $\overline{\binom{0}{2}}SN$. We shall see that this family, denoted by **QsnSN**, can be split into three distinct subfamilies according to the position of the infinite saddle–node. Moreover, we anticipate that one of these three subfamilies yields *all* of the phase portraits of group (A) of codimension–one quadratic systems discussed on page 67.

The study of these three subfamilies will be divided into two chapters (Chapters 6 and 7). In this study we follow the same pattern used in Chapter 5.

6.2 Statement of the results

In this section, we consider the set of all real planar quadratic systems which possess a finite semi–elemental saddle–node $\overline{sn}_{(2)}$ and an infinite semi–elemental saddle–node of type $\overline{\binom{0}{2}}SN$. After the action of the affine group and time homotheties, we may suppose, without loss of generality, that the finite saddle–node is placed at the origin of the plane with the eigenvectors on the axes. We denote this family by **QsnSN**.

The aim of this and the next chapter (Chapters 6 and 7) is studying the class $\overline{\textbf{QsnSN}}$ which is the closure of the set of representatives of **QsnSN** in the parameter space of the specific normal forms which shall be constructed later.

The condition of having a finite saddle–node of all quadratic systems implies that these systems may have up to two other finite singular points.

The family **QsnSN** can be divided into three different subfamilies according to the position of the infinite saddle–node, namely: (A) with the infinite saddle–node in the horizontal axis, (B) with the infinite saddle–node in the vertical axis and (C) with the infinite saddle–node in the bisector of the first and third quadrants. In this chapter we give a partition of the classes $\overline{\textbf{QsnSN(A)}}$ and $\overline{\textbf{QsnSN(B)}}$ according to the normal forms (6.3.1) and (6.3.2). In the normal form (6.3.1), the first class $\overline{\textbf{QsnSN(A)}}$ is partitioned into 85 parts: 23 three–dimensional ones, 37 two–dimensional ones, 20 one–dimensional ones and 5 points. This partition is obtained by considering all the bifurcation surfaces of singularities, one related to the presence of another invariant straight line rather than the one stated in statement *(a)* of Theorem 6.2.1 and one related to connections of separatrices, modulo "islands". In the normal form (6.3.2), the second class $\overline{\textbf{QsnSN(B)}}$ is partitioned into 43 parts: 9 three–dimensional ones, 18 two–dimensional ones, 12 one–dimensional ones and 4 points, which are all delimited by algebraic bifurcation surfaces.

It is worth mentioning that the partitions described above and the number of topological

equivalence classes of phase portraits for each subfamily are due to the choice of a specific normal form. According to Schlomiuk [50], these partitions do not necessarily contain all the phase portraits of the closure within the quadratic class of systems. It may happen that given two different normal forms for a same family, one phase portrait may exist in the closure of one of them but not in the closure of the other. However, the interior of the family in any normal form must contain exactly the same phase portraits.

The results on these two subfamilies can also be found in the paper of Artés, Rezende and Oliveira [10].

Theorem 6.2.1. *There exist* 38 *topologically distinct phase portraits for the closure of the family of quadratic vector fields having a finite saddle–node* $\overline{sn}_{(2)}$ *and an infinite saddle–node of type* $\overline{\binom{0}{2}}SN$ *located in the horizontal axis (the direction defined by the eigenvector with null eigenvalue) and given by the normal form* (6.3.1) *(class* $\overline{\textbf{QsnSN(A)}}$*). The bifurcation diagram for this class is the projective tridimensional space* $\mathbb{RP}^3$*. All these phase portraits are shown in Figures 6.1 and 6.2. Moreover, the following statements hold:*

(a) The manifold defined by the eigenvector with null eigenvalue is always an invariant straight line under the flow;

(b) There exist three phase portraits possessing limit cycle, and they are in the parts V_{11}*,* V_{14} *and* $1S_2$*;*

(c) There exist six phase portraits with nondegenerate graphics, and they are in the parts V_{15}*,* $1S_1$*,* $4S_4$*,* $5S_3$*,* $7S_1$ *and* $1.4L_1$*;*

(d) There exist ten phase portraits with degenerate graphics, and they are in the parts $9S_1$*,* $9S_2$*,* $1.2L_2$*,* $1.9L_1$*,* $5.9L_1$*,* $8.9L_1$*,* P_1*,* P_3*,* P_4 *and* P_5*;*

(e) Any phase portrait of this family can bifurcate from P_1 *of Figure 6.2;*

(f) There exist 29 *topologically distinct phase portraits in* **QsnSN(A)**.

Theorem 6.2.2. *There exist* 25 *topologically distinct phase portraits for the closure of the family of quadratic vector fields having a finite saddle–node* $\overline{sn}_{(2)}$ *and an infinite saddle–node of type* $\overline{\binom{0}{2}}SN$ *located in the vertical axis (direction defined by the eigenvector with non–null eigenvalue) and given by the normal form* (6.3.2) *(class* $\overline{\textbf{QsnSN(B)}}$*). The bifurcation diagram for this class is the projective tridimensional space* $\mathbb{RP}^3$*. All these phase portraits are shown in Fig. 6.3. Moreover, the following statements hold:*

(a) The manifold defined by the eigenvector with non–null eigenvalue is always an invariant straight line under the flow;

(b) There exist four phase portraits with nondegenerate graphic, and they are in the parts $1S_4$, $4S_1$, $1.4L_2$ *and* $1.5L_1$*;*

(c) There exist seven phase portraits with degenerate graphics, and they are in the parts $1.4L_1$, $1.9L_1$, $4.9L_1$, P_1, P_2, P_3 *and* P_5*;*

(d) There exists one phase portrait with a center, and it is in the part $4S_1$*;*

(e) There exists one phase portrait with an integrable saddle, and it is in the part $4S_2$.

(f) Any phase portrait of this family can bifurcate from P_1 *of Figure 6.3;*

(g) There exist 16 *topologically distinct phase portraits in* **QsnSN(B)**.

Corollary 6.2.3. (i) *The phase portrait* $5S_2$ *from family* $\overline{\textbf{QsnSN(A)}}$ *in Figure 6.1 is equivalent to the phase portrait* $5S_3$ *from family* $\overline{\textbf{QsnSN(B)}}$ *in Figure 6.3;*

(ii) *The phase portrait* $1.2L_2$ *from family* $\overline{\textbf{QsnSN(A)}}$ *in Figure 6.2 is equivalent to the phase portrait* $1.4L_1$ *from family* $\overline{\textbf{QsnSN(B)}}$ *in Figure 6.3;*

(iii) *The phase portrait* P_1 *from family* $\overline{\textbf{QsnSN(A)}}$ *in Figure 6.2 is equivalent to the phase portrait* P_1 *from family* $\overline{\textbf{QsnSN(B)}}$ *in Figure 6.3;*

(iv) *The phase portrait* P_3 *from family* $\overline{\textbf{QsnSN(A)}}$ *in Figure 6.2 is equivalent to the phase portrait* P_2 *from family* $\overline{\textbf{QsnSN(B)}}$ *in Figure 6.3.*

For the class **QsnSN(A)**, from its 29 topologically different phase portraits, 9 occur in 3−dimensional parts, 14 in 2−dimensional parts, 5 in 1−dimensional parts and 1 occur in a single 0−dimensional part, and for the class **QsnSN(B)**, from its 16 topologically different phase portraits, 5 occur in 3−dimensional parts, 7 in 2−dimensional parts, 3 in 1−dimensional parts and 1 occur in a single 0−dimensional part.

In Figures 6.1, 6.2 and 6.3 we have denoted all the singular points with a small disk. We have plotted with wide curves the separatrices and we have added some orbits drawn on the picture with thinner lines to avoid confusion in some required cases.

Remark 6.2.4. *It is worth mentioning that a third subclass* $\overline{\textbf{QsnSN(C)}}$ *of* $\overline{\textbf{QsnSN}}$ *must be considered. This subclass consists of planar quadratic systems with a finite saddle–node* $\overline{sn}_{(2)}$ *also situated at the origin (with the eigenvectors in the axes) and an infinite saddle–node of type* $\overline{\binom{0}{2}}SN$ *in the bisector of the first and third quadrants and written in the normal form* (7.3.1)*. This subfamily will be studied in Chapter 7.*

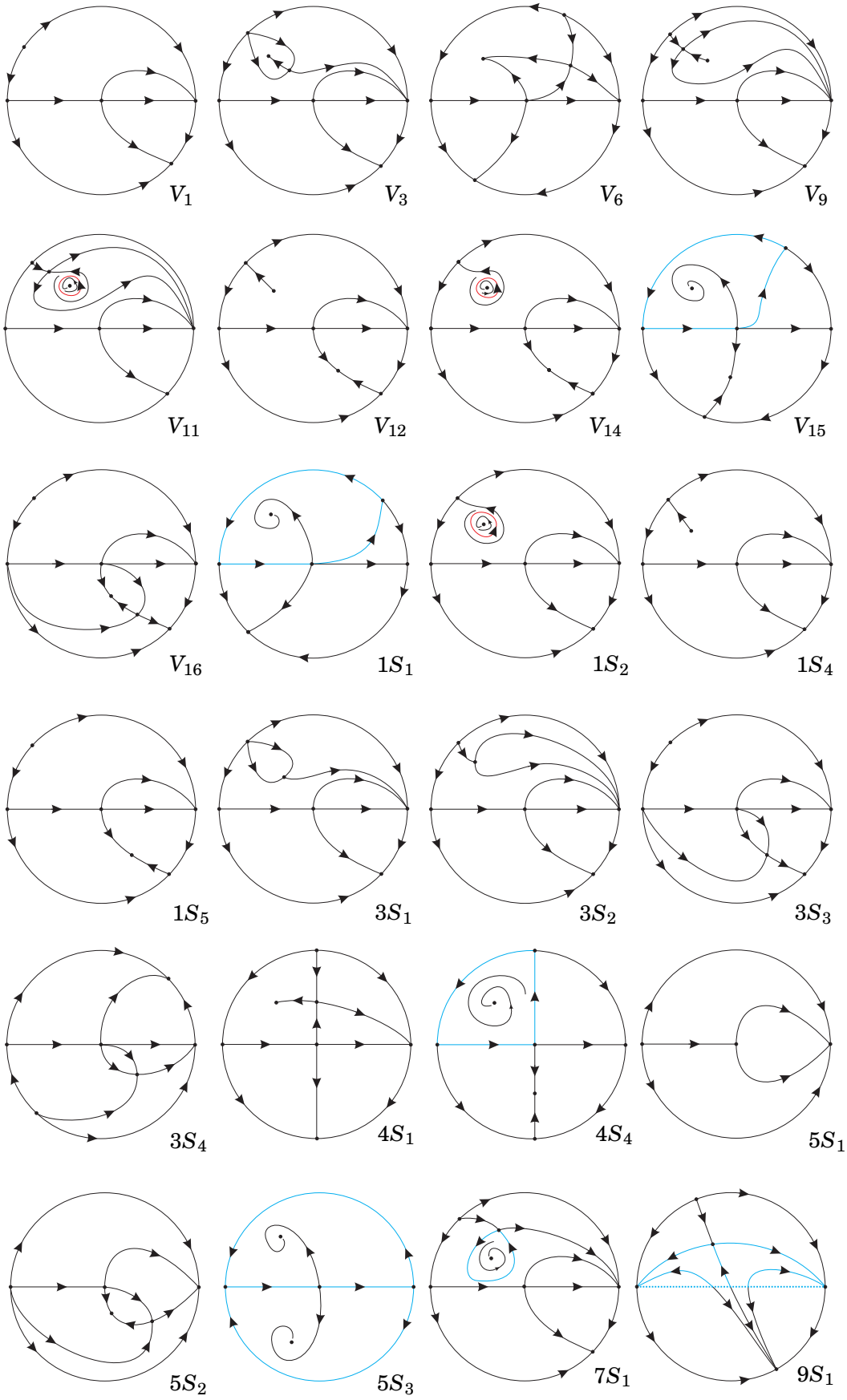

Figure 6.1: Phase portraits for quadratic vector fields with a finite saddle–node $\overline{sn}_{(2)}$ and an infinite saddle–node of type $\binom{0}{2}SN$ in the horizontal axis

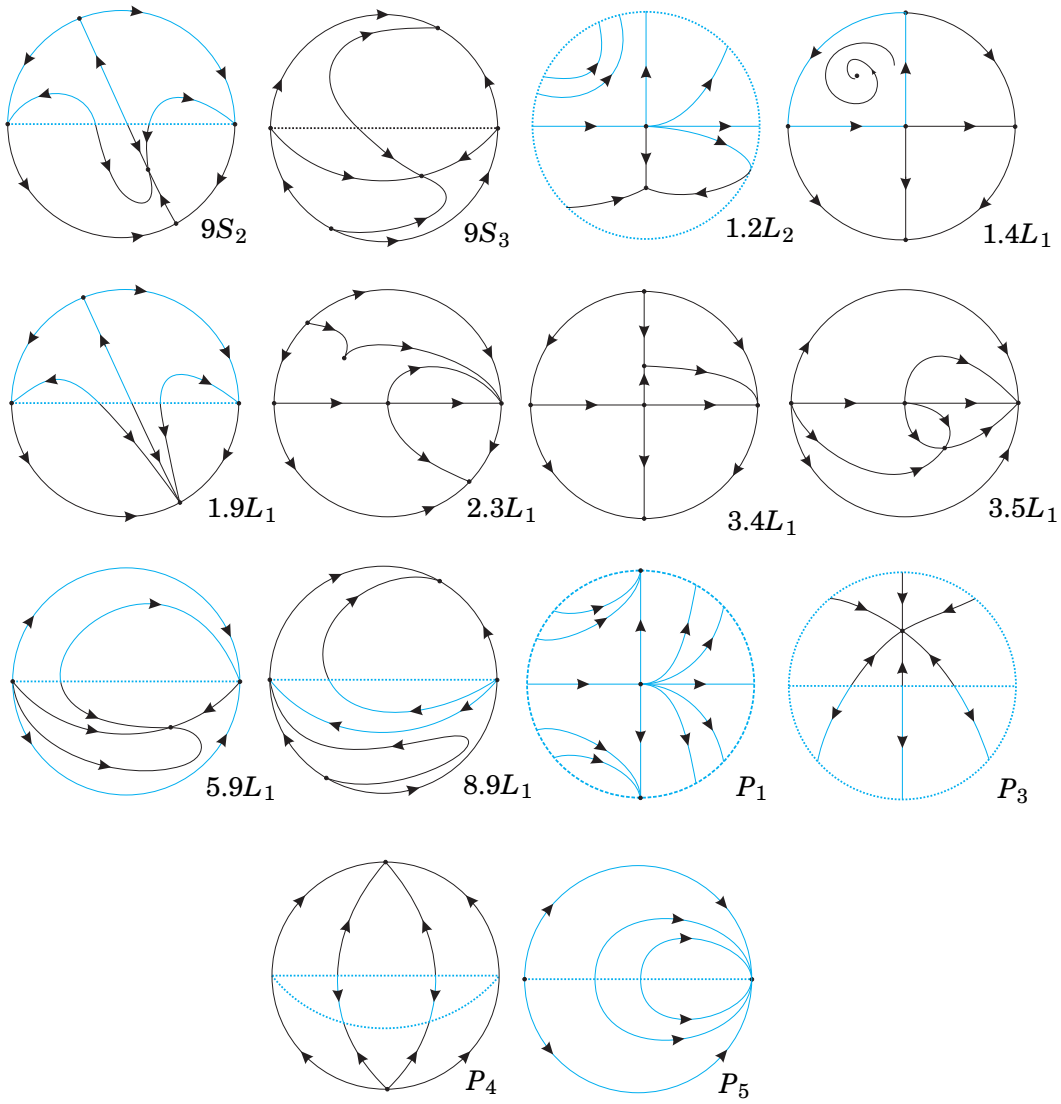

Figure 6.2: Continuation of Figure 6.1

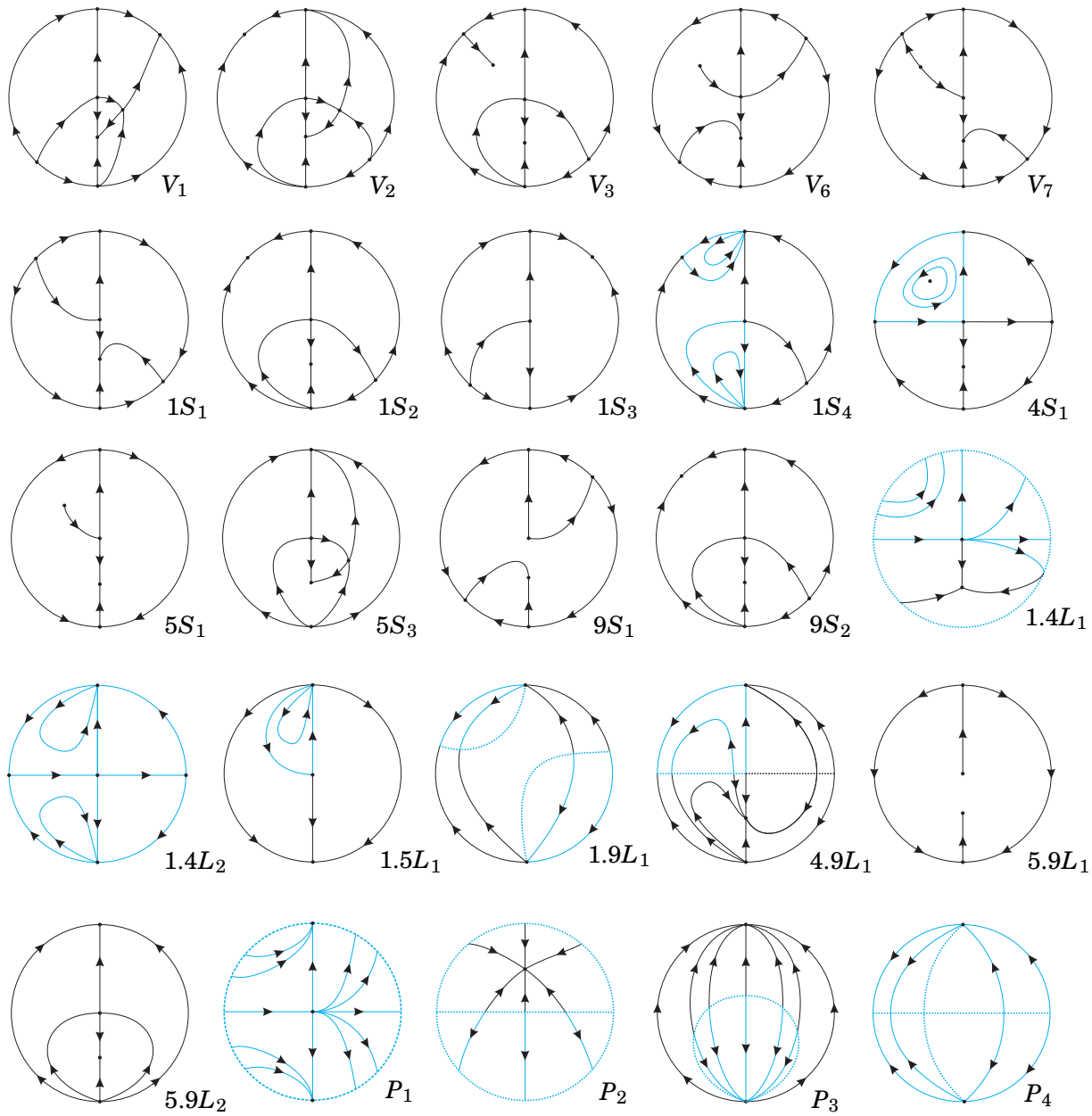

Figure 6.3: Phase portraits for quadratic vector fields with a finite saddle–node $\overline{sn_{(2)}}$ and an infinite saddle–node of type $\binom{0}{2}SN$ in the vertical axis

6.3 Quadratic vector fields with a finite saddle–node $\overline{sn}_{(2)}$ and an infinite saddle–node of type $\overline{\binom{0}{2}}SN$

According to Definition 2.1.1, a singular point r of a planar vector field X in $\mathbb{R}^2$ is semi–elemental, if the determinant of its Jacobian matrix, $\mathrm{D}X(r)$, is zero, but its trace is different from zero.

We recall that in Proposition 2.2.1 (page 23) the normal form of a system possessing a semi–elemental singular point is presented. However, we want this semi–elemental singular point to be a saddle–node.

We note that in the normal form (2.2.2) we already have a semi–elemental point at the origin and its eigenvectors are $(1,0)$ and $(0,1)$ which condition the possible positions of the infinite singular points.

Remark 6.3.1. *We suppose that there exists a $\overline{\binom{0}{2}}SN$ at some point at infinity. If this point is different from either* $[1:0:0]$ *of the local chart U_1, or* $[0:1:0]$ *of the local chart U_2, after a reparametrization of the type $(x,y)\to(x,\alpha y)$, $\alpha\in\mathbb{R}$, this point can be replaced at* $[1:1:0]$ *of the local chart U_1, that is, at the bisector of the first and third quadrants. However, if $\overline{\binom{0}{2}}SN$ is at* $[1:0:0]$ *or* $[0:1:0]$*, we cannot apply this change of coordinates and it requires an independent study for each one of the cases, which are not equivalent due to the position of the infinite saddle–node with respect to the eigenvectors of the finite saddle–node. See Section 3.2 for the notation.*

6.3.1 The normal form adopted for the subclass $\overline{\mathbf{QsnSN(A)}}$

The following result presents the normal form adopted for systems in $\overline{\mathbf{QsnSN(A)}}$.

Proposition 6.3.2. *Every system with a finite semi–elemental double saddle–node $\overline{sn}_{(2)}$ and an infinite saddle–node of type $\overline{\binom{0}{2}}SN$ located in the endpoints of the horizontal axis can be brought via affine transformations and time rescaling to the following normal form*

$$\begin{aligned}\dot{x}&=gx^2+2hxy+ky^2,\\ \dot{y}&=y+gxy+ny^2,\end{aligned}\tag{6.3.1}$$

where g, h, k and n are real parameters and $g\neq 0$.

Proof. We start with system (2.2.2). This system already has a finite semi–elemental saddle–node at the origin (then $g\neq 0$) with its eigenvectors in the direction of the axes. The first step is to

place the point $\overline{\binom{0}{2}}SN$ at the origin of the local chart U_1 with coordinates (w,z). For that, we must guarantee that the origin is a singularity of the flow in U_1,

$$\dot{w} = \ell + (-g+2m)w + (-2h+n)w^2 - kw^3 + wz,$$
$$\dot{z} = (-g-2hw-kw^2)z.$$

Then, we set $\ell = 0$ and, by analyzing the Jacobian of the former expression, we set $m = g/2$ in order to have the eigenvalue associated to the eigenvector on $z = 0$ being null and obtain the normal form (6.3.1). ∎

In order to consider the closure of the family **QsnSN(A)** within the set of representatives of **QsnSN(A)** in the parameter space of the normal form (6.3.1), it is necessary to study the case when $g = 0$, which will be discussed later.

Remark 6.3.3. *We note that* $\{y = 0\}$ *is an invariant straight line under the flow of* (6.3.1).

Systems (6.3.1) depend on the parameter $\lambda = (g,h,k,n) \in \mathbb{R}^4$. We consider systems (6.3.1) which are nonlinear, i.e. $\lambda = (g,h,k,n) \neq 0$. We also consider the affine transformation $X = \alpha x$, $Y = \alpha y$, with $\alpha \neq 0$, and we obtain

$$\dot{X} = \alpha\dot{x} = \alpha(gx^2 + 2hxy + ky^2) = \alpha\left[g\frac{X^2}{\alpha^2} + 2h\frac{XY}{\alpha^2} + k\frac{Y^2}{\alpha^2}\right],$$
$$\dot{Y} = \alpha\dot{y} = \alpha(y + gxy + ny^2) = \alpha\left[\frac{Y}{\alpha} + g\frac{XY}{\alpha^2} + n\frac{Y^2}{\alpha^2}\right].$$

So,

$$\dot{X} = \alpha' gX^2 + 2\alpha' hXY + \alpha' kY^2, \quad \dot{Y} = y + \alpha' gXY + \alpha' nY^2,$$

for $\alpha' = 1/\alpha$, $\alpha \neq 0$.

Then, this transformation takes the system with parameters (g,h,k,n) to a system with parameters $(\alpha' g, \alpha' h, \alpha' k, \alpha' n)$. Hence, instead of considering as parameter space $\mathbb{R}^4$, we may consider $\mathbb{RP}^3$.

But, since for $\alpha' = -1$ all the signs change, we may consider $g \geq 0$ in $[g:h:k:n]$. We now apply the transformation $(x,y,t) \mapsto (-x,y,t)$. This transformation takes the system with parameters (g,h,k,n) to the system with parameters $(-g,h,-k,n)$, which is equivalent to $(g,-h,k,-n)$. So, we may also assume $h \geq 0$.

Since$g \geq 0$ and $g^2+h^2+k^2+n^2 = 1$, then $g = \sqrt{1-(h^2+k^2+n^2)}$, where $0 \leq h^2+k^2+n^2 \leq 1$.

We can therefore view the parameter space as a half–ball $\overline{\mathscr{B}} = \{(h,k,n) \in \mathbb{R}^3; h^2+k^2+n^2 \leq 1, h \geq 0\}$ with base $h=0$ and where two opposite points are identified on the equator. When $h=0$, we identify the point $[g:0:k:n] \in \mathbb{RP}^3$ with $[g:k:n] \in \mathbb{RP}^2$. So, the base of the half–ball $\overline{\mathscr{B}}$ ($h=0$) can be identified with $\mathbb{RP}^2$, which can be viewed as a disk with two opposite points on the circumference (the equator) identified (see Figure 6.4).

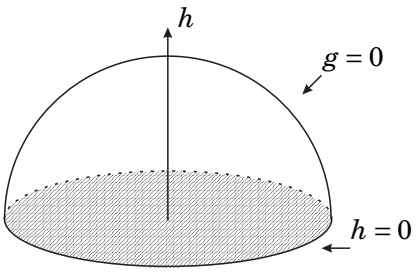

Figure 6.4: The parameter space

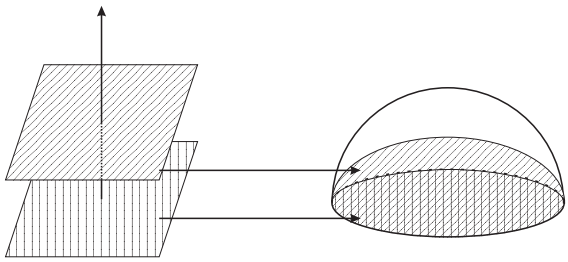

Figure 6.5: Correspondence between planes and ellipsoides

For $g \neq 0$, we get the affine chart:

$$\begin{aligned}
&\mathbb{RP}^3 \setminus \{g=0\} \leftrightarrow \mathbb{R}^3 \\
&[g:h:k:n] \mapsto \left(\frac{h}{g},\frac{k}{g},\frac{n}{g}\right) = (\overline{h},\overline{k},\overline{n}) \\
&[1:\overline{h}:\overline{k}:\overline{n}] \mapsto (\overline{h},\overline{k},\overline{n}).
\end{aligned}$$

The plane $g=0$ in $\mathbb{RP}^3$ corresponds to the equation $h^2+k^2+n^2=1$ (the full sphere $\mathbb{S}^2$) and the line $g=h=0$ in $\mathbb{RP}^3$ corresponds to the equation $k^2+n^2=1$ (the equator $h=0$ of $\mathbb{S}^2$). However, because of symmetry, we only need half sphere and half equator, respectively.

We now consider planes in $\mathbb{R}^3$ of the form $\overline{h}=h_0$, where h_0 is a constant. The projective completion of such a plane in $\mathbb{RP}^3$ has the equation $h-h_0 g=0$. So we see how the slices $\overline{h}=h_0$ need to be completed in the ball (see Figure 6.5). We note that when $g=0$ necessarily we must have $h=0$ on such a slice, and thus the completion of the image of the plane $\overline{h}=h_0$, when visualized in $\mathbb{S}^3$, must include the equator.

The specific equations of the correspondence of the points in the plane $\overline{h}=h_0$ of $\mathbb{R}^3$ (h_0 a constant) onto points in the interior of $\mathbb{S}^2$ ($\mathscr{B} = \{(h,k,n) \in \mathbb{R}^3; h^2+k^2+n^2<1\}$) follows from the

bijection:

$$\mathbb{R}^3 \leftrightarrow \mathscr{B}$$
$$(\overline{h},\overline{k},\overline{n}) \leftrightarrow \left(\frac{\overline{h}}{c},\frac{\overline{k}}{c},\frac{\overline{n}}{c}\right)$$

with $c=\sqrt{\overline{h}^2+\overline{k}^2+\overline{n}^2+1}$. That is, for each plane $\overline{h}=$ constant in $\mathbb{R}^3$, there corresponds an ellipsoid $h^2(1+h_0^2)/h_0^2+k^2+n^2=1$ (see Figure 6.5).

The set defined by $g=0$ and $h=1$ corresponds to the border of the half sphere, while $g=0=h$ is its equator.

In what follows we would have to make a similar study of the geometry of the different surfaces (singularities, intersections, suprema) involved in the bifurcation diagram as it has been done in [6] or Chapter 5 [9]. The conclusion of such a study is that this bifurcation diagram has only one singular slice, $h=0$, plus a symmetry $h\mapsto -h$, so that the only needed slices to be studied are $h=0$ (singular) and $h=1$ (generic). However, there is a much shorter and easier way to detect the same phenomenon and this comes from the next result.

Proposition 6.3.4. *By a rescaling in the variables, we may assume $h=0$ or $h=1$ in the normal form* (6.3.1)*.*

Proof. If $h\neq 0$, we consider the rescaling in the variables given by $(x,y)\mapsto(x,y/h)$ and obtain

$$\dot{x}=gx^2+2xy+\frac{k}{h^2}y^2,\quad \dot{y}=y+gxy+\frac{n}{h}y^2.$$

By recalling the coefficients $k/h^2\mapsto k$ and $n/h\mapsto n$, we obtain system (6.3.1) with $h=1$. Moreover, we must also consider the case when $h=0$. ∎

6.3.2 The normal form adopted for the subclass $\overline{\textbf{QsnSN(B)}}$

The following result states the normal form adopted for systems in $\overline{\textbf{QsnSN(B)}}$.

Proposition 6.3.5. *Every system with a finite semi–elemental double saddle–node $\overline{sn}_{(2)}$ and an infinite saddle–node of type $\overline{\binom{0}{2}}SN$ located in the endpoints of the vertical axis can be brought via affine transformations and time rescaling to the following normal form*

$$\begin{aligned}\dot{x}&=gx^2+2hxy,\\ \dot{y}&=y+\ell x^2+2mxy+2hy^2,\end{aligned}\tag{6.3.2}$$

where g, h, ℓ and m are real parameters and $g \neq 0$.

Proof. Analogously to Proposition 6.3.2, we start with system (2.2.2), but now we want to place the point $\binom{0}{2}\overline{SN}$ at the origin of the local chart U_2. By following the same steps, we set $k = 0$, $n = 2h$ and we obtain the form (6.3.2). ∎

For this family, we also study the case when $g = 0$ in order to consider the closure of the set **QsnSN(B)** within the set of representatives of **QsnSN(B)** in the parameter space of the normal form (6.3.2).

Remark 6.3.6. *We note that $\{x = 0\}$ is an invariant straight line under the flow of* (6.3.2).

We construct the parameter space for systems (6.3.2) in the same way it was constructed for systems (6.3.1), but now with respect to the parameter $[\lambda] = [g : h : \ell : m] \in \mathbb{RP}^3$.

Analogously to the previous family, the bifurcation diagram for this family in $\mathbb{R}^3$ shows only one singular slice, $h = 0$, and a symmetry $h \mapsto -h$. Then, only one generic slice needs to be taken into consideration, and we choose $h = 1$, and this also can be proved in a much easier way with a transformation similar to the previous case as it can be seen in the next result.

Proposition 6.3.7. *By a rescaling in the variables, we may assume $h = 0$ or $h = 1$ in the normal form* (6.3.2).

Proof. If $h \neq 0$, we consider the rescaling in the variables given by $(x, y) \mapsto (x, y/h)$ and obtain

$$\dot{x} = gx^2 + 2xy, \quad \dot{y} = y + \ell h x^2 + 2mxy + 2y^2.$$

By recalling the coefficient $\ell h \mapsto \ell$, we obtain system (6.3.2) with $h = 1$. Moreover, we must also consider the case when $h = 0$. ∎

6.4 The bifurcation diagram of the systems in $\overline{\textbf{QsnSN(A)}}$

In this section we describe the bifurcations surfaces which are needed for completing the study of the family $\overline{\textbf{QsnSN(A)}}$.

6.4.1 Bifurcation surfaces due to the changes in the nature of singularities

For systems (6.3.1) we will always have the origin as a finite singular point, a double saddle–node.

From Chapter 4 we get the formulas which give the bifurcation surfaces of singularities in $\mathbb{R}^{12}$, produced by changes that may occur in the local nature of finite singularities and we also get equivalent formulas for the infinite singular points. These bifurcation surfaces are all algebraic and they are the following:

Bifurcation surfaces in $\mathbb{RP}^3$ due to multiplicities of singularities

($\mathscr{S}_1$) This is the bifurcation surface due to multiplicity of infinite singularities as detected by the coefficients of the divisor $D_{\mathbb{R}}(P,Q;Z) = \sum_{W\in\{Z=0\}\cap\mathbb{CP}^2} I_W(P,Q)W$, (here $I_W(P,Q)$ denotes the intersection multiplicity of $P=0$ with $Q=0$ at the point W situated on the line at infinity, i.e. $Z=0$) whenever $\deg((D_{\mathbb{R}}(P,Q;Z))) > 0$. This occurs when at least one finite singular point collides with at least one infinite point. More precisely this happens whenever the homogenous polynomials of degree two, p_2 and q_2, in p and q have a common root. This is a quartic whose equation is

$$\mu = g^2(gk - 2hn + n^2) = 0.$$

($\mathscr{S}_3$) Since this family already has a saddle–node at the origin, the invariant $\mathbf{D}$ is always zero. The next $T-$comitant related to finite singularities is $\mathbf{T}$. If this $T-$comitant vanishes, it may mean either the existence of another finite semi–elemental point, or the origin being a point of higher multiplicity, or the system being degenerate. The equation of this surface is

$$\mathbf{T} = g^4(h^2 - gk) = 0.$$

($\mathscr{S}_5$) Since this family already has a saddle–node at infinity, the invariant η is always zero. In this sense, we have to consider a bifurcation related to the existence of either the double infinite singularity $\overline{\binom{0}{2}}SN$ plus a simple one, or a triple one. This phenomenon is ruled by the $T-$comitant $\widetilde{M}$. The equation of this surface is

$$\widetilde{M} = 2h - n = 0.$$

The surface of C^∞ bifurcation points due to a strong saddle or a strong focus changing the sign of their traces (weak saddle or weak focus)

($\mathscr{S}_2$) This is the bifurcation surface due to weak finite singularities, which occurs when the trace

of a finite singular point is zero. The equation of this surface is given by

$$\mathscr{T}_4 = g^2(-4h^2 + 4gk + n^2) = 0.$$

We note that this bifurcation surface can either produce a topological change, if the weak point is a focus, or just a C^∞ change, if it is a saddle, except when this bifurcation coincides with a loop bifurcation associated with the same saddle, in which case, the change may also be topological (for an example of this case we refer to Chapter 7).

The surface of C^∞ bifurcation due to a node becoming a focus

($\mathscr{S}_6$) This surface will contain the points of the parameter space where a finite node of the system turns into a focus. This surface is a C^∞ but not a topological bifurcation surface. In fact, when we only cross the surface ($\mathscr{S}_6$) in the bifurcation diagram, the topological phase portraits do not change. However, this surface is relevant for isolating the parts where a limit cycle surrounding an antisaddle cannot exist. According to results of Chapter 4, the equation of this surface is given by $W_4 = 0$, where

$$W_4 = g^4(-48h^4 + 32gh^2k + 16g^2k^2 + 64h^3n - 64ghkn - 24h^2n^2 + 24gkn^2 + n^4).$$

Bifurcation surface in $\mathbb{RP}^3$ due to the presence of another invariant straight line apart from $\{y = 0\}$

($\mathscr{S}_4$) This surface will contain the points of the parameter space where another invariant straight line appears apart from $\{y = 0\}$. This surface is split in some parts. Depending on these parts, the straight line may contain connections of separatrices from different saddles or not. So, in some cases, it may imply a topological bifurcation and, in others, just a C^∞ bifurcation. The equation of this surface is given by

$$\text{Het} = h = 0.$$

These, except ($\mathscr{S}_4$), are all the bifurcation surfaces of singularities of systems (6.3.1) in the parameter space and they are all algebraic. We shall discover another bifurcation surface not necessarily algebraic and on which the systems have global connection of separatrices different from that given by ($\mathscr{S}_4$). The equation of this bifurcation surface can only be determined approximately by means of numerical tools. Using arguments of continuity in the phase portraits we can prove

the existence of this not necessarily algebraic component in the part where it appears, and we can check it numerically. We shall name it the surface ($\mathscr{S}_7$).

We shall foliate the 3−dimensional bifurcation diagram in $\mathbb{RP}^3$ by the planes $h = 0$ and $h = 1$, given by Proposition 6.3.4, plus the open half sphere $g = 0$ and we shall give pictures of the resulting bifurcation diagram on these planar sections on a disk or in an affine chart of $\mathbb{R}^2$.

The following two results study the geometrical behavior of the surfaces, that is, their singularities and their intersection points, or the points where two bifurcation surfaces are tangent.

In what follows we work in the chart of $\mathbb{RP}^3$ corresponding to $g \neq 0$, and we take $g = 1$. To do the study, we shall use Figures 6.7 and 6.8 which are drawn on planes $h = h_0$ of $\mathbb{R}^3$, $h_0 \in \{0, 1\}$, having coordinates (h_0, k, n). In these planes the coordinates are (n, k) where the horizontal line is the n–axis.

As the final bifurcation diagram is quite complex, it is useful to introduce colors which will be used to talk about the bifurcation points. Although the colors are the same used in the study of the triple node, here they play a different role as described below:

(a) the curve obtained from the surface ($\mathscr{S}_1$) is drawn in blue (a finite singular point collides with an infinite one);

(b) the curve obtained from the surface ($\mathscr{S}_2$) is drawn in green (when two finite singular points collide);

(c) the curve obtained from the surface ($\mathscr{S}_3$) is drawn in yellow (when the trace of a singular point becomes zero);

(d) the curve obtained from the surface ($\mathscr{S}_4$) is drawn in purple (presence of an invariant straight line). We draw it as a continuous curve if it implies a topological change or as a dashed curve if not.

(e) the curve obtained from the surface ($\mathscr{S}_5$) is drawn in red (when three infinite singular points collide);

(f) the curve obtained from the surface ($\mathscr{S}_6$) is drawn in black (an antisaddle is on the edge of turning from a node to a focus or vice versa); and

(g) the curve obtained from the surface ($\mathscr{S}_7$) is also drawn in purple (same as for ($\mathscr{S}_4$)) since both surfaces deal with connections of separatrices mostly.

Lemma 6.4.1. *For $g \neq 0$ and $h = 0$, no surface, except ($\mathscr{S}_6$), has any singularity and all of the surfaces coincide at* $[1 : 0 : 0 : 0]$.

Proof. By setting $g = 1$ and restricting the equations of the surfaces to $h = 0$ we obtain: $\mu = k + n^2$, $\mathcal{T}_4 = 4k + n^2$, $\mathbf{T} = -k$, $\widetilde{M} = -n$, $W_4 = 16k^2 + 24kn^2 + n^4$ and Het $\equiv 0$. It is easy too see that μ, $\mathcal{T}_4$, $\mathbf{T}$, $\widetilde{M}$ and Het have no singularities as they are either a line, or a parabola, or null. Surface $(\mathcal{S}_6)$ is a quartic whose only singularity is at $[1:0:0:0]$ (this is the union of two parabolas having a common contact point). Besides, if we solve the system of equations formed by these expressions, we obtain $[1:0:0:0]$ as the unique solution. ∎

Remark 6.4.2. *Everywhere we mention "a contact point" we mean an intersection point between two curves with the same tangency of even order. Everywhere we mention "an intersection point" we mean a transversal intersection point (with different tangencies).*

Lemma 6.4.3. *For $g \neq 0$ and $h = 1$, no surface, except $(\mathcal{S}_6)$, has any singularity. Moreover,*

(i) the point $[1:1:1:0]$ is a contact point among $(\mathcal{S}_2)$, $(\mathcal{S}_3)$ and $(\mathcal{S}_6)$;

(ii) the point $[1:1:1:1]$ is a contact point between $(\mathcal{S}_1)$ and $(\mathcal{S}_3)$;

(iii) the point $[1:1:1:2]$ is an intersection point between $(\mathcal{S}_3)$ and $(\mathcal{S}_5)$;

(iv) the point $[1:1:48/49:6/7]$ is an intersection point between $(\mathcal{S}_1)$ and $(\mathcal{S}_6)$;

(v) the point $[1:1:8/9:2/3]$ is an intersection point between $(\mathcal{S}_2)$ and $(\mathcal{S}_6)$;

(vi) the point $[1:1:0:-6]$ is an intersection point between $(\mathcal{S}_4)$ and $(\mathcal{S}_6)$;

(vii) the point $[1:1:0:-2]$ is an intersection point between $(\mathcal{S}_2)$ and $(\mathcal{S}_4)$;

(viii) the point $[1:1:0:0]$ is an intersection point between $(\mathcal{S}_1)$ and $(\mathcal{S}_4)$;

(ix) the point $[1:1:0:2]$ is an intersection point among all the surfaces, except $(\mathcal{S}_3)$. Besides, surface $(\mathcal{S}_6)$ is singular at this point, surface $(\mathcal{S}_4)$ has a contact point with one of the components of $(\mathcal{S}_6)$ and $(\mathcal{S}_1)$ has a contact point with the other component of $(\mathcal{S}_6)$.

Proof. Analogously to Lemma 6.4.1, by restricting the equations of the surfaces to $g = h = 1$ and solving the system of equation formed by pairs of the restricted expressions, we obtain the result. ∎

Remark 6.4.4. *Even though we are working in $\mathbb{RP}^3$, we have seen that the study can be reduced to the geometry of the curves obtained by intersecting the surfaces with this slice.*

According to Proposition 6.3.4, we shall study the bifurcation diagram having as reference the values $h = 0$ and $h = 1$ (see Figures 6.7 and 6.8) and also the value $h = \infty$, which corresponds to $g = 0$. We perform the bifurcation diagram of all singularities for $h = \infty$ ($g = 0$) by putting $g = 0$ and in the remaining three variables (h,k,n), yielding the point $[h:k:n] \in \mathbb{RP}^2$, we take the chart $h \neq 0$ in which we may assume $h = 1$.

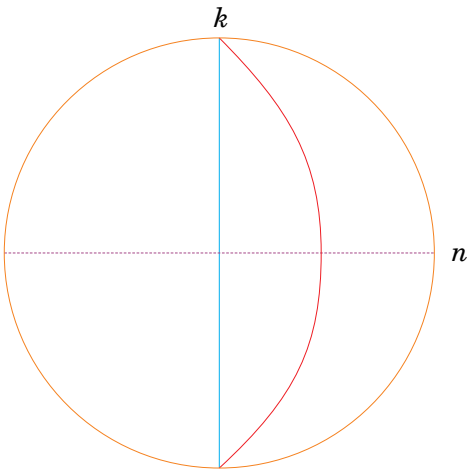

Figure 6.6: Slice of the parameter space for (6.3.1) when $h = \infty$

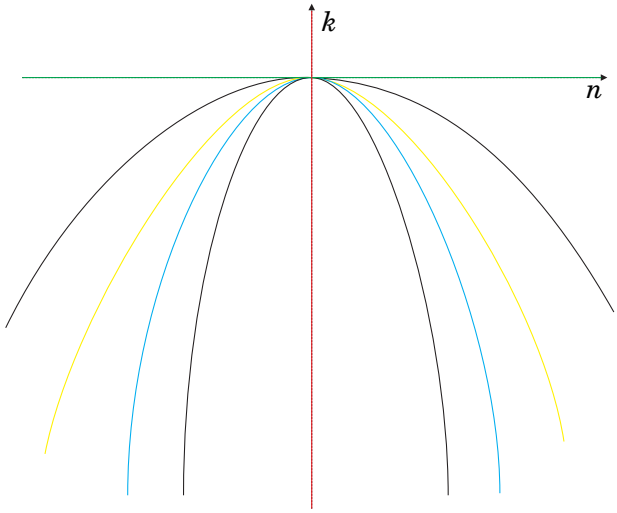

Figure 6.7: Slice of the parameter space for (6.3.1) when $h = 0$

For these values of the parameters, system (6.3.1) becomes

$$\dot{x} = 2xy + ky^2, \quad \dot{y} = y + ny^2, \tag{6.4.1}$$

and the expressions of the bifurcation surfaces for (6.4.1) are given by

$$\mu = \mathscr{T}_4 = \mathbf{T} = W_4 = \mathrm{Het} = 0 \quad \text{and} \quad \widetilde{M} = 2 - n. \tag{6.4.2}$$

Remark 6.4.5. *We note that* $\{y = 0\}$ *is a straight line formed by an infinite number of singularities for system* (6.4.1)*. Then, the phase portraits of such a system must be studied by removing the common factor of the two equations defining it and studying the linear system that remains. The invariant polynomials for linear systems equivalent to the ones for quadratic systems that we use in this study have not been defined, but they are trivial to use for a concrete normal form like* (6.4.1)*.*

The bifurcation curves of singularities (6.4.2) are shown in Figure 6.6. We point out that, although we have drawn in blue the vertical axis k in Figure 6.6, it does not represent surface $(\mathscr{S}_1)$ since it is null by equations (6.4.2), but it has the same geometrical meaning as this surface, i.e. a finite singular has gone to infinity.

The labels used for each part of the bifurcation diagram will follow the same pattern stated in Notation 5.4.11.

Remark 6.4.6. *We point out that the slice* $h = \infty$ *is a bifurcation surface in the parameter space*

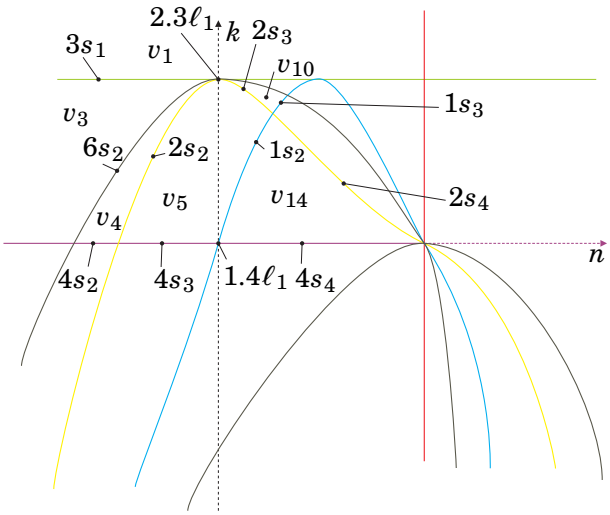

Figure 6.8: Slice of the parameter space for (6.3.1) when $h = 1$

and receives the label $9S$*. We have denoted the curved segments in which the equator splits as* $8.9L_j$.

As an exact drawing of the curves produced by intersecting the surfaces with slices gives us very small parts which are difficult to distinguish, and points of tangency are almost impossible to recognize, we have produced topologically equivalent pictures where parts are enlarged and tangencies are easy to observe. The reader may find the exact pictures in the web page http://mat.uab.es/~artes/articles/qvfsn2SN02/qvfsn2SN02.html.

Remark 6.4.7. *We consider* $g \neq 0$*. It is worth mentioning that if we compare the case of the slices* $h = 0$ *and* $h = 1$ *(here we may take any other* $h > 0$*), we see that a region looking like a "cross" appears on the slice* $h = 1$ *between* $(\mathscr{S}_3)$ *(*$n = 1$*) and* $(\mathscr{S}_4)$ *(*$n = 0$*) and also between* $(\mathscr{S}_5)$ *(*$k = 2$*) and* $k = 0$*. This "cross" exists on every slice given by* $h > 0$ *and, as we take* $h \to 0$*, the region inside the "cross" including the borders tends to the two axes. Furthermore, the rectangle in the middle of the cross tends to* $[1:0:0:0]$.

We recall that the black surface $(\mathscr{S}_6)$ (or W_4) means the turning of a finite antisaddle from a node to a focus. Then, according to the general results about quadratic systems, we could have limit cycles around such point.

6.4.2 Bifurcation surfaces due to connections

We now describe for each set of the partition on $g \neq 0$ and $h = 1$ the local behavior of the flow around all the singular points. Given a concrete value of parameters of each one of the sets in

this slice we compute the global phase portrait with the numerical program P4 [27]. It is worth mentioning that many (but not all) of the phase portraits in this paper can be obtained not only numerically but also by means of perturbations of the systems of codimension one higher.

In this slice we have a partition in 2−dimensional parts bordered by curved polygons, some of them bounded, others bordered by infinity. Provisionally, we use lower–case letters to describe the sets found algebraically so as not to interfere with the final partition described with capital letters. For each 2−dimensional part we obtain a phase portrait which is coherent with those of all their borders, except in one part. Consider the set v_1 in Figure 6.8. In it we have only a saddle–node as finite singularity. When reaching the set $2.3\ell_1$, we are on surfaces $(\mathscr{S}_2)$, $(\mathscr{S}_3)$ and $(\mathscr{S}_6)$ at the same time; this implies the presence of one more finite singularity (in fact, it is a cusp point) which is on the edge of splitting itself and give birth to finite saddle and antisaddle. Now, we consider the segments $2s_2$ and $2s_3$. By the Main Theorem of [61], the corresponding phase portraits of these sets have a first–order weak saddle and a first–order weak focus, respectively. So, on $2s_3$ we have a Hopf bifurcation. This means that either in v_5 or v_{10} we must have a limit cycle. In fact this occurs in v_5. Indeed, as we have a weak saddle on $2s_2$ and we have not detected a loop–type bifurcation surface intersecting this subset, neither its presence is forced to keep the coherence, its corresponding phase portrait is topologically equivalent to the portraits of v_4 and v_5. Since in v_5 we have a phase portrait topologically equivalent to the one on $2s_2$ (without limit cycles) and a phase portrait with limit cycles, this part must be split into two other ones separated by a new surface $(\mathscr{S}_7)$ having at least one element $7S_1$ such that one part has limit cycle and the other does not, and the border $7S_1$ must correspond to a connection between separatrices. After numerical computations we checked that the part v_5 splits into V_5 without limit cycles and V_{11} with one limit cycle, both of which can be seen in Figure 6.13.

The next result assures us the existence of limit cycle in any representative of the subset v_{14} and it is needed to complete the study of $7S_1$.

Lemma 6.4.8. *In v_{14} there is always one limit cycle.*

Proof. We see that the subset v_{14} is characterized by $\mu < 0$, $\mathscr{T}_4 < 0$, $W_4 < 0$, $\widetilde{M} > 0$, $\mathbf{T} > 0$, $k > 0$ and $n > 0$. Any representative of v_{14} has the finite saddle–node at the origin with its eigenvectors on the axes and two more finite singularities, a focus and a node (the focus is due to $W_4 < 0$). We claim that these two other singularities are placed in symmetrical quadrants with respect to the origin (see Figure 6.9). In fact, by computing the exact expression of each singular point (x_1, y_1) and (x_2, y_2) and multiplying their $x-$coordinates and $y-$coordinates we obtain k/μ and $1/\mu$,

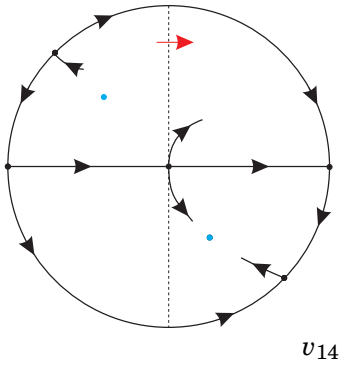

Figure 6.9: The local behavior around each of the finite and infinite singularities of any representative of v_{14}. The red arrow shows the sense of the flow along the $y-$axis and the blue points are the focus and the node with same stability

respectively, which are always negative since $k>0$ and $\mu<0$ in v_{14}. Besides, each one of them is placed in an even quadrant since the product of the coordinates of each antisaddles is never null and any representative gives a negative product. Moreover, both antisaddles have the same stability since the product of their traces is given by $\mu/\mathscr{T}_4$ which is always positive in v_{14}.

The infinite singularities of systems in v_{14} are the saddle–node $\overline{\binom{0}{2}}SN$ (recall the normal form (6.3.1)) and a saddle. In fact, the expression of the singular points in the local chart U_1 are $(0,0)$ and $((-2h+n)/k,0)$. We note that the determinant of the Jacobian matrix of the flow in U_1 at the second singularity is given by

$$-\frac{(2h-n)^2\left(2hn-k-n^2\right)}{k^2}=\frac{\widetilde{M}^2\mu}{k^2},$$

which is negative since $\mu<0$ in v_{14}. Besides, this pair of saddles are in the second and the fourth quadrant because its first coordinate $(-2h+n)/k=-\widetilde{M}/k$ is negative since $\widetilde{M}>0$ and $k>0$ in v_{14}. We also note that the flow along the $y-$axis is such that $\dot{x}>0$.

Since we have a pair of saddle points in the even quadrants, each one of the finite antisaddles is in an even quadrant, no orbit can enter into the second quadrant and no orbit may leave the fourth one and, in addition, these antisaddles, a focus and a node, have the same stability, any phase portrait in v_{14} must have at least one limit cycle in any of the even quadrants. Moreover, the limit cycle is in the second quadrant, because the focus is there since a saddle–node is born in that quadrant on $3s_1$, splits in two points when entering v_3 (both of them remain in the same quadrant since $x_1x_2=k/\mu<0$ and $y_1y_2=1/\mu<0$), the node turns into focus on $6s_2$ and the saddle moves to infinity on $1s_2$ appearing as a node in the fourth quadrant when entering v_{14}. Furthermore, by

the statement (iv) of Section 1.5, it follows the uniqueness of the limit cycle in v_{14}. ■

Now, the following result states that the segment which splits the subset v_5 into the parts V_5 and V_{11} has its endpoints well–determined. We can visualize the image of this surface in the plane $h = 1$ in Figure 6.13.

Proposition 6.4.9. *The endpoints of the part of the curve* $7S_1$ *are* $2.3\ell_1$*, intersection of surfaces* $(\mathscr{S}_2)$ *and* $(\mathscr{S}_3)$*, and* $1.4\ell_1$*, intersection of surfaces* $(\mathscr{S}_1)$ *and* $(\mathscr{S}_4)$*.*

Proof. We write $r_1 = [1 : 1 : 0 : 2]$ and $r_2 = [1 : 1 : 1 : 0]$ for $2.3\ell_1$ and $1.4\ell_1$, respectively. If the starting point were any point of the segments $2s_2$ or $2s_3$, we would have the following incoherences: firstly, if the starting point of $7S_1$ were on $2s_2$, a portion of this subset must refer to a Hopf bifurcation since we have a limit cycle in V_{11}; and secondly, if this starting point were on $2s_3$, a portion of this subset must not refer to a Hopf bifurcation which contradicts the fact that on $2s_3$ we have a first–order weak focus. Finally, the ending point must be r_2 because, if it were located on $4s_3$, we would have a segment between this point and $1.4\ell_1$ along surface $(\mathscr{S}_4)$ with two invariant straight lines and one limit cycle, which contradicts the statement (v) of Section 1.5, and if it were on $1s_2$, we would have a segment between this point and $1.4\ell_1$ along surface $(\mathscr{S}_1)$ without limit cycle which is not compatible with Lemma 6.4.8 since $\mu = 0$ does not produce a graphic. ■

In Figure 6.10 we show the sequence of phase portraits along the subsets pointed out in Figure 6.8.

We cannot be totally sure that this is the unique additional bifurcation curve in this slice. There could exist others which are closed curves which are small enough to escape our numerical research, but the one located is enough to maintain the coherence of the bifurcation diagram. We recall that this kind of studies are always done modulo "islands". For all other two–dimensional parts of the partition of this slice whenever we join two points which are close to two different borders of the part, the two phase portraits are topologically equivalent. So we do not encounter more situations than the one mentioned above.

In Figures 6.11 to 6.13 we show the bifurcation diagrams for family (6.3.1). Since there are two relevant values of h to be taken into consideration (according to Proposition 6.3.4) plus the infinity, the pictures show all the algebraic bifurcation curves and all the nonalgebraic bifurcation ones needed for the coherence of the diagram, which lead to a complete bifurcation diagram for family (6.3.1) modulo islands. In Section 6.7 the reader can look for the topological equivalences among the phase portraits appearing in the various parts and the selected notation for their

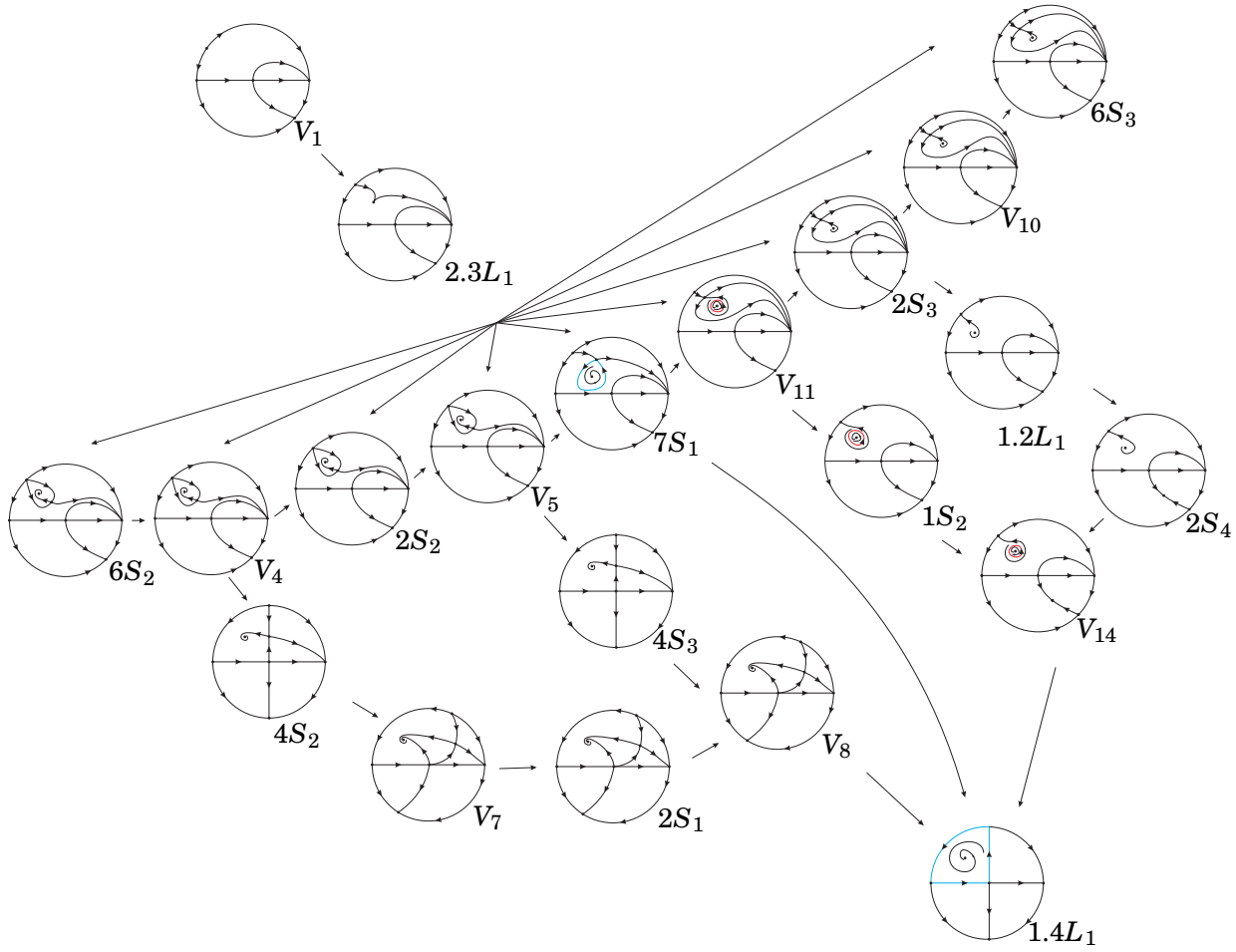

Figure 6.10: Sequence of phase portraits in slice $g = h = 1$ from v_1 to $1.4\ell_1$. We start from v_1. When crossing $2.3\ell_1$, we may choose at least seven "destinations": $6s_2$, v_4, $2s_2$, v_5, $2s_3$, v_{10} and $6s_3$. In each one of these subsets, but v_5, we obtain only one phase portrait. In v_5 we find (at least) three different ones, which means that this subset must be split into (at least) three different parts whose phase portraits are V_5, $7S_1$ and V_{11}. And then we shall follow the arrows to reach the subset $1.4\ell_1$ whose corresponding phase portrait is $1.4L_1$

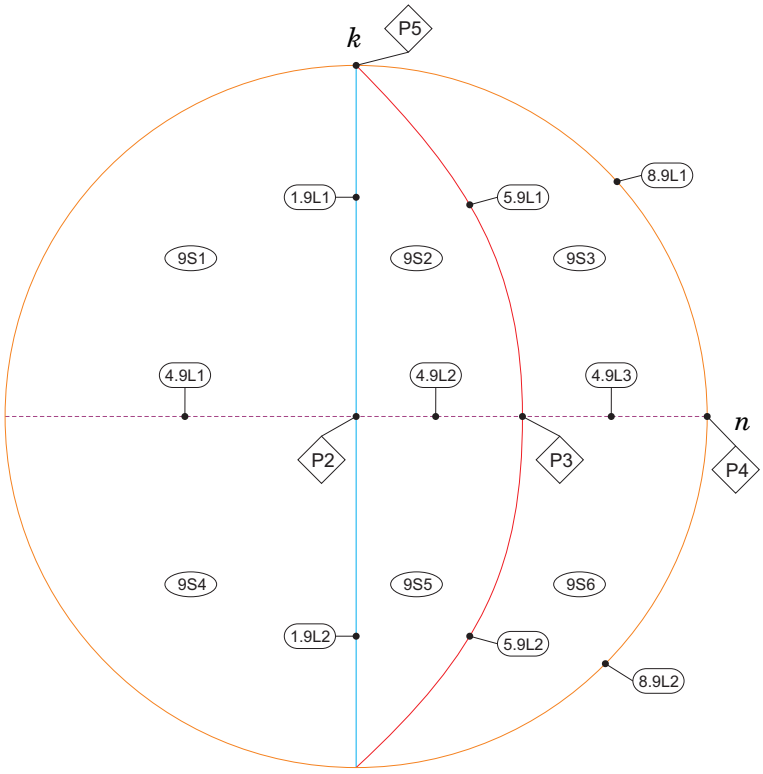

Figure 6.11: Complete bifurcation diagram of $\overline{\mathbf{QsnSN(A)}}$ for slice $h = \infty$

representatives in Figures 6.1 and 6.2. In Figure 6.13, we have colored in light yellow the parts with one limit cycle.

6.5 The bifurcation diagram of the systems in $\overline{\mathbf{QsnSN(B)}}$

Before we describe all the bifurcation surfaces for $\overline{\mathbf{QsnSN(B)}}$, we prove the following result which gives conditions on the parameters for the presence of either a finite star node n^* (whenever any two distinct nontrivial integral curves arrive at the node with distinct slopes), or a finite dicritical node n^d (a node with identical eigenvalues but Jacobian nondiagonal).

Lemma 6.5.1. *Systems* (6.3.2) *always have an* n^**, if* $m = 0$ *and* $h \neq 0$*, or an* n^d*, otherwise.*

Proof. We note that the singular point $(0, -1/(2h))$ has its Jacobian matrix given by

$$\begin{pmatrix} -1 & 0 \\ -m/h & -1 \end{pmatrix}.$$

■

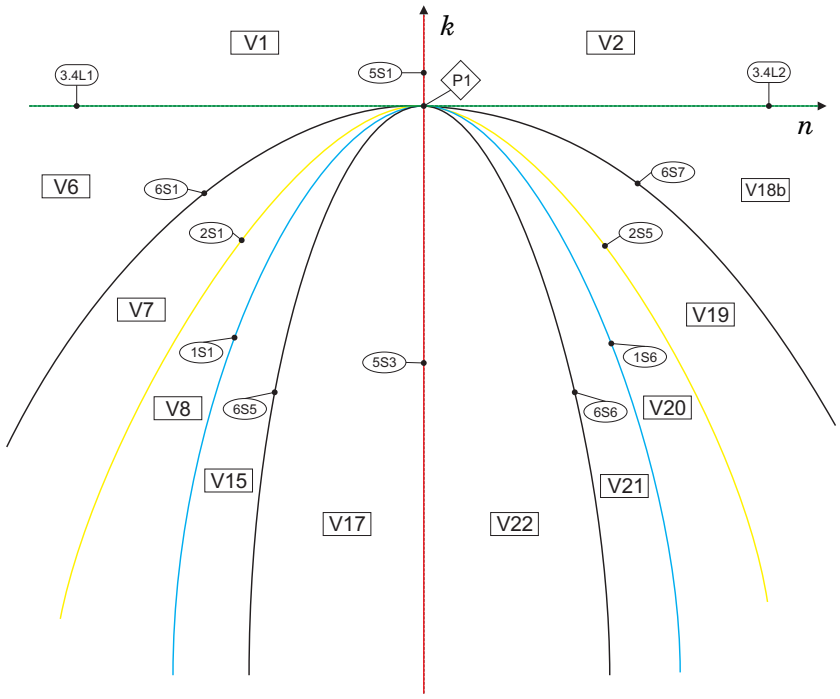

Figure 6.12: Complete bifurcation diagram of $\overline{\mathbf{QsnSN(A)}}$ for slice $h = 0$

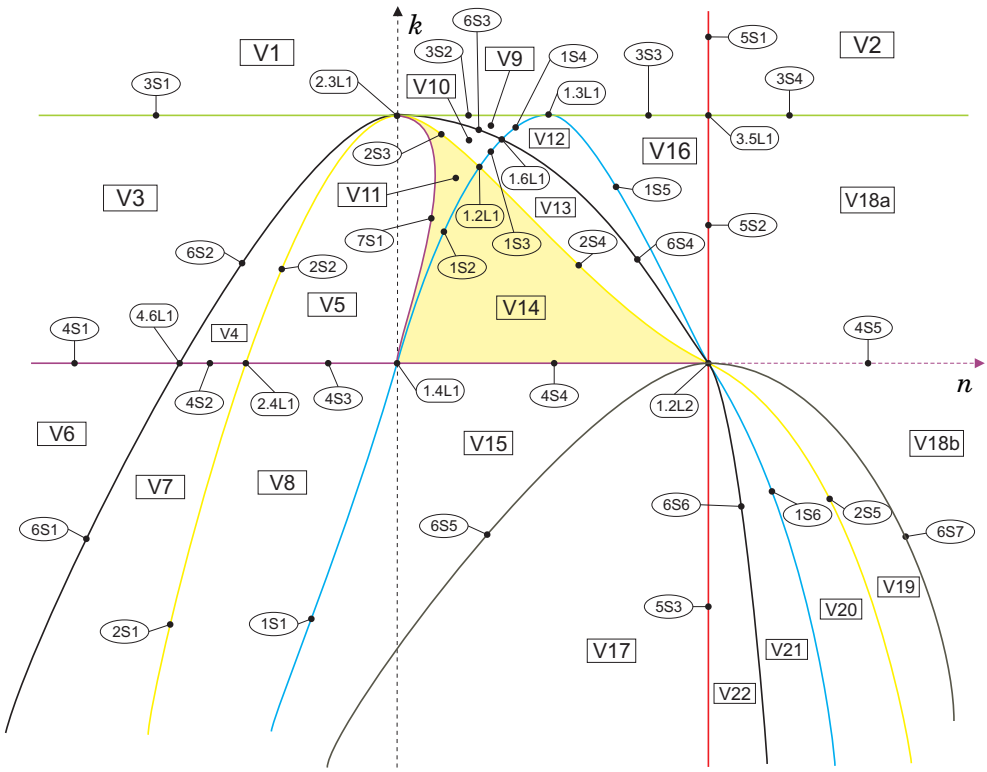

Figure 6.13: Complete bifurcation diagram of $\overline{\mathbf{QsnSN(A)}}$ for slice $h = 1$

6.5.1 Bifurcation surfaces due to the changes in the nature of singularities

The invariants and $T-$comitants needed here are the same as in the previous system except surfaces ($\mathscr{S}_4$) and ($\mathscr{S}_6$); so we shall only give the geometrical meaning and their equations plus a deeper discussion on surface ($\mathscr{S}_6$). For further information about them, see Section 6.4.

Bifurcation surfaces in $\mathbb{RP}^3$ due to multiplicities of singularities

($\mathscr{S}_1$) This is the bifurcation surface due to the multiplicity of infinite singularities. This occurs when at least one finite singular point collides with at least one infinite point. The equation of this surface is

$$\mu = 4h^2(g^2 + 2h\ell - 2gm) = 0.$$

($\mathscr{S}_3$) This is the bifurcation surface is due to either the existence of another finite semi–elemental point, or the origin being a higher multiplicity point, or the system being degenerate. The equation of this surface is given by

$$\mathbf{T} = -g^2h^2 = 0.$$

It only has substantial importance when we consider the planes $g = 0$ or $h = 0$.

($\mathscr{S}_5$) This is the bifurcation surface due to the collision of infinite singularities, i.e. when all three infinite singular points collide. The equation of this surface is

$$\widetilde{M} = (g - 2m)^2 = 0.$$

The surface of C^∞ bifurcation due to a strong saddle or a strong focus changing the sign of their traces (weak saddle or weak focus)

($\mathscr{S}_2$) This is the bifurcation surface due to weak finite singularities, which occurs when their trace is zero. The equation of this surface is given by

$$\mathscr{T}_4 = -16h^3\ell = 0.$$

The surface of C^∞ bifurcation due to a node becoming a focus

($\mathscr{S}_6$) Since W_4 is identically zero for all the bifurcation space, the invariant that captures if a second point may be on the edge of changing from node to focus is W_3. The equation of this surface

is given by

$$W_3 = 64h^4(g^4 + 2g^2h\ell + h^2\ell^2 - 2g^3m) = 0.$$

These are all the bifurcation surfaces of singularities of the systems (6.3.2) in the parameter space and they are all algebraic. We do not expect to discover any other bifurcation surface (neither nonalgebraic nor algebraic one) due to the fact that in all the transitions we make among the parts of the bifurcation diagram of this family we find coherence in the phase portraits when "traveling" from one part to the other.

Analogously to the previous class, we shall foliate the three–dimensional bifurcation diagram in $\mathbb{RP}^3$ by the planes $h = 0$ and $h = 1$, given by Proposition 6.3.7, plus the open half sphere $g = 0$ and we shall give pictures of the resulting bifurcation diagram on these planar sections on a disk or in an affine chart of $\mathbb{R}^2$.

The following three results study the geometrical behavior of the surfaces, that is, their singularities and the simultaneous intersection points among them, or the points where two bifurcation surfaces are tangent, and the presence of a different invariant straight line in the particular case when $\ell = 0$.

In what follows we work in the chart of $\mathbb{RP}^3$ corresponding to $g \neq 0$, and we take $g = 1$. To do the study, we shall use Figures 6.15 and 6.16 which are drawn on planes $h = h_0$ of $\mathbb{R}^3$, $h_0 \in \{0,1\}$, having coordinates (h_0,ℓ,m). In these planes the coordinates are (ℓ,m) where the horizontal line is the $\ell-$axis.

We shall use the same set of colors for the bifurcation surfaces as in the previous case.

Lemma 6.5.2. *All the bifurcation surfaces intersect on $h = 0$, with $g \neq 0$.*

Proof. The equations of surfaces $(\mathscr{S}_1)$, $(\mathscr{S}_2)$, $(\mathscr{S}_3)$ and $(\mathscr{S}_6)$ are identically zero when restricted to the plane $h = 0$, and the equation of $(\mathscr{S}_5)$ is the straight line $2m - 1 = 0$, for all $g \neq 0$, $h \geq 0$ and $m,\ell \in \mathbb{R}$. ∎

Lemma 6.5.3. *For $h = 1$ (with $g \neq 0$), the surfaces have no singularities. Moreover,*

(i) the point $[1:1:-2:1/2]$ is an intersection point between $(\mathscr{S}_5)$ and $(\mathscr{S}_6)$;

(ii) the point $[1:1:0:1/2]$ is an intersection point among $(\mathscr{S}_1)$, $(\mathscr{S}_2)$, $(\mathscr{S}_5)$ and $(\mathscr{S}_6)$. Besides, the intersection between $(\mathscr{S}_1)$ and $(\mathscr{S}_6)$ is in fact a contact point.

Proof. For $g = h = 1$, surface $(\mathscr{S}_1)$ is the straight line $1 + 2\ell - 2m = 0$, which intersects surface $(\mathscr{S}_5)$, which is a double straight line with equation $-1 + 2m = 0$, at the point $[1:1:0:1/2]$; surface

($\mathscr{S}_6$) is the parabola $1+2\ell+\ell^2-2m=0$ passing through the point $[1:1:0:1/2]$ with a 2−order contact with surface ($\mathscr{S}_1$); moreover, surface ($\mathscr{S}_6$) has another intersection point with surface ($\mathscr{S}_5$) at $[1:1:-2:1/2]$; surface ($\mathscr{S}_2$) is the straight line $\ell=0$, which intersects surfaces ($\mathscr{S}_1$), ($\mathscr{S}_5$) and ($\mathscr{S}_6$) at the point $[1:1:0:1/2]$. ■

Lemma 6.5.4. *If $\ell=0$, the straight line $\{y=0\}$ is invariant under the flow of* (6.3.2).

Proof. It is easy to check the result by substituting $\ell=0$ in (6.3.2). ■

According to Proposition 6.3.7, we shall study the bifurcation diagram having as reference the values $h=0$ and $h=1$ (see Figures 6.15 and 6.16) and also the value $h=\infty$, which corresponds to $g=0$. We perform the bifurcation diagram of all singularities for $h=\infty$ ($g=0$) by putting $g=0$ and in the remaining three variables (h,ℓ,m), yielding the point $[h:\ell:m]\in\mathbb{RP}^2$, we take the chart $h\neq 0$ in which we may assume $h=1$.

For these values of the parameters, system (6.3.2) becomes

$$\dot{x}=2xy,\quad \dot{y}=y+\ell x^2+2mxy, \tag{6.5.1}$$

and the expressions of the bifurcation surfaces for (6.5.1) are given by

$$\mu=8\ell,\ \mathscr{T}_4=-16\ell,\ \mathbf{T}=0,\ \widetilde{M}=4m^2 \text{ and } W_3=64\ell^2. \tag{6.5.2}$$

Remark 6.5.5. *We note that $\{y=0\}$ is a straight line of singularities for system* (6.5.1) *when $\ell=0$. To study the phase portraits of system* (6.5.1)*, we proceed as stated in Remark 6.4.5.*

The bifurcation curves of singularities (6.5.2) are shown in Figure 6.14.

Here we also give topologically equivalent figures to the exact drawings of the bifurcation curves. The reader may find the exact pictures in the web page http://mat.uab.es/~artes/articles/qvfsn2SN02/qvfsn2SN02.html.

We recall that the black surface ($\mathscr{S}_6$) (or W_3) means the turning of a finite antisaddle from a node to a focus. Then, according to the general results about quadratic systems, we could have limit cycles around such focus for any set of parameters having $W_3<0$.

In Figures 6.17 to 6.19 we show the bifurcation diagrams for family (6.3.2). Since there are two relevant values of h to be taken into consideration (according to Proposition 6.3.7) plus the infinity, the pictures show all the algebraic bifurcation curves obtained by the invariant polynomials. We

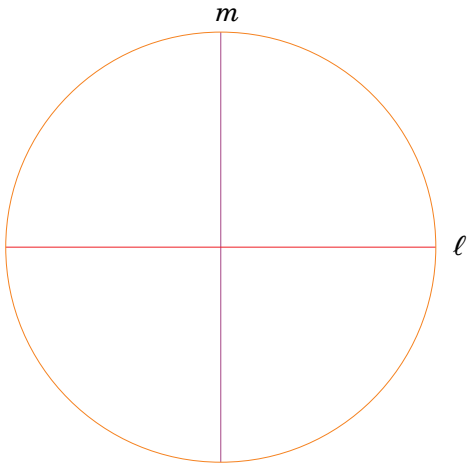

Figure 6.14: Slice of parameter space for (6.3.2) when $h = \infty$

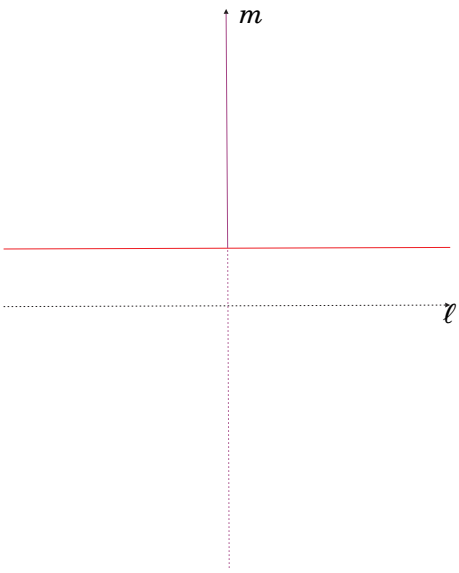

Figure 6.15: Slice of parameter space for (6.3.2) when $h = 0$

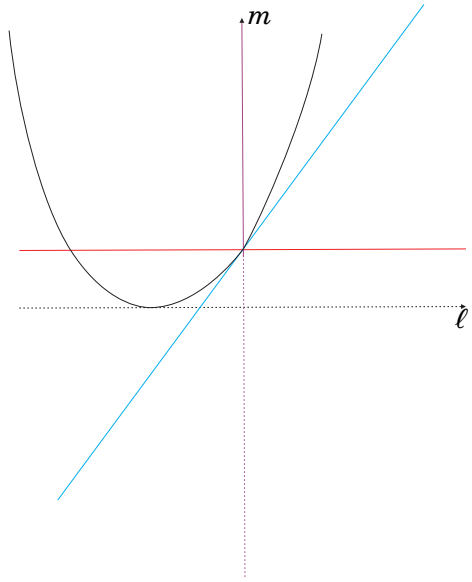

Figure 6.16: Slice of parameter space for (6.3.2) when $h = 1$

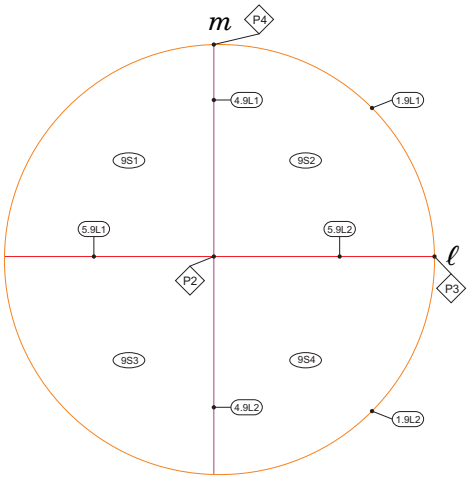

Figure 6.17: Complete bifurcation diagram of $\overline{\textbf{QsnSN(B)}}$ for slice $h = \infty$

observe that nonalgebraic bifurcation curves were not needed for the coherence of the diagram. All of these leads to a complete bifurcation diagram for family (6.3.2) modulo islands. In Section 6.7 the reader can look for the topological equivalences among the phase portraits appearing in the various parts and the selected notation for their representatives in Figure 6.3.

6.6 Other relevant facts about the bifurcation diagrams

The bifurcation diagrams we have obtained for the families $\overline{\textbf{QsnSN(A)}}$ and $\overline{\textbf{QsnSN(B)}}$ are completely coherent, i.e. in each family, by taking any two points in the parameter space and joining them by a continuous curve, along this curve the changes in phase portraits that occur when crossing the different bifurcation surfaces we mention can be completely explained.

Nevertheless, we cannot be sure that these bifurcation diagrams are the complete bifurcation diagrams for $\overline{\textbf{QsnSN(A)}}$ and $\overline{\textbf{QsnSN(B)}}$ due to the possibility of "islands" inside the parts bordered by unmentioned bifurcation surfaces. In case they exist, these "islands" would not mean any modification of the nature of the singular points. So, on the border of these "islands" we could only have bifurcations due to saddle connections or multiple limit cycles.

In case there were more bifurcation surfaces, we should still be able to join two representatives of any two parts of the 85 parts of $\overline{\textbf{QsnSN(A)}}$ or the 43 parts of $\overline{\textbf{QsnSN(B)}}$ found until now with a continuous curve either without crossing such bifurcation surface or, in case the curve crosses it, it must do it an even number of times without tangencies, otherwise one must take into account the multiplicity of the tangency, so the total number must be even. This is why we call these potential

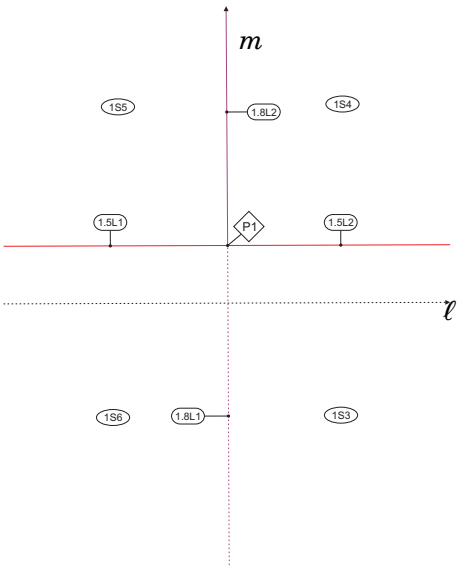

Figure 6.18: Complete bifurcation diagram of **QsnSN(B)** for slice $h = 0$

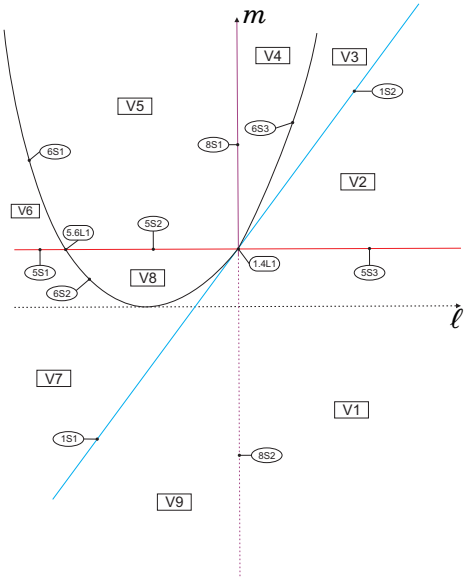

Figure 6.19: Complete bifurcation diagram of **QsnSN(B)** for slice $h = 1$

bifurcation surfaces "*islands*".

However, in none of the two families we have found a different phase portrait which could fit in such an island. The existence of the invariant straight line avoids the existence of a double limit cycle which is the natural candidate for an island (recall the item (iv) of Section 1.5), and also the limited number of separatrices (compared to a generic case) limits greatly the possibilities for phase portraits.

6.7 Completion of the proofs of Theorems 6.2.1 and 6.2.2

In the bifurcation diagram we may have topologically equivalent phase portraits belonging to distinct parts of the parameter space. As here we have finitely many distinct parts of the parameter space, to help us identify or to distinguish phase portraits, we need to introduce some invariants and we actually choose integer–valued invariants. All of them were already used in [39, 6]. These integer–valued invariants, and sometimes symbol–valued invariants, yield a classification which is easier to grasp.

Definition 6.7.1. *We denote by $I_1(S)$ the number of the isolated real finite singular points.*

Definition 6.7.2. *We denote by $I_2(S)$ the sum of the indices of the real finite singular points.*

Definition 6.7.3. *We denote by $I_3(S)$ the number of the real infinite singular points. This number can be ∞ in some cases.*

Definition 6.7.4. *For a given infinite singularity s of a system S, let ℓ_s be the number of global or local separatrices beginning or ending at s and which do not lie on the line at infinity. We have $0 \leq \ell_s \leq 4$. We denote by $I_4(S)$ the sequence of all such ℓ_s when s moves in the set of infinite singular points of the system S. We can start the sequence at anyone of the infinite singular points but all sequences must be listed in a same specific order either clockwise or counter–clockwise along the line of infinity.*

In our case we have used the clockwise sense beginning from the saddle–node at the origin of the local chart U_1 in the pictures shown in Figures 6.1 and 6.2, and the origin of the local chart U_2 in the pictures shown in Figure 6.3.

Definition 6.7.5. *We denote by $I_5(S)$ a digit which gives the number of limit cycles.*

As we have noted previously in Remark 5.4.12, we do not distinguish between phase portraits whose only difference is that in one we have a finite node and in the other a focus. Both phase portraits are topologically equivalent and they can only be distinguished within the C^1 class. In case we may want to distinguish between them, a new invariant may easily be introduced.

Definition 6.7.6. *We denote by $I_6(S)$ the digit 0 or 1 to distinguish the phase portrait which has connection of separatrices outside the straight line $\{y = 0\}$; we use the digit 0 for not having it and 1 for having it.*

Definition 6.7.7. *We denote by $I_7(S)$ the sequence of digits (each one ranging from 0 to 3) such that each digit describes the total number of global or local separatrices ending (or starting) at a finite antisaddle.*

The next three invariants are needed to classify the degenerate phase portraits.

Definition 6.7.8. *We denote by $I_8(S)$ the index of the isolated infinite singular point when there exists another infinite singular which is located in the extreme of a curve of singularities.*

Definition 6.7.9. *We denote by $I_9(S)$ a digit which gives the number of lines with an infinite number of singularities.*

Definition 6.7.10. *We denote by $I_{10}(S)$ a symbol to represent the configuration of the curves of singularities. The symbols are: "><" to represent a hyperbola, "$\cup$" to represent a parabola and "$\times$" to represent two crossing lines.*

Theorem 6.7.11. *Consider the family* $\overline{\textbf{QsnSN(A)}}$ *and all the phase portraits that we have obtained for this family. The values of the affine invariant* $\mathscr{I} = (I_1, I_2, I_3, I_4, I_5, I_6, I_8, I_9)$ *given in the following diagram yield a partition of these phase portraits of the family* $\overline{\textbf{QsnSN(A)}}$.

Furthermore, for each value of $\mathscr{I}$ *in this diagram there corresponds a single phase portrait; i.e.* S *and* S' *are such that* $I(S) = I(S')$*, if and only if* S *and* S' *are topologically equivalent.*

Theorem 6.7.12. *Consider the family* $\overline{\textbf{QsnSN(B)}}$ *and all the phase portraits that we have obtained for this family. The values of the affine invariant* $\mathscr{I} = (I_1, I_2, I_3, I_4, I_7, I_8, I_{10})$ *given in the following diagram yield a partition of these phase portraits of the family* $\overline{\textbf{QsnSN(B)}}$.

Furthermore, for each value of $\mathscr{I}$ *in this diagram there corresponds a single phase portrait; i.e.* S *and* S' *are such that* $I(S) = I(S')$*, if and only if* S *and* S' *are topologically equivalent.*

The bifurcation diagram for $\overline{\textbf{QsnSN(A)}}$ has 85 parts which produce 38 topologically different phase portraits as described in Tables 6.7.1 and 6.7.2. The remaining 47 parts do not produce any new phase portrait which was not included in the 38 previous ones. The difference is basically the presence of a strong focus instead of a node and vice versa.

Similarly, the bifurcation diagram for $\overline{\textbf{QsnSN(B)}}$ has 43 parts which produce 25 topologically different phase portraits as described in Tables 6.7.4 and 6.7.5. The remaining 18 parts do not produce any new phase portrait which was not included in the 25 previous ones. The phase portraits are basically different to each other under some algebro–geometric features related to the position of the orbits.

The phase portraits having neither limit cycle nor graphic have been denoted surrounded by parenthesis, for example (V_1) (in Tables 6.7.1 and 6.7.4); the phase portraits having one limit cycle have been denoted surrounded by brackets, for example $[V_{11}]$ (in Table 6.7.1); the phase portraits having at least one graphic have been denoted surrounded by {}, for example $\{7S_1\}$ (in Table 6.7.1).

Proof. The above two results follow from the results in the previous sections and a careful analysis of the bifurcation diagrams given in Sections 6.4 and 6.5, in Figures 6.11, 6.12, 6.13, 6.17, 6.18 and 6.19, the definition of the invariants I_j and their explicit values for the corresponding phase portraits. ∎

We first make some observations regarding the equivalence relations used in this study: the affine and time rescaling, C^1 and topological equivalences.

The coarsest one among these three is the topological equivalence and the finest is the affine equivalence. We can have two systems which are topologically equivalent but not C^1–equivalent.

For example, we could have a system with a finite antisaddle which is a structurally stable node and in another system with a focus, the two systems being topologically equivalent but belonging to distinct C^1-equivalence classes, separated by the surface $(\mathscr{S}_6)$ on which the node turns into a focus.

In Table 6.7.3 (Table 6.7.6, respectively) we listed in the first column 38 parts (25 parts, respectively) with all the distinct phase portraits of Figures 6.1 and 6.2 (Figure 6.3, respectively). Corresponding to each part listed in column 1 we have in its horizontal block, all parts whose phase portraits are topologically equivalent to the phase portrait appearing in column 1 of the same horizontal block.

In the second column we have put all the parts whose systems yield topologically equivalent phase portraits to those in the first column, but which may have some algebro–geometric features related to the position of the orbits.

In the third (respectively, fourth, and fifth) column we list all parts whose phase portraits have another antisaddle which is a focus (respectively, a node which is at a bifurcation point producing foci close to the node in perturbations, a node–focus to shorten, and a finite weak singular point). In the sixth column of Table 6.7.1 we list all phase portraits which have a triple infinite singularity with multiplicity $\binom{2}{1}$.

Whenever phase portraits appear on a horizontal block in a specific column, the listing is done according to the decreasing dimension of the parts where they appear, always placing the lower dimensions on lower lines.

6.7.1 Proof of the main theorem

The bifurcation diagram described in Section 6.4, plus Tables 6.7.1 and 6.7.2 of the geometrical invariants distinguishing the 38 phase portraits, plus Table 6.7.3 giving the equivalences with the remaining phase portraits lead to the proof of the main statement of Theorem 6.2.1. Analogously, we have the proof of Theorem 6.2.2, but considering the description in Section 6.5 and Tables 6.7.4, 6.7.5 and 6.7.6.

To prove statements *(d)* and *(e)* of Theorem 6.2.2 we recall the Main Theorem of [61] and verify that:

(i) Any representative of $4S_1$ is such that $g \neq 0$ (we may assume $g = 1$), $h > 0$, $\ell = 0$ and $m > 1/2$. Then, we have: $\mathscr{T}_4 = 0$, $\mathscr{T}_3 = 8h^2(2m-1) \neq 0$, $\mathscr{T}_3\mathscr{F} = -8h^4(2m-1)^3 < 0$, $\mathscr{F}_1 = \mathscr{F}_2 = \mathscr{F}_3\mathscr{F}_4 = 0$, which imply that it has a center c;

Table 6.7.1: Geometric classification for the subfamily $\overline{\mathbf{QsnSN(A)}}$: the nondegenerate parts

$$
I_1 = \left\{
\begin{array}{l}
3 \;\&\; I_2 = \left\{
\begin{array}{l}
2 \;\&\; I_3 = \left\{
\begin{array}{l}
2 \;\&\; I_4 = \left\{
\begin{array}{l}
2111 \;\&\; I_5 = \left\{ \begin{array}{l} 1\,[V_{14}], \\ 0\,(V_{12}), \end{array} \right. \\
1111 \;\&\; I_6 = \left\{ \begin{array}{l} 1\,\{4S_4\}, \\ 0\,(V_{15}), \end{array} \right.
\end{array} \right. \\
1\,(5S_3),
\end{array} \right. \\
0 \;\&\; I_3 = \left\{
\begin{array}{l}
2 \;\&\; I_4 = \left\{
\begin{array}{l}
4111 \;\&\; I_5 = \left\{ \begin{array}{l} 1\,[V_{11}], \\ 0\,(V_9), \end{array} \right. \\
2111 \;\&\; I_6 = \left\{ \begin{array}{l} 1\,(4S_1), \\ 0\,(V_6), \end{array} \right. \\
3112\,(V_3), \\
2120\,(V_{16}), \\
3111\,\{7S_1\},
\end{array} \right. \\
1\,(5S_2), \\
\infty\,\{1.2L_2\},
\end{array} \right.
\end{array} \right. \\
2 \;\&\; I_2 = \left\{
\begin{array}{l}
1 \;\&\; I_3 = \left\{
\begin{array}{l}
2 \;\&\; I_4 = \left\{
\begin{array}{l}
2111 \;\&\; I_5 = \left\{ \begin{array}{l} 1\,[1S_2], \\ 0\,(1S_4), \end{array} \right. \\
1111 \;\&\; I_6 = \left\{ \begin{array}{l} 1\,\{1.4L_1\}, \\ 0\,(1S_1), \end{array} \right. \\
2110\,(1S_5),
\end{array} \right. \\
0 \;\&\; I_3 = \left\{
\begin{array}{l}
2 \;\&\; I_4 = \left\{
\begin{array}{l}
2111 \;\&\; I_6 = \left\{ \begin{array}{l} 1\,(3.4L_1), \\ 0\,(3S_4), \end{array} \right. \\
3112\,(3S_1), \\
4111\,(3S_2), \\
2120\,(3S_3), \\
3111\,(2.3L_1),
\end{array} \right. \\
1\,(3.5L_1),
\end{array} \right.
\end{array} \right. \\
1 \;\&\; I_3 = \left\{
\begin{array}{l}
\infty\,\{P_1\}, \\
2\,(V_1), \\
1\,(5S_1).
\end{array} \right.
\end{array} \right.
$$

Table 6.7.2: Geometric classification for the subfamily $\overline{\mathbf{QsnSN(A)}}$: the degenerate parts

$$
I_1 = \left\{
\begin{array}{l}
1 \;\&\; I_2 = \left\{
\begin{array}{l}
1 \;\&\; I_3 = \left\{
\begin{array}{l}
\infty\,\{P_3\}, \\
2 \;\&\; I_8 = \left\{ \begin{array}{l} -1\,\{9S_2\}, \\ 1\,(9S_3), \end{array} \right. \\
1\,\{5.9L_1\},
\end{array} \right. \\
-1\,\{9S_1\},
\end{array} \right. \\
0 \;\&\; I_3 = \left\{
\begin{array}{l}
2 \;\&\; I_8 = \left\{
\begin{array}{l}
1 \;\&\; I_9 = \left\{ \begin{array}{l} 2\,\{P_4\}, \\ 1\,\{8.9L_1\}, \end{array} \right. \\
0\,\{1.9L_1\},
\end{array} \right. \\
1\,\{P_5\}.
\end{array} \right.
\end{array} \right.
$$

Table 6.7.3: Topological equivalences for the subfamily $\overline{\mathbf{QsnSN(A)}}$

Presented phase portrait	Identical under perturbations	Finite antisaddle focus	Finite antisaddle node–focus	Finite weak point	Triple infinite point
V_1	V_2				$1.3L_1$
V_3	V_4, V_5		$6S_2$	$2S_2$	
V_6	V_{18a}, V_{18b} $4S_5$	V_7, V_8, V_{19}, V_{20}	$6S_1$, $6S_7$	$2S_1$, $2S_5$	
V_9		V_{10}	$6S_3$	$2S_3$	
V_{11}					
V_{12}		V_{13}	$6S_4$	$2S_4$	
V_{14}					
V_{15}	V_{21}	V_{17}, V_{22}	$6S_5$, $6S_6$		
V_{16}					
$1S_1$	$1S_6$				
$1S_2$					
$1S_4$		$1S_3$ $1.6L_1$		$1.2L_1$	
$1S_5$					
$3S_1$					
$3S_2$					
$3S_3$					
$3S_4$					
$4S_1$		$4S_2$, $4S_3$	$4.6L_1$	$2.4L_1$	
$4S_4$					
$5S_1$					
$5S_2$					
$5S_3$					
$7S_1$					
$9S_1$	$9S_4$ $4.9L_1$				
$9S_2$	$9S_5$ $4.9L_2$				
$9S_3$	$9S_6$ $4.9L_3$				
$1.2L_2$					
$1.4L_1$					
$1.9L_1$	$1.9L_2$ P_2				
$2.3L_1$					
$3.4L_1$	$3.4L_2$				
$3.5L_1$					
$5.9L_1$	$5.9L_2$				
$8.9L_1$	$8.9L_2$				
P_1					
P_3					
P_4					
P_5					

Table 6.7.4: Geometric classification for the subfamily $\overline{\mathbf{QsnSN(B)}}$: the nondegenerate parts

$$
I_1 = \left\{
\begin{array}{l}
3 \;\&\; I_2 = \left\{
\begin{array}{l}
2 \;\&\; I_3 = \left\{
\begin{array}{l}
2 \;\&\; I_4 = \left\{
\begin{array}{l}
1111 \;\&\; I_7 = \left\{
\begin{array}{l}
32\,(V_6),\\
31\,(V_7),\\
20\,\{4S_1\},
\end{array}\right.\\
1121\,(V_3),
\end{array}\right.\\
1\,(5S_1),
\end{array}\right.\\
0 \;\&\; I_3 = \left\{
\begin{array}{l}
2 \;\&\; I_4 = \left\{
\begin{array}{l}
2120\,(V_2),\\
1121\,\{V_1\},
\end{array}\right.\\
1\,(5S_3),
\end{array}\right.
\end{array}\right.\\
2 \;\&\; I_2 = \left\{
\begin{array}{l}
2 \;\&\; I_3 = \left\{
\begin{array}{l}
2\,(9S_1),\\
1\,(5.9L_1),
\end{array}\right.\\
1 \;\&\; I_3 = \left\{
\begin{array}{l}
\infty\,\{1.4L_1\},\\
2 \;\&\; I_4 = \left\{
\begin{array}{l}
1120\,(1S_2),\\
1111\,(1S_1),
\end{array}\right.
\end{array}\right.\\
0 \;\&\; I_3 = \left\{
\begin{array}{l}
2\,(9S_2),\\
1\,(5.9L_2),
\end{array}\right.
\end{array}\right.\\
1 \;\&\; I_3 = \left\{
\begin{array}{l}
\infty\,\{P_1\},\\
2 \;\&\; I_4 = \left\{
\begin{array}{l}
2121\,\{1S_4\},\\
1111\,\{1.4L_2\},\\
1011\,(1S_3),
\end{array}\right.\\
1\,\{1.5L_1\}.
\end{array}\right.
\end{array}\right.
$$

Table 6.7.5: Geometric classification for the subfamily $\overline{\mathbf{QsnSN(B)}}$: the degenerate parts

$$
I_1 = \left\{
\begin{array}{l}
1 \;\&\; I_3 = \left\{
\begin{array}{l}
\infty\,\{P_2\},\\
2\,\{4.9L_1\},
\end{array}\right.\\
0 \;\&\; I_{10} = \left\{
\begin{array}{l}
>\!<\,\{1.9L_1\},\\
\cup\,\{P_3\},\\
\times\,\{P_4\},
\end{array}\right.
\end{array}\right.
$$

Table 6.7.6: Topological equivalences for the subfamily $\overline{\mathbf{QsnSN(B)}}$

Presented phase portrait	Identical under perturbations	Finite antisaddle focus	Finite antisaddle node–focus	Finite weak point
V_1	V_9			$4S_2$
V_2				
V_3		V_4	$6S_3$	
V_6		V_5	$6S_1$	
V_7		V_8	$6S_2$	
$1S_1$				
$1S_2$				
$1S_3$	$1S_6$			$1.4L_3$
$1S_4$	$1S_5$			
$4S_1$				
$5S_1$		$5S_2$	$5.6L_1$	
$5S_3$				
$9S_1$	$9S_3$			
$9S_2$	$9S_4$			
$1.4L_1$				
$1.4L_2$				
$1.5L_1$	$1.5L_2$			
$1.9L_1$	$1.5L_3$			
$4.9L_1$	$4.9L_2$			
$5.9L_1$				
$5.9L_2$				
P_1				
P_2				
P_3				
P_4				

(ii) Any representative of $4S_2$ is such that $g \neq 0$ (we may assume $g = 1$), $h > 0$, $\ell = 0$ and $m < 1/2$. Then, we have: $\mathscr{T}_4 = 0$, $\mathscr{T}_3 = 8h^2(2m-1) \neq 0$, $\mathscr{T}_3\mathscr{F} = 8h^4(1-2m)^3 > 0$, $\mathscr{F}_1 = \mathscr{F}_2 = \mathscr{F}_3\mathscr{F}_4 = 0$, which imply that it has an integrable saddle $\$$.

We observe that the phase portraits $9S_2$ and $9S_3$ from family $\overline{\textbf{QsnSN(A)}}$ are not equivalent to the phase portrait $4.9L_1$ from family $\overline{\textbf{QsnSN(B)}}$ because the isolated infinite singular point has index 0 in the last phase portrait while its index is -1 and $+1$ in the first two phase portraits, respectively. Moreover, $9S_2$ and $9S_3$ are not equivalent since they are different by the invariant I_8.

However, the phase portrait P_3 from family $\overline{\textbf{QsnSN(A)}}$ is equivalent to the phase portrait P_2 from family $\overline{\textbf{QsnSN(B)}}$ since there are no invariant that distinguishes them. The same argument applies to prove that other two pairs of topologically equivalent phase portraits. This proves Corollary 6.2.3.

Chapter

7

The topological classification of quadratic differential systems with a finite and an infinite semi–elemental saddle–nodes (C)

7.1 Motivation for the study

In Chapter 6, none of the two subfamilies of quadratic systems studied has been able to yield new phase portraits of codimension one. Regarding Remark 6.2.4, the subfamily of quadratic systems possessing a finite semi–elemental saddle–node and an infinite semi–elemental saddle–node $\overline{\binom{0}{2}}SN$ located in the bisector of the first and third quadrants remains to be studied.

As the study of this last subfamily is quite complicated we dedicate this chapter for its analysis and statement of the results. In advance, the subfamily $\overline{\textbf{QsnSN(C)}}$ yields *all* of the phase portraits of group (A) of codimension–one quadratic systems discussed on page 67.

7.2 Statement of the results

In this section, we again consider the set of all real planar quadratic systems which possess a finite semi–elemental saddle–node $\overline{sn}_{(2)}$ and an infinite semi–elemental saddle–node of type

$\overline{\binom{0}{2}}SN$. After the action of the affine group and time homotheties, we may suppose, without loss of generality, that the finite saddle–node is placed at the origin of the plane with the eigenvectors on the axes. We denote this family by **QsnSN**.

In this chapter we conclude the study of the class $\overline{\textbf{QsnSN}}$, which is the closure of the set of representatives of **QsnSN** in the parameter space of the specific normal form which shall be constructed later, by presenting the analysis of the subfamily $\overline{\textbf{QsnSN(C)}}$. The previous two subfamilies $\overline{\textbf{QsnSN(A)}}$ and $\overline{\textbf{QsnSN(B)}}$ were discussed in Chapter 6.

This subfamily $\overline{\textbf{QsnSN(C)}}$ is characterized by possessing the infinite semi–elemental saddle–node $\overline{\binom{0}{2}}SN$ in the bisector of the first and third quadrants. We refer to Remark 6.3.1 in order to understand the difference among the three subfamilies.

In the normal form (7.3.1), the class $\overline{\textbf{QsnSN(C)}}$ is partitioned into 1034 parts: 199 three–dimensional ones, 448 two–dimensional ones, 319 one–dimensional ones and 68 points. This partition is obtained by considering all the bifurcation surfaces of singularities, one related to the presence of invariant straight lines, one related to connections of separatrices, one related to the presence of invariant parabola and one related to the presence of a double limit cycle, modulo "islands".

It is worth mentioning that the partitions described above and the number of topological equivalence classes of phase portraits for each subfamily are due to the choice of a specific normal form. According to Schlomiuk [50], these partitions do not necessarily contain all the phase portraits of the closure within the class of quadratic systems. It may happen that given two different normal forms for a same family, one phase portrait may exist in the closure of one of them but not in the closure of the other. However, the interior of the family in any normal form must contain exactly the same phase portraits.

Theorem 7.2.1. *There exist* 371 *topologically distinct phase portraits for the closure of the family of quadratic vector fields having a finite saddle–node* $\overline{sn}_{(2)}$ *and an infinite saddle–node of type* $\overline{\binom{0}{2}}SN$ *located in the bisector of the first and third quadrants and given by the normal form* (7.3.1) *(class* $\overline{\textbf{QsnSN(C)}}$*). The bifurcation diagram for this class is the projective tridimensional space* $\mathbb{RP}^3$*. All these phase portraits are shown in Figures 7.1 to 7.11. Moreover, the following statements hold:*

(a) There exist 259 *topologically distinct phase portraits in* **QsnSN(C)***;*

(b) There exist 49 *phase portraits possessing at least one simple limit cycle (or an odd number of them taking into account their multiplicity), and they are in the parts* V_5*,* V_{17}*,* V_{27}*,* V_{33}*,* V_{54}*,*

V_{80}, V_{89}, V_{90}, V_{94}, V_{99}, V_{100}, V_{117}, V_{118}, V_{134}, V_{137}, V_{168}, V_{176}, V_{178}, V_{179}, V_{180}, V_{183}, V_{194}, $1S_4$, $1S_{12}$, $1S_{13}$, $1S_{16}$, $1S_{20}$, $1S_{58}$, $1S_{59}$, $1S_{60}$, $1S_{72}$, $2S_{49}$, $2S_{54}$, $2S_{61}$, $4S_{25}$, $4S_{26}$, $5S_5$, $5S_{22}$, $7S_{27}$, $7S_{28}$, $7S_{53}$, $7S_{56}$, $7S_{74}$, $7S_{81}$, $7S_{83}$, $1.4L_3$, $1.5L_6$, $1.7L_4$ *and* $2.5L_{13}$*;*

(c) There exists one phase portrait with at least one double limit cycle (or an odd number of them taking into account their multiplicity), and it is in the part $10S_1$*;*

(d) There exist two phase portraits with at least two limit cycles (or an even number of them taking into account their multiplicity), and they are in the parts V_{88} *and* V_{182}*;*

(e) There exist 107 *phase portraits with nondegenerate graphics (located in only one place in the phase portrait), and they are in the parts* V_6, V_{53}, V_{102}, V_{107}, V_{113}, V_{138}, V_{166}, V_{168}, V_{172}, V_{173}, V_{174}, V_{176}, V_{183}, V_{189}, $1S_5$, $1S_6$, $1S_{14}$, $1S_{15}$, $1S_{21}$, $1S_{25}$, $1S_{26}$, $1S_{28}$, $1S_{30}$, $1S_{33}$, $1S_{36}$, $1S_{37}$, $1S_{40}$, $1S_{43}$, $1S_{44}$, $1S_{45}$, $1S_{55}$, $1S_{59}$, $1S_{60}$, $1S_{65}$, $1S_{66}$, $1S_{71}$, $2S_{62}$, $4S_{13}$, $4S_{36}$, $4S_{51}$, $5S_{23}$, $5S_{33}$, $7S_1$, $7S_2$, $7S_7$, $7S_{10}$, $7S_{17}$, $7S_{22}$, $7S_{27}$, $7S_{29}$, $7S_{31}$, $7S_{32}$, $7S_{33}$, $7S_{41}$, $7S_{42}$, $7S_{52}$, $7S_{57}$, $7S_{58}$, $7S_{70}$, $7S_{71}$, $7S_{72}$, $7S_{74}$, $7S_{77}$, $7S_{78}$, $7S_{79}$, $7S_{81}$, $7S_{83}$, $7S_{85}$, $1.1L_2$, $1.1L_3$, $1.1L_4$, $1.4L_4$, $1.4L_5$, $1.4L_7$, $1.4L_8$, $1.4L_{12}$, $1.4L_{13}$, $1.5L_4$, $1.5L_5$, $1.7L_1$, $1.7L_2$, $1.7L_3$, $1.7L_5$, $1.7L_6$, $1.7L_{18}$, $1.7L_{21}$, $1.7L_{28}$, $1.7L_{29}$, $1.7L_{32}$, $1.7L_{33}$, $2.7L_{18}$, $2.7L_{19}$, $2.7L_{20}$, $2.8L_1$, $2.8L_2$, $4.7L_1$, $5.7L_1$, $5.7L_9$, $5.7L_{14}$, $7.7L_4$, $7.7L_5$, P_{31}, P_{43}, P_{50}, P_{52}, P_{60} *and* P_{65}*;*

(f) There exist 14 *phase portraits with two disjoint graphics, and they are in the parts* V_{169}, V_{177}, $1S_{53}$, $1S_{56}$, $1S_{57}$, $7S_{67}$, $7S_{75}$, $7S_{76}$, $7S_{82}$, $1.7L_{27}$, $1.7L_{30}$, $1.7L_{31}$, $7.7L_6$ *and* $7.7L_7$*;*

(g) There exist 7 *phase portraits with degenerate graphics, and they are in the parts* $1.2L_8$, $1.3L_2$, P_{23}, P_{57}, P_{58}, P_{64} *and* P_{65}.

In Table 7.2.1 we compare the number of phase portraits possessing some geometrical features such as for instance limit cycles or graphics between the class **QsnSN(C)** and its border.

Table 7.2.1: Comparison between the set **QsnSN(C)** and its border

	QsnSN(C)	border of **QsnSN(C)**
Distinct phase portraits	259	112
Phase portraits with exactly one limit cycle	39	10
Phase portraits with two/double limit cycles	2/1	0
Phase portraits with a finite number of nondegenerate graphics	72	14
Phase portraits with an infinite number of nondegenerate graphics	0	35
Phase portraits with degenerate graphics	0	7

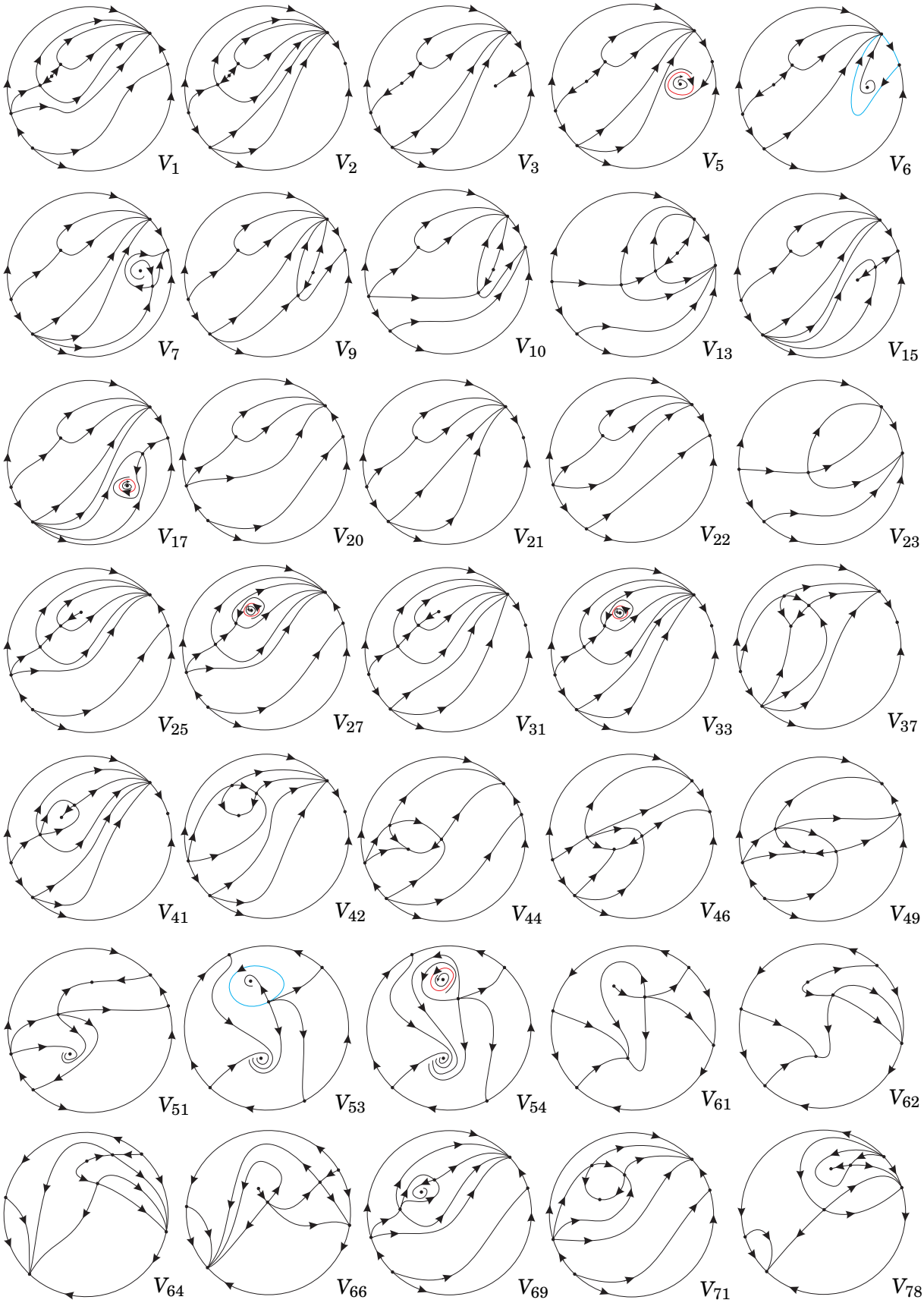

Figure 7.1: Phase portraits for quadratic vector fields with a finite saddle–node $\overline{sn}_{(2)}$ and an infinite saddle–node of type $\binom{0}{2}SN$ in the bisector of first and third quadrants

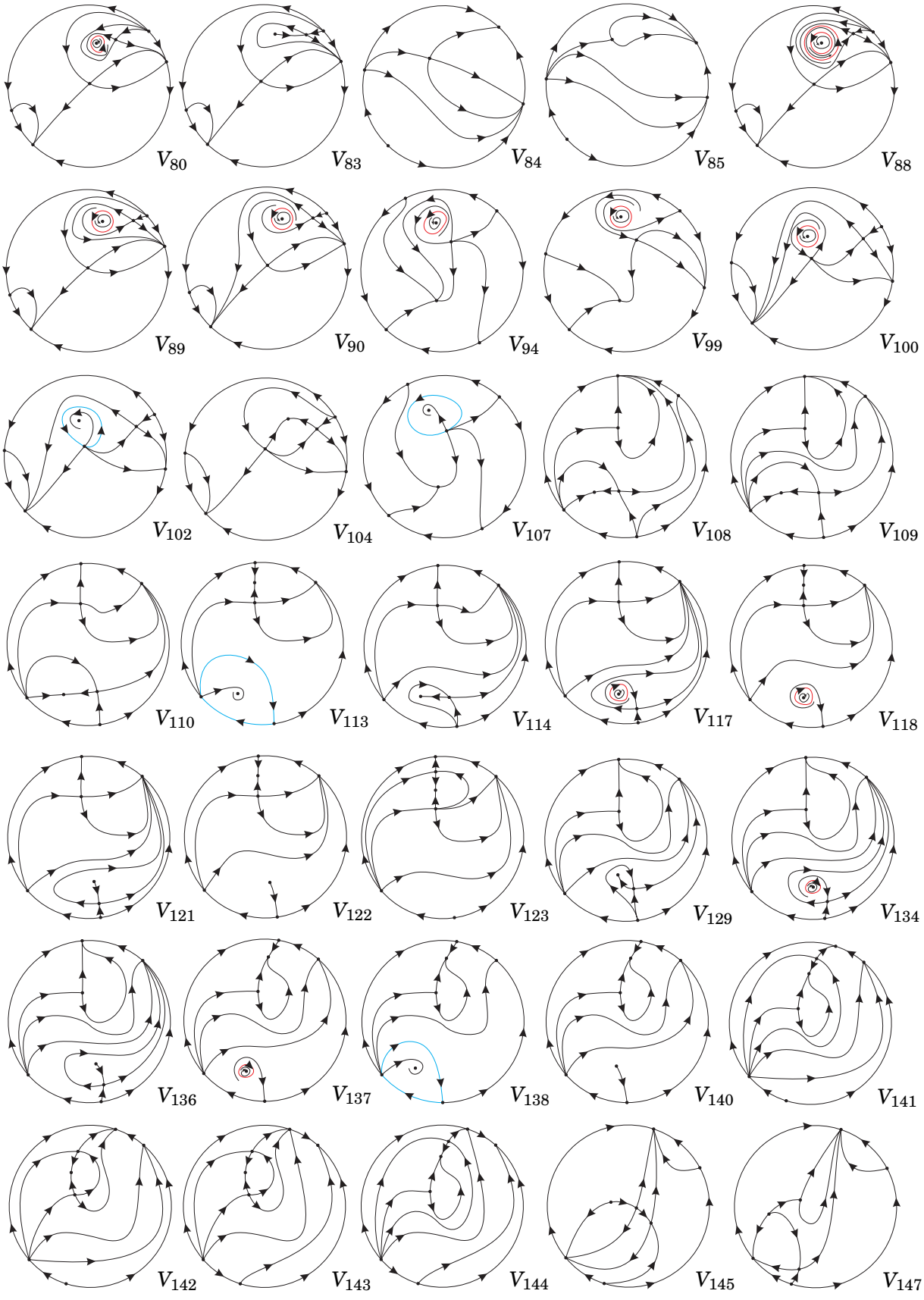

Figure 7.2: Continuation of Figure 7.1

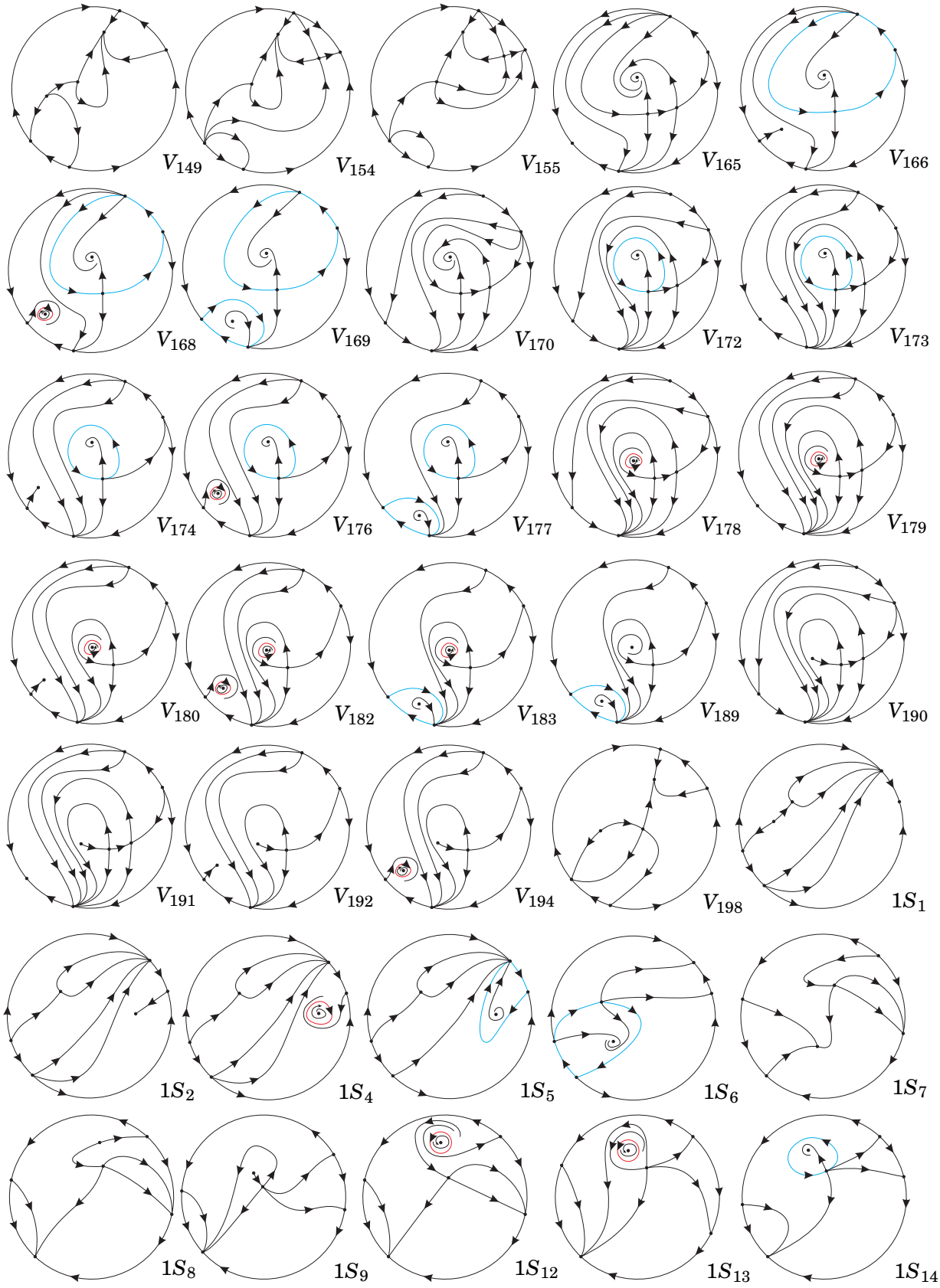

Figure 7.3: Continuation of Figure 7.2

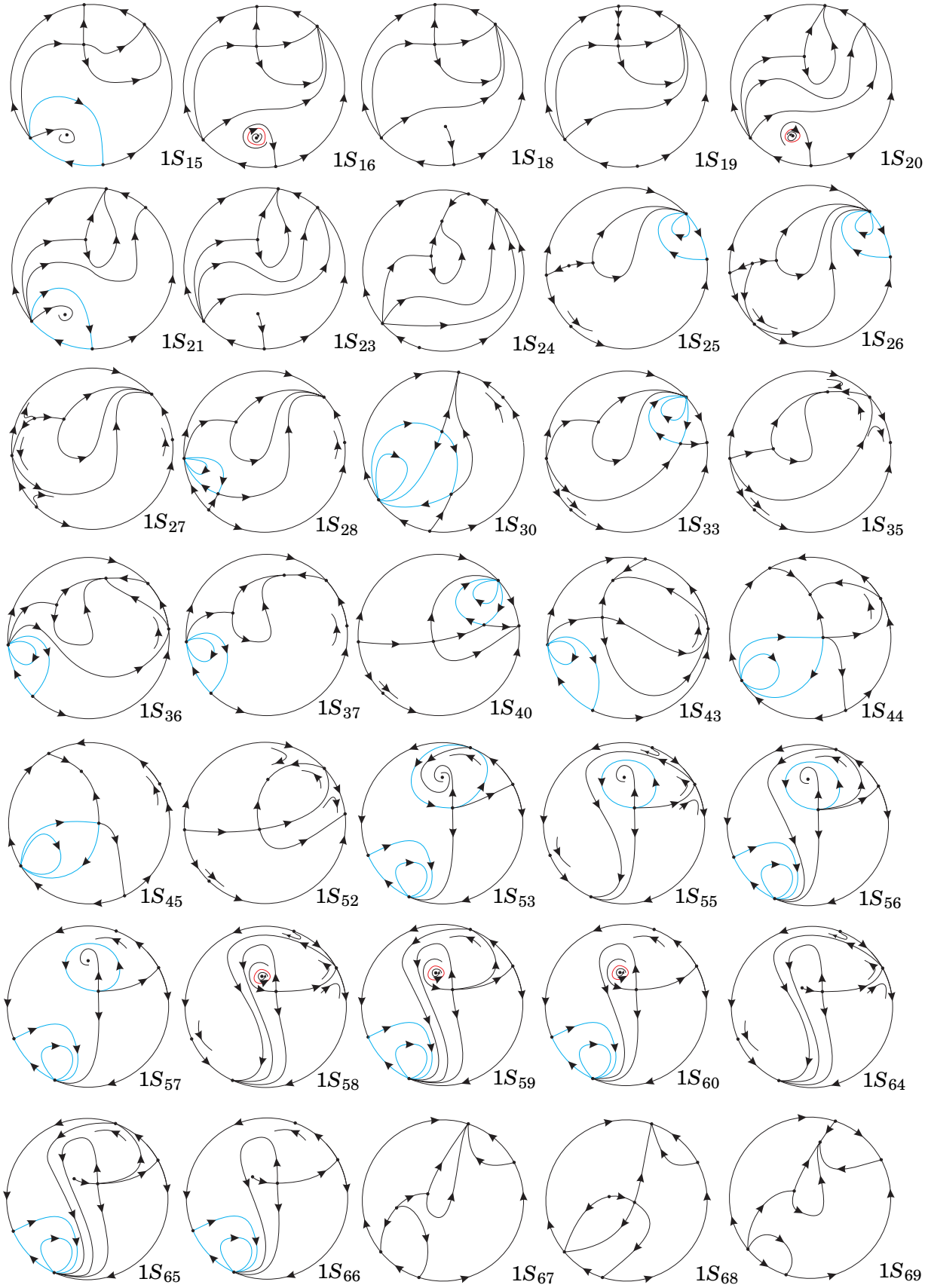

Figure 7.4: Continuation of Figure 7.3

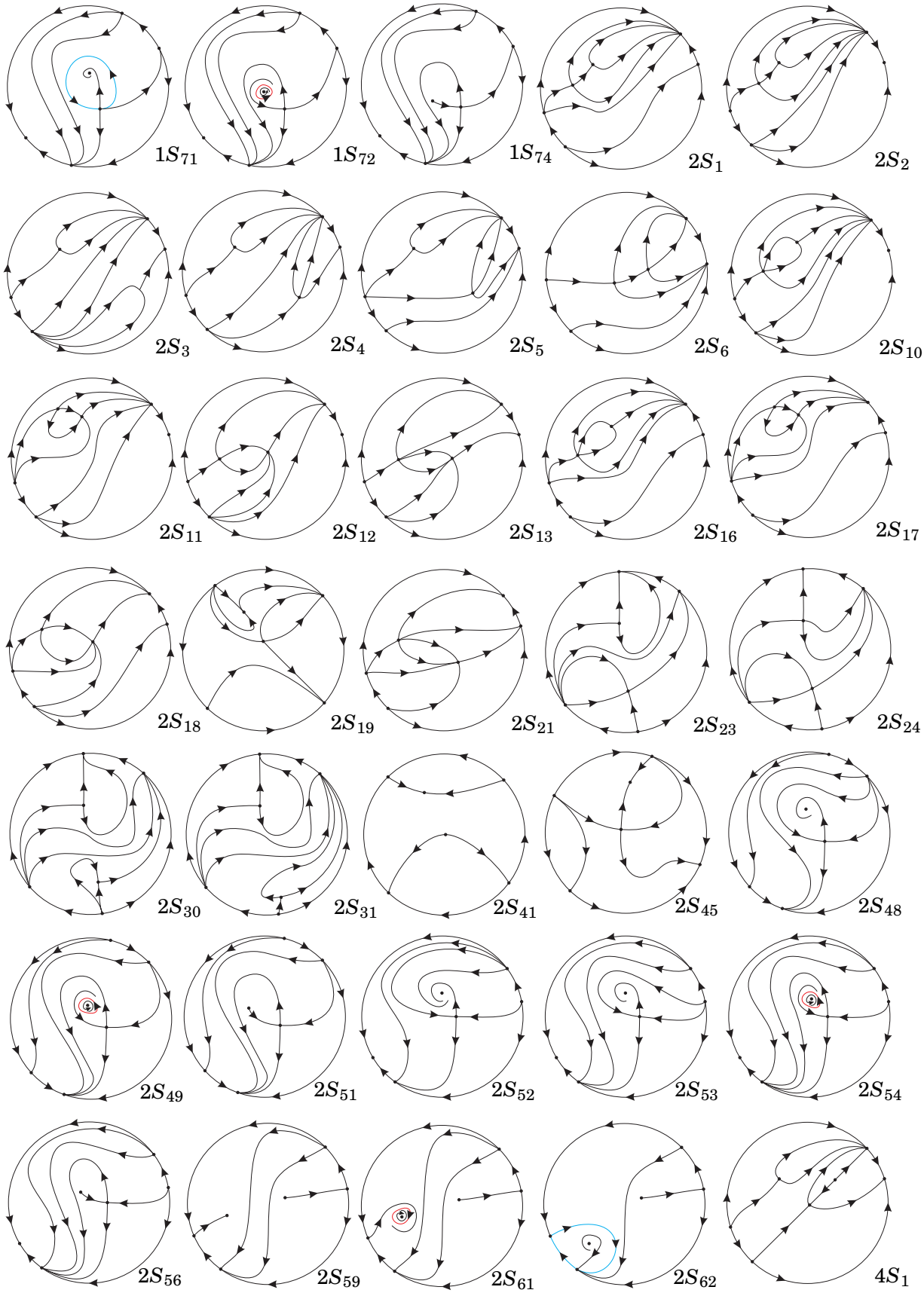

Figure 7.5: Continuation of Figure 7.4

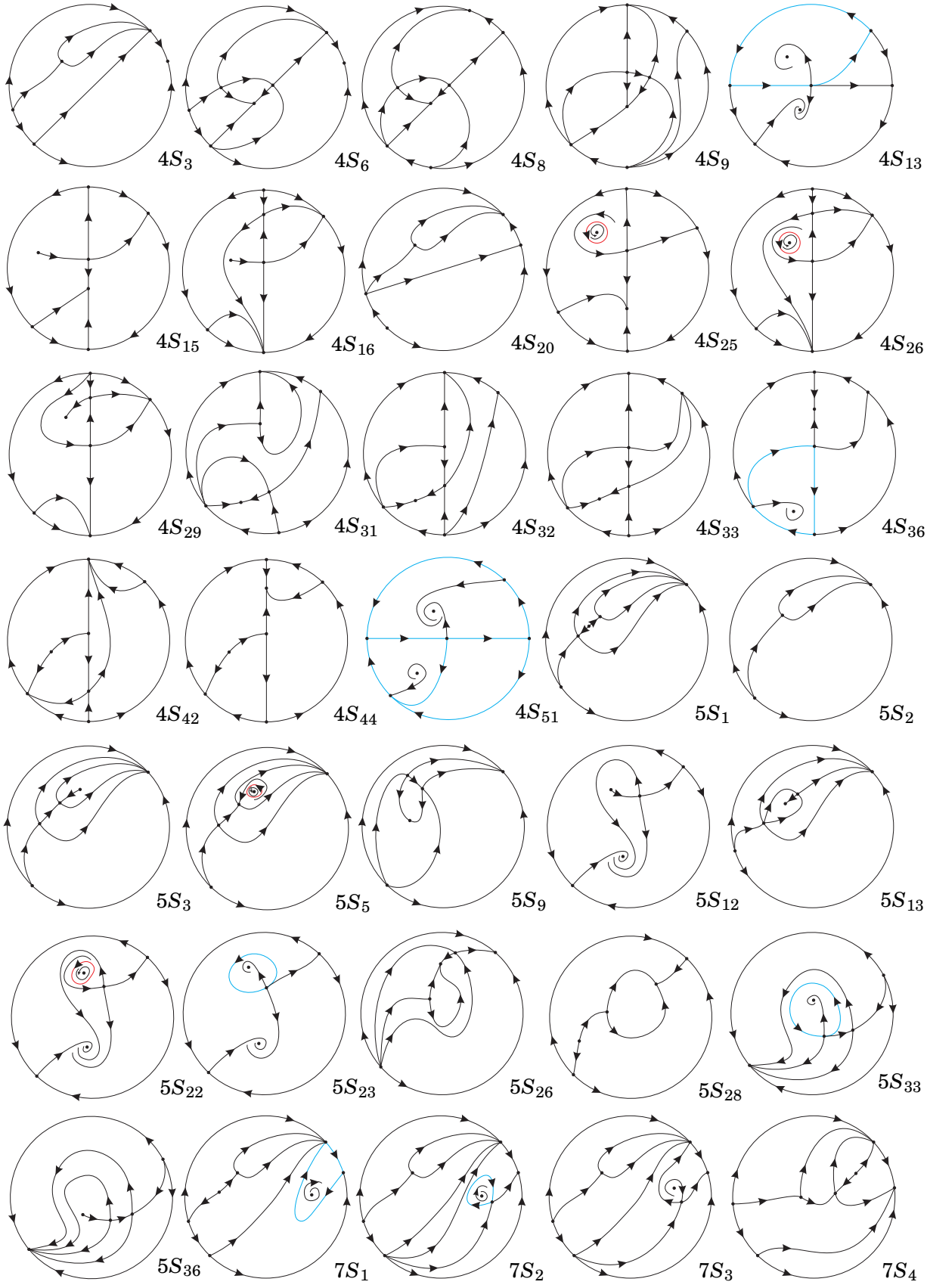

Figure 7.6: Continuation of Figure 7.5

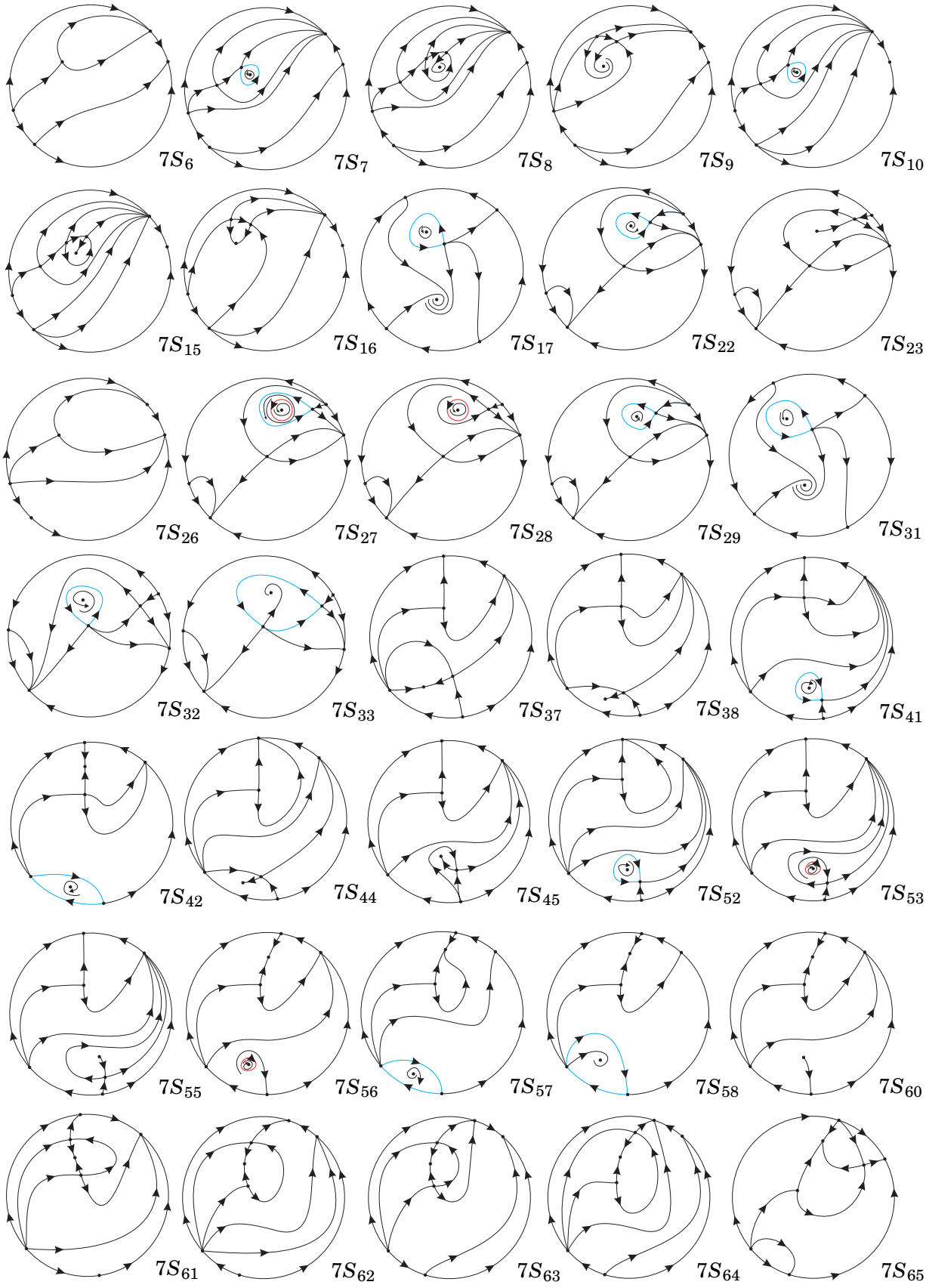

Figure 7.7: Continuation of Figure 7.6

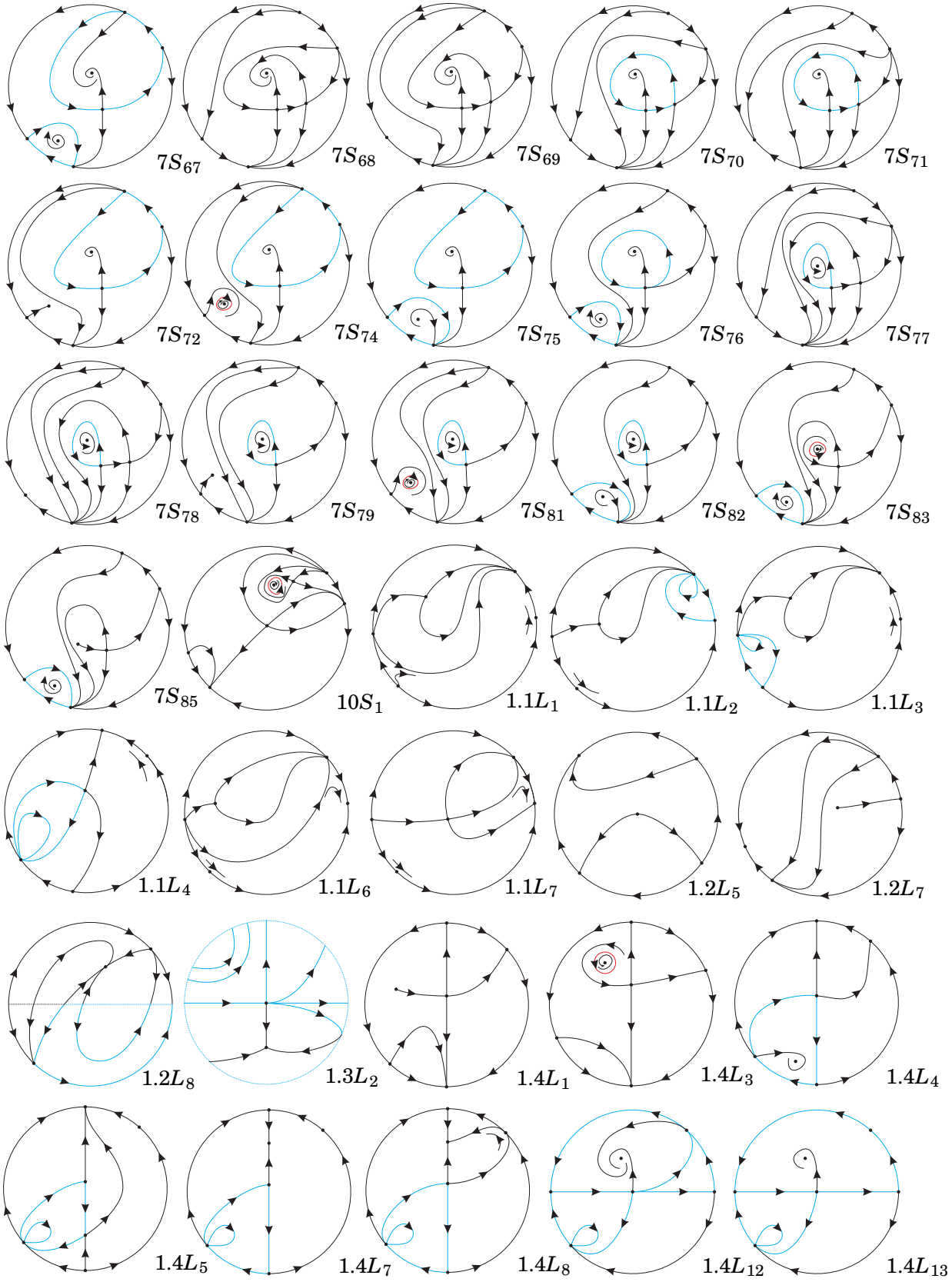

Figure 7.8: Continuation of Figure 7.7

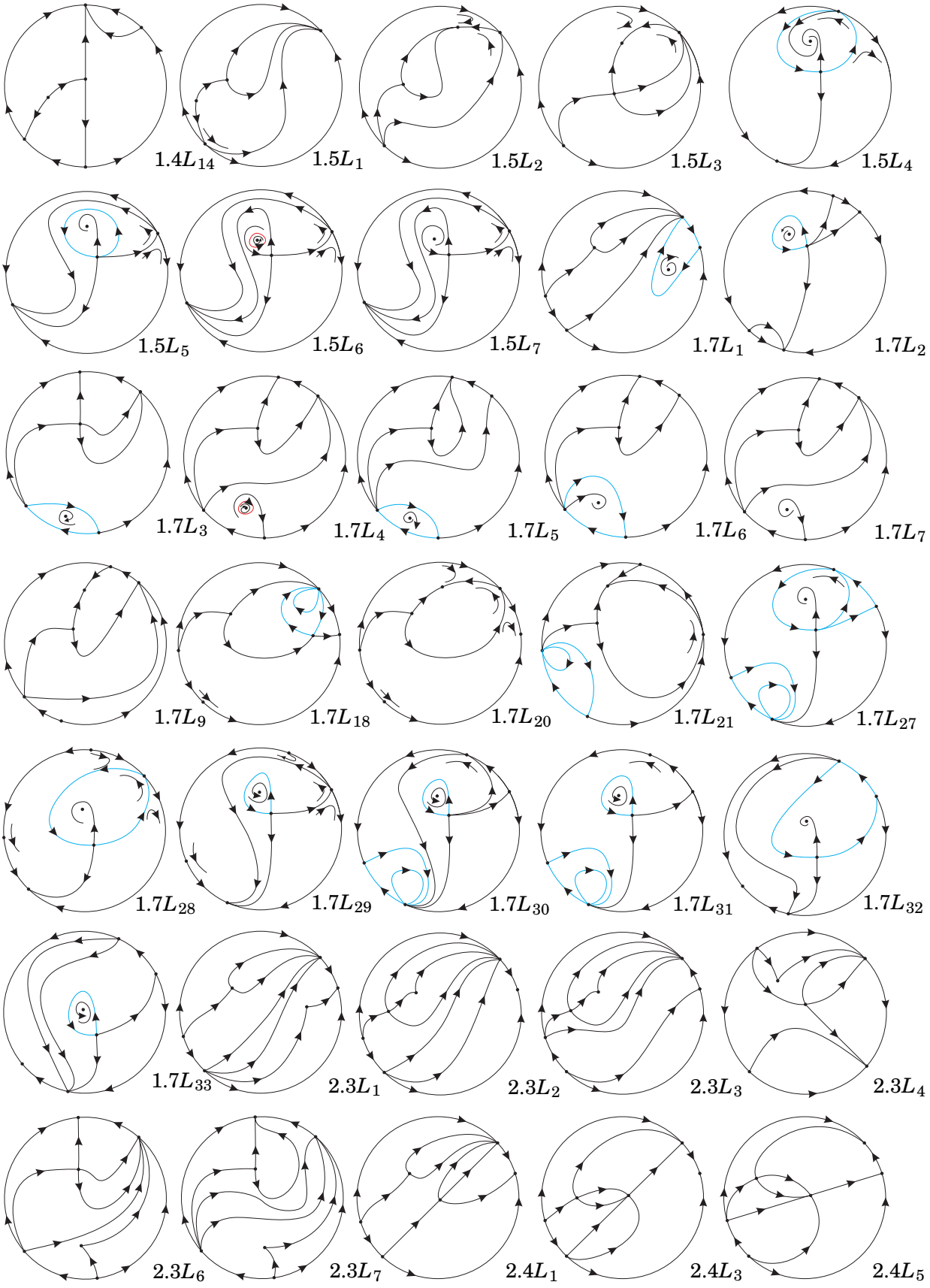

Figure 7.9: Continuation of Figure 7.8

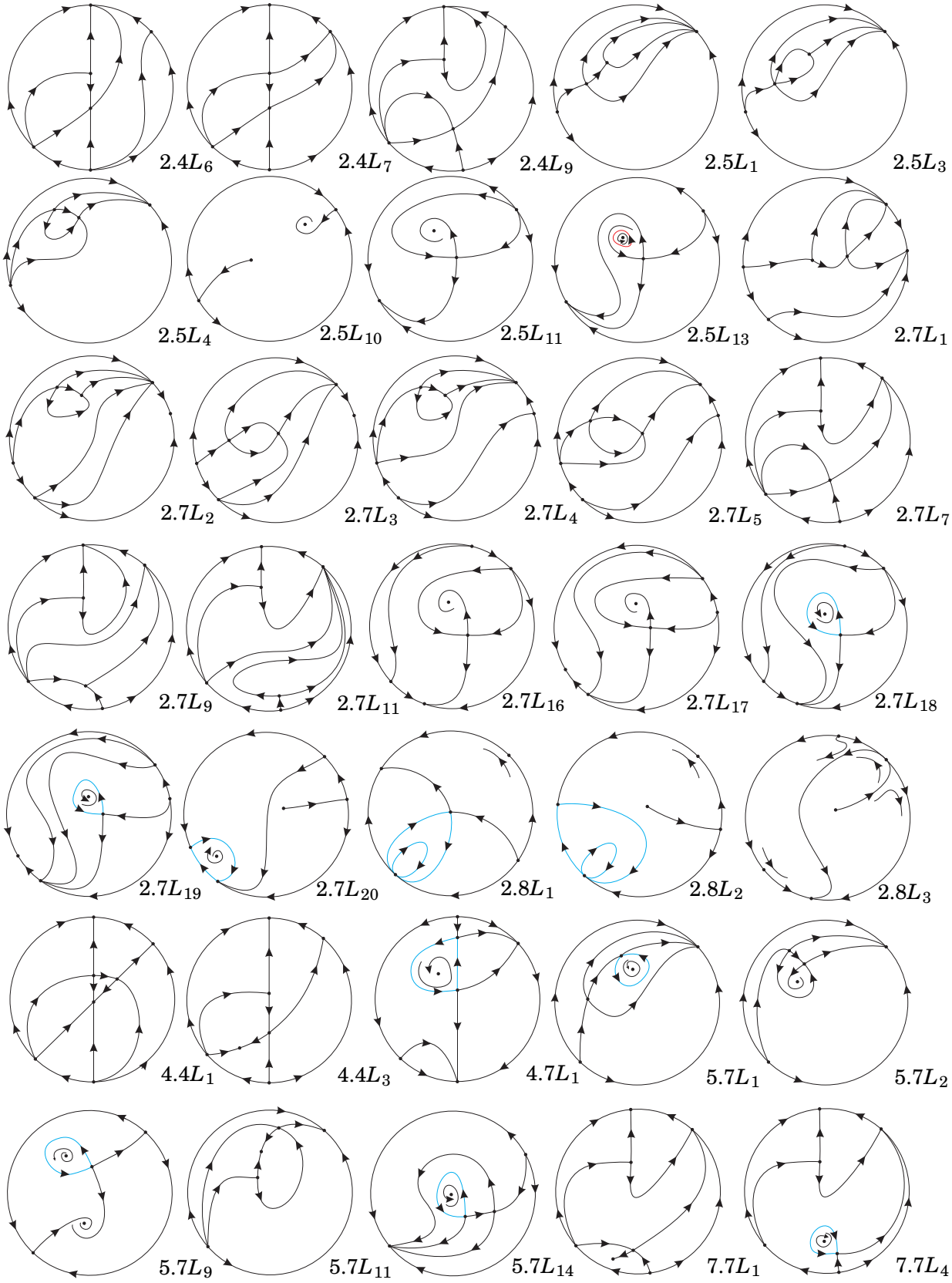

Figure 7.10: Continuation of Figure 7.9

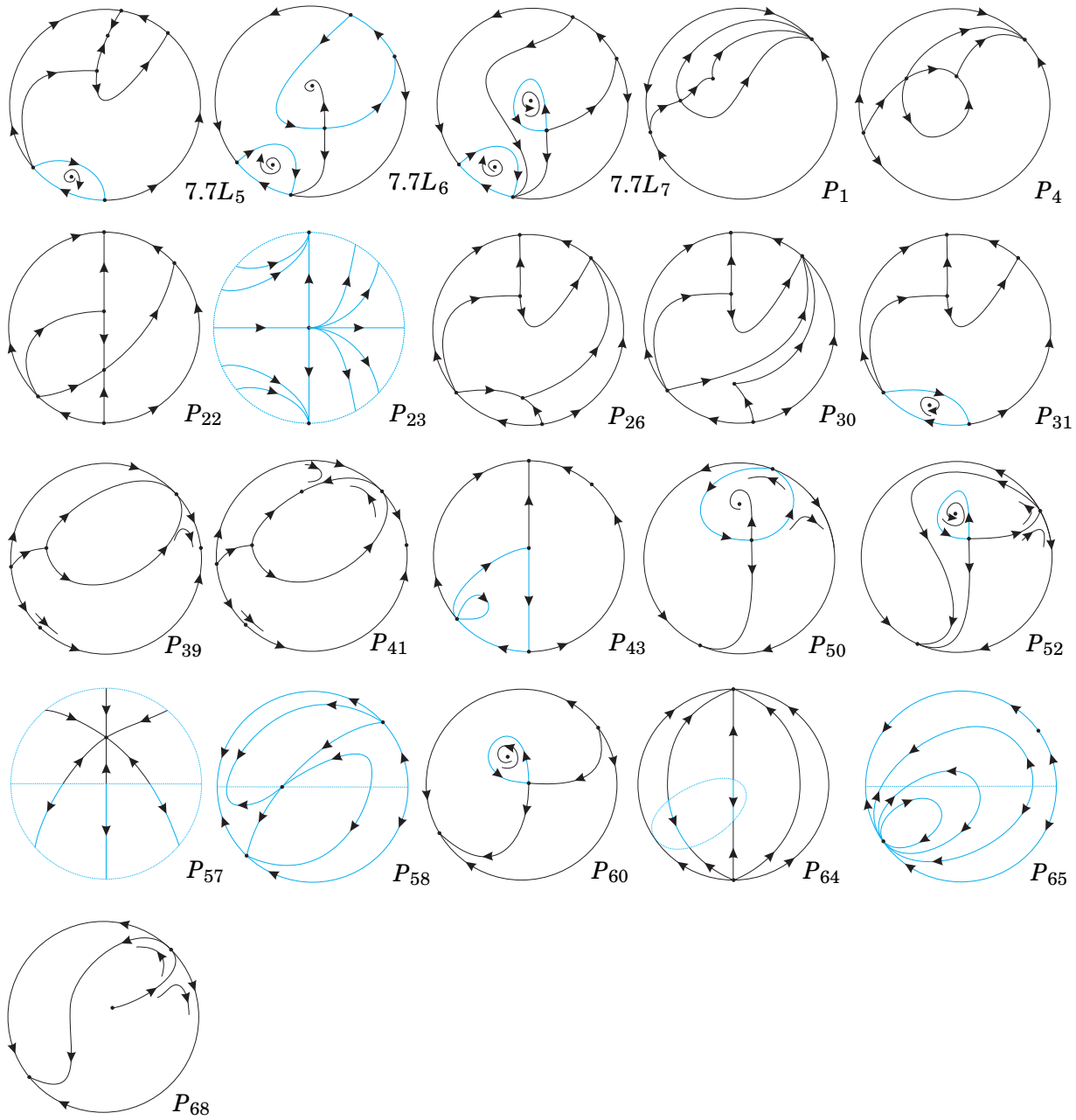

Figure 7.11: Continuation of Figure 7.10

Remark 7.2.2. *Phase portrait P_{65} belongs to two different categories in Theorem 7.2.1 since some of its graphics are nondegenerate.*

Corollary 7.2.3. *There exist* 14 *topologically distinct phase portraits which appear simultaneously in at least two of the three families* $\overline{\textbf{QsnSN(A)}}$, $\overline{\textbf{QsnSN(B)}}$ *and* $\overline{\textbf{QsnSN(C)}}$. *The correspondences are indicated in Table 7.2.2 and the phase portraits in each row are topologically equivalent.*

Table 7.2.2: Topological equivalence among phase portraits from families $\overline{\textbf{QsnSN(A)}}$, $\overline{\textbf{QsnSN(B)}}$ and $\overline{\textbf{QsnSN(C)}}$

$\overline{\textbf{QsnSN(A)}}$	$\overline{\textbf{QsnSN(B)}}$	$\overline{\textbf{QsnSN(C)}}$
V_{15}		$4S_{13}$
$3S_1$		$2.4L_9$
$3S_2$		$2.4L_1$
$3S_3$		$2.4L_3$
$3S_4$		$2.4L_5$
$3.4L_1$		P_{22}
$5S_2$	$5S_3$	
	V_6	$4S_{15}$
	V_7	$4S_{44}$
	$9S_1$	$2S_{41}$
	$5.9L_1$	$2.5L_{10}$
$1.2L_2$	$1.4L_1$	$1.3L_2$
P_1	P_1	P_{23}
P_3	P_2	P_{57}

Corollary 7.2.4. *There exist* 417 *topologically distinct phase portraits in* $\overline{\textbf{QsnSN}}$.

Corollary 7.2.5. *After applying a perturbation, some chosen phase portraits in Figures 7.1 to 7.11 yield all the topologically possible phase portrait of codimension–one from group* (A) *expected to exist (see page 67 for the description of this group). So, the seven codimension–one phase portraits from group* (A) *whose realizability was missing can be constructed after perturbations of some chosen phase portraits from* $\overline{\textbf{QsnSN(C)}}$*; and three codimension–one phase portraits from group* (B) *whose realizability was missing can be constructed after perturbations of some chosen phase portraits from* $\overline{\textbf{QsnSN(C)}}$.

For the class **QsnSN(C)**, from its 259 topologically different phase portraits, 94 occur in three–dimensional parts, 119 in two–dimensional parts, 42 in one–dimensional parts and 4 occur in a single zero–dimensional part.

In Figures 7.1 to 7.11 we have denoted all the singular points with a small disk. We have plotted with wide curves the separatrices and we have added some orbits drawn on the picture with thinner lines to avoid confusion in some required cases.

7.3 Quadratic vector fields with a finite saddle–node $\overline{sn}_{(2)}$ and an infinite saddle–node of type $\overline{\binom{0}{2}}SN$

We consider quadratic differential systems possessing a finite semi–elemental saddle–node $\overline{sn}_{(2)}$ and an infinite semi–elemental saddle–node of type $\overline{\binom{0}{2}}SN$ located in the bisector of the first and third quadrants.

The following result presents the normal form adopted for systems in $\overline{\mathbf{QsnSN(C)}}$.

Proposition 7.3.1. *Every system with a finite semi–elemental double saddle–node $\overline{sn}_{(2)}$ with its eigenvectors in the direction of the axes, with the eigenvector associated with the zero eigenvalue on the horizontal axis, and an infinite saddle–node of type $\overline{\binom{0}{2}}SN$ located in the endpoints of the bisector of the first and third quadrants can be brought via affine transformations and time rescaling to the following normal form*

$$\begin{aligned} \dot{x} &= gx^2 + 2hxy + (-g-2h+n)y^2, \\ \dot{y} &= y + \ell x^2 + (2g+2h-2\ell-n)xy + (2h+\ell+2(-g-2h+n))y^2, \end{aligned} \tag{7.3.1}$$

where g, h, ℓ and n are real parameters and $g \neq 0$.

Proof. We start with system (2.2.2). This system already has a finite semi–elemental saddle–node at the origin (then $g \neq 0$) with its eigenvectors in the direction of the axes. The first step is to place the point $\overline{\binom{0}{2}}SN$ at the point $[1:1:0]$ of the local chart U_1 with coordinates (w,z). For that, we must guarantee that the point $[1:1:0]$ is a singularity of the flow in U_1,

$$\begin{aligned} \dot{w} &= \ell + (-g+2m)w + (-2h+n)w^2 - kw^3 + wz, \\ \dot{z} &= (-g-2hw-kw^2)z. \end{aligned}$$

Then, we set $n = g+2h+k-\ell-2m$ and, by analyzing the Jacobian of the former system after the substitution in n, we set $m = (g-k-2\ell)/2$ in order to have the eigenvalue associated to the eigenvector on $z=0$ being null. Finally, we apply the rotation $k = n-g-2h$ in the parameter space

and obtain the normal form (7.3.1). We note that this rotation is just to simplify the bifurcation diagram. ■

In order to consider the closure of the family **QsnSN(C)** within the set of representatives of **QsnSN(C)** in the parameter space of the normal form (7.3.1), it is necessary to study the case when $g = 0$, which will be discussed later.

We construct the parameter space for systems (7.3.1) in the same way it was constructed for systems (6.3.1) and (6.3.2), but now with respect to the parameter $[\lambda] = [g : h : \ell : n] \in \mathbb{RP}^3$. Due to the symmetry $(x, y, t) \mapsto (-x, -y, t)$ we have $(g, h, \ell, n) \mapsto (-g, -h, -\ell, -n)$, which implies that it is sufficient to consider only $g \geq 0$.

We observe that, except of an affine change of variables and a time rescaling, we can assume $g = 1$ for the case $g \neq 0$.

Before we begin the study of the interactions among the bifurcation surfaces, the next result assures the existence of invariant straight lines under certain conditions.

Lemma 7.3.2. *For all $g \in \mathbb{R}$, systems* (7.3.1) *possess the following invariant straight lines under the specific condition:*

(i) $\{x = 0\}$, *if* $h = (n - g)/2$;

(ii) $\{y = 0\}$, *if* $\ell = 0$;

(iii) $\{y = x - 1/n\}$, *if* $\ell = g$ *and* $n \neq 0$.

Proof. We consider the algebraic curves

$$f_1(x, y) \equiv x = 0, \quad f_2(x, y) \equiv y = 0 \quad \text{and} \quad f_3(x, y) \equiv ny - nx + 1 = 0,$$

and, according to Definition 1.4.1, we show that the polynomials

$$K_1(x, y) = gx + (n - g)y, \quad K_2(x, y) = 1 + (2g + 2h - n)x - 2(g + h - n)y \quad \text{and} \quad K_3(x, y) = ny$$

are the cofactors of $f_1 = 0$, $f_2 = 0$ and $f_3 = 0$, respectively, after restricting systems (7.3.1) to the respective conditions. ■

7.4 The bifurcation diagram of the systems in $\overline{\mathbf{QsnSN(C)}}$

In this section we describe the bifurcation surfaces which are needed for completing the study of the family $\overline{\mathbf{QsnSN(C)}}$.

7.4.1 Bifurcation surfaces due to the changes in the nature of singularities

Most of the invariants and T–comitants needed here have already used in Chapters 5 and 6. So, we shall give only the geometrical meaning and their equations. For further information about them, see Sections 5.4, 6.4 and 6.5.

Bifurcation surfaces in $\mathbb{RP}^3$ due to multiplicities of singularities

($\mathscr{S}_1$) This is the bifurcation surface due to multiplicity of infinite singularities involved with finite singular points. This occurs when at least one finite singular point collides with at least one infinite singular point. This is a quartic whose equation is

$$\mu = n^2(-g^2 - 2gh + 2h\ell + \ell^2 + gn) = 0.$$

($\mathscr{S}_2$) Since this family already has a saddle–node at the origin, the invariant **D** is always zero. The next T–comitant related to finite singularities is **T** (see Proposition 4.5.9). If this T–comitant vanishes, it may mean either the existence of another finite semi–elemental singular point, or the origin being a singular point of higher multiplicity, or the system being degenerate. The equation of this surface is

$$\mathbf{T} = -12g^2(g^2 + 2gh + h^2 - gn) = 0.$$

($\mathscr{S}_5$) Since this family already has a saddle–node at infinity formed by the collision of two infinite singularities, the invariant η is always zero. In this sense, we have to consider a bifurcation related to the existence of either the double infinite singularity $\overline{\binom{0}{2}}\,SN$ plus a simple one, or a triple one. This phenomenon is ruled by the T–comitant $\widetilde{M}$. The equation of this surface is

$$\widetilde{M} = (g + 2h + \ell - n)^2 = 0.$$

The surface of C^∞ bifurcation points due to a strong saddle or a strong focus changing the sign of their traces (weak saddle or weak focus)

($\mathscr{S}_3$) This is the bifurcation surface due to weak finite singularities, which occurs when the trace of a finite singular point is zero. The equation of this surface is given by

$$\mathscr{T}_4 = n(-4g^3 - 8g^2h - 4g^2\ell - 4gh\ell - 8h^2\ell - 4h\ell^2 + 4g^2n + 4g\ell n + \ell^2 n) = 0.$$

We note that this bifurcation surface can either produce a topological change, if the weak point is a focus, or just a C^∞ change, if it is a saddle. However, in the case this bifurcation coincides with a loop bifurcation associated with the same saddle, the change is also topological, as we can see in the analysis of systems (7.3.1) (see page 199).

The surface of C^∞ bifurcation due to a node becoming a focus

($\mathscr{S}_6$) This surface will contain the points of the parameter space where a finite node of the system turns into a focus. This surface is a C^∞ but not a topological bifurcation surface. In fact, when we only cross the surface ($\mathscr{S}_6$) in the bifurcation diagram, the phase portraits do not change topologically. However, this surface is relevant for isolating the parts where a limit cycle surrounding an antisaddle cannot exist. The equation of this surface is given by $W_4 = 0$, where

$$\begin{aligned} W_4 =& n^2(16g^6 + 64g^5h + 64g^4h^2 - 32g^5\ell - 160g^4h\ell - 192g^3h^2\ell - 16g^4\ell^2 + 32g^3h\ell^2 \\ &+ 112g^2h^2\ell^2 - 32gh^3\ell^2 + 32g^3\ell^3 + 64g^2h\ell^3 + 32h^3\ell^3 + 16h^2\ell^4 - 32g^5n \\ &- 64g^4hn + 64g^4\ell n + 160g^3h\ell n + 8g^3\ell^2n - 80g^2h\ell^2n + 16gh^2\ell^2n - 40g^2\ell^3n \\ &- 8gh\ell^3n - 16h^2\ell^3n - 8h\ell^4n + 16g^4n^2 - 32g^3\ell n^2 + 8g^2\ell^2n^2 + 8g\ell^3n^2 + \ell^4n^2). \end{aligned}$$

Bifurcation surface in $\mathbb{RP}^3$ due to the presence of invariant straight lines

($\mathscr{S}_4$) This surface will contain the points of the parameter space where an invariant straight line appears (see Lemma 7.3.2). This surface is split in some parts. Depending on these parts, the straight line may contain connections of separatrices from different points or not. So, in some cases, it may imply a topological bifurcation and, in others, just a C^∞ bifurcation. The equation of this surface is given by

$$\mathrm{Inv} = \ell(\ell - g)(g + 2h - n) = 0.$$

These bifurcation surfaces are all algebraic and they, except ($\mathscr{S}_4$), are the bifurcation surfaces of singularities of systems (7.3.1) in the parameter space. We shall discover other two bifurcation surfaces not necessarily algebraic. On one of them the systems have global connection of separatrices different from that given by ($\mathscr{S}_4$) and on the other the systems possess double limit cycle. The equations of these bifurcation surfaces can only be determined approximately by means of numerical tools. Using arguments of continuity in the phase portraits we can prove the existence of these components not necessarily algebraic in the part where they appear, and we can check

them numerically. We shall name them surfaces ($\mathscr{S}_7$) (connection of separatrices) and ($\mathscr{S}_{10}$) (double limit cycles).

Remark 7.4.1. *On surface ($\mathscr{S}_{10}$), the respective systems have at least one double limit cycle. Although this surface is obtained numerically, we can predict in which portion of the bifurcation diagram it can be placed. It must be in the neighborhood of the points of the bifurcation diagram corresponding to a weak focus $f^{(2)}$ or a weak saddle $s^{(1)}$ which forms a loop. So, according to [61, Main Theorem, item (b_2)], the necessary condition for the existence of weak points of order two or higher is governed by $\mathscr{T}_4 = \mathscr{F}_1 = 0$. The expression of $\mathscr{F}_1$ is given by $\mathscr{F}_1 = -2g^2 - 4gh + 4g\ell + 6h\ell + 2gn - 3\ell n$.*

We shall foliate the 3−dimensional bifurcation diagram in $\mathbb{RP}^3$ by the planes $n = n_0$, n_0 constant, plus the open half sphere $g = 0$ and we shall give pictures of the resulting bifurcation diagram on these planar sections on a disk or in an affine chart of $\mathbb{R}^2$.

In what follows we work in the chart of $\mathbb{RP}^3$ corresponding to $g \neq 0$, and we take $g = 1$. To do the study, we shall use pictures which are drawn on planes $n = n_0$ of $\mathbb{RP}^3$, having coordinates $[1 : h : \ell : n_0]$. In these planes the coordinates are (h, ℓ) where the horizontal line is the h−axis.

As the final bifurcation diagram is quite complex, it is useful to introduce colors which will be used to talk about the bifurcation surfaces. They are the same as described in Section 6.4, on page 105, except for surface ($\mathscr{S}_{10}$) which is drawn in gray.

The following lemmas of this section study the geometrical behavior of the surfaces for $g \neq 0$ (the case $g = 0$ will be considered separately), that is, their singularities, their intersection points and their extrema (maxima and minima) with respect to the coordinate n.

Lemma 7.4.2. *For $gn \neq 0$, surface ($\mathscr{S}_1$) has no singularities and, for $g \neq 0$ and $n = 0$, it has two straight lines of singularities given by $[1 : h : 1 : 0]$ and $[1 : h : -1 - 2h : 0]$.*

Proof. We observe that, for $gn \neq 0$, surface ($\mathscr{S}_1$) with equation $\mu = n^2(-1 - 2h + 2h\ell + \ell^2 + n) = 0$ is the union of a double plane and a conic with no singularities. So, the only singularities of ($\mathscr{S}_1$) will be the intersection between these two components. In this sense, we set $n = 0$ and, solving the expression of the conic with respect to ℓ, we find the straight lines $[1 : h : 1 : 0]$ and $[1 : h : -1 - 2h, 0]$. ∎

Lemma 7.4.3. *For $g \neq 0$, surface ($\mathscr{S}_2$) has no singularities. Moreover, this surface assumes its minimum (with respect to the coordinate n) at $h = -1$.*

Proof. Setting $g \neq 0$, it follows straightforwardly from the expression of $\mathbf{T} = -12(1+2h+h^2-n)$, which is a parabola for each value of n. In addition, if we parametrize this surface, we obtain $[1:h:\ell:(1+h)^2]$ which clearly has a minimum at $h=-1$, which corresponds to $n=0$. ∎

Lemma 7.4.4. *For $gn \neq 0$, surface $(\mathscr{S}_3)$ has a straight line of singularities given by $[1:1/2:-2:n]$. Moreover, in this surface there exist two distinguished points: $[1:1/2:-2:2]$ and $[1:1/2:-2:9/4]$. For $g \neq 0$ and $n=0$, surface $(\mathscr{S}_3)$ has two curves of singularities: the straight line $[1:h:-1-2h:0]$ and the hyperbola $[1:h:-1/h:0]$, and they intersect at the points $[1:-1:1:0]$ and $[1:1/2:-2:0]$.*

Proof. For $gn \neq 0$, surface $(\mathscr{S}_3)$ is the union of a plane and a cubic. As the plane (namely, $\{n=0\}$) has no singularities, we consider only the cubic $C = 4n-8h-4+(4n-4h-8h^2-4)\ell+(n-4h)\ell^2 = 0$. Computing its derivatives, we obtain:

$$\begin{aligned} C_h &\equiv \frac{\partial C}{\partial h} = -4(2+\ell+4h\ell+\ell^2), \\ C_\ell &\equiv \frac{\partial C}{\partial \ell} = -2(2+2h+4h^2+4h\ell-2n-\ell n), \\ C_n &\equiv \frac{\partial C}{\partial n} = (2+\ell)^2, \end{aligned}$$

and solving them (for $g \neq 0$) we get the straight line $[1:1/2:-2:n]$ of singularities. We verify that the determinant of the Hessian of C restricted to this straight line is identically zero. In addition, calculating the discriminant of C with respect to h and ℓ, we obtain, respectively,

$$\begin{aligned} \mathrm{Discrim}_h(C) &= 16(2+\ell)^2(1-2\ell+\ell^2+2\ell n), \\ \mathrm{Discrim}_\ell(C) &= 16(2h-1)^2(1+2h+h^2-n). \end{aligned}$$

So, the resultant of both discriminants with respect to h is

$$\mathrm{Res}_h(\mathrm{Discrim}_h(C), \mathrm{Discrim}_\ell(C)) = 65536(2+\ell)^8(1-2\ell+\ell^2+2\ell n)^4,$$

which vanishes if, and only if, $\ell=-2$ or $n=(-1+2\ell-\ell^2)/(2\ell)$, implying that $n=9/4$ (which is obtained by evaluating the resultant on the line of singularities) is a distinguished point.

Now, we want to investigate the existence of a value of the parameter $n=n_0$ at which the cubic C factorizes, i.e. we want to rewrite C as one of the following forms:

$$C(h,\ell,n_0) = (h-h_0)D_2(h,\ell) \quad \text{or} \quad C(h,\ell,n_0) = (\ell-\ell_0)D_2(h,\ell),$$

where $D_2(h,\ell)$ is a polynomial of degree 2 in the variables h and ℓ. For this, we rewrite the cubic

C in the forms:

$$C_1(h,\ell,n_0) = -4(1+2h-n_0) - 4(1+h+2h^2-n_0)\ell + (-4h+n_0)\ell^2, \text{ and}$$
$$C_2(h,\ell,n_0) = -4 - 4\ell + 4n_0 + 4\ell n_0 + \ell^2 n_0 - 4(2+\ell+\ell^2)h - 8\ell h^2.$$

As we are interested in the set of zeroes of C, we equalize to zero the coefficients of C_1 and C_2 in the variables ℓ and h, respectively, and obtain the systems:

$$\begin{array}{lll} 1+2h-n_0=0, & & 4+4\ell-4n_0-4\ell n_0-\ell^2 n_0=0, \\ 1+h+2h^2-n_0=0, & \text{and} & 2+\ell+\ell^2=0, \\ n_0-4h=0, & & \ell=0. \end{array}$$

Solving the systems above, we see that only the first one is possible and its unique solution is $h = 1/2, n_0 = 2$. Thus, we can factorize the cubic C as $C(h,\ell,2) = -2(2h-1)(2+2\ell+2h\ell+\ell^2)$, implying that $n = 2$ is also a distinguished value of the parameter n.

In the case $g \neq 0$ and $n = 0$, we have $\mathscr{T}_4 \equiv 0$. We denote by F the derivative of $\mathscr{T}_4$ with respect to n, and under the conditions $g \neq 0$ and $n = 0$, we obtain $F = -4(1+2h+\ell)(1+h\ell)$. So, $1+2h+\ell = 0$ and $1+h\ell = 0$ are the singular curves of $(\mathscr{S}_3)$ with $n = 0$, which correspond to the projective curves $[1:h:-1-2h:0]$ and $[1:h:-1/h:0]$. In addition, it is easy to see that both curves intersect at the points $[1:-1:1:0]$ and $[1:1/2:-2:0]$. ∎

Lemma 7.4.5. *For $g \neq 0$, surface $(\mathscr{S}_4)$ has two straight lines of singularities given by* $[1:(n-1)/2:0:n]$ *and* $[1:(n-1)/2:1:n]$.

Proof. For $g \neq 0$, we see that, by the expression $\mathrm{Inv} = \ell(\ell-1)(n-1-2h)$, surface $(\mathscr{S}_4)$ is the union of two parallel planes with a transversal one. The planes themselves have no singularities, so that the singularities of $(\mathscr{S}_4)$ consist of the intersections among them, which are the straight lines $[1:(n-1)/2:0:n]$ and $[1:(n-1)/2:1:n]$. ∎

Lemma 7.4.6. *For $g \neq 0$, surface $(\mathscr{S}_5)$ has no singularities.*

Proof. For $g \neq 0$, it follows directly from the expression of $\widetilde{M} = (1+2h+\ell-n)^2$, which is a plane for each value of n. ∎

Lemma 7.4.7. *For $gn \neq 0$, surface $(\mathscr{S}_6)$ has two curves of singularities:* $[1:(n-1)/2:0:n]$ *(a straight line) and* $[1:(\ell-2)/\ell:\ell:4(4-7\ell+2\ell^2+\ell^3)/(\ell(-4+4\ell+\ell^2))]$. *Moreover, the curve* $[1:(\ell-2)/\ell:\ell:4(4-7\ell+2\ell^2+\ell^3)/(\ell(-4+4\ell+\ell^2))]$ *assumes its extrema (with relation to the coordinate*

n) in the values $\ell=-4$, $\ell=1$, $\ell=(-3\pm\sqrt{41})/4$ *and* $\ell=f^{-1}(n_0)$, *where* $f=4(4-7\ell+2\ell^2+\ell^3)/(\ell(-4+4\ell+\ell^2))$ *and* $n_0=(3-(1548-83\sqrt{249})^{1/3}/3^{2/3}-61/(3(1548-83\sqrt{249}))^{1/3})/2$. *For* $g\neq 0$ *and* $n=0$, *its singularities lie on the two straight lines* $[1:h:1:0]$ *and* $[1:h:-1-2h:0]$ *and on the two curves* $[1:(1-2\ell\pm\sqrt{1-4\ell+5\ell^2-2\ell^3})/\ell^2:\ell:0]$.

Proof. For $g\neq 0$, by the expression of W_4, surface $(\mathscr{S}_6)$ is the union of a (double) plane with a sixth–degree surface, which has singularities by its own. As the plane (namely, $\{n=0\}$) has no singularities, we consider only the sixth–degree surface

$$\begin{aligned}S=&16+64h+64h^2-32\ell-160h\ell-192h^2\ell-16l^2+32h\ell^2+112h^2\ell^2-32h^3\ell^2+32\ell^3\\&+64h\ell^3+32h^3\ell^3+16h^2\ell^4-32n-64hn+64\ell n+160h\ell n+8\ell^2n-80h\ell^2n+16h^2\ell^2n\\&-40\ell^3n-8h\ell^3n-16h^2\ell^3n-8h\ell^4n+16n^2-32\ell n^2+8\ell^2n^2+8\ell^3n^2+\ell^4n^2=0.\end{aligned}$$

Computing the derivatives of S, we have:

$$\begin{aligned}S_h\equiv\frac{\partial S}{\partial h}=&8(\ell-1)(-8-16h+12\ell+32h\ell+8\ell^2+4h\ell^2+12h^2\ell^2+4h\ell^3\\&+8n-12\ell n-2\ell^2n-4h\ell^2n-\ell^3n),\\S_\ell\equiv\frac{\partial S}{\partial \ell}=&4(-8-40h-48h^2-8\ell+16h\ell+56h^2\ell-16h^3\ell+24\ell^2+48h\ell^2\\&+24h^3\ell^2+16h^2\ell^3+16n+40hn+4\ell n-40h\ell n+8h^2\ell n-30\ell^2n\\&-6h\ell^2n-12h^2\ell^2n-8h\ell^3n-8n^2+4\ell n^2+6\ell^2n^2+\ell^3n^2),\\S_n\equiv\frac{\partial S}{\partial n}=&-2(16+32h-32\ell-80h\ell-4\ell^2+40h\ell^2-8h^2\ell^2+20\ell^3+4h\ell^3\\&+8h^2\ell^3+4h\ell^4-16n+32\ell n-8\ell^2n-8\ell^3n-\ell^4n).\end{aligned}$$

Moreover, we calculate the resultant with respect to h of S with each one of its derivatives and we obtain:

$$\begin{aligned}R_h^h\equiv\mathrm{Res}_h(S,S_h)=&-32768\alpha^2\ell^4(\ell-1)^3(16-96\ell+224\ell^2-256\ell^3+144\ell^4-32\ell^5-32n+160\ell n\\&-296\ell^2n+248\ell^3n-88\ell^4n+8\ell^5n+16n^2-64\ell n^2+120\ell^2n^2-112\ell^3n^2\\&+13\ell^4n^2-16\ell^2n^3+16\ell^3n^3),\\R_h^\ell\equiv\mathrm{Res}_h(S,S_\ell)=&32768\alpha^2\ell^4(-4+8\ell-4\ell^2+4n-4\ell n+\ell^2n)^3(-4+8\ell-4\ell^2-2\ell n+\ell^2n),\\R_h^n\equiv\mathrm{Res}_h(S,S_n)=&-4096\alpha^2\ell^4(\ell-1)^2(-16+80\ell-144\ell^2+104\ell^3-16\ell^4-8\ell^5+32n-128\ell n\\&+152\ell^2n-32\ell^3n-24\ell^4n-2\ell^5n-16n^2+48\ell n^2-40\ell^2n^2+7\ell^4n^2+\ell^5n^2),\end{aligned}$$

where $\alpha \equiv -16+28\ell-8\ell^2-4\ell^3-4\ell n+4\ell^2 n+\ell^3 n$. Now, to assure that all the resultants above vanish (and, hence, S and its derivatives), we must have $\ell\alpha=0$.

The case $\ell=0$: If $\ell=0$, then:

$$\begin{aligned} S &= 16(1+2h-n)^2=0,\\ S_h &= 64(1+2h-n)=0,\\ S_\ell &= -32(1+2h-n)(1+3h-n)=0,\\ S_n &= -32(1+2h-n)=0 \end{aligned}$$

if, and only if, $n=1+2h$. So, we obtain a straight line of singularities given by $[1:(n-1)/2:0:n]$.

The case $\alpha=0$: If $\alpha=0$, then

$$n=\frac{4(4-7\ell+2\ell^2+\ell^3)}{\ell(-4+4\ell+\ell^2)},\quad \ell\neq 0,\ \ell\neq 2(-1\pm\sqrt{2}), \tag{7.4.1}$$

and

$$\begin{aligned} S =& 16(\ell-1)(2-\ell+h\ell)^2(16-32\ell+4\ell^2-8h\ell^2+8\ell^3+8h\ell^3+5\ell^4+2h\ell^4\\ &+\ell^5)/(\ell^2(-4+4\ell+\ell^2))=0,\\ S_h =& 32(\ell-1)(2-\ell+h\ell)(16-40\ell+16\ell^2-12h\ell^2+6\ell^3+12h\ell^3+4\ell^4+3h\ell^4\\ &+\ell^5)/(\ell^2(-4+4\ell+\ell^2))=0,\\ S_\ell =& 32(2-\ell+h\ell)(32-64\ell+24h\ell+20\ell^2-56h\ell^2+8h^2\ell^2+6\ell^3+32h\ell^3-20h^2\ell^3\\ &+13\ell^4-5h\ell^4+10h^2\ell^4-4\ell^5+5h\ell^5+3h^2\ell^5-2\ell^6+2h\ell^6)/(\ell^2(-4+4\ell+\ell^2))=0,\\ S_n =& -8(\ell-1)(2-\ell+h\ell)(-8+8\ell+4\ell^2+2h\ell^2+\ell^3)/\ell=0 \end{aligned}$$

if, and only if, $h=(\ell-2)/\ell$. So, we obtain the curve of singularities given by

$$\left[1:\frac{\ell-2}{\ell}:\ell:\frac{4(4-7\ell+2\ell^2+\ell^3)}{\ell(-4+4\ell+\ell^2)}\right].$$

We remark that the conditions in ℓ in equation (7.4.1) are not restrictions since $\alpha\neq 0$ under $\ell=0$ or $\ell=2(-1\pm\sqrt{2})$.

In order to find the extrema of the curve $[1:(\ell-2)/\ell:\ell:4(4-7\ell+2\ell^2+\ell^3)/(\ell(-4+4\ell+\ell^2))]$, we equalize the last coordinate to n and obtain the polynomial $p=-4(\ell-1)^2(4+\ell)+\ell(-4+4\ell+\ell^2)n$.

Computing its discriminant with respect to ℓ, we have:

$$\mathrm{Discrim}_\ell(p) = 256n(125 - 17n - 9n^2 + 2n^3),$$

whose solutions are $n = 0$ and $n = (3 - (1548 - 83\sqrt{249})^{1/3}/3^{2/3} - 61/(3(1548 - 83\sqrt{249}))^{1/3})/2 \approx -3.40133804\ldots$. Besides, we consider the leading coefficient of p in ℓ and solve it with respect to n, obtaining $n = 4$. This proves that p has degree 3 for every n, except when $n = 4$. Finally, solving the equation $p = 0$ by substituting n by the singular values of n, we obtain $\ell = -4$, $\ell = 1$, $\ell = (-3 \pm \sqrt{41})/4$ and $\ell = f^{-1}(n_0)$, where $f = 4(4 - 7\ell + 2\ell^2 + \ell^3)/(\ell(-4 + 4\ell + \ell^2))$ and $n_0 = (3 - (1548 - 83\sqrt{249})^{1/3}/3^{2/3} - 61/(3(1548 - 83\sqrt{249}))^{1/3})/2$, which are the critical values of the curve with respect to n.

Now, restricting W_4 to $g \neq 0$ and $n = 0$, its expression becomes

$$W_4\big|_{g\neq 0, n=0} = 16(\ell - 1)(1 + 2h + \ell)(-1 - 2h + 2\ell + 4h\ell + h^2\ell^2).$$

Under these conditions, $\ell - 1 = 0$, $1 + 2h + \ell = 0$ and $1 + 2h - 2\ell - 4h\ell - h^2\ell^2 = 0$ are the singular curves of $(\mathscr{S}_6)$ with $n = 0$, which correspond to the projective curves $[1 : h : 1 : 0]$, $[1 : h : -1 - 2h : 0]$ and $[1 : (1 - 2\ell \pm \sqrt{1 - 4\ell + 5\ell^2 - 2\ell^3})/\ell^2 : \ell : 0]$. ∎

Lemma 7.4.8. *For $g \neq 0$, the invariant $\mathscr{F}_1$ defined in Remark 7.4.1 has a straight line of singularities given by* $[1 : (3n - 4)/6 : 2/3 : n]$.

Proof. Computing the derivatives of $\mathscr{F}_1$, we have:

$$\frac{\partial \mathscr{F}_1}{\partial h} = 2(3\ell - 2), \quad \frac{\partial \mathscr{F}_1}{\partial \ell} = 4 + 6h - 3n, \quad \frac{\partial \mathscr{F}_1}{\partial n} = 2 - 3\ell,$$

and the unique solution of the homogenous systems formed by them is $h = n/2 - 2/3$, $\ell = 2/3$. So, we obtain the curve of singularities given by $[1 : (3n - 4)/6 : 2/3 : n]$. ∎

Lemma 7.4.9. *For $g \neq 0$, surfaces $(\mathscr{S}_1)$ and $(\mathscr{S}_2)$ intersect along the straight line* $[1 : -1 : \ell : 0]$ *and the parabola* $[1 : h : -h : (1 + h)^2]$. *Moreover, the curve* $[1 : h : -h : (1 + h)^2]$ *assumes its extremum (with relation to the coordinate n) in the value $h = -1$ and, in addition, the contact along this curve is even.*

Proof. Solving the system of equations

$$(\mathscr{S}_1) : n^2(-1 - 2h + 2h\ell + \ell^2 + n) = 0, \quad (\mathscr{S}_2) : -12(1 + 2h + h^2 - n) = 0,$$

we obtain the two solutions $h=-1, n=0$ and $\ell=-h, n=(1+h)^2$, which correspond to the curves $[1:-1:\ell:0]$ and $[1:h:-h:(1+h)^2]$, respectively.

It is easy to see that the extremum of the coordinate n of the curve $[1:h:-h:(1+h)^2]$ is reached at $h=-1$ and its minimum value is $n=0$.

To prove the contact between both surfaces along the curve $\gamma=[1:h:-h:(1+h)^2]$, we apply the affine change of coordinates given by $n=1+2h+h^2-v$, $v\in\mathbb{R}$. Under this transformation, the gradient vector of $(\mathscr{S}_2)$ along the curve γ is $\nabla\mathbf{T}(\gamma)=[1:0:0:-12]$, whereas the gradient vector of $(\mathscr{S}_1)$ along the curve γ is $\nabla\mu(\gamma)=[1:0:0:-1]$, whose last coordinate is always negative. As $\nabla\mu(\gamma)$ does not change its sign, this vector will always point to the same direction in relation to $(\mathscr{S}_2)$ restricted to the previous change of coordinates. Then, the surface $(\mathscr{S}_1)$ remains only on one of the two topological subspaces delimited by the surface $(\mathscr{S}_2)$. ∎

Lemma 7.4.10. *For $g\neq 0$, surfaces $(\mathscr{S}_1)$ and $(\mathscr{S}_3)$ has the plane $\{n=0\}$ as a common component. Besides, the surfaces intersect along the straight lines $[1:h:1:0]$, $[1:h:-1-2h:0]$ and $[1:h:0:1+2h]$, the hyperbola $[1:h:-1/h:0]$ and the curve $[1:-\ell(\ell+3)/4:\ell:(2-3\ell+\ell^3)/2]$. Moreover, this last curve assumes its extrema (with relation to the coordinate n) in the values $\ell=\pm1$ and $\ell=\pm2$.*

Proof. By the equations of both surfaces we observe that $\{n=0\}$ is a common plane for them. As each one of the equations of the surfaces has two factors, we must combine them in pairs and solve the systems we obtain. Thus,

- $-1-2h+2h\ell+\ell^2+n=0,\quad n=0$: it gives the solutions $\ell=1, n=0$ and $h=-(\ell+1)/2, n=0$, which correspond to the curves $[1:h:1:0]$ and $[1:h:-1-2h:0]$, respectively;
- $-4-8h-4\ell-4h\ell-8h^2\ell-4h\ell^2+4n+4\ell n+\ell^2 n=0,\quad n=0$: it gives the solutions $h=-(\ell+1)/2, n=0$ and $h=-1/\ell, n=0$, which correspond to the curves $[1:h:-1-2h:0]$ (repeated) and $[1:h:-1/h:0]$, respectively;
- $-1-2h+2h\ell+\ell^2+n=0,\quad -4-8h-4\ell-4h\ell-8h^2\ell-4h\ell^2+4n+4\ell n+\ell^2 n=0$: it gives the solutions $h=-(\ell+1)/2, n=0$; $\ell=0, n=1+2h$ and $h=-\ell(\ell+3)/4, n=(2-3\ell+\ell^3)/2$, which correspond to the curves $[1:h:-1-2h:0]$ (repeated); $[1:h:0:1+2h]$ and $[1:-\ell(\ell+3)/4:\ell:(2-3\ell+\ell^3)/2]$, respectively.

In order to find the extrema of the curve $[1:-\ell(\ell+3)/4:\ell:(2-3\ell+\ell^3)/2]$, we equalize the last coordinate to n and compute the discriminant of the obtained function:

$$\mathrm{Discrim}_\ell(2n-2+3\ell-\ell^3)=-108(n-2)n,$$

whose solutions are $n = 0$ and $n = 2$. Finally, solving the equation $2n-2+3\ell-\ell^3 = 0$ by substituting n by the zeroes of the discriminant, we obtain $\ell = \pm 1$ and $\ell = \pm 2$, which are the extrema values of the curve with respect to n. ■

Lemma 7.4.11. *For $g \neq 0$, surfaces $(\mathscr{S}_1)$ and $(\mathscr{S}_4)$ intersect along the straight lines $[1 : -1/2 : \ell : 0]$, $[1 : h : 0 : 0]$, $[1 : h : 1 : 0]$, $[1 : h : 0 : 1+2h]$ and $[1 : -\ell/2 : \ell : 1-\ell]$.*

Proof. By solving the equations of both surfaces together, we obtain the five solutions $h = -1/2, n = 0$; $\ell = 0, n = 0$; $\ell = 1, n = 0$; $\ell = 0, n = 1+2h$ and $h = -\ell/2, n = 1-\ell$, which correspond to the straight lines $[1 : -1/2 : \ell : 0]$; $[1 : h : 0 : 0]$; $[1 : h : 1 : 0]$; $[1 : h : 0 : 1+2h]$ and $[1 : -\ell/2 : \ell : 1-\ell]$, respectively. ■

Lemma 7.4.12. *For $g \neq 0$, surfaces $(\mathscr{S}_1)$ and $(\mathscr{S}_5)$ intersect along the straight lines $[1 : h : -1-2h : 0]$ and $[1 : (n-1)/2 : 0 : n]$.*

Proof. As the equation of surface $(\mathscr{S}_1)$ has two factors, we have to compute the intersection of each one of them with the equation of surface $(\mathscr{S}_5)$. Thus,

- $1+2h+\ell-n = 0, \quad n = 0$: it gives the solution $h = -(\ell+1)/2, n = 0$, which corresponds to the curve $[1 : h : -1-2h : 0]$;
- $1+2h+\ell-n = 0, \quad -1-2h+2h\ell+\ell^2+n = 0$: it gives the solution $h = (n-1)/2, \ell = 0$, which corresponds to the curve $[1 : (n-1)/2 : 0 : n]$. ■

Lemma 7.4.13. *For $g \neq 0$, surfaces $(\mathscr{S}_1)$ and $(\mathscr{S}_6)$ has the plane $\{n = 0\}$ as a common component. Besides, the surfaces intersect along the straight lines $[1 : h : 1 : 0]$, $[1 : h : -1-2h : 0]$ and $[1 : -(\ell+1)/2 : \ell : 0]$ and the curves $[1 : h : -(1+2h \pm (1+h)\sqrt{(1+2h)})/h^2 : 0]$ and $[1 : -\ell(\ell+7)/8 : \ell : (\ell-1)^2(\ell+4)/4]$. Moreover, this last curve assumes its extrema (with relation to the coordinate n) in the values $\ell = -4$, $\ell = -7/3$, $\ell = 1$ and $\ell = 8/3$.*

Proof. The proof of this lemma is analogous to the proof of Lemma 7.4.10. By the equations of both surfaces we observe that $\{n = 0\}$ is a common plane for them. As each one of the equations of the surfaces has two factors, we must combine them in pairs and solve the systems we obtain. Thus,

- $-1-2h+2h\ell+\ell^2+n = 0, \quad n = 0$: it gives the solutions $\ell = 1, n = 0$ and $h = -(\ell+1)/2, n = 0$, which correspond to the curves $[1 : h : 1 : 0]$ and $[1 : h : -1-2h : 0]$, respectively;
- $16+64h+64h^2-32\ell-160h\ell-192h^2\ell-16\ell^2+32h\ell^2+112h^2\ell^2-32h^3\ell^2+32\ell^3+64h\ell^3+32h^3\ell^3+16h^2\ell^4-32n-64hn+64\ell n+160h\ell n+8\ell^2 n-80h\ell^2 n+16h^2\ell^2 n-40\ell^3 n-8h\ell^3 n-16h^2\ell^3 n-8h\ell^4 n+16n^2-32\ell n^2+8\ell^2 n^2+8\ell^3 n^2+\ell^4 n^2 = 0, \quad n = 0$: it gives the solutions

$\ell = 1, n = 0$; $\ell = -1-2h, n = 0$ and $\ell = -(1+2h \pm (1+h)\sqrt{(1+2h)})/h^2, n = 0$, which correspond to the curves $[1:h:1:0]$ (repeated); $[1:h:-1-2h:0]$ (repeated) and $[1:h:-(1+2h\pm(1+h)\sqrt{(1+2h)})/h^2:0]$, respectively;

- $-1-2h+2h\ell+\ell^2+n=0, \quad 16+64h+64h^2-32\ell-160h\ell-192h^2\ell-16\ell^2+32h\ell^2+112h^2\ell^2-32h^3\ell^2+32\ell^3+64h\ell^3+32h^3\ell^3+16h^2\ell^4-32n-64hn+64\ell n+160h\ell n+8\ell^2 n-80h\ell^2 n+16h^2\ell^2 n-40\ell^3 n-8h\ell^3 n-16h^2\ell^3 n-8h\ell^4 n+16n^2-32\ell n^2+8\ell^2 n^2+8\ell^3 n^2+\ell^4 n^2=0$: it gives the solutions $h=-(\ell+1)/2, n=0$ and $h=-\ell(\ell+7)/8, n=(\ell-1)^2(\ell+4)/4$, which correspond to the curves $[1:h:-1-2h:0]$ (repeated) and $[1:-\ell(\ell+7)/8:\ell:(\ell-1)^2(\ell+4)/4]$, respectively.

In order to find the extrema of the curve $[1:-\ell(\ell+7)/8:\ell:(\ell-1)^2(\ell+4)/4]$, we equalize the last coordinate to n and compute the discriminant of the obtained function:

$$\mathrm{Discrim}_\ell(4n-(\ell-1)^2(\ell+4)) = 16(125-27n)n,$$

whose solutions are $n=0$ and $n=125/27$. Finally, solving the equation $4n-(\ell-1)^2(\ell+4)=0$ by substituting n by the zeroes of the discriminant, we obtain $\ell=-4$, $\ell=-7/3$, $\ell=1$ and $\ell=8/3$, which are the extrema values of the curve with respect to n. ∎

Lemma 7.4.14. *For $g \neq 0$, surfaces $(\mathscr{S}_2)$ and $(\mathscr{S}_3)$ intersect along the straight line $[1:-1:\ell:0]$ and the curve $[1:h:2h/(h-1):(1+h)^2]$. Moreover, they have a contact of order two along the curve $[1:h:2h/(h-1):(1+h)^2]$, and this curve has the straight line $\{h=1\}$ as an asymptote.*

Proof. The proof of this lemma is analogous to the proof of Lemma 7.4.12. As the equation of surface $(\mathscr{S}_3)$ has two factors, we have to compute the intersection of each one of them with the equation of surface $(\mathscr{S}_2)$. Thus,

- $1+2h+h^2-n=0, \quad n=0$: it gives the solution $h=-1, n=0$, which corresponds to the curve $[1:-1:\ell:0]$;
- $1+2h+h^2-n=0, \quad -4-8h-4\ell-4h\ell-8h^2\ell-4h\ell^2+4n+4\ell n+\ell^2 n=0$: it gives the solution $\ell=2h/(h-1), n=(1+h)^2$, which corresponds to the curve $[1:h:2h/(h-1):(1+h)^2]$.

To prove the contact between both surfaces along the curve $\gamma=[1:h:2h/(h-1):(1+h)^2]$, we apply the affine change of coordinates given by $n=1+2h+h^2-v$, $v\in\mathbb{R}$. Under this transformation, the gradient vector of $(\mathscr{S}_2)$ along the curve γ is $\nabla\mathbf{T}(\gamma)=[1:0:0:-12]$, whereas the gradient vector of $(\mathscr{S}_3)$ along the curve γ is $\nabla\mathscr{T}_4(\gamma)=[1:0:0:-4(2h-1)^2/(h-1)^2]$, whose last coordinate is always negative for all $h\neq 1$. As $\nabla\mathscr{T}_4(\gamma)$ does not change its sign, this vector will always point to the same

direction in relation to $(\mathscr{S}_2)$ restricted to the previous change of coordinates. Then, the surface $(\mathscr{S}_3)$ remains only on one of the two topological subspaces delimited by the surface $(\mathscr{S}_2)$.

Finally, it is easy to see that the curve $[1:h:2h/(h-1):(1+h)^2]$ has an asymptote and it is the straight line $\{h=1\}$, which corresponds to $n=4$. ∎

Lemma 7.4.15. *For $g\neq 0$, surfaces $(\mathscr{S}_2)$ and $(\mathscr{S}_4)$ intersect along the parabolas $[1:h:0:(1+h)^2]$ and $[1:h:1:(1+h)^2]$ and the straight line $[1:0:\ell:1]$. Moreover, the curves $[1:h:0:(1+h)^2]$ and $[1:h:1:(1+h)^2]$ assume their extremum (with relation to the coordinate n) in the value $h=-1$.*

Proof. Solving the system of equations

$$(\mathscr{S}_2):-12(1+2h+h^2-n)=0,\quad (\mathscr{S}_4):\ell(\ell-1)(-1-2h+n)=0,$$

we obtain the three solutions $\ell=0,n=(1+h)^2$, $\ell=1,n=(1+h)^2$ and $h=0,n=1$, which correspond to the curves $[1:h:0:(1+h)^2]$, $[1:h:1:(1+h)^2]$ and $[1:0:\ell:1]$, respectively. It is easy to see that the extrema of the coordinate n of the curves $[1:h:0:(1+h)^2]$ and $[1:h:1:(1+h)^2]$ are reached at $h=-1$ and their minimum value is $n=0$. ∎

Lemma 7.4.16. *For $g\neq 0$, surfaces $(\mathscr{S}_2)$ and $(\mathscr{S}_5)$ intersect along the curve $[1:h:h^2:(1+h)^2]$. Moreover, the curve $[1:h:h^2:(1+h)^2]$ assumes its extrema (with relation to the coordinate n) in the value $h=-1$.*

Proof. Solving the system of equations

$$(\mathscr{S}_2):-12(1+2h+h^2-n)=0,\quad (\mathscr{S}_5):(1+2h+\ell-n)^2=0,$$

we obtain the solution $\ell=h^2,n=(1+h)^2$, which corresponds to the curve $[1:h:h^2:(1+h)^2]$. For the extrema of this curve, see the proof of Lemma 7.4.9. ∎

Lemma 7.4.17. *For $g\neq 0$, surfaces $(\mathscr{S}_2)$ and $(\mathscr{S}_6)$ intersect along the straight line $[1:-1:\ell:0]$ and the curve $[1:h:2h/(h-1):(1+h)^2]$. Moreover, they have a contact of order two along the curve $[1:h:2h/(h-1):(1+h)^2]$ and this curve has the straight line $\{h=1\}$ as an asymptote.*

Proof. The proof of this lemma is analogous to the proof of Lemma 7.4.12. As the equation of surface $(\mathscr{S}_6)$ has two factors, we have to compute the intersection of each one of them with the equation of surface $(\mathscr{S}_2)$. Thus,

- $1+2h+h^2-n=0,\quad n=0$: it gives the solution $h=-1,n=0$, which corresponds to the curve $[1:-1:\ell:0]$;

- $1+2h+h^2-n=0$, $16+64h+64h^2-32\ell-160h\ell-192h^2\ell-16\ell^2+32h\ell^2+112h^2\ell^2-32h^3\ell^2+32\ell^3+64h\ell^3+32h^3\ell^3+16h^2\ell^4-32n-64hn+64\ell n+160h\ell n+8\ell^2n-80h\ell^2n+16h^2\ell^2n-40\ell^3n-8h\ell^3n-16h^2\ell^3n-8h\ell^4n+16n^2-32\ell n^2+8\ell^2n^2+8\ell^3n^2+\ell^4n^2=0$: it gives the solution $\ell=2h/(h-1), n=(1+h)^2$, which corresponds to the curve $[1:h:2h/(h-1):(1+h)^2]$.

To prove the contact between both surfaces along the curve $\gamma=[1:h:2h/(h-1):(1+h)^2]$, we apply the affine change of coordinates given by $n=1+2h+h^2-v$, $v\in\mathbb{R}$. Under this transformation, the gradient vector of $(\mathscr{S}_2)$ along the curve γ is $\nabla\mathbf{T}(\gamma)=[1:0:0:-12]$, whereas the gradient vector of $(\mathscr{S}_6)$ along the curve γ is $\nabla W_4(\gamma)=[1:0:0:-64h^2(1+h)^2/(h-1)^2]$, whose last coordinate is always negative for all $h\neq 1$. As $\nabla W_4(\gamma)$ does not change its sign, this vector will always point to the same direction in relation to $(\mathscr{S}_2)$ restricted to the previous change of coordinates. Then, the surface $(\mathscr{S}_6)$ remains only on one of the two topological subspaces delimited by the surface $(\mathscr{S}_2)$.

For the proof of the asymptote of the curve $[1:h:2h/(h-1):(1+h)^2]$, see the proof of Lemma 7.4.14. ∎

Lemma 7.4.18. *For $g\neq 0$, surfaces $(\mathscr{S}_3)$ and $(\mathscr{S}_4)$ intersect along the straight lines $[1:-1/2:\ell:0]$, $[1:h:0:0]$, $[1:h:1:0]$, $[1:1/2:\ell:2]$, $[1:h:0:1+2h]$ and $[1:-\ell/4:\ell:(2-\ell)/2]$ and the parabola $[1:h:1:8(1+h)^2/9]$. Moreover, this parabola assumes its extremum (with relation to the coordinate n) in the value $h=-1$.*

Proof. Solving the system of equations

$$(\mathscr{S}_3): n(-4-8h-4\ell-4h\ell-8h^2\ell-4h\ell^2+4n+4\ell n+\ell^2n)=0, \quad (\mathscr{S}_4): \ell(\ell-1)(n-1-2h)=0,$$

we obtain the solutions $h=-1/2, n=0$; $\ell=0, n=0$; $\ell=1, n=0$; $h=1/2, n=2$; $\ell=0, n=1+2h$; $h=-\ell/4, n=(2-\ell)/2$ and $\ell=1, n=8(1+h)^2/9$, which correspond to the curves $[1:-1/2:\ell:0]$; $[1:h:0:0]$; $[1:h:1:0]$; $[1:1/2:\ell:2]$; $[1:h:0:1+2h]$; $[1:-\ell/4:\ell:(2-\ell)/2]$ and $[1:h:1:8(1+h)^2/9]$, respectively.

Finally, we see that the extremum of the coordinate n of the curve $[1:h:1:8(1+h)^2/9]$ is reached at $h=-1$ and its minimum value is $n=0$. ∎

Lemma 7.4.19. *For $g\neq 0$, surfaces $(\mathscr{S}_3)$ and $(\mathscr{S}_5)$ intersect along the straight lines $[1:h:-1-2h:0]$, $[1:(n-1)/2:0:n]$ and $[1:(3+n)/6:2(n-3)/3:n]$.*

Proof. As the equation of surface $(\mathscr{S}_3)$ has two factors, we have to compute the intersection of each one of them with the equation of surface $(\mathscr{S}_5)$. Thus,

- $1+2h+\ell-n=0,\quad n=0$: it gives the solution $h=-(\ell+1)/2, n=0$, which corresponds to the curve $[1:h:-1-2h:0]$;
- $1+2h+\ell-n=0,\quad -4-8h-4\ell-4h\ell-8h^2\ell-4h\ell^2+4n+4\ell n+\ell^2 n=0$: it gives the solutions $h=(n-1)/2, \ell=0$ and $h=(3+n)/6, \ell=2(n-3)/3$, which correspond to the curves $[1:(n-1)/2:0:n]$ and $[1:(3+n)/6:2(n-3)/3:n]$, respectively. ■

Lemma 7.4.20. *For $g\neq 0$, surfaces $(\mathscr{S}_3)$ and $(\mathscr{S}_6)$ has the plane $\{n=0\}$ as a common component. Besides, the surfaces intersect along the curves $[1:h:-1-2h:0]$, $[1:-1/\ell:\ell:0]$, $[1:h:1:0]$, $[1:h:-(1+2h\pm(1+h)\sqrt{1+2h})/h^2:0]$, $[1:h:0:1+2h]$, $[1:\ell/(\ell-2):\ell:4(\ell-1)^2/(\ell-2)^2]$ and $[1:(-2+2\ell+\ell^2)/(-4+2\ell+\ell^2):\ell:4(\ell-1)^2(2+\ell)(4+\ell)/(-4+2\ell+\ell^2)^2]$. Moreover, the curve $[1:\ell/(\ell-2):\ell:4(\ell-1)^2/(\ell-2)^2]$ has the straight line $\{\ell=2\}$ as an asymptote and corresponds to a even contact between the surfaces, and the curve $[1:(-2+2\ell+\ell^2)/(-4+2\ell+\ell^2):\ell:4(\ell-1)^2(2+\ell)(4+\ell)/(-4+2\ell+\ell^2)^2]$ assumes its extrema (with relation to the coordinate n) in the values $\ell=-4$, $\ell=-2$, $\ell=1$, $\ell=-3\pm\sqrt{17}$, $\ell=-5\pm\sqrt{21}$ and $\ell=3-\sqrt{21}\pm 4\sqrt{2(13-2\sqrt{21})/17}$.*

Proof. By the equations of both surfaces we observe that $\{n=0\}$ is a common plane for them. As each one of the equations of the surfaces has two factors, we must combine them in pairs and solve the systems we obtain. Thus,

- $-4-8h-4\ell-4h\ell-8h^2\ell-4h\ell^2+4n+4\ell n+\ell^2 n=0,\quad n=0$: it gives the solutions $h=-(\ell+1)/2, n=0$ and $h=-1/\ell, n=0$, which correspond to the curves $[1:h:-1-2h:0]$ and $[1:-1/\ell:\ell:0]$, respectively;
- $16+64h+64h^2-32\ell-160h\ell-192h^2\ell-16\ell^2+32h\ell^2+112h^2\ell^2-32h^3\ell^2+32\ell^3+64h\ell^3+32h^3\ell^3+16h^2\ell^4-32n-64hn+64\ell n+160h\ell n+8\ell^2 n-80h\ell^2 n+16h^2\ell^2 n-40\ell^3 n-8h\ell^3 n-16h^2\ell^3 n-8h\ell^4 n+16n^2-32\ell n^2+8\ell^2 n^2+8\ell^3 n^2+\ell^4 n^2=0,\quad n=0$: it gives the solutions $\ell=1, n=0$; $\ell=-1-2h, n=0$ and $\ell=-(1+2h\pm(1+h)\sqrt{1+2h})/h^2, n=0$, which correspond to the curves $[1:h:1:0]$; $[1:h:-1-2h:0]$ (repeated) and $[1:h:-(1+2h\pm(1+h)\sqrt{1+2h})/h^2:0]$, respectively;
- $-4-8h-4\ell-4h\ell-8h^2\ell-4h\ell^2+4n+4\ell n+\ell^2 n=0,\quad 16+64h+64h^2-32\ell-160h\ell-192h^2\ell-16\ell^2+32h\ell^2+112h^2\ell^2-32h^3\ell^2+32\ell^3+64h\ell^3+32h^3\ell^3+16h^2\ell^4-32n-64hn+64\ell n+160h\ell n+8\ell^2 n-80h\ell^2 n+16h^2\ell^2 n-40\ell^3 n-8h\ell^3 n-16h^2\ell^3 n-8h\ell^4 n+16n^2-32\ell n^2+8\ell^2 n^2+8\ell^3 n^2+\ell^4 n^2=0$: it gives the solutions $h=-(\ell+1)/2, n=0$; $\ell=0, n=1+2h$; $h=\ell/(\ell-2), n=4(\ell-1)^2/(\ell-2)^2$ and $h=(-2+2\ell+\ell^2)/(-4+2\ell+\ell^2), n=4(\ell-1)^2(2+\ell)(4+\ell)/(-4+2\ell+\ell^2)^2$, which correspond to the curves $[1:h:-1-2h:0]$ (repeated); $[1:h:0:1+2h]$; $[1:\ell/(\ell-2):\ell:$

$4(\ell-1)^2/(\ell-2)^2]$ and $[1:(-2+2\ell+\ell^2)/(-4+2\ell+\ell^2):\ell:4(\ell-1)^2(2+\ell)(4+\ell)/(-4+2\ell+\ell^2)^2]$, respectively.

Now, we consider the curve $[1:(-2+2\ell+\ell^2)/(-4+2\ell+\ell^2):\ell:4(\ell-1)^2(2+\ell)(4+\ell)/(-4+2\ell+\ell^2)^2]$. Equalling its last coordinate to n, we obtain the curve $n(-4+2\ell+\ell^2)^2-4(\ell-1)^2(2+\ell)(4+\ell)=0$.

It is easy to see that the curve $[1:\ell/(\ell-2):\ell:4(\ell-1)^2/(\ell-2)^2]$ has an asymptote (with respect to the coordinate n) and it is the straight line $\{\ell=2\}$, which corresponds to $n=4$ (in fact, the limit of $4(\ell-1)^2/(\ell-2)^2$, as $\ell\to\infty$, is 4).

To prove the contact between both surfaces along the curve $\gamma=[1:\ell/(\ell-2):\ell:4(\ell-1)^2/(\ell-2)^2]$, we apply the affine change of coordinates given by $n=(4+8h+4\ell+4h\ell+8h^2\ell+4h\ell^2+v)/(2+\ell)^2$, $v\in\mathbb{R}$. Under this transformation, the gradient vector of $(\mathscr{S}_3)$ along the curve γ is $\nabla\mathbf{T}(\gamma)=[1:0:0:1]$, whereas the gradient vector of $(\mathscr{S}_6)$ along the curve γ is $\nabla W_4(\gamma)=[1:0:0:(64(\ell-1)^2\ell^2)/((\ell-2)^2(2+\ell)^2)]$, whose last coordinate is always positive for all $\ell\neq\pm2$. As $\nabla W_4(\gamma)$ does not change its sign, this vector will always point to the same direction in relation to $(\mathscr{S}_3)$ restricted to the previous change of coordinates. Then, the surface $(\mathscr{S}_6)$ remains only on one of the two topological subspaces delimited by the surface $(\mathscr{S}_3)$.

In order to find the extrema of the curve $[1:(-2+2\ell+\ell^2)/(-4+2\ell+\ell^2):\ell:4(\ell-1)^2(2+\ell)(4+\ell)/(-4+2\ell+\ell^2)^2]$, we equalize the last coordinate to n and compute the discriminant of the obtained function:

$$\mathrm{Discrim}_\ell(n(-4+2\ell+\ell^2)^2-4(\ell-1)^2(2+\ell)(4+\ell))=-4096n(-13500+13167n-4048n^2+400n^3),$$

whose solutions are $n=0$, $n=4$ and $n=3(102-7\sqrt{21})/100$. Finally, solving the equation $n(-4+2\ell+\ell^2)^2-4(\ell-1)^2(2+\ell)(4+\ell)=0$ by substituting n by the zeroes of the discriminant, we obtain $\ell=-4$, $\ell=-2$, $\ell=1$, $\ell=-3\pm\sqrt{17}$, $\ell=-5\pm\sqrt{21}$ and $\ell=3-\sqrt{21}\pm4\sqrt{2(13-2\sqrt{21})/17}$, which are the extremum values of the curve with respect to n. ∎

Lemma 7.4.21. *For $g\neq0$, surface $(\mathscr{S}_3)$ and surface $(\mathscr{S}_{\mathscr{F}_1})$ given by $\{\mathscr{F}_1=0\}$ intersect along the curves $[1:(1-2\ell)/(3\ell-2):\ell:0]$, $[1:h:0:1+2h]$ and $[1:(4-8\ell+3\ell^2\pm\sqrt{3}\sqrt{(2+\ell)^3(3\ell-2)})/(16-24\ell):\ell:(12-24\ell+3\ell^2\pm\sqrt{3}\sqrt{(2+\ell)^3(3\ell-2)})/(8-12\ell)]$. Moreover, this last curves assume their extrema (with relation to the coordinate n) in the values $\ell=-2$, $\ell=7/10$, $\ell=1$ and $\ell=(-7\pm5\sqrt{5})/6$.*

Proof. Solving the system of equations

$$(\mathscr{S}_3):n(-4-8h-4\ell-4h\ell-8h^2\ell-4h\ell^2+4n+4\ell n+\ell^2n)=0,\quad(\mathscr{S}_{\mathscr{F}_1}):-2-4h+4\ell+6h\ell+2n-3\ell n=0,$$

we obtain the solutions $h = (1-2\ell)/(3\ell-2), n = 0$; $\ell = 0, n = 1+2h$ and $h = (4-8\ell+3\ell^2 \pm \sqrt{3} \times \sqrt{(2+\ell)^3(3\ell-2)})/(16-24\ell), n = (12-24\ell+3\ell^2 \pm \sqrt{3}\sqrt{(2+\ell)^3(3\ell-2)})/(8-12\ell)$, which correspond to the curves $[1:(1-2\ell)/(3\ell-2):\ell:0]$; $[1:h:0:1+2h]$ and $[1:(4-8\ell+3\ell^2 \pm \sqrt{3}\sqrt{(2+\ell)^3(3\ell-2)})/(16-24\ell):\ell:(12-24\ell+3\ell^2 \pm \sqrt{3}\sqrt{(2+\ell)^3(3\ell-2)})/(8-12\ell)]$, respectively.

With the purpose to find the extrema of the curves $[1:(4-8\ell+3\ell^2 \pm \sqrt{3}\sqrt{(2+\ell)^3(3\ell-2)})/(16-24\ell):\ell:(12-24\ell+3\ell^2 \pm \sqrt{3}\sqrt{(2+\ell)^3(3\ell-2)})/(8-12\ell)]$, we equalize the last coordinate to n:

$$\begin{aligned}
&(12-24\ell+3\ell^2 \pm \sqrt{3}\sqrt{(2+\ell)^3(3\ell-2)}) - (8-12\ell)n = 0 \Leftrightarrow \\
&\qquad \pm \sqrt{3}\sqrt{(2+\ell)^3(3\ell-2)} = (8-12\ell)n - 12 + 24\ell - 3\ell^2 \Leftrightarrow \\
&\qquad (\pm \sqrt{3}\sqrt{(2+\ell)^3(3\ell-2)})^2 = ((8-12\ell)n - 12 + 24\ell - 3\ell^2)^2 \Leftrightarrow \\
&\qquad p \equiv -64(3-3n+n^2) + 96(n-2)(2n-3)\ell - 48(n-3)(3n-4)\ell^2 - 24(3n-8)\ell^3 = 0,
\end{aligned}$$

and compute the discriminant of the p:

$$\mathrm{Discrim}_\ell(p) = 7077888n^2(4n-9)^3,$$

whose solutions are $n = 0$ and $n = 9/4$. Besides, we consider the leading coefficient of p in ℓ and solve it with respect to n, obtaining $n = 8/3$, which corresponds to the value of the parameter n in which the polynomial p turns from a cubic to a quadratic and after to a cubic polynomial. Finally, solving the equations $12-24\ell+3\ell^2 \pm \sqrt{3}\sqrt{(2+\ell)^3(3\ell-2)}) - (8-12\ell)n = 0$ by substituting n by the zeroes of the discriminant and the bifurcation value of p, we obtain $\ell = -2$, $\ell = 7/10$, $\ell = 1$ and $\ell = (-3 \pm 5\sqrt{5})/6$, which are the extrema values of the curve with respect to n. ■

Lemma 7.4.22. *For $g \neq 0$, surfaces $(\mathscr{S}_4)$ and $(\mathscr{S}_5)$ intersect along the curves $[1:(n-1)/2:0:n]$ and $[1:n/2-1:1:n]$.*

Proof. Solving the system of equations

$$(\mathscr{S}_4): \ell(\ell-1)(n-1-2h) = 0, \quad (\mathscr{S}_5): (1+2h+\ell-n)^2 = 0,$$

we obtain the solutions $h = (n-1)/2, \ell = 0$ and $h = n/2-1, \ell = 1$, which correspond to the curves $[1:(n-1)/2:0:n]$ and $[1:n/2-1:1:n]$, respectively. ■

Lemma 7.4.23. *For $g \neq 0$, surfaces $(\mathscr{S}_4)$ and $(\mathscr{S}_6)$ intersect along the curves $[1:-1/2:\ell:0]$, $[1:h:1:0]$, $[1:(n-1)/2:0:n]$ and $[1:(n-1)/2:-4(n-1)/(n-2)^2:n]$. Moreover, the curve $[1:(n-1)/2:-4(n-1)/(n-2)^2:n]$ assumes its extrema (with relation to the coordinate n) in the value $\ell = 1$.*

Proof. Solving the system of equations

$$
\begin{aligned}
&(\mathscr{S}_4):(\ell-1)(n-1-2h)=0,\\
&(\mathscr{S}_6):n^2(16+64h+64h^2-32\ell-160h\ell-192h^2\ell-16\ell^2+32h\ell^2+112h^2\ell^2\\
&\quad-32h^3\ell^2+32\ell^3+64h\ell^3+32h^3\ell^3+16h^2\ell^4-32n-64hn+64\ell n+160h\ell n\\
&\quad+8\ell^2n-80h\ell^2n+16h^2\ell^2n-40\ell^3n-8h\ell^3n-16h^2\ell^3n-8h\ell^4n+16n^2\\
&\quad-32\ell n^2+8\ell^2n^2+8\ell^3n^2+\ell^4n^2)=0,
\end{aligned}
$$

we obtain the solutions $h=-1/2, n=0$; $\ell=1, n=0$; $h=(n-1)/2, \ell=0$ and $h=(n-1)/2, \ell=-4(n-1)/(n-2)^2$, which correspond to the curves $[1:-1/2:\ell:0]$; $[1:h:1:0]$; $[1:(n-1)/2:0:n]$ and $[1:(n-1)/2:-4(n-1)/(n-2)^2:n]$, respectively.

In order to find the extrema of the curve $[1:(n-1)/2:-4(n-1)/(n-2)^2:n]$, we equalize the third coordinate to ℓ and compute the discriminant of the obtained function:

$$\mathrm{Discrim}_n(\ell(n-2)^2+4(n-1))=-16(\ell-1),$$

whose solutions is $\ell=1$. Finally, solving the equation $\ell(n-2)^2+4(n-1)=0$ by substituting $\ell=1$, we obtain $n=0$, which is the extremum value of the curve with respect to n. ∎

Lemma 7.4.24. *For $g\neq 0$, surfaces $(\mathscr{S}_5)$ and $(\mathscr{S}_6)$ intersect along the curves $[1:h:-1-2h:0]$, $[1:-(\ell+1)/2:\ell:0]$ and $[1:-(16-24\ell+9\ell^2+\ell^3)/(8\ell-6\ell^2):\ell:4(\ell-1)^2(4+\ell)/(\ell(3\ell-4))]$. Moreover, the curve $[1:-(16-24\ell+9\ell^2+\ell^3)/(8\ell-6\ell^2):\ell:4(\ell-1)^2(4+\ell)/(\ell(3\ell-4))]$ assumes its extrema (with relation to the coordinate n) in the values $\ell=-4$, $\ell=1$ and $\ell=f^{-1}(n_0)$, where $f(\ell)=4(\ell-1)^2(4+\ell)/(\ell(3\ell-4))$ and $n_0=(130-4511/(208855+16956\sqrt{471})^{1/3}+(208855+16956\sqrt{471})^{1/3})/27$.*

Proof. As the equation of surface $(\mathscr{S}_6)$ has two factors, we have to compute the intersection of each one of them with the equation of surface $(\mathscr{S}_5)$. Thus,

- $1+2h+\ell-n=0,\quad n=0$: it gives the solution $h=-(\ell+1)/2, n=0$, which corresponds to the curve $[1:h:-1-2h:0]$;
- $1+2h+\ell-n=0,\quad 16+64h+64h^2-32\ell-160h\ell-192h^2\ell-16\ell^2+32h\ell^2+112h^2\ell^2-32h^3\ell^2+32\ell^3+64h\ell^3+32h^3\ell^3+16h^2\ell^4-32n-64hn+64\ell n+160h\ell n+8\ell^2n-80h\ell^2n+16h^2\ell^2n-40\ell^3n-8h\ell^3n-16h^2\ell^3n-8h\ell^4n+16n^2-32\ell n^2+8\ell^2n^2+8\ell^3n^2+\ell^4n^2=0$: it gives the solutions $h=-(\ell+1)/2, n=0$ and $h=-(16-24\ell+9\ell^2+\ell^3)/(8\ell-6\ell^2), n=4(\ell-1)^2(4+\ell)/(\ell(3\ell-4))$, which correspond to the curves $[1:-(\ell+1)/2:\ell:0]$ and $[1:-(16-24\ell+9\ell^2+\ell^3)/(8\ell-6\ell^2):\ell:4(\ell-1)^2(4+\ell)/(\ell(3\ell-4))]$, respectively.

In order to find the extrema of the curve $[1 : -(16-24\ell+9\ell^2+\ell^3)/(8\ell-6\ell^2) : \ell : 4(\ell-1)^2(4+\ell)/(\ell(3\ell-4))]$, we equalize the last coordinate to n and compute the discriminant of the obtained function:

$$\mathrm{Discrim}_\ell(n\ell(3\ell-4)-4(\ell-1)^2(4+\ell)) = 16n(-2000+793n-130n^2+9n^3),$$

whose solutions are $n=0$ and $n=(130-4511/(208855+16956\sqrt{471})^{1/3}+(208855+16956\times\sqrt{471})^{1/3})/27$. Finally, solving the equation $n\ell(3\ell-4)-4(\ell-1)^2(4+\ell)=0$ by substituting n by the zeroes of the discriminant, we obtain $\ell=-4$, $\ell=1$ and $\ell=f^{-1}(n_0)$, where $f(\ell)=4(\ell-1)^2(4+\ell)/(\ell(3\ell-4))$ and $n_0=(130-4511/(208855+16956\sqrt{471})^{1/3}+(208855+16956\sqrt{471})^{1/3})/27$, which are the extrema values of the curve with respect to ℓ. ∎

The purpose now is to find the slices in which the intersection among at least three surfaces or other equivalent phenomena happen. Since there exist 25 distinct curves of intersections or contacts between two any surfaces, we need to study 325 different possible intersections of these surfaces. As the relation is very long, we will reproduce only a few of them deploying the different algebraic techniques used to solve them. The full set of proves can be found on the web page http://mat.uab.es/~artes/articles/qvfsn2SN02/qvfsn2SN02.html.

Remark 7.4.25. *In the next five lemmas we use the following notation. A curve of intersection or contact between two surfaces will be denoted by* solAByC*, where $A<B$ are the numbers of the surfaces involved in the intersection or contact and C is a cardinal. Moreover, these four lemmas illustrate the different techniques we use to solve the intersection among at least three surfaces or other equivalent phenomena.*

Lemma 7.4.26. *Surfaces $(\mathscr{S}_1)$, $(\mathscr{S}_2)$ and $(\mathscr{S}_3)$ intersect in slices when $n=0$ and $n=1$.*

Proof. By Lemmas 7.4.9 and 7.4.10, we have the curves

$$\mathrm{sol12y1} = \left[1 : h : -h : (1+h)^2\right] \quad \text{and} \quad \mathrm{sol13y2} = \left[1 : -\frac{\ell(3+\ell)}{4} : \ell : \frac{2-3\ell+\ell^3}{2}\right].$$

Equalizing each corresponding coordinate:

$$h = -\frac{\ell(3+\ell)}{4}, \quad -h=\ell, \quad (1+h)^2 = \frac{2-3\ell+\ell^3}{2},$$

and solving the system above, we obtain the solutions $h=-1, \ell=1$ and $h=\ell=0$. Since the curves

are parametrized by h and ℓ, we must substitute the solutions of the system in the expressions of the curves and consider the value of the coordinate n. Then,

$$\text{sol12y1}\big|_{h=-1,\ell=1} = [1:-1:1:0] \quad \text{and} \quad \text{sol12y1}\big|_{h=\ell=0} = [1:0:0:1],$$

implying that the values of n where the three surfaces intersect are $n = 0$ and $n = 1$. ■

Lemma 7.4.27. *Surfaces* $(\mathscr{S}_1)$, $(\mathscr{S}_2)$ *and* $(\mathscr{S}_5)$ *intersect in slices when* $n = 0$ *and* $n = 1$.

Proof. By Lemmas 7.4.9 and 7.4.16, we have the curves

$$\text{sol12y1} = \left[1 : h : -h : (1+h)^2\right] \quad \text{and} \quad \text{sol25y1} = \left[1 : h : h^2 : (1+h)^2\right].$$

Equalizing each corresponding coordinate:

$$h = h, \quad -h = h^2, \quad (1+h)^2 = (1+h)^2,$$

and solving the system above, we obtain the solutions $h = -1$ and $h = 0$. Since the curves are parametrized by h, we must substitute the solutions of the system in the expressions of the curves and consider the value of the coordinate n. Then,

$$\text{sol12y1}\big|_{h=-1} = [1:-1:1:0] \quad \text{and} \quad \text{sol25y1}\big|_{h=0} = [1:0:0:1],$$

implying that the values of n where the three surfaces intersect are $n = 0$ and $n = 1$. ■

Lemma 7.4.28. *Surfaces* $(\mathscr{S}_1)$, $(\mathscr{S}_3)$ *and* $(\mathscr{S}_5)$ *intersect in slice when* $n = 3$.

Proof. By Lemmas 7.4.10 and 7.4.19, we have the curves

$$\text{sol13y1} = [1 : h : 0 : 1+2h] \quad \text{and} \quad \text{sol35y2} = \left[1 : \frac{3+n}{6} : \frac{2(n-3)}{3} : n\right].$$

Equalizing each corresponding coordinate:

$$h = \frac{3+n}{6}, \quad \frac{2(n-3)}{3} = 0, \quad 1+2h = n,$$

and solving the system above, we obtain the solution $h = 1, n = 3$. Then, the value of n where the three surfaces intersect is $n = 3$. ■

Lemma 7.4.29. *Surfaces* $(\mathscr{S}_3)$, $(\mathscr{S}_5)$ *and* $(\mathscr{S}_6)$ *intersect in slices when* $n=6$ *and* $n=9$.

Proof. By Lemmas 7.4.19 and 7.4.24, we have the curves

$$\text{sol35y2}=\left[1:\frac{3+n}{6}:\frac{2(n-3)}{3}:n\right] \quad \text{and} \quad \text{sol56y1}=\left[1:\frac{16-24\ell+9\ell^2+\ell^3}{2\ell(3\ell-4)}:\ell:\frac{4(\ell-1)^2(4+\ell)}{\ell(3\ell-4)}\right].$$

Equalizing each corresponding coordinate:

$$\frac{3+n}{6}=\frac{16-24\ell+9\ell^2+\ell^3}{2\ell(3\ell-4)}, \quad \frac{2(n-3)}{3}=\ell, \quad n=\frac{4(\ell-1)^2(4+\ell)}{\ell(3\ell-4)},$$

and solving the system above, we obtain the solutions $\ell=2, n=6$ and $\ell=4, n=9$. Then, the values of n where the three surfaces intersect are $n=6$ and $n=9$. ∎

Lemma 7.4.30. *Surfaces* $(\mathscr{S}_1)$, $(\mathscr{S}_4)$, $(\mathscr{S}_5)$ *and* $(\mathscr{S}_6)$ *intersect in slice when* $n=1$.

Proof. By Lemmas 7.4.12 and 7.4.23, we have the curves

$$\text{sol15y1}=\left[1:\frac{n-1}{2}:0:n\right] \quad \text{and} \quad \text{sol46y2}=\left[1:\frac{n-1}{2}:-\frac{4(n-1)}{(n-2)^2}:n\right].$$

Equalizing each corresponding coordinate:

$$\frac{n-1}{2}=\frac{n-1}{2}, \quad -\frac{4(n-1)}{(n-2)^2}=0, \quad n=n,$$

and solving the system above, we obtain the solution $n=1$. Then, the value of n where the four surfaces intersect is $n=1$. ∎

The next result presents all the algebraic values of n corresponding to singular slices in the bifurcation diagram. Its proof follows from Lemmas 7.4.26 to 7.4.30 and by computing all the remaining 320 different possible intersections or contacts among three or more surfaces.

Lemma 7.4.31. *The full set of needed algebraic singular slices in the bifurcation diagram of family* $\overline{\textbf{QsnSN(C)}}$ *is formed by* 20 *elements which correspond to the values of* n *in* (7.4.2)–(7.4.3).

$$\begin{aligned}
&n_1=9, \quad n_{15}=6, \quad n_{17}=\frac{1}{27}\left(130-\frac{4511}{(208855+16956\sqrt{471})^{1/3}}+(208855+16956\sqrt{471})^{1/3}\right),\\
&n_{19}=125/27, \quad n_{21}=9/2, \quad n_{23}=\frac{3}{100}(102+7\sqrt{21}), \quad n_{25}=4,\\
&n_{27}=\frac{\left(14\sqrt[3]{2}\sqrt[3]{\frac{1}{\alpha}}+2^{2/3}\sqrt[3]{\alpha}-8\right)\left(14\sqrt[3]{2}\sqrt[3]{\frac{1}{\alpha}}+2^{2/3}\sqrt[3]{\alpha}-2\right)\left(14\sqrt[3]{2}\sqrt[3]{\frac{1}{\alpha}}+2^{2/3}\sqrt[3]{\alpha}+7\right)^2}{\left(\sqrt[3]{2}\alpha^{2/3}+98\,2^{2/3}\left(\frac{1}{\alpha}\right)^{2/3}+14\sqrt[3]{2}\sqrt[3]{\frac{1}{\alpha}}+2^{2/3}\sqrt[3]{\alpha}+6\right)^2}, \ \alpha=61-9\sqrt{29},
\end{aligned} \tag{7.4.2}$$

$$\begin{aligned} n_{29} =& 2+\sqrt{2}, \quad n_{31}=3, \quad n_{33}=8/3, \quad n_{37}=9/4, \quad n_{41}=\frac{3}{100}(102-7\sqrt{21}), \\ n_{45} =& 2, \quad n_{55}=1, \quad n_{57}=2-\sqrt{2}, \quad n_{59}=1/2, \quad n_{83}=0, \\ n_{85} =& \frac{1}{2}\left(\frac{3-(1548-83\sqrt{249})^{1/3}}{3^{2/3}}-\frac{61}{(3(1548-83\sqrt{249}))^{1/3}}\right), \quad n_{87}=-\infty. \end{aligned} \tag{7.4.3}$$

The numeration in (7.4.2)–(7.4.3) is not consecutive since we reserve numbers for other slices not algebraically determined and for generic slices.

Now we sum up the content of the previous lemmas. In (7.4.2)–(7.4.3) we list all algebraic values of n where significant phenomena occur for the bifurcation diagram generated by singularities. We first have the two extreme values for n, i.e. $n=-\infty$ (corresponding to $g=0$) and $n=9$. We remark that to perform the bifurcation diagram of all singularities for $n=-\infty$ we set $g=0$ and, in the remaining three variables (h,ℓ,n), yielding the point $[h:\ell:n]$ in $\mathbb{RP}^2$, we take the chart $n\neq 0$ in which we may assume $n=-1$.

In order to determine all the parts generated by the bifurcation surfaces from $(\mathscr{S}_1)$ to $(\mathscr{S}_{10})$, we first draw the horizontal slices of the three–dimensional parameter space which correspond to the explicit values of n obtained in Lemma 7.4.31. However, as it will be discussed later, the presence of nonalgebraic bifurcation surfaces will be detected and the singular slices corresponding to their singular behavior as we move from slice to slice will be approximately determined. We add to each interval of singular values of n an intermediate value for which we represent the bifurcation diagram of singularities. The diagram will remain essentially unchanged in these open intervals except the parts affected by the bifurcation. All the sufficient values of n are shown in equation (7.4.4).

The values indexed by positive odd indices in equation (7.4.4) correspond to explicit values of n for which there exists a bifurcation in the behavior of the systems on the slices. Those indexed by even values are just intermediate points which are necessary to the coherence of the bifurcation diagram.

Due to the presence of many branches of nonalgebraic bifurcation surfaces, we cannot point out exactly neither predict the concrete value of n where the changes in the parameter space happen. Thus, with the purpose to set an order for these changes in the parameter space, we introduce the following notation. If the bifurcation happens between two concrete values of n, then we add or subtract a sufficiently small positive value ε_i or ε_j^* to/from a concrete value of n; this concrete value of n (which is a reference value) can be any of the two values that define

the range where the non–concrete values of n are inserted. The representation ε_i means that the n_i refers to a generic slice, whereas ε_j^* means that the n_j refers to a singular slice. Moreover, considering the values ε_i, ε_i^*, ε_{i+1} and ε_{i+1}^*, it means that $\varepsilon_i < \varepsilon_i^* < \varepsilon_{i+1} < \varepsilon_{i+1}^*$ meanwhile they belong to the same interval determined by algebraic bifurcations.

We now begin the analysis of the bifurcation diagram by studying completely one generic slice and after by moving from slice to slice and explaining all the changes that occur. As an exact drawing of the curves produced by intersecting the surfaces with the slices gives us very small parts which are difficult to distinguish, and points of tangency are almost impossible to recognize, we have produced topologically equivalent figures where parts are enlarged and tangencies are easy to observe.

The reader may find the exact pictures as well as most of the proves of this chapter in the web page http://mat.uab.es/~artes/articles/qvfsn2SN02/qvfsn2SN02.html.

Remark 7.4.32. *We follow the same pattern set out in Notation 5.4.11 to label the parts in the bifurcation diagram for the family* $\overline{\mathbf{QsnSN(C)}}$. *The slice* $n = \infty$ *(which is equivalent to* $n = -\infty$*) is also a bifurcation surface in the parameter space, as observed in Remark 6.4.6, and the labels there should be* $9S$. *However, as the comitant* $\mathbf{T}$ *vanishes for this value of the parameter (we will see this later), all the parts in this slice are part of surface* $(\mathscr{S}_2)$ *and, hence, they are labeled as* $2S_j$ *and* $2.iL_j$. *We have denoted the curved segments in which the equator splits as* $2.8L_j$.

In Figure 7.12 we represent the generic slice of the parameter space when $n = n_0 = 10$, showing only the algebraic surfaces. We note that there are some dashed branches of surface $(\mathscr{S}_3)$ (in yellow) and $(\mathscr{S}_4)$ (in purple). This means the existence of a weak saddle, in the case of surface $(\mathscr{S}_3)$, and the existence of an invariant straight line without connecting separatrices, in the case of surface $(\mathscr{S}_4)$; they do not mean a topological change in the phase portraits but a C^∞ change. In the next figures we will use the same representation for these characteristics of these two surfaces.

With the purpose to explain all the changes in the bifurcation diagram, we would have to present two versions of the picture of each slice: one of them without labels and the other with labels in each new part (as we have done in Chapters 5 and 6).

However, as the number of slices is considerably large (see equation (7.4.4) – 88 slices to be more precise) we would have to present about 176 pictures, which would occupy a large number of pages.

$$
\begin{aligned}
n_0 &= 10 \\
n_1 &= 9 \\
n_2 &= 9-\varepsilon_1 \\
n_3 &= 9-\varepsilon_1^* \\
n_4 &= 9-\varepsilon_2 \\
n_5 &= 9-\varepsilon_2^* \\
n_6 &= 9-\varepsilon_3 \\
n_7 &= 9-\varepsilon_3^* \\
n_8 &= 9-\varepsilon_4 \\
n_9 &= 9-\varepsilon_4^* \\
n_{10} &= 9-\varepsilon_5 \\
n_{11} &= 9-\varepsilon_5^* \\
n_{12} &= 9-\varepsilon_6 \\
n_{13} &= 9-\varepsilon_6^* \\
n_{14} &= 9-\varepsilon_7 \\
n_{15} &= 6 \\
n_{16} &= 119/20 \\
n_{17} &= \tfrac{1}{27}\left(130-\tfrac{4511}{(208855+16956\sqrt{471})^{1/3}}+(208855+16956\sqrt{471})^{1/3}\right) \\
n_{18} &= 21/4 \\
n_{19} &= 125/27 \\
n_{20} &= 114/25 \\
n_{21} &= 9/2 \\
n_{22} &= 108/25 \\
n_{23} &= \tfrac{3}{100}(102+7\sqrt{21}) \\
n_{24} &= 401/100 \\
n_{25} &= 4 \\
n_{26} &= 2304/625 \\
n_{27} &\approx 3.63495307168\ldots \\
n_{28} &= 7/2 \\
n_{29} &= 2+\sqrt{2} \\
n_{30} &= 16/5 \\
n_{31} &= 3 \\
n_{32} &= 14/5 \\
n_{33} &= 8/3 \\
n_{34} &= 8/3-\varepsilon_8 \\
n_{35} &= 8/3-\varepsilon_8^* \\
n_{36} &= 8/3-\varepsilon_9 \\
n_{37} &= 9/4 \\
n_{38} &= 11/5 \\
n_{39} &= 11/5-\varepsilon_9^* \\
n_{40} &= 11/5-\varepsilon_{10} \\
n_{41} &= \tfrac{3}{100}(102-7\sqrt{21}) \\
n_{42} &= \tfrac{3}{100}(102-7\sqrt{21})-\varepsilon_{11} \\
n_{43} &= 2+\varepsilon_{12}^* \\
n_{44} &= 2+\varepsilon_{12} \\
n_{45} &= 2 \\
n_{46} &= 19/10 \\
n_{47} &= 19/10-\varepsilon_{13}^* \\
n_{48} &= 17/10 \\
n_{49} &= 17/10-\varepsilon_{14}^* \\
n_{50} &= 17/10-\varepsilon_{14} \\
n_{51} &= 41/25+\varepsilon_{15}^* \\
n_{52} &= 41/25 \\
n_{53} &= 8/5+\varepsilon_{16}^* \\
n_{54} &= 8/5 \\
n_{55} &= 1 \\
n_{56} &= 81/100 \\
n_{57} &= 2-\sqrt{2} \\
n_{58} &= 9/16 \\
n_{59} &= 1/2 \\
n_{60} &= 9/25 \\
n_{61} &= 9/25-\varepsilon_{17}* \\
n_{62} &= 81/40 \\
n_{63} &= 81/40-\varepsilon_{18}^* \\
n_{64} &= 81/40-\varepsilon_{18} \\
n_{65} &= 81/40-\varepsilon_{19}^* \\
n_{66} &= 81/40-\varepsilon_{19} \\
n_{67} &= 81/40-\varepsilon_{20}^* \\
n_{68} &= 81/40-\varepsilon_{20} \\
n_{69} &= 81/40-\varepsilon_{21}^* \\
n_{70} &= 4/25 \\
n_{71} &= 4/25-\varepsilon_{22}^* \\
n_{72} &= 4/25-\varepsilon_{22} \\
n_{73} &= 4/25-\varepsilon_{23}^* \\
n_{74} &= 4/25-\varepsilon_{23} \\
n_{75} &= 4/25-\varepsilon_{24}^* \\
n_{76} &= 4/25-\varepsilon_{24} \\
n_{77} &= 4/25-\varepsilon_{25}^* \\
n_{78} &= 9/100 \\
n_{79} &= 9/100-\varepsilon_{26}^* \\
n_{80} &= 9/100-\varepsilon_{26} \\
n_{81} &= 9/100-\varepsilon_{27}^* \\
n_{82} &= 1/25 \\
n_{83} &= 0 \\
n_{84} &= -1 \\
n_{85} &= \tfrac{1}{2}\left(\tfrac{3-(1548-83\sqrt{249})^{1/3}}{3^{2/3}}-\tfrac{61}{(3(1548-83\sqrt{249}))^{1/3}}\right) \\
n_{86} &= -4 \\
n_{87} &= -\infty
\end{aligned}
\tag{7.4.4}
$$

Then, we will present only the labeled drawings (just the "important part" in each slice) containing the algebraic and nonalgebraic bifurcation surfaces. In the next section, we prove the existence of such nonalgebraic surfaces and their necessity for the coherence of the bifurcation diagram.

7.4.2 Bifurcation surfaces due to connections

We start this section explaining the generic slice when $n = 10$. In this slice we will make a complete study of all its parts, whereas in the next slices we will only describe the changes. Some singular slices will produce only few changes which are easy to describe, but others can produce simultaneously many changes, even a complete change of all parts and these will need a more detailed description.

As said in last section, in Figure 7.12 we present the slice when $n = 10$ with only the algebraic surfaces. We now place for each set of the partition on this slice the local behavior of the flow around all the singular points. For a specific value of the parameters of each one of the sets in this partition we compute the global phase portrait with the numerical program P4 [3, 27]. In fact, all the phase portraits in this study can be obtained not only numerically but also by means of perturbations of the systems of codimension one.

In this slice we have a partition in 2−dimensional parts bordered by curved polygons, some of them bounded, others bordered by infinity. From now on, we use lower–case letters provisionally to describe the sets found algebraically so not to interfere with the final partition described with capital letters.

For each 2−dimensional part we obtain a phase portrait which is coherent with those of all their borders. Except eight parts, which are shown in Figure 7.12 and named as follows:

- v_5: the curved triangle bordered by yellow and blue curves and infinity;
- v_8: the curved quadrilateral bordered by blue, yellow and black curves and infinity;
- v_{10}: the curved triangle bordered by purple and yellow curves and infinity;
- v_{12}: the pentagon bordered by yellow, purple, green and purple curves and infinity;
- v_{22}: the quadrilateral bordered by two parallel purple and two parallel green curves;
- v_{27}: the curved quadrilateral bordered by yellow, red and black curves and infinity;
- v_{33}: the curved triangle bordered by yellow, red and black curves;
- v_{54}: the curved triangle bordered by purple and yellow curves and infinity;

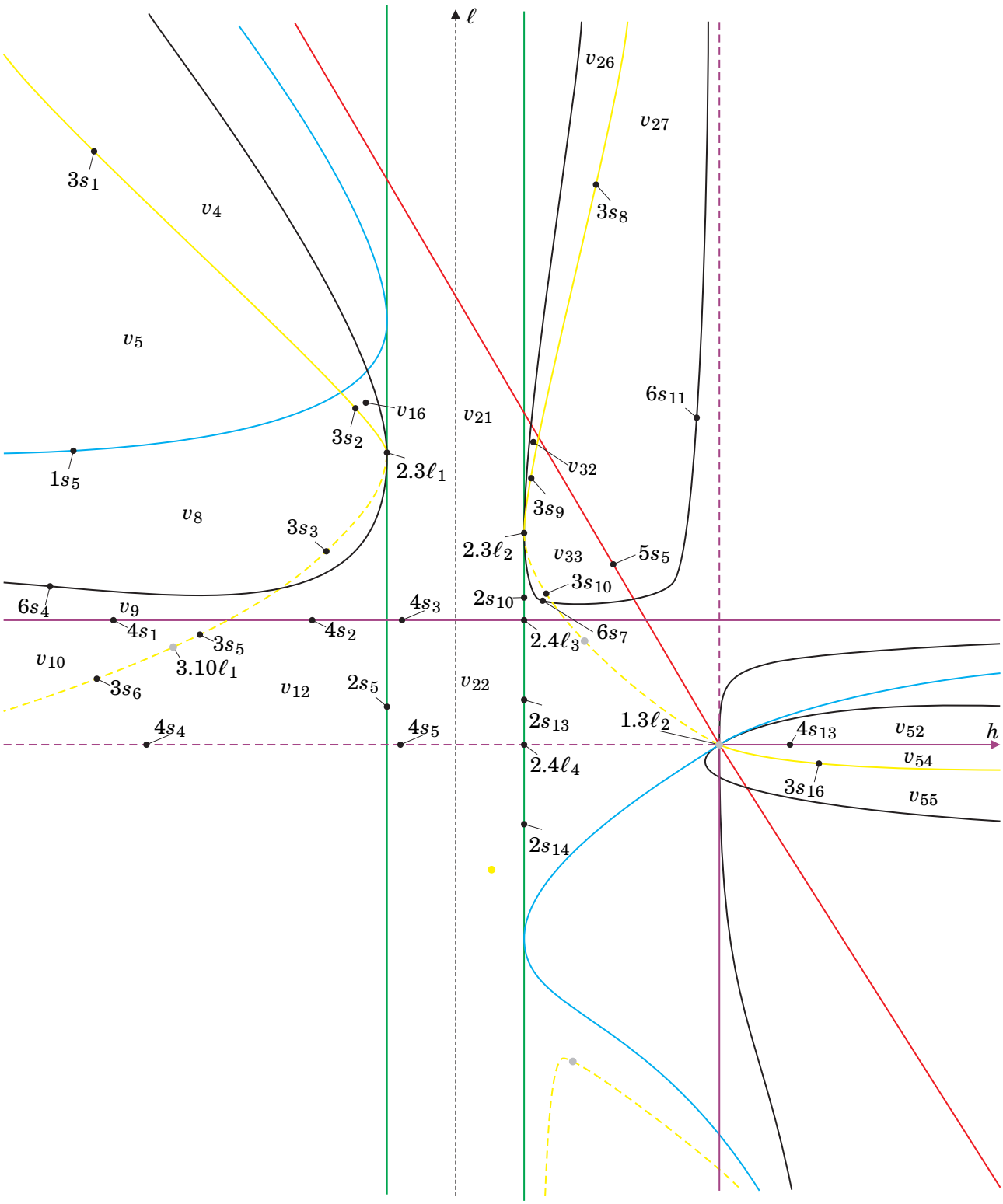

Figure 7.12: Slice of parameter space when $n = 10$ (only algebraic surfaces)

We consider the segment $3s_1$ in Figure 7.12, which is one of the borders of part v_5. On this segment, the corresponding phase portrait possesses a weak focus (of order one) and, consequently, this branch of surface ($\mathscr{S}_3$) corresponds to a Hopf bifurcation. This means that either in v_4 or in v_5 we must have a limit cycle; in fact it is in v_5. The same happens on $3s_2$, one of the borders of part v_8, implying the existence of a limit cycle either in v_8 or in v_{16}; and in fact it is in v_8.

However, in case of part v_5, when approaching $1s_5$ and with the help of the program P4, the limit cycle has already been lost; and in case of part v_8, when approaching $3s_3$ and/or $6s_4$, the limit cycle has also disappeared. After these remarks, each one of the parts v_5 and v_8 must be split into two parts separated by a new surface ($\mathscr{S}_7$) having at least two elements (curves $7S_1$ and $7S_3$ in Figure 7.19) such that one part has limit cycle and the other does not, and the borders $7S_1$ and $7S_3$ correspond to a connection between separatrices. In spite of the necessity of these two branches of surface ($\mathscr{S}_7$), there must exist at least one more element of this surface to make this part of the diagram space coherent. We talk about the element $7S_2$ (see Figure 7.19) which also corresponds to connection of separatrices but different from that happening on $7S_1$ and $7S_3$.

Numerically, it can be checked that part v_5 splits into V_5 with one limit cycle and V_6 without limit cycles, and part v_8 splits into V_7 and V_8 without limit cycles and V_{17} with one limit cycle. Even though parts V_7 and V_8 have no limit cycles, they provide topologically distinct phase portraits since the connection of separatrices on $7S_3$ (respectively, on $7S_1$) is due to the saddle–node $\overline{\binom{0}{2}}SN$ and the finite saddle (respectively, is due to the saddle–node $\overline{\binom{0}{2}}SN$ and an infinite saddle), i.e. connection of separatrices from different points, whereas the connection on $7S_2$ is due to a saddle itself (i.e. a loop–type connection). We plot the complete bifurcation diagram for these two parts in Figure 7.19. We also show the sequence of phase portraits along these subsets in Figure 7.13.

Now, we carry out the analysis of parts v_{10}, v_{12} and v_{22}. We consider part v_9. The respective phase portrait is topologically equivalent to the one in V_8 with the focus turned into a node. On $4s_1$, the separatrix of the infinite saddle–node connects with a separatrix of the finite saddle producing an invariant straight line linking the pair of infinite saddle–nodes. When entering part v_{10}, this connection is broken and the position of the separatrices of the infinite saddle–node and the finite saddle is changed in relation to the position represented in V_9. However, when we approach $4s_4$, the phase portrait in a neighborhood of this segment is topologically different from the one we described just after entering part v_{10}. Indeed, the phase portrait in v_{10} near $4s_1$ possesses a “basin” passing through the saddle–node, i.e. two separatrices of the saddle–node end

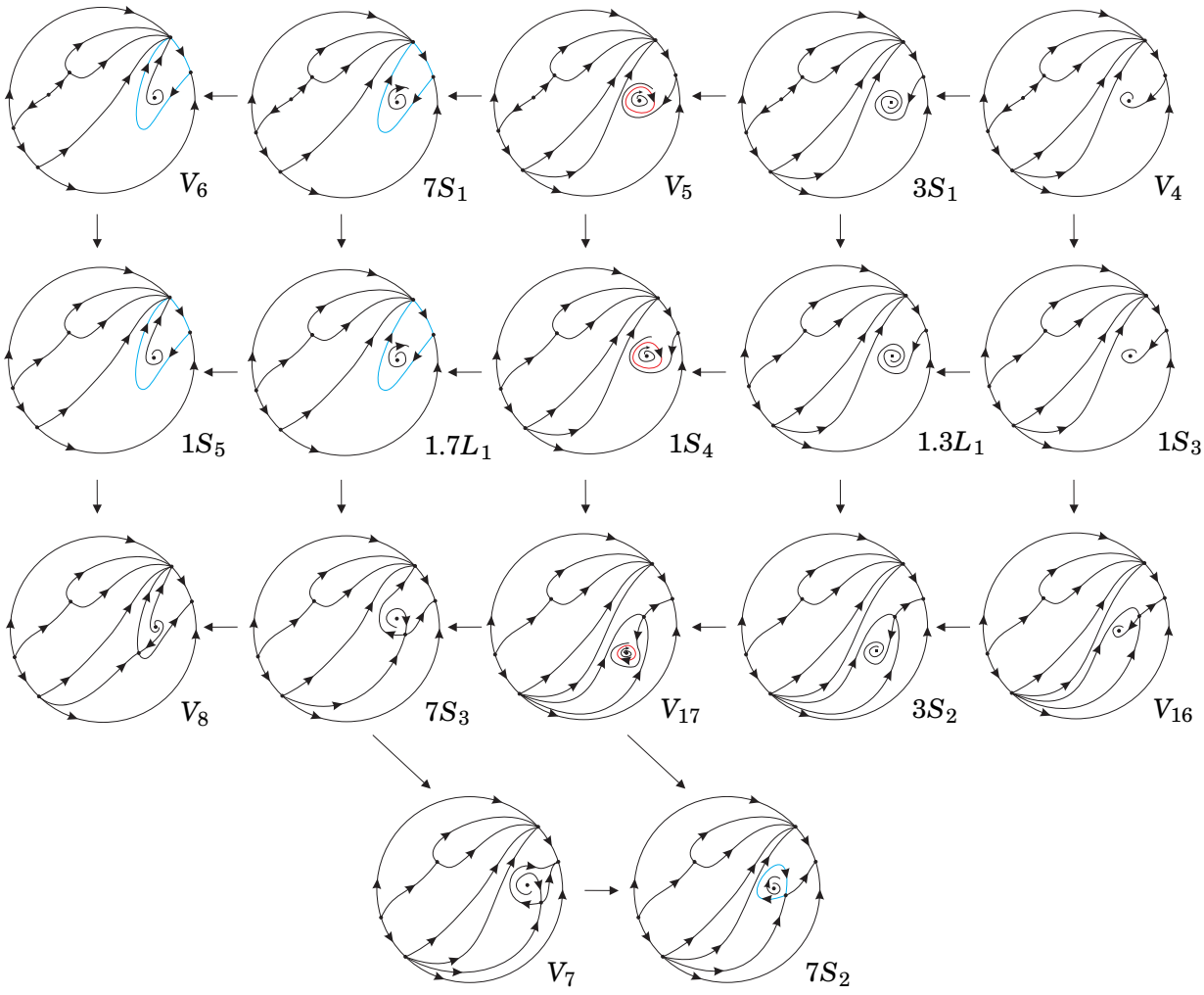

Figure 7.13: Sequence of phase portraits in parts v_5 and v_8 of slice $n = 10$. We start from v_4. We recall that the phase portrait $3S_1$ is equivalent to the phase portrait V_4 up to a weak focus (represented by a little black square) instead of the focus. When crossing $3s_1$, we shall obtain the phase portrait V_5 in subset v_5. From this point we may choose three different ways to reach the subset v_8 by crossing the blue curve: (1) from the phase portrait $1.3L_1$ to the V_{17}; (2) from the phase portrait $1S_4$ to the V_{17}; and (3) from the phase portrait $1.7L_1$ to the V_7, V_8, V_{17}, $1S_4$, $7S_2$ and $7S_3$

at the same infinite singular point, whereas the phase portrait in v_{10} near $4s_4$ does not possess the "basin" and each one of the same two separatrices of the saddle–node ends in different infinite singular points.

As a result, there must exist at least one element $7S_4$ of surface $(\mathscr{S}_7)$ dividing part v_{10} in two "new" parts, V_{10} and V_{11}, which represents a bifurcation due to the connection between a separatrix of a finite saddle–node with a separatrix of a finite saddle. It is worth mentioning that the segments $3s_5$ and $3s_6$ and the point $3.10\ell_1$ refer to the presence of weak saddle (of order one and two, respectively) which implies that part v_{12} is topologically equivalent to v_{10}. Then, part v_{12}

must also be divided in V_{12} and V_{13} by an element $7S_5$ of surface $(\mathscr{S}_7)$ with the same bifurcation as $7S_4$. Coupled with this idea, we have parametrized the yellow surface, "walked" on it and found that there exist a topological change in the phase portraits obtained.

In addition, we have done the same with the green surface (i.e. we have parametrized it) and found that segment $2s_5$ also presents two distinct phase portraits and they are topologically equivalent to the ones described above. This suggests that an element $7S_6$ of surface $(\mathscr{S}_7)$ divides part v_{22} in two "new" ones, V_{22} and V_{23}, where $7S_6$ corresponds to a bifurcation due to the connection between two separatrices from a finite and an infinite saddle–nodes. Therefore, we know that $7S_6$ has one of its endpoints on $2s_5$ (dividing it in $2S_5$ and $2S_6$) and Lemma 7.4.33 assures that the other endpoint is $2.4\ell_3$.

Lemma 7.4.33. *The endpoint of* $7S_6$ *(rather than the one which is on* $2s_5$*) is* $2.4\ell_3$.

Proof. Numerical tools evidence that the endpoint of $7S_6$, rather than the one which is on $2s_5$, is $2.4\ell_3$. In what follows, we prove that this endpoint cannot be on segments $4s_3$ and $2s_{13}$.

If this endpoint were located on $4s_3$, there must exist an invariant straight line linking the pair of infinite saddle–nodes producing a connection between their separatrices. On the other hand, we would have two options. The first one would be that this endpoint of $7S_6$ should correspond to a phase portrait in which the separatrices of the finite saddle–node connects with the invariant straight line, which is itself a connection of two separatrices (see Figure 7.14(a) to visualize the probable movement of the separatrices in $4S_3$), producing a triple connection of separatrices; in addition, the invariant straight line should remain, what would be a contradiction since we would have three non–collinear infinite singular points involved in the "final" connection. And the second option would be the birth of another finite singular point on this straight line which would make the "new" connection possible, but in v_{22} there exists only one finite singular point.

Now, if the endpoint of $7S_6$ were located on $2s_{13}$, then another saddle–node should appear in the finite part and it would send its separatrix associated to the null eigenvalue to an infinite node and one of the other two separatrices would be received by the nodal sector of the other finite saddle–node and the other separatrix would be received by the nodal part of an infinite saddle–node. If there would exist an intersection between $7S_6$ and $2s_{13}$, then a separatrix of a finite saddle–node would have to connect with the separatrix of an infinite saddle–node as sketched in Figure 7.14(b). However, there exists a separatrix in the middle of these two that prevents this connection before the connection between some of these two with the one from the middle. Then, it is impossible to have an intersection between $7S_6$ and $2s_{13}$.

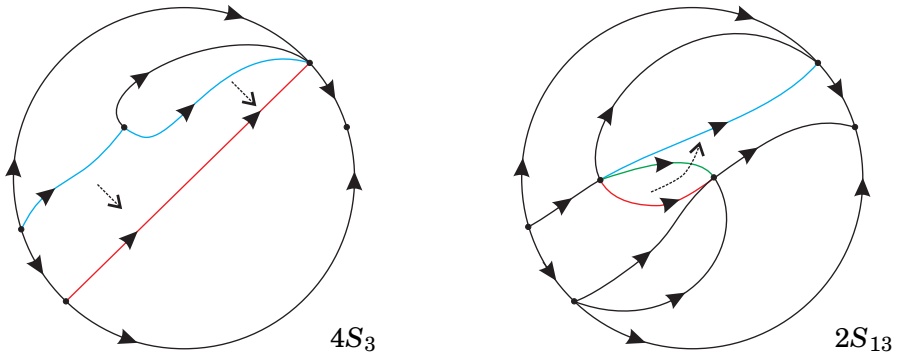

(a) (b)

Figure 7.14: (a) The probable movement of the separatrices to form another connection in phase portrait $4S_3$. The straight line in red is produced by the connection of the separatrices of the infinite saddle–nodes (the characteristic of $4S_3$) and the separatrices in blue of the finite saddle–node would tend to the straight line and provoke a triple connection of separatrices having the invariant straight line remained; (b) The probable movement of the separatrices to form a connection in phase portrait $2S_{13}$. In order to have a phase portrait with characteristics of curve $7S_6$, it would be necessary that the separatrix in red of a finite saddle–node connects with the separatrix of the infinite saddle–node in blue, but before it is necessary that either the red or the blue separatrix connects with the green one

As shown above, the endpoint of $7S_6$ is not on $4s_3$ nor in $2s_{13}$ and this confirms the evidence pointed out by the numerical calculations that $7S_6$ ends at $2.4\ell_3$. ■

We plot the complete bifurcation diagram for these two parts in Figure 7.19. We also show the sequence of phase portraits along these subsets in Figure 7.15.

We now perform the study of parts v_{27} and v_{33}. We consider the segment $3s_8$ in Figure 7.12, which is one of the borders of part v_{27}. Analogously, on this segment, the corresponding phase portrait possesses a weak focus (of order one) and, consequently, this branch of surface ($\mathscr{S}_3$) corresponds to a Hopf bifurcation. This means that either in v_{26} or in v_{27} we must have a limit cycle; in fact it is in v_{27}. The same happens on $3s_9$, one of the borders of part v_{33}, implying the existence of a limit cycle either in v_{32} or in v_{33}; and in fact it is in v_{33}.

However, approaching $6s_{11}$, the limit cycle has been lost, which implies the existence of at least one more element of surface ($\mathscr{S}_7$) (curve $7S_7$ in Figure 7.20); furthermore, the phase portrait in a small neighborhood of $6s_{11}$ is not coherent to that obtained just after making disappear the limit cycle. If we fix a value of the parameter ℓ in order to be in this part and we make the parameter h increase from $3s_8$ towards $6s_{11}$, then we obtain four topologically distinct phase portraits with no separatrix connection inside part v_{27}, which implies the existence of not only one but at least three elements of surface ($\mathscr{S}_7$), the curves $7S_7$, $7S_8$ and $7S_9$ in Figure 7.20; such new phase portraits are V_{27}, with limit cycle, and V_{28}, V_{29} and V_{30}, without limit cycles (see Figure 7.16 for a sequence of

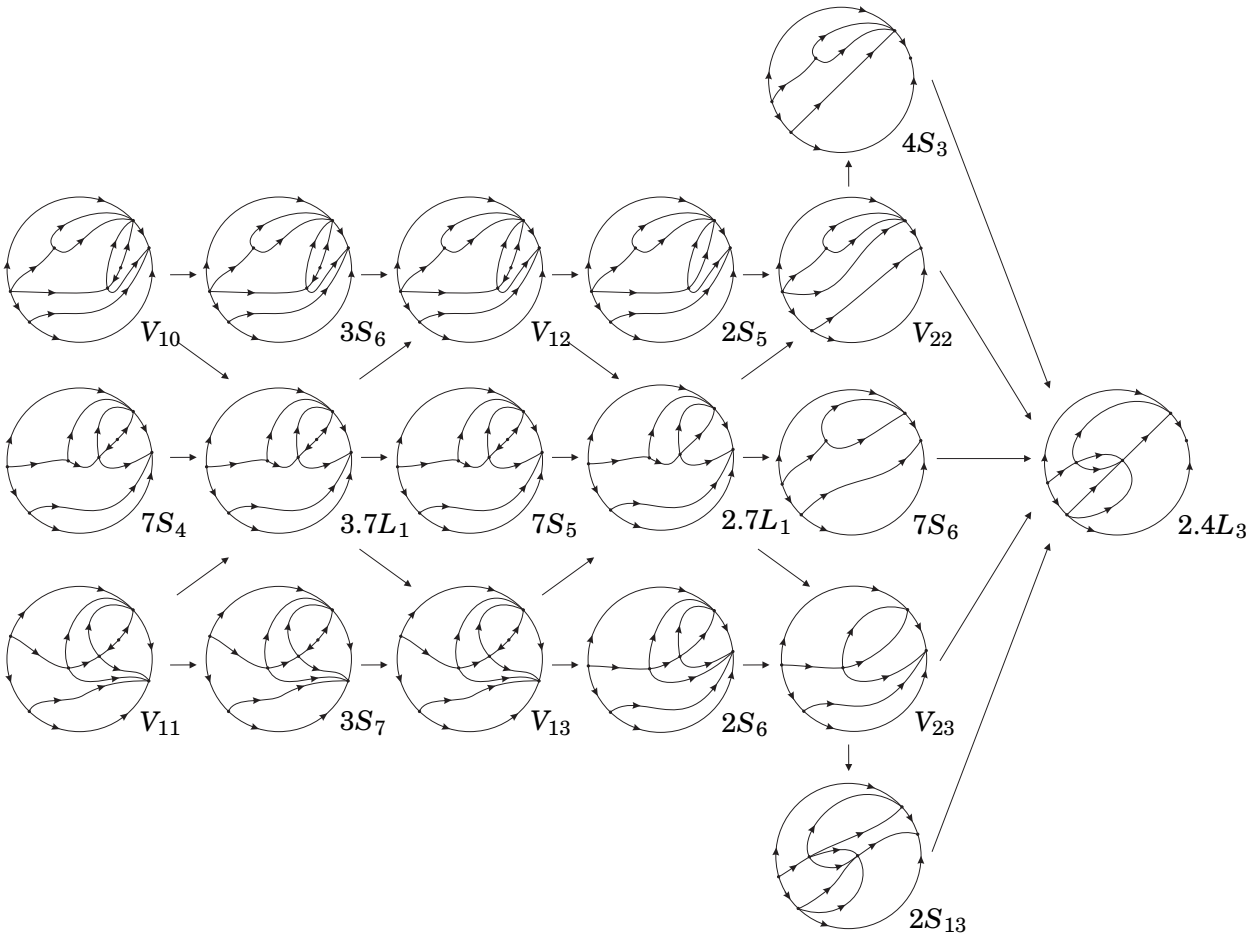

Figure 7.15: Sequence of phase portraits in parts v_{10}, v_{12} and v_{22} of slice $n = 10$. We start from v_{10}. We recall that the phase portraits V_{10}, $3S_6$ and V_{12} are topologically equivalent due to a weak saddle. The same happens to $7S_4$, $3.7L_1$ and $7S_5$, and to V_{11}, $3S_7$ and V_{13}. From V_{12}, $7S_5$ and V_{13}, we cross the segment $2s_5$, where the finite saddle and finte node collide giving birth to a saddle–node, and we have three possibilites: $2S_5$, $2.7L_1$ and $2S_{16}$. Entering part v_{22}, this just–born saddle–node disappears; this part was divided in three and the respective phase portraits V_{22}, $7S_6$ and V_{23} are topologically distinct among them, and they tend to the phase portrait $2.4L_3$ either directly or passing through $4S_3$ and $2S_{13}$

phase portraits in these parts). As the segment $5s_5$ corresponds to changes in the infinite singular points, the finite part of the phase portraits remain unchanged and these elements of surface $(\mathscr{S}_7)$ intersect $5s_5$. Consequently, v_{33} is also split into four parts having the same behavior in the finite part with relation to the corresponding "new" parts in v_{27}; such new phase portraits are V_{33}, with limit cycle, and V_{34}, V_{35} and V_{36}, without limit cycles, and the branches of surface $(\mathscr{S}_7)$ which are the continuation of the segments $7S_7$, $7S_8$ and $7S_9$ are, respectively, $7S_{10}$, $7S_{11}$ and $7S_{12}$.

Remark 7.4.34. *One of the separatrices in the connection on the curves* $7S_7$, $7S_8$, $7S_9$, $7S_{10}$, $7S_{11}$ *and* $7S_{12}$ *is always from a finite saddle.*

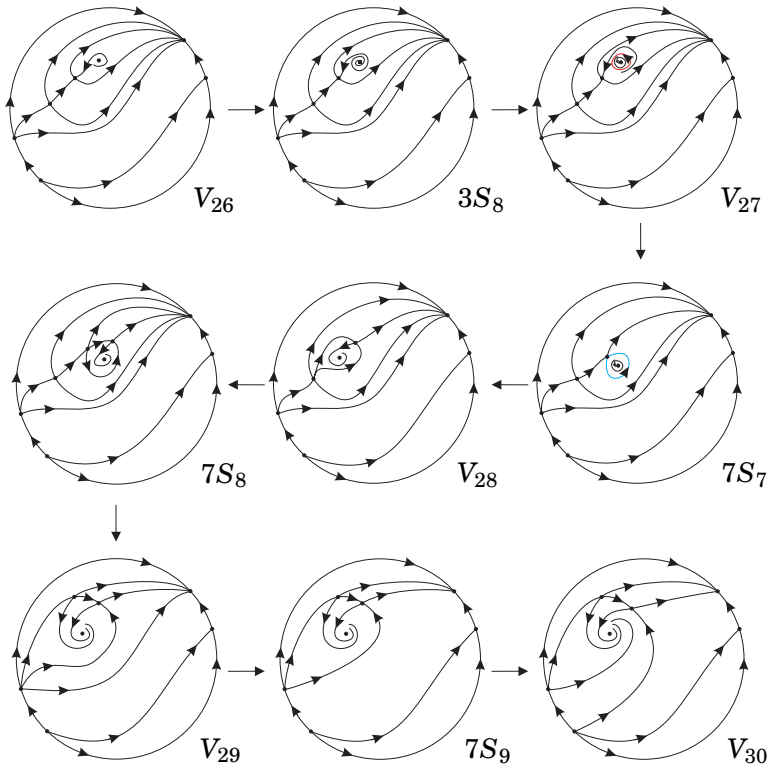

Figure 7.16: Sequence of phase portraits in part v_{27} of slice $n = 10$. We start from v_{26}. We recall that the phase portrait $3S_8$ is equivalent to the phase portrait V_{26} up to a weak focus (represented by a little black square) in place of the focus. When crossing $3s_8$, we shall obtain the phase portrait V_{27} in subset v_{27} possessing a limit cycle. Then, on $7S_7$ two separatrices of the finite saddle connect themselves producing a loop; this loop is broken and one of the separatrices of the saddle goes towards the focus and the other comes from the nodal part of the saddle–node in V_{28}; thus, that separatrix of the saddle coming from the nodal sector of the saddle–node connects with one of the separatrices of the saddle–node producing another separatrices connection on $7S_8$; after this connection is broken, the separatrix of the saddle–node goes towards the focus and the separatrix of the saddle comes from the infinite saddle–node, characterizing part V_{29}; then, on $7S_9$ one more connection of separatrices is produced between the same separatrix of the saddle and the separatrix of the infinite saddle–node; and, finally, on V_{30} this separatrices connection is broken and the separatrix of the infinite saddle–node goes towards the focus and the separatrix of the saddle comes from the infinite node

Lemma 7.4.35. *The curve $7S_7$ has one of its ends at the point $2.3\ell_2$.*

Proof. Numerical analysis suggests that the curve $7S_7$, which corresponds to a loop–type bifurcation, has one of its ends at the point $2.3\ell_2$. Indeed, if the starting point of $7S_7$ were any point of segments $3s_9$ or $3s_{10}$, we would have the following incoherences. Firstly, if this starting point were on $3s_9$, then a portion of this subset must not refer to a Hopf bifurcation, which contradicts the fact that on $3s_9$ we have a weak focus of order one. Secondly, if the starting point were on $3s_{10}$, then a portion of this segment must also refer to a Hopf bifurcation since we a limit cycle in V_{33}, which is also a contradiction. ∎

Since the subsets $3s_{10}$ and $6s_7$ correspond respectively to the presence of a weak saddle and the node–focus bifurcation, they do not imply a topological change in the phase portrait. Under these circumstances, the segments $7S_{11}$ and $7S_{12}$ intersect both subsets $3s_{10}$ and $6s_7$ causing only C^∞ changes in the phase portraits and they will end on segment $2s_{10}$ dividing it in three new parts: $2S_{10}$, $2S_{11}$ and $2S_{12}$. The reason why they do not cross $2s_{10}$ is that, if they did so, the connection of the separatrices would have to remain. However, in part v_{21} there exists only one finite singular point (namely, $\overline{sn}_{(2)}$), i.e. the finite saddle and node that existed on the right side of $2s_{10}$ have collapsed on this segment and become a complex point after crossing it. Following this idea, Remark 7.4.34 has no sense in part v_{21}. In Figure 7.17 we show the sequence of phase portraits from part $2.3L_2$ to $2S_{12}$.

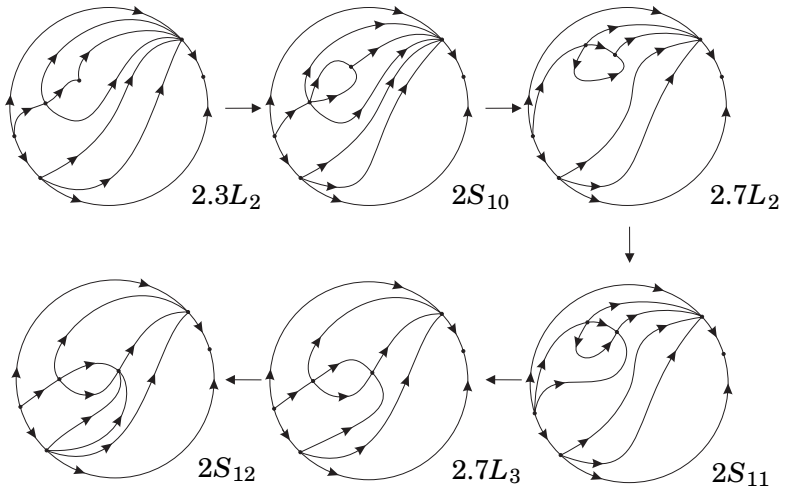

Figure 7.17: Sequence of phase portraits in part $2s_{10}$ of slice $n = 10$. We start from $2.3\ell_2$. This part produces only one phase portrait $2.3L_2$ which possesses finite saddle–node and a cusp (we remark that this point is the intersection of many surfaces, inducing a degeneracy — the cusp point). On $2S_{10}$ the cusp turns into a saddle–node having two of its separatrices sent from the nodal part of the remaining saddle–node. At $2.7L_2$, one separatrix of one saddle–node connects with one separatrix of the other saddle–node and, on $2S_{11}$, this connection is broken and we have the creation of two "basins" which intersect at the two saddle–nodes. Then, on $2.7L_3$ a connection of separatrices is produced between the separatrix of the infinite saddle–node and one separatrix of one of the finite saddle–nodes and, finally, on $2S_{12}$ this connection is broken and we obtain the portrait above

Finally, we analyze part v_{54}. We start in part v_{52}. In this portion of the parameter space, the corresponding phase portrait possesses the saddle–node and two foci in the finite part and saddle–nodes and saddles at infinity. When we cross the curve $4s_{13}$, its phase portrait possesses $\{(x,0);\, x \in \mathbb{R}\}$ as an invariant straight line linking the infinite saddles. The presence of this invariant straight line produces a connection of separatrices between one from a saddle and the other from the finite saddle–node (the one associated to the null eigenvalue). Entering part v_{54}, this invariant line

disappears and the separatrices in question change position, which forces the separatrix of the saddle–node start from its own nodal sector, forming a graphic.

On the other hand, we start from part v_{55}. There, the corresponding phase portrait also possesses the saddle–node and two foci in the finite part and saddle–nodes and saddles at infinity. On $3s_{16}$, which is a common border of parts v_{54} and v_{55}, the corresponding phase portrait possesses a weak focus (of order one) and, consequently, this branch of surface ($\mathscr{S}_3$) corresponds to a Hopf bifurcation. This means that either in v_{54} or in v_{55} we must have a limit cycle; in fact it is in v_{54}.

After these remarks, we conclude that part v_{54} must be split into two parts separated by a new surface ($\mathscr{S}_7$) having at least one element $7S_{17}$ (see Figure 7.20) such that one part has limit cycle and the other does not, and the border $7S_{17}$ corresponds to a connection of two separatrices of the same saddle–node in a loop, because the limit cycle disappears and one of the phase portraits in v_{54} possesses a graphic attached to the saddle–node.

Lemma 7.4.36 assures that the segment $7S_{17}$ starts from (or ends at) $1.3\ell_2$ and is not bounded.

Lemma 7.4.36. *The segment $7S_{17}$ starts from (or ends at) $1.3\ell_2$ and is not bounded.*

Proof. If $7S_{17}$ started on $3s_{16}$, there would exist a portion of this segment without limit cycles, which is a contradiction since it corresponds to a Hopf bifurcation. On the other hand, if $7S_{17}$ started on $4s_{13}$, two types of connection of separatrices should happen: the connection between the separatrix of the infinite saddle with the separatrix of the finite saddle–node associated to the null eigenvalue (creating an invariant straight line) and the loop–type connection in the finite saddle–node. If both connections happen, there must exist a degenerate portion of $4s_{13}$ in which this segment would start. Using numerical tools, we verify that $7S_{17}$ starts from $1.3\ell_2$. Moreover, using the same arguments, the segment $7S_{17}$ can end neither on $3s_{16}$ nor on $4s_{13}$, implying that it is unbounded. ∎

We can check numerically that part v_{54} splits into V_{53}, without limit cycles, and V_{54}, with limit cycle. We plot the complete bifurcation diagram for these two parts in Figure 7.20. We also show the sequence of phase portraits along these subsets in Figure 7.18.

Having analyzed all the parts pointed out on page 169 and explained the existence of all possible nonalgebraic surfaces in there (modulo islands), we have finished the study of the generic slice $n = 10$ for the family $\overline{\mathbf{QsnSN(C)}}$. However, we cannot be sure that these are all the additional bifurcation curves in this slice. There could exist others which are closed curves small enough to escape our numerical research. For all other two–dimensional parts of the partition of this slice, whenever we join two points which are close to different borders of the part, the two phase

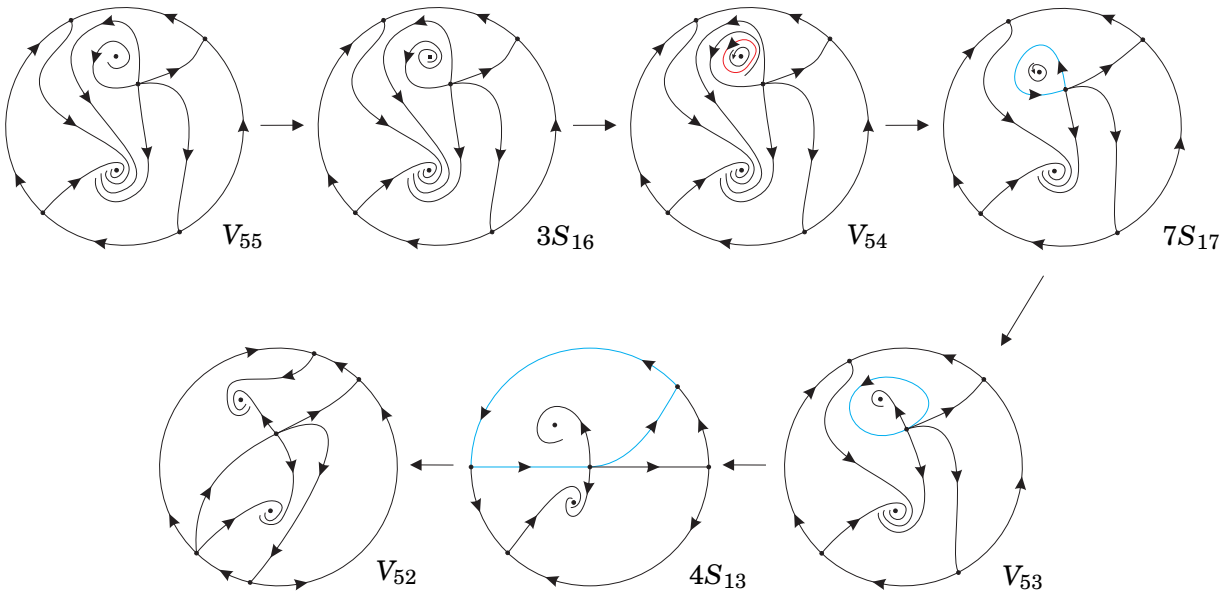

Figure 7.18: Sequence of phase portraits in part v_{54} of slice $n = 10$. We start in v_{55}, whose corresponding phase portrait is V_{55}. On $3s_{16}$, one of the foci becomes weak (represented as a small square in $3S_{16}$) and it gives birth to a limit cycle when we enter part v_{54}; see phase portrait V_{54}. Then, on $7S_{17}$, two separatrices of the saddle–node connect forming a loop, which "kills" the limit cycle. After that, we obtain the portrait V_{53} in which there exists no connection of separatrices but only a graphic. A graphic remains when we lie on $4s_{13}$, but the corresponding phase portrait $4S_{13}$ possesses an invariant straight line and connection of separatrices. Finally, in v_{52} the graphic disappears and we obtain the phase portrait V_{52}

portraits are topologically equivalent. So, we do not encounter more situations than the ones mentioned above. In short, it is expected that the complete bifurcation diagram for $n = 10$ is the one shown in Figures 7.19 and 7.20. In these and the next figures, we have colored in light yellow the parts with one limit cycle, in light green the parts with two limit cycles, in black the labels referring to new parts which are created in a slice and in red the labels corresponding to parts which has already appeared in previous slices.

The next step is to decrease the values of n, according to equation (7.4.4), and make an analogous study for each one of the slices that we need to consider and also look for changes when going from one slice to the next one.

For all values of n greater than zero, the second and third quadrants of the bifurcation diagram remain unchanged (i.e., for all $n > 0$, there exist no topological bifurcations in the second and third quadrants in the parameter space). So, as we move from $n > 9$ towards infinity, all the slices are topologically equivalent to slice $n = 10$ and, at the limit to infinity, the bifurcation diagram tends to be the one shown in Figure 7.21.

We now start decreasing the values of n in order to explain as much as we can the bifurcations

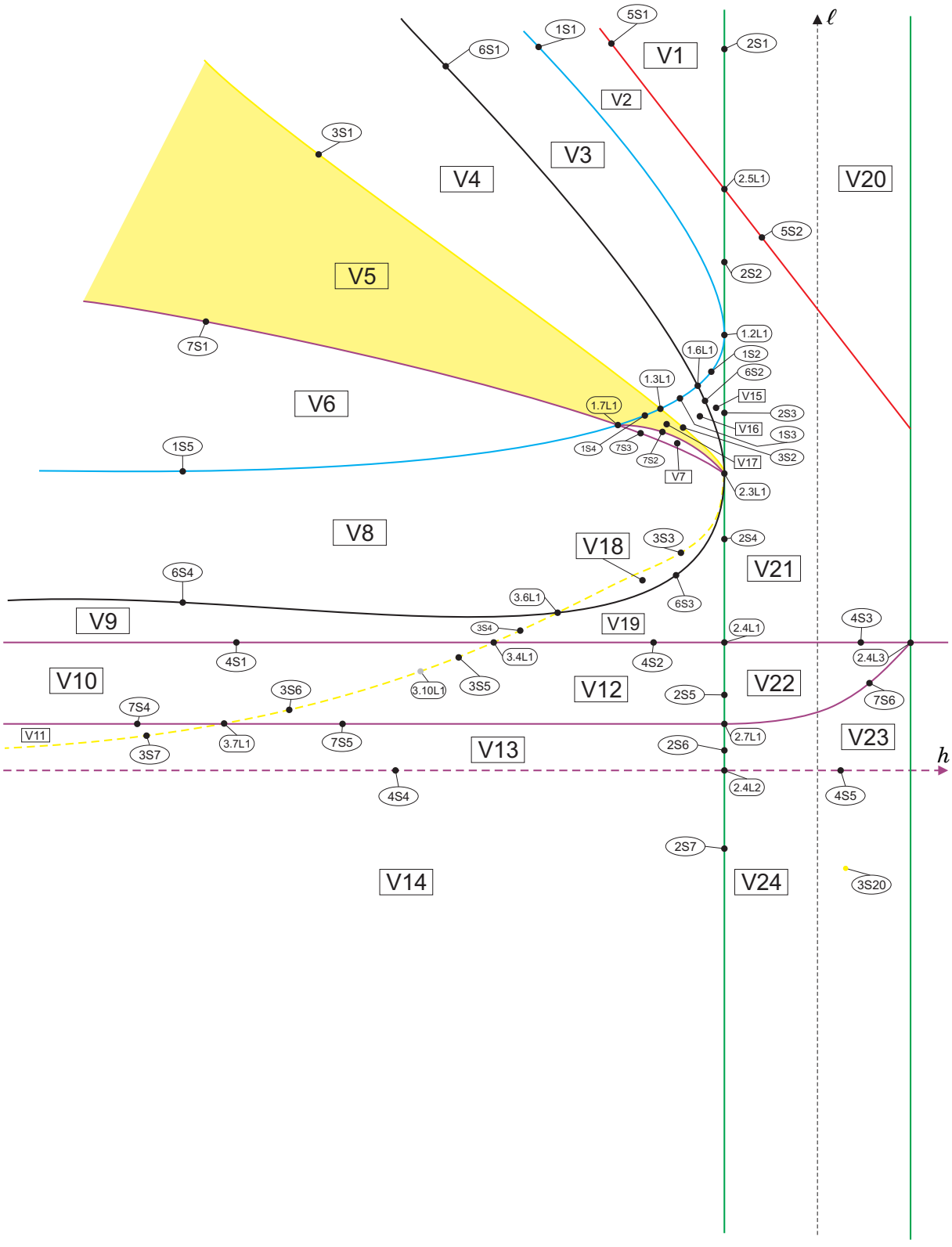

Figure 7.19: Complete bifurcation diagram for slice $n = 10$ (second and third quadrants)

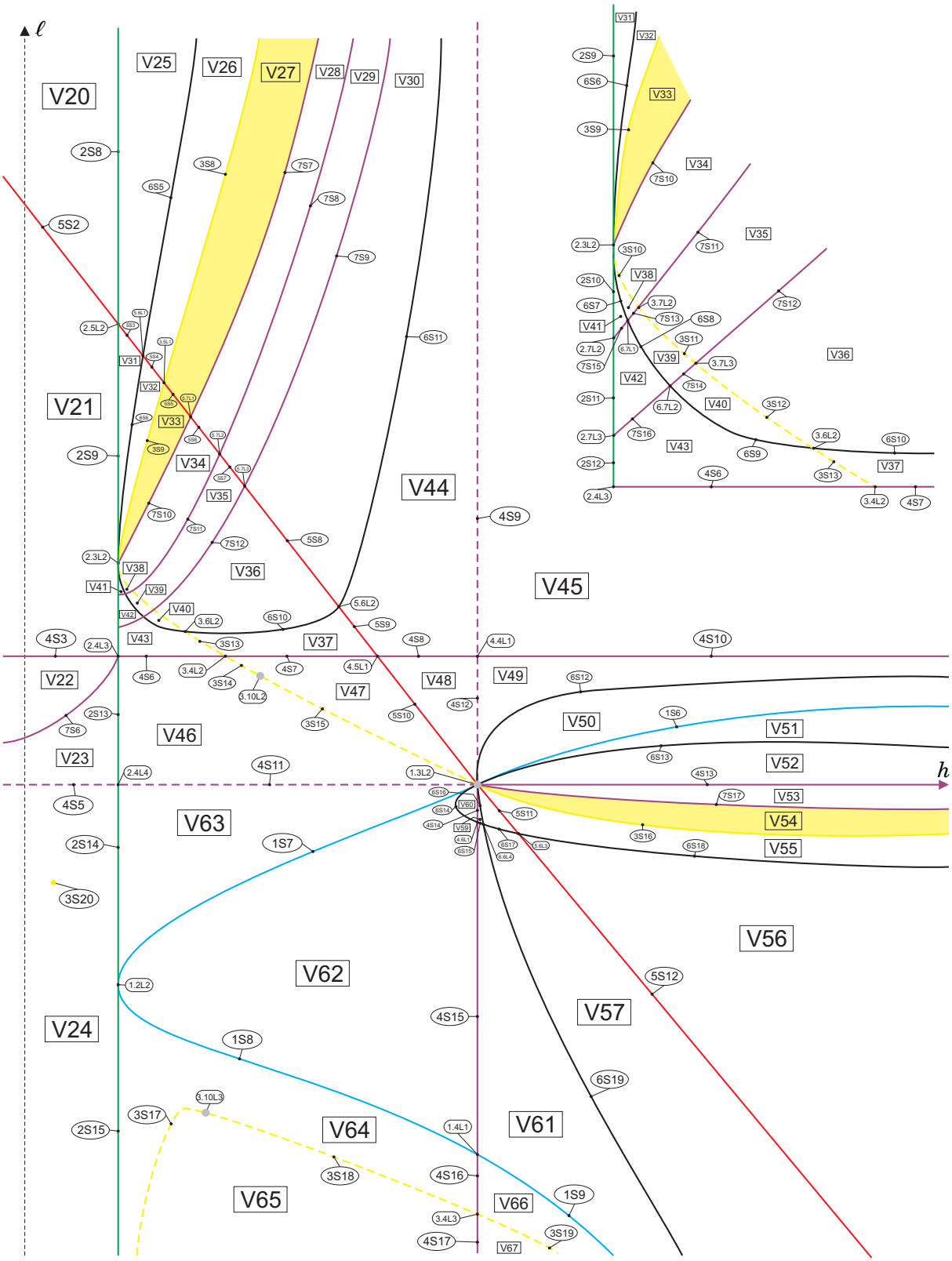

Figure 7.20: Complete bifurcation diagram for slice $n = 10$ (first and fourth quadrants)

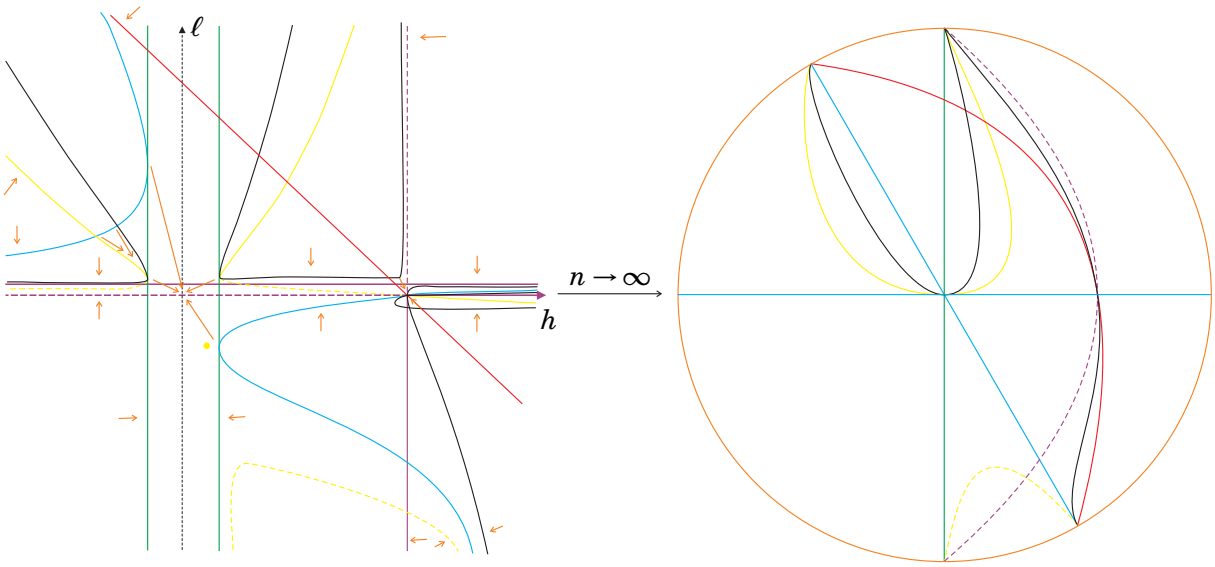

Figure 7.21: The transition from $n > 9$ to infinity. The orange arrows show the movement the curves must do as $n \to \infty$

in the parameter space.

We consider the curved triangles in the first quadrant of slice $n = 10$: V_{31}, V_{32} and V_{33}, all having $2.3\ell_2$ as a common vertex. As we move down from $n = 10$ to $n = 9$ (a singular slice), these three triangles collapse in a single point ($2.5L_2$) and, for values of $n < 9$, but very close to it, two triangles V_{68} and V_{69} appear in the upper part limited by the red curve. In addition, as we have already proved, there exist some elements of surface ($\mathscr{S}_7$) near these triangles and we either have the purple bifurcations persisting next to the triangles, or not. The first possibility is true, because after numerical analysis for values of n less than 9, but very close to it, we still verify the same changes in the phase portraits as shown in the sequence in Figure 7.16. As the endpoint of the curve $7S_7$ is $2.3\ell_2$ (see Lemma 7.4.35) and this point collapses and reappears in the part over the red curve, it is natural that $7S_7$ follows the same movement. However, the other elements of surface ($\mathscr{S}_7$) in this part remain starting from the segment $2s_{10}$. These facts are illustrated in Figures 7.22 to 7.35. For the transition of the slices drawn in these figures, it is clear that we need at least 13 values of n (apart from $n = 9$) to have coherence in the bifurcation diagram. Those values of n cannot be concretely determined, but we know they lie on the open interval between $n = 6$ and $n = 9$.

Figures 7.26 to 7.35 illustrate needed slices for the coherence of the bifurcation diagram. The intersection points between the purple curves with the green curve will “go up” in the sense of

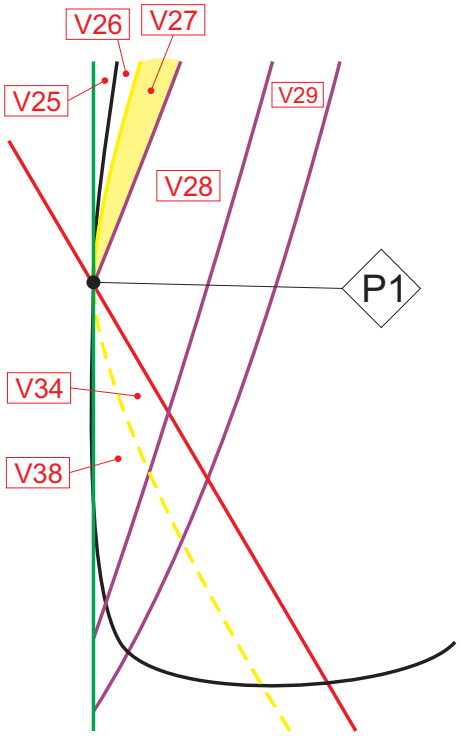

Figure 7.22: Slice of parameter space when $n = 9$ (see Figure 7.20)

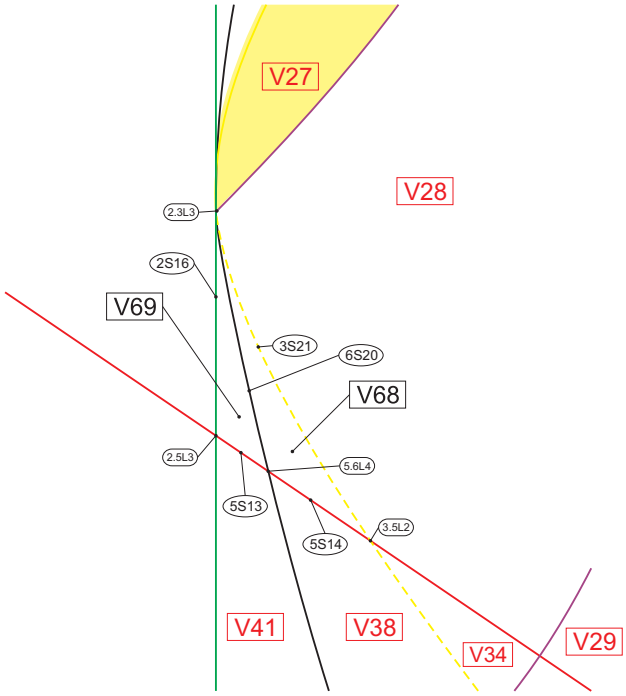

Figure 7.23: Slice of parameter space when $n = 9 - \varepsilon_1$ (see Figure 7.22)

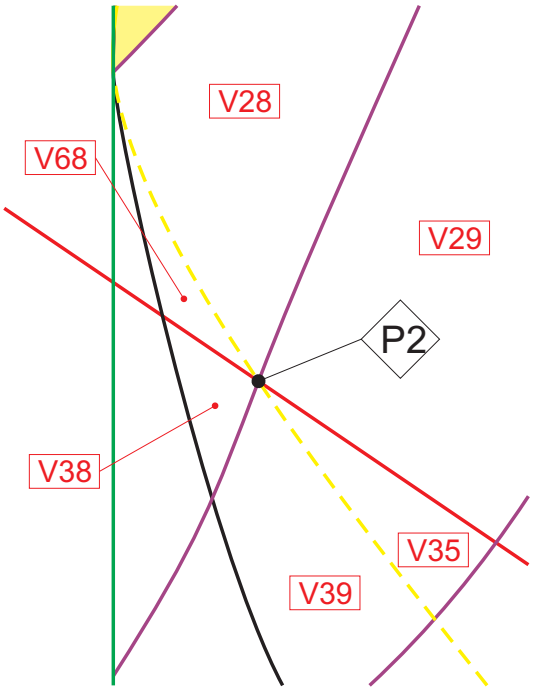

Figure 7.24: Slice of parameter space when $n = 9 - \varepsilon_1^*$ (see Figure 7.23)

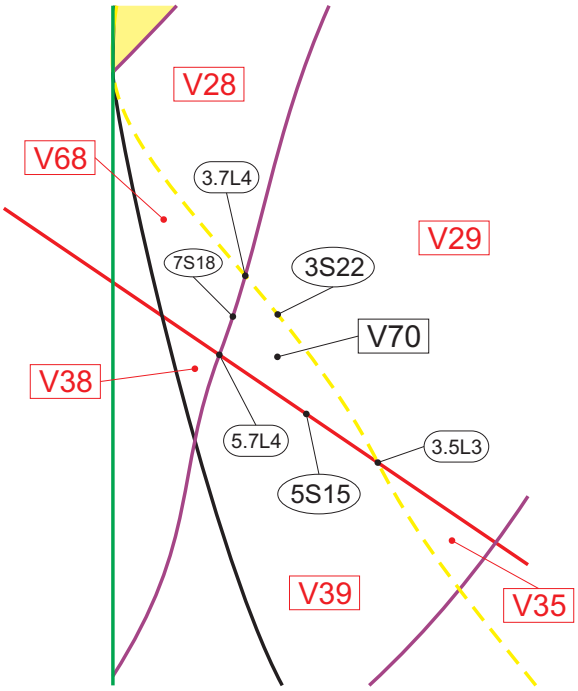

Figure 7.25: Slice of parameter space when $n = 9 - \varepsilon_2$ (see Figure 7.24)

increasing ℓ and cross the intersection point between the red and green curves (this intersection is renamed as different slices succeed). Consequently, the same will happen to the entire purple segments. However, there exist other bifurcation curves intersecting these purple curves. Then, the slices within these figures show step by step the movement of these purple curves until they are all in the upper part limited by the red curve. Each one of Tables 7.4.1 to 7.4.7 presents the "dead" and the "born" parts (of higher dimension in that slice) in the transition from one generic slice to another passing through a singular slice in the middle of them from $n = 10$ to $n = 9 - \varepsilon_7$.

Table 7.4.1: Transition from slice $n = 10$ to $n = 9 - \varepsilon_1$

"Dead" parts	**Parts in singular slice**	**"Born" parts**
V_{31}, V_{32}, V_{33}	P_1	V_{68}, V_{69}

Table 7.4.2: Transition from slice $n = 9 - \varepsilon_1$ to $n = 9 - \varepsilon_2$

"Dead" parts	**Parts in singular slice**	**"Born" parts**
V_{34}	P_2	V_{70}

Table 7.4.3: Transition from slice $n = 9 - \varepsilon_2$ to $n = 9 - \varepsilon_3$

"Dead" parts	**Parts in singular slice**	**"Born" parts**
V_{38}	P_3	V_{71}

Table 7.4.4: Transition from slice $n = 9 - \varepsilon_3$ to $n = 9 - \varepsilon_4$

"Dead" parts	**Parts in singular slice**	**"Born" parts**
V_{41}	P_4	$2S_{17}$

Table 7.4.5: Transition from slice $n = 9 - \varepsilon_4$ to $n = 9 - \varepsilon_5$

"Dead" parts	**Parts in singular slice**	**"Born" parts**
V_{35}	P_5	V_{72}

In Figures 7.36 to 7.39 we still remain in the first quadrant and they show the interaction among the algebraic surfaces ($\mathscr{S}_3$), ($\mathscr{S}_5$) and ($\mathscr{S}_6$), and it is not necessary to consider nonalge-

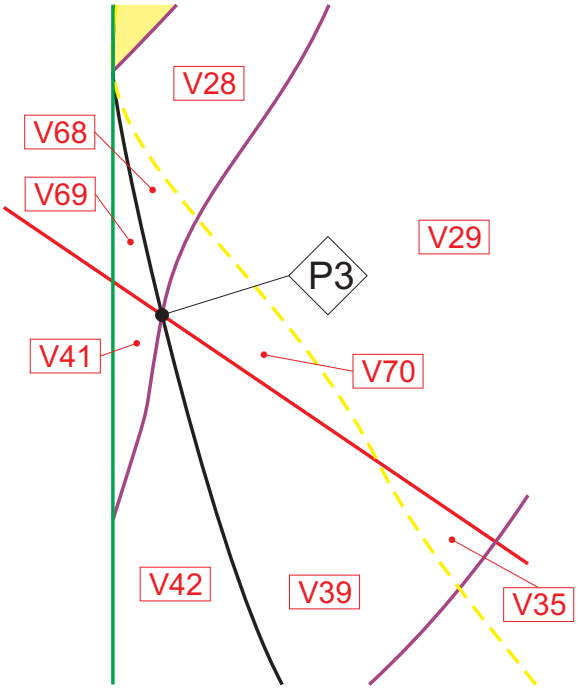

Figure 7.26: Slice of parameter space when $n = 9 - \varepsilon_2^*$ (see Figure 7.25)

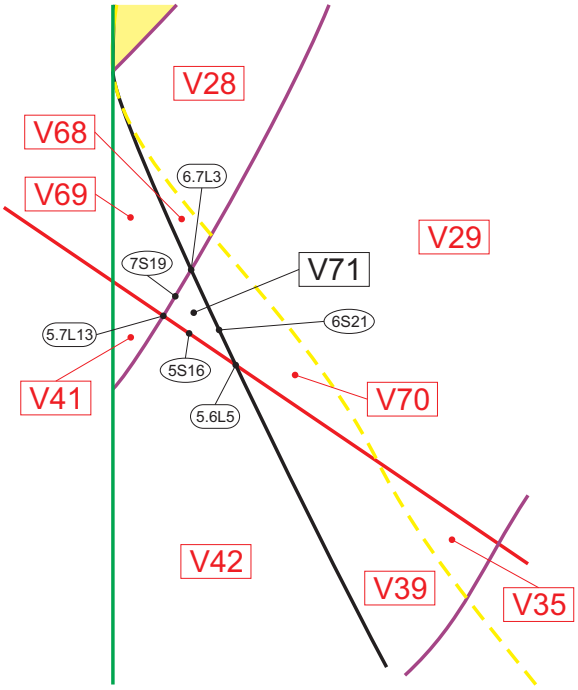

Figure 7.27: Slice of parameter space when $n = 9 - \varepsilon_3$ (see Figure 7.26)

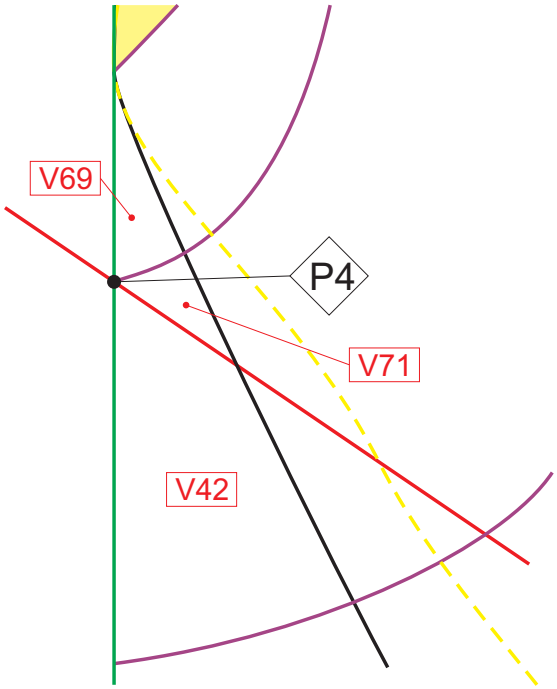

Figure 7.28: Slice of parameter space when $n = 9 - \varepsilon_3^*$ (see Figure 7.27)

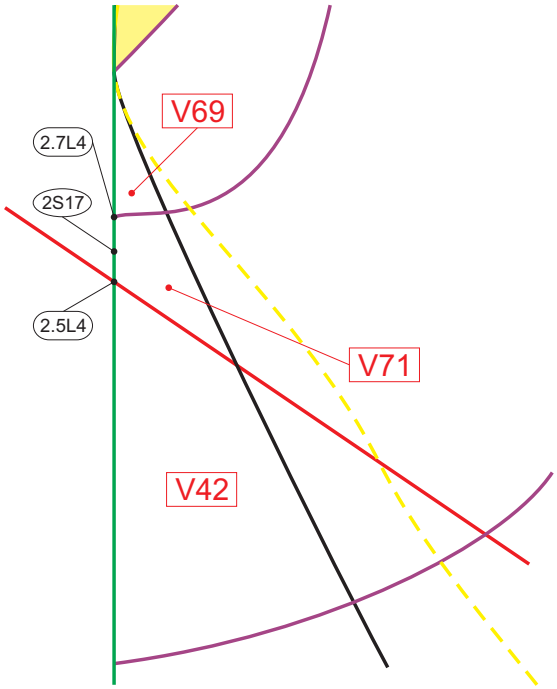

Figure 7.29: Slice of parameter space when $n = 9 - \varepsilon_4$ (see Figure 7.28)

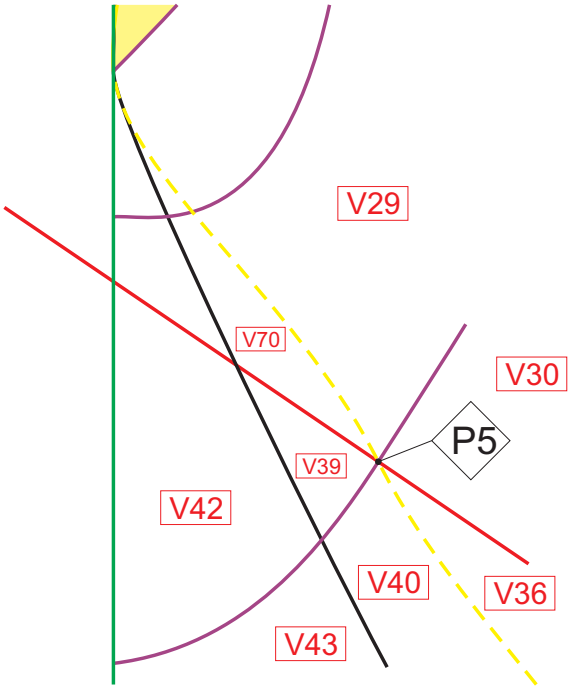

Figure 7.30: Slice of parameter space when $n = 9 - \varepsilon_4^*$ (see Figure 7.29)

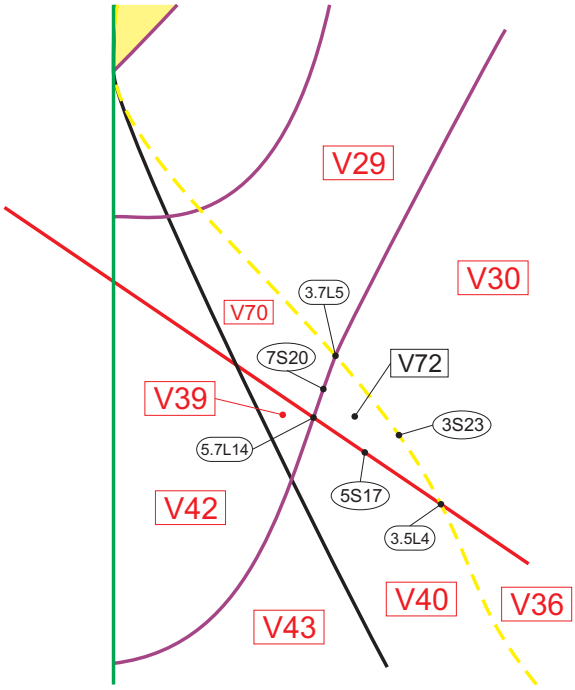

Figure 7.31: Slice of parameter space when $n = 9 - \varepsilon_5$ (see Figure 7.30)

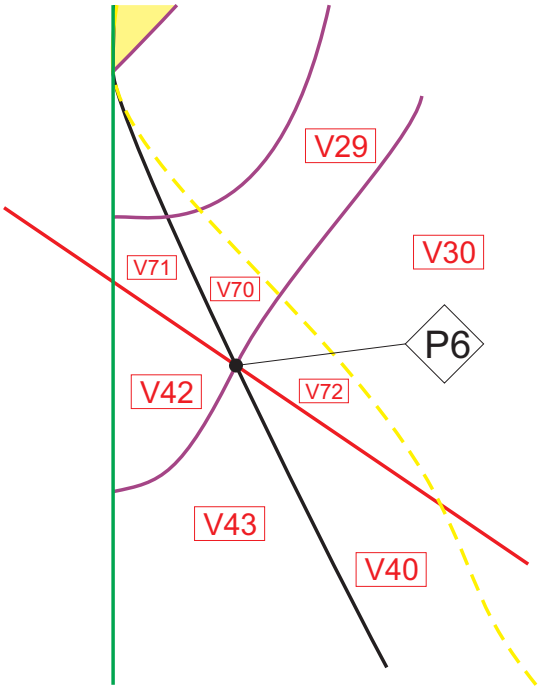

Figure 7.32: Slice of parameter space when $n = 9 - \varepsilon_5^*$ (see Figure 7.31)

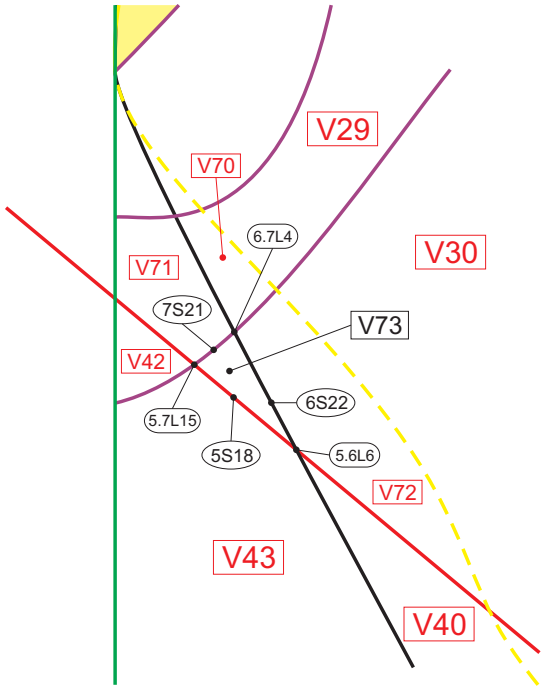

Figure 7.33: Slice of parameter space when $n = 9 - \varepsilon_6$ (see Figure 7.32)

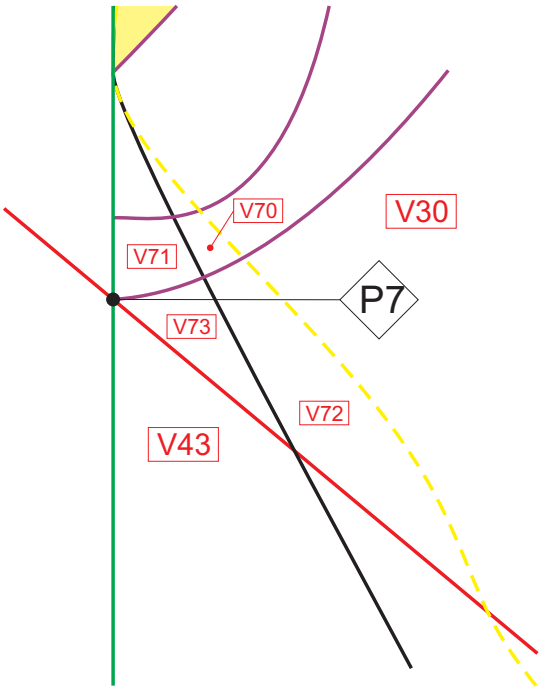

Figure 7.34: Slice of parameter space when $n = 9 - \varepsilon_6^*$ (see Figure 7.33)

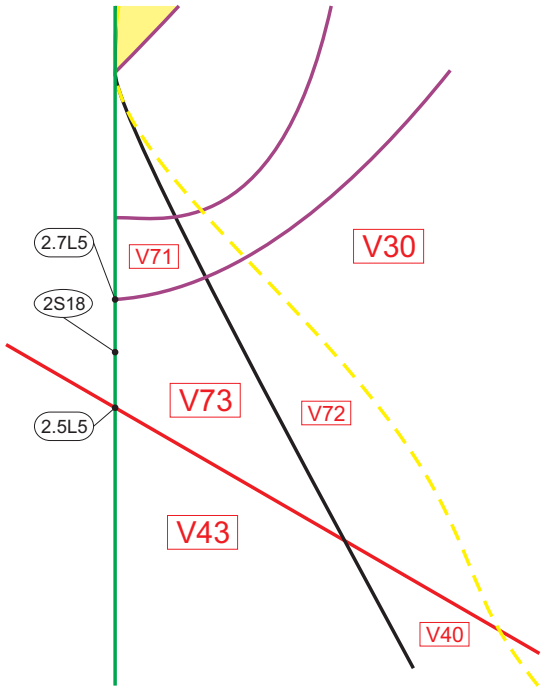

Figure 7.35: Slice of parameter space when $n = 9 - \varepsilon_7$ (see Figure 7.34)

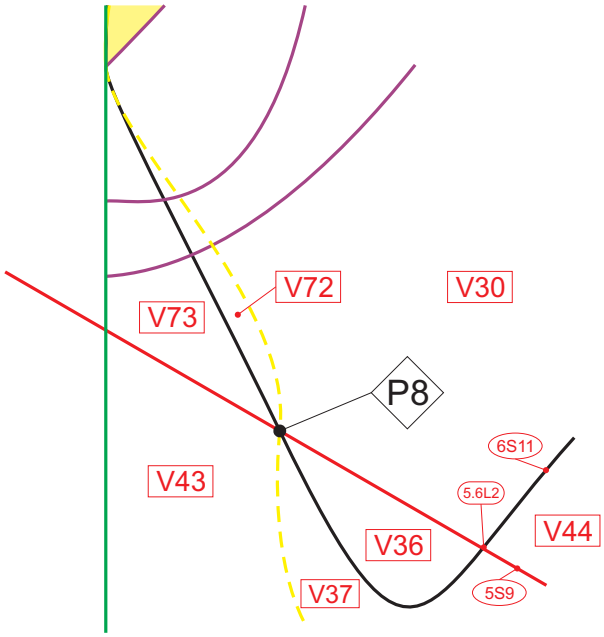

Figure 7.36: Slice of parameter space when $n = 6$ (see Figure 7.35)

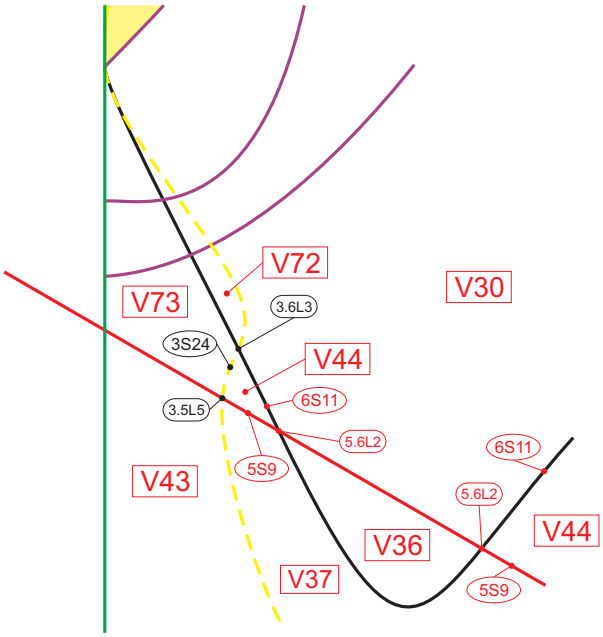

Figure 7.37: Slice of parameter space when $n = 119/20$ (see Figure 7.36)

Table 7.4.6: Transition from slice $n = 9 - \varepsilon_5$ to $n = 9 - \varepsilon_6$

"Dead" parts	**Parts in singular slice**	**"Born" parts**
V_{39}	P_6	V_{73}

Table 7.4.7: Transition from slice $n = 9 - \varepsilon_6$ to $n = 9 - \varepsilon_7$

"Dead" parts	**Parts in singular slice**	**"Born" parts**
V_{42}	P_7	$2S_{18}$

braic bifurcation surfaces to keep the coherence. Neither their existence is needed in the fourth quadrant shown in Figures 7.40 and 7.41. We observe that, even if $n = 125/27$ is a critical value corresponding to a singular slice, the intersection produced here is not labeled as a point but a line due to the fact that it is a contact point and, when we pass to the next (generic) slice, this contact point becomes two transversal ones but its characteristic remains; so, there exists no sense in changing its label. There will exist more situations like this in what follows. Tables 7.4.8 to 7.4.10 show the death and birth of parts from slice $n = 9 - \varepsilon_7$ to $n = 114/25$.

Table 7.4.8: Transition from slice $n = 9 - \varepsilon_7$ to $n = 119/20$. The "born" part V_{44}^* is not new since it will join later with V_{44} (see Figure 7.39)

"Dead" parts	**Parts in singular slice**	**"Born" parts**
V_{40}	P_8	V_{44}^*

Table 7.4.9: Transition from slice $n = 119/20$ to $n = 21/4$. The symbol '$\emptyset$' means that no new part was "born"

"Dead" parts	**Parts in singular slice**	**"Born" parts**
V_{36}	$5.6L_2$	$\emptyset$

Table 7.4.10: Transition from slice $n = 21/4$ to $n = 114/25$. The symbol '$\emptyset$' means that no part was "dead"

"Dead" parts	**Parts in singular slice**	**"Born" parts**
$\emptyset$	$1.6L_2$	V_{36}

Returning back to the first quadrant, the point in gray corresponds to a weak saddle of second

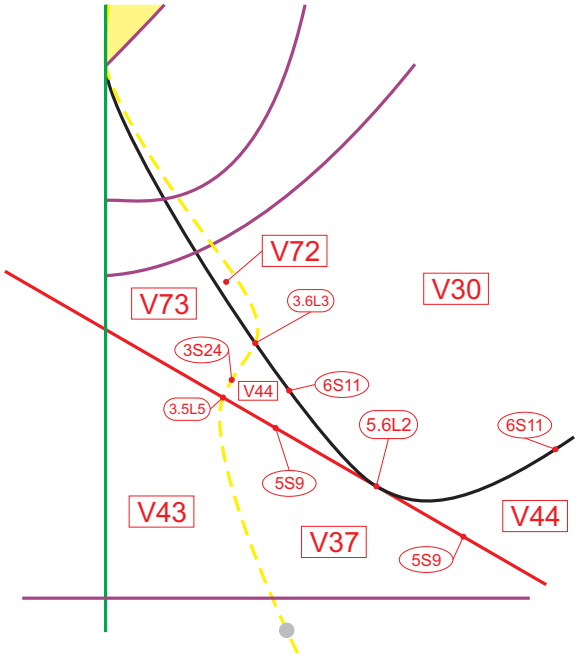

Figure 7.38: Slice of parameter space when $n = n_{17} \approx 5.8908\ldots$ (see Figure 7.37)

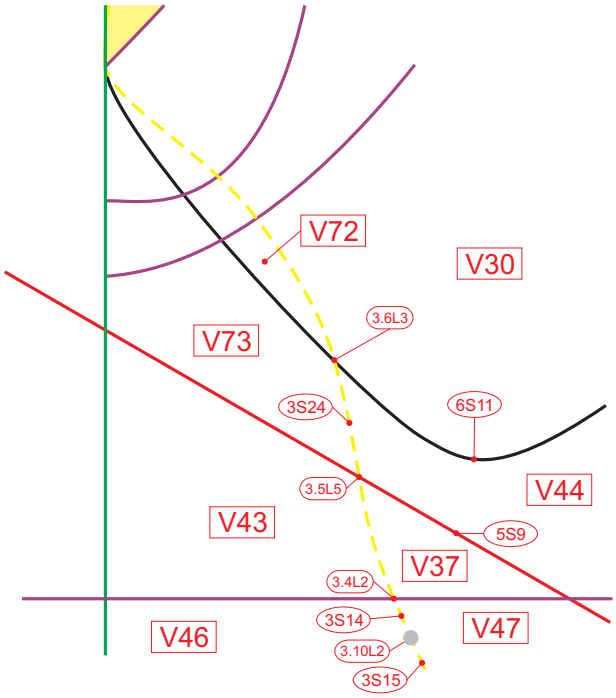

Figure 7.39: Slice of parameter space when $n = 21/4$ (see Figure 7.38)

order (see the point $3.10L_2$ in Figure 7.20). When $n = 9/2$, the curved triangle bordered by yellow (plus the gray point), purple and red curves bordering V_{37} ($3S_{13}$, $4S_7$, $5S_9$ and $3.10L_2$) collapses and reappears creating new parts, as seen in Figures 7.42 and 7.43. Table 7.4.11 shows the "dead" and "born" parts after this bifurcation.

Table 7.4.11: Transition from slice $n = 21/4$ to $n = 108/25$

"Dead" parts	**Parts in singular slice**	**"Born" parts**
V_{37}	P_9	V_{75}

Moving back to the forth quadrant to the continuation of the movement shown in Figures 7.40 and 7.41, the black curve produces the same movement as before but now contacting the yellow curve, according to Figures 7.44 and 7.45, and Table 7.4.12 presents the new parts.

In Figure 7.46 we represent fourth quadrant of the slice of the parameter space when $n = 4$. When $n > 4$, there exists a point of intersection among surfaces $(\mathscr{S}_2)$, $(\mathscr{S}_3)$ and $(\mathscr{S}_6)$; more precisely, the point $2.3L_3$ in Figure 7.23. According to Lemmas 7.4.14, 7.4.17 and 7.4.20, the expression of this point (or, seen in the projective space, this curve) is $[1 : h : 2h/(h-1) : (1+h)^2]$. As $h \to 1^+$, we

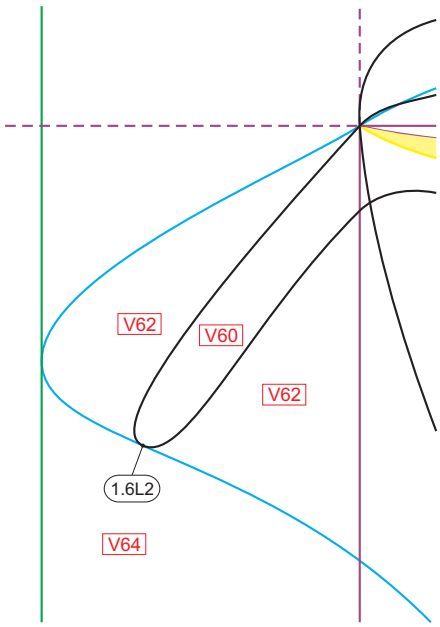

Figure 7.40: Slice of parameter space when n = 125/27 (see Figure 7.20)

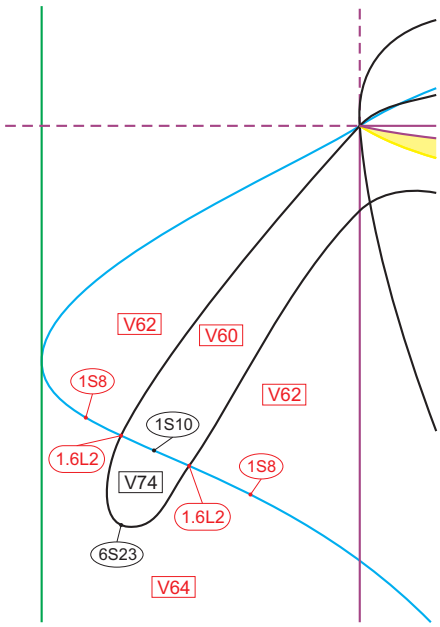

Figure 7.41: Slice of parameter space when n = 114/25 (see Figure 7.40)

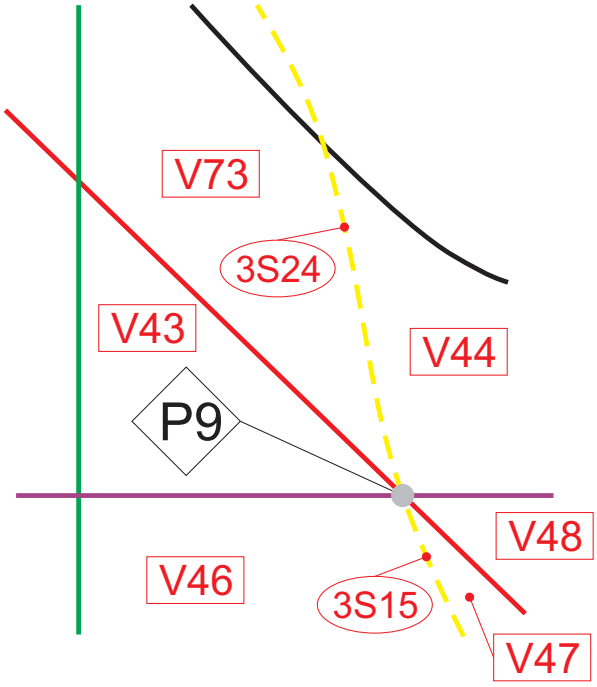

Figure 7.42: Slice of parameter space when n = 9/2 (see Figure 7.39)

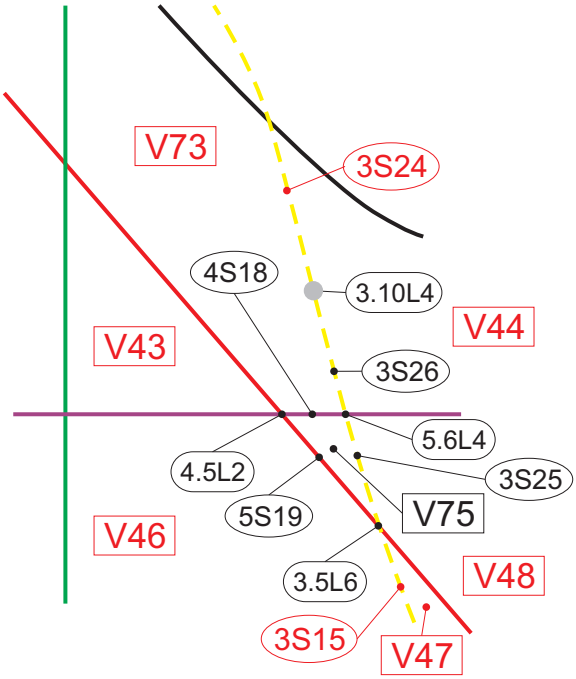

Figure 7.43: Slice of parameter space when n = 108/25 (see Figure 7.42)

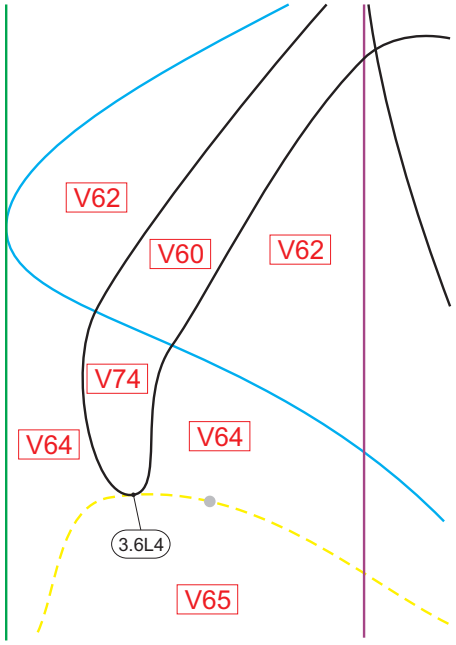

Figure 7.44: Slice of parameter space when $n = 3(102+7\sqrt{21})/100$ (see Figure 7.41)

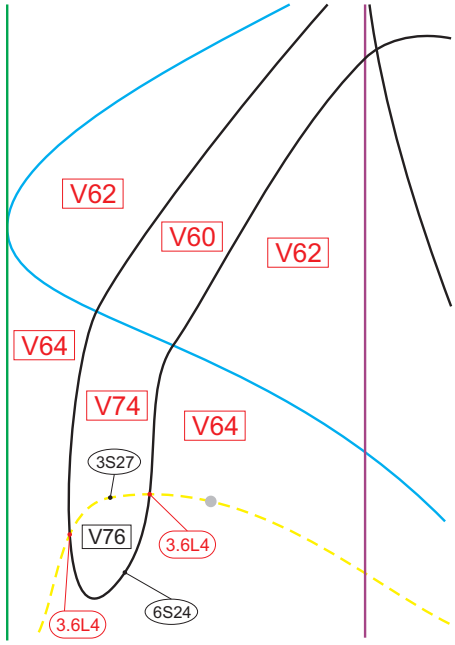

Figure 7.45: Slice of parameter space when $n = 401/100$ (see Figure 7.44)

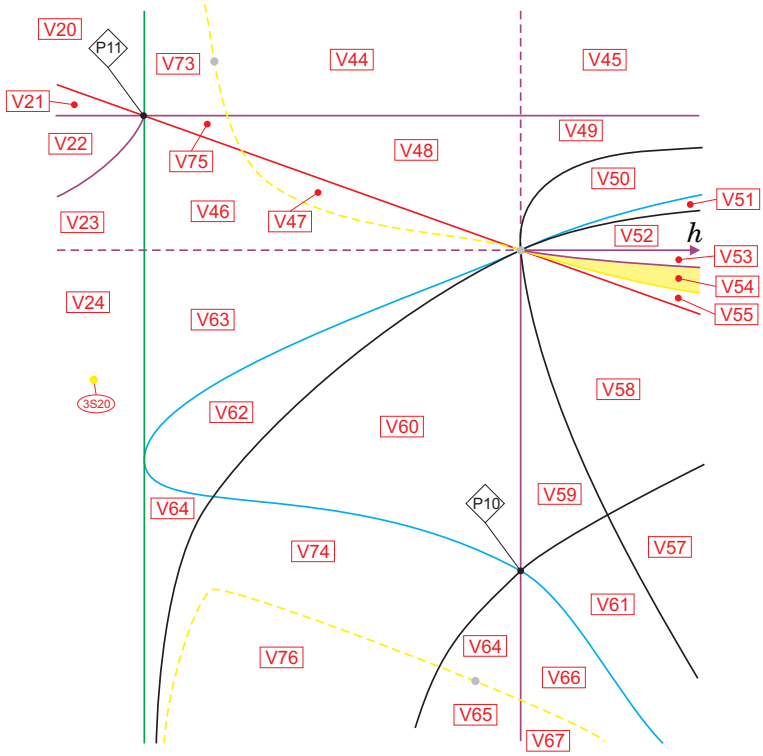

Figure 7.46: Slice of parameter space when $n = 4$ (see Figures 7.20, 7.42 and 7.45)

Table 7.4.12: Transition from slice $n = 114/25$ to $n = 401/100$. The symbol '$\emptyset$' means that no part was "dead"

"Dead" parts	**Parts in singular slice**	**"Born" parts**
$\emptyset$	$3.6L_4$	V_{76}

have $n \to 4^+$ and $2.3L_3$ goes to $+\infty$ (since the coordinate ℓ goes to $+\infty$). An analogous argument is applied to the point $3.6L_4$ in Figure 7.45 (the one in the left side) and we conclude it also goes to $-\infty$. Thus, we conclude that the segment $6S_{24}$ in Figure 7.45 breaks apart, obtaining the configuration shown in Figure 7.46. Moreover, there exist two portions of collapsing of curves, forming the points P_{10} and P_{11}. Considering the next slice when $n = 2304/625$, the collapsed curves separate and form three curved triangles: V_{77}, V_{84} and V_{85}. Furthermore, the expressions for the points $2.3L_3$ and $3.6L_4$ now make sense and the points coincide at infinity and appear as $2.3L_4$ in the lower part of the slice. Together with them, four more elements of surface ($\mathscr{S}_7$) must exist in order to keep the coherence of the bifurcation diagram. We plot a portion of the slice when $n = 2304/625$ in Figure 7.47. See in Table 7.4.13 the parts which disappeared and were created when we pass through slice $n = 4$.

Table 7.4.13: Transition from slice $n > 4$ to $n = 2304/645$. The notation V_{62}^* means that only one of the two apparently disconnected parts of V_{62} in Figure 7.45 has died. Moreover, the point $2.7L_5$ in Figure 7.35 tends to P_{64} as $n \to \infty$ "killing" all the above volumes (and respective borders) and $2.7L_6$ comes from P_{64} (when $n = -\infty$) "bringing" a new set of volumes and borders

"Dead" parts	**Parts in singular slice**	**"Born" parts**
V_{62}^*	P_{10}	V_{77}
V_{26}, V_{27}, V_{28}, V_{29}, V_{30}, V_{68}, V_{69}, V_{70}, V_{71}, V_{72}	P_{64}	V_{78}, V_{79}, V_{80}, V_{81}, V_{82}, V_{83}
$2.7L_5$	P_{64}	$2.7L_6$
V_{43}	P_{11}	V_{84}, V_{85}

In Figures 7.48 to 7.51 we show the movement of the gray point $3.10L_3$ and the purple straight line containing segment $4S_{16}$, when n moves down from $n = n_{27} \approx 3.6349\ldots$ to $n = n_{31} = 3$. Tables 7.4.14 and 7.4.15 presents the death and birth of parts in this transition.

When $n = 3$, surfaces ($\mathscr{S}_3$) and ($\mathscr{S}_5$) do not intersect transversally, possessing a point of contact, as we can see in Figure 7.52 and in Table 7.4.16. We note that in the next slice when $n = 14/5$ there exists another part with limit cycles (V_{87}) as represented in Figure 7.53. In the sequence, we claim that at $n = 8/3$ the point $3.10L_4$ goes to infinity (more precisely, to the point P_{64}). Indeed, according

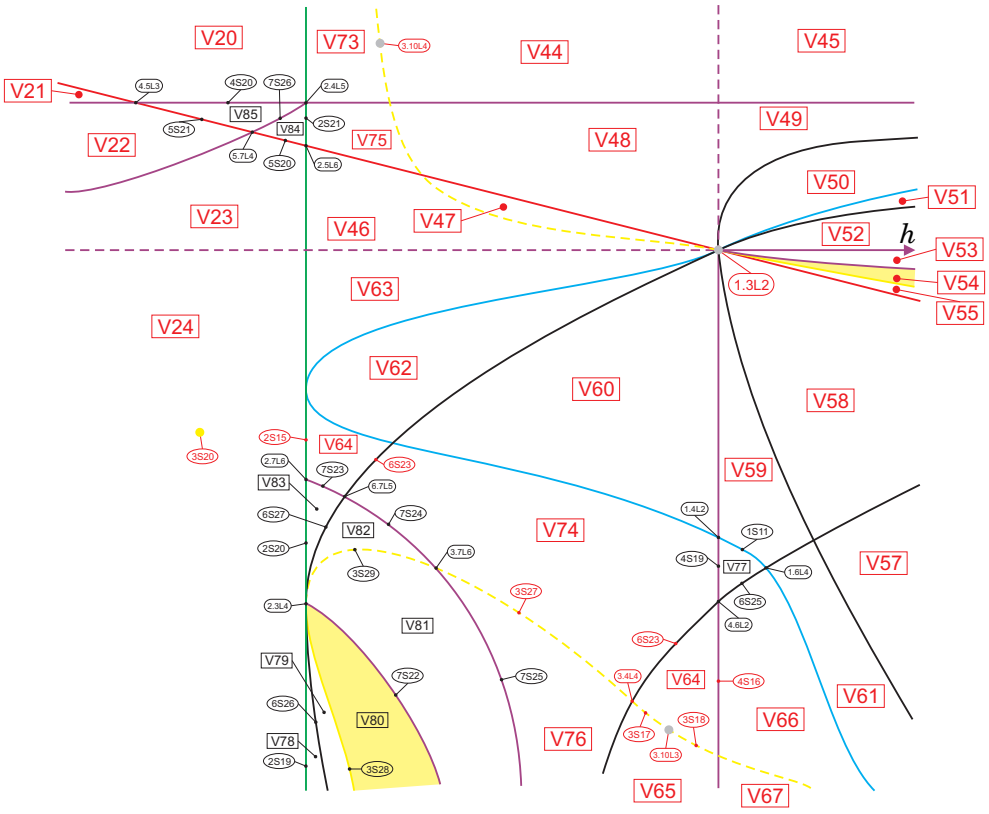

Figure 7.47: Slice of parameter space when $n = 2304/625$ (see Figure 7.46)

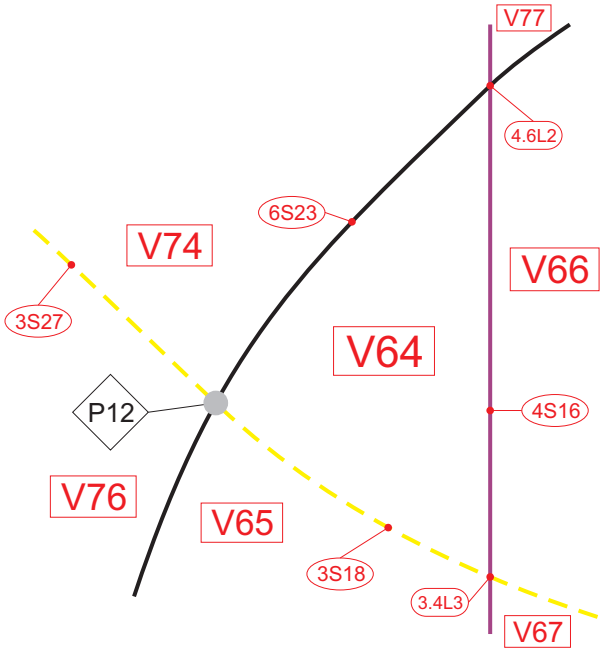

Figure 7.48: Slice of parameter space when $n = n_{27} \approx 3.6349\ldots$ (see Figure 7.47)

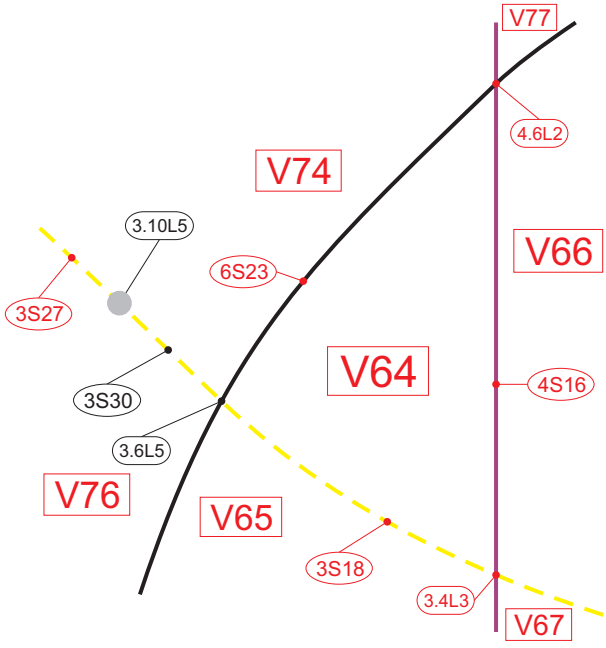

Figure 7.49: Slice of parameter space when $n = 7/2$ (see Figure 7.48)

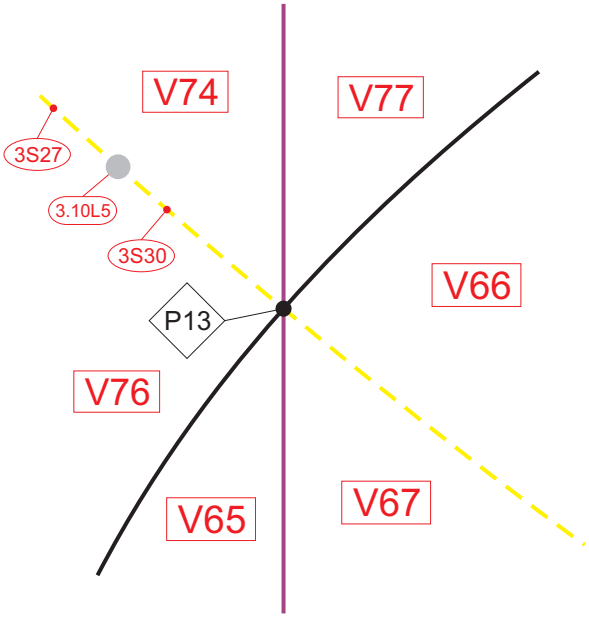

Figure 7.50: Slice of parameter space when $n = 2+\sqrt{2}$ (see Figure 7.49)

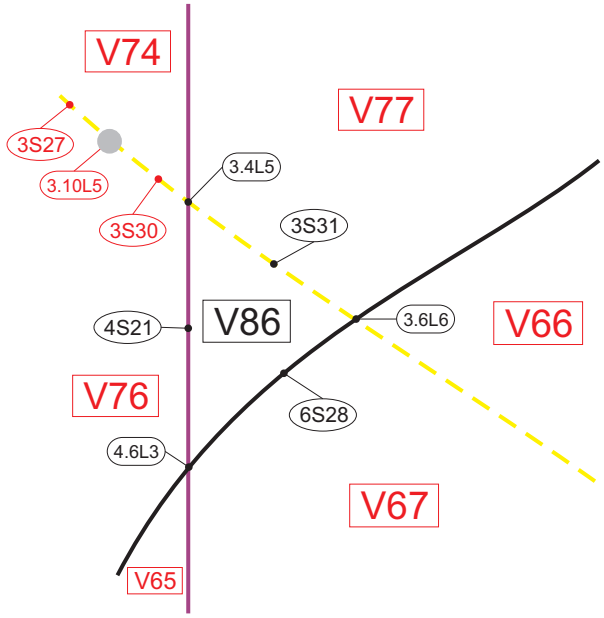

Figure 7.51: Slice of parameter space when $n = 16/5$ (see Figure 7.50)

Table 7.4.14: Transition from slice $n = 2304/625$ to $n = 7/2$

"Dead" parts	**Parts in singular slice**	**"Born" parts**
$3S_{12}$	P_{12}	$3S_{30}$

Table 7.4.15: Transition from slice $n = 7/2$ to $n = 16/5$. The notation V_{64}^* means that only one of the two apparently disconnected parts of V_{64} in Figure 7.49 has died

"Dead" parts	**Parts in singular slice**	**"Born" parts**
V_{64}^*	P_{13}	V_{86}

to Lemma 7.4.21, the expression of this point is

$$\left[1 : \frac{4-8\ell+3\ell^2-\sqrt{3}\sqrt{(2+\ell)^3(3\ell-2)}}{16-24\ell} : \ell : \frac{12-24\ell+3\ell^2-\sqrt{3}\sqrt{(2+\ell)^3(3\ell-2)}}{8-12\ell}\right].$$

Considering the last coordinate, we write

$$\frac{12-24\ell+3\ell^2-\sqrt{3}\sqrt{(2+\ell)^3(3\ell-2)}}{8-12\ell} = n$$

and solve it with respect to n, obtaining three solutions. Now, if we substitute the value $n = 8/3$ in

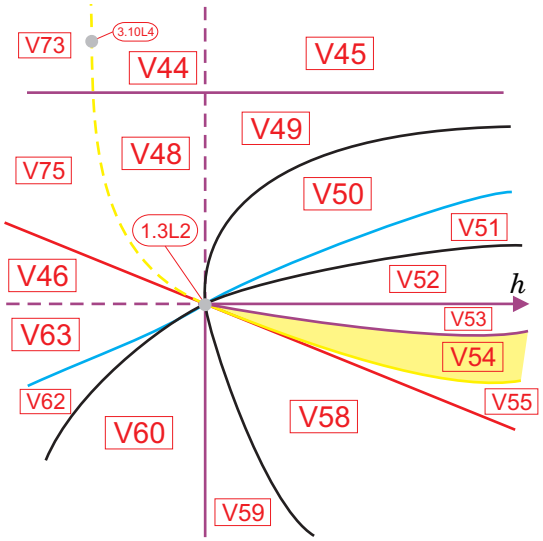

Figure 7.52: Slice of parameter space when $n = 3$ (see Figure 7.47)

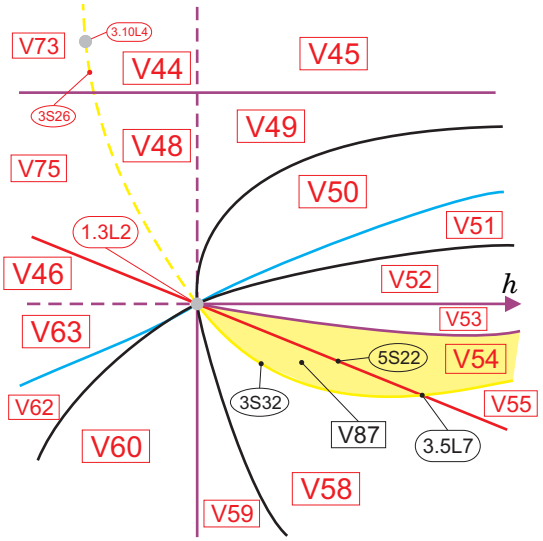

Figure 7.53: Slice of parameter space when $n = 14/5$ (see Figure 7.52)

these solutions, they are not defined, since $3n-8$ is a factor in the three denominators, proving our claim. The parameter space at this level is shown in Figure 7.54.

Table 7.4.16: Transition from slice $n > 3$ to $n = 14/5$

"Dead" parts	**Parts in singular slice**	**"Born" parts**
V_{47}	$1.3L_2$	V_{87}

However, when we move down the value of n, the expression above makes sense again and the point reappears as $3.6L_6$ in the parameter space, but in the lower part (in the fourth quadrant), according to Figure 7.55 (this figure is an ampliation of a portion of Figure 7.47). When this point reappears, it "brings" the curves $7S_{22}$ (loop–type connection) and $7S_{25}$ (heteroclinic connection between the finite saddle–node and the finite saddle), making them intersect $3S_{28}$. This phenomenon can be verified by fixing $n < 8/3$, but sufficiently close to this value, and parameterizing the segment $3S_{28}$ in the coordinate ℓ, for example, and for each value of h, we construct the phase portrait with the program P4 and verify that the connections of separatrices which correspond to the curves $7S_{22}$ and $7S_{25}$ occur on this segment. In addition, we must have an element of surface ($\mathscr{S}_{10}$) which corresponds to a bifurcation of double limit cycle in order to keep the coherence in the bifurcation diagram. Lemma 7.4.37 assures the existence of such surface.

Lemma 7.4.37. *Segment* $10S_1$ *corresponds to a bifurcation of double limit cycle and its borders*

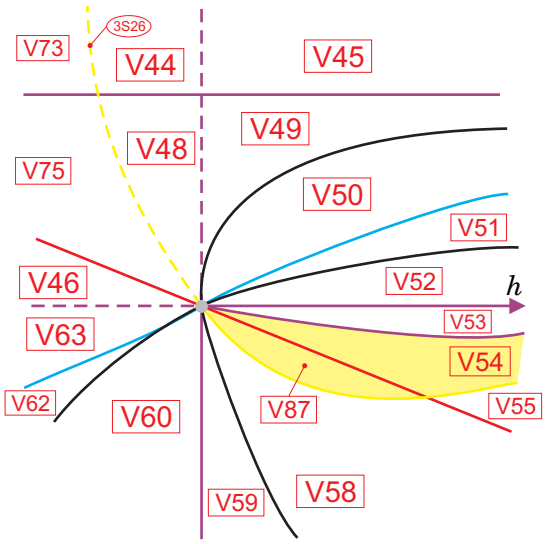

Figure 7.54: Slice of parameter space when $n = 8/3$ (see Figure 7.53)

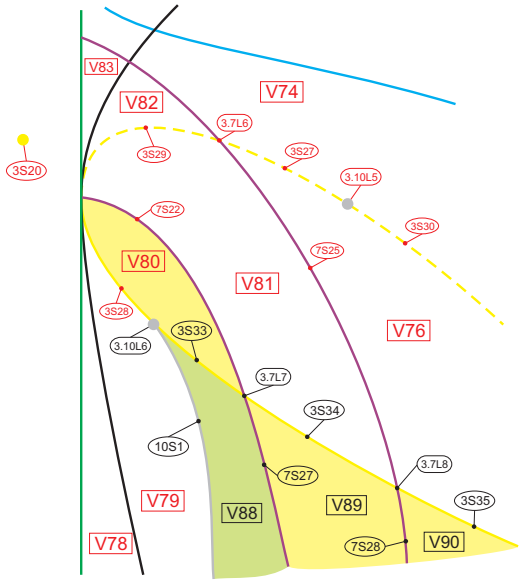

Figure 7.55: Slice of parameter space when $n = 8/3 - \varepsilon_8$ (see Figure 7.47)

are $3.10L_6$ *and* P_{64} *(this last one from slice* $n = -\infty$*).*

Proof. We consider Figure 7.55. Part V_{80} first appeared in slice when $n = 2304/625$ and its corresponding phase portrait possesses a limit cycle. We note that on the segments $3S_{28}$, $3S_{33}$, $3S_{34}$, $3S_{35}$ and on their linking points the phase portraits possess a weak focus of order at least one and, consequently, they refer to a Hopf bifurcation. If we are in part V_{80} and cross the segment $3S_{28}$, we enter part V_{79} and the limit cycle is lost. Following this idea, the same should happen if we cross the segment $3S_{33}$, but that is not what happens. After crossing this segment, the limit cycle persisted when entering part V_{88}. In fact the Hopf bifurcation creates a second limit cycle.

We can confirm this by moving along a different path. There exist no limit cycles in the phase portraits of parts V_{81} and V_{76} and, after crossing the segments $3S_{34}$ and $3S_{35}$, respectively, we enter in parts V_{89} and V_{90}, whose corresponding phase portraits have a limit cycle. As the segment $7S_{28}$ is the continuation of $7S_{25}$, it refers to a heteroclinic connection of separatrices between the finite saddle–node and the finite saddle, and it also possesses a limit cycle, since the separatrix which enrolls in the limit cycle is not involved in the connection. Now, considering the segment $7S_{27}$, we know it is the continuation of $7S_{22}$ and, hence, a loop–type bifurcation happens on it. So, we have two possibilities after crossing it and entering in part V_{88}: either the limit cycle dies, or another one is created. In fact the second possibility is which happens, since there already exist at least one limit cycle in V_{88}, confirming that there exist two limit cycles in the representatives

of part V_{88}.

We note that these two limit cycles are around the same focus, because there exists only one focus in this portion of the parameter space. Then, as in part V_{79} we do not have limit cycles and in V_{88} we have two of them (around the same focus), there must exist at least one element $10S_1$ of surface $(\mathscr{S}_{10})$ dividing these two parts and corresponding to the presence of a double limit cycle.

Now, it remains to prove where $10S_1$ starts from. As we have already discussed, the point $3.10L_4$ (corresponding to the presence of a weak saddle of order two) went to infinity and returned back in the lower part of the forth quadrant, being labeled as $3.10L_6$ and corresponding to the presence of a weak focus of order two. With this in mind, it is more comprehensible that leaving part V_{80} and crossing the yellow curves, we enter in two topologically distinct parts, one with limit cycles and the other without them. The linking point $3.10L_6$ of the segments $3S_{28}$ and $3S_{33}$ is responsible for this, i.e. if we "walk" along the segment $3S_{28}$, which does not possess limit cycle, and cross $3.10L_6$, the focus becomes weaker and a Hopf bifurcation happens, implying the birth of a limit cycle in the representatives of $3S_{33}$. Then, by this argument and by numerical evidences, the segment $10S_1$ starts from $3.10L_6$. Since surface $(\mathscr{S}_{10})$ has been born at P_{64} in slice $n = 8/3$, this point is still a border of $10S_1$. ∎

We show in Figure 7.56 an ampliation of the neighborhood in the parameter space of the point $3.10L_6$ with the corresponding phase portraits. Table 7.4.17 presents the "dead" and "born" parts when we go from slice $n = 14/5$ to $n = 8/3 - \varepsilon_8$.

Table 7.4.17: Transition from slice $n = 14/5$ to $n = 8/3 - \varepsilon_8$

"Dead" parts	**Parts in singular slice**	**"Born" parts**
$3.10L_4$	P_{64}	V_{88}, V_{89}, V_{90}

We now continue moving down the values of n and the next important value to be considered is $n = n_{35} = 8/3 - \varepsilon_8^*$. At this level, the point $3.10L_5$ (see Figure 7.55) moves towards the intersection between yellow and purple curves $(3.7L_6)$, which cannot be precisely determined, and crosses it. This movement does not imply topological changes in the phase portraits since $3.10L_5$ corresponds to a weak saddle of order two. We show the movement just described in Figures 7.57 and 7.58, and in Table 7.4.18.

Considering the next singular slice, we analyze the case when $n = 9/4$. According to Lemma 7.4.4, in this value of n, surface $(\mathscr{S}_3)$ has a line of singularities of degree of degeneration at least three; in fact, when $n = 9/4$, a branch of this surface becomes a cusp after the collision of the point

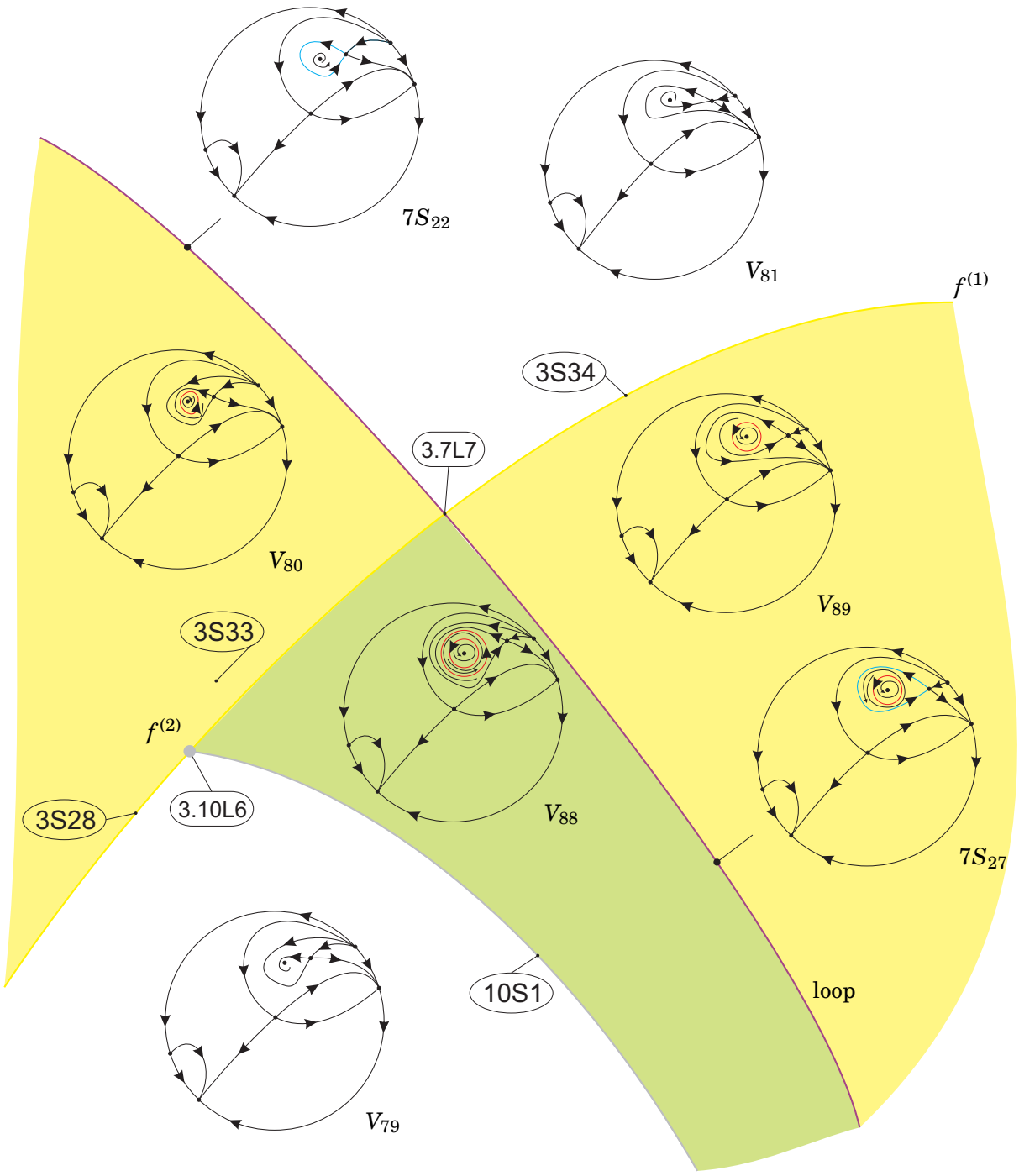

Figure 7.56: Neighborhood in the parameter space of the point $3.10L_6$ with the corresponding phase portraits: the existence of double limit cycle through a $f^{(2)}$

Table 7.4.18: Transition from slice $n = 8/3 - \varepsilon_8$ to $n = 8/3 - \varepsilon_9$

"Dead" parts	**Parts in singular slice**	**"Born" parts**
$3S_{27}$	P_{14}	$3S_{36}$

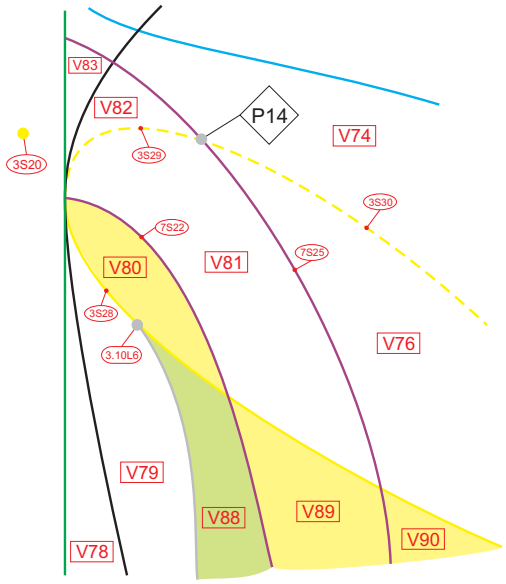

Figure 7.57: Slice of parameter space when $n = 8/3 - \varepsilon_8^*$ (see Figure 7.55)

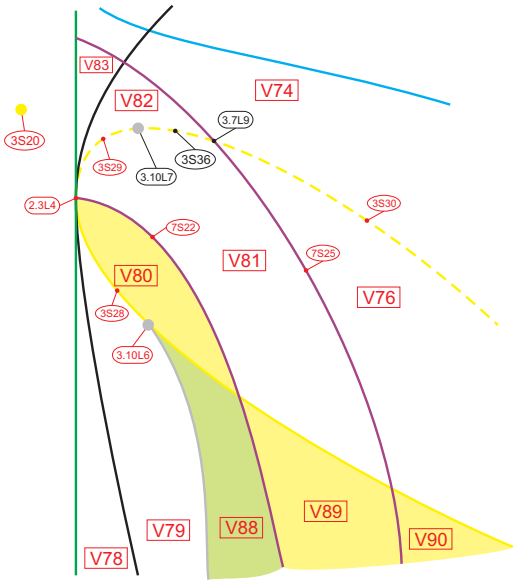

Figure 7.58: Slice of parameter space when $n = 8/3 - \varepsilon_9$ (see Figure 7.57)

$2.3L_4$ (which is also a common point of surfaces $(\mathscr{S}_2)$, $(\mathscr{S}_6)$ and $(\mathscr{S}_7)$; see Figure 7.58) with $3S_{20}$ (a projective line or a single point in each slice) which corresponds to two complex singular points with null trace. In addition to this collision, the points $3.10L_6$ and $3.10L_7$ also collapse and make part of this cusp point of surface $(\mathscr{S}_3)$, as we can see in Figure 7.59. It is worth mentioning that the corresponding phase portrait of this cusp point, P_{15}, possesses a singularity (a nilpotent cusp) that grasps simultaneously the properties of a weak saddle of order two and a weak focus of order two; besides, this focus is in the edge of turning into a node. We also note that the part with two limit cycles has remained at this level and it will "survive a bit longer".

The next phenomenon is that the same branch of yellow curve produces itself a loop for values of $n < 9/4$, but close to it, and we arrive at the Figure 7.60. We have verified that the purple curves behaves as represented in Figure 7.60 and that the part of two limit cycles still persists. However, the elements characterized by possessing a weak point of order two do not persist, since their expression has no image for values of $n \in (-2, 9/4)$.

So, there may arise a question. If there exists no element implying the presence of a weak

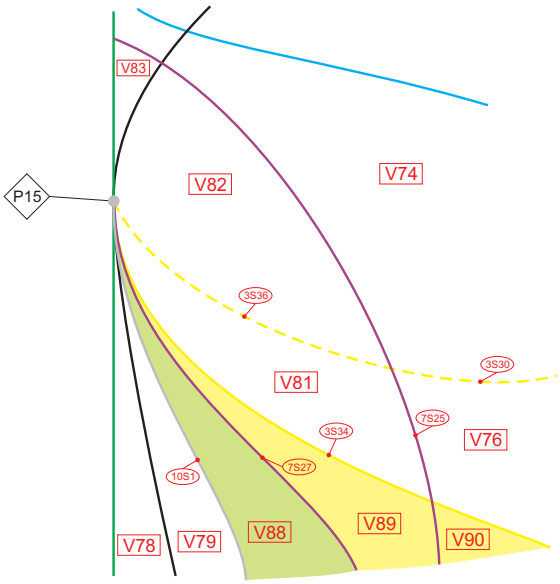

Figure 7.59: Slice of parameter space when $n = 9/4$ (see Figure 7.58)

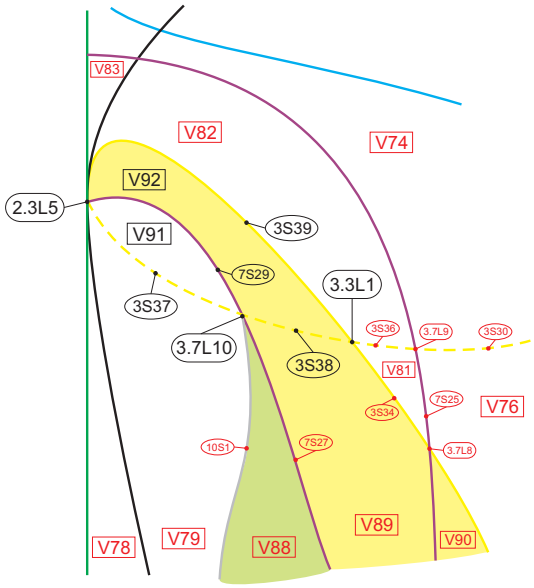

Figure 7.60: Slice of parameter space when $n = 11/5$ (see Figure 7.59)

focus of order two, where does the bifurcation surface of double limit cycle start from? This starts from a weak saddle of order one which produces a loop itself (as suggested in the description of surface ($\mathscr{S}_3$) on page 147). In the case of planar differential systems, we know that the stability of a homoclinic loop through a saddle is determined in first approximation by the trace of the saddle. If the trace is nonzero, a loop bifurcation leads to the birth (or death) of a unique limit cycle when the two separatrices of the saddle cross each other, and we strongly use this fact in the results of this thesis. However, according to Joyal and Rousseau [36], when the trace of the saddle point vanishes, we can have several limit cycles rising in a loop bifurcation (the authors prove this phenomenon using the Poincaré return map in the neighborhood of the loop).

In simple words, when an elementary saddle forms a loop, the interior stability of the loop is ruled by the trace of the saddle. It is unstable, if the trace is positive, and it is stable, if the trace is negative. Thus, if along a set of parameters while the loop persists the trace changes its sign, a limit cycle must bifurcate.

The most interesting phenomenon that happens in the family $\overline{\mathbf{QsnSN(C)}}$ is the fact that we can pass from a (generalized) Hopf bifurcation to a (generalized) loop bifurcation continuously as we can see in Figures 7.58 to 7.60.

Remark 7.4.38. *The terms "generalized" used twice above refer respectively to a Hopf bifurcation associated with a weak focus of order two and a loop bifurcation associated with a weak saddle of*

order one.

We show in Figure 7.61 an ampliation of the neighborhood in the parameter space of the point $3.7L_{10}$ with the corresponding phase portraits. Table 7.4.19 shows the "dead" and "born" parts when we go from slice $n = 8/3 - \varepsilon_9$ to $n = 11/5$.

Table 7.4.19: Transition from slice $n = 8/3 - \varepsilon_9$ to $n = 11/5$

"Dead" parts	**Parts in singular slice**	**"Born" parts**
V_{80}	P_{15}	V_{91}, V_{92}

In what follows, the point $3.7L_9$ moves towards the point $3.3L_1$, they intersect and new parts are created as can be visualized in Figures 7.62 and 7.63. Table 7.4.20 shows the "dead" and "born" parts when we go from slice $n = 11/5$ to $n = 11/5 - \varepsilon_{10}$.

Table 7.4.20: Transition from slice $n = 11/5$ to $n = 11/5 - \varepsilon_{10}$

"Dead" parts	**Parts in singular slice**	**"Born" parts**
V_{81}	P_{16}	V_{93}

In Figures 7.64 to 7.67, we show the movement of the curves in yellow and purple when we decrease n from $n_{41} = 3(102 - 7\sqrt{21})/100$ (including this value) to $n_{45} = 2$, creating contact points with other curves and after intersecting them transversally in two points. Tables 7.4.21 and 7.4.22 indicate the "dead" and "born" parts during this transition.

Table 7.4.21: Transition from slice $n = 11/5 - \varepsilon_{10}$ to $n = 3(102 - 7\sqrt{21})/100 - \varepsilon_{11}$. The symbol '$\emptyset$' means that no part was "dead"

"Dead" parts	**Parts in singular slice**	**"Born" parts**
$\emptyset$	$3.6L_8$	V_{94}

Table 7.4.22: Transition from slice $n = 3(102 - 7\sqrt{21})/100 - \varepsilon_{11}$ to $n = 2 + \varepsilon_{12}$. The symbol '$\emptyset$' means that no part was "dead"

"Dead" parts	**Parts in singular slice**	**"Born" parts**
$\emptyset$	$5.7L_5$	V_{95}

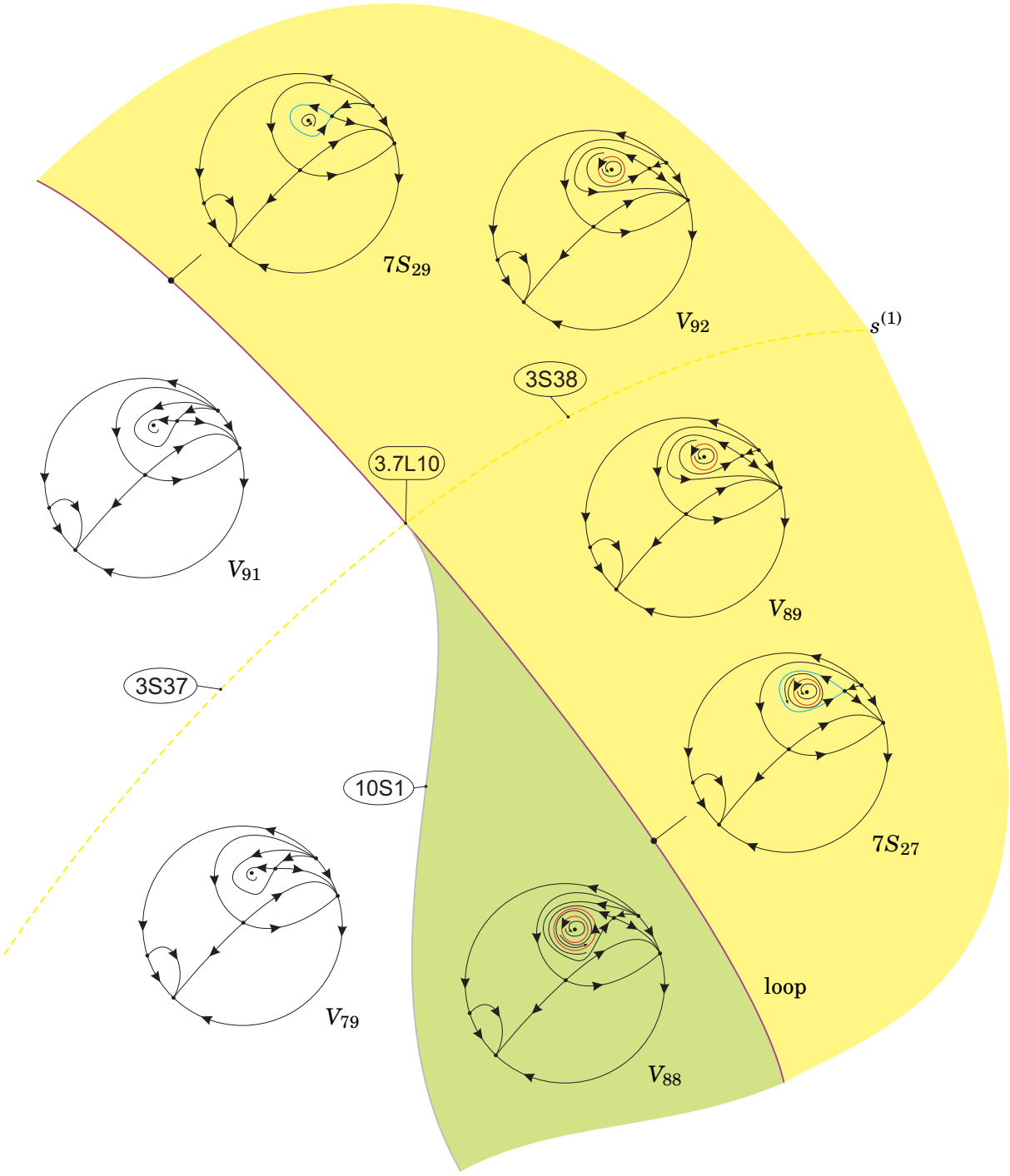

Figure 7.61: Neighborhood in the parameter space of the point $3.10L_6$ with the corresponding phase portraits: the existence of double limit cycle through a $s^{(1)}$

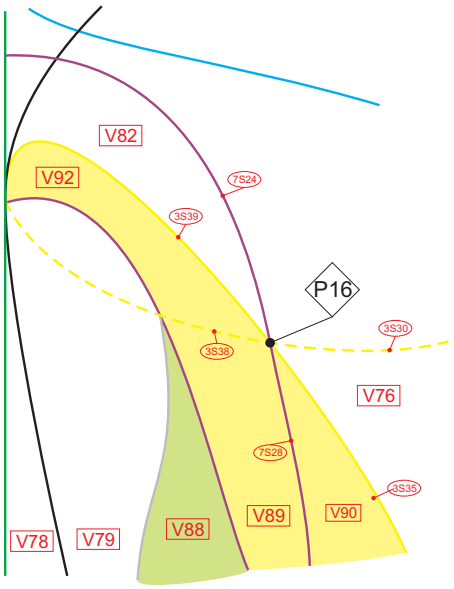

Figure 7.62: Slice of parameter space when $n = 11/5 - \varepsilon_9^*$ (see Figure 7.60)

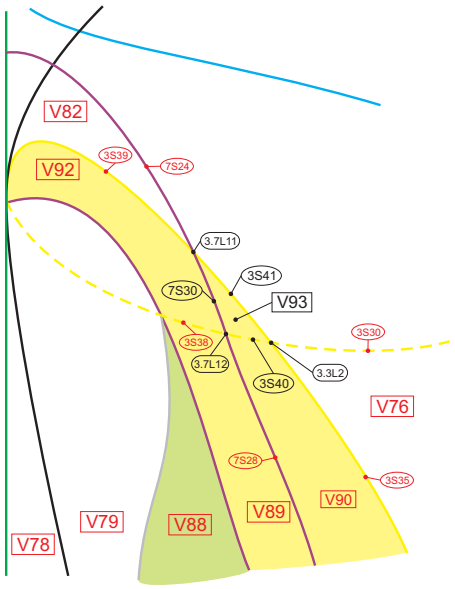

Figure 7.63: Slice of parameter space when $n = 11/5 - \varepsilon_{10}$ (see Figure 7.62)

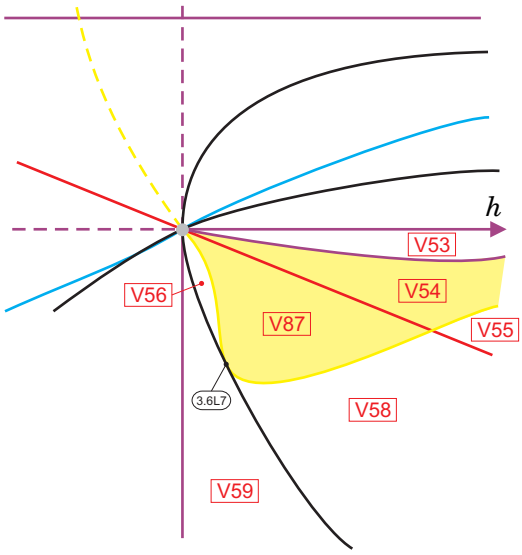

Figure 7.64: Slice of parameter space when $n = 3(102 - 7\sqrt{21})/100$ (see Figure 7.54)

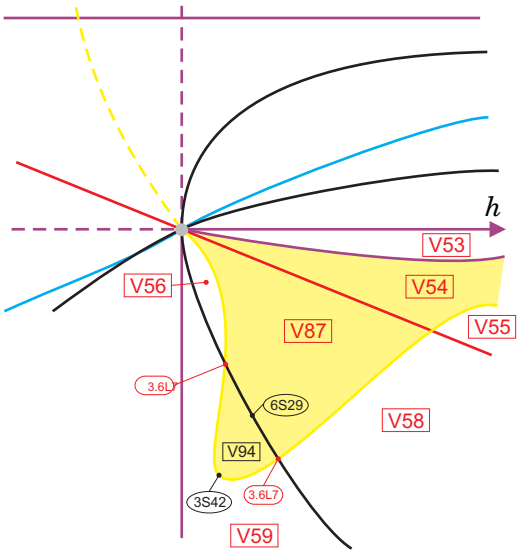

Figure 7.65: Slice of parameter space when $n = 3(102 - 7\sqrt{21})/100 - \varepsilon_{11}$ (see Figure 7.64)

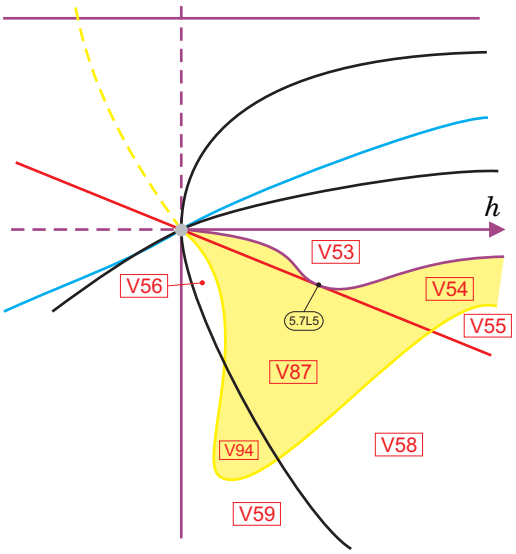

Figure 7.66: Slice of parameter space when $n = 2+\varepsilon_{12}^{*}$ (see Figure 7.65)

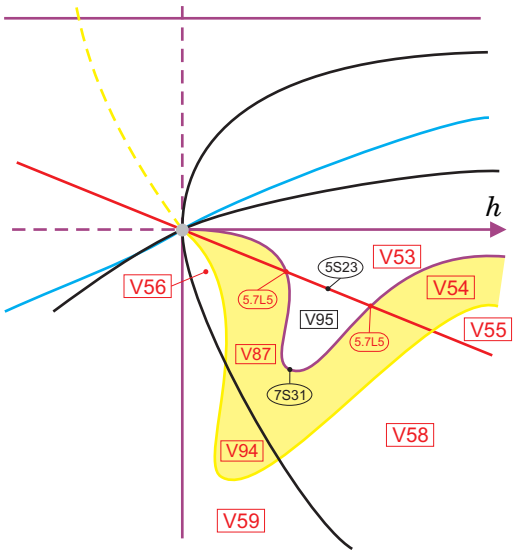

Figure 7.67: Slice of parameter space when $n = 2+\varepsilon_{12}$ (see Figure 7.66)

We recall that surface $(\mathscr{S}_3)$ is the union of a plane and a cubic, and the proof of Lemma 7.4.4 assures that, if $n = 2$, this cubic can be factorized in a line plus a conic: $-4(2h-1)(2+2\ell+2h\ell+\ell^2)$. It is to say that this surface changes its behavior when we move to $n = 2$ and some parts in the bifurcation diagram die and others are created. See Figure 7.68 which illustrates the slice when $n = 2$ (we only show the first and fourth quadrants) and Table 7.4.23 which indicates the "dead" and "born" parts when we cross slice $n = 2$.

Table 7.4.23: Transition from slice $n = 2+\varepsilon_{12}$ to $n = 19/10$. The notation V_{56}^{*} means that only one of the two apparently disconnected parts of V_{56} in Figure 7.67 has died

"Dead" parts	**Parts in singular slice**	**"Born" parts**
V_{44}	$3.4L_6$	V_{96}
V_{48}	$3.4L_7$	V_{97}, V_{98}
V_{56}^{*}	$3.4L_8$	V_{99}
V_{65}	P_{64}	V_{101}, V_{102}, V_{103}, V_{104}
V_{76}	$3.4L_9$	V_{100}

If we consider the next slice when $n = 19/10$, the factorization is not possible and we obtain the slice shown in Figure 7.69. We note that in the lower part of this slice the elements of surfaces $(\mathscr{S}_7)$ and $(\mathscr{S}_{10})$ intersect with an element of surface $(\mathscr{S}_4)$. This fact was verified by "walking" along two segments parallel to an element of surface $(\mathscr{S}_4)$ containing $4S_{27}$ in this slice both left and right sides. On the right side (upper part), starting from part V_{101}, the phase portrait possesses a limit

cycle and the separatrix which enrolls around it comes from the finite saddle–node. However, after "walking down" a little more, we observed that the limit cycle died and the separatrix which goes towards the focus comes from the finite saddle, implying that we have crossed a loop bifurcation. A little below, a heteroclinic bifurcation between finite singularities also happens.

On the other hand, on the left side, starting from part V_{90} and going down, we first cross the heteroclinic connection and, after, the loop connection, but in this case, instead of meaning the death of the limit cycle, it means the birth of a second one. A little below, these two limit cycles die in a double–limit–cycle bifurcation. A bit further down, we cross surface ($\mathscr{S}_6$), so the focus becomes a node and no limit cycles are possible anymore. Also, surface ($\mathscr{S}_4$) crosses surface ($\mathscr{S}_6$) forcing part V_{88} to be bounded now. Then, the only point where surface ($\mathscr{S}_{10}$) may end is $4.7L_1$, in which we have two heteroclinic connections between the finite saddle and the finite saddle–node. As it is shown in the paper of Dumortier, Roussarie and Rousseau [28], the graphic in $4.7L_1$ has cyclicity two which is compatible with the fact that this part borders a part with two limit cycles around the same focus and a part with double limit cycle. Figure 7.70 shows an ampliation of the neighborhood in the parameter space of the point $4.7L_1$ with the corresponding phase portraits.

In what follows, this point $4.7L_1$ "goes up" in the sense of increasing ℓ along the segment of surface ($\mathscr{S}_4$). The next singular slice to be considered is when it crosses the intersection $3.4L_{12}$ between yellow and purple curves (see Figure 7.71). In addition, the point $3.7L_{10}$ tends towards $4.7L_1$ and, after the bifurcation, all the parts of surface ($\mathscr{S}_3$) close to the new part $4.7L_2$ will be below it. So, there is no more intersection between the weak–saddle phenomenon and the loop phenomenon on the left side of vertical purple. This avoids the existence of part V_{88}. Then, part V_{88} must have shrunk as n tends to $19/10 - \varepsilon_{13}^*$ and disappeared in P_{21}. On the right side of the vertical purple it still exists an intersection between weak–saddle and loop bifurcations ($3.7L_{13}$), but the loop takes place with the separatrices of the finite saddle–node and, thus, the weak saddle is not related to any limit cycle (see Figure 7.72). Table 7.4.24 indicates the "dead" and "born" parts in this transition.

Table 7.4.24: Transition from slice $n = 19/10$ to $n = 17/10$

"Dead" parts	**Parts in singular slice**	**"Born" parts**
V_{88}, V_{89}, V_{90}	P_{21}	V_{105}, V_{106}

Now, it is the turn of the purple curve $7S_{31}$ (see Figure 7.69) to "go down" in the parameter space, as shown in Figures 7.73 to 7.78. Firstly, part of it becomes tangent to the red curve $5S_{22}$ at

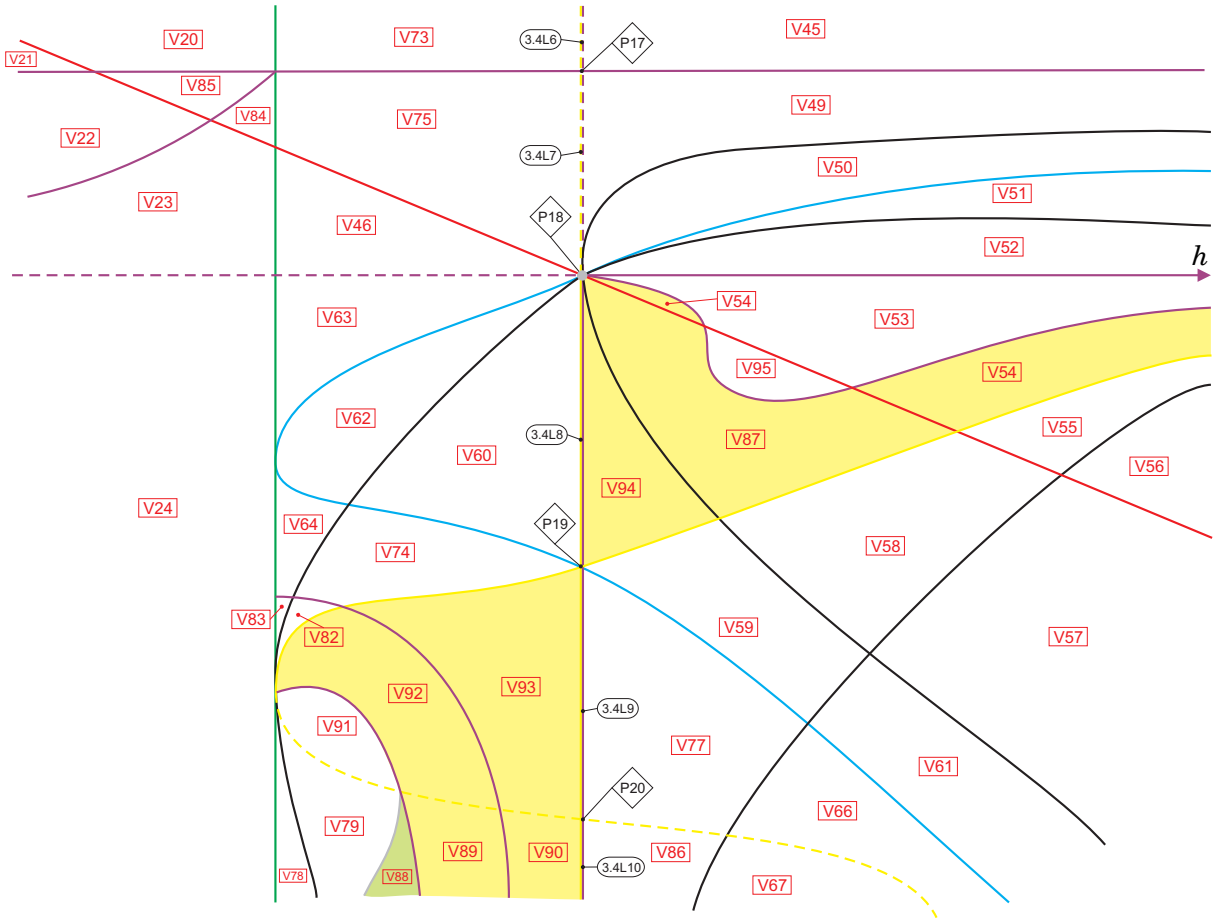

Figure 7.68: Slice of parameter space when $n = 2$ (see Figures 7.47, 7.63 and 7.67)

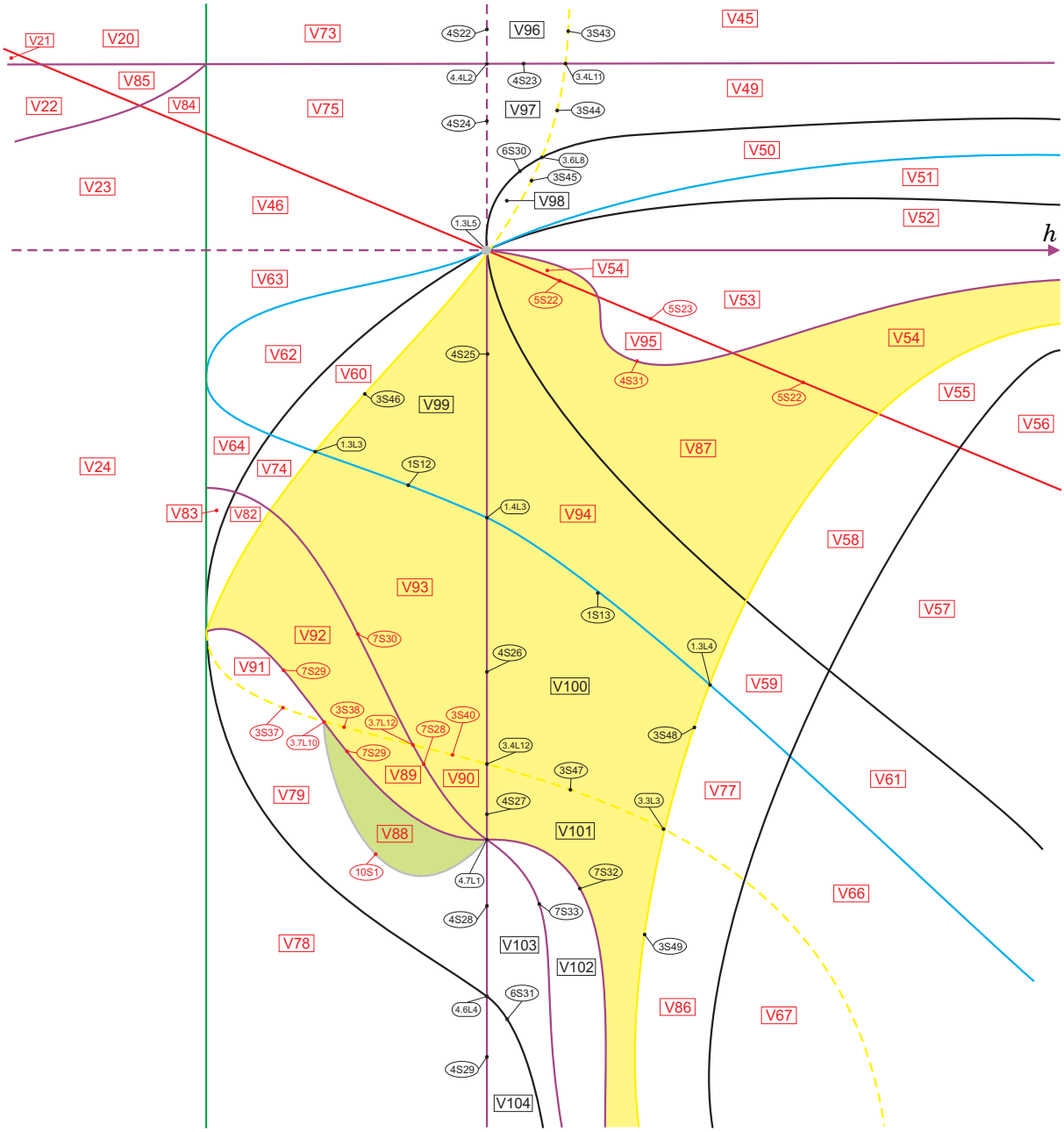

Figure 7.69: Slice of parameter space when $n = 19/10$ (see Figure 7.68)

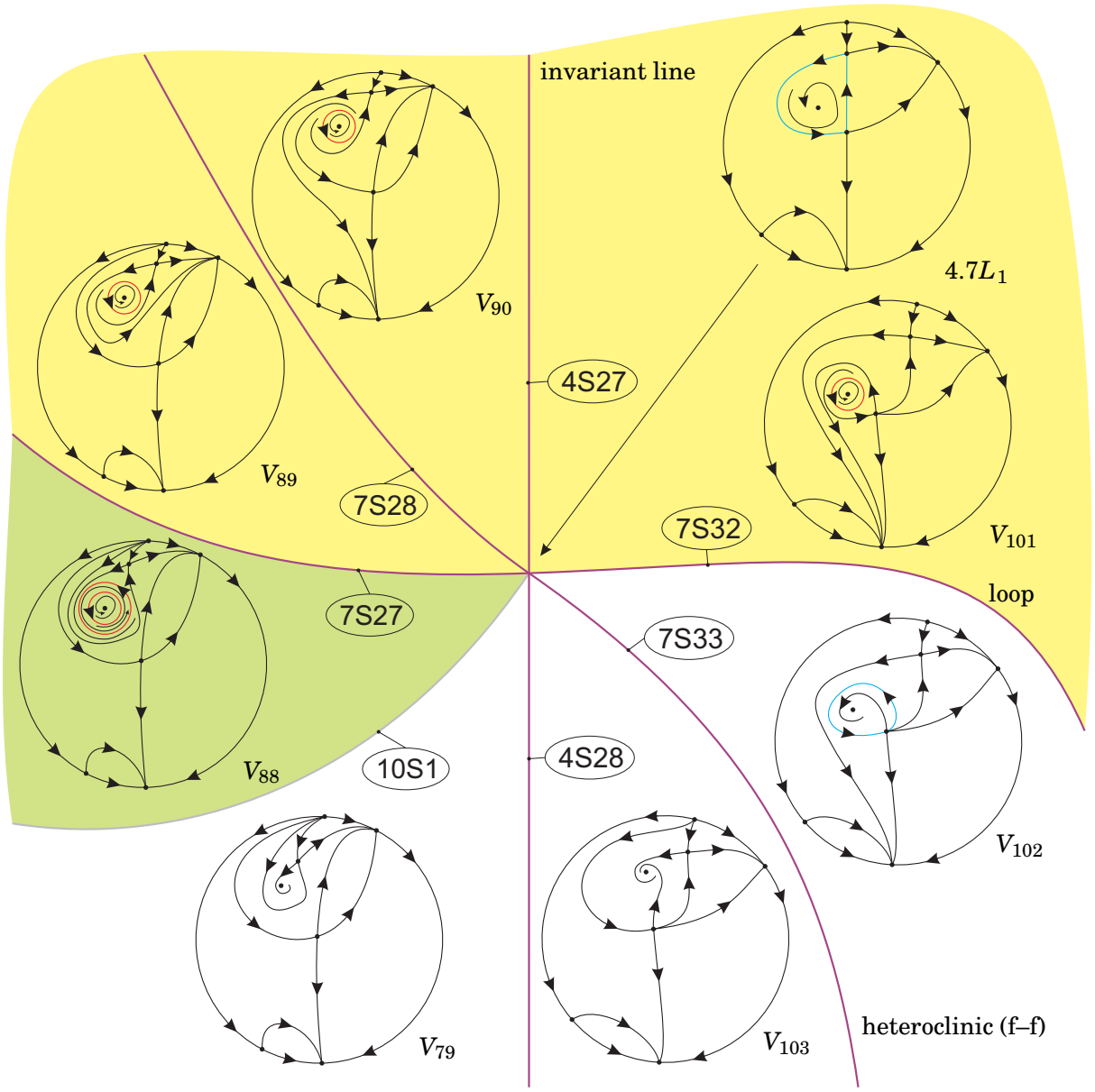

Figure 7.70: Neighborhood in the parameter space of the point $4.7L_1$ with the corresponding phase portraits: the existence of double limit cycle through a finite–to–finite heteroclinic and a loop bifurcations

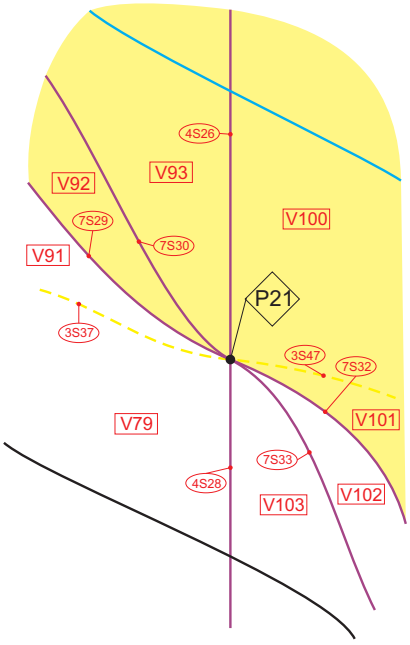

Figure 7.71: Slice of parameter space when $n = 19/10 - \varepsilon_{13}^{*}$ (see Figure 7.69)

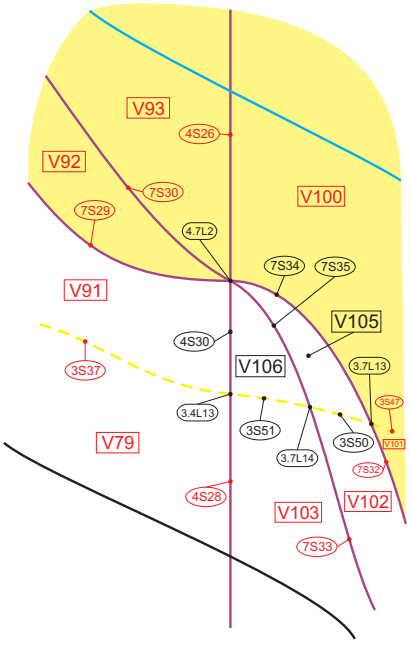

Figure 7.72: Slice of parameter space when $n = 17/10$ (see Figure 7.71)

the point $1.3L_5$ making disappear a portion of part V_{54}; then, the tangency is lost and it continues to move down contacting and intersecting the black and the blue curves yielding the curves $6.7L_6$ and $1.7L_2$, respectively. The first crossing produces new part V_{107}, but the second crossing (see Figure 7.78) does no produce a new part as we will see in the next step. Tables 7.4.25, 7.4.26 and 7.4.27 indicate the "dead" and "born" parts in the transition from slice $n = 17/10$ to $n = 8/5$.

Table 7.4.25: Transition from slice $n = 17/10$ to $n = 17/10 - \varepsilon_{14}$. The notation V_{54}^{*} means that only one of the two apparently disconnected parts of V_{54} in Figure 7.67 has died. The symbol '$\emptyset$' means that no part was created

"Dead" parts	**Parts in singular slice**	**"Born" parts**
V_{54}^{*}	$1.3L_5$	$\emptyset$

Table 7.4.26: Transition from slice $n = 17/10 - \varepsilon_{14}$ to $n = 41/25$. The symbol '$\emptyset$' means that no part was "dead"

"Dead" parts	**Parts in singular slice**	**"Born" parts**
$\emptyset$	$6.7L_6$	V_{107}

When we reach the value $n = 1$, some considerable changes happen to the behavior of the

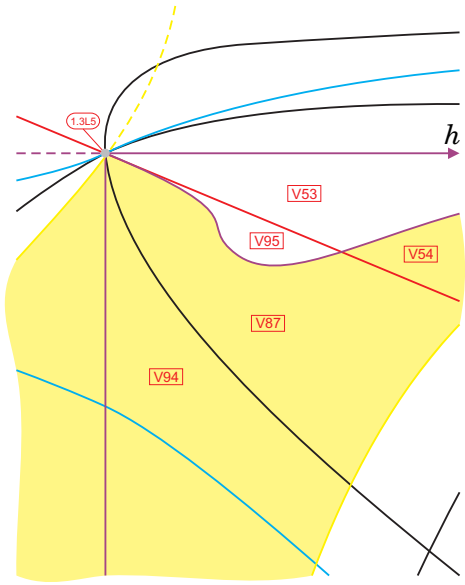

Figure 7.73: Slice of parameter space when $n = 17/10 - \varepsilon_{14}^{*}$ (see Figure 7.69)

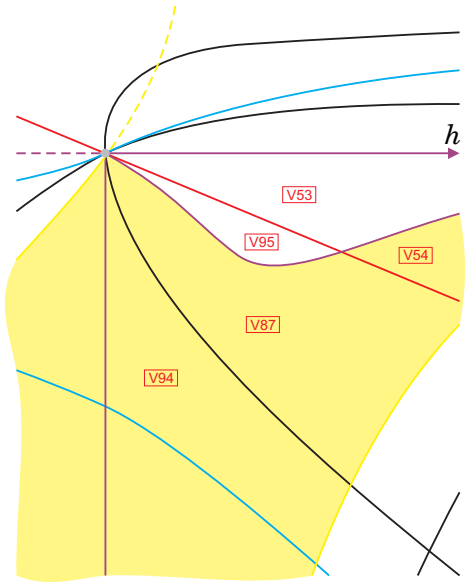

Figure 7.74: Slice of parameter space when $n = 17/10 - \varepsilon_{14}$ (see Figure 7.73)

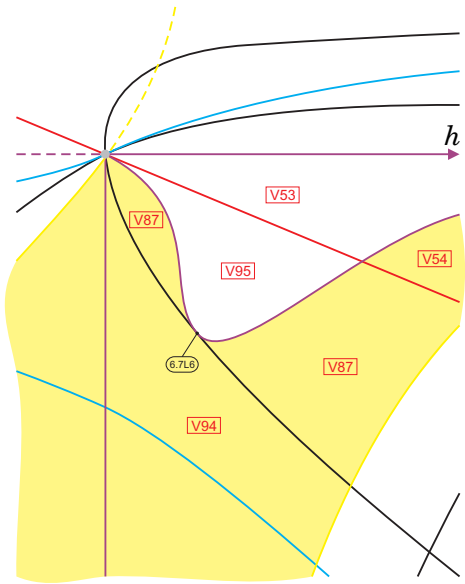

Figure 7.75: Slice of parameter space when $n = 41/25 + \varepsilon_{15}^{*}$ (see Figure 7.74)

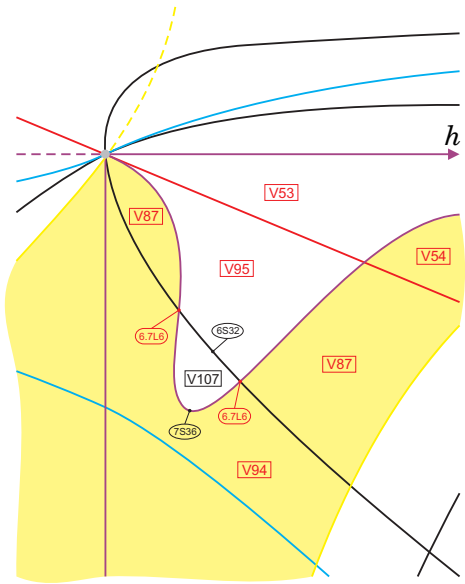

Figure 7.76: Slice of parameter space when $n = 41/25$ (see Figure 7.75)

Table 7.4.27: Transition from slice $n = 41/25$ to $n = 8/5$. The symbol '$\varnothing$' means that no part was "dead". The "born" part V^*_{105} is not new since it will join later with V_{105} (see Figure 7.80)

"Dead" parts	**Parts in singular slice**	**"Born" parts**
$\varnothing$	$1.7L_2$	V^*_{105}

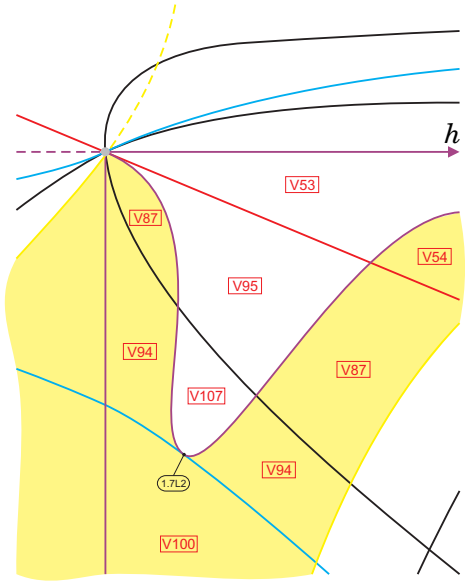

Figure 7.77: Slice of parameter space when $n = 8/5 + \varepsilon^*_{16}$ (see Figure 7.76)

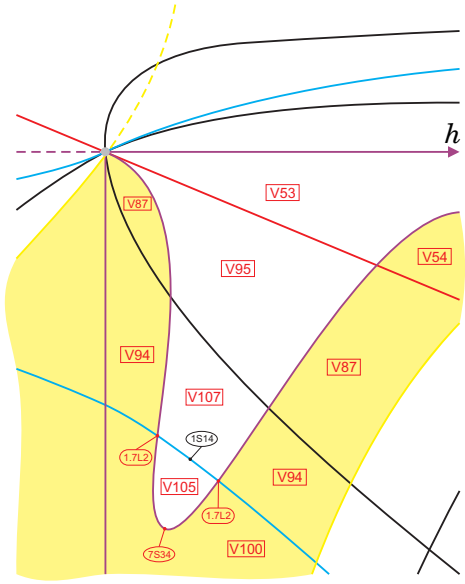

Figure 7.78: Slice of parameter space when $n = 8/5$ (see Figure 7.77)

curves. The purple vertical line and one component of the green lines collide (since their expressions have the common factor h) and all the elements which were in between of them have collapsed in some parts of this vertical line. See Figure 7.79. However, they separate again for $n < 1$ and many new parts appear between them, as shown in Figure 7.80. All these "dead" and "born" parts are indicated in Table 7.4.28.

Table 7.4.28: Transition from slice $n = 8/5$ to $n = 81/100$. Compare Figures 7.69 and 7.80: all parts between the two vertical lines collapse. The lines split again and generate new parts. Parts V_{88}, V_{89} and V_{90} had already disappeared some slices above

"Dead" parts	**Parts in singular slice**	**"Born" parts**
V_{46}, V_{60}, V_{62}, V_{63}, V_{64}, V_{73}, V_{74}, V_{75}, V_{78}, V_{82}, V_{83}, V_{91}, V_{92}, V_{93}, V_{99}	$2.4L_6$, $2.4L_7$, $2.4L_8$	from V_{108} to V_{125}

We note that most of the new parts in slice $n = 81/100$ are concentred in the rectangle bounded

by green, vertical purple and two horizontal purple curves (we call it *Region 1*), including elements of nonalgebraic surfaces whose existence are necessary for the coherence of that part of the bifurcation diagram. Moreover, we remark that the rest of the changes will occur in the portion of the parameter space in the right side of the vertical purple line (we call it *Region 2*).

In *Region 1*, the three intersection points among green, black and yellow curves ($2.3L_6$), green and blue curves ($1.2L_3$), and green and red curves ($2.5L_7$) are the continuation of the intersections $2.3L_5$, $1.2L_2$ and $2.5L_6$, respectively, but with a different ordering they were before. Moreover, the purple segment $7S_{26}$ which separated parts V_{84} and V_{85} (see Figure 7.79) and which started from an intersection of green and horizontal purple curves (P_{22}), now it is called $7S_{38}$ and starts from an intersection of horizontal purple and vertical purple curves ($4.4L_3$, in the right top of *Region 1*), splitting parts V_{109} and V_{110}. In addition, more elements of surface ($\mathscr{S}_7$) were necessary for the coherence and their existence and shape was verified numerically; four of them refer to heteroclinic bifurcations ($7S_{39}$, $7S_{40}$, $7S_{41}$ and $7S_{43}$) and one of them corresponds to loop bifurcation ($7S_{42}$).

In *Region 2*, at the level $n = 81/100$ all the algebraic curves remain and intersect at a single point $1.3L_7$ together with an element of a heteroclinic bifurcation. But the two disjoint elements of loop bifurcation $7S_{34}$ in Figures 7.72 and 7.78 which border two temporary disjoint parts of part V_{105} will have a common point at P_{23} in Figure 7.79 and will remain joined and unlinked from any other bifurcation surface. Segment $7S_{34}$ was purposely drawn in Figure 7.80 with a beak to show its movement of separation from $1.3L_7$.

In Figures 7.81 to 7.84 we sketch the movement of the intersection between yellow and purple $3.4L_{14}$ along the vertical purple curve ($\mathscr{S}_4$) as it crosses surface ($\mathscr{S}_6$) and another component of ($\mathscr{S}_4$). We note that the intersection shown in Figure 7.83 shows it having a tangency between $3S_{56}$ and $7S_{38}$. However, this could not be the case and we could have this transition needing some more steps as a different crossing between $3S_{56}$ and $7S_{38}$ can happen. This intersection cannot be detected algebraically. Anyway, since surface ($\mathscr{S}_3$) in this surroundings only means the presence of a weak saddle and there is no possible loop, this has no effects in the number of topologically different phase portraits. Tables 7.4.29 and 7.4.30 indicate the "dead" and "born" parts in the transition from slice $n = 81/100$ to $n = 9/25$.

For the next slices, the intersection between purple and green $2.7L_7$, which is located in the left top of *Region 1*, will "sweep" the segments from $2S_{24}$ up to $2S_{28}$. Consequently, surface $7S_{38}$ will also "sweep" most of the parts in *Region 1*, producing new phase portraits. Due to its nature

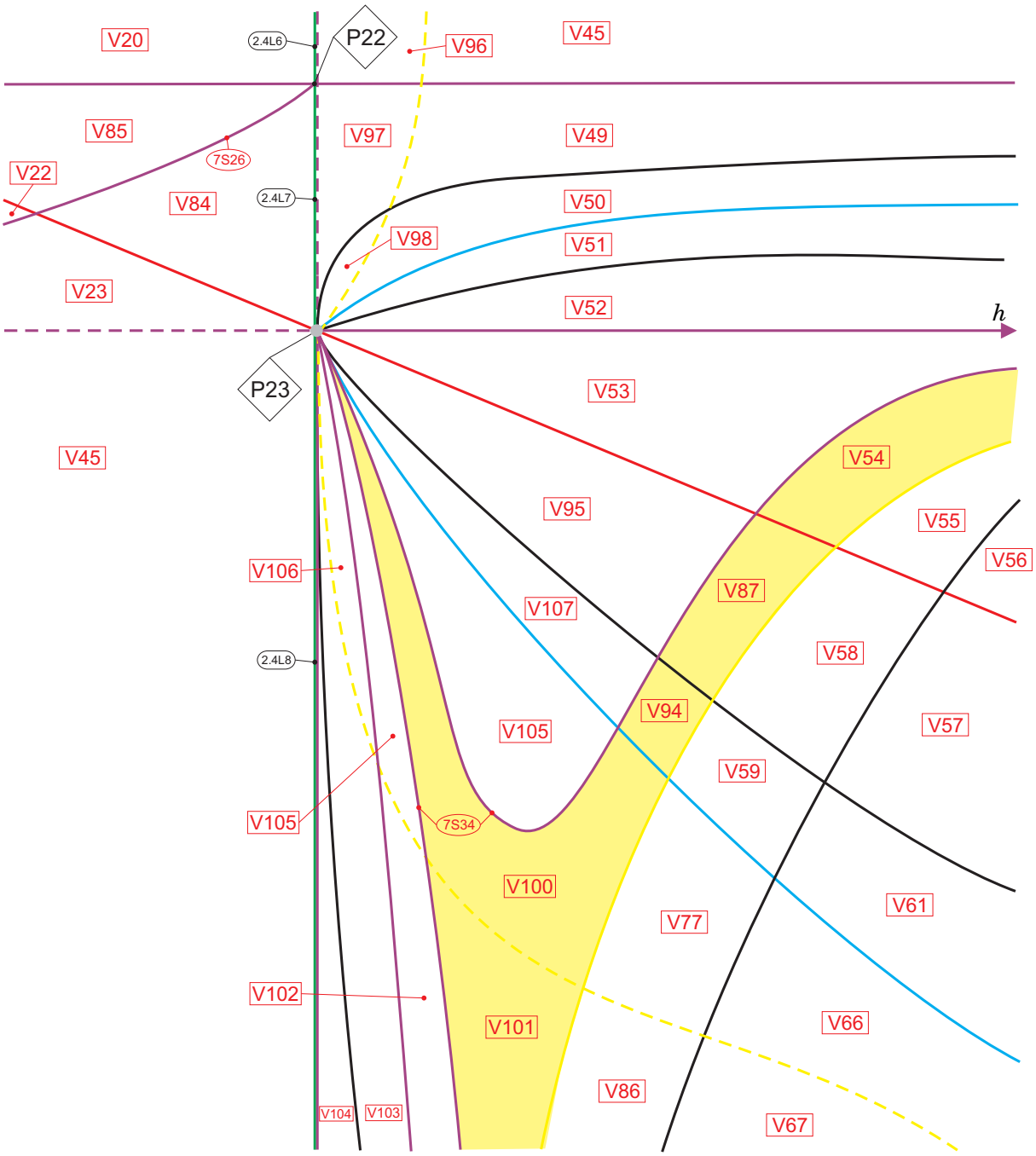

Figure 7.79: Slice of parameter space when $n = 1$ (see Figures 7.69, 7.72 and 7.78)

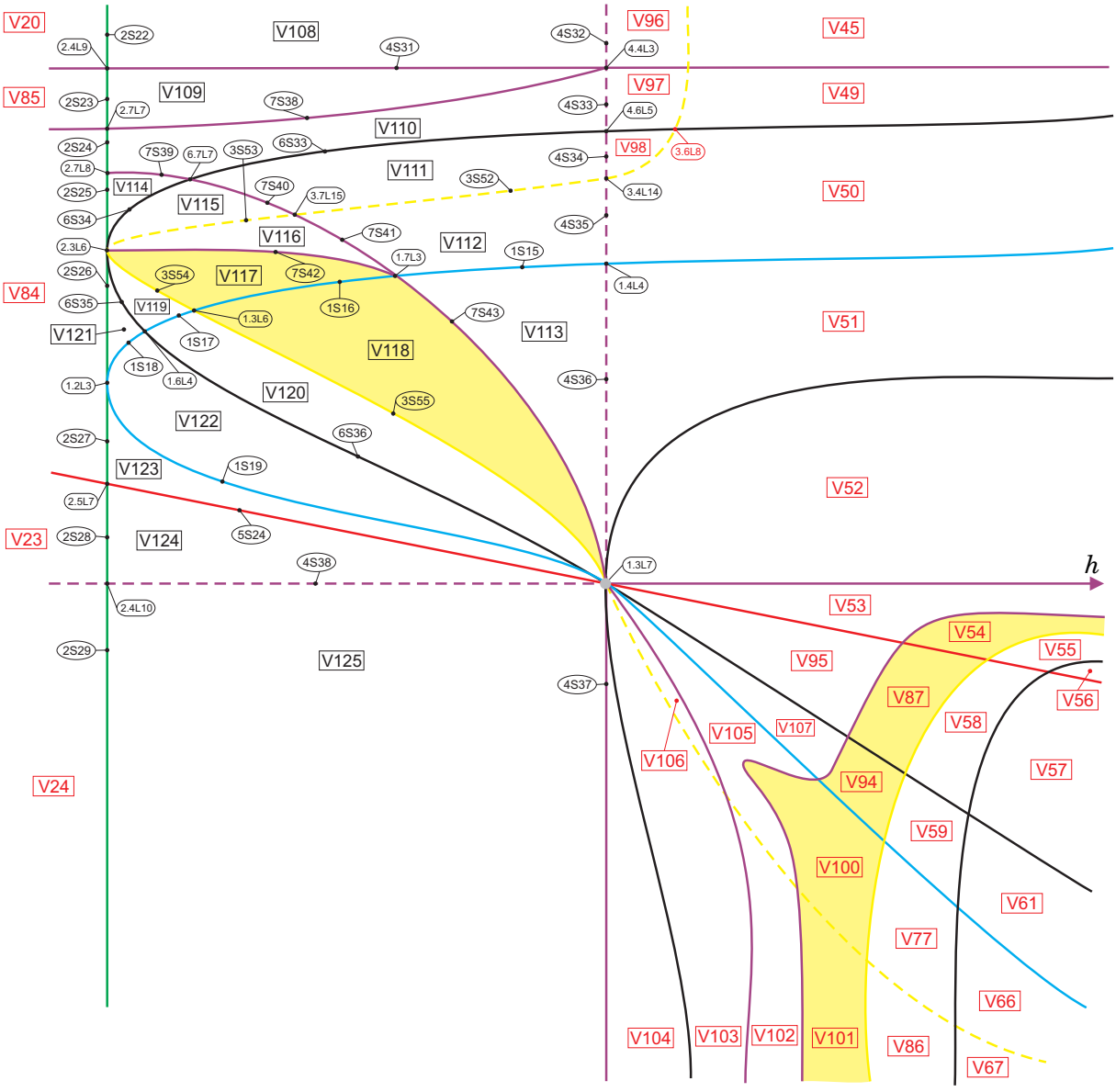

Figure 7.80: Slice of parameter space when $n = 81/100$ (see Figure 7.79)

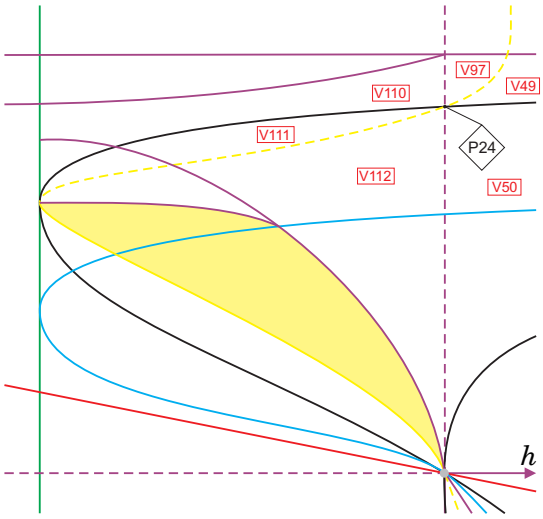

Figure 7.81: Slice of parameter space when $n = 2 - \sqrt{2}$ (see Figure 7.80)

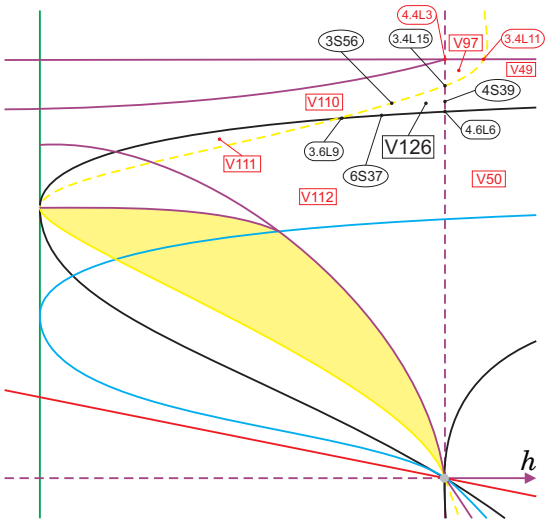

Figure 7.82: Slice of parameter space when $n = 9/16$ (see Figure 7.81)

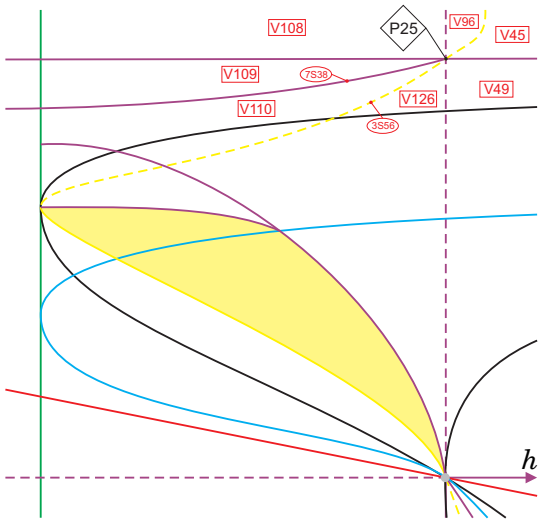

Figure 7.83: Slice of parameter space when $n = 1/2$ (see Figure 7.82)

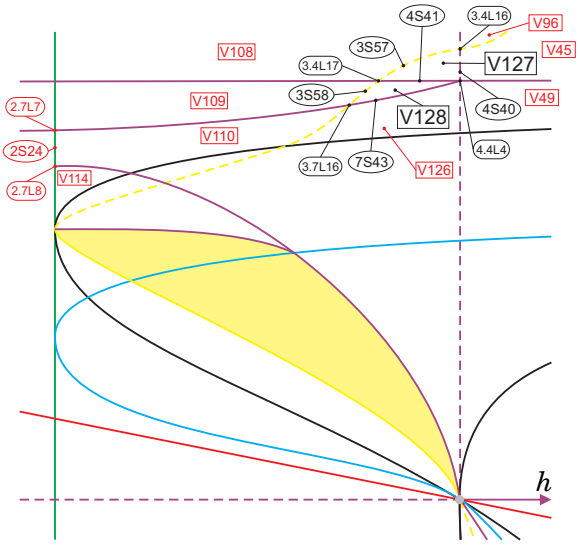

Figure 7.84: Slice of parameter space when $n = 9/25$ (see Figure 7.83)

Table 7.4.29: Transition from slice $n = 81/100$ to $n = 9/16$

"Dead" parts	**Parts in singular slice**	**"Born" parts**
V_{98}	P_{24}	V_{126}

Table 7.4.30: Transition from slice $n = 9/16$ to $n = 9/25$

"Dead" parts	**Parts in singular slice**	**"Born" parts**
V_{97}	P_{25}	V_{127}, V_{128}

of being nonalgebraic, we cannot precise the order of the intersection and contact points with the other curves, but any other order different from the one we present in Figures 7.85 to 7.106 will not bring about new phase portraits rather than the ones which have been created. Moreover, Tables 7.4.31 to 7.4.41 present the "dead" and "born" parts in the transition from slice $n = 9/25$ to $n = 1/25$.

Table 7.4.31: Transition from slice $n = 9/25$ to $n = 81/40$

"Dead" parts	**Parts in singular slice**	**"Born" parts**
$2S_{24}$	P_{26}	V_{129}

Table 7.4.32: Transition from slice $n = 81/40$ to $n = 81/40 - \varepsilon_{18}$

"Dead" parts	**Parts in singular slice**	**"Born" parts**
$7S_{39}$	P_{27}	V_{130}, V_{131}

Table 7.4.33: Transition from slice $n = 81/40 - \varepsilon_{18}$ to $n = 81/40 - \varepsilon_{19}$

"Dead" parts	**Parts in singular slice**	**"Born" parts**
V_{110}	P_{28}	V_{132}

Table 7.4.34: Transition from slice $n = 81/40 - \varepsilon_{19}$ to $n = 81/40 - \varepsilon_{20}$

"Dead" parts	**Parts in singular slice**	**"Born" parts**
V_{111}	P_{29}	V_{133}

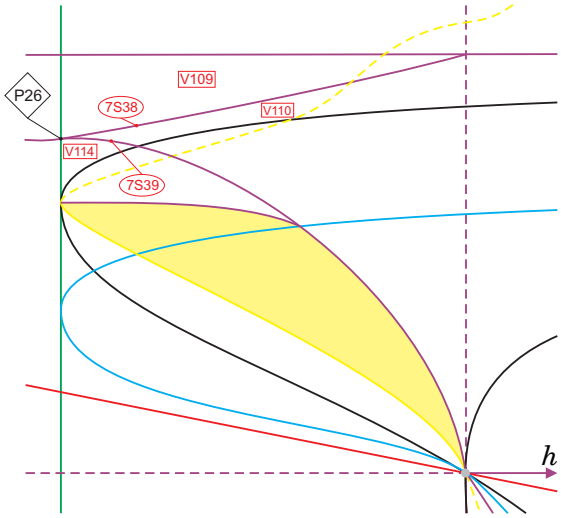

Figure 7.85: Slice of parameter space when $n = 9/25 - \varepsilon_{17}^{*}$ (see Figure 7.84)

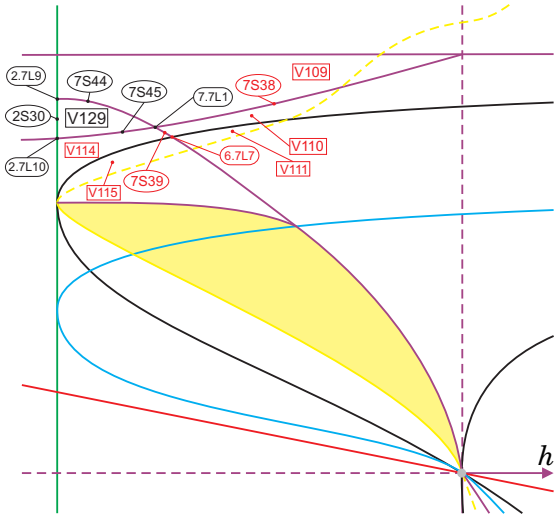

Figure 7.86: Slice of parameter space when $n = 81/40$ (see Figure 7.85)

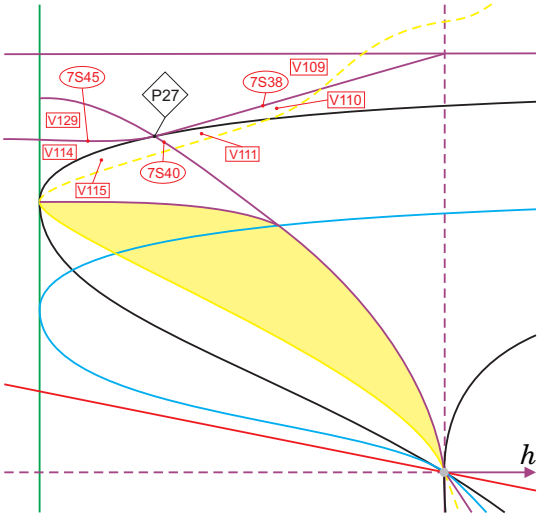

Figure 7.87: Slice of parameter space when $n = 81/40 - \varepsilon_{18}^{*}$ (see Figure 7.86)

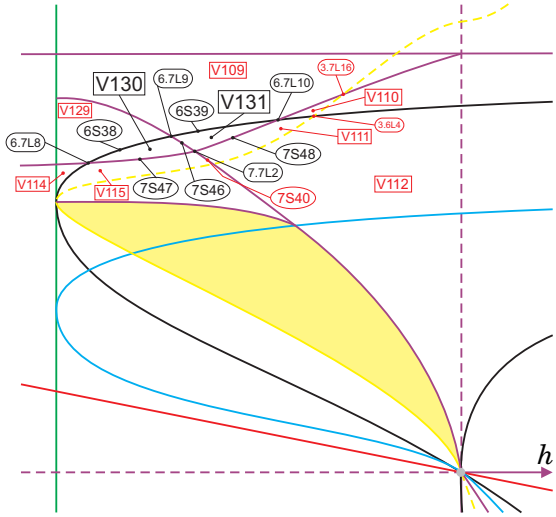

Figure 7.88: Slice of parameter space when $n = 81/40 - \varepsilon_{18}$ (see Figure 7.87)

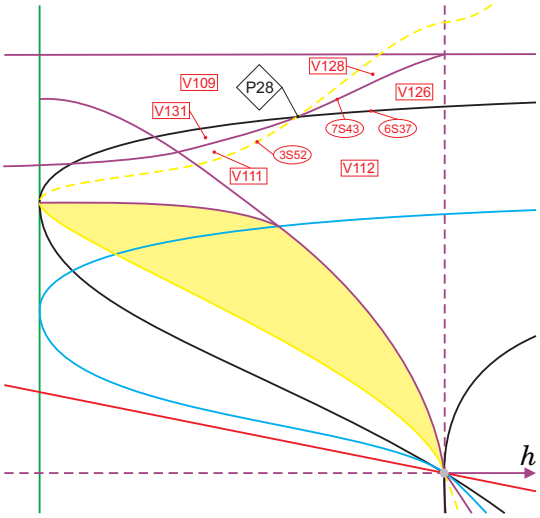

Figure 7.89: Slice of parameter space when $n = 81/40 - \varepsilon_{19}^*$ (see Figure 7.88)

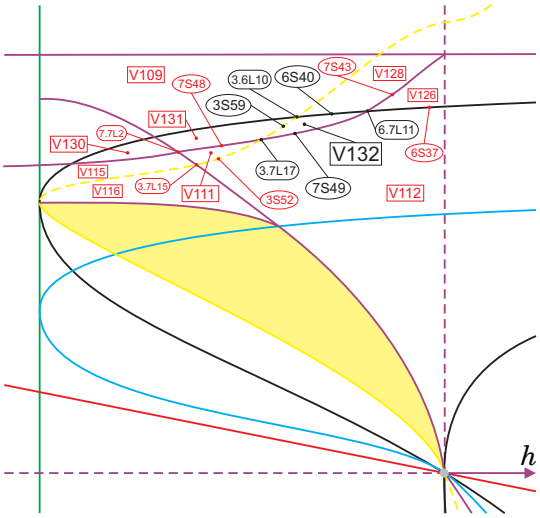

Figure 7.90: Slice of parameter space when $n = 81/40 - \varepsilon_{19}$ (see Figure 7.89)

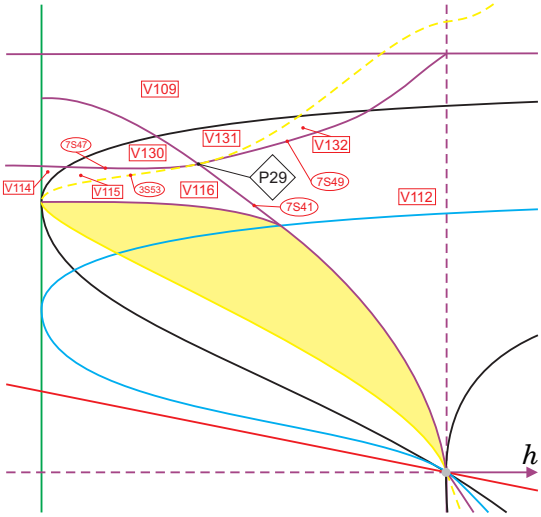

Figure 7.91: Slice of parameter space when $n = 81/40 - \varepsilon_{20}^*$ (see Figure 7.90)

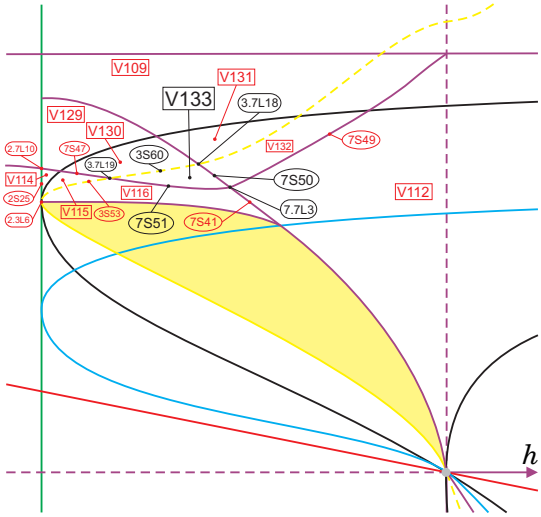

Figure 7.92: Slice of parameter space when $n = 81/40 - \varepsilon_{20}$ (see Figure 7.91)

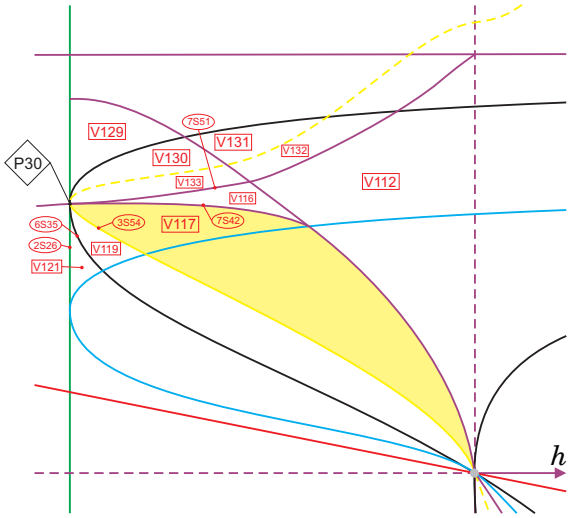

Figure 7.93: Slice of parameter space when $n = 81/40 - \varepsilon_{21}^*$ (see Figure 7.92)

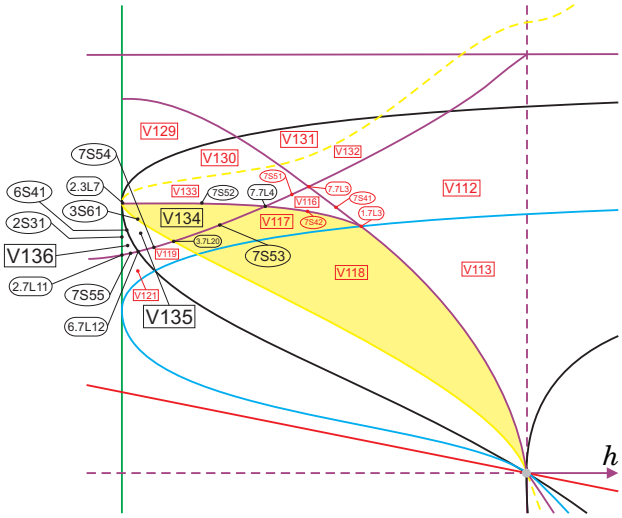

Figure 7.94: Slice of parameter space when $n = 4/25$ (see Figure 7.93)

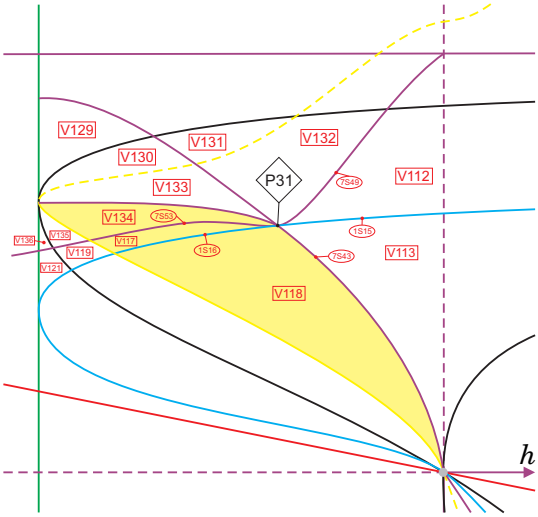

Figure 7.95: Slice of parameter space when $n = 4/25 - \varepsilon_{22}^*$ (see Figure 7.94)

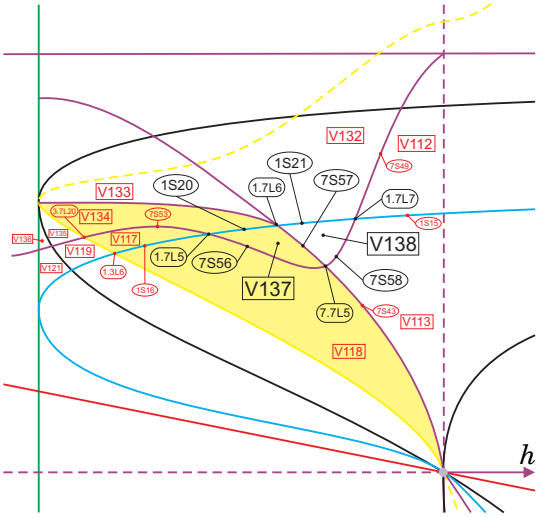

Figure 7.96: Slice of parameter space when $n = 4/25 - \varepsilon_{22}$ (see Figure 7.95)

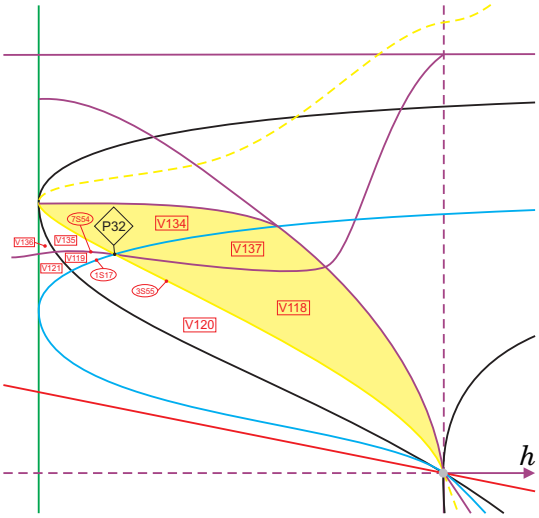

Figure 7.97: Slice of parameter space when $n = 4/25 - \varepsilon_{23}^*$ (see Figure 7.96)

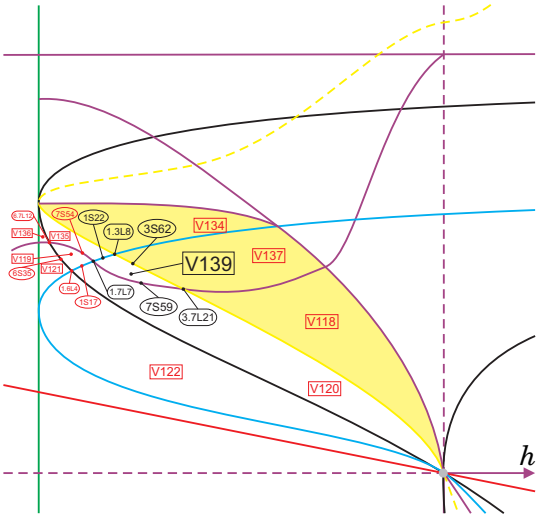

Figure 7.98: Slice of parameter space when $n = 4/25 - \varepsilon_{23}$ (see Figure 7.97)

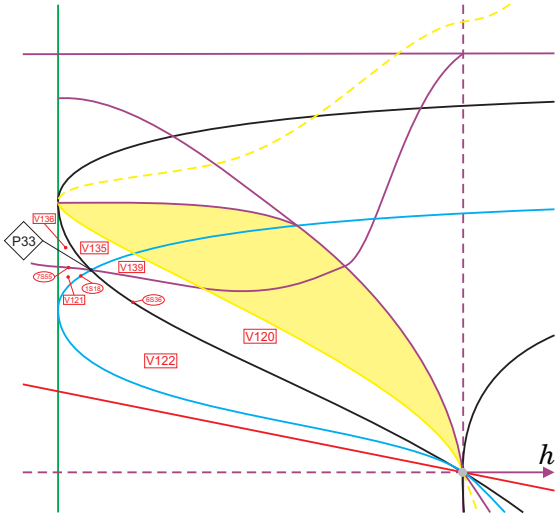

Figure 7.99: Slice of parameter space when $n = 4/25 - \varepsilon_{24}^*$ (see Figure 7.98)

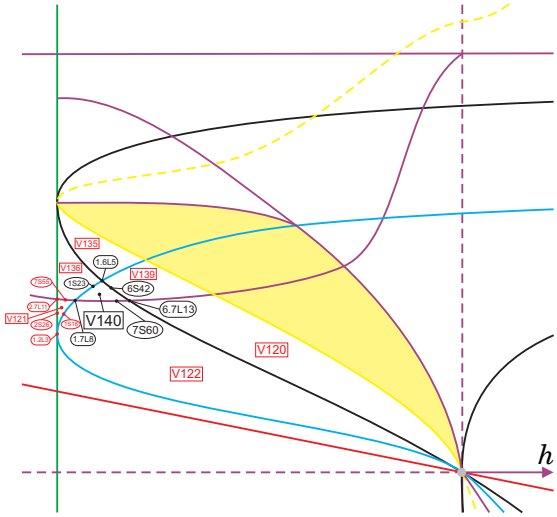

Figure 7.100: Slice of parameter space when $n = 4/25 - \varepsilon_{24}$ (see Figure 7.99)

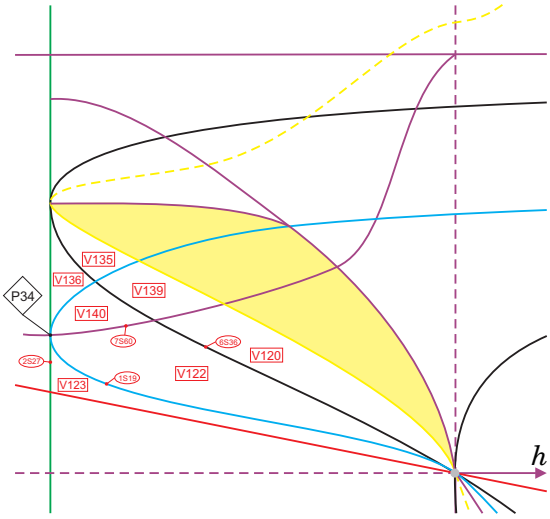

Figure 7.101: Slice of parameter space when $n = 4/25 - \varepsilon^*_{25}$ (see Figure 7.100)

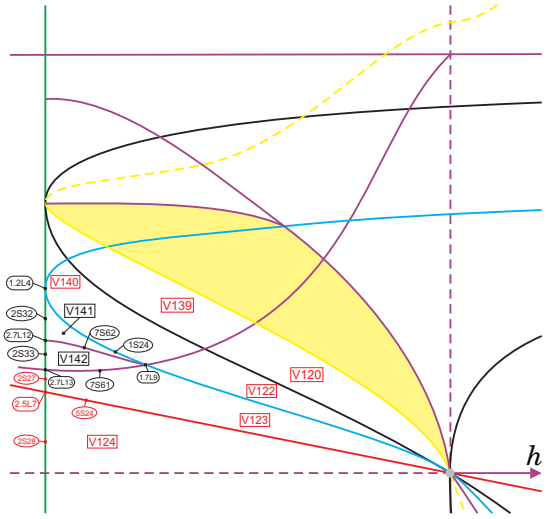

Figure 7.102: Slice of parameter space when $n = 9/100$ (see Figure 7.101)

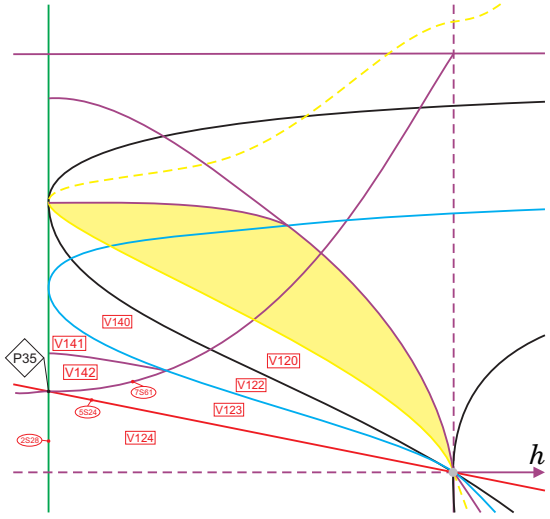

Figure 7.103: Slice of parameter space when $n = 9/100 - \varepsilon^*_{26}$ (see Figure 7.102)

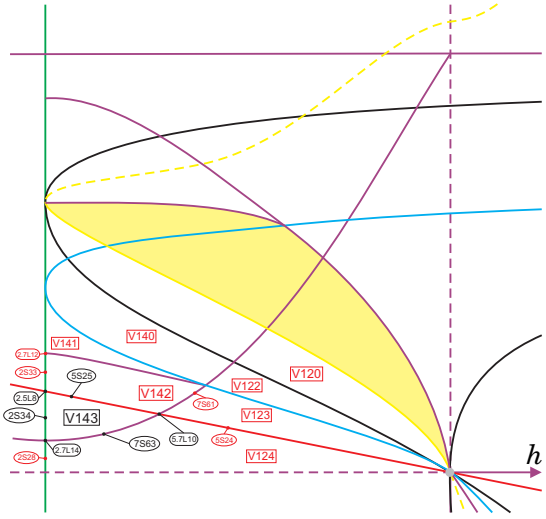

Figure 7.104: Slice of parameter space when $n = 9/100 - \varepsilon_{26}$ (see Figure 7.103)

Table 7.4.35: Transition from slice $n = 81/40 - \varepsilon_{20}$ to $n = 4/25$

"Dead" parts	**Parts in singular slice**	**"Born" parts**
V_{114}, V_{115}	P_{30}	$V_{134}, V_{135}, V_{136}$

Table 7.4.36: Transition from slice $n = 4/25$ to $n = 4/25 - \varepsilon_{22}$

"Dead" parts	**Parts in singular slice**	**"Born" parts**
V_{116}	P_{31}	V_{137}, V_{138}

Table 7.4.37: Transition from slice $n = 4/25 - \varepsilon_{22}$ to $n = 4/25 - \varepsilon_{23}$

"Dead" parts	**Parts in singular slice**	**"Born" parts**
V_{117}	P_{32}	V_{139}

Table 7.4.38: Transition from slice $n = 4/25 - \varepsilon_{23}$ to $n = 4/25 - \varepsilon_{24}$

"Dead" parts	**Parts in singular slice**	**"Born" parts**
V_{119}	P_{33}	V_{140}

Table 7.4.39: Transition from slice $n = 4/25 - \varepsilon_{24}$ to $n = 9/100$

"Dead" parts	**Parts in singular slice**	**"Born" parts**
V_{121}	P_{34}	V_{141}, V_{142}

Table 7.4.40: Transition from slice $n = 9/100$ to $n = 9/100 - \varepsilon_{26}$

"Dead" parts	**Parts in singular slice**	**"Born" parts**
$2S_{27}$	P_{35}	V_{143}

Table 7.4.41: Transition from slice $n = 9/100 - \varepsilon_{26}$ to $n = 1/25$

"Dead" parts	**Parts in singular slice**	**"Born" parts**
$2S_{33}$	P_{36}	V_{144}

We now consider the slice when $n = 0$. At this level almost all the invariant polynomials we use to describe the bifurcation diagram vanish and, hence, we need to consider other ones which

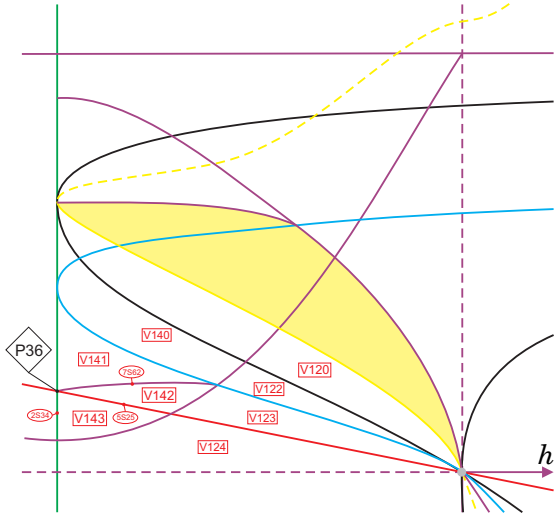

Figure 7.105: Slice of parameter space when $n = 9/100 - \varepsilon^*_{27}$ (see Figure 7.104)

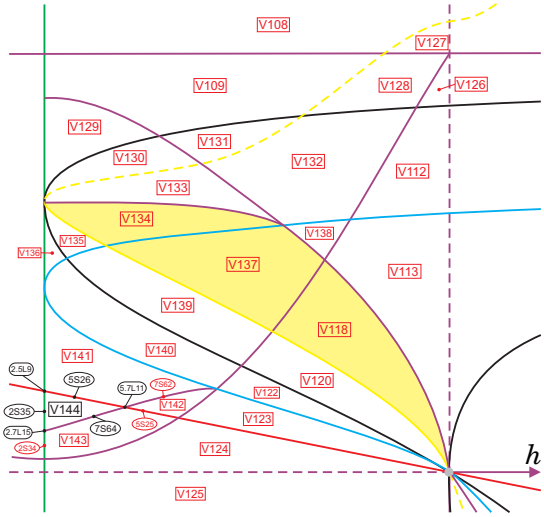

Figure 7.106: Slice of parameter space when $n = 1/25$ (see Figure 7.105)

will play a similar role. For this value of n, systems (7.3.1) get the form:

$$\begin{aligned} \dot{x} &= gx^2 + 2hxy + (-g-2h)y^2, \\ \dot{y} &= y + \ell x^2 + (2g+2h-2\ell)xy + (2h+\ell+2(-g-2h))y^2, \end{aligned} \tag{7.4.5}$$

and for systems (7.4.5), we calculate

$$\begin{aligned} \mu = \mathcal{T}_4 = W_4 \equiv 0, \quad \mathbf{T} = -48(h+1)^4(\ell-1)^2, \\ \mathrm{Inv} = \ell(1+2h)(1-\ell), \quad \widetilde{M} = (1+2h+\ell)^2. \end{aligned} \tag{7.4.6}$$

Then, we need new comitants which indicate: (i) when a second finite singular point collides with an infinite singular point, (ii) when a second finite singular point becomes weak and (iii) when a second node turns into a focus. The next invariant polynomials we need are, respectively:

(i) $\mu_1 = -4(g+h)^2(g-\ell)$ (drawn in blue);

(ii) $\mathscr{B}_1 = 2g^2 + 2h\ell$ (drawn in yellow);

(iii) $W_7 = -12(g+h)^4(g^4 + 2g^3h - 2g^3\ell - 4g^2h\ell - h^2\ell^2)$ (drawn in black).

Moreover, by the time we were analyzing this slice, we verified that there exist some parts in the bifurcation diagram corresponding to the presence of invariant parabolas passing through the origin in the phase portraits. Lemma 7.4.39 assures the existence of two straight lines in the bifurcation diagram with such a characteristic.

Lemma 7.4.39. *For $g \neq 0$ and $n = 0$, phase portraits possess invariant parabolas passing through the origin if either $h = 0$ or $\ell = 1/2$.*

Proof. We fix $g = 1$ and $n = 0$. First, we suppose $h = 0$. Then, systems (7.4.5) become

$$\dot{x} = x^2 - y^2, \quad \dot{y} = y + \ell x^2 + (2 - 2\ell)xy + (\ell - 2)y^2. \tag{7.4.7}$$

We look for invariant parabolas of the form

$$\mathscr{P} = Ax^2 + By^2 + Cxy + Dx + Ey + F = 0,$$

but as it passes through the origin we set $F = 0$.

If $\mathscr{C} = Ux + Vy + W$ is a cofactor of $\mathscr{P}$, then

$$\frac{\partial \mathscr{P}}{\partial x}\dot{x} + \frac{\partial \mathscr{P}}{\partial y}\dot{y} = \mathscr{C}\,\mathscr{P},$$

which is equivalent to

$$\begin{aligned}
&-DWx - E(W-1)y + (2D + E - 2DU - 2AW)x^2/2 + (C + 2hD + E + 2hE - EU - DV \\
&- CW)xy + (4B - 2D - 4hD - 3E - 4hE - 2EV - 2BW)y^2/2 + (4A + C - 2AU)x^3/2 \\
&+ (4hA + B + 2C + 2hC - CU - AV)x^2y + (-4A - 8hA + 4B + 8hB - 3C - 2BU - 2CV)xy^2/2 \\
&+ (-3B - 4hB - C - 2hC - BV)y^3 = 0.
\end{aligned}$$

Equating to zero all the coefficients of the previous equation and solving this system in the variables A, B, C, D, E, U, V and W, we obtain the solution

$$A = -C/2,\ B = -C/2,\ D = 0,\ E = -C/(2\ell),\ U = 2(\ell - 1),\ V = 2(\ell - 1),\ W = 1$$

and, hence,

$$\mathscr{P} = -\frac{C(\ell(x-y)^2 + y)}{2\ell} = 0 \quad \text{and} \quad \mathscr{C} = 1 - 2(\ell - 1)x + 2(\ell - 1)y.$$

Applying the change of coordinates $x = X + Y$, $y = Y$, renaming X, Y by x, y and setting $C = 2$, we see that $\mathscr{P}$ can be brought to the parabola

$$\mathscr{P} = -\frac{\ell x^2 + y}{\ell} = 0.$$

An analogous construction can be applied for the case $\ell = 1/2$ and we obtain the invariant parabola

$$\mathscr{P} = -\frac{2x + (1+2h)x^2 + 2y}{1+2h} = 0.$$

■

Remark 7.4.40. *By Lemma 7.4.39, the straight lines* $\{h = 0\} \cup \{\ell = 1/2\}$ *in the bifurcation diagram correspond to the presence of invariant parabolas passing through the origin in the phase portraits, and they will be part of surface* $(\mathscr{S}_7)$ *and colored in purple. Sometimes this invariant parabola will not coincide with connection of separatrices, so these respective parts are drawn in dashed lines in Figure 7.107, otherwise they are drawn in a continuous line.*

Remark 7.4.41. *For* $g \neq 0$ *and* $n = 0$*, the corresponding phase portraits on the line* $\{h + \ell = 0\}$ *in the bifurcation diagram possess an infinite singular point of type* $\widehat{\binom{1}{2}}E - H$*, which is a bifurcation between the types* $\widehat{\binom{1}{2}}PEP - H$ *and* $\widehat{\binom{1}{2}}E - PHP$*. Such a straight line is needed for the coherence of the bifurcation diagram.*

We observe that, since $\mu \equiv 0$ for $g \neq 0$ and $n = 0$ (i.e. this slice is entirely contained in surface $(\mathscr{S}_1)$), all the "generic" parts on this slice are labeled as $1S_j$, the lines are labeled as $1.iL_j$ and the points as points. We could have also used surfaces $(\mathscr{S}_3)$ or $(\mathscr{S}_6)$ for the same reason, but we have used $(\mathscr{S}_1)$ for its higher relevance on singularities. In Figure 7.107, we present the slice when $n = 0$ with each part properly labeled.

In Table 7.4.42 we indicate the death of all volumetric parts from slice $n = 1/25$ to $n = 0$ and in Table 7.4.43, the birth of new parts at $n = -1$ from slice $n = 0$.

Since there exists no symmetry in the parameter n of foliation of the parameter space as this happened to systems (5.3.1), (6.3.1) and (6.3.2), for systems (7.3.1) we need to consider negative values for the parameter n according to (7.4.4). So, we consider the next generic slice when $n = -1$. In Figure 7.108 we present this slice, but we note that the portion bordered by $4S_{51}$ and $4S_{52}$ (the fourth quadrant) is presented only with the volume parts labeled. We show a zoom of this part in Figure 7.109. In addition, the dashed vertical line in black represents the $\ell-$axis and we draw it only for reference.

We highlight that in part V_{182} there exist two limit cycles in the phase portrait, but each one around different foci. Each one of the limit cycles can be created (or lost) either by Hopf bifurcation on $3S_{70}$ or $3S_{75}$, or by loop bifurcation on $7S_{81}$ or $7S_{83}$.

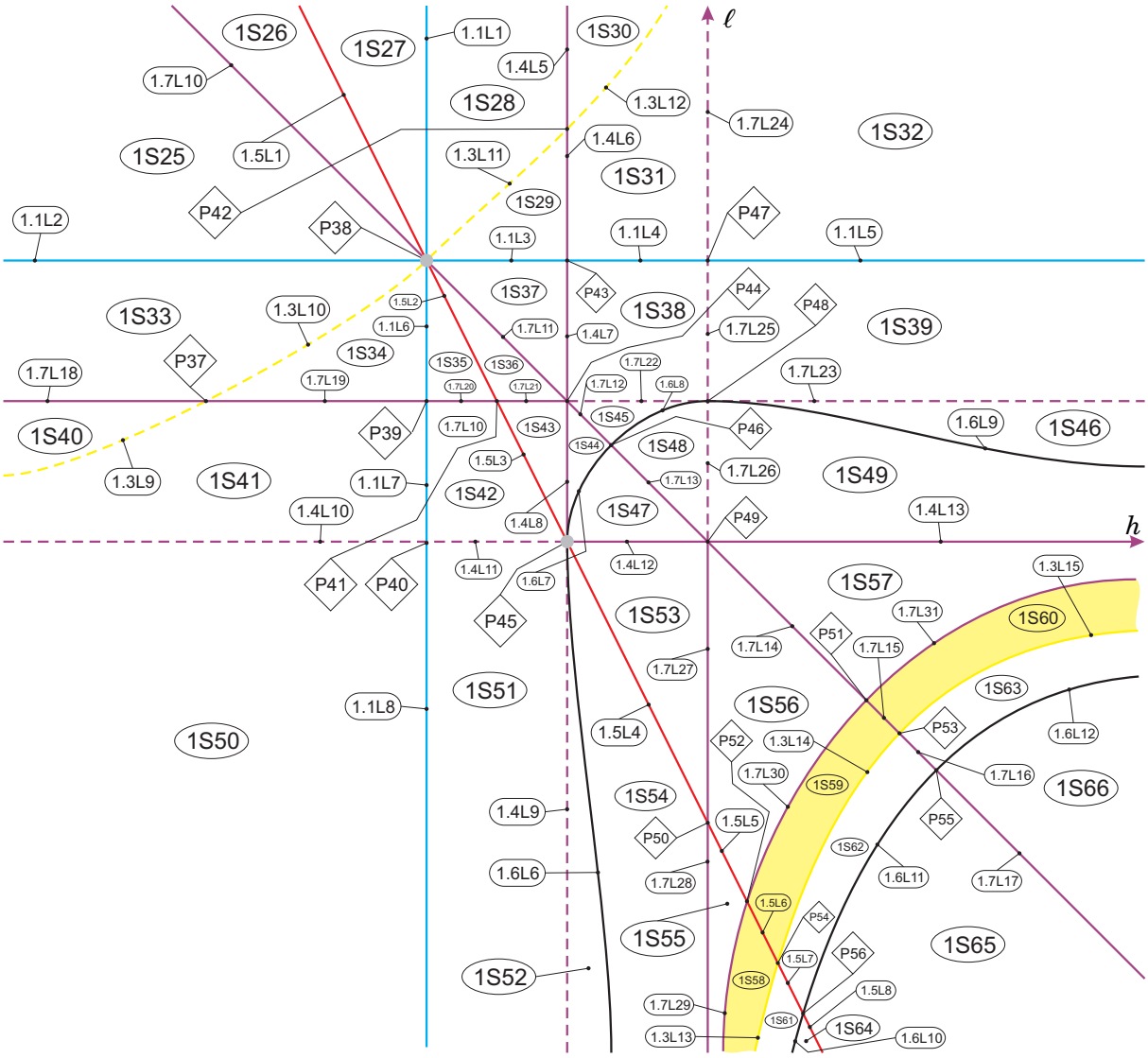

Figure 7.107: Slice of parameter space when $n = 0$ (see Figures 7.80 and 7.106)

Table 7.4.42: Transition from slice $n = 1/25$ to $n = 0$

"Dead" parts	**Parts in slice $n = 0$**	**"Dead" parts**	**Parts in slice $n = 0$**	**"Dead" parts**	**Parts in slice $n = 0$**
V_1	$1S_{27}$	V_{52}	$1S_{47}$, $1S_{48}$, $1S_{49}$	V_{109}	$1.1L_3$
V_2	$1.5L_1$	V_{53}	$1S_{53}$, $1S_{56}$, $1S_{57}$	V_{112}	P_{43}
V_3	$1S_{26}$	V_{54}	$1S_{59}$, $1S_{60}$	V_{113}	$1.4L_7$
V_4	$1.7L_{10}$	V_{55}	$1S_{62}$, $1S_{63}$	V_{118}	$1S_{43}$
V_5	$1.7L_{10}$	V_{56}	$1S_{65}$, $1S_{66}$	V_{120}	$1.5L_3$
V_6	$1S_{25}$	V_{57}	$1.5L_8$	V_{122}	$1.5L_3$
V_7	P_{38}	V_{58}	$1.5L_7$	V_{123}	$1.5L_3$
V_8	$1.1L_2$	V_{59}	$1.5L_7$	V_{124}	$1S_{42}$
V_9	$1.1L_2$	V_{61}	$1.5L_8$	V_{125}	$1S_{51}$
V_{10}	$1S_{33}$	V_{66}	$1.5L_8$	V_{126}	P_{43}
V_{11}	$1S_{40}$	V_{67}	$1S_{64}$	V_{127}	$1S_{29}$
V_{12}	$1S_{34}$	V_{77}	$1.5L_7$	V_{128}	$1.1L_3$
V_{13}	$1S_{41}$	V_{84}	P_{38}	V_{129}	P_{38}
V_{14}	$1S_{50}$	V_{85}	P_{38}	V_{130}	P_{38}
V_{15}	P_{38}	V_{86}	$1S_{61}$	V_{131}	$1.1L_3$
V_{16}	P_{38}	V_{87}	$1.5L_6$	V_{132}	$1.1L_3$
V_{17}	P_{38}	V_{94}	$1.5L_6$	V_{133}	P_{38}
V_{18}	P_{38}	V_{95}	$1.5L_5$	V_{134}	P_{38}
V_{19}	P_{38}	V_{96}	$1S_{30}$	V_{135}	P_{38}
V_{20}	$1.1L_1$	V_{100}	$1.5L_6$	V_{136}	P_{38}
V_{21}	P_{38}	V_{101}	$1S_{58}$	V_{137}	$1S_{36}$
V_{22}	$1.1L_6$	V_{102}	$1S_{55}$	V_{138}	$1S_{37}$
V_{23}	$1.1L_7$	V_{103}	$1S_{54}$	V_{139}	$1.5L_2$
V_{24}	$1.1L_8$	V_{104}	$1S_{52}$	V_{140}	$1.5L_2$
V_{45}	$1S_{31}$, $1S_{32}$	V_{105}	$1.5L_5$	V_{141}	$1.5L_2$
V_{49}	$1.1L_4$, $1.1L_5$	V_{106}	$1.5L_4$	V_{142}	$1.5L_2$
V_{50}	$1.1L_4$, $1.1L_5$	V_{107}	$1.5L_5$	V_{143}	$1.7L_{20}$
V_{51}	$1S_{38}$, $1S_{39}$, $1S_{44}$, $1S_{45}$, $1S_{46}$	V_{108}	$1S_{28}$	V_{144}	$1S_{35}$

Table 7.4.43: Transition from slice $n=-1$ to $n=0$

"Dead" parts	**Parts in slice** $n=0$	**"Dead" parts**	**Parts in slice** $n=0$
V_{145}	$1S_{30}$	V_{172}	$1S_{55}$
V_{146}	$1S_{29}$, $1S_{31}$, $1S_{32}$	V_{173}	$1.5L_5$
V_{147}	$1S_{27}$, $1S_{28}$	V_{174}	$1.5L_5$
V_{148}	$1.5L_1$	V_{175}	$1.5L_5$
V_{149}	$1.5L_1$	V_{176}	$1S_{56}$
V_{150}	$1.1L_3$, $1.1L_4$, $1.1L_5$	V_{177}	$1S_{57}$
V_{151}	$1.5L_1$	V_{178}	$1S_{58}$
V_{152}	$1S_{25}$, $1S_{26}$	V_{179}	$1.5L_6$
V_{153}	$1.1L_2$	V_{180}	$1.5L_6$
V_{154}	$1S_{33}$	V_{181}	$1.5L_6$
V_{155}	$1S_{40}$	V_{182}	$1S_{59}$
V_{156}	$1S_{41}$, $1S_{42}$	V_{183}	$1S_{60}$
V_{157}	$1S_{34}$, $1S_{35}$	V_{184}	$1S_{61}$
V_{158}	$1.5L_2$	V_{185}	$1.5L_7$
V_{159}	$1S_{36}$, $1S_{37}$, $1S_{43}$	V_{186}	$1.5L_7$
V_{160}	$1S_{38}$, $1S_{39}$, $1S_{44}$, $1S_{45}$, $1S_{46}$	V_{187}	$1.5L_7$
V_{161}	$1S_{47}$, $1S_{48}$, $1S_{49}$	V_{188}	$1S_{62}$
V_{162}	$1S_{50}$, $1S_{51}$	V_{189}	$1S_{63}$
V_{163}	$1S_{52}$	V_{190}	$1S_{64}$
V_{164}	$1S_{54}$	V_{191}	$1.5L_8$
V_{165}	P_{50}	V_{192}	$1.5L_8$
V_{166}	$1.5L_4$	V_{193}	$1.5L_8$
V_{167}	$1.5L_4$	V_{194}	$1S_{65}$
V_{168}	$1S_{53}$	V_{195}	$1S_{66}$
V_{169}	$1.4L_{13}$	V_{196}	$1.1L_2$
V_{170}	$1.7L_{28}$	V_{197}	$1.1L_3$
V_{171}	$1.7L_{27}$	V_{198}	$1.1L_4$, $1.1L_5$

There also exists the possibility of both limit cycles being created (or lost) at the same time either by Hopf bifurcation on $3.3L_4$, or by loop bifurcation on $7.7L_7$. We present in Figure 7.110 the phase portraits in a neighborhood of V_{182}.

In Figures 7.111 and 7.112 we present the movement of a branch of surface ($\mathscr{S}_6$) which contacts another branch of the same surface and, then, they intersect transversally in two points. Table 7.4.44 indicates the "dead" and "born" parts in this transition.

Following the values of n in (7.4.4), the last slice we need to described is when $n=-\infty$. However, on page 182 we have already discussed about the behavior of the surfaces as $n\to\infty$. Due to the symmetry in g (see page 145), the slices $n=-\infty$ and $n=\infty$ are symmetrical. These slices

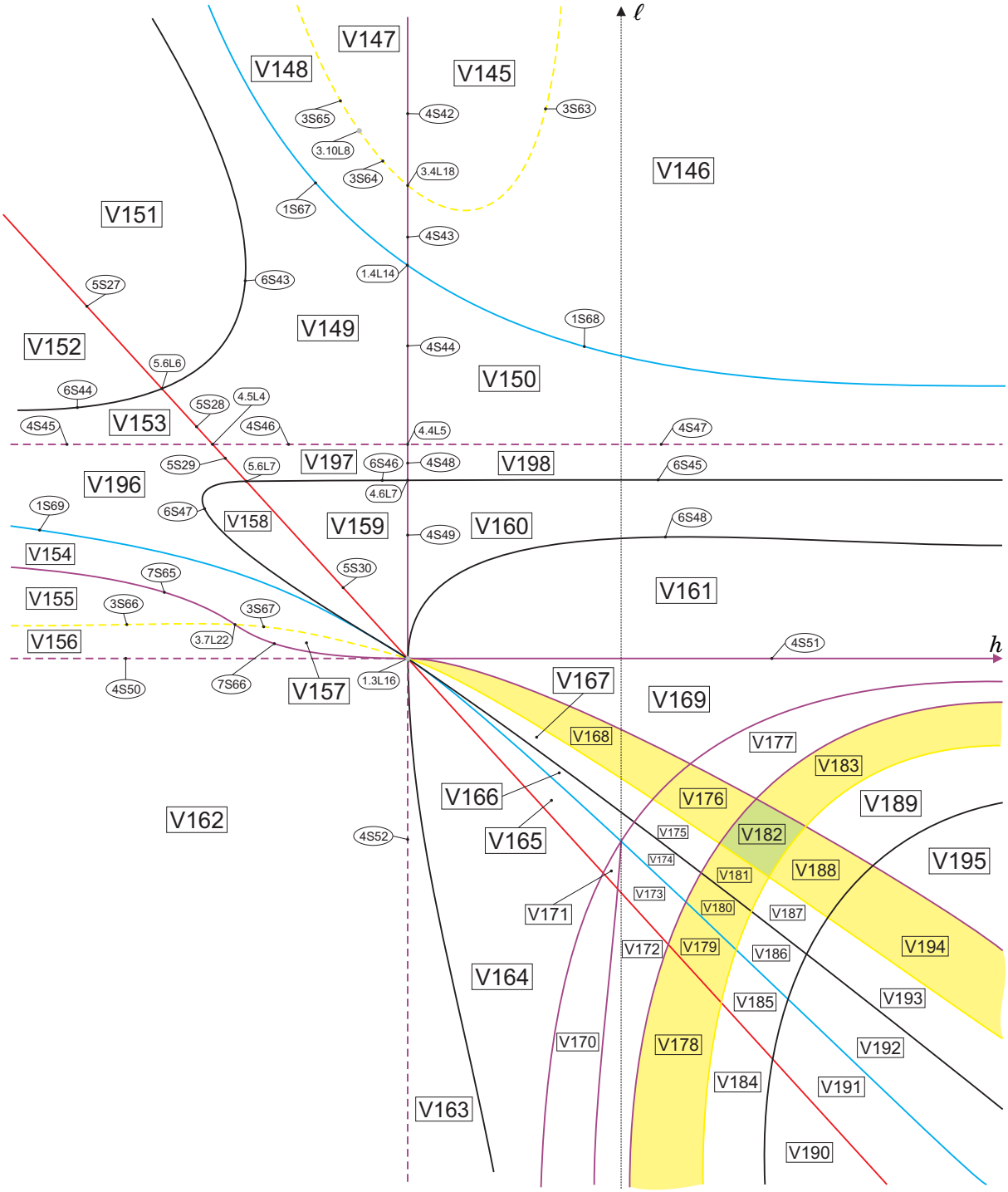

Figure 7.108: Slice of parameter space when $n = -1$ (see Figure 7.107)

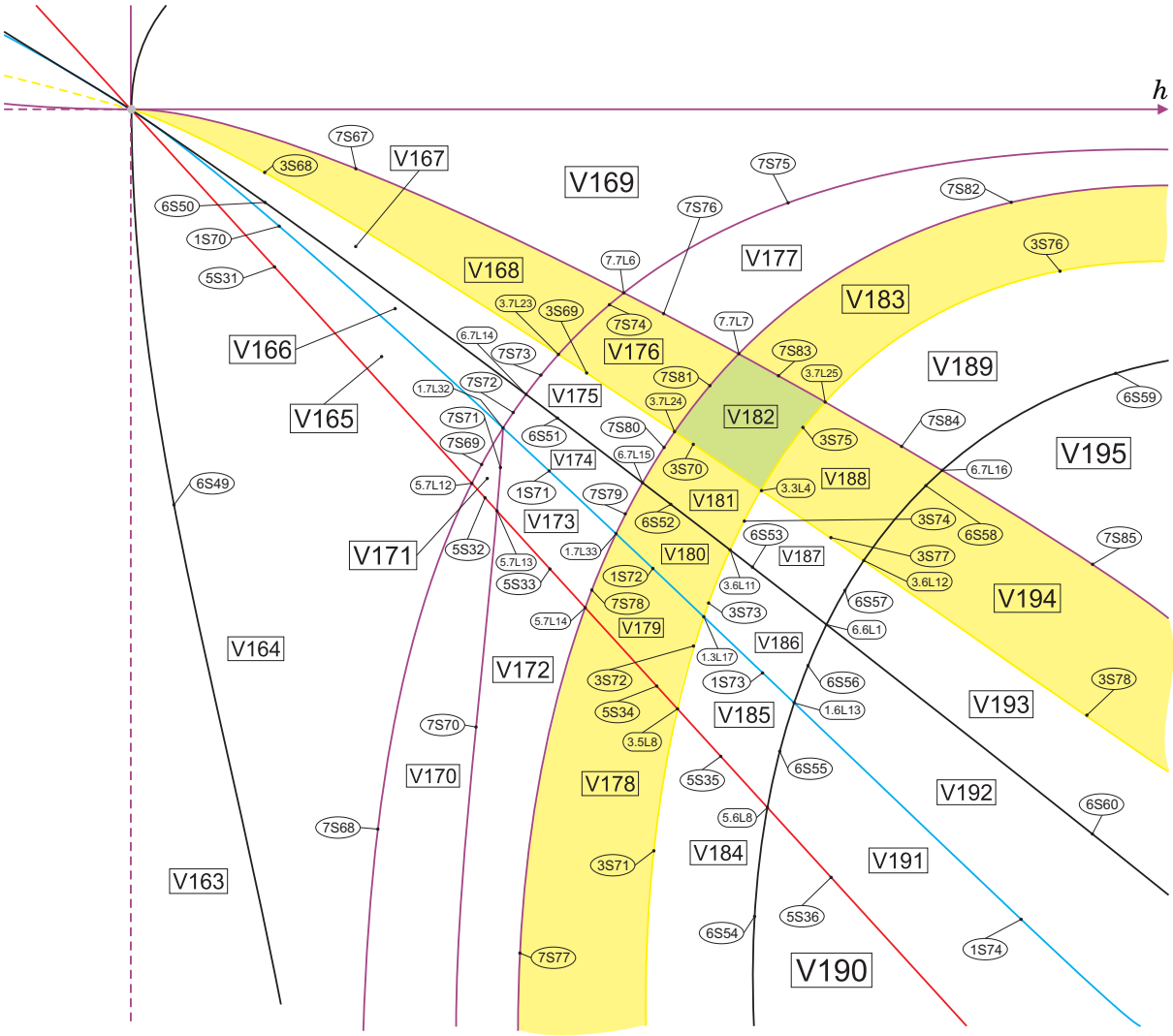

Figure 7.109: Slice of parameter space when $n = -1$ (zoom) (see Figure 7.108)

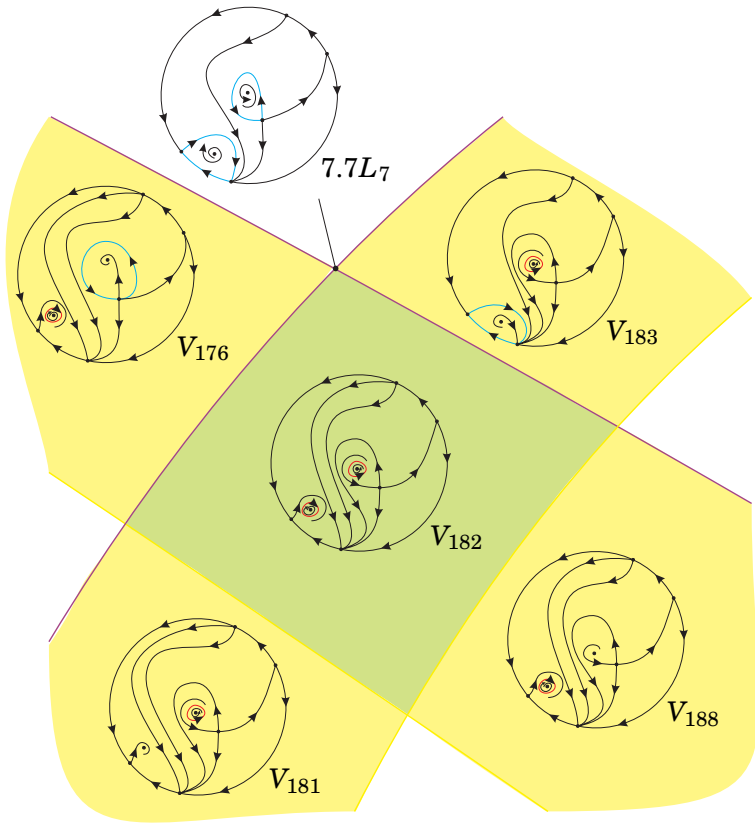

Figure 7.110: Phase portraits in a neighborhood of V_{182}

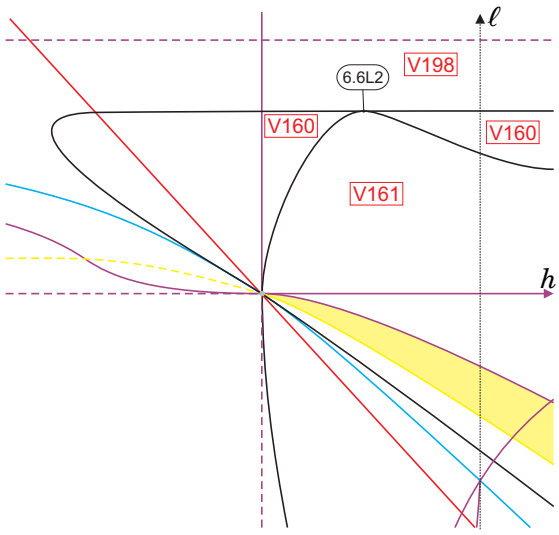

Figure 7.111: Slice of parameter space when $n \approx -3'4013\ldots$ (see Figure 7.108)

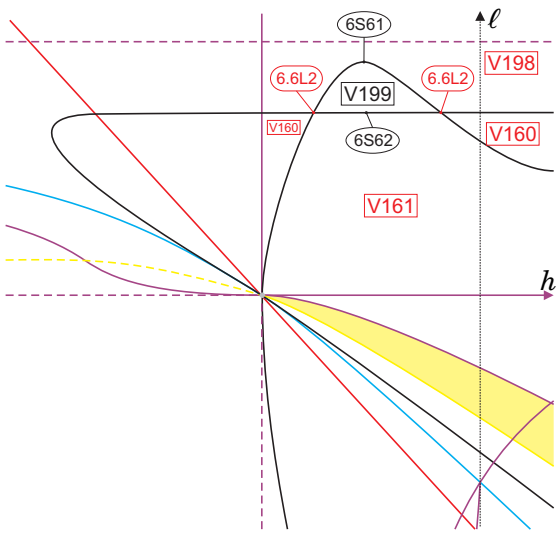

Figure 7.112: Slice of parameter space when $n = -4$ (see Figure 7.111)

Table 7.4.44: Transition from slice $n=-1$ to $n=-4$. The symbol '$\emptyset$' means that no part was "dead"

"Dead" parts	**Parts in singular slice**	**"Born" parts**
$\emptyset$	$6.6L_2$	V_{199}

correspond to $g=0$ and $n\neq 0$. Setting $g=0$ and $n=-1$, systems (7.3.1) become

$$\dot{x}=2hxy-(1+2h)y^2,\quad \dot{y}=y+\ell x^2+(1+2h-2\ell)xy+(2h+\ell-2(1+2h))y^2, \tag{7.4.8}$$

for which we calculate

$$\begin{aligned}&\mu=\ell(2h+\ell),\quad \mathbf{T}\equiv 0,\quad \mathcal{T}_4=\ell(8h^2+\ell+4h\ell),\quad \mathrm{Inv}=-\ell^2(1+2h),\\ &\widetilde{M}=(2h+\ell+1)^2,\quad W_4=\ell^3(16h^2+32h^3+\ell+8h\ell+16h^2\ell).\end{aligned} \tag{7.4.9}$$

As $\mathbf{T}$ vanishes as $n\to-\infty$, we need to consider the next comitant which is responsible for the multiplicity of finite singular points (see Table 4.5.2). This next comitant is $\mathbf{R}=h^2\ell^2$, whose set of zeroes will be called surface ($\mathscr{S}_{11}$) and colored in green. In Figure 7.113 we present the slice when $n=-\infty$ properly labeled.

In Table 7.4.45 we indicate the death of all volumetric parts from slice $n=-4$ to $n=-\infty$ and in Table 7.4.46, the birth of new parts at $n=10$ from slice $n=\infty$ (see Figure 7.21 where nonalgebraic bifurcations and labels must be considered from Figure 7.113 with proper symmetry).

Since there is coherence between the generic slices bordering the most singular slices $n=1$, $n=0$ and $n=-\infty$ with their respective generic side slices, no more slices are needed for the complete coherence of the bifurcation diagram. So, all the values of n in (7.4.4) are sufficient for the coherence of the bifurcation diagram. Thus, we can affirm that we have described a complete bifurcation diagram for family $\overline{\mathbf{QsnSN(C)}}$ modulo islands, as discussed in Section 6.6.

7.5 Completion of the proof of the main theorem

In the bifurcation diagram we may have topologically equivalent phase portraits belonging to distinct parts of the parameter space. As here we have 1034 distinct parts of the parameter space, to help us identify or to distinguish phase portraits, we need to introduce some invariants and we actually choose integer–valued, character and symbol invariants. Some of them were already used in Chapters 5 and 6, but we recall them and introduce some needed ones. These invariants

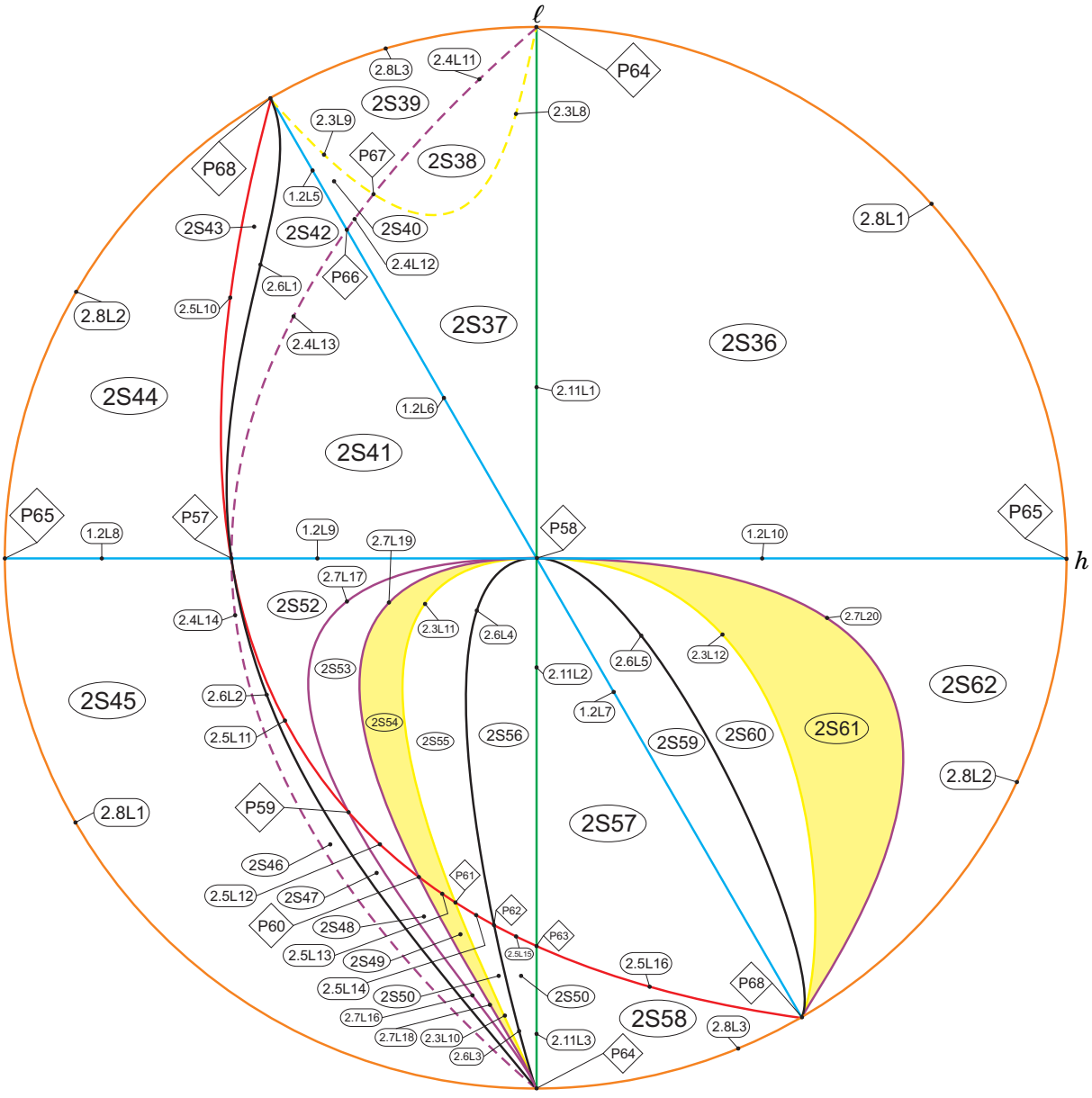

Figure 7.113: Slice of parameter space when $n = -\infty$

Table 7.4.45: Transition from slice $n = -4$ to $n = -\infty$

"Dead" parts	**Parts in slice** $n = -\infty$	**"Dead" parts**	**Parts in slice** $n = -\infty$
V_{145}	$2S_{38}$	V_{173}	$2S_{53}$
V_{146}	$2S_{36}$, $2S_{37}$	V_{174}	P_{58}
V_{147}	$2S_{39}$	V_{175}	P_{58}
V_{148}	$2S_{40}$	V_{176}	P_{58}
V_{149}	$2S_{42}$	V_{177}	$1.2L_{10}$
V_{150}	$2S_{41}$, $1.2L_{10}$	V_{178}	$2S_{49}$
V_{151}	$2S_{43}$	V_{179}	$2S_{54}$
V_{152}	$2S_{44}$	V_{180}	P_{58}
V_{153}	$1.2L_8$	V_{181}	P_{58}
V_{154}	$1.2L_8$	V_{182}	P_{58}
V_{155}	$1.2L_8$	V_{183}	$1.2L_{10}$
V_{156}	$1.2L_8$	V_{184}	$2S_{50}$
V_{157}	$1.2L_8$	V_{185}	$2S_{55}$
V_{158}	P_{57}	V_{186}	P_{58}
V_{159}	P_{57}	V_{187}	P_{58}
V_{160}	$1.2L_9$, $1.2L_{10}$	V_{188}	P_{58}
V_{161}	$1.2L_9$, $1.2L_{10}$	V_{189}	$1.2L_{10}$
V_{162}	$2S_{45}$	V_{190}	$2S_{51}$, $2S_{58}$
V_{163}	$2S_{46}$	V_{191}	$2S_{56}$, $2S_{57}$
V_{164}	$2S_{47}$	V_{192}	$2S_{59}$
V_{165}	$2S_{52}$	V_{193}	$2S_{60}$
V_{166}	P_{58}	V_{194}	$2S_{61}$
V_{167}	P_{58}	V_{195}	$2S_{62}$
V_{168}	P_{58}	V_{196}	$1.2L_8$
V_{169}	$1.2L_{10}$	V_{197}	P_{57}
V_{170}	$2.7L_{16}$	V_{198}	$1.2L_9$, $1.2L_{10}$
V_{171}	$2.7L_{17}$	V_{199}	$1.2L_9$
V_{172}	$2S_{48}$		

yield a classification which is easier to grasp.

Definition 7.5.1. *We denote by $I_1(S)$ the number of the real finite singular points. We note that this number can also be infinity, which is represented by ∞.*

Definition 7.5.2. *We denote by $I_2(S)$ the sum of the indices of the isolated real finite singular points.*

Definition 7.5.3. *We denote by $I_3(S)$ the number of the real infinite singular points.*

Definition 7.5.4. *For a given infinite singularity s of a system S, let ℓ_s be the number of global or local separatrices beginning or ending at s and which do not lie on the line at infinity. We have*

Table 7.4.46: Transition from slice $n = 10$ to $n = \infty$

"Dead" parts	**Parts in slice** $n = -\infty$	**"Dead" parts**	**Parts in slice** $n = -\infty$
V_1	$2S_{58}$	V_{35}	$2S_{53}$
V_2	$2S_{57}$	V_{36}	$2S_{52}$
V_3	$2S_{59}$	V_{37}	P_{57}
V_4	$2S_{60}$	V_{38}	P_{58}
V_5	$2S_{61}$	V_{39}	P_{58}
V_6	$2S_{62}$	V_{40}	$1.2L_9$
V_7	P_{58}	V_{41}	P_{58}
V_8	$1.2L_{10}$	V_{42}	P_{58}
V_9	$1.2L_{10}$	V_{43}	$1.2L_9$
V_{10}	$1.2L_{10}$	V_{44}	$2S_{46}$
V_{11}	$1.2L_{10}$	V_{45}	$2S_{45}$
V_{12}	$1.2L_{10}$	V_{46}	$1.2L_9$
V_{13}	$1.2L_{10}$	V_{47}	$1.2L_9$
V_{14}	$2S_{36}$	V_{48}	P_{57}
V_{15}	P_{58}	V_{49}	$1.2L_8$
V_{16}	P_{58}	V_{50}	$1.2L_8$
V_{17}	P_{58}	V_{51}	$1.2L_8$
V_{18}	P_{58}	V_{52}	$1.2L_8$
V_{19}	P_{58}	V_{53}	$1.2L_8$
V_{20}	$2.11L_3$	V_{54}	$1.2L_8$
V_{21}	$2.11L_2$	V_{55}	$1.2L_8$
V_{22}	P_{58}	V_{56}	$2S_{44}$
V_{23}	P_{58}	V_{57}	$2S_{43}$
V_{24}	$2.11L_1$	V_{58}	P_{57}
V_{25}	$2S_{51}$	V_{59}	P_{57}
V_{26}	$2S_{50}$	V_{60}	P_{57}
V_{27}	$2S_{49}$	V_{61}	$2S_{42}$,
V_{28}	$2.7L_{18}$	V_{62}	$2S_{41}$
V_{29}	$2S_{48}$	V_{63}	$1.2L_9$
V_{30}	$2S_{47}$	V_{64}	$2S_{37}$
V_{31}	$2S_{56}$	V_{65}	$2S_{38}$
V_{32}	$2S_{55}$	V_{66}	$2S_{40}$
V_{33}	$2S_{54}$	V_{67}	$2S_{39}$
V_{34}	$2.7L_{19}$		

$0 \le \ell_s \le 4$. *We denote by* $I_4(S)$ *the sequence of all such* ℓ_s *when* s *moves in the set of infinite singular points of the system* S. *We start the sequence at the infinite singular point which receives (or sends) the greatest number of separatrices and take the direction which yields the greatest absolute value, e.g. the values* 2110 *and* 2011 *for this invariant are symmetrical (and, therefore, they are the same), so we consider* 2110.

Definition 7.5.5. *We denote by $I_5(S)$ the sequence of digits between parenthesis and separated by commas, if there is more than one digit, denoting the number of limit cycles around foci.*

Definition 7.5.6. *We denote by $I_6(S)$ the sequence of digits (ranging from 0 to 5) between parenthesis and separated by commas, if there is more than one digit, meaning the existence or the nonexistence of separatrices connection, where "0" means no separatrices connection, "1" means a loop–type connection, "2" means a connection of separatrices from two finite singular points, "3" means a connection of separatrices from one finite singular point to an infinite one, "4" means a connection of separatrices from nonadjacent infinite singular points, and "5" means a connection of separatrices from adjacent infinite singular points.*

Definition 7.5.7. *We denote by $I_7(S)$ the sequence of digits (ranging from 0 to 4) between parenthesis and separated by commas which describes the number of local or global separatrices starting or ending at the nodal sector of the finite saddle–node and at each finite antisaddle or each limit cycle.*

Definition 7.5.8. *We denote by $I_8(S)$ the sequence of two digits (each one ranging from 0 to 2) between parenthesis and separated by commas which describes the total number of local or global separatrices linking the finite multiple singular points to the infinite multiple singular points in each local chart. For example, "$(1,0)$" means that there exist only one separatrix linking the finite multiple singular point to the infinite multiple singular point in the local chart U_1 whereas there exists no linking separatrix going to the local chart U_2.*

Definition 7.5.9. *We denote by $I_9(S)$ a character from the set $\{f,\infty\}$ describing the origin of the orbits that arrive to a finite antisaddle, where "f" means that all the separatrices arrive from finite singular points and "∞" means that at least one separatrix arrives from an infinite singular point. We observe that this invariant makes sense only in the case of the existence of only one antisaddle.*

Definition 7.5.10. *We denote by $I_{10}(S)$ a digit (ranging from 0 to 2) describing the connection of separatrices involving the separatrices of finite saddle–nodes, where "0" means that the connection is produced by separatrices associated with nonzero eigenvalues, "1" means that one of the separatrices in the connection is associated with a zero eigenvalue and "2" means that both of the separatrices are associated with zero eigenvalues.*

Definition 7.5.11. *We denote by $I_{11}(S)$ an element from the set $\{a,N,SN\}$ which describes the singular point which would receive one or two separatrices of the finite elemental saddle, if the*

finite saddle–node disappears. Here, "a" means an antisaddle, "N" means an infinite node and "SN" means $\overline{\binom{0}{2}}SN$.

Definition 7.5.12. *We denote by* $I_{12}(S)$ *an element from the set* $\{s,d\}$ *describing if the stability of the focus inside a graphic is the* ***s****ame as or* ***d****ifferent from the nodal part of the finite saddle–node.*

Definition 7.5.13. *We denote by* $I_{13}(S)$ *an element from the set* $\{S,SN\}$ *describing the origin of the middle separatrix (of three) received by the nodal sector of the finite saddle–node. Here, "S" means an infinite saddle and "SN" means* $\overline{\binom{0}{2}}SN$.

Definition 7.5.14. *We denote by* $I_{14}(S)$ *a character from the set* $\{f,\infty\}$ *describing the nature of the singular point which sends or receives a separatrix to or from a limit cycle.*

Definition 7.5.15. *We denote by* $I_{15}(S)$ *the sum of the indices of the isolated infinite multiple singular points (considered in only one local chart).*

Definition 7.5.16. *We denote by* $I_{16}(S)$ *a character from the set* $\{H,P\}$*, where* H *determines that a finite antisaddle sends (or receives) orbits to (from) a parabolic sector of a multiple infinite singular point situated in the local chart where the parabolic sector is accompanied by other hyperbolic sectors, and* P *denotes that the parabolic sector is the only sector of the infinite singular point in that local chart. This invariant is needed to distinguish* $1.5L_3$ *from* $1.5L_4$.

Definition 7.5.17. *We denote by* $I_{17}(S)$ *a symbol to represent the configuration of the curves of singularities. The symbols are: "−" to represent a straight line and "*$\cup$*" to represent a parabola.*

Definition 7.5.18. *We denote by* $I_{18}(S)$ *a character from the set* $\{n,y\}$ *describing the nonexistence ("n") or the existence ("y") of graphics.*

Definition 7.5.19. *We denote by* $I_{19}(S)$ *a character from the set* $\{c,s\}$ *describing the position of the separatrix of the finite saddle–node associated with the eigenvector with zero eigenvalue which arrives to (or leaves from)* $\overline{\binom{0}{2}}SN$ *when this point receives* 3 *separatrices. We use "c" for the central position and "s" for the lateral (side) position.*

Definition 7.5.20. *We denote by* $I_{20}(S)$ *a character from the set* $\{s,d\}$ *describing if each point of the pair of infinite saddle–nodes sends (or receives) two separatrices to/from the* ***s****ame or* ***d****ifferent finite saddle–nodes. This invariant only makes sense in case of existence of two finite saddle–nodes.*

As we have noted previously in Remark 5.4.12, we do not distinguish between phase portraits whose only difference is that in one we have a finite node and in the other a focus. Both phase

portraits are topologically equivalent and they can only be distinguished within the C^1 class. In case we may want to distinguish between them, a new invariant may easily be introduced.

Theorem 7.5.21. *Consider the family* $\overline{\mathbf{QsnSN(C)}}$ *and all the phase portraits that we have obtained for this family. The values of the affine invariant* $\mathscr{I} = (I_1, I_2, I_3, I_4, I_5, I_6, I_7, I_8, I_9, I_{10}, I_{11}, I_{12}, I_{13}, I_{14}, I_{15}, I_{16}, I_{17}, I_{18}, I_{19}, I_{20})$ *given in the following diagram yield a partition of these phase portraits of the family* $\overline{\mathbf{QsnSN(C)}}$.

Furthermore, for each value of $\mathscr{I}$ *in this diagram there corresponds a single phase portrait; i.e.* S *and* S' *are such that* $I(S) = I(S')$*, if and only if* S *and* S' *are topologically equivalent.*

The bifurcation diagram for $\overline{\mathbf{QsnSN(C)}}$ has 1034 parts which produce 371 topologically different phase portraits as described in Tables 7.5.2 to 7.5.11. The remaining 663 parts do not produce any new phase portrait which was not included in the 371 previous ones. The difference is basically the presence of a strong focus instead of a node and vice versa and weak points.

The phase portraits having neither limit cycle nor graphic have been denoted surrounded by parenthesis, for example $(5S_2)$; the phase portraits having one or two limit cycles have been denoted surrounded by brackets, for example $[V_{80}]$, possessing one limit cycle, and $[[V_{88}]]$, possessing two limit cycles; the phase portraits having one or two graphics have been denoted surrounded by $\{*\}$ or $\{\{*\}\}$, for example $\{1S_{28}\}$ and $\{\{1S_{57}\}\}$; the phase portraits having one limit cycle and one graphic have been denoted surrounded by $[\{*\}]$, for example $[\{1S_{60}\}]$.

Proof of Theorem 7.5.21. The above result follows from the results in the previous sections and a careful analysis of the bifurcation diagrams given in Section 7.4, in Figures 7.19 to 7.113, the definition of the invariants I_j and their explicit values for the corresponding phase portraits. ■

We recall some observations regarding the equivalence relations used in this study: the affine and time rescaling, C^1 and topological equivalences.

The coarsest one among these three is the topological equivalence and the finest is the affine equivalence. We can have two systems which are topologically equivalent but not C^1–equivalent. For example, we could have a system with a finite antisaddle which is a structurally stable node and in another system with a focus, the two systems being topologically equivalent but belonging to distinct C^1–equivalence classes, separated by the surface $(\mathscr{S}_6)$ on which the node turns into a focus.

In Tables 7.5.12 to 7.5.25 we listed in the first column 371 parts with all the distinct phase portraits of Figures 7.1 to 7.11. Corresponding to each part listed in column 1 we have in its

horizontal block, all parts whose phase portraits are topologically equivalent to the phase portrait appearing in column 1 of the same horizontal block.

In the second column we have put all the parts whose systems yield topologically equivalent phase portraits to those in the first column, but which may have some algebro–geometric features related to the position of the orbits. In the third column we have presented all the parts which are topologically equivalent to the ones from the first column having a focus instead of a node.

In the fourth (respectively, fifth; sixth; seventh; and eightieth) column we have listed all parts whose phase portraits have a node which is at a bifurcation point producing foci close to the node in perturbations, a node–focus to shorten (respectively, a finite weak singular point; belong to disconnected parts; possess an invariant curve not yielding a connection of separatrices; and have symmetry).

The last column refers to other reasons associated to different geometrical aspects and they are described as follows:

(1) it possesses a $\overline{sn}_{(4)}$ as a finite singular point;

(2) it possesses a $\overline{\binom{2}{1}}N$ at infinity;

(3) $3S_{20}$ is the singularity of the surface $(\mathscr{S}_3)$, i.e. of the invariant polinomial $\mathscr{T}_4$, where the two finite complex singularities are weak;

(4) it possesses a $\widehat{\binom{1}{2}}E-H$ at infinity;

(5) the antisaddle is triple;

(6) it possesses a $\widehat{\binom{2}{3}}N$ at infinity;

Whenever phase portraits appear on a horizontal block in a specific column, the listing is done according to the decreasing dimension of the parts where they appear, always placing the lower dimensions on lower lines.

7.5.1 Proof of the main theorem

The bifurcation diagram described in Section 7.4, plus Tables 7.5.2 to 7.5.11 of the geometrical invariants distinguishing the 371 phase portraits, plus Tables 7.5.12 to 7.5.31 giving the equivalences with the remaining phase portraits lead to the proof of the main statement of Theorem 7.2.1.

Moreover, the phase portraits P_3 from family $\overline{\textbf{QsnSN(A)}}$, P_2 from family $\overline{\textbf{QsnSN(B)}}$ and P_{57} from family $\overline{\textbf{QsnSN(C)}}$ are topologically equivalent since there exists no geometrical invariant

that distinguishes them. It has been needed to have the curve at infinity filled up with an infinite number of singularities to have a common element in the three families. The same argument is applied to prove the equivalence of the two other triplets. Also, there are 10 more cases of coincidences between phase portraits of family $\overline{\textbf{QsnSN(C)}}$ and one of either $\overline{\textbf{QsnSN(A)}}$ or $\overline{\textbf{QsnSN(B)}}$ and we have discovered another equivalence between $5S_2$ from $\overline{\textbf{QsnSN(A)}}$ and $5S_3$ from $\overline{\textbf{QsnSN(B)}}$ which have no equivalence in $\overline{\textbf{QsnSN(C)}}$. This proves Corollary 7.2.3.

Now, summing all the topologically distinct phase portraits from families $\overline{\textbf{QsnSN(A)}}$, $\overline{\textbf{QsnSN(B)}}$ and $\overline{\textbf{QsnSN(C)}}$ and subtracting the intersections among them, according to Corollary 7.2.3, we obtain $38+25+371-17=417$ topologically distinct phase portraits in $\overline{\textbf{QsnSN}}$, and we prove Corollary 7.2.4.

In the family $\overline{\textbf{QsnSN(C)}}$, all the phase portraits corresponding to parts of volume yield all the topologically possible phase portraits of codimension one from group (A) (see page 67 for the description of this group). Many of them had already been discovered being realizable, and others which realization was missing have been found within the perturbations of family $\overline{\textbf{QsnSN(C)}}$. In the next example we perturbe one phase portrait from family $\overline{\textbf{QsnSN(C)}}$ and obtain one phase portrait of codimension one which was missing. Also three new phase portraits of group (B) can be found from perturbations of family $\overline{\textbf{QsnSN(C)}}$.

Example 7.5.22. *Phase portrait V_{177} yields an example of the "wanted" case A_{66} of codimension one. Indeed, by adding the small perturbation $x^2/100$ in a representative of the part V_{177} we obtain the following system:*

$$\dot{x}=x^2+12xy/5-22y^2/5+x^2/100,\quad \dot{y}=y-x^2/10+28xy/5-13y^2/2, \tag{7.5.1}$$

and, hence, the infinite saddle–node $\overline{\binom{0}{2}}SN$ splits into a saddle and a node, and we obtain the phase portrait A_{66} of codimension one, as shown in Figure 7.114. ■

By applying perturbations to the phase portraits of family $\overline{\textbf{QsnSN(C)}}$ we obtain the "wanted" new phase portraits of codimension one in Table 7.5.1. Then, Corollary 7.2.5 is proved.

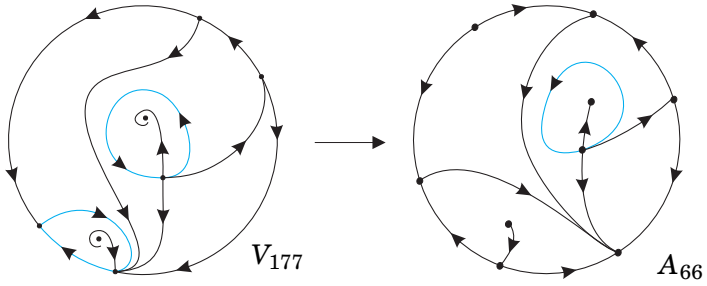

Figure 7.114: The perturbation of phase portrait V_{177} yielding the structurally unstable phase portrait A_{66}

Table 7.5.1: New codimension–one phase portraits obtained after perturbations

Phase portrait from $\overline{\mathbf{QsnSN(C)}}$	Splitting $\overline{\binom{0}{2}}SN$	Splitting $\overline{sn}_{(2)}$
V_{29}	A_{49}	B_{33}
V_{35}	—	B_{34}
V_{36}	—	B_{36}
V_{102}	A_{44}	—
V_{170}	A_{50}	—
V_{172}	A_{37}	—
V_{174}	A_{73}	—
V_{177}	A_{66}	—
$2S_{34}$	A_{51}	—

Table 7.5.2: Geometric classification for the family **QsnSN(C)**

$$
I_1 = \left\{
\begin{array}{l}
1 \,\&\, I_2 = \left\{
\begin{array}{l}
-1\,\{2.8L_1\},\\
0 \,\&\, I_3 = \left\{
\begin{array}{l}
1\,(5S_2),\\
2 \,\&\, I_4 = \left\{
\begin{array}{l}
1110\,\{P_{43}\},\\
2100\,(P_{39}),\\
2101 \,\&\, I_{18} = \left\{ \begin{array}{l} y\,(1.1L_4),\\ n\,(1.1L_7), \end{array} \right.\\
2111\,(7S_6),\\
2120\,(7S_{26}),\\
2210 \,\&\, I_{18} = \left\{ \begin{array}{l} y\,(1.1L_3),\\ n\,(4S_{20}), \end{array} \right.\\
2211\,(V_{23}),\\
3101\,\{1.1L_2\},\\
3110\,(4S_3),\\
3120\,(V_{84}),\\
3200 \,\&\, I_8 = \left\{ \begin{array}{l} (1,0)\,(1.1L_1),\\ (0,2)\,(1.1L_6), \end{array} \right.\\
3211 \,\&\, I_8 = \left\{ \begin{array}{l} (1,0)\,(V_{20}),\\ (0,2)\,(V_{22}), \end{array} \right.\\
3220\,(V_{85}),\\
4120\,(V_{21}),\\
5211\,(V_1),
\end{array} \right.\\
\infty\,\{P_{23}\},
\end{array} \right.\\
1 \,\&\, I_3 = \left\{
\begin{array}{l}
1\,(P_{68}),\\
2 \,\&\, I_4 = \left\{
\begin{array}{l}
1110\,\{2.8L_2\},\\
1111\,(1.2L_5),\\
2100\,(2.8L_3),\\
2120\,(1.2L_7),
\end{array} \right.
\end{array} \right.
\end{array} \right.\\
2 \,\&\, I_2 = \left\{
\begin{array}{l}
-1 \,\&\, I_4 = \left\{
\begin{array}{l}
2210\,\{1.4L_5\},\\
3101\,\{1.7L_{18}\},\\
3201 \,\&\, I_8 = \left\{ \begin{array}{l} (1,0)\,\{1S_{40}\},\\ (1,2)\,\{1S_{30}\}, \end{array} \right.\\
3310\,\{1S_{28}\},\\
4201\,\{1S_{33}\},
\end{array} \right.\\
0 \,\&\, I_3 = \mathscr{A}_1 \textit{ (next page)}\\
1 \,\&\, I_3 = \mathscr{A}_2 \textit{ (next page)}\\
2 \,\&\, I_3 = \mathscr{A}_3 \textit{ (next page)}
\end{array} \right.\\
3 \,\&\, I_2 = \mathscr{A}_4 \textit{ (next page)}\\
\infty \,\&\, I_2 = \mathscr{A}_5 \textit{ (next page)}
\end{array} \right.
$$

Table 7.5.3: Geometric classification for the family **QsnSN(C)** *(cont.)*

$$
I_1=\begin{cases}
\overset{\mathscr{A}_1}{\begin{bmatrix} I_1=2, \\ I_2=0 \end{bmatrix}} \;\&\; I_3=\begin{cases}
1\;\&\; I_4=\begin{cases}
11\,\{P_{60}\},\\
21\;\&\; I_5=\begin{cases} (0)\;\&\; I_6=\begin{cases} (0)\,(2.5L_{11}),\\ (2)\,(P_4),\end{cases}\\ (1)\,[2.5L_{13}],\end{cases}\\
22\,(2.5L_4),\\
31\;\&\; I_7=\begin{cases} (0,2)\,(2.5L_3),\\ (1)\,(P_1),\end{cases}\\
41\,(2.5L_1),
\end{cases}\\
2\;\&\; I_4=\begin{cases}
2111\;\&\; I_6=\begin{cases} (3)\;\&\; I_7=\begin{cases} (1)\,(2.7L_{16}),\\ (1,2)\,(2.4L_5),\end{cases}\\ (2,3)\,(P_{22}),\end{cases}\\
2120\;\&\; I_7=\begin{cases} (1)\,(2.7L_{17}),\\ (1,2)\,(2.4L_3),\end{cases}\\
2121\;\&\; I_6=\begin{cases} (0)\;\&\; I_{20}=\begin{cases} s\,(2S_{13}),\\ d\,(2S_{21}),\end{cases}\\ (2)\,(2.4L_7),\\ (3,3)\,(P_{26}),\end{cases}\\
2211\;\&\; I_6=\begin{cases} (0)\,(2S_{45}),\\ (1)\,\{2.7L_{18}\},\\ (3)\,(2.7L_5),\end{cases}\\
2221\;\&\; I_6=\begin{cases} (0)\,(2S_{18}),\\ (2)\,(2.4L_6),\end{cases}\\
3120\;\&\; I_6=\begin{cases} (0)\,(2S_{52}),\\ (1)\,\{2.7L_{19}\},\\ (3)\,(2.7L_3),\end{cases}\\
3121\;\&\; I_7=\begin{cases} (1,0)\,(2.7L_7),\\ (0)\,(P_{30}),\end{cases}\\
3130\,(2S_{12}),\\
3131\,(2S_{24}),\\
3211\;\&\; I_5=\begin{cases} (0)\;\&\; I_6=\begin{cases} (0)\;\&\; I_7=\begin{cases} (1,0)\,(2S_{51}),\\ (2,0)\,(2S_{48}),\end{cases}\\ (2)\;\&\; I_7=\begin{cases} (1,0)\,(2.7L_4),\\ (3,0)\,(2.7L_1),\end{cases}\\ (3)\,(2.4L_9),\end{cases}\\ (1)\,[2S_{49}],\end{cases}\\
\mathscr{A}_6\ \textit{(next page)}
\end{cases}\\
2\;\&\; I_2=\begin{cases} 1\;\&\; I_3=\mathscr{A}_2\ \textit{(next page)}\\ 2\;\&\; I_3=\mathscr{A}_3\ \textit{(next page)}\end{cases}\\
3\;\&\; I_2=\mathscr{A}_4\ \textit{(next page)}\\
\infty\;\&\; I_2=\mathscr{A}_5\ \textit{(next page)}
\end{cases}
$$

Table 7.5.4: Geometric classification for the family **QsnSN(C)** *(cont.)*

$$
I_1 = \left\{ \begin{array}{l}
\begin{matrix}\mathscr{A}_6 \\ \begin{bmatrix} I_1=2, \\ I_2=0, \\ I_3=2 \end{bmatrix}\end{matrix} \;\&\; I_4 = \left\{ \begin{array}{l}
3212\,(2.3L_4), \\
3220\,(2S_{53}), \\
3221\,(2.7L_9), \\
3231\,(2.3L_7), \\
3232\,(2S_{30}), \\
3311\;\&\; I_8 = \left\{ \begin{array}{l} (2,0)\,(2S_{17}), \\ (3,0)\,(2S_6), \end{array} \right. \\
3321\,(2S_{19}), \\
4111\,(2.4L_1), \\
4120\;\&\; I_5 = \left\{ \begin{array}{l} (0)\;\&\; I_6 = \left\{ \begin{array}{l} (0)\,(2S_{56}), \\ (2)\,(2.7L_2), \end{array} \right. \\ (1)\,[2S_{54}], \end{array} \right. \\
4121\;\&\; I_6 = \left\{ \begin{array}{l} (0)\,(2.3L_6), \\ (3)\,(2.7L_{11}), \end{array} \right. \\
4131\,(2.3L_1), \\
4141\,(2S_3), \\
4211\;\&\; I_7 = \left\{ \begin{array}{l} (0,2)\,(2S_{16}), \\ (1)\,(2.3L_3), \end{array} \right. \\
4212\,(2S_5), \\
4220\,(2S_{11}), \\
4221\,(2S_{23}), \\
4231\,(2S_{31}), \\
5120\;\&\; I_7 = \left\{ \begin{array}{l} (1,2)\,(2.3L_2), \\ (0,2)\,(2S_{10}), \end{array} \right. \\
5121\,(2S_4), \\
5211\,(2S_1), \\
6120\,(2S_2),
\end{array} \right. \\
2\;\&\; I_2 = \left\{ \begin{array}{l}
\begin{matrix}\mathscr{A}_2 \\ \begin{bmatrix} I_1=2, \\ I_2=1 \end{bmatrix}\end{matrix} \;\&\; I_3 = \left\{ \begin{array}{l}
1\;\&\; I_4 = \left\{ \begin{array}{l}
21\;\&\; I_7 = \left\{ \begin{array}{l} (0,2)\,(P_{41}), \\ (1,1)\,\{P_{50}\}, \end{array} \right. \\
22\;\&\; I_6 = \left\{ \begin{array}{l} (0)\;\&\; I_7 = \left\{ \begin{array}{l} (0,3)\,(1.5L_2), \\ (2,1)\,\{1.5L_5\}, \end{array} \right. \\ (1)\,\{P_{52}\}, \end{array} \right. \\
31\;\&\; I_{16} = \left\{ \begin{array}{l} H\,\{1.5L_4\}, \\ P\,(1.5L_3), \end{array} \right. \\
32\;\&\; I_5 = \left\{ \begin{array}{l} (0)\;\&\; I_7 = \left\{ \begin{array}{l} (0,2)\,(1.5L_1), \\ (1,1)\,(1.5L_7), \end{array} \right. \\ (1)\,[1.5L_6], \end{array} \right.
\end{array} \right. \\
\mathscr{A}_2' \textit{ (next page)}
\end{array} \right. \\
2\;\&\; I_3 = \mathscr{A}_3 \textit{ (next page)}
\end{array} \right. \\
3\;\&\; I_2 = \mathscr{A}_4 \textit{ (next page)} \\
\infty\;\&\; I_2 = \mathscr{A}_5 \textit{ (next page)}
\end{array} \right.
$$

Table 7.5.5: Geometric classification for the family **QsnSN(C)** *(cont.)*

$$
I_1=\begin{cases}
\mathscr{A}_2' \\
\begin{bmatrix} I_1=2, \\ I_2=1 \end{bmatrix} \;\&\; I_3=\begin{cases}
2\;\&\; I_4=\begin{cases}
1110\;\&\; I_7=\begin{cases}(0,2)\,\{1.4L_7\},\\(1,1)\,\{1.4L_{13}\},\end{cases}\\
2100\;\&\; I_7=\begin{cases}(0,2)\,(1.7L_{20}),\\(1,1)\,\{1.7L_{28}\},\end{cases}\\
2101\;\&\; I_7=\begin{cases}(0,3)\,\{1S_{37}\},\\(1,0)\,\{\{1.7L_{31}\}\},\\(1,2)\;\&\; I_8=\begin{cases}(1,0)\,(1S_{52}),\\(2,0)\,\{1S_{45}\},\end{cases}\\(2,1)\,\{\{1S_{57}\}\},\end{cases}\\
2111\;\&\; I_5=\begin{cases}(0)\;\&\; I_6=\begin{cases}(0)\;\&\; I_7=\begin{cases}(0,4)\,(1S_{69}),\\(1,3)\,(1S_7),\\(2,2)\,(1S_6),\\(3,1)\,\{1S_{14}\},\end{cases}\\(1)\,\{1.7L_2\},\\(3)\;\&\; I_7=\begin{cases}(0,2)\,(1.4L_{14}),\\(1,1)\;\&\; I_9=\begin{cases}f\,(1.4L_1),\\\infty\,(1.4L_4),\end{cases}\\(1,3)\,\{1.4L_8\},\\(2,2)\,\{1.4L_{12}\},\end{cases}\\(3,5)\,\{\{P_{31}\}\},\end{cases}\\(1)\,[1.4L_3],\end{cases}\\
2120\;\&\; I_7=\begin{cases}(0,2)\,(1.7L_9),\\(1,1)\,(1.7L_{32}),\end{cases}\\
2121\;\&\; I_5=\begin{cases}(0)\;\&\; I_6=\begin{cases}(0)\,\{1S_{44}\},\\(3)\;\&\; I_7=\begin{cases}(0,1)\,(1.7L_7),\\(0,3)\,\{1.7L_{21}\},\\(1,2)\,\{\{1.7L_{27}\}\},\end{cases}\\(5)\,\{1.7L_3\},\end{cases}\\(1)\,[1.7L_4],\end{cases}\\
2200\;\&\; I_6=\begin{cases}(0)\;\&\; I_7=\begin{cases}(0,3)\,(1S_{35}),\\(2,1)\,\{1S_{55}\},\end{cases}\\(1)\,\{1.7L_{29}\},\end{cases}\\
\mathscr{A}_7\ \textit{(next page)}
\end{cases}\\
\infty\,\{1.3L_2\},
\end{cases}\\
2\;\&\; I_2=2\;\&\; I_3=\mathscr{A}_3\ \textit{(next page)}\\
3\;\&\; I_2=\mathscr{A}_4\ \textit{(next page)}\\
\infty\;\&\; I_2=\mathscr{A}_5\ \textit{(next page)}
\end{cases}
$$

Table 7.5.6: Geometric classification for the family **QsnSN(C)** *(cont.)*

$$
I_1=\left\{\begin{array}{l}
\begin{bmatrix}\mathscr{A}_7\\ I_1=2,\\ I_2=1,\\ I_3=2\end{bmatrix}\ \&\ I_4=\left\{\begin{array}{l}
2211\ \&\ I_5=\left\{\begin{array}{l}(0)\ \&\ I_8=\left\{\begin{array}{l}(1,1)\,(1S_{68}),\\ (2,0)\,(1S_8),\end{array}\right.\\ (1)\,[1S_{12}],\end{array}\right.\\
3101\ \&\ I_5=\left\{\begin{array}{l}(0)\ \&\ I_8=\left\{\begin{array}{l}(0,2)\,\{1S_{25}\},\\ (1,1)\,\{1S_{66}\},\end{array}\right.\\ (1)\,[\{1S_{60}\}],\end{array}\right.\\
3111\ \&\ I_5=\left\{\begin{array}{l}(0)\ \&\ I_6=\left\{\begin{array}{l}(0)\ \&\ I_7=\left\{\begin{array}{l}(0,3)\,(1S_{67}),\\ (2,1)\,(1S_9),\end{array}\right.\\ (3)\,\{1.7L_6\},\end{array}\right.\\ (1)\,[1S_{13}],\end{array}\right.\\
3120\ \&\ I_6=\left\{\begin{array}{l}(0)\ \&\ I_7=\left\{\begin{array}{l}(0,3)\,(1S_{24}),\\ (1,2)\,(1S_{19}),\\ (2,1)\,\{1S_{71}\},\end{array}\right.\\ (1)\,\{1.7L_{33}\},\end{array}\right.\\
3121\ \&\ I_5=\left\{\begin{array}{l}(0)\ \&\ I_6=\left\{\begin{array}{l}(0)\ \&\ I_7=\left\{\begin{array}{l}(1,1)\ \&\ I_{18}=\left\{\begin{array}{l}y\,\{1S_{15}\},\\ n\,(1S_{18}),\end{array}\right.\\ (1,3)\,\{\{1S_{56}\}\},\\ (2,2)\,\{\{1S_{53}\}\},\\ (3,1)\,\{1S_{43}\},\\ (4,0)\,\{1S_{36}\},\end{array}\right.\\ (1)\,\{\{1.7L_{30}\}\},\end{array}\right.\\ (1)\,[1S_{16}],\end{array}\right.\\
3200\ \&\ I_5=\left\{\begin{array}{l}(0)\ \&\ I_7=\left\{\begin{array}{l}(0,2)\,(1S_{27}),\\ (1,1)\,(1S_{64}),\end{array}\right.\\ (1)\,[1S_{58}],\end{array}\right.\\
3211\,\{1.7L_5\},\\
3221\ \&\ I_5=\left\{\begin{array}{l}(0)\,(1S_{23}),\\ (1)\,[1S_{20}],\end{array}\right.\\
4111\,\{1.7L_1\},\\
4120\ \&\ I_5=\left\{\begin{array}{l}(0)\ \&\ I_7=\left\{\begin{array}{l}(0,2)\,(1S_1),\\ (1,1)\,(1S_{74}),\end{array}\right.\\ (1)\,[1S_{72}],\end{array}\right.\\
4121\ \&\ I_5=\left\{\begin{array}{l}(0)\ \&\ I_7=\left\{\begin{array}{l}(0,1)\,(1S_2),\\ (0,3)\,\{1S_{26}\},\\ (2,1)\,\{1S_{65}\},\end{array}\right.\\ (1)\ \&\ I_{18}=\left\{\begin{array}{l}y\,[\{1S_{59}\}],\\ n\,[1S_4],\end{array}\right.\end{array}\right.\\
4211\,\{1S_{21}\},\\
5111\,\{1S_5\},
\end{array}\right.\\
2\ \&\ I_2=2\ \&\ I_3=\mathscr{A}_3\ \textit{(next page)}\\
3\ \&\ I_2=\mathscr{A}_4\ \textit{(next page)}\\
\infty\ \&\ I_2=\mathscr{A}_5\ \textit{(next page)}
\end{array}\right.
$$

Table 7.5.7: Geometric classification for the family **QsnSN(C)** *(cont.)*

$$
I_1=\left\{\begin{array}{l}
\begin{bmatrix}\mathscr{A}_3\\ I_1=2,\\ I_2=2\end{bmatrix}\ \&\ I_3=\left\{\begin{array}{l}
1\,(2.5L_{10}),\\
2\ \&\ I_4=\left\{\begin{array}{l}
1111\,(2S_{41}),\\
2111\,\{2.7L_{20}\},\\
2121\ \&\ I_5=\left\{\begin{array}{l}(0)\,(2S_{59}),\\(1)\,[2S_{61}],\end{array}\right.\\
3111\,\{2S_{62}\},
\end{array}\right.
\end{array}\right.\\
\begin{bmatrix}\mathscr{A}_4\\ [I_1=3]\end{bmatrix}\ \&\ I_2=\left\{\begin{array}{l}
0\ \&\ I_3=\left\{\begin{array}{l}
1\ \&\ I_4=\left\{\begin{array}{l}
21\ \&\ I_7=\left\{\begin{array}{l}(0,2)\,(5.7L_{11}),\\(1,1)\,(5.7L_2),\end{array}\right.\\
22\,(5S_9),\\
31\ \&\ I_6=\left\{\begin{array}{l}
(0)\ \&\ I_7=\left\{\begin{array}{l}(0,3)\,(5S_{26}),\\(2,1)\ \&\ I_{18}=\left\{\begin{array}{l}y\,\{5S_{33}\},\\n\,(5S_{13}),\end{array}\right.\end{array}\right.\\
(1)\,\{5.7L_1\},\\
(2)\,\{5.7L_{14}\},
\end{array}\right.\\
41\ \&\ I_5=\left\{\begin{array}{l}
(0)\ \&\ I_7=\left\{\begin{array}{l}(0,2)\,(5S_1),\\(1,1)\,(5S_3),\\(2,1)\,(5S_{36}),\end{array}\right.\\
(1)\,[5S_5],
\end{array}\right.\\
2111\ \&\ I_6=\left\{\begin{array}{l}(3)\,(4S_8),\\(1,5)\,\{7.7L_4\},\\(2,3)\,(4.4L_3),\end{array}\right.\\
2120\,(4S_6),\\
2121\ \&\ I_6=\left\{\begin{array}{l}
(0)\ \&\ I_8=\left\{\begin{array}{l}(1,1)\,(V_{49}),\\(2,0)\,(V_{46}),\end{array}\right.\\
(2)\,(4S_{33}),\\
(3,3)\,(7.7L_1),
\end{array}\right.\\
2211\ \&\ I_6=\left\{\begin{array}{l}
(2)\ \&\ I_7=\left\{\begin{array}{l}(0,3)\,(7S_{65}),\\(2,1)\,(7S_{33}),\end{array}\right.\\
(3)\ \&\ I_{10}=\left\{\begin{array}{l}0\ \&\ I_{11}=\left\{\begin{array}{l}N\,(7S_{63}),\\SN\,(7S_9),\end{array}\right.\\1\,(7S_{68}),\end{array}\right.\\
(2,2)\,\{4.7L_1\},\\
(2,3)\,(4.4L_1),
\end{array}\right.\\
2221\ \&\ I_6=\left\{\begin{array}{l}
(0)\ \&\ I_7=\left\{\begin{array}{l}(1,3)\ \&\ I_{11}=\left\{\begin{array}{l}N\,(V_{155}),\\SN\,(V_{44}),\end{array}\right.\\(2,2)\,(V_{104}),\end{array}\right.\\
(2)\ \&\ I_7=\left\{\begin{array}{l}(0,2)\,(4S_{32}),\\(1,1)\,(4S_{29}),\end{array}\right.
\end{array}\right.\\
3120\ \&\ I_{10}=\left\{\begin{array}{l}0\,(7S_{69}),\\1\ \&\ I_{11}=\left\{\begin{array}{l}N\,(7S_{16}),\\SN\,(7S_{61}),\end{array}\right.\end{array}\right.\\
\mathscr{A}_8\ \textit{(next page)}
\end{array}\right.\\
2\ \&\ I_3=\mathscr{A}_9\ \textit{(next page)}
\end{array}\right.\\
\infty\ \&\ I_2=\mathscr{A}_5\ \textit{(next page)}
\end{array}\right.
$$

Table 7.5.8: Geometric classification for the family **QsnSN(C)** *(cont.)*

$$
I_1=\left\{\begin{array}{l}
\mathscr{A}_8\ \begin{bmatrix} I_1=3,\\ I_2=0,\\ I_3=2\end{bmatrix}\ \&\ I_4=\left\{\begin{array}{l}
3121\ \&\ I_5=\left\{\begin{array}{l}
(0)\ \&\ I_6=\left\{\begin{array}{l}(0)\,(V_{122}),\\ (3)\ \&\ I_7=\left\{\begin{array}{l}(0,2)\,(7S_{37}),\\(1,1)\,(7S_{38}),\end{array}\right.\end{array}\right.\\
(1)\,[V_{118}],
\end{array}\right.\\
3130\ \&\ I_7=\left\{\begin{array}{l}
(1,3)\ \&\ I_{11}=\left\{\begin{array}{l}N\,(V_{37}),\\SN\,(V_{165}),\end{array}\right.\\
(2,2)\,(V_{123}),
\end{array}\right.\\
3131\,(V_{110}),\\
3211\ \&\ I_5=\left\{\begin{array}{l}
(0)\ \&\ I_6=\left\{\begin{array}{l}
(0)\ \&\ I_7=\left\{\begin{array}{l}(0,4)\,(V_{154}),\\(3,1)\,(V_{102}),\end{array}\right.\\
(1)\,\{7S_{32}\},\\
(2)\ \&\ I_7=\left\{\begin{array}{l}
(0,2)\ \&\ I_8=\left\{\begin{array}{l}(0,0)\ \&\ I_{11}=\left\{\begin{array}{l}a\,(4S_{42}),\\N\,(7S_{64}),\end{array}\right.\\(1,0)\,(7S_4),\end{array}\right.\\
(1,1)\ \&\ I_8=\left\{\begin{array}{l}(0,0)\,(7S_{70}),\\(1,0)\ \&\ I_{10}=\left\{\begin{array}{l}0\ \&\ I_{11}=\left\{\begin{array}{l}a\,(4S_{16}),\\SN\,(7S_8),\end{array}\right.\\1\,(7S_{71}),\end{array}\right.\\(2,0)\,(7S_{23}),\end{array}\right.
\end{array}\right.\\
(3)\,(4S_{31}),
\end{array}\right.\\
(1)\ \&\ I_{10}=\left\{\begin{array}{l}0\,[4S_{26}],\\1\,[7S_{28}],\end{array}\right.
\end{array}\right.\\
3212\ \&\ I_5=\left\{\begin{array}{l}
(0)\ \&\ I_{12}=\left\{\begin{array}{l}s\,\{7S_{22}\},\\d\,\{7S_{29}\},\end{array}\right.\\
(1)\,[\{7S_{27}\}],
\end{array}\right.\\
3221\ \&\ I_7=\left\{\begin{array}{l}
(0,1)\ \&\ I_8=\left\{\begin{array}{l}(0,1)\,(7S_{44}),\\(1,1)\,(7S_{45}),\end{array}\right.\\
(1,4)\,(4S_9),
\end{array}\right.\\
3231\,\{7S_{52}\},\\
3232\,(V_{129}),\\
3311\ \&\ I_5=\left\{\begin{array}{l}
(0)\ \&\ I_8=\left\{\begin{array}{l}
(1,0)\ \&\ I_9=\left\{\begin{array}{l}
f\ \&\ I_{11}=\left\{\begin{array}{l}N\,(V_{143}),\\SN\ \&\ I_{19}=\left\{\begin{array}{l}c\,(V_{170}),\\s\,(V_{71}),\end{array}\right.\end{array}\right.\\
\infty\ \&\ I_{11}=\left\{\begin{array}{l}a\,(V_{145}),\\N\,(V_{13}),\end{array}\right.
\end{array}\right.\\
(2,0)\,(V_{64}),
\end{array}\right.\\
(1)\,[V_{90}],
\end{array}\right.\\
3321\ \&\ I_5=\left\{\begin{array}{l}
(0)\ \&\ I_7=\left\{\begin{array}{l}(0,2)\,(V_{108}),\\(1,1)\,(V_{78}),\end{array}\right.\\
(1)\ \&\ I_{12}=\left\{\begin{array}{l}s\,[V_{80}],\\d\,[10S_1],\end{array}\right.\\
(2)\,[[V_{88}]],
\end{array}\right.\\
\mathscr{A}_8'\ \textit{(next page)}
\end{array}\right.\\
3\ \&\ I_2=2\ \&\ I_3=\mathscr{A}_9\ \textit{(next page)}\\
\infty\ \&\ I_2=\mathscr{A}_5\ \textit{(next page)}
\end{array}\right.
$$

Table 7.5.9: Geometric classification for the family **QsnSN(C)** *(cont.)*

$$
I_1=\begin{cases}
\mathscr{A}_8' \\
\begin{bmatrix} I_1=3, \\ I_2=0, \\ I_3=2 \end{bmatrix} \ \&\ I_4=\begin{cases}
4111\,(4S_1), \\
4120\,(7S_{62}), \\
4121\ \&\ I_5=\begin{cases}
(0)\ \&\ I_6=\begin{cases} (0)\,(V_{66}), \\ (1)\,\{7S_{41}\}, \end{cases} \\
(1)\ \&\ I_6=\begin{cases} (3)\ \&\ I_8=\begin{cases} (1,1)\,(7S_{55}), \\ (2,0)\,(7S_3), \end{cases} \\ (0)\,[V_{100}], \\ (3)\,[7S_{53}], \end{cases}
\end{cases} \\
4131\,\{7S_2\}, \\
4141\ \&\ I_5=\begin{cases} (0)\,(V_{15}), \\ (1)\,[V_{17}], \end{cases} \\
4211\ \&\ I_6=\begin{cases}
(0)\ \&\ I_7=\begin{cases} (0,3)\ \&\ I_7=\begin{cases} f\,(V_{144}), \\ \infty\,(V_{147}), \end{cases} \\ (2,1)\ \&\ I_{11}=\begin{cases} a\,\{V_{172}\}, \\ SN\,(V_{69}), \end{cases} \end{cases} \\
(1)\ \&\ I_{11}=\begin{cases} a\,\{7S_{77}\}, \\ SN\,\{7S_7\}, \end{cases}
\end{cases} \\
4212\ \&\ I_5=\begin{cases}
(0)\ \&\ I_7=\begin{cases} (0,2)\,(V_{10}), \\ (1,1)\,(V_{83}), \end{cases} \\
(1)\,[V_{89}],
\end{cases} \\
4220\ \&\ I_{11}=\begin{cases} N\,(V_{42}), \\ SN\,(V_{142}), \end{cases} \\
4221\ \&\ I_7=\begin{cases} (0,2)\,(V_{109}), \\ (1,1)\,(V_{114}), \end{cases} \\
4231\ \&\ I_5=\begin{cases}
(0)\ \&\ I_8=\begin{cases} (1,0)\,(V_{136}), \\ (2,0)\,(V_7), \end{cases} \\
(1)\,[V_{134}],
\end{cases} \\
5120\ \&\ I_6=\begin{cases}
(0)\ \&\ I_7=\begin{cases} (0,3)\,(V_{141}), \\ (2,1)\ \&\ I_{11}=\begin{cases} a\,\{V_{173}\}, \\ N\,(V_{41}), \end{cases} \end{cases} \\
(1)\ \&\ I_{11}=\begin{cases} a\,\{7S_{78}\}, \\ N\,\{7S_{10}\}, \end{cases}
\end{cases} \\
5121\ \&\ I_5=\begin{cases}
(0)\ \&\ I_7=\begin{cases} (0,2)\,(V_9), \\ (1,1)\,(V_{121}), \end{cases} \\
(1)\,[V_{117}],
\end{cases} \\
5211\ \&\ I_5=\begin{cases}
(0)\ \&\ I_{11}=\begin{cases} a\,(V_{190}), \\ SN\,(V_{25}), \end{cases} \\
(1)\ \&\ I_{11}=\begin{cases} a\,[V_{178}], \\ SN\,[V_{27}], \end{cases}
\end{cases} \\
6120\ \&\ I_5=\begin{cases}
(0)\ \&\ I_6=\begin{cases} (0)\ \&\ I_7=\begin{cases} (0,2)\,(V_2), \\ (1,1)\ \&\ I_{11}=\begin{cases} a\,(V_{191}), \\ N\,(V_{31}), \end{cases} \end{cases} \\ (2)\,(7S_{15}), \end{cases} \\
(1)\ \&\ I_{11}=\begin{cases} a\,[V_{179}], \\ N\,[V_{33}], \end{cases}
\end{cases}
\end{cases} \\
3\ \&\ I_2=2\ \&\ I_3=\mathscr{A}_9\ \textit{(next page)} \\
\infty\ \&\ I_2=\mathscr{A}_5\ \textit{(next page)}
\end{cases}
$$

Table 7.5.10: Geometric classification for the family **QsnSN(C)** *(cont.)*

$$
I_1=\left\{\begin{array}{l}
\begin{matrix}\mathscr{A}_9\\ \begin{bmatrix} I_1=3,\\ I_2=2\end{bmatrix}\end{matrix}\ \&\ I_3=\left\{\begin{array}{l}
1\ \&\ I_5=\left\{\begin{array}{l}
(0)\ \&\ I_6=\left\{\begin{array}{l}
(0)\ \&\ I_7=\left\{\begin{array}{l}(0,2,3)\,(5S_{28}),\\ (1,1,3)\,(5S_{12}),\\ (2,1,2)\,\{5S_{23}\},\end{array}\right.\\
(1)\,\{5.7L_9\},
\end{array}\right.\\
(1)\,[5S_{22}],
\end{array}\right.\\
2\ \&\ I_4=\left\{\begin{array}{l}
1111\ \&\ I_5=\left\{\begin{array}{l}
(0)\ \&\ I_6=\left\{\begin{array}{l}
(0)\ \&\ I_7=\left\{\begin{array}{l}(0,3,4)\,(V_{149}),\\ (2,1,4)\,(V_{61}),\\ (3,1,3)\ \&\ I_{13}=\left\{\begin{array}{l}S\,(V_{107}),\\ SN\,\{V_{53}\},\end{array}\right.\end{array}\right.\\
(1)\ \&\ I_{13}=\left\{\begin{array}{l}S\,\{7S_{31}\},\\ SN\,\{7S_{17}\},\end{array}\right.\\
(3)\ \&\ I_7=\left\{\begin{array}{l}(0,2,3)\,(4S_{44}),\\ (1,1,3)\,(4S_{15}),\\ (2,1,2)\,\{4S_{13}\},\end{array}\right.
\end{array}\right.\\
(1)\ \&\ I_6=\left\{\begin{array}{l}(0)\ \&\ I_{13}=\left\{\begin{array}{l}S\,[V_{94}],\\ SN\,[V_{54}],\end{array}\right.\\ (3)\,[4S_{25}],\end{array}\right.
\end{array}\right.\\
2111\ \&\ I_5=\left\{\begin{array}{l}
(0)\ \&\ I_6=\left\{\begin{array}{l}
(0)\ \&\ I_7=\left\{\begin{array}{l}(1,2,3)\ \&\ I_8=\left\{\begin{array}{l}(1,0)\,(V_{198}),\\ (2,0)\,(V_{62}),\end{array}\right.\\ (2,2,2)\,(V_{51}),\end{array}\right.\\
(3)\ \&\ I_8=\left\{\begin{array}{l}(0,1)\,\{4S_{51}\},\\ (1,1)\,(4S_{36}),\end{array}\right.\\
(3,5)\ \&\ I_7=\left\{\begin{array}{l}(0,0,2)\,\{\{7.7L_6\}\},\\ (1,0,1)\,\{7.7L_5\},\end{array}\right.
\end{array}\right.\\
(1)\,[V_{99}],
\end{array}\right.\\
2121\ \&\ I_5=\left\{\begin{array}{l}
(0)\ \&\ I_6=\left\{\begin{array}{l}
(3)\ \&\ I_7=\left\{\begin{array}{l}(0,1,2)\,(7S_{72}),\\ (1,1,1)\,(7S_{60}),\end{array}\right.\\
(5)\ \&\ I_{11}=\left\{\begin{array}{l}s\,\{\{7S_{67}\}\},\\ d\,\{7S_{42}\},\end{array}\right.
\end{array}\right.\\
(1)\ \&\ I_7=\left\{\begin{array}{l}(0,1,2)\,[7S_{56}],\\ (1,1,1)\,[\{7S_{74}\}],\end{array}\right.
\end{array}\right.\\
3111\ \&\ I_6=\left\{\begin{array}{l}
(3)\ \&\ I_7=\left\{\begin{array}{l}(0,1,2)\,\{7S_{58}\},\\ (1,1,1)\,\{\{7S_{75}\}\},\end{array}\right.\\
(5)\ \&\ I_7=\left\{\begin{array}{l}(0,0,3)\,\{7S_{57}\},\\ (2,0,1)\,\{\{7S_{76}\}\},\end{array}\right.\\
(1,5)\,\{\{7.7L_7\}\},
\end{array}\right.\\
3121\ \&\ I_5=\left\{\begin{array}{l}
(0)\ \&\ I_6=\left\{\begin{array}{l}
(0)\ \&\ I_7=\left\{\begin{array}{l}(0,1,3)\,(V_{140}),\\ (1,1,2)\ \&\ I_8=\left\{\begin{array}{l}(1,1)\ \&\ I_{18}=\left\{\begin{array}{l}1\,\{V_{166}\},\\ 2\,\{\{V_{169}\}\},\end{array}\right.\\ (2,1)\,\{V_{113}\},\end{array}\right.\\ (2,1,1)\,\{V_{174}\},\end{array}\right.\\
(1)\,\{7S_{79}\},
\end{array}\right.\\
(1)\ \&\ I_6=\left\{\begin{array}{l}(0)\ \&\ I_7=\left\{\begin{array}{l}(0,1,3)\,[V_{137}],\\ (1,1,2)\,[\{V_{168}\}],\\ (2,1,1)\,[\{V_{176}\}],\end{array}\right.\\ (1)\,[\{7S_{81}\}],\end{array}\right.
\end{array}\right.\\
\mathscr{A}_{10}\ \textit{(next page)}
\end{array}\right.\\
\infty\ \&\ I_2=\mathscr{A}_5\ \textit{(next page)}
\end{array}\right.
$$

Table 7.5.11: Geometric classification for the family **QsnSN(C)** *(cont.)*

$$
I_1 = \left\{ \begin{array}{l}
\begin{matrix} \mathscr{A}_{10} \\ \left[\begin{matrix} I_1 = 3, \\ I_2 = 2, \\ I_3 = 2 \end{matrix}\right] \end{matrix} \;\&\; I_4 = \left\{ \begin{array}{l}
4111 \;\&\; I_5 = \left\{ \begin{array}{l}
(0) \;\&\; I_6 = \left\{ \begin{array}{l} (0) \;\&\; I_{18} = \left\{ \begin{array}{l} 1\,\{V_{138}\}, \\ 2\,\{\{V_{177}\}\}, \end{array} \right. \\ (1)\,\{\{7S_{82}\}\}, \\ (5) \;\&\; I_7 = \left\{ \begin{array}{l} (0,2,0)\,\{7S_1\}, \\ (1,1,0)\,\{7S_{85}\}, \end{array} \right. \end{array} \right. \\
(1)\,[\{7S_{83}\}],
\end{array} \right. \\
4121 \;\&\; I_5 = \left\{ \begin{array}{l}
(0) \;\&\; I_7 = \left\{ \begin{array}{l} (0,2,1)\,(V_3), \\ (1,1,1)\,(V_{192}), \end{array} \right. \\
(1) \;\&\; I_7 = \left\{ \begin{array}{l} (0,2,1)\,[V_5], \\ (1,1,1) \;\&\; I_{14} = \left\{ \begin{array}{l} f\,[V_{180}], \\ \infty\,[V_{194}], \end{array} \right. \end{array} \right. \\
(1,1)\,[[V_{182}]],
\end{array} \right. \\
5111 \;\&\; I_5 = \left\{ \begin{array}{l}
(0) \;\&\; I_7 = \left\{ \begin{array}{l} (0,1,2)\,\{V_6\}, \\ (1,1,1)\,\{V_{189}\}, \end{array} \right. \\
(1)\,[\{V_{183}\}],
\end{array} \right.
\end{array} \right. \\
\begin{matrix} \mathscr{A}_5 \\ [I_1 = \infty] \end{matrix} \;\&\; I_2 = \left\{ \begin{array}{l}
0 \;\&\; I_{15} = \left\{ \begin{array}{l} 0\,\{P_{58}\}, \\ 1 \;\&\; I_{17} = \left\{ \begin{array}{l} -\,\{P_{65}\}, \\ \cup\,\{P_{64}\}, \end{array} \right. \end{array} \right. \\
1 \;\&\; I_3 = \left\{ \begin{array}{l} 2\,\{1.2L_8\}, \\ \infty\,\{P_{57}\}. \end{array} \right.
\end{array} \right.
\end{array} \right.
$$

Table 7.5.12: Topological equivalences for the family **QsnSN(C)**

Presented phase portrait	Identical under perturbations	Finite antisaddle focus	Finite antisaddle node–focus	Finite weak point	Disconnected parts	Possessing invariant curve (no separatrix)	Symmetry	Other reasons
V_1								
V_2								
V_3		V_4	$6S_1$	$3S_1$				
V_5								
V_6								
V_7								
V_9	V_{19}	V_8, V_{18}	$6S_3$, $6S_4$ $3.6L_1$	$3S_3$, $3S_4$				
V_{10}	V_{12}		$3.10L_1$	$3S_5$, $3S_6$				
V_{13}	V_{11}, V_{14}			$3S_7$		$4S_4$		
V_{15}		V_{16}	$6S_2$	$3S_2$				
V_{17}								
V_{20}								$2.11{L_3}^{(1)}$
V_{21}								${1.2L_1}^{(2)}$, ${2.11L_2}^{(1)}$
V_{22}								
V_{23}	V_{24}					$4S_{15}$		${3S_{20}}^{(3)}$ ${1.2L_2}^{(2)}$, ${2.11L_2}^{(1)}$
V_{25}		V_{26}	$6S_5$	$3S_8$				
V_{27}								

Table 7.5.13: Topological equivalences for the family **QsnSN(C)** *(cont.)*

Presented phase portrait	Identical under perturbations	Finite antisaddle focus	Finite antisaddle node–focus	Finite weak point	Disconnected parts	Possessing invariant curve (no separatrix)	Symmetry	Other reasons
V_{31}		V_{32}	$6S_6$	$3S_9$				
V_{33}								
V_{37}	V_{43}	V_{36}, V_{40}	$6S_9$, $6S_{10}$ $3.6L_2$	$3S_{12}$, $3S_{13}$				
V_{41}		V_{34}, V_{38}	$6S_7$	$3S_{10}$				
V_{42}		V_{35}, V_{39}	$6S_8$	$3S_{11}$				
V_{44}	V_{45}, V_{73}, V_{96}	V_{30}, V_{72}	$6S_{11}$, $6S_{22}$ $3.6L_3$	$3S_{23}$, $3S_{24}$, $3S_{26}$, $3S_{43}$ $3.10L_4$				
V_{46}	V_{47}, V_{63}			$3S_{14}$, $3S_{15}$ $3.10L_2$		$4S_{11}$		
V_{49}	V_{48}, V_{75}, V_{97}	V_{50}, V_{98}	$6S_{12}$, $6S_{30}$	$3S_{25}$, $3S_{44}$, $3S_{45}$ $3.4L_7$, $3.6L_8$		$4S_{12}$, $4S_{24}$		
V_{51}		V_{52}	$6S_{13}$					
V_{53}								
V_{54}								
V_{61}		V_{55}, V_{56}, V_{57} V_{58}, V_{59}	$6S_{15}$, $6S_{16}$, $6S_{17}$ $6S_{18}$, $6S_{19}$ $3.6L_7$, $6.6L_1$	$3S_{16}$, $3S_{32}$, $3S_{42}$				

Table 7.5.14: Topological equivalences for the family **QsnSN(C)** *(cont.)*

Presented phase portrait	Identical under perturbations	Finite antisaddle focus	Finite antisaddle node–focus	Finite weak point	Disconnected parts	Possessing invariant curve (no separatrix)	Symmetry	Other reasons
V_{62}		V_{60}	$6S_{14}$	$3S_{46}$				
V_{64}	V_{65}	V_{74}, V_{76}	$6S_{23}$, $6S_{24}$ $3.6L_4$, $3.6L_5$ P_{12}	$3S_{17}$, $3S_{18}$, $3S_{27}$ $3S_{30}$, $3S_{35}$, $3S_{41}$ $3.3L_2$, $3.10L_3$, $3.10L_5$				
V_{66}	V_{67}	V_{77}, V_{86}	$6S_{25}$, $6S_{28}$	$3S_{19}$, $3S_{31}$, $3S_{48}$, $3S_{49}$ $3.3L_3$, $3.6L_6$				
V_{69}		V_{28}, V_{68}	$6S_{20}$	$3S_{21}$				
V_{71}		V_{29}, V_{70}	$6S_{21}$	$3S_{22}$				
V_{78}		V_{79}, V_{91}	$6S_{26}$	$3S_{28}$, $3S_{37}$ $3.10L_6$				
V_{80}				$3S_{33}$				
V_{83}		V_{81}, V_{82}	$6S_{27}$	$3S_{29}$, $3S_{34}$, $3S_{36}$, $3S_{39}$ $3.3L_1$, $3.10L_7$				
V_{84}								$1.2L_3{}^{(2)}$
V_{85}								$1.2L_4{}^{(2)}$
V_{88}								
V_{89}	V_{92}			$3S_{38}$				
V_{90}	V_{93}			$3S_{40}$				

Table 7.5.15: Topological equivalences for the family **QsnSN(C)** *(cont.)*

Presented phase portrait	Identical under perturbations	Finite antisaddle focus	Finite antisaddle node–focus	Finite weak point	Disconnected parts	Possessing invariant curve (no separatrix)	Symmetry	Other reasons
V_{94}		V_{87}	$6S_{29}$					
V_{99}								
V_{100}	V_{101}			$3S_{47}$				
V_{102}	V_{105}			$3S_{50}$				
V_{104}		V_{103}, V_{106}	$6S_{31}$	$3S_{51}$	V_{125}, V_{126}	$4S_{37}$, $4S_{38}$		
V_{107}		V_{95}	$6S_{32}$					
V_{108}	V_{127}			$3S_{57}$				
V_{109}	V_{128}	V_{131}, V_{132}	$6S_{39}$, $6S_{40}$ $3.6L_{10}$	$3S_{58}$, $3S_{59}$				
V_{110}	V_{126}	V_{111}, V_{112}	$6S_{33}$, $6S_{37}$ $3.6L_{9}$	$3S_{52}$, $3S_{56}$				
V_{113}								
V_{114}		V_{115}, V_{116}	$6S_{34}$	$3S_{53}$				
V_{117}								
V_{118}								
V_{121}		V_{119}	$6S_{35}$	$3S_{54}$				
V_{122}		V_{120}	$6S_{36}$	$3S_{55}$				
V_{123}								

Table 7.5.16: Topological equivalences for the family **QsnSN(C)** *(cont.)*

Presented phase portrait	Identical under perturbations	Finite antisaddle focus	Finite antisaddle node–focus	Finite weak point	Disconnected parts	Possessing invariant curve (no separatrix)	Symmetry	Other reasons
V_{129}		V_{130}, V_{133}	$6S_{38}$	$3S_{60}$				
V_{134}								
V_{136}		V_{135}	$6S_{41}$	$3S_{61}$				
V_{137}								
V_{138}								
V_{140}		V_{139}	$6S_{42}$	$3S_{62}$				
V_{141}								
V_{142}								
V_{143}								
V_{144}								
V_{145}	V_{144}			$3S_{63}$				
V_{147}	V_{148}			$3S_{64}$, $3S_{56}$ $3.10L_8$				
V_{149}	V_{153}, V_{158} V_{196}, V_{197}	V_{151}, V_{152} V_{159}	$6S_{43}$, $6S_{44}$ $6S_{46}$, $6S_{47}$			$4S_{45}$, $4S_{46}$		
V_{154}	V_{157}			$3S_{67}$				
V_{155}	V_{156}, V_{162}, V_{163}	V_{164}	$6S_{49}$	$3S_{66}$		$4S_{50}$, $4S_{52}$		
V_{165}								
V_{166}		V_{167}	$6S_{50}$	$3S_{68}$				

Table 7.5.17: Topological equivalences for the family **QsnSN(C)** *(cont.)*

Presented phase portrait	Identical under perturbations	Finite antisaddle focus	Finite antisaddle node–focus	Finite weak point	Disconnected parts	Possessing invariant curve (no separatrix)	Symmetry	Other reasons
V_{168}								
V_{169}								
V_{170}							V_{171}	
V_{172}								
V_{173}								
V_{174}		V_{175}	$6S_{51}$	$3S_{69}$				
V_{176}								
V_{177}								
V_{178}								
V_{179}				$3S_{72}$				
V_{180}		V_{181}	$6S_{52}$	$3S_{70}$				
V_{182}								
V_{183}								
V_{189}		V_{195}	$6S_{59}$	$3S_{76}$				
V_{190}		V_{184}	$6S_{54}$	$3S_{71}$				
V_{191}		V_{185}	$6S_{55}$					
V_{192}	V_{186}, V_{187}, V_{193}		$6S_{53}$, $6S_{56}$ $6S_{57}$, $6S_{60}$ $3.6L_{11}$, $3.6L_{12}$ $6.6L_2$	$3S_{73}$, $3S_{74}$ $3S_{77}$, $3S_{78}$ $3.3L_4$				

Table 7.5.18: Topological equivalences for the family **QsnSN(C)** *(cont.)*

Presented phase portrait	Identical under perturbations	Finite antisaddle focus	Finite antisaddle node–focus	Finite weak point	Disconnected parts	Possessing invariant curve (no separatrix)	Symmetry	Other reasons
V_{194}		V_{188}	$6S_{59}$	$3S_{76}$				
V_{198}	V_{150}	$V_{160}, V_{161}, V_{199}$	$6S_{45}, 6S_{48}$ $6S_{61}, 6S_{62}$ $6.6L_3$			$4S_{47}$		
$1S_1$								
$1S_2$		$1S_3$	$1.6L_1$	$1.3L_1$				
$1S_4$								
$1S_5$								
$1S_6$								
$1S_7$								
$1S_8$		$1S_{10}$	$1.6L_2$	$1.3L_3$				
$1S_9$		$1S_{11}$	$1.6L_3$	$1.3L_4$				
$1S_{12}$								
$1S_{13}$								
$1S_{14}$								
$1S_{15}$								
$1S_{16}$								
$1S_{18}$		$1S_{17}$	$1.6L_4$	$1.3L_6$				
$1S_{19}$					$1S_{70}$			
$1S_{20}$								
$1S_{21}$								
$1S_{23}$		$1S_{22}$	$1.6L_5$	$1.3L_8$				

Table 7.5.19: Topological equivalences for the family **QsnSN(C)** *(cont.)*

Presented phase portrait	Identical under perturbations	Finite antisaddle focus	Finite antisaddle node–focus	Finite weak point	Disconnected parts	Possessing invariant curve (no separatrix)	Symmetry	Other reasons
$1S_{24}$								
$1S_{25}$								$1.7L_{10}{}^{(4)}$
$1S_{26}$								
$1S_{27}$								
$1S_{28}$	$1S_{29}$			$1.3L_{11}$				
$1S_{30}$	$1S_{31}$, $1S_{32}$			$1.3L_{12}$		$1.7L_{24}$		
$1S_{33}$	$1S_{34}$			$1.3L_{10}$				
$1S_{35}$								
$1S_{36}$								
$1S_{37}$								$1.7L_{11}{}^{(4)}$
$1S_{40}$	$1S_{41}$, $1S_{50}$			$1.3L_{9}$		$1.4L_{10}$		
$1S_{43}$								
$1S_{44}$		$1S_{47}$	$1.6L_{7}$					
$1S_{45}$	$1S_{38}$, $1S_{39}$ $1S_{46}$	$1S_{48}$, $1S_{49}$	$1.6L_{8}$, $1.6L_{9}$ P_{48}			$1.7L_{22}$, $1.7L_{23}$ $1.7L_{25}$, $1.7L_{26}$		$1.7L_{12}{}^{(4)}$, $1.7L_{13}{}^{(4)}$ $P_{46}{}^{(4)}$
$1S_{52}$	$1S_{42}$, $1S_{51}$	$1S_{54}$	$1.6L_{6}$			$1.4L_{9}$, $1.4L_{11}$		
$1S_{53}$								
$1S_{55}$								
$1S_{56}$								
$1S_{57}$								$1.7L_{14}{}^{(4)}$

Table 7.5.20: Topological equivalences for the family **QsnSN(C)** *(cont.)*

Presented phase portrait	Identical under perturbations	Finite antisaddle focus	Finite antisaddle node–focus	Finite weak point	Disconnected parts	Possessing invariant curve (no separatrix)	Symmetry	Other reasons
$1S_{58}$								
$1S_{59}$								
$1S_{60}$								$1.7L_{15}{}^{(4)}$
$1S_{64}$		$1S_{61}$	$1.6L_{10}$	$1.3L_{13}$				
$1S_{65}$		$1S_{62}$	$1.6L_{11}$	$1.3L_{14}$				
$1S_{66}$		$1S_{63}$	$1.6L_{12}$	$1.3L_{15}$			$P_{53}{}^{(4)}$, $P_{55}{}^{(4)}$	$1.7L_{16}{}^{(4)}$, $1.7L_{17}{}^{(4)}$
$1S_{67}$								
$1S_{68}$								
$1S_{69}$								
$1S_{71}$								
$1S_{72}$								
$1S_{74}$		$1S_{73}$	$1.6L_{13}$	$1.3L_{17}$				
$2S_1$							$2S_8$	
$2S_2$					$2S_9$			
$2S_3$								
$2S_4$					$2S_{26}$			
$2S_5$					$2S_{20}$			
$2S_6$	$2S_7$				$2S_{15}$	$2.4L_2$		
$2S_{10}$					$2S_{32}$			
$2S_{11}$					$2S_{33}$			
$2S_{12}$					$2S_{27}$			

Table 7.5.21: Topological equivalences for the family **QsnSN(C)** *(cont.)*

Presented phase portrait	Identical under perturbations	Finite antisaddle focus	Finite antisaddle node–focus	Finite weak point	Disconnected parts	Possessing invariant curve (no separatrix)	Symmetry	Other reasons
$2S_{13}$	$2S_{14}$					$2.4L_4$		
$2S_{16}$					$2S_{35}$			
$2S_{17}$					$2S_{34}$			
$2S_{18}$					$2S_{28}$, $2S_{29}$	$2.4L_{10}$		
$2S_{19}$					$2S_{22}$			
$2S_{21}$								
$2S_{22}$								
$2S_{23}$					$2S_{25}$			
$2S_{24}$								
$2S_{30}$								
$2S_{31}$								
$2S_{41}$	$2S_{42}$, $2S_{44}$	$2S_{43}$	$2.6L_1$			$2.4L_{13}$		
$2S_{45}$	$2S_{36}$, $2S_{46}$	$2S_{47}$	$2.6L_2$	$2.3L_8$, $2.3L_{12}$		$2.4L_{11}$, $2.2L_{12}$, $2.4L_{14}$		${2S_{37}}^{(5)}$, ${2S_{38}}^{(5)}$ ${2S_{39}}^{(5)}$, ${2S_{40}}^{(5)}$ ${P_{67}}^{(5)}$
$2S_{48}$								
$2S_{49}$								
$2S_{51}$		$2S_{50}$	$2.6L_3$	$2.3L_{10}$				${2S_{58}}^{(5)}$
$2S_{52}$								
$2S_{53}$								

Table 7.5.22: Topological equivalences for the family **QsnSN(C)** *(cont.)*

Presented phase portrait	Identical under perturbations	Finite antisaddle focus	Finite antisaddle node–focus	Finite weak point	Disconnected parts	Possessing invariant curve (no separatrix)	Symmetry	Other reasons
$2S_{54}$								
$2S_{56}$		$2S_{55}$	$2.6L_4$	$2.3L_{11}$				$2S_{57}^{(5)}$
$2S_{59}$		$2S_{60}$	$2.6L_5$	$2.3L_{12}$				
$2S_{61}$								
$2S_{62}$								
$4S_1$	$4S_2$			$3.4L_1$				
$4S_3$								
$4S_6$	$4S_7$			$3.4L_2$				
$4S_8$	$4S_{10}$, $4S_{18}$, $4S_{23}$			$3.4L_4$, $3.4L_{11}$				
$4S_9$	$4S_{22}$			$3.4L_6$				
$4S_{13}$								
$4S_{15}$		$4S_{14}$	$4.6L_1$	$3.4L_8$				
$4S_{16}$	$4S_{17}$	$4S_{19}$, $4S_{21}$	$4.6L_2$, $4.6L_3$ P_{13}	$3.4L_3$, $3.4L_5$ $3.4L_9$, $3.4L_{10}$ P_{20}				
$4S_{20}$								
$4S_{25}$								
$4S_{26}$	$4S_{27}$			$3.4L_{12}$				

Table 7.5.23: Topological equivalences for the family **QsnSN(C)** *(cont.)*

Presented phase portrait	Identical under perturbations	Finite antisaddle focus	Finite antisaddle node–focus	Finite weak point	Disconnected parts	Possessing invariant curve (no separatrix)	Symmetry	Other reasons
$4S_{29}$	$4S_{30}$	$4S_{28}$	$4.6L_4$	$3.4L_{13}$				
$4S_{31}$	$4S_{41}$			$3.4L_{17}$				
$4S_{32}$	$4S_{40}$			$3.4L_{16}$				
$4S_{33}$	$4S_{39}$	$4S_{34}$, $4S_{35}$	$4.6L_5$, $4.6L_6$ P_{24}	$3.4L_{14}$, $3.4L_{15}$				
$4S_{36}$								
$4S_{42}$	$4S_{43}$			$3.4L_{18}$				
$4S_{44}$	$4S_{48}$	$4S_{49}$	$4.6L_7$			$4.4L_5$		
$4S_{51}$								
$5S_1$								
$5S_2$	$5S_{20}$, $5S_{21}$ $5.7L_4$					$4.5L_3$ ${P_{38}}^{(6)}$, ${P_{63}}^{(1)}$		
$5S_3$		$5S_4$	$5.6L_1$	$3.5L_1$				
$5S_5$					$5S_{34}$			
$5S_9$	$5S_8$, $5S_{10}$, $5S_{16}$ $5S_{18}$, $5S_{19}$ $5.7L_{10}$	$5S_7$, $5S_{15}$ $5S_{17}$ $5.7L_3$, $5.7L_6$ $5.7L_7$, $5.7L_{12}$ P_5	$5.6L_4$, $5.6L_5$ P_6, P_8	$3.5L_3$, $3.5L_4$ $3.5L_5$, $3.5L_6$ P_9	$5S_{24}$, $5S_{25}$ $5S_{31}$, $5S_{32}$	$4.5L_1$, $4.5L_2$		

Table 7.5.24: Topological equivalences for the family **QsnSN(C)** *(cont.)*

Presented phase portrait	Identical under perturbations	Finite antisaddle focus	Finite antisaddle node–focus	Finite weak point	Disconnected parts	Possessing invariant curve (no separatrix)	Symmetry	Other reasons
$5S_{12}$		$5S_{11}$	$5.6L_2$	$3.5L_7$				
$5S_{13}$		$5S_6$, $5S_{14}$	$5.6L_3$	$3.5L_2$				
$5S_{22}$								
$5S_{23}$								
$5S_{26}$								
$5S_{28}$	$5S_{29}$	$5S_{27}$, $5S_{30}$	$5.6L_6$, $5.6L_7$			$4.5L_4$		
$5S_{33}$								
$5S_{36}$		$5S_{35}$	$5.6L_8$	$3.5L_8$				
$7S_1$								
$7S_2$								
$7S_3$								
$7S_4$	$7S_5$			$3.7L_1$				
$7S_6$								
$7S_7$								
$7S_8$	$7S_{18}$	$7S_{19}$	$6.7L_3$	$3.7L_4$				
$7S_9$	$7S_{20}$	$7S_{21}$	$6.7L_4$	$3.7L_5$				
$7S_{10}$								
$7S_{15}$		$7S_{11}$, $7S_{13}$	$6.7L_1$	$3.7L_2$				
$7S_{16}$		$7S_{12}$, $7S_{14}$	$6.7L_2$	$3.7L_3$				

Table 7.5.25: Topological equivalences for the family **QsnSN(C)** *(cont.)*

Presented phase portrait	Identical under perturbations	Finite antisaddle focus	Finite antisaddle node–focus	Finite weak point	Disconnected parts	Possessing invariant curve (no separatrix)	Symmetry	Other reasons
$7S_{17}$								
$7S_{22}$				$3.7L_7$				
$7S_{23}$		$7S_{24}$, $7S_{25}$ $3.7L_6$	$6.7L_5$	$3.7L_8$, $3.7L_9$, $3.7L_{11}$ P_{14}, P_{16}				
$7S_{26}$								
$7S_{27}$								
$7S_{28}$	$7S_{30}$			$3.7L_{12}$				
$7S_{29}$				$3.7L_{10}$				
$7S_{31}$		$7S_{36}$		$3.7L_{12}$				
$7S_{32}$	$7S_{34}$			$3.7L_{13}$				
$7S_{33}$	$7S_{35}$			$3.7L_{14}$				
$7S_{37}$	$7S_{43}$	$7S_{48}$, $7S_{49}$	$6.7L_{10}$, $6.7L_{11}$ P_{28}	$3.7L_{16}$, $3.7L_{17}$				
$7S_{38}$		$7S_{39}$, $7S_{40}$	$6.7L_7$	$3.7L_{15}$				
$7S_{41}$								
$7S_{42}$								
$7S_{44}$		$7S_{46}$, $7S_{50}$	$6.7L_9$	$3.7L_{18}$				
$7S_{45}$		$7S_{47}$, $7S_{51}$	$6.7L_8$	$3.7L_{19}$				

Table 7.5.26: Topological equivalences for the family **QsnSN(C)** *(cont.)*

Presented phase portrait	Identical under perturbations	Finite antisaddle focus	Finite antisaddle node–focus	Finite weak point	Disconnected parts	Possessing invariant curve (no separatrix)	Symmetry	Other reasons
$7S_{52}$								
$7S_{53}$								
$7S_{55}$		$7S_{54}$	$6.7L_{12}$	$3.7L_{20}$				
$7S_{56}$								
$7S_{57}$								
$7S_{58}$								
$7S_{60}$		$7S_{59}$	$6.7L_{13}$	$3.7L_{21}$				
$7S_{61}$								
$7S_{62}$								
$7S_{63}$								
$7S_{64}$								
$7S_{65}$		$7S_{66}$		$3.7L_{22}$				
$7S_{67}$								
$7S_{68}$								
$7S_{69}$								
$7S_{70}$								
$7S_{71}$								
$7S_{72}$		$7S_{73}$	$6.7L_{14}$	$3.7L_{23}$				
$7S_{74}$								
$7S_{75}$								
$7S_{76}$								
$7S_{77}$								

Table 7.5.27: Topological equivalences for the family **QsnSN(C)** *(cont.)*

Presented phase portrait	Identical under perturbations	Finite antisaddle focus	Finite antisaddle node–focus	Finite weak point	Disconnected parts	Possessing invariant curve (no separatrix)	Symmetry	Other reasons
$7S_{78}$								
$7S_{79}$		$7S_{80}$	$6.7L_{15}$	$3.7L_{24}$				
$7S_{81}$								
$7S_{82}$								
$7S_{83}$								
$7S_{85}$		$7S_{84}$	$6.7L_{16}$	$3.7L_{25}$				
$10S_1$								
$1.1L_1$								
$1.1L_2$								
$1.1L_3$								
$1.1L_4$	$1.1L_5$					P_{47}		
$1.1L_6$								
$1.1L_7$	$1.1L_8$					P_{40}		
$1.2L_5$	$1.2L_6$					P_{66}		
$1.2L_7$								
$1.2L_8$	$1.2L_9$, $1.2L_{10}$							
$1.3L_2$					$1.3L_5$, $1.3L_7$, $1.3L_{16}$ P_{18}, P_{45}			
$1.4L_1$		$1.4L_2$		P_{19}		P_{10}		
$1.4L_3$								

Table 7.5.28: Topological equivalences for the family **QsnSN(C)** *(cont.)*

Presented phase portrait	Identical under perturbations	Finite antisaddle focus	Finite antisaddle node–focus	Finite weak point	Disconnected parts	Possessing invariant curve (no separatrix)	Symmetry	Other reasons
$1.4L_4$								
$1.4L_5$								
$1.4L_7$								$P_{44}{}^{(4)}$
$1.4L_8$								
$1.4L_{12}$								
$1.4L_{13}$								$P_{49}{}^{(4)}$
$1.4L_{14}$								
$1.5L_1$								
$1.5L_2$								
$1.5L_3$								
$1.5L_4$								
$1.5L_5$								
$1.5L_6$								
$1.5L_7$		$1.5L_8$	P_{56}	P_{54}				
$1.7L_1$								
$1.7L_2$								
$1.7L_3$								
$1.7L_4$								
$1.7L_5$								
$1.7L_6$								
$1.7L_7$		$1.7L_8$	P_{32}	P_{33}				
$1.7L_9$								
$1.7L_{18}$	$1.7L_{19}$			P_{37}				
$1.7L_{20}$								

Table 7.5.29: Topological equivalences for the family **QsnSN(C)** *(cont.)*

Presented phase portrait	Identical under perturbations	Finite antisaddle focus	Finite antisaddle node–focus	Finite weak point	Disconnected parts	Possessing invariant curve (no separatrix)	Symmetry	Other reasons
$1.7L_{21}$								
$1.7L_{27}$								
$1.7L_{28}$								
$1.7L_{29}$								
$1.7L_{30}$								
$1.7L_{31}$								$P_{51}{}^{(4)}$
$1.7L_{32}$								
$1.7L_{33}$								
$2.3L_1$								
$2.3L_2$								
$2.3L_3$								
$2.3L_4$	$2.3L_5$			P_{15}				
$2.3L_6$								
$2.3L_7$								
$2.4L_1$								
$2.4L_3$								
$2.4L_5$								
$2.4L_6$					$2.4L_8$			
$2.4L_7$								
$2.4L_9$								
$2.5L_1$							$2.5L_2$	
$2.5L_3$					$2.5L_9$			
$2.5L_4$					$2.5L_5$, $2.5L_6$ $2.5L_7$, $2.5L_8$ P_7, P_{35}	P_{11}		
$2.5L_{10}$								

Table 7.5.30: Topological equivalences for the family **QsnSN(C)** *(cont.)*

Presented phase portrait	Identical under perturbations	Finite antisaddle focus	Finite antisaddle node–focus	Finite weak point	Disconnected parts	Possessing invariant curve (no separatrix)	Symmetry	Other reasons
$2.5L_{11}$	$2.5L_{12}$, $2.5L_{14}$ P_{59}	$2.5L_{15}$	P_{62}	P_{61}				$2.5L_{16}{}^{(5)}$
$2.5L_{13}$								
$2.7L_1$					$2.7L_6$			
$2.7L_2$					$2.7L_{12}$			
$2.7L_3$					$2.7L_{13}$			
$2.7L_4$					$2.7L_{15}$			
$2.7L_5$					$2.7L_{14}$			
$2.7L_7$					$2.7L_8$			
$2.7L_9$					$2.7L_{10}$			
$2.7L_{11}$								
$2.7L_{16}$								
$2.7L_{17}$								
$2.7L_{18}$								
$2.7L_{19}$								
$2.7L_{20}$								
$2.8L_1$								
$2.8L_2$								
$2.8L_3$								
$4.4L_1$	$4.4L_2$			P_{17}				
$4.4L_3$	$4.4L_4$			P_{25}				
$4.7L_1$	$4.7L_2$			P_{21}				
$5.7L_2$	$5.7L_4$	$5.7L_5$	P_3	P_2	$5.7L_{13}$			
$5.7L_9$								

Table 7.5.31: Topological equivalences for the family **QsnSN(C)** *(cont.)*

Presented phase portrait	Identical under perturbations	Finite antisaddle focus	Finite antisaddle node–focus	Finite weak point	Disconnected parts	Possessing invariant curve (no separatrix)	Symmetry	Other reasons
$5.7L_{11}$								
$5.7L_{14}$								
$7.7L_1$	$7.7L_3$	$7.7L_2$	P_{27}	P_{29}	$5.7L_{13}$			
$7.7L_4$								
$7.7L_5$								
$7.7L_6$								
$7.7L_7$								
P_1								
P_4					P_{36}			
P_{22}								
P_{23}								
P_{26}								
P_{30}								
P_{31}								
P_{39}								
P_{41}								
P_{43}								
P_{50}								
P_{52}								
P_{57}								
P_{58}								
P_{60}								
P_{64}								
P_{65}								
P_{68}								

Chapter

8

The complete classification of quadratic differential systems with invariant hyperbolas

8.1 Introduction and statement of main results

Quadratic systems with an invariant algebraic curve have been studied by many authors. For example, Schlomiuk and Vulpe [52, 56] have studied quadratic systems with invariant straight lines, Qin Yuan-xum [48] has investigated the quadratic systems having an ellipse as limit cycle, Druzhkova [24] has presented the necessary and sufficient conditions for the existence and the uniqueness of an invariant algebraic curve of second degree in terms of the coefficients of quadratic systems and Cairó and Llibre [18] have studied the quadratic systems having invariant algebraic conics in order to investigate the Darboux integrability of such systems.

The motivation for studying the systems in the quadratic class is not only because of their usefulness in many applications but also for theoretical reasons, as discussed by Schlomiuk and Vulpe in the introduction of [52]. The study of nondegenerate quadratic systems could be done using normal forms and applying the invariant theory.

Here we consider quadratic differential systems, i.e. systems (1.4.1) with $m = 2$. We always assume that the polynomials P and Q are coprime. Otherwise, doing a rescaling of the time, systems (1.4.1) can be reduced to linear or constant systems. Quadratic systems under this assumption are

called *nondegenerate quadratic systems*.

Definition 1.4.1 of algebraic invariant curve will be very useful in this chapter since our purpose is to classify all nondegenerate quadratic systems possessing an invariant hyperbola.

The main goal of this chapter is to investigate nondegenerate quadratic systems having invariant hyperbolas and this study is done applying the invariant theory. More precisely, denoting by $\mathbf{QS_f}$ the class of all quadratic systems possessing a finite number of singularities (finite and infinite), in this chapter we provide necessary and sufficient conditions for a quadratic system in $\mathbf{QS_f}$ to have invariant hyperbolas. We also determine the invariant criteria which provide the number and multiplicity of such hyperbolas.

Definition 8.1.1. *We say that an invariant conic*

$$\Phi(x,y) = p + qx + ry + sx^2 + 2txy + uy^2 = 0,\ (s,t,u) \neq (0,0,0),\ (p,q,r,s,t,u) \in \mathbb{C}^6$$

*for a quadratic vector field X has **multiplicity** m, if there exists a sequence of real quadratic vector fields X_k converging to X, such that each X_k has m distinct (complex) invariant conics $\Phi_k^1 = 0, \ldots, \Phi_k^m = 0$, converging to $\Phi = 0$ as $k \to \infty$, and this does not occur for $m+1$. In the case when an invariant conic $\Phi(x,y) = 0$ has multiplicity one we call it **simple**.*

The main results of this chapter are stated in the following theorem. They can also be found in the paper of Oliveira, Rezende and Vulpe [44].

Theorem 8.1.2. **(*A*)** *The conditions $\eta \geq 0$, $M \neq 0$ and $\gamma_1 = \gamma_2 = 0$ are necessary for a quadratic system in the class $\mathbf{QS_f}$ to possess at least one invariant hyperbola.*

(*B*) *Assume that for a system in the class $\mathbf{QS_f}$ the condition $\gamma_1 = \gamma_2 = 0$ is satisfied.*

- **(B_1)** *If $\eta > 0$, then the necessary and sufficient conditions for this system to possess at least one invariant hyperbola are given in Figure 8.1, where we can also find the number and multiplicity of such hyperbolas.*
- **(B_2)** *In the case $\eta = 0$ and $M \neq 0$, the corresponding necessary and sufficient conditions for this system to possess at least one invariant hyperbola are given in Figure 8.2, where we can also find the number and multiplicity of such hyperbolas.*
- **(B_3)** *In the case of the existence of a family $(\mathscr{F})$ $(\mathscr{F} \in \{\mathscr{F}_1, \ldots, \mathscr{F}_5\})$ of invariant hyperbolas, we give necessary and sufficient conditions which characterize the geometric properties of this family (including the number of singularities) (see Remark 8.1.4).*

(*C*) *Figures 8.1 and 8.2 actually contain the global bifurcation diagram in the $12-$dimensional space of parameters of the systems belonging to family $\mathbf{QS_f}$, which possess at least one in-*

variant hyperbola. The corresponding conditions are given in terms of invariant polynomials with respect to the group of affine transformations and time rescaling.

Remark 8.1.3. *In the case of the existence of two hyperbolas, we denote them by $\mathscr{H}^p$, if their asymptotes are parallel, and by $\mathscr{H}$, if there exists at least one pair of nonparallel asymptotes. We denote by $\mathscr{H}_k$ ($k=2,3$) a hyperbola with multiplicity k; by $\mathscr{H}_2^p$ a double hyperbola, which, after perturbation, splits into two $\mathscr{H}^p$; and by $\mathscr{H}_3^p$ a triple hyperbola which splits into two $\mathscr{H}^p$ and one $\mathscr{H}$.*

Remark 8.1.4. *(i) Consider the three families $\Phi_s(x,y)=2s-r(x-y)+2xy=0$, $s\in\{-1,0,1\}$, $r\in\mathbb{R}$ of hyperbolas. These are three distinct families (see Figure 8.3) which we denote, respectively, by $\mathscr{F}_1$, $\mathscr{F}_2$ and $\mathscr{F}_3$. We observe that, for each one of the three families, any two hyperbolas have distinct parallel asymptotes.*

(ii) Consider the two families $\widetilde{\Phi}_s(x,y)=(4-sq)/2+qx+sy+2xy=0$, $s\in\{0,1\}$, ($q\in\mathbb{R}$) of hyperbolas. These families are distinct and we denote them, respectively, by $\mathscr{F}_4$, $\mathscr{F}_5$ (see Figure 8.4). We observe that, for each family, any two hyperbolas have only one common asymptote.

The invariants and comitants of differential equations used for proving our main result are obtained following the theory of algebraic invariants of polynomial differential systems developed by Sibirsky and his disciples which is discussed in Chapter 4.

8.1.1 The main invariants and comitants associated with invariant hyperbolas

Using the elements of the minimal polynomial basis given in Section 4.4, we construct the affine invariants, T−comitants and CT−comitants associated with invariant hyperbolas.

$$
\begin{aligned}
\gamma_1(a) =& A_1^2(3A_6+2A_7)-2A_6(A_8+A_{12}),\\
\gamma_2(a) =& 9A_1^2A_2(23252A_3+23689A_4)-1440A_2A_5(3A_{10}+13A_{11})-1280A_{13}(2A_{17}+A_{18}\\
&+23A_{19}-4A_{20})-320A_{24}(50A_8+3A_{10}+45A_{11}-18A_{12})+120A_1A_6(6718A_8\\
&+4033A_9+3542A_{11}+2786A_{12})+30A_1A_{15}(14980A_3-2029A_4-48266A_5)\\
&-30A_1A_7(76626A_1^2-15173A_8+11797A_{10}+16427A_{11}-30153A_{12})\\
&+8A_2A_7(75515A_6-32954A_7)+2A_2A_3(33057A_8-98759A_{12})-60480A_1^2A_{24}\\
&+A_2A_4(68605A_8-131816A_9+131073A_{10}+129953A_{11})-2A_2(141267A_6^2\\
&-208741A_5A_{12}+3200A_2A_{13}),
\end{aligned}
$$

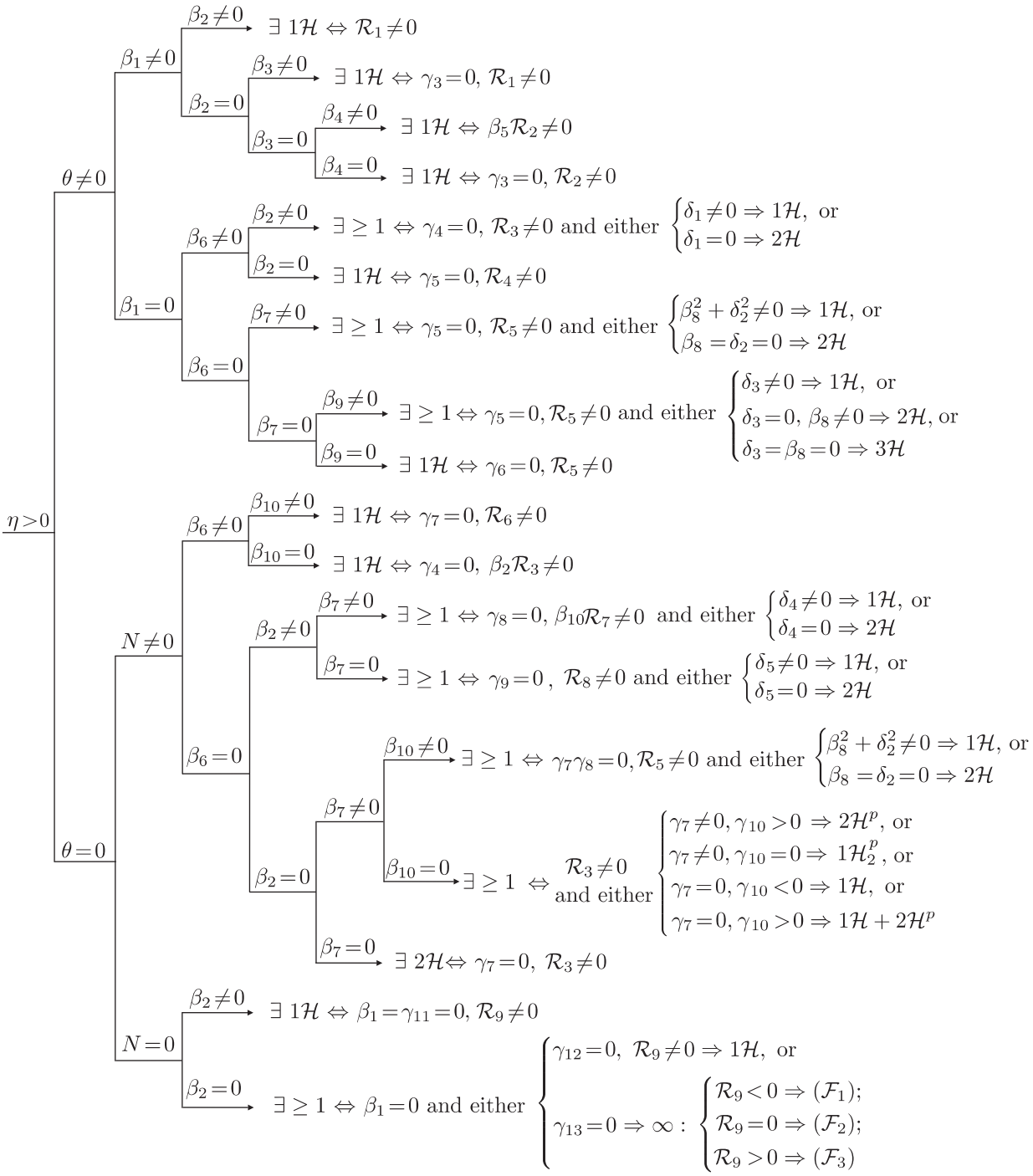

Figure 8.1: The existence of invariant hyperbola: the case $\eta>0$

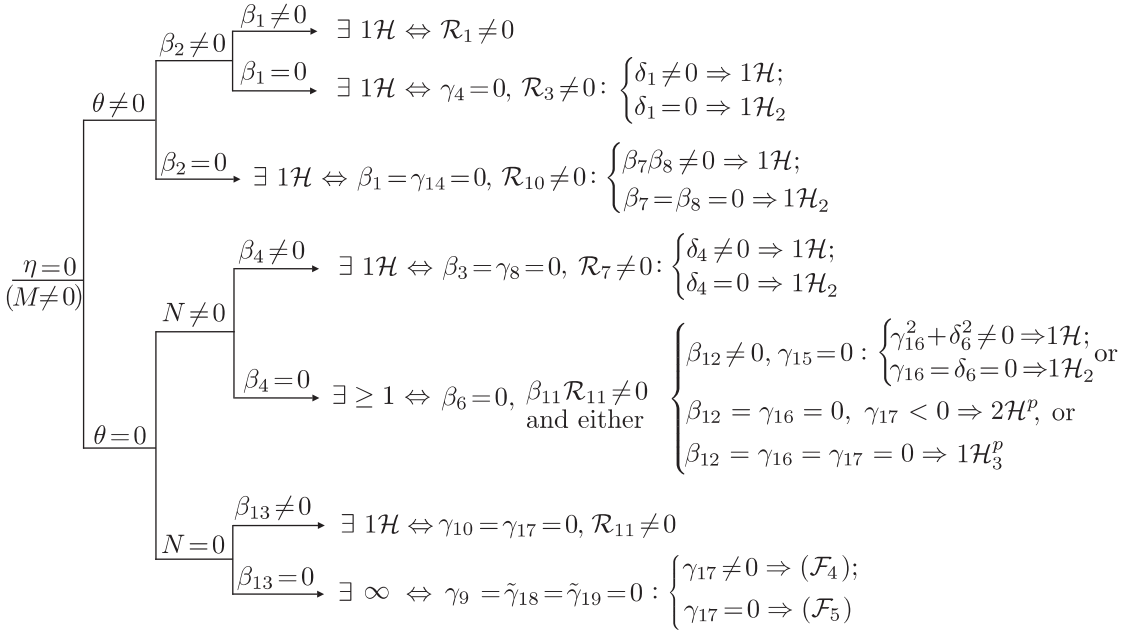

Figure 8.2: The existence of invariant hyperbola: the case $\eta=0$

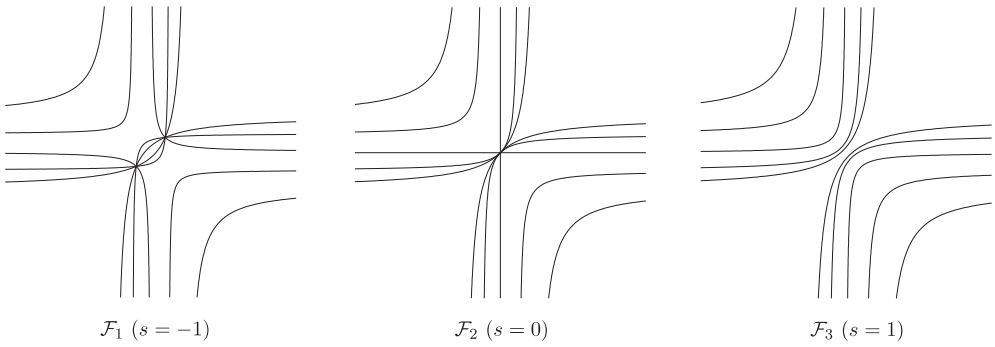

Figure 8.3: The families of invariant hyperbolas $\Phi_s(x,y)=2s-r(x-y)+2xy=0$ ($r\in\mathbb{R}$, $s\in\{-1,0,1\}$)

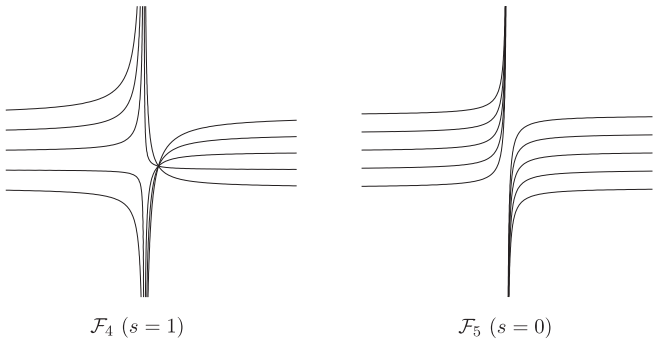

Figure 8.4: The families of invariant hyperbolas $\widetilde{\Phi}_s(x,y)=(4-sq)/2+qx+sy+2xy=0$ ($q\in\mathbb{R}$, $s\in\{0,1\}$)

$$\gamma_3(a) = 843696A_5A_6A_{10} + A_1(-27(689078A_8 + 419172A_9 - 2907149A_{10} - 2621619A_{11})A_{13} - 26(21057A_3A_{23} + 49005A_4A_{23} - 166774A_3A_{24} + 115641A_4A_{24})).$$

$$\gamma_4(a) = -9A_4^2(14A_{17} + A_{21}) + A_5^2(-560A_{17} - 518A_{18} + 881A_{19} - 28A_{20} + 509A_{21}) - A_4(171A_8^2 + 3A_8(367A_9 - 107A_{10}) + 4(99A_9^2 + 93A_9A_{11} + A_5(-63A_{18} - 69A_{19} + 7A_{20} + 24A_{21}))) + 72A_{23}A_{24},$$

$$\gamma_5(a) = -488A_2^3A_4 + A_2(12(4468A_8^2 + 32A_9^2 - 915A_{10}^2 + 320A_9A_{11} - 3898A_{10}A_{11} - 3331A_{11}^2 + 2A_8(78A_9 + 199A_{10} + 2433A_{11})) + 2A_5(25488A_{18} - 60259A_{19} - 16824A_{21}) + 779A_4A_{21}) + 4(7380A_{10}A_{31} - 24(A_{10} + 41A_{11})A_{33} + A_8(33453A_{31} + 19588A_{32} - 468A_{33} - 19120A_{34}) + 96A_9(-A_{33} + A_{34}) + 556A_4A_{41} - A_5(27773A_{38} + 41538A_{39} - 2304A_{41} + 5544A_{42})),$$

$$\gamma_6(a) = 2A_{20} - 33A_{21},$$

$$\gamma_7(a) = A_1(64A_3 - 541A_4)A_7 + 86A_8A_{13} + 128A_9A_{13} - 54A_{10}A_{13} - 128A_3A_{22} + 256A_5A_{22} + 101A_3A_{24} - 27A_4A_{24},$$

$$\gamma_8(a) = 3063A_4A_9^2 - 42A_7^2(304A_8 + 43(A_9 - 11A_{10})) - 6A_3A_9(159A_8 + 28A_9 + 409A_{10}) + 2100A_2A_9A_{13} + 3150A_2A_7A_{16} + 24A_3^2(34A_{19} - 11A_{20}) + 840A_5^2A_{21} - 932A_2A_3A_{22} + 525A_2A_4A_{22} + 844A_{22}^2 - 630A_{13}A_{33},$$

$$\gamma_9(a) = 2A_8 - 6A_9 + A_{10},$$

$$\gamma_{10}(a) = 3A_8 + A_{11},$$

$$\gamma_{11}(a) = -5A_7A_8 + A_7A_9 + 10A_3A_{14},$$

$$\gamma_{12}(a) = 25A_2^2A_3 + 18A_{12}^2,$$

$$\gamma_{13}(a) = A_2,$$

$$\gamma_{14}(a) = A_2A_4 + 18A_2A_5 - 236A_{23} + 188A_{24},$$

$$\gamma_{15}(a,x,y) = 144T_1T_7^2 - T_1^3(T_{12} + 2T_{13}) - 4(T_9T_{11} + 4T_7T_{15} + 50T_3T_{23} + 2T_4T_{23} + 2T_3T_{24} + 4T_4T_{24}),$$

$$\gamma_{16}(a,x,y) = T_{15},$$

$$\gamma_{17}(a,x,y) = T_{11},$$

$$\tilde{\gamma}_{18}(a,x,y) = C_1(C_2,C_2)^{(2)} - 2C_2(C_1,C_2)^{(2)},$$

$$\tilde{\gamma}_{19}(a,x,y) = D_1(C_1,C_2)^{(2)} - ((C_2,C_2)^{(2)},C_0)^{(1)},$$

$$\delta_1(a) = 9A_8 + 31A_9 + 6A_{10},$$

$$\delta_2(a) = 41A_8 + 44A_9 + 32A_{10},$$

$$\delta_3(a) = 3A_{19} - 4A_{17},$$

$$\delta_4(a) = -5A_2A_3 + 3A_2A_4 + A_{22},$$

$$\delta_5(a) = 62A_8 + 102A_9 - 125A_{10},$$

$$\delta_6(a) = 2T_3 + 3T_4,$$

$$\beta_1(a) = 3A_1^2 - 2A_8 - 2A_{12},$$

$$\beta_2(a) = 2A_7 - 9A_6,$$

$$\beta_3(a) = A_6,$$

$$\beta_4(a) = -5A_4 + 8A_5,$$

$$\beta_5(a) = A_4,$$

$$\beta_6(a) = A_1,$$

$$\beta_7(a) = 8A_3 - 3A_4 - 4A_5,$$

$$\beta_8(a) = 24A_3 + 11A_4 + 20A_5,$$

$$\beta_9(a) = -8A_3 + 11A_4 + 4A_5,$$

$$\beta_{10}(a) = 8A_3 + 27A_4 - 54A_5,$$

$$\beta_{11}(a,x,y) = T_1^2 - 20T_3 - 8T_4,$$

$$\beta_{12}(a,x,y) = T_1,$$

$$\beta_{13}(a,x,y) = T_3,$$

$$\mathscr{R}_1(a) = -2A_7(12A_1^2 + A_8 + A_{12}) + 5A_6(A_{10} + A_{11}) - 2A_1(A_{23} - A_{24}) + 2A_5(A_{14} + A_{15}) + A_6(9A_8 + 7A_{12}),$$

$$\mathscr{R}_2(a) = A_8 + A_9 - 2A_{10},$$

$$\mathscr{R}_3(a) = A_9,$$

$$\mathscr{R}_4(a) = -3A_1^2A_{11} + 4A_4A_{19},$$

$$\mathscr{R}_5(a,x,y) = (2C_0(T_8 - 8T_9 - 2D_2^2) + C_1(6T_7 - T_6) - (C_1,T_5)^{(1)} + 6D_1(C_1D_2 - T_5) - 9D_1^2C_2),$$

$$\mathscr{R}_6(a) = -213A_2A_6 + A_1(2057A_8 - 1264A_9 + 677A_{10} + 1107A_{12}) + 746(A_{27} - A_{28}),$$

$$\mathscr{R}_7(a) = -6A_7^2 - A_4A_8 + 2A_3A_9 - 5A_4A_9 + 4A_4A_{10} - 2A_2A_{13},$$

$$\mathscr{R}_8(a) = A_{10},$$

$$\mathscr{R}_9(a) = -5A_8 + 3A_9,$$

$$\mathscr{R}_{10}(a) = 7A_8 + 5A_{10} + 11A_{11},$$

$$\mathscr{R}_{11}(a,x,y) = T_{16}.$$

8.1.2 Preliminary results involving the use of polynomial invariants

Considering the GL−comitant $C_2(a,x,y) = y\,p_2(a,x,y) - x\,q_2(a,x,y)$ as a cubic binary form of x and y, we calculate

$$\eta(a) = \text{Discrim}[C_2,\xi], \quad \widetilde{M}(a,x,y) = \text{Hessian}[C_2],$$

where $\xi = y/x$ or $\xi = x/y$. Following [57], we have the next assertion.

Lemma 8.1.5. *The number of distinct roots (real and imaginary) of the polynomial $C_2(a,x,y) \not\equiv 0$ is determined by the following conditions:*

(i) 3 *real, if* $\eta > 0$*;*

(ii) 1 *real and* 2 *imaginary, if* $\eta < 0$*;*

(iii) 2 *real* (1 *double), if* $\eta = 0$ *and* $\widetilde{M} \neq 0$*;*

(iv) 1 *real (triple), if* $\eta = \widetilde{M} = 0$.

Moreover, for each one of these cases the quadratic systems (1.5.1) *can be brought via a linear transformation to one of the following canonical systems* $(\mathbf{S}_I) - (\mathbf{S}_{IV})$*:*

$$\begin{cases} \dot{x} &= a + cx + dy + gx^2 + (h-1)xy, \\ \dot{y} &= b + ex + fy + (g-1)xy + hy^2; \end{cases} \qquad (\mathbf{S}_I)$$

$$\begin{cases} \dot{x} &= a + cx + dy + gx^2 + (h+1)xy, \\ \dot{y} &= b + ex + fy - x^2 + gxy + hy^2; \end{cases} \qquad (\mathbf{S}_{II})$$

$$\begin{cases} \dot{x} &= a + cx + dy + gx^2 + hxy, \\ \dot{y} &= b + ex + fy + (g-1)xy + hy^2; \end{cases} \qquad (\mathbf{S}_{III})$$

$$\begin{cases} \dot{x} &= a + cx + dy + gx^2 + hxy, \\ \dot{y} &= b + ex + fy - x^2 + gxy + hy^2. \end{cases} \qquad (\mathbf{S}_{IV})$$

Proof. We consider the polynomial $C_2 = y\,p_2(x,y) - x\,q_2(x,y) \not\equiv 0$ as a cubic binary form. It is well–known that there exists $g \in \text{GL}(2,\mathbb{R})$, $g(x,y) = (u,v)$, such that the transformed binary form $g\,C_2(a,x,y) = C_2(a,g^{-1}(u,v))$ is one of the following 4 canonical forms:

$$(i)\ xy(x-y); \quad (ii)\ x(x^2+y^2); \quad (iii)\ x^2y; \quad (iv)\ x^3.$$

We note that each of such canonical forms corresponds to one of the cases enumerated in the statement of Lemma 8.1.5. On the other hand, applying the same transformation g to an initial

system (1.5.1) and calculating its polynomial $C_2(a(g),u,v)$ for the transformed system, Definition 4.4.1 implies the following relation:

$$C_2(a(g),u,v) = \det(g) C_2(a,x,y) = \det(g) C_2(a,g^{-1}(u,v)) = \lambda C_2(a,g^{-1}(u,v)),$$

where we may consider $\lambda = 1$ (via a time rescaling). Therefore, considering the expression for $C_2(x,y) = y\,p_2(x,y) - x\,q_2(x,y)$, we construct the canonical forms of quadratic homogeneous systems having their polynomials C_2 the indicated canonical forms $(i)-(iv)$ and we arrive at the systems $(\mathbf{S}_I)-(\mathbf{S}_{IV})$, respectively. This completes the proof of Lemma 8.1.5. ∎

Lemma 8.1.6. *If a quadratic system* (1.5.1) *possesses a nonparabolic irreducible conic, then the conditions* $\gamma_1 = \gamma_2 = 0$ *hold.*

Proof. According to [19], a system (1.5.1) possessing a second order nonparabolic irreducible curve as an algebraic particular integral can be written in the form

$$\dot{x} = a\,\Phi(x,y) + \Phi'_y(gx+hy+k), \quad \dot{y} = b\,\Phi(x,y) - \Phi'_x(gx+hy+k),$$

where a,b,g,h,k are real parameters and $\Phi(x,y)$ is the conic

$$\Phi(x,y) \equiv p + qx + ry + sx^2 + 2txy + uy^2 = 0. \tag{8.1.1}$$

A straightforward calculation gives $\gamma_1 = \gamma_2 = 0$ for the above systems and this completes the proof of the lemma. ∎

Assume that a conic (8.1.1) is an affine algebraic invariant curve for quadratic systems (1.5.1), which we rewrite in the form:

$$\begin{aligned} \dot{x} &= a + cx + dy + gx^2 + 2hxy + ky^2 \equiv P(x,y), \\ \dot{y} &= b + ex + fy + lx^2 + 2mxy + ny^2 \equiv Q(x,y). \end{aligned} \tag{8.1.2}$$

Remark 8.1.7. *Following [38], we construct the determinant*

$$\Delta = \begin{vmatrix} s & t & q/2 \\ t & u & r/2 \\ q/2 & r/2 & p \end{vmatrix},$$

associated with the conic (8.1.1)*. By [38], this conic is nondegenerate (i.e. it could not be presented in* $\mathbb{C}[x,y]$ *as a product of lines) if, and only if,* $\Delta \neq 0$.

In order to detect if an invariant conic (8.1.1) of a system (8.1.2) has the multiplicity greater than one, we shall use the notion of *k-th extactic curve* $\mathscr{E}_k(X)$ of the vector field X associated with systems (8.1.2). This curve is defined in the paper [20, Definition 5.1] as follows:

$$\mathscr{E}_k(X) = \det \begin{pmatrix} v_1 & v_2 & \dots & v_\ell \\ X(v_1) & X(v_2) & \dots & X(v_\ell) \\ \cdot & \cdot & & \cdot \\ \cdot & \cdot & \dots & \cdot \\ \cdot & \cdot & & \cdot \\ X^{\ell-1}(v_1) & X^{\ell-1}(v_2) & \dots & X^{\ell-1}(v_\ell) \end{pmatrix},$$

where $v_1, v_2, \dots, v_l$ are the basis of $\mathbb{C}_n[x,y]$, the $\mathbb{C}-$vector space of polynomials in $\mathbb{C}_n[x,y]$ and $\ell = (k+1)(k+2)/2$. Here $X^0(v_i) = v_i$ and $X^j(v_1) = X(X^{j-1}(v_1))$.

Considering Definition 8.1.1 of multiplicity of an invariant curve and according to [20], the following statement holds:

Lemma 8.1.8. *If an invariant curve* $\Phi(x,y) = 0$ *of degree* k *has multiplicity* m*, then* $\Phi(x,y)^m$ *divides* $\mathscr{E}_k(X)$.

We shall apply Lemma 8.1.8 in order to detect additional conditions for a conic to be multiple.

According to Definition 1.4.1 of invariant curve (see page 14) and considering the cofactor $K = Ux + Vy + W \in \mathbb{R}[x,y]$, the following identity holds:

$$\frac{\partial \Phi}{\partial x} P(x,y) + \frac{\partial \Phi}{\partial y} Q(x,y) = \Phi(x,y)(Ux + Vy + W).$$

This identity yields a system of 10 equations for determining the 9 unknown parameters p, q, r, s, t, u, U, V, W:

$$\begin{aligned} Eq_1 &\equiv s(2g - U) + 2\ell t = 0, \\ Eq_2 &\equiv 2t(g + 2m - U) + s(4h - V) + 2\ell u = 0, \\ Eq_3 &\equiv 2t(2h + n - V) + u(4m - U) + 2ks = 0, \\ Eq_4 &\equiv u(2n - V) + 2kt = 0, \\ Eq_5 &\equiv q(g - U) + s(2c - W) + 2et + \ell r = 0, \end{aligned} \tag{8.1.3}$$

$$\begin{aligned}
Eq_6 &\equiv r(2m-U)+q(2h-V)+2t(c+f-W)+2(ds+eu)=0,\\
Eq_7 &\equiv r(n-V)+u(2f-W)+2dt+kq=0,\\
Eq_8 &\equiv q(c-W)+2(as+bt)+er-pU=0,\\
Eq_9 &\equiv r(f-W)+2(bu+at)+dq-pV=0,\\
Eq_{10} &\equiv aq+br-pW=0.
\end{aligned} \tag{8.1.4}$$

8.2 The proof of the Main Theorem

Assuming that a quadratic system (8.1.2) in $\mathbf{QS_f}$ has an invariant hyperbola (8.1.1), we conclude that this system must possess at least two real distinct infinite singularities. So, according to Lemmas 8.1.5 and 8.1.6, the conditions $\eta \geq 0$, $\widetilde{M} \neq 0$ and $\gamma_1 = \gamma_2 = 0$ have to be fulfilled.

In what follows, supposing that the conditions $\gamma_1 = \gamma_2 = 0$ hold, we shall examine two families of quadratic systems (8.1.2): systems with three real distinct infinite singularities (corresponding to the condition $\eta > 0$) and systems with two real distinct infinite singularities (corresponding to the conditions $\eta = 0$ and $\widetilde{M} \neq 0$).

8.2.1 Systems with three real infinite singularities and $\theta \neq 0$

In this case, according to Lemma 8.1.5, systems (8.1.2) could be brought via a linear transformation to the following family of systems:

$$\begin{aligned}
\dot{x} &= a+cx+dy+gx^2+(h-1)xy,\\
\dot{y} &= b+ex+fy+(g-1)xy+hy^2.
\end{aligned} \tag{8.2.1}$$

For this systems we calculate

$$C_2(x,y)=xy(x-y),\quad \theta=-(g-1)(h-1)(g+h)/2 \tag{8.2.2}$$

and we shall prove the next lemma.

Lemma 8.2.1. *Assume that for a system* (8.2.1) *the conditions* $\theta \neq 0$ *and* $\gamma_1 = 0$ *hold. Then, this system could be brought via an affine transformation to the for*

$$\dot{x}=a+cx+gx^2+(h-1)xy,\quad \dot{y}=b-cy+(g-1)xy+hy^2. \tag{8.2.3}$$

Proof. Since $\theta \neq 0$, the condition $(g-1)(h-1)(g+h) \neq 0$ holds and, due to a translation, we may assume $d = e = 0$ for systems (8.2.1). Then, we calculate

$$\gamma_1 = \frac{1}{64}(g-1)^2(h-1)^2\mathscr{D}_1\mathscr{D}_2\mathscr{D}_3,$$

where

$$\mathscr{D}_1 = c + f, \;\; \mathscr{D}_2 = c(g+4h-1) + f(1+g-2h),$$
$$\mathscr{D}_3 = c(1-2g+h) + f(4g+h-1).$$

So, due to $\theta \neq 0$ (i.e. $(g-1)(h-1) \neq 0$), the condition $\gamma_1 = 0$ is equivalent to $\mathscr{D}_1\mathscr{D}_2\mathscr{D}_3 = 0$. We claim that, without loss of generality, we may assume $\mathscr{D}_1 = c + f = 0$, as the other cases could be brought to this one via an affine transformation.

Indeed, assume first $\mathscr{D}_1 \neq 0$ and $\mathscr{D}_2 = 0$. Then, as $g + h \neq 0$ (due to $\theta \neq 0$), we apply to systems (8.2.1) with $d = e = 0$ the affine transformation

$$x' = y - x - (c-f)/(g+h), \quad y' = -x \tag{8.2.4}$$

and we get the systems

$$\dot{x'} = a' + c'x' + g'x'^2 + (h'-1)x'y', \quad \dot{y'} = b' + f'y' + (g'-1)x'y' + h'y'^2. \tag{8.2.5}$$

These systems have the following new parameters:

$$\begin{gathered} a' = \left[c^2h - f^2g + cf(g-h) - (a-b)(g+h)^2\right]/(g+h)^2, \\ b' = -a, \quad c' = (cg - 2fg - ch)/(g+h), \\ f' = (c - f - cg + 2fg + fh)/(g+h), \quad g' = h, \quad h' = 1 - g - h. \end{gathered} \tag{8.2.6}$$

A straightforward computation gives

$$\mathscr{D}_1' = c' + f' = \left[c(g+4h-1) + f(1+g-2h)\right]/(g+h) = \mathscr{D}_2/(g+h) = 0$$

and, hence, we replace the condition $\mathscr{D}_2 = 0$ by $\mathscr{D}_1 = 0$ via an affine transformation.

Suppose now $\mathscr{D}_1 \neq 0$ and $\mathscr{D}_3 = 0$. Then, we apply to systems (8.2.1) the affine transformation

$$x'' = -y, \quad y'' = x - y + (c-f)/(g+h)$$

and we get the systems

$$\dot{x''} = a'' + c''x'' + g''x''^2 + (h'' - 1)x''y'', \quad \dot{y''} = b'' + f''y'' + (g'' - 1)x''y'' + h''y''^2,$$

having the following new parameters:

$$a'' = -b, \quad b'' = \left[f^2 g - c^2 h + cf(-g + h) + (a - b)(g + h)^2\right]/(g + h)^2,$$
$$c'' = (c - f - cg + 2fg + fh)/(g + h),$$
$$f'' = (cg - 2fg - ch)/(g + h), \quad g'' = 1 - g - h, \quad h'' = g.$$

We calculate

$$\mathscr{D}_1'' = c'' + f'' = \left[c(1 - 2g + h) + f(4g + h - 1)\right]/(g + h) = \mathscr{D}_3/(g + h) = 0.$$

Thus, our claim is proved and this completes the proof of the lemma. ∎

Lemma 8.2.2. *A system* (8.2.3) *possesses an invariant hyperbola of the indicated form if, and only if, the respective conditions are satisfied:*

I. $\Phi(x, y) = p + qx + ry + 2xy \;\Leftrightarrow\; \mathscr{B}_1 \equiv b(2h - 1) - a(2g - 1) = 0,\ (2h - 1)^2 + (2g - 1)^2 \neq 0,\ a^2 + b^2 \neq 0;$

II. $\Phi(x, y) = p + qx + ry + 2x(x - y) \;\Leftrightarrow$ *either*

(i) $c = 0,\ \mathscr{B}_2 \equiv b(1 - 2h) + 2a(g + 2h - 1) = 0,\ (2h - 1)^2 + (g + 2h - 1)^2 \neq 0,\ a^2 + b^2 \neq 0;$
(ii) $h = 1/3,\ \mathscr{B}_2' \equiv (1 + 3g)^2(b - 2a + 6ag) + 6c^2(1 - 3g) = 0,\ a \neq 0;$

III. $\Phi(x, y) = p + qx + ry + 2y(x - y) \;\Leftrightarrow$ *either*

(i) $c = 0,\ \mathscr{B}_3 \equiv a(1 - 2g) + 2b(2g + h - 1) = 0,\ (2g - 1)^2 + (2g + h - 1)^2 \neq 0,\ a^2 + b^2 \neq 0;$
(ii) $g = 1/3,\ \mathscr{B}_3' \equiv (1 + 3h)^2(a - 2b + 6bh) + 6c^2(1 - 3h) = 0,\ b \neq 0.$

Proof. Since for systems (8.2.3) we have $C_2 = xy(x - y)$ (i.e. the infinite singularities are located at the "ends" of the lines $x = 0$, $y = 0$ and $x - y = 0$), it is clear that if a hyperbola is invariant for these systems, then its homogeneous quadratic part has one of the following forms: $(i)\ kxy$, $(ii)\ kx(x - y)$, $(iii)\ ky(x - y)$, where k is a real nonzero constant. Obviously we may assume $k = 2$ (otherwise, instead of hyperbola (8.1.1), we could consider $2\Phi(x, y)/k = 0$).

Considering equations (8.1.3), we examine each one of the above mentioned possibilities.

(i) $\Phi(x,y) = p + qx + ry + 2xy$: in this case we obtain

$$t = 1,\ q = r = s = u = 0,\ U = 2g - 1,\ V = 2h - 1,\ W = 0,$$
$$Eq_8 = p(1-2g) + 2b,\ \ Eq_9 = p(1-2h) + 2a,$$
$$Eq_1 = Eq_2 = Eq_3 = Eq_4 = Eq_5 = Eq_6 = Eq_7 = Eq_{10} = 0.$$

Calculating the resultant of the nonvanishing equations with respect to the parameter p, we obtain

$$\mathrm{Res}_p(Eq_8, Eq_9) = a(1-2g) + b(2h-1) = \mathscr{B}_1.$$

So, if $(2h-1)^2 + (2g-1)^2 \neq 0$, then the hyperbola exists if, and only if, $\mathscr{B}_1 = 0$. We may assume $2h - 1 \neq 0$, otherwise the change $(x,y,a,b,c,g,h) \mapsto (y,x,b,a,-c,h,g)$ (which preserves systems (8.2.3)) could be applied. Then, we get

$$p = 2a/(2h-1),\ \ b = a(2g-1)/(2h-1),\ \ \Phi(x,y) = \frac{2a}{2h-1} + 2xy = 0$$

and, clearly, for the irreducibility of the hyperbola, the condition $a^2 + b^2 \neq 0$ must hold. This completes the proof of the statement **I.** of the lemma.

(ii) $\Phi(x,y) = p + qx + ry + 2x(x-y)$: since $g + h \neq 0$ (due to $\theta \neq 0$), we obtain

$$s = 2,\ t = -1,\ r = u = 0,\ q = 4c/(g+h),\ U = 2g,\ V = 2h - 1,\ W = -hq/2,$$
$$Eq_8 = 4a - 2b - 2gp + 4c^2(g-h)/(g+h)^2,$$
$$Eq_9 = p(1-2h) - 2a,\quad Eq_{10} = 2c(2a - hp)/(g+h),$$
$$Eq_1 = Eq_2 = Eq_3 = Eq_4 = Eq_5 = Eq_6 = Eq_7 = 0.$$

1) Assume first $c \neq 0$. Then, considering equations $Eq_9 = 0$ and $Eq_{10} = 0$, we obtain $p(3h-1) = 0$. Taking into account the relations above, we get the hyperbola

$$\Phi(x,y) = p + 4cx/(g+h) + 2x(x-y) = 0$$

which evidently is degenerate if $p = 0$. So, $p \neq 0$ and this implies $h = 1/3$. Then, from equation $Eq_9 = 0$, we obtain $p = 6a$. Since $\theta = (g-1)(3g+1)/9 \neq 0$, we have

$$Eq_9 = Eq_{10} = 0,\ \ Eq_8 = -2\mathscr{B}_2'/(3g+1)^2.$$

So, equation $Eq_8 = 0$ gives $\mathscr{B}_2' = 0$ and then systems (8.2.3) with $h = 1/3$ possess the hyperbola

$$\Phi(x,y) = 6a + \frac{12c}{3g+1}x + 2x(x-y) = 0,$$

which is nondegenerate if, and only if, $a \neq 0$.

2) Suppose now $c = 0$. In this case, it remains only two nonvanishing equations:

$$Eq_8 = 4a - 2b - 2gp = 0, \quad Eq_9 = p(1-2h) - 2a = 0.$$

Calculating the resultant of these equations with respect to the parameter p, we obtain

$$\mathrm{Res}_p(Eq_8, Eq_9) = b(1-2h) + 2a(g+2h-1) = \mathscr{B}_2.$$

If $(1-2h)^2 + (g+2h-1)^2 \neq 0$ (which is equivalent to $(1-2h)^2 + g^2 \neq 0$), then the condition $\mathscr{B}_2' = 0$ is necessary and sufficient for a system (8.2.3) with $c = 0$ to possess the invariant hyperbola

$$\Phi(x,y) = p + 2x(x-y) = 0,$$

where p is the parameter determined from equation $Eq_9 = 0$ (if $2h - 1 \neq 0$), or $Eq_8 = 0$ (if $g \neq 0$). We observe that the hyperbola is nondegenerate if, and only if, $p \neq 0$ which, due to the mentioned equations, is equivalent to $a^2 + b^2 \neq 0$.

Thus the statement **II.** of the lemma is proved.

(iii) $\Phi(x,y) = p + qx + ry + 2y(x-y)$: we observe that, due to the change $(x,y,a,b,c,g,h) \mapsto (y,x,b,a,-c,h,g)$ (which preserves systems (8.2.3)), this case could be brought to the previous one and, hence, the conditions could be constructed directly applying this change. This completes the proof of Lemma 8.2.2. ∎

In what follows the next remark will be useful.

Remark 8.2.3. *Consider systems* (8.2.3). *(i) The change* $(x,y,a,b,c,g,h) \mapsto (y,x,b,a,-c,h,g)$ *which preserves these systems replaces the parameter* g *by* h *and* h *by* g. *(ii) Moreover, if* $c = 0$, *then having the relation* $(2h-1)(2g-1)(1-2g-2h) = 0$ *(respectively,* $(4h-1)(4g-1)(3-4g-4h) = 0$*) due to a change we may assume* $2h - 1 = 0$ *(respectively,* $4h - 1 = 0$*).*

To prove the statement *(ii)* it is sufficient to observe that, in the case $2g - 1 = 0$ (respectively, $4g - 1 = 0$), we could apply the change given in the statement *(i)* (with $c = 0$), whereas, in the case

$1-2g-2h=0$ (respectively, $3-4g-4h=0$), we apply the change

$$(x,y,a,b,g,h)\mapsto(y-x,-x,b-a,-a,h,1-g-h),$$

which conserves systems (8.2.3) with $c=0$.

Next, we determine the invariant criteria which are equivalent to the conditions given by Lemma 8.2.2.

Lemma 8.2.4. *Assume that for a quadratic system* (8.1.2) *the conditions* $\eta>0$, $\theta\neq 0$ *and* $\gamma_1=\gamma_2=0$ *hold. Then, this system possesses at least one invariant hyperbola if, and only if, one of the following sets of the conditions are satisfied:*

(i) If $\beta_1\neq 0$ *then either*

$(i.1)$ $\beta_2\neq 0$, $\mathscr{R}_1\neq 0$;

$(i.2)$ $\beta_2=0$, $\beta_3\neq 0$, $\gamma_3=0$, $\mathscr{R}_1\neq 0$;

$(i.3)$ $\beta_2=\beta_3=0$, $\beta_4\beta_5\mathscr{R}_2\neq 0$;

$(i.4)$ $\beta_2=\beta_3=\beta_4=0$, $\gamma_3=0$,$\mathscr{R}_2\neq 0$;

(ii) If $\beta_1=0$ *then either*

$(ii.1)$ $\beta_6\neq 0$, $\beta_2\neq 0$, $\gamma_4=0$, $\mathscr{R}_3\neq 0$;

$(ii.2)$ $\beta_6\neq 0$, $\beta_2=0$, $\gamma_5=0$, $\mathscr{R}_4\neq 0$;

$(ii.3)$ $\beta_6=0$, $\beta_7\neq 0$, $\gamma_5=0$, $\mathscr{R}_5\neq 0$;

$(ii.4)$ $\beta_6=0$, $\beta_7=0$, $\beta_9\neq 0$, $\gamma_5=0$, $\mathscr{R}_5\neq 0$;

$(ii.5)$ $\beta_6=0$, $\beta_7=0$, $\beta_9=0$, $\gamma_6=0$, $\mathscr{R}_5\neq 0$.

Proof. Assume that for a quadratic system (8.1.2) the conditions $\eta>0$, $\theta\neq 0$ and $\gamma_1=0$ are fulfilled. According to Lemma 8.2.1, due to an affine transformation and time rescaling, this system can be brought to the canonical form (8.2.3), for which we calculate

$$\begin{aligned}
\gamma_2&=-1575c^2(g-1)^2(h-1)^2(g+h)(3g-1)(3h-1)(3g+3h-4)\mathscr{B}_1,\\
\beta_1&=-c^2(g-1)(h-1)(3g-1)(3h-1)/4,\\
\beta_2&=-c(g-h)(3g+3h-4)/2.
\end{aligned}\tag{8.2.7}$$

The case $\beta_1\neq 0$

According to Lemma 8.1.6, the condition $\gamma_2=0$ is necessary for the existence of an invariant hyperbola. Since $\theta\beta_1\neq 0$, the condition $\gamma_2=0$ is equivalent to $(3g+3h-4)\mathscr{B}_1=0$.

The subcase $\beta_2 \neq 0$. Then, $(3g+3h-4) \neq 0$ and the condition $\gamma_2 = 0$ gives $\mathscr{B}_1 = 0$. Moreover, the condition $\beta_2 \neq 0$ yields $g-h \neq 0$ and this implies $(2h-1)^2+(2g-1)^2 \neq 0$. According to Lemma 8.2.2, systems (8.2.3) possess an invariant hyperbola, which is nondegenerate if, and only if, $a^2+b^2 \neq 0$.

On the other hand, for these systems we calculate

$$\mathscr{R}_1 = -3c(a-b)(g-1)^2(h-1)^2(g+h)(3g-1)(3h-1)/8$$

and we claim that, for $\mathscr{B}_1 = 0$, the condition $\mathscr{R}_1 = 0$ is equivalent to $a = b = 0$. Indeed, as the equation $\mathscr{B}_1 = 0$ is linear homogeneous in a and b, as well as the equation $a-b=0$, calculating the respective determinant we obtain $-2(g+h) \neq 0$ due to $\theta \neq 0$. This proves our claim and hence the statement $(i.1)$ of Lemma 8.2.4 is proved.

The subcase $\beta_2 = 0$. Since $\beta_1 \neq 0$ (i.e. $c \neq 0$), we get $(g-h)(3g+3h-4) = 0$. On the other hand, for systems (8.2.3) we have

$$\beta_3 = -c(g-h)(g-1)(h-1)/4$$

and we consider two possibilities: $\beta_3 \neq 0$ and $\beta_3 = 0$.

The possibility $\beta_3 \neq 0$. In this case, we have $g-h \neq 0$ and the condition $\beta_2 = 0$ implies $3g+3h-4=0$, i.e. $g = 4/3-h$. So, the condition $(2h-1)^2+(2g-1)^2 \neq 0$ for systems (8.2.3) becomes $(2h-1)^2+(6h-5)^2 \neq 0$ and obviously this condition is satisfied.

For systems (8.2.3) with $g = 4/3-h$ we calculate

$$\begin{aligned}
&\gamma_3 = 22971c(h-1)^3(3h-1)^3\mathscr{B}_1, \quad \mathscr{R}_1 = (a-b)c(h-1)^3(3h-1)^3/6,\\
&\beta_1 = -c^2(h-1)^2(3h-1)^2/4, \quad \beta_3 = -c(h-1)(3h-2)(3h-1)/18.
\end{aligned}$$

So, due to $\beta_1 \neq 0$, the condition $\gamma_3 = 0$ is equivalent to $\mathscr{B}_1 = 0$. Moreover, if in addition $\mathscr{R}_1 = 0$ (i.e. $a-b=0$), we get $a = b = 0$, because the determinant of the systems of linear equations

$$3\mathscr{B}_1 = a(5-6h)-3b(2h-1) = 0, \quad a-b=0$$

with respect to the parameters a and b equals $4(3h-2) \neq 0$ due to the condition $\beta_3 \neq 0$. So, the statement $(i.2)$ of the lemma is proved.

The possibility $\beta_3 = 0$. Due to $\beta_1 \neq 0$ (i.e. $c(g-1)(h-1) \neq 0$), we get $g = h$ and for systems (8.2.3) we calculate

$$\begin{aligned}\gamma_2 =& 6300c^2h(h-1)^4(3h-2)(3h-1)^2\mathscr{B}_1,\\ \theta =& -h(h-1)^2,\ \ \beta_1 = -c^2(h-1)^2(3h-1)^2/4,\\ \beta_4 =& 2h(3h-2),\ \ \beta_5 = -2h^2(2h-1).\end{aligned}$$

So, due to the condition $\theta\beta_1 \neq 0$, we obtain that the necessary condition $\gamma_2 = 0$ is equivalent to $\mathscr{B}_1(3h-2) = 0$ and we shall consider two cases: $\beta_4 \neq 0$ and $\beta_4 = 0$.

1) *The case* $\beta_4 \neq 0$. Therefore, $3h-2 \neq 0$ and this implies $\mathscr{B}_1 = 0$. Considering Lemma 8.2.2, the condition $(2h-1)^2 + (2g-1)^2 \neq 0$ for $g = h$ becomes $2h-1 \neq 0$. So, for the existence of an invariant hyperbola the condition $\beta_5 \neq 0$ is necessary. Moreover, this hyperbola is nondegenerate if, and only if, $a^2 + b^2 \neq 0$. Since, for these systems, we have

$$\mathscr{R}_2 = (a+b)(h-1)^2(3h-1)/2,\ \ \mathscr{B}_1 = -(2h-1)(a-b)$$

and we conclude that, when $\mathscr{B}_1 = 0$, the condition $\mathscr{R}_2 \neq 0$ is equivalent to $a^2 + b^2 \neq 0$ and this completes the proof of the statement $(i.3)$ of the lemma.

2) *The case* $\beta_4 = 0$. Then, due to $\theta \neq 0$, we get $h = 2/3$ and arrive at the 3−parametric family of systems

$$\dot{x} = a + cx + 2x^2/3 - xy/3, \quad \dot{y} = b - cy - xy/3 + 2y^2/3. \tag{8.2.8}$$

For these systems we calculate

$$\gamma_3 = 7657c\mathscr{B}_1/9, \quad \beta_1 = -c^2/36, \quad \mathscr{R}_2 = (a+b)/18,$$

where $\mathscr{B}_1 = (b-a)/3$. Since for these systems the condition $(2h-1)^2 + (2g-1)^2 = 2/9 \neq 0$ holds, according to Lemma 8.2.2, we conclude that the statement $(i.4)$ of the lemma is proved.

The case $\beta_1 = 0$

Considering (8.2.7) and the condition $\theta \neq 0$, we get $c(3g-1)(3h-1) = 0$. On the other hand, for systems (8.2.3) we calculate

$$\beta_6 = -c(g-1)(h-1)/2$$

and we shall consider two subcases: $\beta_6 \neq 0$ and $\beta_6 = 0$.

The subcase $\beta_6 \neq 0$. Then, $c \neq 0$ and the condition $\beta_1 = 0$ implies $(3g-1)(3h-1) = 0$. Therefore, due to Remark 8.2.3, we may assume $h = 1/3$ and this leads to the following 4−parametric family of systems

$$\dot{x} = a + cx + gx^2 - 2xy/3, \quad \dot{y} = b - cy + (g-1)xy + y^2/3, \tag{8.2.9}$$

which is a subfamily of (8.2.3). According to Lemma 8.2.2, the above systems possess a nondegenerate hyperbola if, and only if, either $\mathscr{B}_1 = a(1-2g) - b/3 = 0$ and $a^2 + b^2 \neq 0$ (the statement **I.**), or $\mathscr{B}_2' = (1+3g)^2(b-2a+6ag) + 6c^2(1-3g) = 0$ and $a \neq 0$ (the statement **II.**). We observe that in the first case, when $a(1-2g) - b/3 = 0$, the condition $a^2 + b^2 \neq 0$ is equivalent to $a \neq 0$.

On the other hand, for these systems we calculate

$$\gamma_4 = -16(g-1)^2(3g-1)^2\mathscr{B}_1\mathscr{B}_2'/81, \quad \beta_6 = c(g-1)/3,$$
$$\beta_2 = c(g-1)(3g-1)/2, \quad \mathscr{R}_3 = a(3g-1)^3/18.$$

So, we consider two possibilities: $\beta_2 \neq 0$ and $\beta_2 = 0$.

The possibility $\beta_2 \neq 0$. In this case, $(g-1)(3g-1) \neq 0$ and the conditions $\gamma_4 = 0$ and $\mathscr{R}_3 \neq 0$ are equivalent to $\mathscr{B}_1\mathscr{B}_2' = 0$ and $a \neq 0$, respectively. This completes the proof of the statement $(ii.1)$.

The possibility $\beta_2 = 0$. Due to the condition $\beta_6 \neq 0$, we get $g = 1/3$ and this leads to the following 3−parametric family of systems

$$\dot{x} = a + cx + x^2/3 - 2xy/3, \quad \dot{y} = b - cy - 2xy/3 + y^2/3. \tag{8.2.10}$$

Since $c \neq 0$ (due to $\beta_6 \neq 0$), according to Lemma 8.2.2, these systems possess a nondegenerate invariant hyperbola if, and only if, one of the following sets conditions are fulfilled:

$$\mathscr{B}_1 = (a-b)/3 = 0, \quad a^2 + b^2 \neq 0;$$
$$\mathscr{B}_2' = 4b = 0, \quad a \neq 0; \quad \mathscr{B}_3' = 4a = 0, \quad b \neq 0.$$

We observe that the last two conditions are equivalent to $ab = 0$ and $a^2 + b^2 \neq 0$.

On the other hand, for systems (8.2.10) we calculate

$$\gamma_5 = 16\mathscr{B}_1\mathscr{B}_2'\mathscr{B}_3'/27, \quad \mathscr{R}_4 = 128(a^2 - ab + b^2)/6561.$$

It is clear that the condition $\mathscr{R}_4 = 0$ is equivalent to $a^2 + b^2 = 0$. So, the statement $(ii.2)$ is proved.

The subcase $\beta_6 = 0$. Since $\theta \neq 0$ (i.e. $(g-1)(h-1) \neq 0$), the condition $\beta_6 = 0$ yields $c = 0$. Therefore, according to Lemma 8.2.2, systems (8.2.3) with $c = 0$ possess a nondegenerate invariant hyperbola if, and only if, one of the following sets of conditions holds:

$$\begin{aligned}
&\mathscr{B}_1 \equiv b(2h-1) - a(2g-1) = 0, && (2h-1)^2 + (2g-1)^2 \neq 0, \ \ a^2 + b^2 \neq 0;\\
&\mathscr{B}_2 \equiv b(1-2h) + 2a(g+2h-1) = 0, && (2h-1)^2 + (g+2h-1)^2 \neq 0, \ \ a^2 + b^2 \neq 0;\\
&\mathscr{B}_3 \equiv a(1-2g) + 2b(2g+h-1) = 0, && (2g-1)^2 + (2g+h-1)^2 \neq 0, \ \ a^2 + b^2 \neq 0.
\end{aligned}$$

Considering the following three expressions

$$\alpha_1 = 2g - 1, \quad \alpha_2 = 2h - 1, \quad \alpha_3 = 1 - 2g - 2h,$$

we observe that the condition $(2h-1)^2 + (2g-1)^2 \neq 0$ (respectively, $(2h-1)^2 + (g+2h-1)^2 \neq 0$; $(2g-1)^2 + (2g+h-1)^2 \neq 0$) is equivalent to $\alpha_1^2 + \alpha_2^2 \neq 0$ (respectively, $\alpha_2^2 + \alpha_3^2 \neq 0$; $\alpha_1^2 + \alpha_3^2 \neq 0$).

On the other hand, for these systems we calculate

$$\begin{aligned}
\gamma_5 &= -288(g-1)(h-1)(g+h)\mathscr{B}_1\mathscr{B}_2\mathscr{B}_3,\\
\theta &= -(g-1)(h-1)(g+h)/2,\\
\beta_7 &= 2\alpha_1\alpha_2\alpha_3, \quad \beta_9 = 2(\alpha_1\alpha_2 + \alpha_1\alpha_3 + \alpha_2\alpha_3),\\
\mathscr{R}_5 &= 36(bx - ay)\big[(g-1)^2x^2 + 2(g+h+gh-1)xy + (h-1)^2y^2\big].
\end{aligned}$$

We observe that, if $\alpha_1 = \alpha_2 = 0$ (respectively, $\alpha_2 = \alpha_3 = 0$; $\alpha_1 = \alpha_3 = 0$), then the factor $\mathscr{B}_1$ (respectively, $\mathscr{B}_2$; $\mathscr{B}_3$) vanishes identically. Considering the values of the invariant polynomials β_7 and β_9, we conclude that two of the factors α_i $(i = 1,2,3)$ vanish if, and only if, $\beta_7 = \beta_9 = 0$. So, we have to consider two subcases: $\beta_7^2 + \beta_9^2 \neq 0$ and $\beta_7^2 + \beta_9^2 = 0$.

The possibility $\beta_7^2 + \beta_9^2 \neq 0$. In this case, due to $\theta \neq 0$, the conditions $\gamma_5 = 0$ and $\mathscr{R}_5 \neq 0$ are equivalent to $\mathscr{B}_1\mathscr{B}_2\mathscr{B}_3 = 0$ and $a^2 + b^2 \neq 0$, respectively. So, by Lemma 8.2.2 there exists at least

one hyperbola and, hence, the statements $(ii.3)$ and $(ii.4)$ are valid.

The possibility $\beta_7^2+\beta_9^2=0$. As it was mentioned above, in this case two of the factors α_i $(i=1,2,3)$ vanish. Considering Remark 8.2.3, without loss of generality, we may assume $\alpha_1=\alpha_2=0$.

Thus, we have $g=h=1/2$ and we get the family of systems

$$\frac{dx}{dt}=a+x^2/2-xy/2,\quad \frac{dy}{dt}=b-xy/2+y^2/2. \tag{8.2.11}$$

Since $c=0$ and the conditions of the statement **I.** of Lemma 8.2.2 are not satisfied for these systems, according to Lemma 8.2.2, the above systems possess a nondegenerate invariant hyperbola if, and only if, $a^2+b^2\neq 0$ and either $\mathscr{B}_2=a=0$ or $\mathscr{B}_3=b=0$. For systems (8.2.11) we calculate

$$\gamma_6=-9\mathscr{B}_2\mathscr{B}_3,\quad \mathscr{R}_5=9(bx-ay)(x+y)^2$$

and we conclude that the statement $(ii.5)$ of the lemma holds.

As all the cases are examined, Lemma 8.2.4 is proved. ∎

The next lemma is related to the number of the invariant hyperbolas that quadratic systems with $\eta>0$ and $\theta\neq 0$ could have.

Lemma 8.2.5. *Assume that for a quadratic system* (8.1.2) *the conditions* $\eta>0$, $\theta\neq 0$ *and* $\gamma_1=\gamma_2=0$ *are satisfied. Then, this system possesses:*

(𝒜) two nondegenerate invariant hyperbolas if, and only if, either

($\mathscr{A}_1$) if $\beta_1=0$, $\beta_6\neq 0$, $\beta_2\neq 0$, $\gamma_4=0$, $\mathscr{R}_3\neq 0$ *and* $\delta_1=0$, *or*

($\mathscr{A}_2$) if $\beta_1=0$, $\beta_6=0$, $\beta_7\neq 0$, $\gamma_5=0$, $\mathscr{R}_5\neq 0$ *and* $\beta_8=\delta_2=0$, *or*

($\mathscr{A}_3$) if $\beta_1=0$, $\beta_6=\beta_7=0$, $\beta_9\neq 0$, $\gamma_5=0$, $\mathscr{R}_5\neq 0$ *and* $\delta_3=0$, $\beta_8\neq 0$;

(ℬ) three nondegenerate invariant hyperbolas if, and only if, $\beta_1=0$, $\beta_6=\beta_7=0$, $\beta_9\neq 0$, $\gamma_5=0$, $\mathscr{R}_5\neq 0$ *and* $\delta_3=\beta_8=0$.

Proof. For systems (8.2.3) we have

$$\beta_6=-c(g-1)(h-1)/2,\quad \theta=-(g-1)(h-1)(g+h)/2,$$
$$\beta_1=-c^2(g-1)(h-1)(3g-1)(3h-1)/4.$$

The case $\beta_6 \neq 0$

Then, $c \neq 0$ and, according to Lemma 8.2.2, we could have at least two hyperbolas only if the conditions given either by the statements **I.** and **II.**; (ii) (i.e. $\mathscr{B}_1 = \mathscr{B}_2' = 0$ and $h = 1/3$), or by the statements **I.** and **III.**; (ii) (i.e. $\mathscr{B}_1 = \mathscr{B}_3' = 0$ and $g = 1/3$) are satisfied. Therefore, the condition $(3g-1)(3h-1) = 0$ is necessary. This condition is governed by the invariant polynomial β_1. So, we assume $\beta_1 = 0$ and, due to Remark 8.2.3, we may consider $h = 1/3$. Then, we calculate

$$\gamma_4 = -16(g-1)^2(3g-1)^2\mathscr{B}_1\mathscr{B}_2'/81, \quad \beta_1 = 0,$$
$$\theta = (g-1)(1+3g)/9 \neq 0, \quad \beta_2 = c(g-1)(3g-1)/2.$$

Solving the systems of equations $\mathscr{B}_1\Big|_{h=1/3} = \mathscr{B}_2' = 0$ with respect to a and b we obtain

$$a = \frac{6c^2(3g-1)}{(1+3g)^2} \equiv A_0, \quad b = -\frac{18c^2(2g-1)(3g-1)}{(1+3g)^2} \equiv B_0.$$

In this case, we get the family of systems

$$\dot{x} = A_0 + cx + gx^2 - 2xy/3, \quad \dot{y} = B_0 - cy + (g-1)xy + y^2/3, \tag{8.2.12}$$

which possess two nondegenerate invariant hyperbolas:

$$\Phi_1(x,y) = -\frac{36c^2(3g-1)}{(1+3g)^2} + 2xy = 0,$$
$$\Phi_2(x,y) = -\frac{36c^2(3g-1)}{(1+3g)^2} + \frac{12c}{1+3g}x + 2x(x-y) = 0,$$

where $c(3g-1) \neq 0$, due to $a \neq 0$. Thus, for the nondegeneracy of the hyperbolas above, the condition $c(3g-1) \neq 0$ (i.e. $\beta_2 \neq 0$) is necessary.

Since the condition $\gamma_4 = 0$ gives $\mathscr{B}_1\mathscr{B}_2' = 0$, it remains to find out the invariant polynomial which, in addition to γ_4, is responsible for the relation $\mathscr{B}_1 = \mathscr{B}_2' = 0$. We observe that in the case $\mathscr{B}_1 = 0$ (i.e. $b = 3a(1-2g)$) we have

$$\delta_1 = (3g-1)\big[a(1+3g)^2 - 6c^2(3g-1)\big]/18 = (3g-1)\mathscr{B}_2'/18.$$

It remains to observe that in the considered case we have $\mathscr{R}_3 = a(3g-1)^3/18 \neq 0$ and that, due to the condition $\beta_2 \neq 0$ (i.e. $c(3g-1) \neq 0$), Lemma 8.2.2 assures we could not have a third hyperbola

of the form $\Phi(x,y) = p + qx + ry + 2y(x-y) = 0$. This completes the proof of the statement $(\mathscr{A}_1)$ of the lemma.

The case $\beta_6 = 0$

Then, $c = 0$ and we calculate for systems (8.2.3)

$$\beta_7 = 2\alpha_1\alpha_2\alpha_3, \quad \beta_9 = 2(\alpha_1\alpha_2 + \alpha_1\alpha_3 + \alpha_2\alpha_3), \quad \beta_8 = 2(4g-1)(4h-1)(3-4g-4h),$$

where $\alpha_1 = 2g-1$, $\alpha_2 = 2h-1$ and $\alpha_3 = 1-2g-2h$.

The subcase $\beta_7 \neq 0$. Then, $\alpha_1\alpha_2\alpha_3 \neq 0$ and we consider two possibilities: $\beta_8 \neq 0$ and $\beta_8 = 0$.

The possibility $\beta_8 \neq 0$. We claim that in this case we could not have more than one hyperbola. Indeed, as $c = 0$, we observe that all five polynomials $\mathscr{B}_i$ $(i = 1,2,3)$, $\mathscr{B}_2'$ and $\mathscr{B}_3'$ are linear (and homogeneous) with respect to a and b and the condition $a^2 + b^2 \neq 0$ must hold. So, in order to have nonzero solutions in (a,b) of the equations

$$\mathscr{U} = \mathscr{V} = 0, \quad \mathscr{U}, \mathscr{V} \in \{\mathscr{B}_1, \mathscr{B}_2, \mathscr{B}_3, \mathscr{B}_2', \mathscr{B}_3'\}, \ \ \mathscr{U} \neq \mathscr{V}$$

it is necessary that the corresponding determinants $\det(\mathscr{U},\mathscr{V}) = 0$. We have for each couple, respectively:

$$\begin{aligned}
&(\omega_1)\ \det(\mathscr{B}_1,\mathscr{B}_2) = -(2h-1)(4h-1) = 0;\\
&(\omega_2)\ \det(\mathscr{B}_1,\mathscr{B}_3) = -(2g-1)(4g-1) = 0;\\
&(\omega_3)\ \det(\mathscr{B}_2,\mathscr{B}_3) = (1-2g-2h)(3-4g-4h) = 0;\\
&(\omega_4)\ \det(\mathscr{B}_1,\mathscr{B}_2')\big|_{h=1/3} = (3g+1)^2/3;\\
&(\omega_5)\ \det(\mathscr{B}_1,\mathscr{B}_3')\big|_{g=1/3} = (3h+1)^2/3;\\
&(\omega_6)\ \det(\mathscr{B}_2',\mathscr{B}_3)\big|_{\{c=0,\,h=1/3\}} = (1+3g)^2(6g-1)(12g-5)/3 = 0;\\
&(\omega_7)\ \det(\mathscr{B}_2,\mathscr{B}_3')\big|_{\{c=0,\,g=1/3\}} = (1+3h)^2(6h-1)(12h-5)/3 = 0;\\
&(\omega_8)\ \det(\mathscr{B}_2',\mathscr{B}_3')\big|_{\{h=1/3,\,g=1/3\}} = -16 \neq 0.
\end{aligned} \tag{8.2.13}$$

We observe that the determinant (ω_8) is not zero. Moreover, since $\beta_7 \neq 0$ and $\beta_8 \neq 0$, we deduce that none of the determinants (ω_i) $(i = 1,2,3)$ could vanish.

On the other hand, for systems (8.2.3) with $c = 0$ we have $\theta = (g-1)(3g+1)/9$ in the case $h = 1/3$

and $\theta = (h-1)(3h+1)/9$ in the case $g = 1/3$. Therefore, due to $\theta \neq 0$, in the cases (ω_4) and (ω_5) we also could not have zero determinants.

Thus, it remains to consider the cases (ω_6) and (ω_7). Considering Remark 8.2.3, we observe that the case (ω_7) could be brought to the case (ω_6). So, assuming $h = 1/3$ we calculate

$$\beta_7 = 2(2g-1)(6g-1)/9, \quad \beta_8 = -2(4g-1)(12g-5)/9, \quad \theta = (g-1)(3g+1)/9,$$

and, hence, the determinant corresponding to the case (ω_6) could not be zero due to $\theta\beta_7\beta_8 \neq 0$. This completes the proof of our claim.

The possibility $\beta_8 = 0$. In this case, we get $(4g-1)(4h-1)(3-4g-4h) = 0$ and, due to Remark 8.2.3, we may assume $h = 1/4$. Then, $\det(\mathscr{B}_1, \mathscr{B}_2) = 0$ (see the case (ω_1)) and we obtain $\mathscr{B}_1 = (2a-b-4ag)/2 = -\mathscr{B}_2 = 0$. Since in this case we have

$$\delta_2 = 2(2g-1)(4g-1)(b-2a+4ag), \quad \beta_7 = (2g-1)(4g-1)/2,$$

we conclude that, due to $\beta_7 \neq 0$, the condition $2a-b-4ag = 0$ is equivalent to $\delta_2 = 0$. So, setting $b = 2a(1-2g)$, we arrive at the family of systems

$$\dot{x} = a + gx^2 - 3xy/4, \quad \dot{y} = 2a(1-2g) + (g-1)xy + y^2/4. \tag{8.2.14}$$

These systems possess the invariant hyperbolas

$$\Phi_1''(x,y) = -4a + 2xy = 0, \quad \Phi_2''(x,y) = 4a + 2x(x-y) = 0,$$

which are nondegenerate if, and only if, $a \neq 0$. Since for these systems we have

$$\mathscr{R}_5 = 9a(2x - 4gx - y)\left[16(g-1)^2x^2 + 8(5g-3)xy + 9y^2\right]/4,$$

the condition $a \neq 0$ is equivalent to $\mathscr{R}_5 \neq 0$. On the other hand, for these systems we calculate

$$\mathscr{B}_3 = -2a(2g-1)(4g-1), \quad \mathscr{B}_3'\big|_{h=1/4} = 49a/24$$

and, due to $\beta_7\mathscr{R}_5 \neq 0$, we get $\mathscr{B}_3\mathscr{B}_3' \neq 0$, i.e. systems (8.2.14) could not possess a third hyperbola. This completes the proof of the statement $(\mathscr{A}_2)$.

The subcase $\beta_7 = 0$. Then, $(2g-1)(2h-1)(1-2g-2h) = 0$ and, due to Remark 8.2.3, we may assume $h = 1/2$. So, by Lemma 8.2.2, we must have $g(2g-1) \neq 0$ and this is equivalent to $\beta_9 = -4g(2g-1) \neq 0$. Herein, we have $\det(\mathscr{B}_1, \mathscr{B}_2) = 0$ and we obtain $\mathscr{B}_1 = a(1-2g) = 0$ and $\mathscr{B}_2 = 2ag = 0$. This implies $a = 0$, which is equivalent to $\delta_3 = 16a^2g^2(2g-1)^2 = 0$ due to $\beta_9 \neq 0$. So, we get the family of systems

$$\dot{x} = gx^2 - xy/2, \quad \dot{y} = b + (g-1)xy + y^2/2 \tag{8.2.15}$$

which possess the following two hyperbolas

$$\Phi_1(x,y) = -\frac{2b}{2g-1} + 2xy = 0, \quad \Phi_2(x,y) = -\frac{b}{g} + 2x(x-y) = 0.$$

These hyperbolas are nondegenerate if, and only if, $b \neq 0$ which is equivalent to $\mathscr{R}_5 = 9bx\big[4(g-1)^2x^2 + 4(3g-1)xy + y^2\big] \neq 0$.

For the above systems we have $\mathscr{B}_3 = b(4g-1)$ and $\mathscr{B}_3' = 25b/4$. Since $b \neq 0$, only the condition $\mathscr{B}_3 = 0$ could be satisfied and this implies $g = 1/4$. It is not too hard to find out that in this case we get the third hyperbola:

$$\Phi_3(x,y) = -4b + 2y(x-y) = 0.$$

We observe that for the systems above $\beta_8 = -2(4g-1)^2$ and, hence, the third hyperbola exists if, and only if, $\beta_8 = 0$. So, the statements $(\mathscr{A}_3)$ and $(\mathscr{B})$ are proved.

Since all the possibilities are examined, Lemma 8.2.5 is proved. ∎

8.2.2 Systems with three real infinite singularities and $\theta = 0$

Considering (8.2.2) for systems (8.2.1), we get $(g-1)(h-1)(g+h) = 0$ and we may assume $g = -h$, otherwise in the case $g = 1$ (respectively, $h = 1$) we apply the change $(x,y,g,h) \mapsto (-y, x-y, 1-g-h, g)$ (respectively, $(x,y,g,h) \mapsto (y-x, -x, h, 1-g-h)$), which preserves the quadratic parts of systems (8.2.1).

So, $g = -h$ and for systems (8.2.1) we calculate $\widetilde{N} = 9(h^2-1)(x-y)^2$. We consider two cases: $\widetilde{N} \neq 0$ and $\widetilde{N} = 0$.

The case $\widetilde{N} \neq 0$

Then, $(h-1)(h+1) \neq 0$ and due to a translation we may assume $d = e = 0$ and this leads to the family of systems

$$\dot{x} = a + cx - hx^2 + (h-1)xy, \quad \dot{y} = b + fy - (h+1)xy + hy^2. \tag{8.2.16}$$

Remark 8.2.6. *We observe that due to the change* $(x,y,a,b,c,f,h)\mapsto(y,x,b,a,f,c,-h)$ *which conserves systems* (8.2.16) *we can change the sign of the parameter* h.

Lemma 8.2.7. *A system* (8.2.16) *with* $(h-1)(h+1)\neq 0$ *possesses at least one nondegenerate invariant hyperbola of the indicated form if, and only if, the following conditions are satisfied, respectively:*

I. $\Phi(x,y)=p+qr+ry+2xy \;\Leftrightarrow\; c+f=0,\ \mathscr{E}_1\equiv a(2h+1)+b(2h-1)=0,\ a^2+b^2\neq 0;$

II. $\Phi(x,y)=p+qr+ry+2x(x-y) \;\Leftrightarrow\; c-f=0$ *and either*

(i) $(2h-1)(3h-1)\neq 0,\ \mathscr{E}_2\equiv 2c^2(h-1)(2h-1)+(3h-1)^2(b-2a+2ah-2bh)=0,\ a\neq 0;$

(ii) $h=1/3,\ c=0,\ a\neq 0,\ 4a-b\geq 0;$

(iii) $h=1/2,\ a=0,\ b+4c^2\neq 0;$

III. $\Phi(x,y)=p+qr+ry+2y(x-y) \;\Leftrightarrow\; c-f=0$ *and either*

(i) $(2h+1)(3h+1)\neq 0,\ \mathscr{E}_3\equiv 2c^2(h+1)(2h+1)+(3h+1)^2(a-2b-2bh+2ah)=0,\ b\neq 0;$

(ii) $h=-1/3,\ c=0,\ b\neq 0,\ 4b-a\geq 0;$

(iii) $h=-1/2,\ b=0,\ a+4c^2\neq 0.$

Proof. As it was mentioned in the proof of Lemma 8.2.2 (see page 285), we may assume that the quadratic part of an invariant hyperbola has one of the following forms: $(i)\ 2xy$, $(ii)\ 2x(x-y)$, $(iii)\ 2y(x-y)$. Considering the equations (8.1.3), we examine each one of these possibilities.

(i) $\Phi(x,y)=p+qx+ry+2xy$: in this case, due to $\widetilde{N}\neq 0$ (i.e. $(h-1)(h+1)\neq 0$), we obtain

$$t=1,\ q=r=s=u=0,\ U=-2h-1,\ V=2h-1,\ W=c+f,$$
$$Eq_8=p(1+2h)+2b,\ \ Eq_9=p(1-2h)+2a,\ \ Eq_{10}=-p(c+f),$$
$$Eq_1=Eq_2=Eq_3=Eq_4=Eq_5=Eq_6=Eq_7=0.$$

Since in this case the hyperbola has the form $\Phi(x,y)=p+2xy$, it is clear that $p\neq 0$, otherwise we get a degenerate hyperbola. So, the condition $c+f=0$ is necessary.

Calculating the resultant of the nonvanishing equations with respect to the parameter p we obtain

$$\mathrm{Res}_p(Eq_8,Eq_9)=2[a(2h+1)+b(2h-1)]=2\mathscr{E}_1.$$

Since $(2h-1)^2+(2h+1)^2\neq 0$, we conclude that an invariant hyperbola exists if, and only if,

$\mathscr{E}_1 = 0$. Due to Remark 8.2.6, we may assume $2h-1 \neq 0$. Then, we get

$$p = 2a/(2h-1),\ \ b = a(2h+1)/(2h-1),\ \ \Phi(x,y) = \frac{2a}{2h-1} + 2xy = 0$$

and, clearly, for the nondegeneracy of the hyperbola, the condition $a \neq 0$ must hold.

This completes the proof of the statement **I.** of the lemma.

(ii) $\Phi(x,y) = p + qx + ry + 2x(x-y)$: since $(h-1)(h+1) \neq 0$ (due to $N \neq 0$), we obtain

$$\begin{gathered} s = 2,\ t = -1,\ r = u = 0,\ U = -2h,\ V = 2h-1,\ W = (4c+hq)/2, \\ Eq_6 = 2(c-f),\ \ Eq_8 = 4a - 2b + 2hp - cg - hq^2/2, \\ Eq_9 = p(1-2h) - 2a, \quad Eq_{10} = -2cp + aq - hpq/2, \\ Eq_1 = Eq_2 = Eq_3 = Eq_4 = Eq_5 = Eq_7 = 0. \end{gathered} \tag{8.2.17}$$

We observe that the equation $Eq_6 = 0$ implies the condition $c - f = 0$.

1) Assume first $(2h-1)(3h-1) \neq 0$. Then, considering the equation $Eq_9 = 0$, we obtain $p = 2a/(1-2h)$. As the hyperbola $\Phi(x,y) = p + qx + 2x(x-y) = 0$ has to be nondegenerate, the condition $p \neq 0$ holds and this implies $a \neq 0$. Therefore, from

$$Eq_{10} = \frac{a(4c - q + 3hq)}{2h-1} = 0,$$

due to $3h - 1 \neq 0$, we obtain $q = 4c/(1-3h)$ and, then, we get

$$Eq_8 = \frac{2\mathscr{E}_2}{(2h-1)(3h-1)^2} = 0.$$

So, we deduce that the conditions $c - f = 0$, $\mathscr{E}_2 = 0$ and $a \neq 0$ are necessary and sufficient for the existence of a nondegenerate hyperbola of systems (8.2.16) in the case $(2h-1)(3h-1) \neq 0$.

2) Suppose now $h = 1/3$. Then, considering (8.2.17), we have $Eq_9 = (p - 6a)/3 = 0$, i.e. $p = 6a \neq 0$ (otherwise, we get a degenerate hyperbola). Therefore, the equation $Eq_{10} = -12ac = 0$ yields $c = 0$. Herein, the equation $Eq_8 = 0$ becomes $Eq_8 = \left[12(4a-b) - q^2\right]/6 = 0$ and obviously for the existence of a real solution for the parameter q of hyperbola the condition $4a - b \geq 0$ must be satisfied.

Thus, in the case $h = 1/3$, we have at least one nondegenerate hyperbola if, and only if, the conditions $f = c = 0$, $4a - b \geq 0$ and $a \neq 0$ hold.

3) Assume finally $h = 1/2$. In this case, we get $Eq_9 = -2a = 0$, i.e. $a = 0$, and we have

$$Eq_8 = -2b + p - cq - q^2/4 = 0, \;\; Eq_{10} = -p(8c + q)/4 = 0, \;\; \Phi(x, y) = p + qx + 2x(x - y).$$

Therefore, $p \neq 0$ and we obtain $q = -8c$ and $p = 2(b + 4c^2) \neq 0$. This completes the proof of the statement **II.** of the lemma.

(iii) $\Phi(x, y) = p + qx + ry + 2y(x - y)$: we observe that, due to the change $(x, y, a, b, c, f, h) \mapsto (y, x, b, a, c, f, -h)$ (which preserves systems (8.2.16)), this case could be brought to the previous one and, hence, the conditions could be constructed directly applying this change.

Thus, Lemma 8.2.7 is proved. ■

We shall construct now the affine invariant conditions for the existence of at least one invariant hyperbola for quadratic systems in the considered family.

Lemma 8.2.8. *Assume that for a quadratic system* (8.1.2) *the conditions* $\eta > 0$, $\theta = 0$, $\widetilde{N} \neq 0$ *and* $\gamma_1 = \gamma_2 = 0$ *hold. Then, this system possesses at least one nondegenerate invariant hyperbola if, and only if, one of the following sets of the conditions are satisfied:*

(i) If $\beta_6 \neq 0$ *then either*

$(i.1)$ $\beta_{10} \neq 0$, $\gamma_7 = 0$, $\mathscr{R}_6 \neq 0$;

$(i.2)$ $\beta_{10} = 0$, $\gamma_4 = 0$, $\beta_2 \mathscr{R}_3 \neq 0$;

(ii) If $\beta_6 = 0$ *then either*

$(ii.1)$ $\beta_2 \neq 0$, $\beta_7 \neq 0$, $\gamma_8 = 0$, $\beta_{10} \mathscr{R}_7 \neq 0$;

$(ii.2)$ $\beta_2 \neq 0$, $\beta_7 = 0$, $\gamma_9 = 0$, $\mathscr{R}_8 \neq 0$;

$(ii.3)$ $\beta_2 = 0$, $\beta_7 \neq 0$, $\beta_{10} \neq 0$, $\gamma_7 \gamma_8 = 0$, $\mathscr{R}_5 \neq 0$;

$(ii.4)$ $\beta_2 = 0$, $\beta_7 \neq 0$, $\beta_{10} = 0$, $\mathscr{R}_3 \neq 0$, $\gamma_7 \neq 0$, $\gamma_{10} \geq 0$;

$(ii.5)$ $\beta_2 = 0$, $\beta_7 \neq 0$, $\beta_{10} = 0$, $\mathscr{R}_3 \neq 0$, $\gamma_7 = 0$;

$(ii.6)$ $\beta_2 = 0$, $\beta_7 = 0$, $\gamma_7 = 0$, $\mathscr{R}_3 \neq 0$.

Proof. Assume that for a quadratic system (8.1.2) the conditions $\eta > 0$, $\theta = 0$ and $\widetilde{N} \neq 0$ are fulfilled. As it was mentioned earlier, due to an affine transformation and time rescaling, this system could be brought to the canonical form (8.2.16), for which we calculate

$$\gamma_1 = (c - f)^2 (c + f)(h - 1)^2 (h + 1)^2 (3h - 1)(3h + 1)/64,$$
$$\beta_6 = (c - f)(h - 1)(h + 1)/4, \quad \beta_{10} = -2(3h - 1)(3h + 1).$$

The subcase $\beta_6 \neq 0$. By Lemma 8.1.6, for the existence of a nondegenerate invariant hyperbola of systems (8.2.16), the condition $\gamma_1 = 0$ is necessary and this condition is equivalent to $(c+f)(3h-1)(3h+1) = 0$. We examine two possibilities: $\beta_{10} \neq 0$ and $\beta_{10} = 0$.

The possibility $\beta_{10} \neq 0$. Then, we obtain $f = -c$ (this implies $\gamma_2 = 0$) and we have

$$\gamma_7 = 8(h-1)(h+1)\mathscr{E}_1.$$

Therefore, due to $\beta_6 \neq 0$, the condition $\gamma_7 = 0$ is equivalent to $\mathscr{E}_1 = 0$. So, we have $a = \lambda(2h-1)$, $b = -\lambda(2h+1)$ (where $\lambda \neq 0$ is an arbitrary parameter) and, then, we calculate

$$\mathscr{R}_6 = -632\lambda c(h-1)(h+1).$$

Since $\beta_6 \neq 0$, we deduce that the condition $\mathscr{R}_6 \neq 0$ is equivalent to $a^2 + b^2 \neq 0$. This completes the proof of the statement $(i.1)$ of the lemma.

The possibility $\beta_{10} = 0$. Then, we have $(3h-1)(3h+1) = 0$ and, by Remark 8.2.6, we may assume $h = 1/3$. Then, we get the 4−parametric family of systems

$$\dot{x} = a + cx - x^2/3 - 2xy/3, \quad \dot{y} = b + fy - 4xy/3 + y^2/3, \tag{8.2.18}$$

for which we calculate $\gamma_1 = 0$ and

$$\gamma_2 = 44800(c-f)^2(c+f)(2c-f)/243, \quad \beta_6 = -2(c-f)/9, \quad \beta_2 = -4(2c-f)/9.$$

Since $\beta_6 \neq 0$ (i.e. $c - f \neq 0$), by Lemma 8.1.6, the necessary condition $\gamma_2 = 0$ gives $(c+f)(2c-f) = 0$. We claim that for the existence of an invariant hyperbola the condition $2c - f \neq 0$ (i.e. $\beta_2 \neq 0$) must be satisfied. Indeed, setting $f = 2c$ we obtain $\beta_6 = 2c/9 \neq 0$. However, according to Lemma 8.2.7, for the existence of a hyperbola of systems (8.2.18), it is necessary the condition $(c+f)(c-f) = 0$, which for $f = 2c$ becomes $-3c^2 = 0$. The obtained contradiction proves our claim.

Thus, the condition $\beta_2 \neq 0$ is necessary and, then, we have $f = -c$. By Lemma 8.2.7, in the case $h = 1/3$ we have an invariant hyperbola (which is of the form $\Phi(x,y) = p + qx + ry + 2xy = 0$) if, and only if, $\mathscr{E}_1 = (5a-b)/3 = 0$ and $a^2 + b^2 \neq 0$.

On the other hand, for systems (8.2.18) with $f=-c$ we calculate

$$\gamma_4=-4096c^2\mathscr{E}_1/243,\quad \beta_6=-4c/9,\quad \mathscr{R}_3=-4a/9.$$

So, the statement $(i.2)$ of the lemma is proved.

The subcase $\beta_6=0$. Then, $f=c$ (this implies $\gamma_2=0$) and we calculate

$$\gamma_8=42(h-1)(h+1)\mathscr{E}_2\mathscr{E}_3,\ \ \beta_2=c(h-1)(h+1)/2,\ \ \beta_7=-2(2h-1)(2h+1),$$
$$\beta_{10}=-2(3h-1)(3h+1),\ \ \mathscr{R}_7=-(h-1)(h+1)U(a,b,c,h)/4,$$

where $U(a,b,c,h)=2c^2(h-1)(h+1)-b(h+1)(3h-1)^2+a(h-1)(3h+1)^2$.

The possibility $\beta_2\neq 0$. Then, $c\neq 0$ and we shall consider two cases: $\beta_7\neq 0$ and $\beta_7=0$.

1) *The case* $\beta_7\neq 0$. We observe that in this case, for the existence of a nondegenerate hyperbola, the condition $\beta_{10}\neq 0$ is necessary. Indeed, since $f=c\neq 0$ and $(2h-1)(2h+1)\neq 0$, according to Lemma 8.2.7 (see the statements **II.** and **III.**), for the existence of at least one nondegenerate invariant hyperbola it is necessary and sufficient $(3h-1)(3h+1)\neq 0$ and either $\mathscr{E}_2=0$ and $a\neq 0$, or $\mathscr{E}_3=0$ and $b\neq 0$.

We claim that the condition $a\neq 0$ (when $\mathscr{E}_2=0$), as well as the condition $b\neq 0$ (when $\mathscr{E}_3=0$), is equivalent to $U(a,b,c,h)\neq 0$. Indeed, as $\mathscr{E}_2$, as well as $\mathscr{E}_3$, and $U(a,b,c,h)$ are linear polynomials in a and b, then the equations $\mathscr{E}_2=U(a,b,c,h)=0$ (respectively, $\mathscr{E}_2=U(a,b,c,h)=0$) with respect to a and b gives $a=0$ and $b=2c^2(h-1)/(3h-1)^2$ (respectively, $b=0$ and $a=-2c^2(h+1)/(3h+1)^2$). This proves our claim.

It remains to observe that the condition $\mathscr{E}_2\mathscr{E}_3=0$ is equivalent to $\gamma_8=0$. So, this completes the proof of the statement $(ii.1)$ of the lemma.

2) *The case* $\beta_7=0$. Then, by Remark 8.2.6, we may assume $h=1/2$ and, since $f=c$, by Lemma 8.2.7, for the existence of a nondegenerate hyperbola of systems (8.2.16) (with $h=1/2$ and $f=c$), the conditions $a=0$ and $b+4c^2\neq 0$ are necessary. On the other hand, we calculate

$$\gamma_9=3a/2,\quad \mathscr{R}_8=(7a+b+4c^2)/8$$

and clearly these invariant polynomials govern the above conditions. So, the statement $(ii.2)$ of the lemma is proved.

The possibility $\beta_2 = 0$. In this case we have $f = c = 0$.

1) *The case* $\beta_7 \neq 0$. Then, $(2h-1)(2h+1) \neq 0$.

a) *The subcase* $\beta_{10} \neq 0$. In this case $(3h-1)(3h+1) \neq 0$. By Lemma 8.2.7, we could have an invariant hyperbola if, and only if, $\mathscr{E}_1\mathscr{E}_2\mathscr{E}_3 = 0$. On the other hand, for systems (8.2.16) with $f = c = 0$ we have

$$\gamma_7\gamma_8 = -336(h-1)^2(1+h)^2\mathscr{E}_1\mathscr{E}_2\mathscr{E}_3,$$

$$\mathscr{R}_5 = 36(bx-ay)(x-y)\left[(1+h)^2x-(h-1)^2y\right]$$

and, therefore, the condition $\mathscr{R}_5 \neq 0$ is equivalent to $a^2+b^2 \neq 0$. This completes the proof of the statement $(ii.3)$ of the lemma.

b) *The subcase* $\beta_{10} = 0$. Then, we have $(3h-1)(3h+1) = 0$ and, by Remark 8.2.6, we may assume $h = 1/3$. By Lemma 8.2.7, we could have an invariant hyperbola if, and only if, either the conditions **I.** or **II.**; (ii) of Lemma 8.2.7 are satisfied. In this case we calculate

$$\gamma_7 = -64\mathscr{E}_1/9, \quad \gamma_{10} = 8(4a-b)/27, \quad \mathscr{R}_3 = -4a/9$$

and, hence, the condition $\mathscr{R}_3 \neq 0$ implies the nondegeneracy of the hyperbola. Therefore, in the case $\gamma_7 \neq 0$ the condition $\gamma_{10} \geq 0$ must hold and this leads to the statement $(ii.4)$ of the lemma, whereas for $\gamma_7 = 0$ the statement $(ii.5)$ of the lemma holds.

2) *The case* $\beta_7 = 0$. Then, $(2h-1)(2h+1) = 0$ and, by Remark 8.2.6, we may assume $h = 1/2$. By Lemma 8.2.7, we could have an invariant hyperbola if, and only if, either the conditions $\mathscr{E}_1 = 2a = 0$ and $b \neq 0$ (see statement **I.**), or $a = 0$ and $b \neq 0$ (see statement **II.**; (iii) of the lemma) are fulfilled. As we could see, the conditions coincides and, hence, by this lemma we have two hyperbolas: the asymptotes of one of them are parallel to the lines $x = 0$ and $y = 0$, whereas the asymptotes of the other hyperbola are parallel to the lines $x = 0$ and $y = x$.

On the other hand, for systems (8.2.16) (with $h = 1/2$ and $f = c = 0$) we calculate

$$\gamma_7 = -12a, \quad \mathscr{R}_3 = \quad (5a-b)/16$$

and this leads to the statement $(ii.6)$ of the lemma.

Since all the possibilities are considered, Lemma 8.2.8 is proved. ∎

Lemma 8.2.9. *Assume that for a quadratic system* (8.1.2) *the conditions* $\eta > 0$, $\theta = 0$, $\tilde{N} \neq 0$ *and* $\gamma_1 = \gamma_2 = 0$ *are satisfied. Then, this system possesses:*

($\mathscr{A}$) three distinct nondegenerate invariant hyperbolas (1 $\mathscr{H}$ and 2 $\mathscr{H}^p$) if, and only if, $\beta_6 = \beta_2 = \beta_{10} = \gamma_7 = 0$, $\beta_7\mathscr{R}_3 \neq 0$ *and* $\gamma_{10} > 0$;

($\mathscr{B}$) two distinct nondegenerate invariant hyperbolas if, and only if, $\beta_6 = 0$ *and either*

($\mathscr{B}_1$) $\beta_2 \neq 0$, $\beta_7 \neq 0$, $\gamma_8 = 0$, $\beta_{10}\mathscr{R}_7 \neq 0$ *and* $\delta_4 = 0$ *($\Rightarrow$ 2 $\mathscr{H}$), or*

($\mathscr{B}_2$) $\beta_2 \neq 0$, $\beta_7 = 0$, $\gamma_9 = 0$, $\mathscr{R}_8 \neq 0$ *and* $\delta_5 = 0$ *($\Rightarrow$ 2 $\mathscr{H}$), or*

($\mathscr{B}_3$) $\beta_2 = 0$, $\beta_7 \neq 0$, $\beta_{10} \neq 0$, $\gamma_7\gamma_8 = 0$, $\mathscr{R}_5 \neq 0$ *and* $\beta_8 = \delta_2 = 0$ *($\Rightarrow$ 2 $\mathscr{H}$), or*

($\mathscr{B}_4$) $\beta_2 = 0$, $\beta_7 \neq 0$, $\beta_{10} = 0$, $\gamma_7 \neq 0$, $\mathscr{R}_3 \neq 0$ *and* $\gamma_{10} > 0$ *($\Rightarrow$ 2 $\mathscr{H}^p$), or*

($\mathscr{B}_5$) $\beta_2 = 0$, $\beta_7 = 0$, $\gamma_7 = 0$, $\mathscr{R}_3 \neq 0$ *($\Rightarrow$ 2 $\mathscr{H}$);*

($\mathscr{C}$) one double ($\mathscr{H}_2^p$) nondegenerate invariant hyperbola if, and only if, $\beta_6 = \beta_2 = 0$, $\beta_7 \neq 0$, $\beta_{10} = 0$, $\gamma_7 \neq 0$, $\mathscr{R}_3 \neq 0$ *and* $\gamma_{10} = 0$.

Proof. For systems (8.2.16) we calculate

$$\begin{aligned} \beta_6 &= (c-f)(h-1)(h+1)/4, \quad \beta_7 = -2(2h+1)(2h-1), \\ \beta_{10} &= -2(3h+1)(3h-1), \quad \beta_2 = \big[(c+f)(h^2-1) - 8(c-f)h\big]/4. \end{aligned} \tag{8.2.19}$$

According to Lemma 8.2.7, in order to have at least two nondegenerate invariant hyperbolas, the condition $c - f = 0$ must hold. This condition is governed by the invariant polynomial β_6 and in what follows we assume $\beta_6 = 0$ (i.e. $f = c$).

The case $\beta_2 \neq 0$. Then, we have $c \neq 0$ and the conditions given by the statement **I.** of Lemma 8.2.7 could not be satisfied.

The case $\beta_7 \neq 0$. We observe that in this case, due to $c \neq 0$, we could have two nondegenerate invariant hyperbolas if, and only if, $(3h-1)(3h+1) \neq 0$ (i.e. $\beta_{10} \neq 0$), $\mathscr{E}_2 = \mathscr{E}_3 = 0$ and $ab \neq 0$. The systems of equations $\mathscr{E}_2 = \mathscr{E}_3 = 0$ with respect to the parameters a and b gives the solution

$$a = -\frac{2c^2(1+h)^3(2h-1)}{(3h-1)^2(1+3h)^2} \equiv a_0, \qquad b = -\frac{2c^2(h-1)^3(1+2h)}{(3h-1)^2(1+3h)^2} \equiv b_0, \tag{8.2.20}$$

which exists and $ab \neq 0$ due to the condition $(2h-1)(2h+1)(3h-1)(3h+1) \neq 0$.

In this case systems (8.2.16) with $a = a_0$ and $b = b_0$ possess the following two hyperbolas

$$\begin{aligned} \Phi_1^{(1)}(x,y) &= \frac{4c^2(1+h)^3}{(3h-1)^2(1+3h)^2} - \frac{4c}{3h-1}x + 2x(x-y) = 0, \\ \Phi_2^{(1)}(x,y) &= \frac{4c^2(h-1)^3}{(3h-1)^2(1+3h)^2} - \frac{4c}{1+3h}y + 2y(x-y) = 0. \end{aligned}$$

Since $c \neq 0$, by Lemma 8.2.7, we could not have a third invariant hyperbola.

Now, we need the invariant polynomials which govern the condition $\mathscr{E}_2 = \mathscr{E}_3 = 0$. Firstly, we recall that for these systems we have $\gamma_8 = 42(h-1)(h+1)\mathscr{E}_2\mathscr{E}_3$ and, hence, the condition $\gamma_8 = 0$ is necessary. In order to set $\mathscr{E}_2 = 0$, we use the following parametrization:

$$c = c_1(3h-1)^2, \;\; a = a_1(2h-1)$$

and, then, the condition $\mathscr{E}_2 = 0$ gives $b = 2(h-1)(a_1 + c_1^2)$. Herein, for systems (8.2.16) with

$$f = c = c_1(3h-1)^2, \;\; a = a_1(2h-1), \;\; b = 2(h-1)(a_1 + c_1^2)$$

we calculate

$$\mathscr{E}_3 = 3\big[2c_1^2(1+h)^3 + a_1(1+3h)^2\big], \quad \delta_4 = (h-1)(2h-1)\mathscr{E}_3/2$$

and, hence, the condition $\mathscr{E}_3 = 0$ is equivalent to $\delta_4 = 0$.

It remains to observe that in this case $\mathscr{R}_7 = -3a_1(h-1)^4(h+1)/4 \neq 0$, otherwise $a_1 = 0$ and, then, the condition $\delta_4 = 0$ implies $c_1 = 0$, i.e. $c = 0$ and this contradicts to $\beta_2 \neq 0$. So, we arrive at the statement $(\mathscr{B}_1)$ of the lemma.

The case $\beta_7 = 0$. Then, $(2h-1)(2h+1) = 0$ and, by Remark 8.2.6, we may assume $h = 1/2$. In this case, by Lemma 8.2.7, in order to have at least two hyperbolas, the conditions **II.**; (iii) and **III.**; (i) have to be satisfied simultaneously. Therefore, we arrive at the conditions

$$a = 0, \;\; b + 4c^2 \neq 0, \;\; \mathscr{E}_3 = (50a - 75b + 24c^2)/4 = 0$$

and, as $a = 0$, we have $b = 24c^2/75$ and $b + 4c^2 = 108c^2/25 \neq 0$ due to $\beta_2 \neq 0$. So, we get the family of systems

$$\dot{x} = cx - x(x+y)/2, \quad \dot{y} = 8c^2/25 + cy - y(3x-y)/2 \tag{8.2.21}$$

which possess the following two hyperbolas

$$\Phi_1^{(2)}(x,y) = 216c^2/25 - 8cx + 2x(x-y) = 0, \quad \Phi_2^{(2)}(x,y) = -8c^2/25 - 8cy/5 + 2y(x-y) = 0.$$

These hyperbolas are nondegenerate due to $\beta_2 \neq 0$ (i.e. $c \neq 0$).

We need to determine the affine invariant conditions which are equivalent to $a = \mathscr{E}_3 = 0$. For

systems (8.2.16) with $f = c$ and $h = 1/2$ we calculate

$$\gamma_9 = 3a/2, \quad \delta_5 = -3(25b - 8c^2)/2$$

and obviously these invariant polynomials govern the mentioned conditions. It remains to observe that for systems (8.2.21) we have $\mathscr{R}_8 = 108c^2/25 \neq 0$ due to $\beta_2 \neq 0$. This completes the proof of the statement ($\mathscr{B}_2$) of the lemma.

The case $\beta_2 = 0$. Then, $c = 0$ and, by Lemma 8.2.7, systems (8.2.16) with $f = c = 0$ could possess at least two nondegenerate invariant hyperbolas if, and only if, one of the following sets of conditions hold:

$$\begin{aligned}
&(\phi_1)\ \ \mathscr{E}_1 = \mathscr{E}_2 = 0,\ \ (2h-1)(3h-1) \neq 0,\ \ a \neq 0;\\
&(\phi_2)\ \ \mathscr{E}_1 = \mathscr{E}_3 = 0,\ \ (2h+1)(3h+1) \neq 0,\ \ b \neq 0;\\
&(\phi_3)\ \ \mathscr{E}_2 = \mathscr{E}_3 = 0,\ \ (2h-1)(2h+1)(3h-1)(3h+1) \neq 0,\ \ ab \neq 0;\\
&(\phi_4)\ \ \mathscr{E}_1 = 0,\ \ h = 1/3,\ \ a \neq 0,\ \ 4a - b \geq 0;\\
&(\phi_5)\ \ \mathscr{E}_1 = a = 0,\ \ h = 1/2,\ \ b \neq 0;\\
&(\phi_6)\ \ \mathscr{E}_1 = 0,\ \ h = -1/3,\ \ b \neq 0,\ \ 4b - a \geq 0;\\
&(\phi_7)\ \ \mathscr{E}_1 = b = 0,\ \ h = -1/2,\ \ a \neq 0.
\end{aligned} \tag{8.2.22}$$

As for systems (8.2.16) with $f = c = 0$ we have

$$\beta_7 = -2(2h+1)(2h-1), \quad \beta_{10} = -2(3h+1)(3h-1),$$

we consider two subcases: $\beta_7 \neq 0$ and $\beta_7 = 0$.

The subcase $\beta_7 \neq 0$. Then, $(2h+1)(2h-1) \neq 0$ and we examine two possibilities: $\beta_{10} \neq 0$ and $\beta_{10} = 0$.

1) *The possibility* $\beta_{10} \neq 0$. In this case $(3h+1)(3h-1) \neq 0$. We observe that, due to $f = c = 0$, all the polynomials $\mathscr{E}_i$ are linear (homogeneous) with respect to the parameters a and b. So, each one of the sets of conditions (ϕ_1)–(ϕ_3) could be compatible only if the corresponding determinant vanishes, i.e.

$$\begin{aligned}
&\det(\mathscr{E}_1, \mathscr{E}_2) \Rightarrow \ \ -(2h-1)(3h-1)^2(4h-1) = 0,\\
&\det(\mathscr{E}_1, \mathscr{E}_3) \Rightarrow \ \ (2h+1)(3h+1)^2(4h+1) = 0,\\
&\det(\mathscr{E}_2, \mathscr{E}_3) \Rightarrow \ \ -3(3h-1)^2(3h+1)^2 = 0,
\end{aligned} \tag{8.2.23}$$

otherwise we get the trivial solution $a = b = 0$. Clearly, the third determinant could not be zero due to the condition $\beta_{10} \neq 0$, i.e. the set of conditions (ϕ_3) is incompatible in this case. As regarding the conditions (ϕ_1) (respectively, (ϕ_2)), we observe that they could be compatible only if $4h - 1 = 0$ (respectively, $4h + 1 = 0$).

On the other hand, we have $\beta_8 = -6(4h - 1)(4h + 1)$ and we conclude that,[for the existence of two hyperbolas in these case the condition $\beta_8 = 0$ is necessary.

Assuming $\beta_8 = 0$, we may consider $h = 1/4$ due to Remark 8.2.6 and we obtain

$$\mathscr{E}_1 = (3a - b)/2 = -16\mathscr{E}_2 = 0.$$

So, we get $b = 3a$ and we arrive at the systems

$$\dot{x} = a - x^2/4 - 3xy/4, \quad \dot{y} = 3a - 5xy/4 + y^2/4, \tag{8.2.24}$$

which possess the following two invariant hyperbolas

$$\Phi_1^{(3)}(x, y) = -4a + 2xy = 0, \quad \Phi_2^{(3)}(x, y) = 4a + 2x(x - y) = 0.$$

Clearly, these hyperbolas are nondegenerate if, and only if, $a \neq 0$.

On the other hand, for systems (8.2.16) with $f = c = 0$ and $h = 1/4$ we have

$$\gamma_7 = -15(3a - b), \ \ \gamma_8 = 15435(3a - 5b)(3a - b)/8192,$$
$$\delta_2 = -6(3a - b), \ \ \mathscr{R}_5 = 9(bx - ay)(25x - 9y)(x - y)/4.$$

We observe that the conditions $\mathscr{E}_1 = \mathscr{E}_2 = 0$ and $a \neq 0$ are equivalent to $\gamma_7 = 0$ and $\mathscr{R}_5 \neq 0$. However, in order to insert this possibility in the generic diagram (see Figure 8.1), we remark that these conditions are equivalent to $\gamma_7\gamma_8 = \delta_2 = 0$ and $\mathscr{R}_5 \neq 0$.

It remains to observe that for the systems above we have $\mathscr{E}_3 = 147a/8 \neq 0$ and, hence, we could not have the third hyperbola. So, the statement $(\mathscr{B}_3)$ of the lemma is proved.

2) *The possibility* $\beta_{10} = 0$. In this case $(3h+1)(3h-1) = 0$ and, without loss of generality, we may assume $h = 1/3$ due to the change $(x, y, a, b, h) \mapsto (y, x, b, a, -h)$, which conserves systems (8.2.16) with $f = c = 0$ and transfers the conditions (ϕ_6) to (ϕ_4).

So, $h = 1/3$ and we arrive at the conditions

$$\mathscr{E}_1 = (5a - b)/3 = 0, \;\; 4a - b \geq 0, \;\; a \neq 0,$$

which imply $b = 5a$ and $4a - b = -a \geq 0$. Then, setting $a = -3z^2 \leq 0$ we get the family of systems

$$\dot{x} = -3z^2 - x^2/3 - 2xy/3, \quad \dot{y} = -15z^2 - 4xy/3 + y^2/3, \tag{8.2.25}$$

which possess the following three invariant hyperbolas

$$\Phi_1^{(4)}(x, y) = 18z^2 + 2xy = 0, \quad \Phi_{2,3}^{(4)}(x, y) = -18z^2 \pm 6zx + 2x(x - y) = 0.$$

These hyperbolas are nondegenerate if, and only if, $z \neq 0$ and the hyperbolas $\Phi_{2,3}^{(4)}(x, y) = 0$ have parallel asymptotes, i.e. we have two hyperbolas $\mathscr{H}^p$. Since for systems (8.2.25) we have $\mathscr{E}_3 = -140z^2 \neq 0$, we deduce that these systems could not have an invariant hyperbola with the asymptotes $y = 0$ and $y = x$.

Remark 8.2.10. *We claim that, if the conditions* (ϕ_4) *are satisfied except the condition* $\mathscr{E}_1 = 0$*, then the corresponding systems possess exactly two distinct nondegenerate invariant hyperbolas if* $4a - b > 0$ *and* $a \neq 0$*, and these hyperbolas collapse and we get a hyperbola of multiplicity two if* $4a - b = 0$.

Indeed, providing that the conditions of Remark 8.2.10 hold and setting a new parameter z as follows: $4a - b = 3z^2 \geq 0$, we arrive at the family of systems

$$\dot{x} = a - x^2/3 - 2xy/3, \quad \dot{y} = 4a - 3z^2 - 4xy/3 + y^2/3. \tag{8.2.26}$$

These systems possess the following two invariant hyperbolas

$$\widehat{\Phi}_{2,3}^{(4)}(x, y) = 6a \pm 6zx + 2x(x - y) = 0,$$

which are nondegenerate if, and only if, $a \neq 0$. We observe that, if in addition the condition $5a - b = a + 3z^2 = 0$ (i.e. $a = -3z^2$) holds, we get the family of systems (8.2.25). We also observe that the two hyperbolas $\widehat{\Phi}_{2,3}(x, y) = 0$ are distinct if $z \neq 0$ (i.e. $4a - b > 0$) whereas in the case $4a - b = 0$ these hyperbolas collapse and we get a hyperbola of multiplicity two.

Thus, we arrive at the following statement:

- if $\mathscr{E}_1 \neq 0$, $4a-b>0$ and $a\neq 0$ we have 2 invariant hyperbolas $\mathscr{H}^p$;
- if $\mathscr{E}_1 \neq 0$, $4a-b=0$ and $a\neq 0$ we have one double invariant hyperbola $\mathscr{H}^p_2$.
- if $\mathscr{E}_1 = 0$, $4a-b>0$ and $a\neq 0$ we have 3 invariant hyperbolas (two of them being $\mathscr{H}^p$);

To determine the corresponding invariant conditions, for systems (8.2.16) with $c=f=0$ and $h=1/3$ we calculate

$$\gamma_7 = -64(5a-b)/27, \quad \gamma_{10} = 8(4a-b)/27, \quad \mathscr{R}_3 = -4a/9.$$

Considering the conditions above, it is easy to observe that the corresponding invariant conditions are given by the statements $(\mathscr{B}_4)$, $(\mathscr{C})$ and $(\mathscr{A})$, respectively.

The subcase $\beta_7 = 0$. Then, $(2h+1)(2h-1)=0$ and, by Remark 8.2.6, we may assume $h = 1/2$. Considering (8.2.23), we conclude that only the case (ϕ_5) could be satisfied and we get the additional conditions: $a=0,\ b\neq 0$. Therefore, we arrive at the family of systems

$$\dot{x} = -x^2/2 - xy/2, \quad \dot{y} = b - 3xy/2 + y^2/2, \tag{8.2.27}$$

which possess the following two hyperbolas

$$\Phi^{(5)}_1,(x,y) = -b+2xy = 0, \quad \Phi^{(5)}_2(x,y) = 2b+2x(x-y) = 0.$$

We observe that the condition $a=0$ is equivalent to $\gamma_7 = -12a = 0$. As regarding the condition $b\neq 0$, in the case $a=0$, it is equivalent to $\mathscr{R}_3 = -b/16 \neq 0$. Since for these systems we have $\mathscr{E}_3 = 75b/4 \neq 0$, we deduce that we could not have a third nondegenerate invariant hyperbola. This completes the proof of the statement $(\mathscr{B}_5)$ of the lemma.

Since all the cases are examined, Lemma 8.2.9 is proved. ∎

The case $\widetilde{N}=0$

As $\theta = -(g-1)(h-1)(g+h)/2 = 0$, we observe that the condition $\widetilde{N}=0$ implies the vanishing of two factors of θ. We may assume $g=1=h$, otherwise in the case $g+h=0$ and $g-1\neq 0$ (respectively, $h-1\neq 0$) we apply the change $(x,y,g,h)\mapsto(-y,x-y,1-g-h,g)$ (respectively, $(x,y,g,h)\mapsto (y-x,-x,h,1-g-h)$) which preserves the form of systems (8.2.1).

So, $g = h = 1$ and due to an additional translation systems (8.2.1) become

$$\dot{x} = a + dy + x^2, \quad \dot{y} = b + ex + y^2. \tag{8.2.28}$$

Lemma 8.2.11. *A system* (8.2.28) *possesses at least one nondegenerate invariant hyperbola of the indicated form if, an only if, the respective conditions are satisfied:*

I. $\Phi(x,y) = p + qr + ry + 2xy \;\Leftrightarrow\; d = e = 0$ *and* $a - b = 0$*;*

II. $\Phi(x,y) = p + qr + ry + 2x(x-y) \;\Leftrightarrow\; d = 0,\ \mathscr{M}_1 \equiv 64a - 16b - e^2 = 0,\ 16a + e^2 \neq 0$*;*

III. $\Phi(x,y) = p + qr + ry + 2y(x-y) \;\Leftrightarrow\; e = 0,\ \mathscr{M}_2 \equiv 64b - 16a - d^2 = 0,\ 16b + d^2 \neq 0.$

Proof. As it was mentioned in the proof of Lemma 8.2.2 (see page 285), we may assume that the quadratic part of an invariant hyperbola has one of the following forms: $(i)\ 2xy$, $(ii)\ 2x(x-y)$, $(iii)\ 2y(x-y)$. Considering the equations (8.1.3), we examine each one of these possibilities.

(i) $\Phi(x,y) = p + qx + ry + 2xy$: in this case we obtain

$$t = 1,\ s = u = 0,\ p = (4b + q^2 + qr)/2,\ U = 1,\ V = 1,\ W = -(q+r)/2,$$
$$Eq_9 = (4a - 4b - q^2 + r^2)/2,\ \ Eq_{10} = 4aq + 4b(q+2r) + q(q+r)^2,$$
$$Eq_1 = Eq_2 = Eq_3 = Eq_4 = Eq_5 = Eq_6 = Eq_7 = Eq_8 = 0.$$

Calculating the resultant of the nonvanishing equations with respect to the parameter r we obtain

$$\mathrm{Res}_r(Eq_9, Eq_{10}) = (a-b)(4b+q^2)^2/4.$$

If $b = -q^2/4$, then we get the hyperbola $\Phi(x,y) = (r+2x)(q+2y)/2 = 0$, which is degenerate.

Thus, $b = a$ and we obtain

$$Eq_9 = -(q-r)(q+r)/2 = 0,\ \ Eq_{10} = (q+r)(8a + q^2 + qr)/4 = 0.$$

It is not too difficult to observe that the case $q + r \neq 0$ (then $q = r$) leads to degenerate hyperbola (as we obtain $b = a = -q^2/4$, see the case above). So, $q = -r$ and the above equations are satisfied. This leads to the invariant hyperbola $\Phi(x,y) = 2a - rx + ry + 2xy = 0$. Considering Remark 8.1.7, we calculate $\Delta = -(4a + r^2)/2$. So, the hyperbola above is nondegenerate if, and only if, $4a + r^2 \neq 0$.

Thus, any system belonging to the family

$$\dot{x} = a + x^2, \quad \dot{y} = a + y^2 \tag{8.2.29}$$

possesses an 1−parametric family of nondegenerate invariant hyperbolas $\Phi(x,y) = 2a - r(x-y) + 2xy = 0$, where $r \in \mathbb{R}$ is a parameter satisfying the relation $4a + r^2 \neq 0$. This completes the proof of the statement **I.** of the lemma.

(ii) $\Phi(x,y) = p + qx + ry + 2x(x-y)$: in this case we obtain

$$s = 2,\ t = -1,\ u = 0,\ p = (8a - 4b + 4de - 2e^2 + q^2)/4,$$
$$r = 2d - e - q,\ U = 2,\ V = 1,\ W = -(2e+q)/2,\ \ Eq_7 = -2d$$

and, hence, the condition $d = 0$ is necessary. Then, we calculate

$$Eq_1 = Eq_2 = Eq_3 = Eq_4 = Eq_5 = Eq_6 = Eq_7 = Eq_8 = 0,$$
$$Eq_9 = -4a + b - (2e^2 + 6eq + 3q^2)/4,$$
$$Eq_{10} = \left[16a(e+q) - 4b(4e+3q) + (2e+q)(q^2 - 2e^2)\right]/8$$

and

$$\mathrm{Res}_q(Eq_9, Eq_{10}) = -(64a - 16b - e^2)(4a - 4b - e^2)^2/256.$$

1) Assume first $64a - 16b - e^2 = 0$. Then, $b = 4a - e^2/16$ and we obtain

$$Eq_9 = -3(e+2q)(3e+2q)/16 = 0,\ \ Eq_{10} = -(3e+2q)(64a + 4e^2 - eq - 2q^2)/32 = 0.$$

1a) If $q = -3e/2$, then all the equations vanish and we arrive at the invariant hyperbola

$$\Phi(x,y) = -2a + e^2/8 + e(-3x+y)/2 + 2x(x-y) = 0$$

for which we calculate $\Delta = (16a + e^2)/8$. Therefore, this hyperbola is nondegenerate if, and only if, $16a + e^2 \neq 0$.

1b) In the case $3e + 2q \neq 0$ we have $q = -e/2 \neq 0$ and the equation $Eq_{10} = 0$ implies $e(16a + e^2) = 0$. Therefore, due to $e \neq 0$ we obtain $16a + e^2 = 0$. However, in this case we have the hyperbola

$$\Phi(x,y) = -(16a + 3e^2)/8 - e(x+y)/2 + 2x(x-y) = 0,$$

whose determinant equals $(16a + e^2)/8$ and, hence, the condition above leads to a nondegenerate hyperbola.

2) Suppose now $4a - 4b - e^2 = 0$, i.e. $b = a - e^2/4$. Herein, we obtain

$$Eq_9 = -3\left[4a + (e+q)^2\right]/4 = 0, \;\; Eq_{10} = q\left[4a + (e+q)^2\right]/8 = 0$$

and the hyperbola

$$\Phi(x,y) = 2x(x-y) + qx - (e+q)y + (4a - e^2 + q^2)/4 = 0,$$

for which we calculate $\Delta = -[4a + (e+q)^2]/4$. Obviously, the condition $Eq_9 = 0$ implies $\Delta = 0$ and, hence, the invariant hyperbola is degenerate. So, in the case $d = 0$ and $4a - 4b - e^2 = 0$, systems (8.2.28) could not possess a nondegenerate invariant hyperbola and the statement **II.** of the lemma is proved.

(iii) $\Phi(x,y) = p + qx + ry + 2y(x-y)$: we observe that due to the change $(x,y,a,b,d,e) \mapsto (y,x,b,a,e,d)$ (which preserves systems (8.2.28)) this case could be brought to the previous one and, hence, the conditions could be constructed directly applying this change.

Thus Lemma 8.2.11 is proved. ∎

Lemma 8.2.12. *Assume that for a quadratic system* (8.1.2) *the conditions* $\eta > 0$ *and* $\theta = \widetilde{N} = 0$ *hold. Then, this system could possess either a single nondegenerate invariant hyperbola or a family of these hyperbolas. More precisely, it possesses:*

(i) one irreducible invariant hyperbola if, and only if, $\beta_1 = 0$, $\mathscr{R}_9 \neq 0$ *and either* $(i.1)$ $\beta_2 \neq 0$ *and* $\gamma_{11} = 0$, *or* $(i.2)$ $\beta_2 = \gamma_{12} = 0$;

(ii) a family of such hyperbolas if, and only if, $\beta_1 = \beta_2 = \gamma_{13} = 0$.

Moreover, the family of hyperbolas corresponds to $(\mathscr{F}_1)$ *(respectively,* $(\mathscr{F}_2)$*;* $(\mathscr{F}_3)$*) (see Figure 8.3) if* $\mathscr{R}_9 < 0$ *(respectively,* $\mathscr{R}_9 = 0$*;* $\mathscr{R}_9 > 0$*).*

Proof. For systems (8.2.28) we calculate

$$\begin{aligned}
\beta_1 &= 4de, \quad \beta_2 = -2(d+e),\\
\gamma_{11} &= 19de(d+e) + e\mathscr{M}_1 + d\mathscr{M}_2,\\
\mathscr{R}_9\big|_{d=0} &= \left[5(16a + e^2) - \mathscr{M}_1\right]/2,\\
\mathscr{R}_9\big|_{e=0} &= \left[5(16b + d^2) - \mathscr{M}_2\right]/2.
\end{aligned}$$

By Lemma 8.2.11, the condition $de = 0$ (i.e. $\beta_1 = 0$) is necessary for a system (8.2.28) to possess an invariant hyperbola.

The subcase $\beta_2 \neq 0$. Then, $d^2 + e^2 \neq 0$ and considering the values of the above invariant polynomials, by Lemma 8.2.11, we deduce that the statement $(i.1)$ of the lemma is proved.

The subcase $\beta_2 = 0$. In this case we get $d = e = 0$ and we calculate

$$\gamma_{13} = 4(a-b), \quad \mathscr{R}_9 = 8(a+b), \quad \gamma_{12} = -128(a-4b)(4a-b) = \mathscr{M}_1\mathscr{M}_2/2.$$

Therefore, by Lemma 8.2.11, in the case $\gamma_{12} = 0$ we arrive at the statement $(i.2)$, whereas for $\gamma_{13} = 0$ we arrive at the statement (ii) of the lemma.

It remains to observe that, if systems (8.2.28) possess the mentioned family of invariant hyperbolas, then they have the form (8.2.29), depending on the parameter a. We may assume $a \in \{-1, 0, 1\}$ due to the rescaling $(x, y, t) \mapsto (|a|^{1/2}x, |a|^{1/2}y, |a|^{-1/2}t)$. In such a way, we arrive at the three families mentioned in Remark 8.1.4. ∎

8.2.3 Systems with two real distinct infinite singularities and $\theta \neq 0$

For this family of systems, by Lemma 8.1.5, the conditions $\eta = 0$ and $\widetilde{M} \neq 0$ are satisfied and, then, via a linear transformation and time rescaling, systems (8.1.2) could be brought to the following family of systems:

$$\begin{aligned} \dot{x} &= a + cx + dy + gx^2 + hxy, \\ \dot{y} &= b + ex + fy + (g-1)xy + hy^2. \end{aligned} \tag{8.2.30}$$

For this systems we calculate

$$C_2(x, y) = x^2 y, \quad \theta = -h^2(g-1)/2 \tag{8.2.31}$$

and, since $\theta \neq 0$, due to a translation we may assume $d = e = 0$. So, in what follows we consider the family of systems

$$\begin{aligned} \dot{x} &= a + cx + gx^2 + hxy, \\ \dot{y} &= b + fy + (g-1)xy + hy^2. \end{aligned} \tag{8.2.32}$$

Lemma 8.2.13. *A system* (8.2.32) *could not posses more than one nondegenerate invariant hyperbola. And it possesses one such hyperbola if, an only if,* $c + f = 0$, $\mathscr{G}_1 \equiv a(1-2g) + 2bh = 0$ *and*

$a \neq 0$.

Proof. Since $C_2 = x^2 y$, we may assume that the quadratic part of an invariant hyperbola has the form $2xy$. Considering equations (8.1.3) and the condition $\theta \neq 0$ (i.e. $h(g-1) \neq 0$), for systems (8.2.32) we obtain

$$t = 1,\ s = u = q = r = 0,\ p = a/h,\ U = 2g - 1,\ V = 2h,\ W = c + f,$$
$$Eq_8 = (a - 2ag + 2bh)/h = \mathscr{G}_1/h,\ \ Eq_{10} = -a(c+f)/h,$$
$$Eq_1 = Eq_2 = Eq_3 = Eq_4 = Eq_5 = Eq_6 = Eq_7 = Eq_9 = 0.$$

Since the hyperbola (8.1.1) in this case becomes $\Phi(x,y) = a/h + 2xy = 0$, the condition $a \neq 0$ is necessary in order to have a nondegenerate invariant hyperbola. Then, the equation $Eq_{10} = 0$ implies $c + f = 0$ and the condition $Eq_8/h = 0$ yields $\mathscr{G}_1 = 0$. Since $h \neq 0$, we set $b = a(2g-1)/(2h)$ and this leads to the family of systems

$$\dot{x} = a + cx + gx^2 + hxy, \quad \dot{y} = \frac{a(2g-1)}{2h} - cy + (g-1)xy + hy^2, \tag{8.2.33}$$

which possess the following nondegenerate invariant hyperbola

$$\Phi(x,y) = \frac{a}{h} + 2xy = 0.$$

This completes the proof of the lemma. ∎

Next, we determine the corresponding affine invariant conditions.

Lemma 8.2.14. *Assume that for a quadratic system* (8.1.2) *the conditions* $\eta = 0$, $\widetilde{M} \neq 0$ *and* $\theta \neq 0$ *hold. Then, this system possesses a single nondegenerate invariant hyperbola (which could be simple or double) if, and only if, one of the following sets of the conditions holds:*

(i) $\beta_2\beta_1 \neq 0$, $\gamma_1 = \gamma_2 = 0$, $\mathscr{R}_1 \neq 0$*: simple;*

(ii) $\beta_2 \neq 0$, $\beta_1 = \gamma_1 = \gamma_4 = 0$, $\mathscr{R}_3 \neq 0$*: simple if* $\delta_1 \neq 0$ *and double if* $\delta_1 = 0$*;*

(iii) $\beta_2 = \beta_1 = \gamma_{14} = 0$, $\mathscr{R}_{10} \neq 0$*: simple if* $\beta_7\beta_8 \neq 0$ *and double if* $\beta_7\beta_8 = 0$.

Proof. For systems (8.2.32) we calculate

$$\gamma_1 = (2c - f)(c+f)^2 h^4 (g-1)^2/32, \quad \beta_2 = h^2(2c - f)/2.$$

According to Lemma 8.1.6, for the existence of a nondegenerate invariant hyperbola the condition $\gamma_1 = 0$ is necessary and, therefore, we consider two cases: $\beta_2 \neq 0$ and $\beta_2 = 0$.

The case $\beta_2 \neq 0$

Then, $2c - f \neq 0$ and the condition $\gamma_1 = 0$ implies $f = -c$. So, we calculate

$$\gamma_2 = 14175c^2h^5(g-1)^2(3g-1)\mathscr{G}_1, \quad \beta_2 = 3ch^2/2,$$
$$\beta_1 = -3c^2h^2(g-1)(3g-1)/4, \quad \mathscr{R}_1 = -9achh^4(g-1)^2(3g-1)/8$$

and we examine two subcases: $\beta_1 \neq 0$ and $\beta_1 = 0$.

The subcase $\beta_1 \neq 0$. Then, the necessary condition $\gamma_2 = 0$ (see Lemma 8.1.6) gives $\mathscr{G}_1 = 0$ and, by Lemma 8.2.13, systems (8.2.32) possess an invariant hyperbola. We claim that this hyperbola could not be double. Indeed, since the condition $\theta \neq 0$ holds, we apply Lemma 8.2.5 which provides necessary and sufficient conditions in order to have at least two hyperbolas. According to this lemma, the condition $\beta_1 = 0$ is necessary for the existence of at least two hyperbolas. So, it is clear that in this case the hyperbola of systems (8.2.33) could not be double due to $\beta_1 \neq 0$. This completes the proof of the statement (i) of the lemma.

The subcase $\beta_1 = 0$. Due to $\beta_2 \neq 0$ (i.e. $c \neq 0$), we have $g = 1/3$ and, then, $\gamma_2 = 0$ and

$$\gamma_4 = 16h^6(a+6bh)^2/3 = 48h^6\mathscr{G}_1^2, \quad \mathscr{R}_3 = 3bh^3/2.$$

Therefore, the condition $\gamma_4 = 0$ is equivalent to $\mathscr{G}_1 = 0$ and in this case $\mathscr{R}_3 \neq 0$ gives $b \neq 0$ which is equivalent to $a \neq 0$. By Lemma 8.2.13, systems (8.2.32) possess a nondegenerate hyperbola. We claim that this hyperbola is double if, and only if, the condition $a = -12c^2$ holds.

Indeed, as we would like after some perturbation to have two hyperbolas, then the respective conditions provided by Lemma 8.2.5 must hold. We calculate:

$$\beta_1 = 0, \ \ \beta_2 = 3ch^2/2, \ \ \beta_6 = ch/3, \ \ \gamma_4 = 0, \ \ \delta_1 = -(a+12c^2)h^2/4$$

and, since $\beta_6 \neq 0$ (due to $\beta_2 \neq 0$), we could have a double hyperbola only if the identities provided by the statement $(\mathscr{A}_1)$ are satisfied. Therefore, the condition $\delta_1 = 0$ is necessary and, due to $\theta \neq 0$ (i.e. $h \neq 0$), we obtain $a = -12c^2$.

So, our claim is proved and we get the family of systems

$$\dot{x} = -12c^2 + cx + x^2/3 + hxy, \quad \dot{y} = 2c^2/h - cy - 2xy/3 + hy^2, \tag{8.2.34}$$

which possess the hyperbola $\Phi(x,y) = -12c^2/h + 2xy = 0$. The perturbed systems

$$\begin{aligned} \dot{x} &= -\frac{18c^2(2h+\varepsilon)(3h+\varepsilon)}{(3h-\varepsilon)^2} + cx + x^2/3 + (h+\varepsilon)xy, \\ \dot{y} &= \frac{6c^2(3h+\varepsilon)}{(3h-\varepsilon)^2} - cy - 2xy/3 + hy^2, \quad |\varepsilon| \ll 1 \end{aligned} \tag{8.2.35}$$

possess the following two distinct invariant hyperbolas:

$$\Phi_1^\varepsilon(x,y) = -\frac{36c^2(3h+\varepsilon)}{(3h-\varepsilon)^2} + 2xy = 0, \quad \Phi_2^\varepsilon(x,y) = -\frac{36c^2(3h+\varepsilon)}{(3h-\varepsilon)^2} - \frac{12c\varepsilon}{3h-\varepsilon}\, y + 2y(x+\varepsilon y) = 0.$$

It remains to observe that the hyperbola $\Phi(x,y) = -12c^2/h + 2xy = 0$ could not be triple, because in this case for systems (8.2.34) the necessary conditions provided by the statement ($\mathscr{B}$) of Lemma 8.2.5 to have three invariant hyperbolas are not satisfied: we have $\beta_6 \neq 0$.

Thus the statement (ii) of the lemma is proved.

The case $\beta_2 = 0$

Then, $f = 2c$ and this implies $\gamma_1 = 0$. On the other hand, we calculate

$$\gamma_2 = -14175ac^2(g-1)^3(1+3g)h^5, \quad \beta_1 = -9c^2(g-1)^2h^2/16$$

and, since $f = 2c$, according to Lemma 8.2.13, the condition $c = 0$ is necessary in order to have a nondegenerate invariant hyperbola. The condition $c = 0$ is equivalent to $\beta_1 = 0$ and this implies $\gamma_2 = 0$. It remains to detect invariant polynomials which govern the conditions $\mathscr{G}_1 = 0$ and $a \neq 0$. For $c = 0$ we have

$$\gamma_{14} = 80h^3\big[a(1-2g) + 2bh\big] = 80h^3\mathscr{G}_1, \quad \mathscr{R}_{10} = -4ah^2.$$

So, for $\beta_1 = \beta_2 = 0$, $\gamma_{14} = 0$ and $\mathscr{R}_{10} \neq 0$, systems (8.2.33) (with $c = 0$) possess the invariant hyperbola $\Phi(x,y) = a/h + 2xy = 0$.

Next, we shall determine the conditions under which this hyperbola is simple or double. In accordance with Lemma 8.2.5, we calculate:

$$\beta_1 = \beta_6 = 0, \beta_7 = -8(2g-1)h^2.$$

We examine two possibilities: $\beta_7 \neq 0$ and $\beta_7 = 0$.

The possibility $\beta_7 \neq 0$. According to Lemma 8.2.5, for systems (8.2.33) with $c = 0$ could be satisfied only the identities given by the statement ($\mathscr{A}_2$). So, we have to impose the following conditions:

$$\gamma_5 = \beta_8 = \delta_2 = 0.$$

We have $\beta_8 = -32(4g-1)h^2 = 0$, which implies $g = 1/4$. Then, we obtain $\gamma_5 = \delta_2 = 0$ and we get the family of systems

$$\dot{x} = a + x^2/4 + hxy, \quad \dot{y} = -a/(4h) - 3xy/4 + hy^2, \tag{8.2.36}$$

which possess the hyperbola $\Phi(x,y) = a/h + 2xy = 0$. On the other hand, we observe that the perturbed systems

$$\dot{x} = a + \frac{\varepsilon}{2h} + x^2/4 + (h+\varepsilon)xy, \quad \dot{y} = -a/(4h) - 3xy/4 + hy^2, \tag{8.2.37}$$

possess the following two distinct invariant hyperbolas:

$$\Phi_1^\varepsilon(x,y) = a/h + 2xy = 0, \quad \Phi_2^\varepsilon(x,y) = a/h + 2y(x+\varepsilon y) = 0.$$

Since $\beta_7 \neq 0$, according to Lemma 8.2.5, the hyperbola $\Phi(x,y) = a/h + 2xy = 0$ could not be triple.

The possibility $\beta_7 = 0$. In this case we get $g = 1/2$ and this implies $\gamma_8 = \delta_3 = 0$. Hence, the identities given by the statement ($\mathscr{A}_3$) of Lemma 8.2.5 are satisfied. In this case we obtain the family of systems

$$\dot{x} = a + x^2/2 + hxy, \quad \dot{y} = -xy/2 + hy^2, \tag{8.2.38}$$

which possess the hyperbola $\Phi(x,y) = a/h + 2xy = 0$. On the other hand, we observe that the perturbed systems

$$\dot{x} = a + x^2/2 + (h+\varepsilon)xy, \quad \dot{y} = -xy/2 + hy^2, \tag{8.2.39}$$

possess the following two distinct invariant hyperbolas:

$$\Phi_1^\varepsilon(x,y) = \frac{2a}{2h+\varepsilon} + 2xy = 0, \quad \Phi_2^\varepsilon(x,y) = a/h + 2y(x+\varepsilon y) = 0.$$

Since for systems (8.2.38) we have $\beta_8 = -32h^2 \neq 0$, according to Lemma 8.2.5, the hyperbola $\Phi(x,y) = a/h + 2xy = 0$ could not be triple.

It remains to observe that the conditions of the statement ($\mathscr{B}$) of Lemma 8.2.5 in order to have three invariant hyperbolas could not be satisfied for systems (8.2.33) (i.e. the necessary conditions

for these systems to possess a triple hyperbola). Indeed, for systems (8.2.33) we have

$$\beta_7 = -8(2g-1)h^2, \quad \beta_8 = -32(4g-1)h^2, \quad \theta = -(g-1)h^2/2$$

and, hence, the conditions $\beta_7 = 0$ and $\beta_8 = 0$ are incompatible due to $\theta \neq 0$.

As all the cases are examined, we deduce that Lemma 8.2.14 is proved. ■

8.2.4 Systems with two real distinct infinite singularities and $\theta = 0$

By Lemma 8.1.5, via a linear transformation, systems (8.1.2) could be brought to the systems (8.2.30) for which we have

$$\theta = -h^2(g-1)/2, \quad \beta_4 = 2h^2, \quad \widetilde{N} = (g^2-1)^2x^2 + 2h(g-1)xy + h^2y^2. \tag{8.2.40}$$

We shall consider to cases: $\widetilde{N} \neq 0$ and $\widetilde{N} = 0$.

The case $\widetilde{N} \neq 0$

Since $\theta = 0$, we obtain $h(g-1) = 0$ and $(g^2-1)^2 + h^2 \neq 0$. So, we examine two subcases: $\beta_4 \neq 0$ and $\beta_4 = 0$.

The subcase $\beta_4 \neq 0$. Then, $h \neq 0$ (this implies $\widetilde{N} \neq 0$) and we get $g = 1$. Applying a translation and the additional rescaling $y \to y/h$, we may assume $c = f = 0$ and $h = 1$. So, in what follows we consider the family of systems

$$\dot{x} = a + dy + x^2 + xy, \quad \dot{y} = b + ex + y^2. \tag{8.2.41}$$

Lemma 8.2.15. *A system* (8.2.41) *possesses a nondegenerate invariant hyperbola if, and only if,* $e = 0$, $\mathscr{L}_1 \equiv 9a - 18b + d^2 = 0$ *and* $a + d^2 \neq 0$.

Proof. Since $C_2 = x^2y$, we determine that the quadratic part of an invariant hyperbola has the form $2xy$. Considering equations (8.1.3) for systems (8.2.41), we obtain

$$t = 1,\ s = u = 0,\ \ r = 2d,\ p = 2b + 2de + dq + q^2/2,$$
$$U = 1,\ V = 2,\ W = -(q+r)/2,\ \ Eq_5 = e,$$
$$Eq_1 = Eq_2 = Eq_3 = Eq_4 = Eq_6 = Eq_7 = Eq_8 = 0.$$

Therefore, the condition $Eq_5 = 0$ yields $e = 0$ and, then, we have

$$Eq_9 = 2a - 4b + 2d^2 - q^2, \quad Eq_{10} = aq + b(4d + q) + q(2d + q)^2/4.$$

Clearly, in order to have a common solution of the equations $Eq_9 = Eq_{10} = 0$ with respect to the parameter q, the condition

$$\mathrm{Res}_q\,(Eq_9, Eq_{10}) = (a + d^2)^2(9a - 18b + d^2)/2 = 0$$

is necessary. We claim that the condition $a + d^2 = 0$ leads to a degenerate hyperbola. Indeed, setting $a = -d^2$, we get $Eq_9 = -(4b + q^2) = 0$. On the other hand, we get the hyperbola

$$\Phi(x, y) = 2b + dq + q^2/2 + qx + 2dy + 2xy = 0$$

for which, by considering Remark 8.1.7, we calculate $\Delta = -(4b + q^2)/2$. Therefore, the equation $Eq_9 = -(4b + q^2) = 0$ leads to a degenerate invariant hyperbola. This proves our claim.

So, $a + d^2 \neq 0$ and we set $b = (9a + d^2)/18$. Then, $Eq_9 = 0$ gives $(4d - 3q)(4d + 3q) = 0$ and we examine two subcases: $q = 4d/3$ and $q = -4d/3$.

1) Assuming $q = 4d/3$, we get $Eq_{10} = 4d(a + d^2) = 0$. Since $a + d^2 \neq 0$, we have $d = 0$ and this leads to the family of systems

$$\dot{x} = a + x^2 + xy, \quad \dot{y} = a/2 + y^2. \tag{8.2.42}$$

These systems possess the invariant hyperbola $\Phi(x, y) = a + 2xy = 0$.

2) Suppose now $q = -4d/3$. This implies $Eq_{10} = 0$ and we obtain the systems

$$\dot{x} = a + dy + x^2 + xy, \quad \dot{y} = (9a + d^2)/18 + y^2, \tag{8.2.43}$$

which possess the invariant hyperbola

$$\Phi_1(x, y) = (3a - d^2)/3 - 2d(2x - 3y)/3 + 2xy = 0.$$

Its determinant Δ equals $-(a + d^2)$ and, hence, the hyperbola is nondegenerate if, and only if, $a + d^2 \neq 0$.

It remains to observe that the family of systems (8.2.42) is a subfamily of the family (8.2.43) (corresponding to $d = 0$) and this completes the proof of the lemma. ■

The subcase $\beta_4 = 0$. This implies $h = 0$ and the condition $\widetilde{N} \neq 0$ gives $g^2 - 1 \neq 0$. Using a translation, we may assume $e = f = 0$ and we arrive at the family of systems

$$\dot{x} = a + cx + dy + gx^2, \quad \dot{y} = b + (g-1)xy. \tag{8.2.44}$$

Lemma 8.2.16. *A system* (8.2.44) *possesses at least one nondegenerate invariant hyperbola if, and only if,* $d = 0$, $2g - 1 \neq 0$ *and either*

(i) $3g - 1 \neq 0$, $\mathcal{K}_1 \equiv c^2(1-2g) + a(3g-1)^2 = 0$ *and* $b \neq 0$, *or*

(ii) $g = 1/3$, $c = 0$, $a \leq 0$ *and* $b \neq 0$.

Moreover, in the second case we have two hyperbolas ($\mathcal{H}^p$), *if* $a < 0$, *and we have one double hyperbola* ($\mathcal{H}_2^p$), *if* $a = 0$.

Proof. We assume that the quadratic part of an invariant hyperbola has the form $2xy$ and considering equations (8.1.3), for systems (8.2.44) we obtain

$$t = 1,\ s = u = q = 0,\ U = 2g - 1,\ V = 0,\ W = c - gr/2,$$
$$Eq_7 = 2d,\ \ Eq_8 = 2b + p(1-2g),\ \ Eq_9 = 2a - cr + gr^2/2,$$
$$Eq_{10} = br - cp + gpr/2,\ \ Eq_1 = Eq_2 = Eq_3 = Eq_4 = Eq_5 = Eq_6 = 0.$$

Therefore, the condition $Eq_7 = 0$ yields $d = 0$ and we claim that the condition $2g - 1 \neq 0$ must hold. Indeed, supposing $g = 1/2$, the equation $Eq_8 = 0$ yields $b = 0$ and then

$$Eq_9 = 2a + r(r - 4c)/4 = 0, \quad Eq_{10} = p(r - 4c)/4 = 0.$$

Since $p \neq 0$ (otherwise we get a degenerate hyperbola), we obtain $r = 4c$. However, in this case $Eq_9 = 0$ implies $a = 0$ and we arrive at degenerate systems. This completes the proof of our claim.

Thus, we have $2g - 1 \neq 0$ and, then, the equation $Eq_8 = 0$ gives $p = 2b/(2g-1)$ and we obtain:

$$Eq_{10} = b(2c + r - 3gr))/(1 - 2g).$$

Since in this case the hyperbola is of the form

$$\Phi(x,y)=\frac{2b}{2g-1}+ry+2xy=0,$$

it is clear that the condition $b\neq 0$ must hold and, therefore, we get $2c+r(1-3g)=0$.

1) Assume first $3g-1\neq 0$. Then, we obtain $r=2c/(3g-1)$ and the equation $Eq_9=0$ becomes

$$Eq_9=\frac{2}{(3g-1)^2}\left[c^2(1-2g)+a(3g-1)^2\right]=\frac{2}{(3g-1)^2}\mathscr{K}_1=0.$$

The condition $\mathscr{K}_1=0$ implies $a=c^2(2g-1)/(3g-1)^2$ and we arrive at the family of systems

$$\dot{x}=\frac{c^2(2g-1)}{(3g-1)^2}+cx+gx^2,\quad \dot{y}=b+(g-1)xy, \tag{8.2.45}$$

possessing the invariant hyperbola

$$\Phi(x,y)=\frac{2b}{2g-1}+\frac{2c}{3g-1}y+2xy=0,$$

which is nondegenerate if, and only if, $b\neq 0$.

2) Suppose now $g=1/3$. In this case the equation $Eq_{10}=0$ yields $c=0$ and, then, we get $p=-6b$ and the equation $Eq_9=0$ becomes $Eq_9=(12a+r^2)/6=0$. Therefore, for the existence of an invariant hyperbola, the condition $a\leq 0$ is necessary. In this case, setting $a=-3z^2\leq 0$, we arrive at the family of systems

$$\dot{x}=-3z^2+x^2/3,\quad \dot{y}=b-2xy/3, \tag{8.2.46}$$

possessing the following two invariant hyperbolas

$$\Phi_{1,2}(x,y)=-6b\pm 6z\,y+2xy=0,$$

which are nondegenerate if, and only if, $b\neq 0$. Clearly, these hyperbolas coincide (and we obtain the double one) if $z=0$. ■

Lemma 8.2.17. *Assume that for a quadratic system* (8.1.2) *the conditions* $\eta=0$, $\widetilde{M}\neq 0$, $\theta=0$ *and* $\widetilde{N}\neq 0$ *are satisfied. Then, this system could possess either a single nondegenerate invariant hyperbola, or two distinct* ($\mathscr{H}^p$) *such hyperbolas, or one triple invariant hyperbola. More precisely,*

it possesses:

(i) one nondegenerate invariant hyperbola if, and only if, either

(i.1) $\beta_4 \neq 0$, $\beta_3 = \gamma_8 = 0$ *and* $\mathscr{R}_7 \neq 0$ *(simple, if* $\delta_4 \neq 0$*, and double, if* $\delta_4 = 0$*), or*

(i.2) $\beta_4 = \beta_6 = 0$, $\beta_{11}\mathscr{R}_{11} \neq 0$, $\beta_{12} \neq 0$ *and* $\gamma_{15} = 0$ *(simple, if* $\gamma_{16}^2 + \delta_6^2 \neq 0$*, and double, if* $\gamma_{16} = \delta_6 = 0$*);*

(ii) two distinct nondegenerate invariant hyperbolas ($\mathscr{H}^p$) *if, and only if,* $\beta_4 = \beta_6 = 0$, $\beta_{11}\mathscr{R}_{11} \neq 0$, $\beta_{12} = \gamma_{16} = 0$ *and* $\gamma_{17} < 0$ *(both simple);*

(iii) one triple nondegenerate invariant hyperbola (which splits into three distinct hyperbolas, two of them being ($\mathscr{H}^p$)*) if, and only if,* $\beta_4 = \beta_6 = 0$, $\beta_{11}\mathscr{R}_{11} \neq 0$, $\beta_{12} = \gamma_{16} = 0$ *and* $\gamma_{17} = 0$.

Proof. Assume that for a quadratic system (8.1.2) the conditions $\eta = 0$, $\widetilde{M} \neq 0$, $\theta = 0$ and $\widetilde{N} \neq 0$ are satisfied.

The case $\beta_4 \neq 0$. As it was shown earlier, in this case via an affine transformation and time rescaling, the system could be brought to the form (8.2.41), for which we calculate

$$\gamma_1 = -9de^2/8, \quad \beta_3 = -e/4,$$

and, by Lemma 8.2.15, the condition $\beta_3 = 0$ is necessary in order to have an invariant hyperbola. In this case we obtain

$$\gamma_8 = 42(9a - 18b + d^2)^2 = 42\mathscr{L}_1^2, \quad \mathscr{R}_7 = -\mathscr{L}_1/8 - (a + d^2)/3$$

and, considering Lemma 8.2.15, for $\beta_3 = \gamma_8 = 0$ we get systems (8.2.43) possessing the hyperbola $\Phi(x, y) = (3a - d^2)/3 - 2d(2x - 3y)/3 + 2xy = 0$. To detect its multiplicity we apply Lemma 8.1.8 setting $k = 2$. So, in order to have the polynomial $\Phi(x, y)$ as a double factor in $\mathscr{E}_k$, we force its cofactor in $\mathscr{E}_2$ to be zero along the curve $\Phi(x, y) = 0$ (i.e. we set $y = (-3a + d^2 + 4dx)/(6(d + x))$). We obtain

$$\frac{\mathscr{E}_2}{\Phi(x, y)} = \frac{(a + d^2)^4(81a + 17d^2)}{2^{11}3^{12}(d + x)^{10}}(7d + 15x)(3a + d^2 + 4dx + 6x^2)^{10} = 0$$

and, since $a + d^2 \neq 0$ (see Lemma 8.2.15), we get $81a + 17d^2 = 0$. So, we obtain the family of systems

$$\dot{x} = -17d^2/81 + dy + x^2 + xy, \quad \dot{y} = -4d^2/81 + y^2, \tag{8.2.47}$$

which possess the invariant hyperbola: $\Phi(x,y) = -44d^2/81 - 4dx/3 + 2dy + 2xy = 0$. The perturbed systems

$$\dot{x} = -\frac{d^2(17-2\varepsilon+\varepsilon^2)}{(\varepsilon^2-9)^2} + dy + x^2 + (1+\varepsilon)xy, \quad \dot{y} = -\frac{4d^2}{(\varepsilon^2-9)^2} + y^2, \tag{8.2.48}$$

possess the two hyperbolas:

$$\Phi_1^\varepsilon(x,y) = -\frac{4d^2(11-4\varepsilon+\varepsilon^2}{(\varepsilon^2-9)^2(1+\varepsilon)} - \frac{4d}{(1+\varepsilon)(3+\varepsilon)}x + \frac{2d}{1+\varepsilon}y + 2xy = 0,$$
$$\Phi_2^\varepsilon(x,y) = \frac{4d^2(11+4\varepsilon+\varepsilon^2}{(\varepsilon^2-9)^2(\varepsilon-1)} - \frac{4d}{(1-\varepsilon)(3-\varepsilon)}x - \frac{6d}{\varepsilon-3}y + 2y(x+\varepsilon y) = 0.$$

We observe that for systems (8.2.43) we have $\delta_4 = (81a + 17d^2)/6$ and $\beta_7 = -8$. Therefore, if $\delta_4 = 0$, the invariant hyperbola is double and, by Lemma 8.2.5, it could not be triple due to $\beta_7 \neq 0$. This completes the proof of the statement $(i.1)$ of the lemma.

The case $\beta_4 = 0$. Then, we arrive at the family of systems (8.2.44), for which we have

$$\beta_6 = d(g^2-1)/4, \quad \widetilde{N} = 4(g^2-1)x^2, \quad \beta_{11} = 4(2g-1)^2x^2, \quad \beta_{12} = (3g-1)x,$$

So, due to $\widetilde{N} \neq 0$, the necessary conditions $d = 0$ and $2g - 1 \neq 0$ (see Lemma 8.2.16) are equivalent to $\beta_6 = 0$ and $\beta_{11} \neq 0$, respectively.

The subcase $\beta_{12} \neq 0$. In this case $3g - 1 \neq 0$ and, then, by Lemma 8.2.16, a nondegenerate invariant hyperbola exists if, and only if, $\mathscr{K}_1 = 0$ and $b \neq 0$. On the other hand, for systems (8.2.44) with $d = 0$ we calculate

$$\gamma_{15} = 4(g-1)^2(3g-1)\mathscr{K}_1x^5, \quad \mathscr{R}_{11} = -3b(g-1)^2x^4$$

and, hence, the above conditions are governed by the invariant polynomials γ_{15} and $\mathscr{R}_{11}$. So, we get systems (8.2.45) possessing the hyperbola $\Phi(x,y) = 2b/(2g-1) + 2cy/(3g-1) + 2xy = 0$.

According to Lemma 8.1.8, we calculate the polynomial $\mathscr{E}_2$ and we observe that $\mathscr{E}_2$ contains the polynomial $\Phi(x,y)$ as a simple factor.

In order to have this polynomial as a double factor in $\mathscr{E}_2$, we force its cofactor in $\mathscr{E}_2$ to be zero

along the curve $\Phi(x,y)=0$ (i.e we set $y=b(3g-1)/((2g-1)(c-x+3gx))$). We obtain

$$\frac{\mathscr{E}_2}{\Phi(x,y)}=\frac{288b^3(g-1)[c+(3g-1)x]^3}{(2g-1)^3(3g-1)^{16}}\big[c(2g-1)+g(3g-1)x\big]^{10}\times$$
$$\big[c^2(31-87g+62g^2)+6c(3g-2)(3g-1)^2x+(3g-1)^3(4g-1)x^2\big]=0$$

and, since $(2g-1)(3g-1)\neq 0$, we get $c=0$ and either $g=1/4$ or $g=0$. However, in the second case we get degenerate systems. So, $g=1/4$ and we arrive at the family of systems

$$\dot{x}=x^2/4,\quad \dot{y}=b-3xy/4, \tag{8.2.49}$$

which possess the hyperbola $\Phi(x,y)=-4b+2xy=0$. On the other hand, the perturbed systems

$$\dot{x}=-2b\varepsilon+\varepsilon xy+x^2/4,\quad \dot{y}=b-3xy/4 \tag{8.2.50}$$

possess the two invariant hyperbolas

$$\Phi_1^{\varepsilon}(x,y)=-4b+2xy=0,\quad \Phi_2^{\varepsilon}(x,y)=-4b+2y(x+\varepsilon y)=0.$$

It remains to determine the invariant polynomials which govern the conditions $c=0$ and $g=1/4$. We observe that for systems (8.2.45) we have $\gamma_{16}=-c(g-1)^2x^3/2$ and $\delta_6=(g-1)(4g-1)x^2/2$.

To deduce that the hyperbola $\Phi(x,y)=-4b+2xy=0$ could not be triple it is sufficient to calculate $\mathscr{E}_2$ for systems (8.2.49):

$$\mathscr{E}_2=-\frac{135x^{15}}{65536}\Phi(x,y)^2(5b-3xy)(17b-7xy)$$

and to observe that the cofactor of $\Phi(x,y)^2$ could not vanish along the curve $\Phi(x,y)=0$. This leads to the statement $(i.2)$ of the lemma.

The subcase $\beta_{12}=0$. Then, $g=1/3$ and, by Lemma 8.2.16, at least one nondegenerate invariant hyperbola exists if, and only if, $c=0$, $a\leq 0$ and $b\neq 0$. On the other hand, for systems (8.2.44) with $d=0$ and $g=1/3$ we calculate

$$\gamma_{16}=-2cx^3/9,\quad \gamma_{17}=32ax^2/9,\quad \mathscr{R}_{11}=-4bx^4/3$$

Therefore, the condition $c=0$ (respectively, $b\neq 0$; $a\leq 0$) is equivalent to $\gamma_{16}=0$ (respectively, $\mathscr{R}_{11}\neq 0$; $\gamma_{17}\leq 0$).

1) *The possibility* $\gamma_{17} < 0$. By Lemma 8.2.16, in this case we arrive at systems (8.2.46) with $z \neq 0$ possessing the two hyperbolas $\Phi_{1,2}(x,y) = -6b \pm 6z\,y + 2xy = 0$. We claim that none of the hyperbolas could be double. Indeed, calculating $\mathscr{E}_2$ (see Lemma 8.1.8), we obtain:

$$\mathscr{E}_2 = -\frac{2560(x^2-9z^2)^6}{177147}\Phi_1\Phi_2(2bx-x^2y-3yz^2)(3bx^2-x^3y+27bz^2-27xyz^2).$$

So, each hyperbola appears as a factor of degree one. Imposing the cofactor of Φ_1 (respectively, Φ_2) to vanish along the curve $\Phi_1(x,y) = 0$ (respectively, $\Phi_2(x,y) = 0$), i.e. setting $x = 3(b - zy)/y$ (respectively, $x = 3(b + zy)/y$), we obtain

$$\frac{\mathscr{E}_2}{\Phi_{1,2}} = 3732480b^6z^2(b \mp 2yz)^{10}/y^{13} \neq 0$$

due to $bz \neq 0$. This proves our claim and we arrive at the statement (ii) of the lemma.

2) *The possibility* $\gamma_{17} = 0$. In this case we have $z = 0$ and this leads to the systems

$$\dot{x} = x^2/3, \quad \dot{y} = b - 2xy/3, \tag{8.2.51}$$

possessing the hyperbola $\Phi(x,y) = -6b + 2xy = 0$. Calculating $\mathscr{E}_2$ for this systems, we obtain that $\Phi(x,y)$ is a triple factor of $\mathscr{E}_2$. According to Lemma 8.1.8, this hyperbola could be triple. And, in fact, it is triple as it is shown by the following perturbed systems:

$$\dot{x} = -12b^2\varepsilon^2 + x^2/3, \quad \dot{y} = b - 2xy/3 + 3b\varepsilon^2y^2, \tag{8.2.52}$$

possessing the three invariant hyperbolas:

$$\Phi_{1,2} = -6b \pm 6b\varepsilon\,y + 2xy = 0, \quad \Phi_3 = -6b + 2y(x - 3b\varepsilon^2y).$$

So, we arrive at the statement (iii) of Lemma 8.2.17 and this completes the proof of this lemma. ■

The case $\widetilde{N} = 0$

Considering (8.2.40), the condition $\widetilde{N} = 0$ implies $h = 0$ and $g = \pm 1$. On the other hand, for (8.2.30) with $h = 0$ we have $\beta_{13} = (g-1)^2x^2/4$ and we consider two cases: $\beta_{13} \neq 0$ and $\beta_{13} = 0$.

The subcase $\beta_{13} \neq 0$. Then, $g-1 \neq 0$ (this implies $g=-1$) and due to a translation we may assume $e=f=0$. So, we get the following family of systems

$$\dot{x} = a + cx + dy - x^2, \quad \dot{y} = b - 2xy. \tag{8.2.53}$$

Lemma 8.2.18. *A system* (8.2.53) *possesses at least one nondegenerate invariant hyperbola if, and only if,* $d=0$, $16a+3c^2=0$ *and* $b \neq 0$.

Proof. We again assume that the quadratic part of an invariant hyperbola has the form $2xy$ and considering equations (8.1.3) for systems (8.2.53), we obtain

$$t=1,\ s=u=q=0,\ p=-2b/3,\ r=-c/2,\ U=-3,$$
$$V=0,\ W=c+r/2,\ \ Eq_7=2d,\ \ Eq_9=(16a+3c^2)/8,$$
$$Eq_1=Eq_2=Eq_3=Eq_4=Eq_5=Eq_6=Eq_8=Eq_{10}=0.$$

Therefore, the conditions $Eq_7=0$ and $Eq_9=0$ yield $d=0$ and $16a+3c^2=0$. In this case we get the systems

$$\dot{x} = -3c^2/16 + cx - x^2, \quad \dot{y} = b - 2xy, \tag{8.2.54}$$

which possess the invariant hyperbola

$$\Phi(x,y) = -2b/3 - cy/2 + 2xy = 0.$$

Obviously, this hyperbola is nondegenerate if, and only if, $b \neq 0$. So, Lemma 8.2.18 is proved. ■

The subcase $\beta_{13}=0$. Then, $g=1$ and due to a translation we may assume $c=0$. So, we get the following family of systems

$$\dot{x} = a + dy + x^2, \quad \dot{y} = b + ex + fy. \tag{8.2.55}$$

Lemma 8.2.19. *A system* (8.2.55) *could not possess a finite number of hyperbolas. And it possesses a family of nondegenerate invariant hyperbolas if, and only if,* $d=e=0$ *and* $4a+f^2=0$.

Proof. Considering equations (8.1.3) and the fact that the quadratic part of an invariant hyper-

bola has the form $2xy$, for systems (8.2.55) we calculate

$$t = 1,\ s = u = 0,\ U = 1,\ \ V = 0,\ \ W = f - r/2,$$
$$Eq_5 = 2e,\ \ Eq_7 = 2d,\ \ Eq_1 = Eq_2 = Eq_3 = Eq_4 = Eq_6 = 0.$$

Therefore, the conditions $Eq_5 = 0$ and $Eq_7 = 0$ yield $d = e = 0$ and, then, we have

$$Eq_8 = 2b - p - fq + qr/2,\ \ Eq_9 = (4a + r^2)/2,\ \ Eq_{10} = aq + br - p(2f - r)/2.$$

The equations $Eq_8 = Eq_{10} = 0$ have a common solution with respect to the parameter q only if

$$\mathrm{Res}_q(Eq_8, Eq_{10}) = -2ab + p(a + f^2) - fr(b + p) + r^2(2b + p)/4 = 0.$$

On the other hand, in order to have a common solution of the above equations with respect to r, the following condition is necessary:

$$\mathrm{Res}_r\left(Eq_9, \mathrm{Res}_q(Eq_8, Eq_{10})\right) = (4a + f^2)(4ab^2 + f^2p^2)/4 = 0.$$

We claim, that the condition $4a + f^2 = 0$ is necessary for the existence of a nondegenerate invariant hyperbola.

Indeed, supposing $4a + f^2 \neq 0$, we deduce that the condition $4ab^2 + f^2p^2 = 0$ must hold.

1) Assume first $f \neq 0$. If $b = 0$, then we get $p = 0$ and the equation $Eq_{10} = 0$ gives $aq = 0$. In the case $q = 0$ we obtain a degenerate hyperbola. If $a = 0$, then the equation $Eq_9 = 0$ implies $r = 0$ and we again get a degenerate hyperbola.

Thus, $b \neq 0$ and, hence, $a \leq 0$. We set $a = -z^2 \leq 0$ and, consequently, $r = \pm 2z$ and $p = \pm 2bz/f$. It is not too hard to convince ourselves that all four possibilities lead either to degenerate hyperbolas, or to the equality $4a + f^2 = 0$, which contradicts our assumption.

2) Suppose now $f = 0$. This implies $ab = 0$ and, since $b \neq 0$ (otherwise we get degenerate systems), we have $a = 0$ and this again contradicts to $4a + f^2 \neq 0$. This completes the proof of our claim.

Thus, $4a + f^2 = 0$ and, setting $a = -f^2/4$, we arrive at the family of systems

$$\dot{x} = -f^2/4 + x^2, \quad \dot{y} = b + fy, \tag{8.2.56}$$

which possess the following family of invariant hyperbolas

$$\Phi(x,y) = (4b - fq)/2 + qx + fy + 2xy = 0,$$

depending on the free parameter q. Since the corresponding determinant Δ (see Remark 8.1.7) for this family equals $fq - 2b$, we conclude that all the hyperbolas are nondegenerate, except the hyperbola, for which the equality $fq - 2b = 0$ holds. Thus, the lemma is proved. ∎

We observe that in the above systems we may assume $b = 1$. Indeed, if $b = 0$, then $f \neq 0$ (otherwise we get a degenerate system) and, therefore, due to the translation $y \to y + b'/f$ with $b' \neq 0$ and the addition rescaling $y \to b'y$, we get $b' = 1$. Moreover, in this case we may assume $f \in \{0,1\}$ due to rescaling $(x,y,t) \mapsto (fx, fy, t/f)$ when $f \neq 0$. This leads to the two families of hyperbolas mentioned in Remark 8.1.4.

Lemma 8.2.20. *Assume that for a quadratic system* (8.1.2) *the conditions* $\eta = 0$, $\widetilde{M} \neq 0$ $\theta = 0$ *and* $\widetilde{N} = 0$ *hold. Then, this system could possess either a single nondegenerate invariant hyperbola, or a family of such hyperbolas. More precisely, this system possess*

(i) one simple nondegenerate invariant hyperbola if, and only if, $\beta_{13} \neq 0$, $\gamma_{10} = \gamma_{17} = 0$ *and* $\mathscr{R}_{11} \neq 0$*;*

(ii) one family of nondegenerate invariant hyperbolas if, and only if, $\beta_{13} = \gamma_9 = \tilde{\gamma}_{18} = \tilde{\gamma}_{19} = 0$.

Moreover, the family of hyperbolas corresponds to $(\mathscr{F}_4)$ *(respectively,* $(\mathscr{F}_5)$*) (see Figure 8.4), if* $\gamma_{17} \neq 0$ *(respectively,* $\gamma_{17} = 0$*).*

Proof. Assume that for a quadratic system (8.1.2) the conditions $\eta = 0$, $\widetilde{M} \neq 0$ $\theta = 0$ and $\widetilde{N} = 0$ hold.

The subcase $\beta_{13} \neq 0$. In this case we consider systems (8.2.53) for which we calculate

$$\gamma_{10} = 14d^2, \quad \mathscr{R}_{11} = -12bx^4 + 6dxy^2(cx + dy), \quad \gamma_{17} = 8(16a + 3c^2)x^2 - 4dy(14cx + 9dy).$$

So, for $\gamma_{10} = \gamma_{17} = 0$ and $\mathscr{R}_{11} \neq 0$ we get systems (8.2.54) possessing the hyperbola $\Phi(x,y) = -2b/3 - cy/2 + 2xy = 0$. We claim that this hyperbola is a simple one. Indeed, calculating $\mathscr{E}_2$, we obtain that the polynomial $\Phi(x,y)$ is a factor of degree one in $\mathscr{E}_2$. So, setting $y = -4b/(3(c-4x))$ (i.e. $\Phi(x,y) \equiv 0$), we get

$$\frac{\mathscr{E}_2}{\Phi(x,y)} = -2^{-24}5b^3(c-4x)^3(3c-4x)^{12}/3 \neq 0$$

due to $b \neq 0$. So, the hyperbola above could not be double and this proves our claim. Thus the statement (i) of lemma is proved.

The subcase $\beta_{13} = 0$. Then, we consider systems (8.2.55) and we calculate

$$\gamma_9 = -6d^2, \quad \tilde{\gamma}_{18} = 8ex^4, \quad \tilde{\gamma}_{19} = 4(4a + f^2)x.$$

So, the conditions $d = e = 0$ are equivalent to $\gamma_9 = \tilde{\gamma}_{18} = 0$ and $4a + f^2 = 0$ is equivalent to $\tilde{\gamma}_{19} = 0$.

Considering Lemma 8.2.19 we arrive at the statement (ii).

It remains to observe that for systems (8.2.55) with $d = e = 0$ and $a = -f^2/4$ we have $\gamma_{17} = 8f^2x^2$ and this invariant polynomial governs the condition $f = 0$.

As all the cases are examined, Lemma 8.2.20 is proved. ∎

To complete the proof of Theorem 8.1.2 we remark that both generic families of quadratic systems (with three and with two distinct real infinite singularities) are examined and now we could compare the obtained results with the statements of Theorem 8.1.2.

So, comparing the statements of Lemmas 8.2.4, 8.2.5, 8.2.8, 8.2.9 and 8.2.12 with the conditions given by Figure 8.1, it is not too difficult to conclude that the statement $\boldsymbol{(B_1)}$ of Theorem 8.1.2 is valid.

Analogously, comparing the statements of Lemmas 8.2.14, 8.2.17 and 8.2.20 with the conditions given by Figure 8.2, we deduce that the statement $\boldsymbol{(B_2)}$ of Theorem 8.1.2 is valid.

Since the type of each of the five families $\mathscr{F}_1$–$\mathscr{F}_5$ is determined inside the proof of the respective lemma, we conclude that the Theorem 8.1.2 is completely proved.

Chapter

9

Final considerations

The object of study of this thesis was the family of quadratic differential systems in the plane and the main goal was to classify three families of such systems. Essentially here we consider two classification problems: one is on the topological classification of some families of quadratic systems and the other is to classify the family of quadratic systems possessing invariant hyperbolas with respect to their number and their multiplicity.

For both problems, we used the theory of affine invariant polynomials (comitants and invariants) developed by Sibirsky and his former students, especially by Vulpe. This theory has been used by many researchers in the field of the quadratic class of differential systems. One of the reasons why invariant polynomials are widely used is because of the possibility of constructing algebraic or semi–algebraic sets of objects having a specific geometric property. Then, building a "bridge" between geometry and algebra of quadratic systems, we have the control of all possible algebraic bifurcation in its parameter space under some geometrical restriction.

In the case of the topological classification of phase portraits, due to the normal form adopted for each one of the families, we have worked with three–parametric and four–parametric systems, but the bifurcation diagram is always tridimensional. The normal form we used for systems possessing a finite semi–elemental triple node belonging to the class $\mathbf{QT\overline{N}}$ possesses three parameters and its bifurcation diagram is $\mathbb{R}^3$, whereas the normal forms we used for systems possessing a finite semi–elemental saddle–node and an infinite saddle–node of type $\overline{\binom{0}{2}}SN$ belonging to the class $\overline{\mathbf{QsnSN}}$ possess four parameters and their bifurcation diagram is $\mathbb{RP}^3$. It is worth mentioning that not all the bifurcations in the parameter space were purely algebraic; we detected the

presence of many nonalgebraic bifurcations referring mainly to connection of separatrices.

As an illustration, the table below shows the number of regions in the bifurcation diagram and the number of topologically distinct phase portraits of different families of quadratic systems using the theory of affine invariant polynomials as well as the number of some geometric objects present in the phase portraits (limit cycles and graphics).

	$\overline{\mathbf{QW2}}$	$\overline{\mathbf{QTN}}$	$\overline{\mathbf{QsnSN(A)}}$	$\overline{\mathbf{QsnSN(B)}}$	$\overline{\mathbf{QsnSN(C)}}$	$\overline{\mathbf{QsnSN}}$
Parts in the bifurcation diagram	373	63	85	43	1034	senseless
Topologically distinct phase portraits	126	28	38	25	371	417
Phase portraits with one limit cycle	17	3	3	0	49	52
Phase portraits with two limit cycles	3 (1,1)	0	0	0	1 (2) 1 (1,1)	2
Phase portraits with nondegenerate graphics	19	4	6	4	118	128
Phase portraits with degenerate graphics	0	0	10	7	7	21

In the table above, when a phase portrait possesses two limit cycles, we exhibit their number followed by their configuration by denoting i (j), where i is the number of phase portraits with two limit cycles and (j) is their configuration as for example (j) could be $(1,1)$ (one limit cycle around each one of the two foci) or (2) (two limit cycles around only one focus).

In the other case, the classification was in the sense of giving necessary and sufficient conditions in terms of affine invariant polynomials for the existence and multiplicity of invariant hyperbolas in quadratic differential systems. The parameter space considered here is $\mathbb{R}^{12}$, but after affine transformations and time homotheties, we reduce this dimension to five. The problem about hyperbolas we considered here can be extended so as to include all conics. Our purpose is to classify all quadratic differential systems possessing invariant irreducible conics, and to achieve this goal it remains to find out necessary and sufficient conditions for the existence of invariant ellipses and invariant parabolas in quadratic systems. This is a joint work with Vulpe and Schlomiuk and it will be finished in the next years.

Now, being more specific in the case of topological classification of phase portraits, the families we analyzed and presented in this thesis are themselves interesting because of the degree of complexity of their study. Moreover, the results we obtained contribute to the topological classification of the whole class of quadratic systems. We are aware that our efforts to this classification correspond to a small grain in the vast class of quadratic systems, but we believe it is not in vain.

However, although we have indirectly contributed to the topological classification of quadratic differential systems, we have enriched the specific case of classifying topologically all the unstable quadratic systems of codimension one. The main way to do this is to consider phase portraits of quadratic systems of higher codimension and submit them to perturbations in order to obtain codimension–one phase portraits. The stage of this research was already advanced, but the proof of the realization or nonrealization of some topological possible phase portraits was missing. With this study, it was possible to decrease the number of the missing cases, but it was not sufficient to cover all of them.

In order to annihilate these missing cases, we intend to analyze other families of quadratic systems which are worth studying, namely: (i) with a finite semi–elemental triple saddle; (ii) with a finite node with one direction (n^d) and an infinite saddle–node of type $\overline{\binom{0}{2}}SN$; (iii) with a weak focus of order one and an infinite saddle–node of type $\overline{\binom{0}{2}}SN$; and (iv) with a finite saddle–node and an infinite saddle–node of type $\overline{\binom{1}{1}}SN$. However, we cannot guarantee that we will finish the study of the unstable quadratic systems of codimension one by analyzing the families above; we may need to consider other families different from these ones with other specific geometric characteristics which may lead to the desired cases.

Bibliography

[1] H. AMANN, *Ordinary differential equations: an introduction to nonlinear analysis*. New York: de Gruyter, 1990.

[2] A. A. ANDRONOV, E. A. LEONTOVICH, I. I. GORDON, A. G. MAIER, *Qualitative theory of second–order dynamic systems*. Israel Program for Scientific Translations (Halsted Press, A division of John Wiley & Sons, NY-Toronto, Ontario), 1973.

[3] J. C. ARTÉS, F. DUMORTIER, C. HERSSENS, J. LLIBRE, P. DE MAESSCHALCK, *Computer program P4 to study phase portraits of planar polynomial differential equations*. Available at: <http://mat.uab.es/~artes/p4/p4.htm>, 2005.

[4] J. C. ARTÉS, R. KOOIJ, J. LLIBRE, *Structurally stable quadratic vector fields*, Memoires Amer. Math. Soc. **134 (639)** (1998).

[5] J. C. ARTÉS, J. LLIBRE, *Structurally unstable quadratic systems of codimension 1*, Preprint, 2014.

[6] J. C. ARTÉS, J. LLIBRE, D. SCHLOMIUK, *The geometry of quadratic differential systems with a weak focus of second order*, Internat. J. Bifur. Chaos Appl. Sci. Engrg. **16** (2006), 3127–3194.

[7] J. C. ARTÉS, J. LLIBRE, D. SCHLOMIUK, N. VULPE, *From topological to geometric equivalence in the classification of singularities at infinity for quadratic vector fields*, To appear in Rocky Mountain J. Math. **43** (2013).

[8] J. C. ARTÉS, J. LLIBRE, N. VULPE, *Singular points of quadratic systems: a complete classification in the coefficient space*, Internat. J. Bifur. Chaos Appl. Sci. Engrg. **18** (2008), 313–362.

[9] J. C. ARTÉS, A. C. REZENDE, R. D. S. OLIVEIRA, *Global phase portraits of quadratic polynomial differential systems with a semi–elemental triple node*, Internat. J. Bifur. Chaos Appl. Sci. Engrg. **23** (2013), 21pp.

[10] J. C. ARTÉS, A. C. REZENDE, R. D. S. OLIVEIRA, *The geometry of quadratic polynomial differential systems with a finite and an infinite saddle–node* (A,B), Internat. J. Bifur. Chaos Appl. Sci. Engrg. **24** (2014), 30pp.

[11] V. A. BALTAG, N. VULPE, *Affine–invariant conditions for determining the number and multiplicity of singular points of quadratic differential systems*, Izv. Akad. Nauk Respub. Moldova Mat. **1** (1993), 39–48.

[12] N. N. BAUTIN, *On periodic solutions of a system of differential equations*, Prikl. Mat. Meh. **18** (1954).

[13] I. BENDIXSON, *Sur les courbes définies par des équations différentielles*, Acta Math. **24** (1901), 1–88.

[14] E. BIERSTONE, P.D. MILMAN, *Semi-analytic and subanalytic sets*. Inst. Hautestudes Sci. Publ. Math. **67** (1988), 5–42.

[15] F. BRAUER, *Basic ideas of mathematical epidemiology*, in: C. Castillo-Chavez, S. Blower Sally, P. van den Driessche, D. Kirschner, A.A. Yakubu, Mathematical approaches for emerging and reemerging infectious diseases, The IMA volumes in mathematics and its applications, New York: Springer-Verlag, 2002, 31–65.

[16] G. BOOLE, *Exposition of a general theory of linear transformations*. Camb. Math. J. **3** (1841-2), 1–20, 106–119.

[17] D. BOULARAS, I. CALIN, L. TIMOCHOUK, N. VULPE, *$T-$comitants of quadratic systems: a study via the translation invariants*, Delft University of Technology, Faculty of Technical Mathematics and Informatics, v. 90, 1996.

[18] L. CAIRÓ, J. LLIBRE, *Darbouxian first integrals and invariants for real quadratic systems having an invariant conic*, J. Phys. A: Math. Gen. **35** (2002), 589–608.

[19] C. CHRISTOPHER, *Quadratic systems having a parabola as an integral curve*. Proc. Roy. Soc. Edinburgh Sect. A, **112A** (1989), 113–134.

[20] C. CHRISTOPHER, J. LLIBRE, J. V. PEREIRA, *Multiplicity of invariant algebraic curves in polynomial vector fields*. Pacific J. Math. **229** (2007), 63–117.

[21] B. COLL, J. LLIBRE, *Limit cycles for a quadratic system with an invariant straight line and some evolution of phase portraits*, Qualitative Theory of Differential Equations, Colloq. Math. Soc. János Bolyai, Bolyai Institut, Szeged, Hungria. **53** (1988), 111–123.

[22] W. A. COPPEL, *A survey of quadratic systems*, J. Differ. Equat. **2** (1966), 293–304.

[23] G. DARBOUX, *Mémoire sur les équations différentielles algébriques du premier ordre et du premier degré (mélanges)*, Bull. Sci. Math. **124A** (1878), 60–96, 123–144, 151–200.

[24] T. A. DRUZHKOVA, *The algebraic integrals of a certain differential equation*. Differ. Equ. **4** (1968).

[25] F. DUMORTIER. *Singularities of vector fields on the plane*. J. Differ. Equat. **23** (1977), 53–106.

[26] F. DUMORTIER, P. FIDDELAERS, *Quadratic models for general local* 3*–parameter bifurcations on the plane*, Trans. Amer. Math. Soc. **326** (1991), 101–126.

[27] F. DUMORTIER, J. LLIBRE, J. C. ARTÉS, *Qualitative theory of planar differential systems*. New York: Springer, 2006.

[28] F. DUMORTIER, R. ROUSSARIE, C. ROUSSEAU, *Hilbert's 16th problem for quadratic vector fields*, J. Differ. Equat. **110** (1994), 86–133.

[29] H. EVES, *An introduction to the history of mathematics*. Philadelphia: Saunders College Publishing, 1990.

[30] W. FULTON, *Algebraic curves: an introduction to algebraic geometry*, New York: W.A. Benjamin, Inc, 1969.

[31] J. H. GRACE, A. YOUNG, *The algebra of invariants*. New York: Stechert, 1941.

[32] R. HARTSHORNE, *Algebraic geometry*. New York: Springer, 1997.

[33] D. HILBERT, *Mathematical problems*. Reprinted from Bull. Amer. Math. Soc. **8** (1902), 437–479. Bull. Amer. Math. Soc. (N.S.) **37** (2000), 407–436.

[34] D. HILBERT, *Mathematische probleme*. In Nachr. Ges. Wiss., editor, Second Internat. Congress Math. Paris, 1900, Göttingen Math.-Phys. Kl. (1900), 253–297.

[35] Q. JIANG, J. LLIBRE, *Qualitative classification of singular points*, Qual. Theory Dyn. Syst. **6** (2005), 87–167.

[36] P. JOYAL, C. ROUSSEAU, *Saddle quantities and applications*, J. Diff. Eqns. **78** (1989), 374–399.

[37] W.O. KERMACK, A.G. MCKENDRICK, *A contribution to the mathematical theory of epidemics*, Proc. Roy. Soc. London **115** (1927), 700–721.

[38] J. D. LAWRENCE, *A catalog of special planar curves*. Dover Publication, 1972.

[39] J. LLIBRE, D. SCHLOMIUK, *The geometry of quadratic differential systems with a weak focus of third order*, Canad. J. Mat. **56** (2004), 310–343.

[40] J. LLIBRE, C. VALLS, *Integrability of a SIS model*, J. Math. Anal. Appl. **344** (2008), 574–578.

[41] I. NIKOLAEV, N. VULPE, *Topological classification of quadratic systems at infinity*, J. London Math. Soc. **55** (1997), 473–488.

[42] M.C. NUCCI, P.G.L. LEACH, *An integrable SIS model*, J. Math. Anal. Appl. **290** (2004), 506–518.

[43] R. D. S. OLIVEIRA, A. C. REZENDE, *Global phase portraits of a SIS model*. Appl. Math. Comput. **219** (2013), 4924–4930.

[44] R. D. S. OLIVEIRA, A. C. REZENDE, N. VULPE, *Family of quadratic differential systems with invariant hyperbolas: a complete classification in the space* $\mathbb{R}^{12}$. Cadernos de Matemática. **15** (2014), 19–75.

[45] P. J. OLVER, *Classical invariant theory*. London Mathematical Society Students Texts, 44. Cambridge: Cambridge University Press, 1999.

[46] H. POINCARÉ, *Sur l'intégration algébrique des équations différentielles du premier ordre et du premier degré*. Rend. Circ. Mat. Palermo **5** (1891), 161–191.

[47] H. POINCARÉ, *Mémoire sur les courbes définies par une équation différentielle*. Edit. Jacques Gabay, Paris (1993). Reprinted from the original papers published in the Journal de Mathématiques **7** (1881) 375–422, **8** (1882) 251–296, **1** (1885) 167–244, and **2** (1886) 151–217.

[48] QIN YUAN-XUN, *On the algebraic limit cycles of second degree of the differential equation* $dy/dx = \Sigma_{0\le i+j\le 2} a_{ij}x^i y^j / \Sigma_{0\le i+j\le 2} b_{ij}x^i y^j$. Chin. Math. Acta. **8** (1996).

[49] D. SCHLOMIUK, *Basic algebro–geometric concepts in the study of planar polynomial vector fields*, Publ. Mat. **41** (1997), 269–295.

[50] D. SCHLOMIUK, *Topological and polynomial invariants, moduli spaces, in classification problems of polynomial vector fields*, Publ. Mat. **58** (2014), suppl., 461–496.

[51] D. SCHLOMIUK, J. PAL, *On the geometry in the neighborhood of infinity of quadratic differential systems with a weak focus*, Qual. Theory Dyn. Syst. **2** (2001), 1–43.

[52] D. SCHLOMIUK, N. VULPE, *Planar quadratic differential systems with invariant straight lines of at least five total multiplicity*, Qual. Theory Dyn. Syst. **5** (2004), 135–194.

[53] D. SCHLOMIUK, N. VULPE, *Geometry of quadratic differential systems in the neighborhood of infinity*, J. Diff. Eqns. **215** (2005), 357–400.

[54] D. SCHLOMIUK, N. VULPE, *Integrals and phase portraits of planar quadratic differential systems with invariant lines of total multiplicity four*, Bul. Acad. Ştiinţe Repub. Mold. Mat. **1** (2008), 27–83.

[55] D. SCHLOMIUK, N. VULPE, *Planar quadratic differential systems with invariant straight lines of total multiplicity four*, Nonlinear Anal. **68** (2008), 681–715.

[56] D. SCHLOMIUK, N. VULPE, *Integrals and phase portraits of planar quadratic differential systems with invariant lines of at least five total multiplicity*, Rocky Mountain J. Math., **38** (2008), 1–60.

[57] K. S. SIBIRSKY, *Introduction to the algebraic theory of invariants of differential equations*. Nonlinear Sci. Theory Appl. Manchester: Manchester University Press, 1988.

[58] J. SOTOMAYOR, *Lições de equações diferenciais ordinárias*. Projeto Euclides. Rio de Janeiro: IMPA, 1979.

[59] C. VARGAS-DE-LÉON, *Stability analysis of a SIS epidemic model with standard incidence*, Foro RED-Mat **28** (2011).

[60] N. VULPE, *Polynomial bases of comitants of differential systems and their applications in qualitative theory*, Kishinev: Shtiintsa, 1986.

[61] N. VULPE, *Characterization of the finite weak singularities of quadratic systems via invariant theory*, Nonlinear Anal. **74** (2011), 6553–6582.

[62] Y. Q. YE, S. L. CAI, L. S. CHEN, K. C. HUANG, D. J. LUO, Z. E. MA, E. N. WANG, M. S. WANG, X. A. YANG, *Theory of limit cycles*, Trans. of Mathematical Monographs, **66**. Providence: Amer. Math. Soc., 2 edition.

Index